AD-A136 610 JETTY STABILITY STUDY OREGON INLET NORTH CAROLINA HYDRAULIC MODEL INVESTIGATION(U) COASTAL ENGINEERING RESEARCH CENTER VICKSBURG MS R D CARVER ET AL. SEP 83

1/5

UNCLASSIFIED CERC-TR-83-3 F/G 13/2 NL

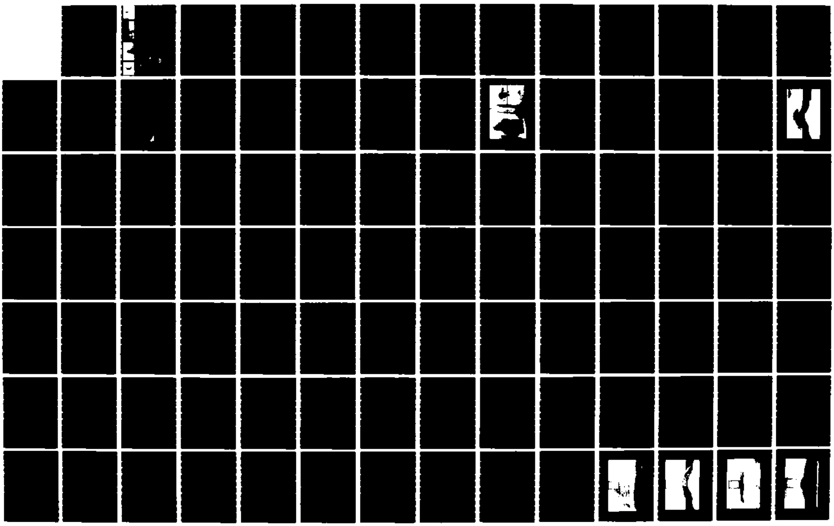

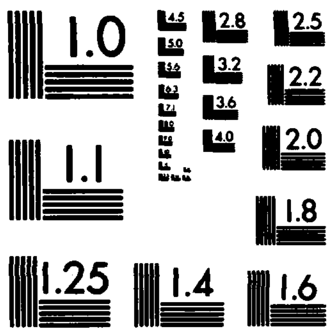

MICROCOPY RESOLUTION TEST CHART
NATIONAL BUREAU OF STANDARDS-1963-A

(12)

US Army Corps
of Engineers

TECHNICAL REPORT CERC-83-3

JETTY STABILITY STUDY, OREGON INLET, NORTH CAROLINA

Hydraulic Model Investigation

by

Robert D. Carver, D. Donald Davidson
Coastal Engineering Research Center
U. S. Army Engineer Waterways Experiment Station
P. O. Box 631, Vicksburg, Miss. 39180

September 1983

Final Report

Approved For Public Release; Distribution Unlimited

Prepared for U. S. Army Engineer District, Wilmington
Wilmington, North Carolina 28402

Unclassified

SECURITY CLASSIFICATION OF THIS PAGE (When Data Entered)

REPORT DOCUMENTATION PAGE		READ INSTRUCTIONS BEFORE COMPLETING FORM
1. REPORT NUMBER Technical Report CERC-83-3	2. GOVT ACCESSION NO. AD-A136610	3. RECIPIENT'S CATALOG NUMBER
4. TITLE (and Subtitle) JETTY STABILITY STUDY, OREGON INLET, NORTH CAROLINA; Hydraulic Model Investigation		5. TYPE OF REPORT & PERIOD COVERED Final report 6. PERFORMING ORG. REPORT NUMBER
7. AUTHOR(s) Robert D. Carver D. Donald Davidson		8. CONTRACT OR GRANT NUMBER(s)
9. PERFORMING ORGANIZATION NAME AND ADDRESS U. S. Army Engineer Waterways Experiment Station Coastal Engineering Research Center P. O. Box 631, Vicksburg, Miss. 39180		10. PROGRAM ELEMENT, PROJECT, TASK AREA & WORK UNIT NUMBERS
11. CONTROLLING OFFICE NAME AND ADDRESS U. S. Army Engineer District, Wilmington P. O. Box 1890 Wilmington, N. C. 28402		12. REPORT DATE September 1983 13. NUMBER OF PAGES 446
14. MONITORING AGENCY NAME & ADDRESS(if different from Controlling Office)		15. SECURITY CLASS. (of this report) Unclassified 15a. DECLASSIFICATION/DOWNGRADING SCHEDULE

16. DISTRIBUTION STATEMENT (of this Report)

Approved for public release; distribution unlimited.

17. DISTRIBUTION STATEMENT (of the abstract entered in Block 20, if different from Report)

18. SUPPLEMENTARY NOTES

Available from National Technical Information Service, 5285 Port Royal Road, Springfield, Va. 22161.

19. KEY WORDS (Continue on reverse side if necessary and identify by block number)

Hydraulic models
Inlets (Waterways)
Jetties
Shore protection
Water waves

20. ABSTRACT (Continue on reverse side if necessary and identify by block number)

An undistorted-scale hydraulic model study was conducted to provide input for design optimization of a rubble-mound jetty system proposed for Oregon Inlet, North Carolina. Two-dimensional (trunk) tests consisted of (a) developing stable stone and dolos sections (base designs) for a depth-limited breaking wave of 15 sec, 13.6 ft at a design swl of +5.5 ft; (b) subjecting the stable base designs obtained at the +5.5 ft swl to storm-surge hydrographs with peak levels of +6.5, +7.5, +8.5, +9.5, +10.5, and +11.5 ft

(Continued)

DD FORM 1 JAN 73 1473 EDITION OF 1 NOV 65 IS OBSOLETE

Unclassified

SECURITY CLASSIFICATION OF THIS PAGE (When Data Entered)

20. ABSTRACT (Continued).

NGVD and obtaining damage as a function of swl; (c) redesigning the armoring schemes for stable sections at +7.5 ft swl with a depth-limited breaking wave of 15 sec, 15.5 ft and subjecting these plans to storm-surge hydrographs of +8.5, +9.5, +10.5, and +11.5 ft NGVD and again determining damage as a function of swl; and (d) redesigning both the stone and dolos sections for stability at an swl of +9.5 ft with a depth-limited breaking wave of 15 sec, 17.2 ft. Three-dimensional tests were conducted to determine stable stone and dolos head sections for 15-sec, 17.6-ft waves at angles of wave attack equal to 0, 22.5, 45, 67.5, and 90 deg.

Two-dimensional test results of base designs at swl's of +5.5, +7.5, and +9.5 ft correlated well with the seaside armor requirement predicted by the Hudson Stability Equation. Stability coefficients for the range of conditions investigated were determined to be 2.3 and 8.3 for stone and dolosse, respectively. Results of storm-surge hydrograph tests showed that as opposed to the stone designs, the dolos sections experienced significantly more rapid deterioration when subjected to wave heights in excess of the design height.

During three-dimensional tests of the selected head geometries, 30-ton stone and 14-ton dolosse proved to be stable for 15-sec, 17.6-ft breaking and nonbreaking waves at angles of wave attack equal to 0.0, 22.5, 45, 67.5, and 90 deg. The 30-ton stone and 14-ton dolos breakwater head designs correspond to stability coefficients of 1.3 and 4.0, respectively. Also, based on total armor area reproduced, no particular angle of wave attack was significantly more damaging than the others for either armor type.

Additional two-dimensional tests (Phase II) conducted to satisfy prototype foundation problems produced stable designs for (a) an all dolos section, (b) protection with dolosse on the crown and side slopes and stone on the toe, and (c) protection with stone on the crown and toe, and dolosse on the side slopes.

PREFACE

The model investigation reported herein was requested by the U. S. Army Engineer District, Wilmington (SAW), in a letter to the U. S. Army Engineer Waterways Experiment Station (WES), dated 16 September 1974. Funding authorization was initially granted by SAW on Intra-Army order No. SAWRS-75-20, dated 9 July 1975.

Model tests were conducted at WES during the period January 1976 to October 1982, under the general direction of Mr. H. B. Simmons, Chief of the Hydraulics Laboratory; Dr. R. W. Whalin, former Chief of the Wave Dynamics Division; and Mr. D. D. Davidson, Chief of the Wave Research Branch. Tests were conducted by Messrs. R. D. Carver, Research Hydraulic Engineer; C. R. Herrington and C. Lewis, Engineering Technicians; and L. J. Brown, Engineering Aid. The Wave Dynamics Division and its personnel were combined with and transferred to the Coastal Engineering Research Center of WES on 1 July 1983 under the supervision of Dr. R. W. Whalin, Chief of the Center. This report was prepared by Messrs. Carver and Davidson. Messrs. Lim Vallianos and Tom Jarrett of SAW provided prototype information and coordinated plans for the model tests with Messrs. Davidson and Carver of WES.

Liaison was maintained during the course of the investigation by means of conferences, progress reports, and telephone conversations.

Commanders and Directors of WES during the conduct of this study and the preparation and publication of this report were COL John L. Cannon, CE, COL Nelson P. Conover, CE, and COL Tilford C. Creel, CE. Technical Director was Mr. F. R. Brown.

CONTENTS

CONVERSION FACTORS, U. S. CUSTOMARY TO METRIC (SI) UNITS OF MEASUREMENT

U. S. customary units of measurement used in this report can be converted to metric (SI) units as follows:

Multiply	By	To Obtain
feet	0.3048	metres
inches	25.4	millimetres
pounds (mass)	0.4535924	kilograms
pounds (mass) per cubic foot	16.01846	kilograms per cubic metre
square feet	0.09290304	square metres
tons (2,000 lb, mass)	907.1847	kilograms

JETTY STABILITY STUDY, OREGON INLET, NORTH CAROLINA

Hydraulic Model Investigation

PART I: INTRODUCTION

The Prototype

1. The northernmost opening through the barrier reef of the North Carolina coast is Oregon Inlet (Figure 1). Its existence was first noted in 1585. With an intervening history of closing and opening, it has maintained a continuous migratory watercourse since 1846. Oregon Inlet is of major hydrological significance in that it is the only existing communicator between the sounds of northeastern North Carolina and the Atlantic Ocean.

2. The area immediately adjacent to Oregon Inlet includes all of Dare County, North Carolina. Principal economic activities include services, recreation, commercial fishing, seafood processing, and boat building. The existing project channel depth of 14 ft* across the ocean bar at Oregon Inlet is not deep enough nor stable enough for safe navigation by operators of commercial fishing vessels from North Carolina and other out-of-State ports.

3. In an effort to provide safe passage for commercial fishing craft and other commercial ships, the U. S. Army Engineer District, Wilmington (SAW), has proposed a channel improvement and stabilization project for Oregon Inlet. The proposed project will include a 20-ft-deep and 400-ft-wide channel through the ocean bar at Oregon Inlet. Protection for the new channel will be provided by rubble-mound jetties.

The Problem

4. A need for stability model tests of the jetties arises from the intent of SAW to develop a jetty design, which is optimum in terms of cost-effectiveness. In other words, the selection of structural features, particularly armor cover, is to be based on a least-cost alternative in terms of

---

* A table of factors for converting U. S. customary units of measurement to metric (SI) units is presented on page 4.

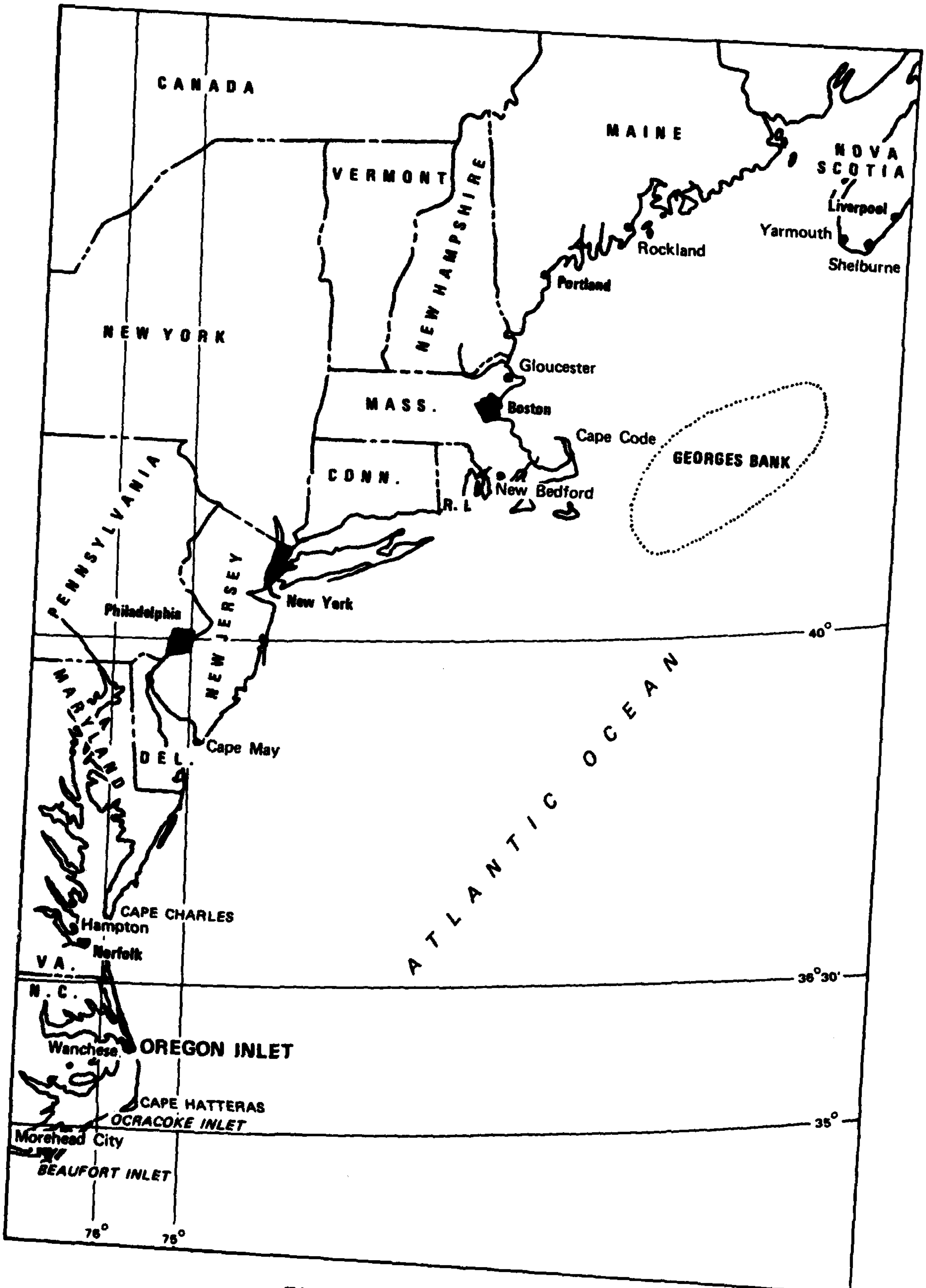

Figure 1. Location map

combined capitalized initial construction costs and expected annual maintenance costs. Determination of the annual costs necessitates, as input, relationships of damage to wave heights exceeding a given design wave height. Some general information of this type is available for quarrystone, quadripods, dolos, and tribars when it is expected that a structure would experience little or no wave overtopping (Hudson 1958, Jackson 1968, Carver and Davidson 1977). However, this latter point does not apply to the case at hand, and accordingly, the available data concerning damages are not directly applicable to the intended optimum design analysis. Specifically, the jetty structures proposed for Oregon Inlet will be exposed to surges (extratropical and tropical storms) and wave action generated by storms of hurricane intensity, and it is expected that the proposed structures will suffer numerous major wave overtopping events during the project life.

5. Model tests to determine the optimum jetty design were conducted during the period in which SAW was continuing the engineering evaluation of other aspects associated with the stabilization of the inlet. Specifically, the analysis of the foundation on which the jetty structures would be constructed revealed the existence of a weak clay layer lying under the offshore sand deposits. The weakness of this clay layer poses significant problems with the jetties, particularly if scour during construction reduces the thickness of the sand layer to a critical point. If the sand thickness is reduced and channel scour occurs immediately adjacent to the jetties, there is a possibility that the foundation could slip toward the channel under certain loading conditions caused by the jetties.

6. The significance of the weak clay layer, vis-a-vis the jetty design, was not fully realized until after the completion of the two-dimensional (2-d) stability tests aimed at determining an optimum jetty design. Consequently, SAW requested a second series of 2-d stability tests to evaluate several alternative jetty cross-sectional designs that would reduce the total weight of the structures. Therefore in this report, the original series of 2-d tests conducted to determine the optimum jetty design and the three-dimensional (3-d) tests on the jetty head will be designated as the Phase I testing program, whereas the test to reduce the overall weight of the jetties will be designated as Phase II.

Purpose and Approach of Phase I Model Study

7. The purpose of the Phase I model study was to conduct a sufficient number of 2-d and 3-d stability tests to provide data required for the design optimization described in paragraph 4. Specifically, the following 2-d tests were conducted:

a. Stable stone and dolos jetty sections (base designs) were determined for the most severe breaking wave conditions that experimentally could be made to attack the structures at a design still-water level (swl) of +5.5 ft NGVD.*

b. Once the base designs were determined at the +5.5 ft swl, they were subjected to storm-surge hydrographs with maximum swl's of +6.5, +7.5, +8.5, +9.5, +10.5, and +11.5 ft (using the most severe breaking wave condition that experimentally could be made to attack the structure at each swl) and damage was obtained as a function of swl.

c. Both armoring schemes were redesigned for stability for the most severe breaking wave condition at an swl of +7.5 ft and these plans were subjected to storm-surge hydrographs with maximum swl's of +8.5, +9.5, +10.5, and +11.5 ft (using the most severe breaking wave condition at each swl) and again damage was determined as a function of swl.

d. Finally, both the stone and dolos sections were redesigned for stability for the most severe breaking wave condition at an swl of +9.5 ft.

Three-dimensional tests were conducted to determine stable stone and dolos head sections for 15-sec, 17.6-ft waves at 0-, 22.5-, 45-, 67.5-, and 90-deg angles of wave attack.

---

* All elevations and still-water levels (el and swl, respectively) cited herein are in feet referred to the National Geodetic Vertical Datum (NGVD); though on some figures, photographs, and plates "ft msl" is used.

PART II: THE MODEL

Design of Model

8. Tests were conducted at geometrically undistorted linear scales of 1:33 (2-d tests) and 1:48 (3-d tests), model to prototype. Scale selection was determined by the absolute size of model breakwater sections necessary to ensure the preclusion of stability scale effects (Hudson 1975), capabilities of the available wave generator, and depth of water at the toe of the breakwater. Based on Froude's model law (Stevens et al. 1942) and the linear scales of 1:33 and 1:48, the following model-prototype relations were derived. Dimensions are in terms of length (L) and time (T).

		Model-Prototype Scale Relation	
Characteristic	Dimension	2-d Tests	3-d Tests
Length	L	$L_r = 1:33$	$L_r = 1:48$
Area	L^2	$A_r = 1:1,089$	$A_r = 1:2,304$
Volume	L^3	$V_r = 1:35,937$	$V_r = 1:110,592$
Time	T	$T_r = 1:5.74$	$T_r = 1:6.93$

9. The specific weight of water used in the model was assumed to be 62.4 pcf and that of seawater is 64.0 pcf; specific weights of model breakwater construction materials were not identical with their prototype counterparts. These variables were related using the following transference equation:

$$\frac{(W_a)_m}{(W_a)_p} = \frac{(\gamma_a)_m}{(\gamma_a)_p}\left(\frac{L_m}{L_p}\right)^3\left[\frac{(S_a)_p - 1}{(S_a)_m - 1}\right]^3$$

where

subscripts m and p = model and prototype quantities, respectively

W_a = weight of an individual armor unit, lb

γ_a = specific weight of an individual armor unit, pcf

L_m/L_p = linear scale of the model

S_a = specific gravity of an individual armor unit relative to the water in which the breakwater is constructed, i.e., $S_a = \gamma_a/\gamma_w$, where γ_w is the specific weight of water, pcf

10. Plans 1, 2, 3, 4, 4A, 5, 6, and 7 used a cast-in-place concrete crownwall 20 ft wide, 5 ft thick, and poured in 20-ft-long sections. To ensure dynamic similarity, model crownwall sections reproduced both prototype geometry and weight. The 150-ton prototype sections were reproduced by 8.14-lb model sections. These sections, made of concrete and cast separately from the structure, had one layer of first-underlayer stone glued to the bottom to simulate bonding resulting from cast-in-place prototype construction techniques. Actual prototype resistances of the concrete crown were not known; however, the modeling approach used is believed to be reasonably close to being in similitude and, if anything, the model friction is probably slightly less than that in the full scale. Consequently, a stable model concrete crown should certainly be expected to be stable in the prototype when exposed to the conditions tested.

Test Facilities and Equipment

11. Companion concrete wave flumes, 5 and 6.6 ft wide, 4 ft deep, and 119 ft long, were used for the 2-d tests (Figure 2). The flumes are equipped with a common vertical-displacement, wave generator capable of producing sinusoidal waves of various periods and heights. Test waves of the required characteristics were generated by varying the frequency and amplitude of the plunger motion. Location of test sections in each of the parallel flumes was 85 ft from the wave generator. Local prototype bathymetry was represented by a 1V-on-20H slope for a simulated prototype distance of 611 ft (18.5 ft model) seaward of the test sections (Figure 2).

12. A concrete wave flume (Figure 3), 35.5 ft wide, 3.5 ft deep, and 90 ft long, was used for the 3-d tests. This flume is equipped with a horizontal displacement wave generator capable of producing sinusoidal waves of various periods and heights. Test waves of the required characteristics were generated by varying the frequency and amplitude of the plunger motion. During calibration of both test facilities, changes in water-surface elevation as a function of time were measured by electrical wave-height gages located where the toe of the test sections would be constructed. Water-surface elevations were recorded on chart paper by an electrically operated oscillograph. Electrical output of the wave gages was directly proportional to their submergence depth.

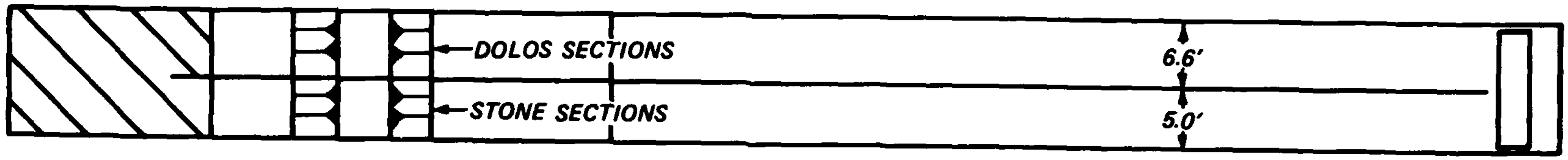

a. PLAN VIEW

b. ELEVATION VIEW

Figure 2. Two-dimensional wave flume cross section

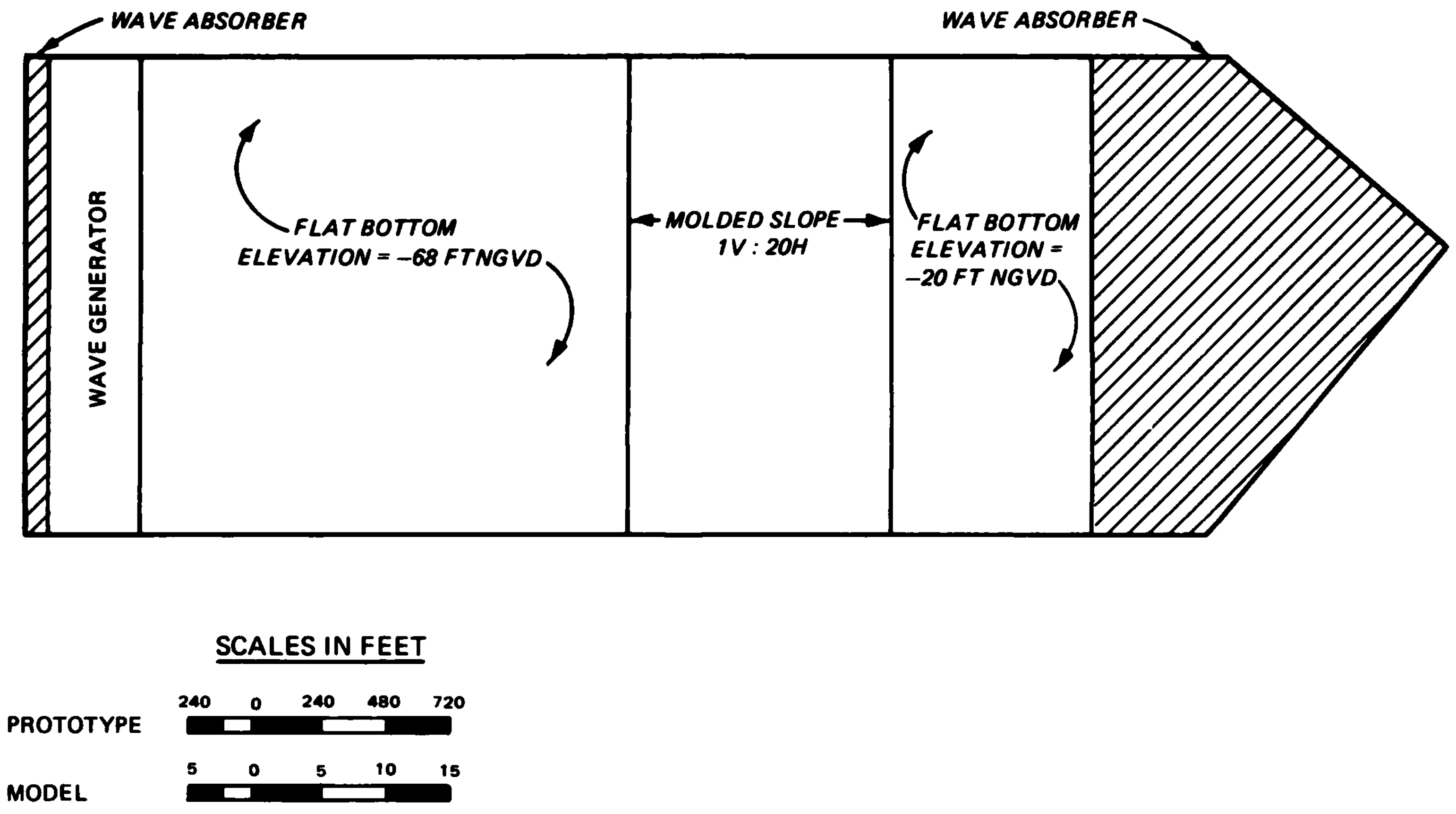

Figure 3. Plan view of three-dimensional wave tank

Test Procedures

Calibration of the test facility

13. Normal procedure at the U. S. Army Engineer Waterways Experiment Station (WES) is to calibrate the wave facility without the breakwater structure in the facility. This is the most accurate means of calibrating and is analogous to the prototype conditions for which the measured and/or hindcast wave data were determined. In both the 2-d and 3-d test facilities, electrical resistance-type wave gages were positioned in the wave flume at a point that would coincide with the toe of the proposed breakwater section, and the wave generator was calibrated for various selected wave conditions at the selected model scales.

14. Once calibration was completed, stone and dolos test sections with the geometric characteristics proposed for use at Oregon Inlet were constructed, respectively, in the parallel flumes and the wave generator was "tuned" to determine the most severe breaking wave that could be experimentally made to attack the structures; that is, for each swl (or water depth) and wave period, the wave generator stroke was varied until the most severe wave condition relative to armor unit stability was obtained. Observations of incident wave forms at the structures showed that the most severe breaking wave condition occurred for both the stone- and dolos-armored sections using the same generator conditions; thus simultaneous testing was possible. Model observations of the wave periods considered for the major storm conditions (11, 13, 15 sec) indicated that for each swl, the 15-sec period wave was the most severe. Therefore subsequent full-length stability tests were conducted using only the 15-sec wave period. Various combinations of duration, swl, and wave height were run for the various test plans. The individual test conditions (swl-wave height versus time hydrographs) are described for each particular test plan in PART III.

Method of constructing test sections

15. All model-jetty sections were constructed to reproduce, as closely as possible, results of the usual methods of constructing prototype jetties. Core material was compacted and smoothed to grade with hand trowels as it was dumped by bucket or shovel in an effort to simulate the natural consolidation that would occur due to wave action during prototype construction. Once the core material was in place, the underlayer was added by shovel and smoothed

to grade by hand or with trowels to simulate individual or controlled random placement. No excessive pressure or compaction was applied to any of the underlayer stone placements. Armor units used in the cover layers were placed in a random manner, i.e., laid down in such a way that no intentional interlocking of the units was obtained. Model elevations were contolled with an engineer's level to a tolerance of $\pm$0.01 ft (i.e., 0.33 and 0.48 ft prototype for scales of 1:33 and 1:48, respectively).

Test setup

16. A typical 2-d stability test consisted of simultaneously subjecting the stone and dolos test sections to attack by test waves of a given height and period for whatever test duration was specified. The testing time on each structure is accumulative since the test sections were subjected to wave attack in approximately 30-sec intervals between which the wave generator was stopped and the waves allowed to decay to zero height. This procedure was necessary to prevent the structures from being subjected to an undefined wave system created by reflections from the model boundaries and wave generator. If no specific wave duration was prespecified, the newly built test sections were subjected to a short duration (15 to 30 min, prototype) of shakedown using a wave equal in height to about one-half of the proposed design wave. This procedure merely provided a means of allowing some measure of consolidation and armor-unit seating that would normally occur during construction of the prototype structure. The test sections were then directly subjected to the design wave condition for a sufficient length of time to assure damage had stabilized, i.e., until all significant deterioration of the breakwater material has stopped or until complete failure occurs. Test waves did at times remove a few loose armor units without causing significant damage.

17. All base design test sections (both 2-d and 3-d) were rebuilt and repeat tests were conducted for every condition tested. The 2-d test sections that were subjected to water levels and wave conditions exceeding the no-damage base conditions were also rebuilt prior to the testing of each new hydrograph.

18. Behavior of the 2-d test sections during wave attack, including the extent of damage, was determined by counting the number of units displaced (number method), using the WES sounding method, and making and documenting visual observations. The 3-d test results were evaluated by visual observations and the number method. Damage evaluation for site-specific model

studies is normally accomplished by visual observation on the basis that after the initial movement or displacement of unnested armor units (such units are generally present on any newly constructed structure, but their displacement does not significantly affect the cover layer) occurs, minor displacement of the primary armor units and stone (insufficient to allow leaching of the first underlayer stone through the primary cover layer) constitutes an acceptable no-damage criterion. This definition of no-damage can only be observed in a subjective manner and, by itself, is not a quantitative measure of degree of damage. Consequently, additional damage-evaluation methods were necessary for the 2-d tests. The different methods of obtaining damage were performed by highly trained personnel experienced in executing breakwater stability investigations. Visual observations were recorded by before- and after-testing photographs and written descriptions. Photographs and written descriptions of all significant test results are included in this report.

Methods of determining damage

19. Observation. In optimizing a breakwater design, it is initially advantageous to evaluate stability test results simply by observing movement of armor material. Armor unit movement decreases as the initial design is refined or it increases as the no-damage criterion is exceeded, making quantitative comparison of stability by observation difficult. Based on this study's need to evaluate degrees of damage, two quantitative methods that are utilized throughout the world are used in conjunction with visual observations.

20. Number method. A popular method used in several foreign laboratories is to count the number of armor units displaced from the test section (or from specified areas on the test section) and express this number as a percentage of the total number of armor units (or the total number of units in the specified area from which units were displaced). This method is relatively easy to accomplish and is operationally simple and quick. The drawback to this method is that some movement may be unintentionally overlooked, consolidation is not considered, and initial movement during shakedown tests is not necessarily detrimental.

21. Sounding method. WES developed the sounding method of measuring percent damage during the early 1950's. This method has proven to be valid and, even though most of the 2-d stability test results delineated herein are reported in terms of both the number and sounding method, the sounding method

and the observations that go with it are used as the primary basis for comparison.

22. Details of the WES sounding technique are described as follows. To use the WES damage measurement technique, the cross-sectional area occupied by armor units is determined for each stability test section. Armor unit area is obtained from elevations (soundings) measured on a gridded pattern (a) prior to placing the armor on the underlayer, (b) after the armor has been placed but before the section has been subjected to wave attack, and (c) after wave attack. Elevations are obtained with a sounding rod (Figure 4) equipped with a circular spirit level for plumbing, a scale graduated in thousandths of a foot, and a ball-and-socket foot for adjustment to the irregular surface of the breakwater slope. The diameter of the circular foot of the sounding rod was related to the size of the material being sounded by the following equation:

$$d = c \left(\frac{W_a}{\gamma_a}\right)^{1/3}$$

where

d = sounding foot diameter, in.

c = coefficient ($c = 6.8$ for stone; $c = 13.7$ for dolosse)

W_a = weight of an armor unit, lb

γ_a = specific weight of an armor unit, pcf

A previously conducted series of sounding tests in which both the size of armor stones and dolosse and the diameter of the sounding foot were varied indicated that the above relationship would give a measured thickness which appeared (by observation) to be an acceptable two-layer thickness.

23. Sounding data for each test section were obtained as follows. After the core material and first underlayer were in place, soundings were taken along rows beginning at and parallel to the center line of the structure and extending in 0.20-ft increments to the seaward and channelward edges of the armor (the spacing between some rows was slightly more or less than 0.20 ft to provide better resolution in the vicinity of slope changes or armor material size interfaces). On each parallel row, 16 or 24 sounding points, spaced at 0.20-ft increments, were measured. This distance represented the middle

Figure 4. Sounding jetty before wave attack

3 and 4.6 ft of the 5- and 6.6-ft-wide test sections; the 1 ft of the structure next to each wall was not considered because of possible discontinuity effects. Soundings were taken at the identical points once the armor was in place and again after the structure had been subjected to wave attack.

24. Sounding data from each stability test were reduced in the following manner. Individual sounding points obtained on each parallel row were averaged to yield an average elevation at the bottom of the armor layer before the armor was placed and then at the top of the armor before and after testing. The cross-sectional armor area before testing and the area from which armor units were displaced (either downslope or off the section) were calculated from these data. Damage was determined from the following relationship:

$$\text{Percent Damage} = \frac{A_2}{A_1} (100)$$

where

A_1 = area before testing, ft^2

A_2 = area from which units have been displaced, ft^2

The percentage given by the WES sounding technique is a measurement of the area or volume of armor material that has been moved from its original location (either downslope or off structure). It has a distinct advantage over the number method in that it quantifies downslope movement. It must be realized, however, that the sounding method presents an average damage value and tends to minimize spot damage (small concentrations of damage, one or two armor units wide). Thus soundings must be accompanied and documented with observations and visual aids. All WES sounding data are accompanied by such observations.

PART III: TWO-DIMENSIONAL STABILITY TESTS

Tests Conducted at a Design swl of +5.5 ft

Selection of test conditions

25. The objective of the 2-d stability tests at the +5.5 ft swl was to determine for depth-limited breaking wave attack a stable design for both a stone and dolos armored structure using a water depth at the structure toe of 9.0 ft. Initially, swl's of -2.5, -1.6, and +5.5 ft were considered. Observations of Plan 1 (Plate 1) under wave attack indicated that the most critical breaking waves which could experimentally be made to attack the section for the selected swl's and wave periods were as follows:

swl ft NGVD	Wave Period sec	Maximum Breaking Wave Height, ft
-2.5	8	5.2
-2.5	11	5.4
-2.5	14	5.7
-1.6	8	5.7
-1.6	11	6.0
-1.6	14	6.3
+5.5	11	12.2
+5.5	13	12.7
+5.5	15	13.6

Model observations indicated that for a given swl, the longest wave period considered was always the most detrimental to stability of the section. Therefore full-length stability tests were conducted using only wave periods of 14 and 15 sec. During testing of Plan 1, it was observed that the highest swl produced the most damage; consequently, subsequent plans were tested at an swl of +5.5 ft with 15-sec, 13.6-ft waves. All wave heights at swl's of +5.5 ft or above produced severe overtopping for all plans tested.

Plans tested and general results

26. A total of 10 plans (six with stone and four with dolosse) were tested before optimum 2-d stone and dolos designs were obtained for the +5.5 ft design swl. All plans used a bottom toe elevation of -9.0 ft, and armor slopes of 1V on 1.5H (both sea side and channel side); channel-side toe protection was provided by 2-ton stone. Although tidal flow was not

represented in the stability model, the sponsor planned an extra wide toe protection on the channel side of all plans tested to minimize the probability of undermining due to the interaction of tidal currents and wind waves. Plans 1, 2, 3, 4, 4A, 5, 6, and 7 used a concrete crownwall 20 ft wide, 5 ft thick, and poured in 20-ft-long sections. Crown protection for Plans 4B and 8 was provided by three rows of 18-ton stone. Details of the plans tested and general results follow:

a. Plan 1 (Plate 1 and Photos 1 and 2) was constructed to a crown elevation of +10.5. Armor-stone weights for the primary armor (W_1) and the toe-protection armor (W_3) were 8 and 2 tons, respectively. Plan 1 was initially subjected to 14-sec, 5.7-ft waves at an swl of -2.5 ft. This wave condition produced minor displacement of the seaward 2-ton, toe-protection stone as illustrated in Photos 3 and 4. The swl was raised to -1.6 ft and the structure was subjected to 14-sec, 6.3-ft waves. This condition produced some minor reshuffling of the seaward 2-ton stone, but no significant changes in the condition of the structure were observed. Photos 5 and 6 show the structure after testing at this swl. Upon raising the swl to +5.5 ft, the structure was attacked with 15-sec, 13.6-ft waves that resulted in severe damage to the sea side of the structure. This wave condition moved both 2- and 8-ton armor stone from the sea side of the structure over the crownwall and redeposited them on the channel side. Approximately 20 percent and 40 percent by volume of the 8- and 2-ton stone, respectively, were moved over the crownwall. Movement of sea-side armor over the crownwall was so extensive that it was difficult to evaluate the movement of channel-side armor. Probably 10 to 25 percent of the 8-ton, channel-side armor suffered downslope displacement. Even though individual sections shifted slightly, the overall integrity of the crownwall was not affected by this wave condition. Damage by the sounding method was not taken during exploratory testing. Photos 7 and 8 show the after-testing condition of the structure.

b. Plan 2 (Plate 2 and Photos 9 and 10) used 11.5- and 8.0-ton stone sea side and channel side, respectively. The crown was constructed to an elevation of +10.5 and the 11.5-ton primary armor on the sea-side slope was extended into the toe area. Testing with 15-sec, 13.6-ft waves at an swl of +5.5 ft caused moderate damage to both the sea- and channel-side armor. Approximately 25 percent by volume of the 11.5-ton, sea-side armor was displaced downslope and eight of these units were washed across the crownwall and redeposited on the channel-side slope. Also 15 to 20 percent by volume of the 8.0-ton channel-side armor suffered downslope displacement, with 14 units being rolled onto the toe-protection stone. Even though individual sections shifted slightly, the overall integrity of the crownwall was not affected by this wave condition. Soundings were not taken. Photos 11 and 12 show the after-testing condition of the structure.

c. Plan 3 (Plate 3 and Photos 13 and 14) was constructed to a crown elevation of +10.5 and used 11.5-ton armor both sea side and channel side. The sea-side armor incurred moderate damage while the channel-side armor suffered only minor damage under attack of 15-sec, 13.6-ft waves. About 20 to 25 percent by volume of the sea-side armor was displaced downslope and seven of these units were moved across the crownwall. The crownwall was stable. Photos 15 and 16 show the after-testing condition of the structure.

d. Plan 4 (Plate 4 and Photos 17 and 18) used 15.0- and 11.5-ton stone sea side and channel side, respectively. The crown was constructed to an elevation of +11.5. Figure 5 shows the structure under attack of 15-sec, 13.6-ft waves which caused only minor damage. The after-testing condition of the structure is shown in Photos 19 and 20.

e. Plan 4A (Plate 5 and Photo 21) was the same as Plan 4 except for cross-sectional changes which increased the volume of armor stone and decreased the volume of first-underlayer stone. The structure suffered only minor damage under wave attack and the crownwall was stable. Photo 22 shows the after-testing condition of the structure.

f. Plan 4B (Plate 6 and Photos 23 and 24) was similar to Plan 4A except that crown protection was provided by three rows of 18.0-ton stone. This gave an average crown width of 20.7 ft relative to 20.0 ft in Plan 4A. The 18-ton capstone was chinked with quarry-run stone (W_6) to simulate construction of an access roadway. The structure suffered only minor damage under wave attack with four channel-side armor units being rolled onto the toe-protection stone. Most of the chinking stone was washed from the crown to the channelward slope; however, the capstones suffered no significant damage. Some of the capstones shifted slightly as they sought a more stable orientation during wave attack, but none were displaced nor were any gaps opened in the crown. The after-testing condition of the structure is shown in Photos 25 and 26. During the repeat test of this plan, the sponsor requested that swl-wave height combinations (for which the model was already calibrated) be conducted to aid in determining under which sea-state conditions roadway material would not be removed. Wave heights up to the maximum breaking conditions at swl's of -2.5 and -1.6 ft (paragraph 25) were conducted and did not adversely affect the roadway material. As in the original test, the 13.6-ft, 15-sec wave at the +5.5 ft swl removed almost all the roadway material.

g. Plan 5 (Plate 7 and Photos 27 and 28) was constructed to a crown elevation of +10.5 and used 3.25-ton dolosse both sea side and channel side. Attack of 15-sec, 13.6-ft waves produced severe damage with 25 to 35 percent by volume of the sea-side armor units being displaced downslope. Two sea-side armor units were washed across the crownwall. Channel-side armor was extensively displaced with 35 units being washed onto the toe-protection stone. Extensive channelward displacement of the crownwall was

Figure 5. End view of Plan 4 under attack of 15-sec, 13.6-ft waves at a +5.5 ft swl

experienced with individual sections being moved from 3 to 9 ft. Soundings were not taken. Photos 29 and 30 show the after-testing condition of the structure.

h. Plan 6 (Plate 8 and Photos 31 and 32) was similar to Plan 5, except that an 18-ft apron of 3.25-ton dolosse (2 layers thick) was added to the sea-side toe of the structure. The stability response of the structure was more favorable than Plan 5 with 10 to 15 percent by volume of the sea-side armor being displaced downslope from near the crownwall. Three sea-side armor units were displaced across the crownwall. The channel-side dolosse incurred moderate displacement with 15 units being displaced onto the toe-protection stone. Moderate channelward displacement of the crownwall was experienced with individual sections being moved from 1 to 6 ft. Photos 33 and 34 show the after-testing condition of the structure.

i. Plan 7 (Plate 9 and Photos 35 and 36) was constructed to a crown elevation of +11.0 and used 3.25-ton dolosse both sea side and channel side. The structure suffered minor damage under wave attack with four sea-side armor units being washed across the crownwall and five channel-side armor units being rolled onto the toe-protection stone. The crownwall was stable. Photos 37 and 38 show the after-testing condition of the structure.

j. Plan 8 (Plate 10 and Photos 39 and 40) was constructed to a crown elevation of +13.0 and used 3.25-ton dolosse both sea side and channel side. Crown protection was provided by three rows of 18.0-ton stone which gave an average crown width of 20.7 ft. The 18-ton capstone was chinked with quarry-run stone (W_5). The structure suffered minor damage under wave attack with eight sea-side armor units being washed onto or over the capstone. Two channel-side armor units were rolled onto the toe-protection stone. Most of the chinking stone was washed from the crown to the channelward slope; however, the capstones suffered no significant damage. Some of the capstones shifted slightly as they sought a more stable orientation during wave attack, but none were displaced nor were any gaps opened in the crown. The after-testing condition of the structure is shown in Photos 41 and 42.

27. The 2-ton, channel-side, toe-protection stone used on all plans described in paragraph 26 proved to be stable. It should be noted that for all the 2-d tests conducted herein, the seaward exposed core material or bedding layer deteriorated into the first row of the toe-protection material. This was reasonable since the tests were conducted on a fixed-bed bottom and it was not possible for the material to sink into the substrata. It is surmised that in the prototype, the bedding material and/or the first row of toe protection will stabilize into the sand bottom. Each of the plans described in paragraph 26 was exposed to wave attack until it stabilized, i.e., until all significant movement of material had abated and results for each

plan were verified by at least one repeat test. The number of units listed as having moved out of a given area is an average for two or more tests; and since the after-testing photographs are of one representative run, the numbers given in the text may not correspond exactly to the number of displaced units observable in the photographs.

Summary of damage and selection of optimum plans

28. Damage for Plans 2, 3, 4, 4A, 4B, 5, 6, 7, and 8 computed by the number method is shown in Table 1. Table 1 also includes damage values computed by the WES sounding method for all armor areas of Plans 3, 4, 4A, 4B, 7, and 8 and the sea-side armor of Plan 6. Armor movement in Plan 1 was so extensive that it was not possible to accurately quantify damage by the number method. Armor movement of Plans 2 and 5 was extensive enough that based on model observations, they were not considered viable alternatives and therefore soundings were of no practical value. Movement of the crownwall in Plan 6 prevented acquisition of sounding data for the channel-side armor. Based on the damage values presented in Table 1 and the initial cost (as estimated by the sponsor) of the structures, Plans 4B and 8 were selected as the optimum stone and dolos designs.

Effects of Higher Storm Surges on the Design Sections swl of +5.5 ft

Storm-surge hydrograph

29. In nature, as a storm intensifies, the swl rises, reaches some maximum value, and then falls as the storm dissipates. Storm surge is a function of time. In stability model tests, it is not operationally practicable to attempt to exactly reproduce this storm surge curve, i.e., it is not practicable to continually vary the swl and the wave conditions associated with it. However, the storm-surge hydrograph can be reasonably approximated by a stepped hydrograph. The stepped hydrograph is drawn so that the area under it approximately equals the area under the predicted storm-surge hydrograph. Model tests can be expediently conducted using a stepped hydrograph. The only effect, if any, of the stepped curve on stability-test results is to make them slightly conservative due to the finite step length at the peak of the hydrograph.

30. Typical storm-surge hydrographs representative of conditions along the North Carolina coast were determined by the sponsor. These predicted

hydrographs and their stepped counterparts for maximum storm surges of +6.5 through +11.5 are shown in Plates 11-16. Specific test conditions for the hydrographs are given in Table 2. Stability tests exactly followed the swl's and times predicted by the stepped hydrographs. Both test plans were completely rebuilt between hydrographs.

31. Test results for the hydrographs can be summarized as follows:

a. For a maximum storm surge of +6.5:

(1) Plan 4B incurred minor damage. Photos 43 and 44 show the structure after testing step 3.

(2) Plan 8 sustained minor damage. Photos 45 and 46 show the structure after testing step 3.

b. For a maximum storm surge of +7.5:

(1) Plan 4B received moderate damage. Even though several capstones were displaced, the crown was not breached. Photos 47 and 48 show the structure after testing step 5.

(2) Plan 8 suffered severe damage with large quantities of sea-side armor being moved onto and across the crown. As damage progressed and the sea side of the structure weakened, capstones from the front of the crown were allowed to move down the seaward slope. Photos 49 and 50 show the structure after testing step 5.

c. For a maximum storm surge of +8.5:

(1) Plan 4B sustained moderate damage. Most of the damage was limited to the seaward-slope armor and the seaward portion of the crown. Photos 51 and 52 show the structure after testing step 7.

(2) Plan 8 suffered very severe damage. There was extensive displacement of sea-side slope and toe armor and crown armor. Photos 53 and 54 show the structure after testing step 7.

d. For a maximum storm surge of +9.5:

(1) Plan 4B exhibited a damage pattern similar to the +8.5 hydrograph except there was some reduction in damage to the beach-side and crown armor. Photos 55 and 56 show the structure after step 9.

(2) Plan 8 showed a stability response (very severe damage) almost identical with the +8.5 hydrograph. Photos 57 and 58 show the structure after step 9.

e. For a maximum storm surge of +10.5:

(1) Plan 4B incurred moderate damage. Most of the damage was limited to the seaward-slope armor and the seaward portion of the crown. Photos 59 and 60 show the structure after step 11.

(2) Plan 8 showed a stability response (very severe damage) similar to the +8.5 and +9.5 hydrographs except there was some reduction in damage to the channel-side and crown armor. Photos 61 and 62 show the structure after step 11.

f. For a maximum storm surge of +11.5:

(1) Plan 4B showed a damage pattern (moderate damage) similar to the +10.5 hydrograph except there appeared to be some increase in damage to the crown and beach-side armor. Photos 63 and 64 show the structure after step 13.

(2) Plan 8 experienced severe damage; however, relative to the +9.5 and +10.5 hydrographs, there appeared to be some decrease in damage to both the crown and channel-side armor. Photos 65 and 66 show the structure after step 13.

32. Damage results for the hydrographs are shown in Table 3 and Figures 6-9. Typical comparative jetty cross sections (before and after wave attack) are given in Appendix A for +8.5, +9.5, +10.5, and +11.5 surges. The plots in Figures 6-9 present damage as a function of relative wave height (H/H_D) where H_D equals the design-wave height of 13.6 ft and H is the maximum wave height within a given storm-surge hydrograph. These data show that for both plans, once an swl of +8.5 ft ($H/H_D = 1.2$) is reached, the damage curves tend to flatten, i.e., there is a trend for damage to increase as progressively higher hydrographs are tested until a peak surge of +8.5 is reached and then for peak surges from +8.5 to +11.5 ($H/H_D = 1.38$) damage values fluctuate. As shown in Figure 6, it appeared that damage for Plan 4B determined by the number method had reached a peak at an H/H_D of 1.2. Hydrograph tests at H/H_D's of 1.26 and 1.32 showed a trend of decreasing damage; however, damage in all three armor areas abruptly increased at $H/H_D = 1.38$. It is also interesting to note that Plan 4B withstood peak surges up through +11.5 ($H/H_D = 1.38$) without sustaining severe damage, whereas Plan 8 was severely damaged by peak surges of +7.5 ($H/H_D = 1.14$) and larger.

33. The damage data reported above are presented in numbers for each method of evaluating damage; however, it must be realized that the representation of the damage may be biased by the evaluation method used and/or the extent of damage. For example, the sounding method is based on measuring in-place volume of material before and after testing, but in the case of severe damage this method does not account for sea-side material that has replaced crown or channel-side material. Further, the manner in which damage occurs may bias the results in that for high-damage situations on dolos sections, the sea-side dolosse are swept over the crown and engulf the channel-side

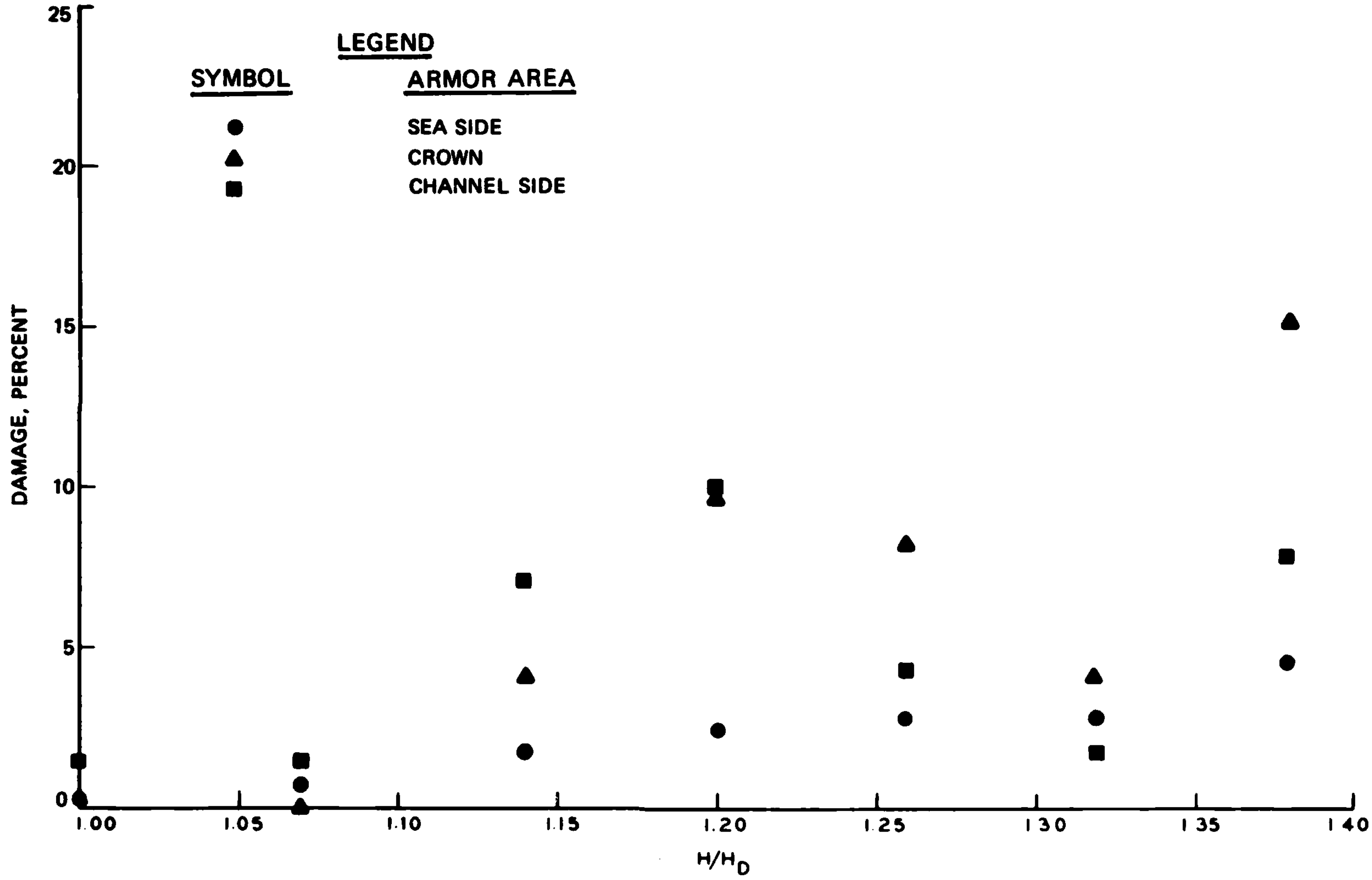

Figure 6. Damage as a function of H/H_D for Plan 4B, number method

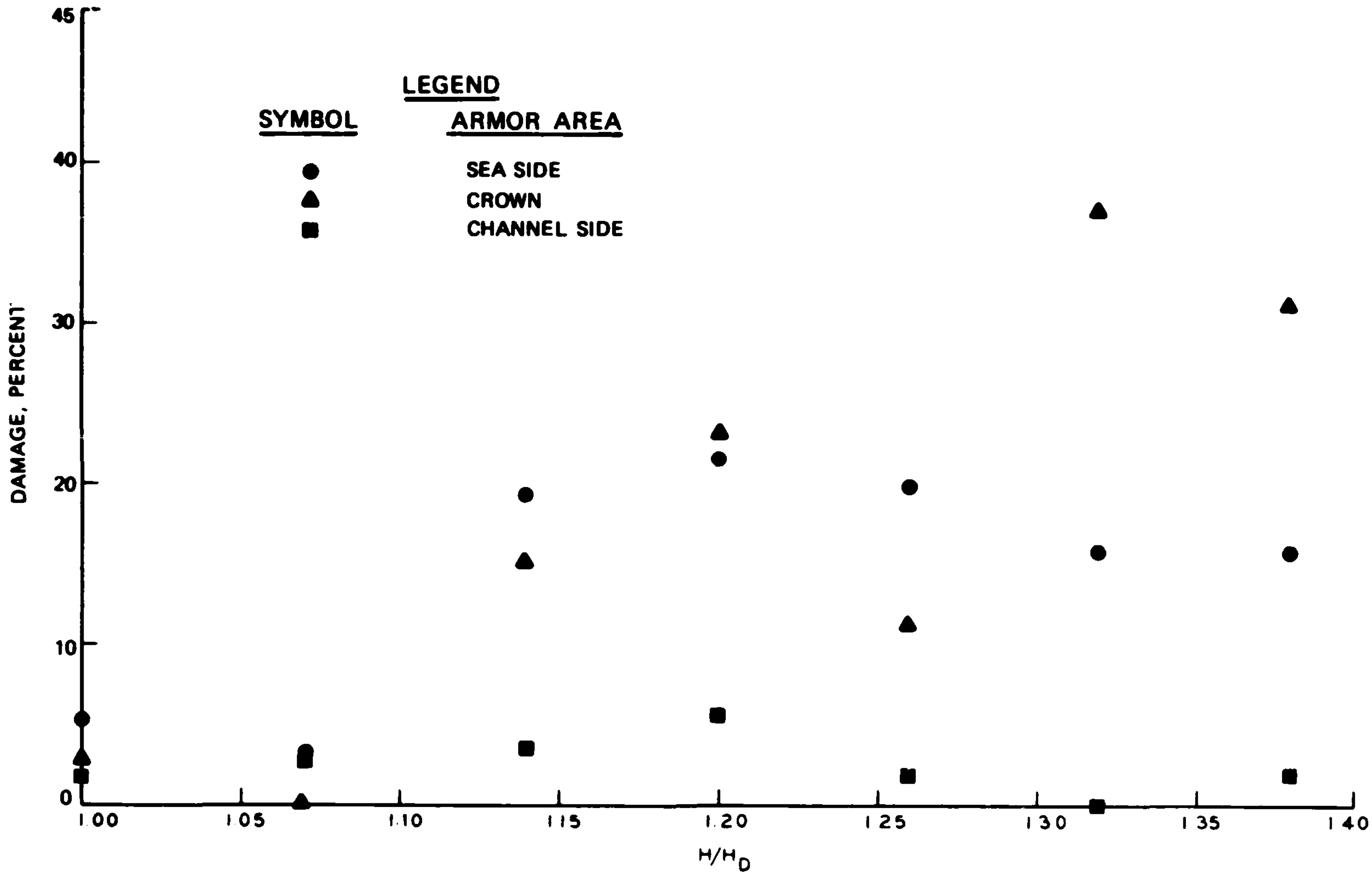

Figure 7. Damage as a function of H/H_D for Plan 4B, sounding method

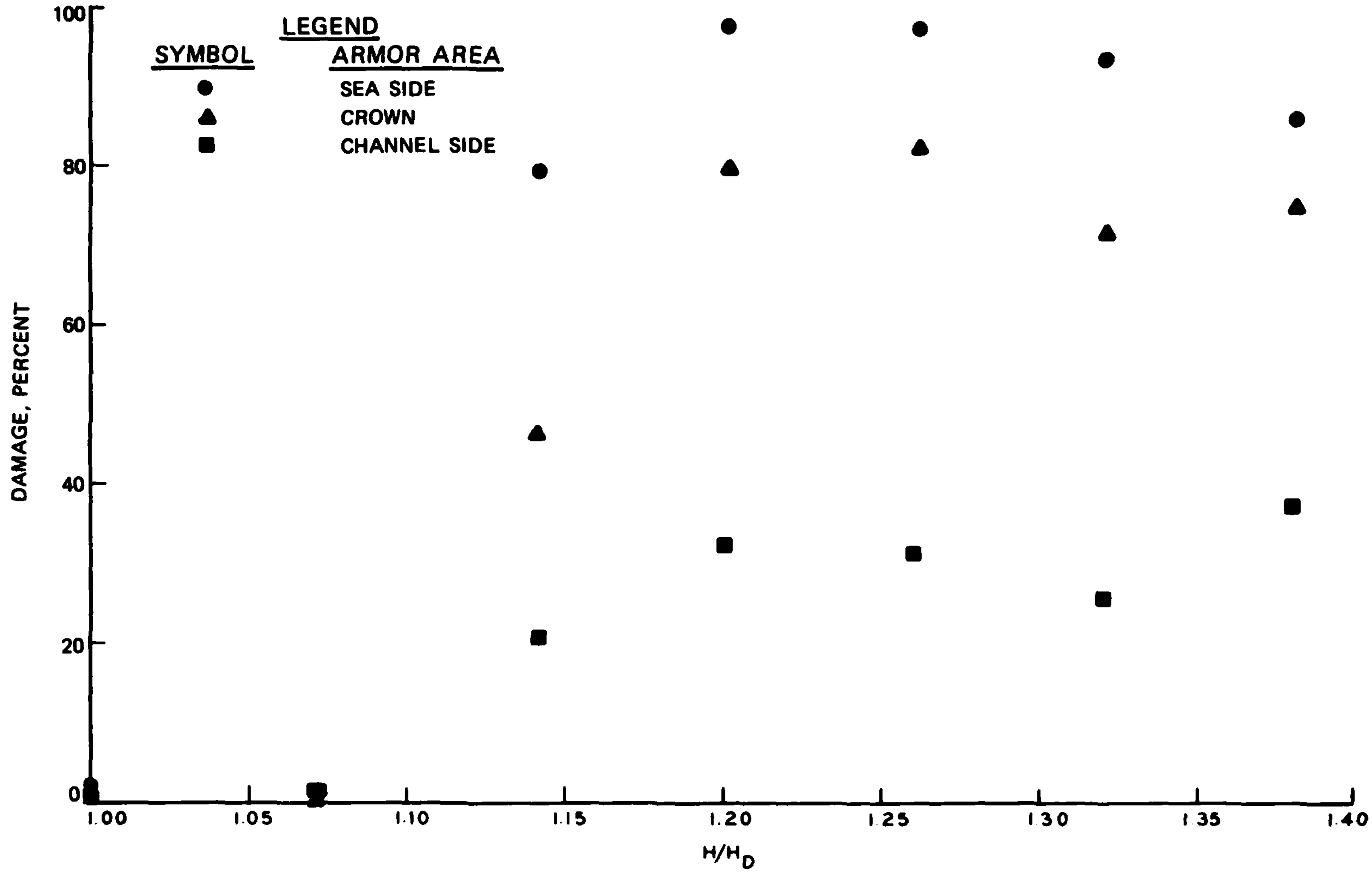

Figure 8. Damage as a function of H/H_D for Plan 8, number method

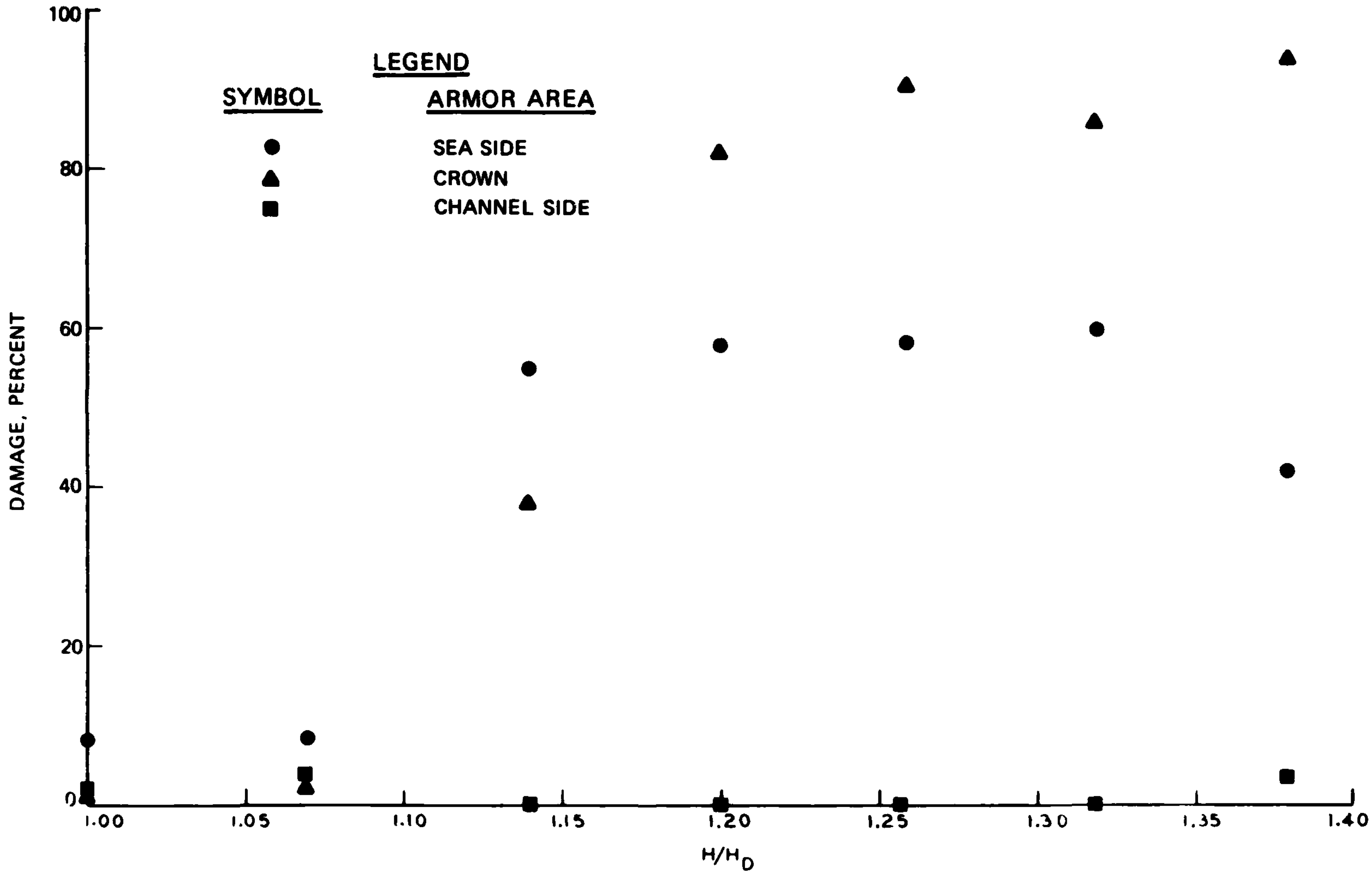

Figure 9. Damage as a function of H/H_D for Plan 8, sounding method

dolosse prior to their having a chance to be displaced. One of these reasons is probably why low or no damage is shown for the channel side of Plan 8 in Figure 9. The explanation stated above is not to question the data taken in this study for there are no better methods known worldwide, but it is to caution against overreliance on the precise results when large damages are indicated.

Simulation of two successive +7.5 storm hydrographs on the design sections

34. Plans 4B and 8 were also tested for two successive +7.5 hydrographs. The purpose of this simulation was to determine if two successive storms with peak surges of +7.5 would be more damaging than one +7.5 storm. The rationale for these tests was to investigate the consequences of being unable to make repairs before a second storm damages the structures. Even though the probability of this occurrence may be small, these results comprise additional information that can be factored into the final cost comparison of the two plans. Original and stepped hydrographs for the successive surges are shown in Plate 17 and specific test conditions are given in Table 4.

35. Test results for the successive hydrographs can be summarized as follows:

a. Plan 4B sustained moderate damage during the first hydrograph (steps 1-5). Most of the damage was limited to the seaward-slope and crown armor. During testing of the second hydrograph (steps 6-10), there was a slight increase in damage to the sea- and channel-side armor; however, there was a substantial increase in damage to the crown armor. This seems plausible since some sea-side armor migrated downslope during the first hydrograph, thereby making the crown armor more vulnerable to direct wave attack during the second hydrograph. Photos 67 and 68 show the structure after testing step 5, whereas Photos 69 and 70 show it after step 10.

b. Plan 8 incurred extensive damage to both the sea-side and crown armor during testing of steps 1-5. There was a continued movement of sea-side armor and a substantial increase in damage to the crown armor during testing of steps 6-10. Photos 71 and 72 show the structure after testing step 5, and Photos 73 and 74 show it after step 10.

36. Damage for the successive hydrographs, as computed by both the number and sounding methods, is given in Table 5. These data substantiate the observations presented in paragraph 35.

Tests Conducted at a Design swl of +7.5 ft

Selection of initial armor weight

37. It was determined (paragraphs 26-28) that a sea-side stone weight of 15 tons (Plan 4B) and a sea-side dolos weight of 3.25 tons (Plan 8) would be stable for a design wave height of 13.6 ft at an swl of +5.5 ft. It was hoped that the Hudson Stability Equation (HSE), which has proven successful in predicting armor weights for nonovertopping structures, could be used in conjunction with test results of Plans 4B and 8 to determine the sea-side armor weights required to withstand a design wave of 15.5 ft at an swl of +7.5 ft.

38. The HSE (Hudson 1958) is as follows:

$$W_a = \frac{\gamma_a H^3}{K_D (S_a - 1)^3 \cot \alpha} \qquad (1)$$

where

W_a = weight of an individual armor unit, lb

γ_a = specific weight of the armor unit, pcf

H = wave height, ft

K_D = stability coefficient which is a function of the armor unit shape, method of placement, structure geometry, etc.

S_a = specific gravity of the armor unit relative to the water in which the breakwater is constructed

α = angle between the horizontal and the seaward face of the breakwater

Solving the above equation with $H = 13.6$ ft , $\cot \alpha = 1.5$ and $\gamma_r = 165$ and 150 pcf, respectively, yields a K_D value of 2.35 for the 15-ton stone and 16.0 for the 3.25-ton dolosse. Using these values of K_D and a design-wave height of 15.5, predicted stable armor weights for an swl of +7.5 ft are 22.0 and 5.0 tons for the stone and dolosse, respectively. Therefore, initial stability tests were conducted with 22.0-ton stone and 5.0-ton dolosse.

Plans tested and general results

39. Details of the plans tested and general results were as follows:

a. Plan 4C (Plate 18 and Photos 75 and 76) was constructed to a crown elevation of +13.0 and used armor slopes of 1V on 1.5H both sea side and channel side. Sea-side slope and toe and crown protection was afforded by 22.0-ton stone while the channel side of the structure was armored with 11.5-ton stone.

Attack of 15-sec, 15.5-ft waves at an swl of +7.5 ft produced significant damage to the sea side and crown of the structure; however, the channel-side armor experienced only minor damage. Photos 77 and 78 show the after-testing condition of the structure. Observations of Plan 4C under wave attack indicated that a large portion of the damage was probably initiated by seaward sliding of the sea-side toe armor. Initially, it appeared that the toe armor would slide and allow the sea-side slope of the structure to flatten. Finally, displacement of the crown armor would be initiated as more wave energy was allowed to reach it. It is felt that the sliding of the toe armor which occurred in the model was not a realistic simulation of the prototype because sliding resistance between the prototype toe armor and the sand sea floor should be significantly greater than the sliding resistance between the model armor and the flume's concrete floor. Therefore it was decided to determine the stability response of the 22-ton armor in the absence of toe slippage.

b. Plan 4D (Plate 19 and Photos 79 and 80) was the same as Plan 4C except that a small wooden strip was placed along the toe of the structure to prevent seaward sliding of the toe armor, and the crown elevation was raised slightly to +13.5 to accommodate vertical sheet piling which will be used in the core of the prototype structure. Attack of 15-sec, 15.5-ft waves produced only minor damage to all portions of the structure. The after-testing stability condition of the breakwater is shown in Photos 81 and 82.

c. Plan 9 (Plate 20 and Photos 83 and 84) was constructed to a crown elevation of +13.5 and used armor slopes of 1V on 1.5H both sea side and channel side. Both the channel and seaward slopes and the seaward toe were armored with 5-ton dolosse. Crown protection was provided by three rows of 22-ton stone. As shown in Photos 85 and 86, attack of 15-sec, 15.5-ft waves produced extensive damage to both the sea-side and crown armor; however, the channel-side armor experienced only minor damage. Based on these results, it was apparent that 5-ton dolosse were not adequate for the sea side of the structure; however, it was felt that the 22.0-ton crown armor might be acceptable provided the sea-side armor did not experience a high degree of movement. Also, based on the movement experienced by the 5-ton dolosse and previous experience, it was thought that a sea-side armor weight in the range of 8 to 10 tons would probably be suitable. A dolos weight of 9.25 tons was readily available and therefore was selected for testing.

d. Plan 10 (Plate 21 and Photos 87 and 88) was the same as Plan 9 except the sea-side dolos weight was increased to 9.25 tons. Attack by 15-sec, 15.5-ft waves produced only minor damage. Five to six sea-side armor units were displaced onto or over the crown; however, the structure did stabilize and it was determined that the amount of movement experienced was acceptable (Photos 89 and 90).

40. The 2-ton, channel-side toe-protection stone used on all plans

described in paragraph 39 proved to be stable. Each of the plans described in paragraph 39 was exposed to wave attack until it stabilized, i.e., until all significant movement of material had abated and results for each plan were verified by at least one repeat test.

Summary of damage

41. Damage for Plans 4C, 4D, 9, and 10 computed by both the number and sounding method is presented in Table 6. These data verify the observations made in paragraphs 39 and 40, i.e., Plans 4C and 9 were damaged too extensively to be acceptable base designs while the damage incurred by Plans 4D and 10 was within acceptable limits for base designs.

Effects of Higher Storm Surges on the Design Sections swl of +7.5 ft

42. Initially, it was planned to conduct hydrograph tests with maximum surges from +8.5 to +11.5; however, during the course of testing, it was observed that the dolos armor was exhibiting significantly less damage in the range $1.1 \leq H/H_D \leq 1.2$ than had been obtained with the +5.5 ft design swl (Plan 8). Therefore, in an effort to determine if the dolos armor would again experience severe damage at high values of H/H_D, it was decided to test Plan 10 with a +14.5 hydrograph ($H/H_D = 1.38$).

43. Predicted and stepped hydrographs for storm surges of +8.5 through +11.5 and +14.5 are shown in Plates 22-26. Specific test conditions for the hydrographs are presented in Table 7. Stability tests exactly followed the swl's and times predicted by the stepped hydrographs with both plans being completely rebuilt between hydrograph tests.

44. Test results for the hydrographs can be summarized as follows:

a. Maximum storm surge of +8.5:

(1) Plan 4D incurred only minor damage. Photos 91 and 92 show the structure after testing step 3.

(2) Plan 10 sustained only minor damage. Photos 93 and 94 show the structure after testing step 3.

b. Maximum storm surge of +9.5:

(1) Plan 4D received minor to moderate damage. As shown in Photos 95 and 96, most of the damage was limited to the seaward- and channelward-slope armor.

(2) Plan 10 experienced moderate damage. As illustrated in Photos 97 and 98, most of the damage was limited to the

seaward slope and the toe armor and the seaward portion of the crown.

c. Maximum storm surge of +10.5:

(1) Plan 4D exhibited minor to moderate damage. As shown in Photos 99 and 100, most of the damage was limited to the seaward- and channelward-slope armor and the seaward portion of the crown.

(2) Plan 10 demonstrated a stability response similar to that for the +9.5 hydrograph; however, the damage appeared to be slightly less. Photos 101 and 102 show the structure after step 7.

d. Maximum storm surge of +11.5:

(1) Plan 4D exhibited a stability response similar to that for the +10.5 hydrograph except there appeared to be some increase in damage. Photos 103 and 104 show the structure after step 9.

(2) Plan 10 again experienced moderate damage similar to that observed for the +9.5 and +10.5 hydrographs. Photos 105 and 106 show the structure after step 9.

e. Maximum storm surge of +14.5:

(1) Plan 10 experienced severe damage. There was extensive movement of sea-side armor across the crown and crown armor was displaced both seaward and channelward (Photos 107 and 108).

45. Damage results for the hydrographs are presented in Table 8 and Figures 10-12. The plots shown in Figures 10-12 present damage as a function of relative wave height (H/H_D) where H_D equals the design-wave height of 15.5 ft and H is the maximum wave height within a given storm-surge hydrograph. These data show that for Plan 4D, there was a general tendency for sea-side and crown damage to increase as progressively higher hydrographs were tested; however, the sea-side damage incurred by Plan 10 appeared to peak at an swl of +9.5 ft (H/H_D = 1.11) but then began to increase again at an swl of +11.5 ft (H/H_D = 1.21). Comparative cross sections (before and after wave attack) of Plans 4D and 10 are presented in Appendix A for the various hydrographs tested.

Tests Conducted at a Design swl of +9.5 ft

Selection of armor weights

46. As reported in paragraphs 39 through 41, it was determined that a sea-side stone weight of 22 tons (Plan 4D) and a sea-side dolos weight of 9.25

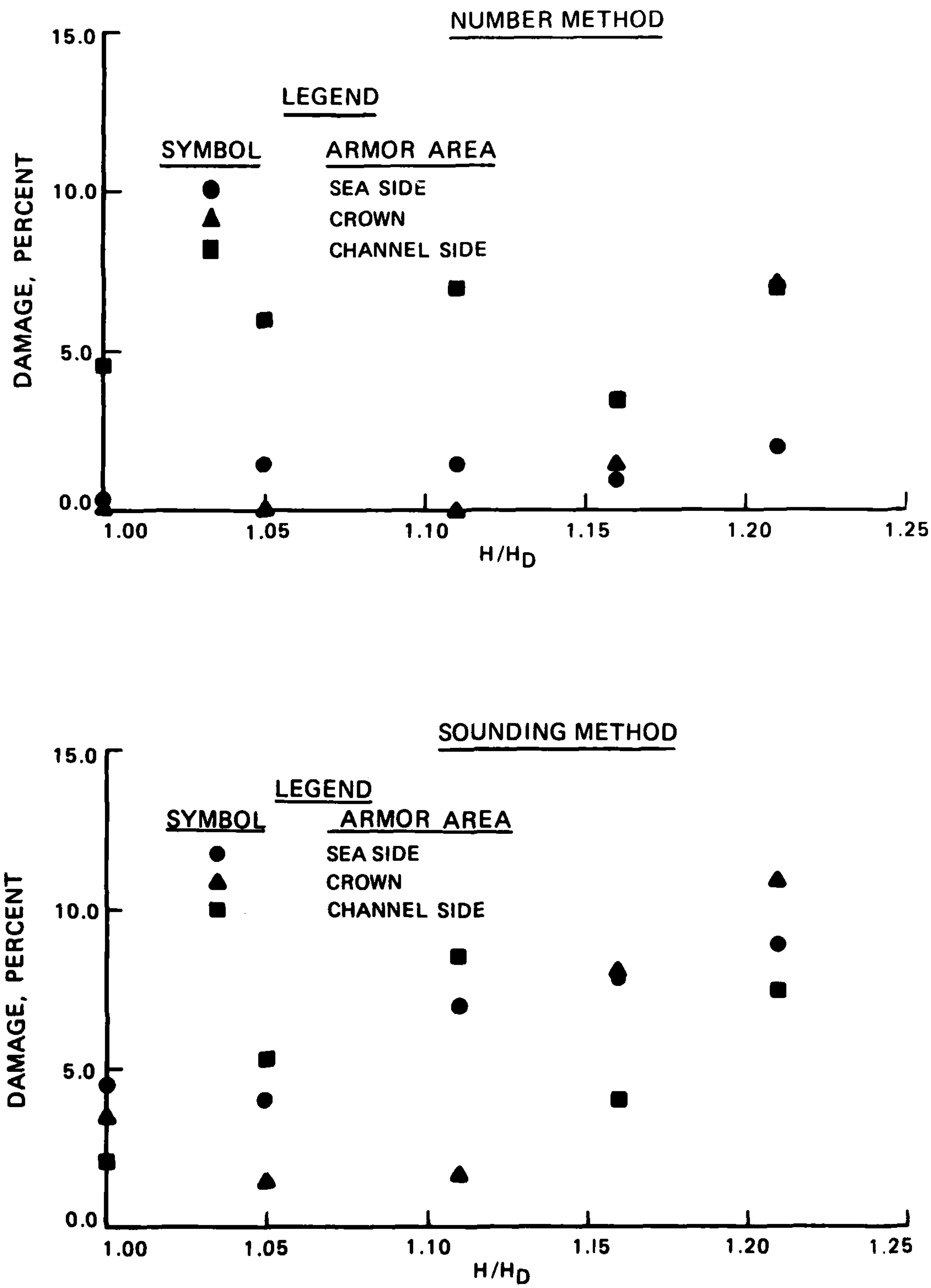

Figure 10. Damage as a function of H/H_D for Plan 4D

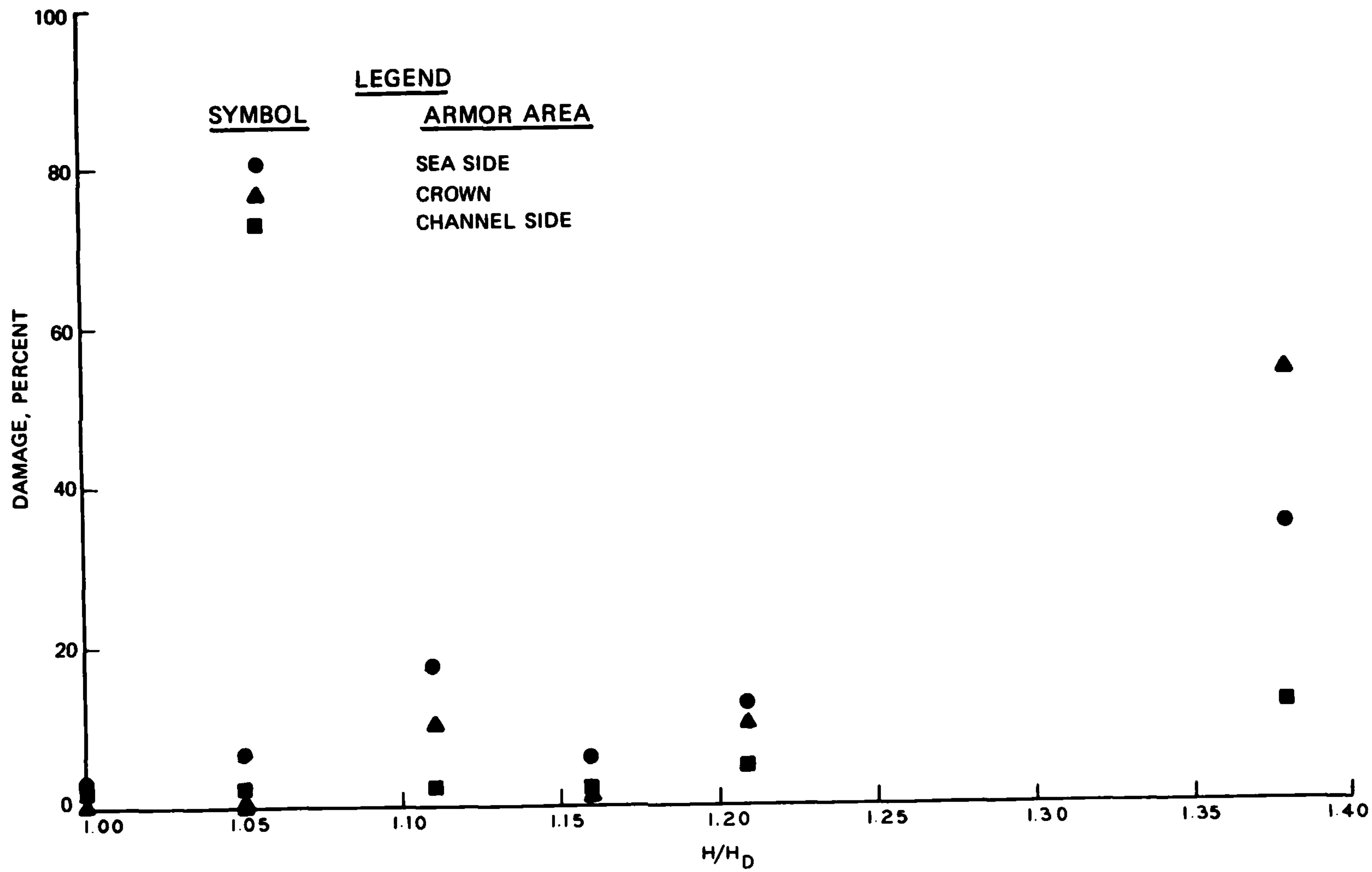

Figure 11. Damage as a function of H/H_D for Plan 10, number method

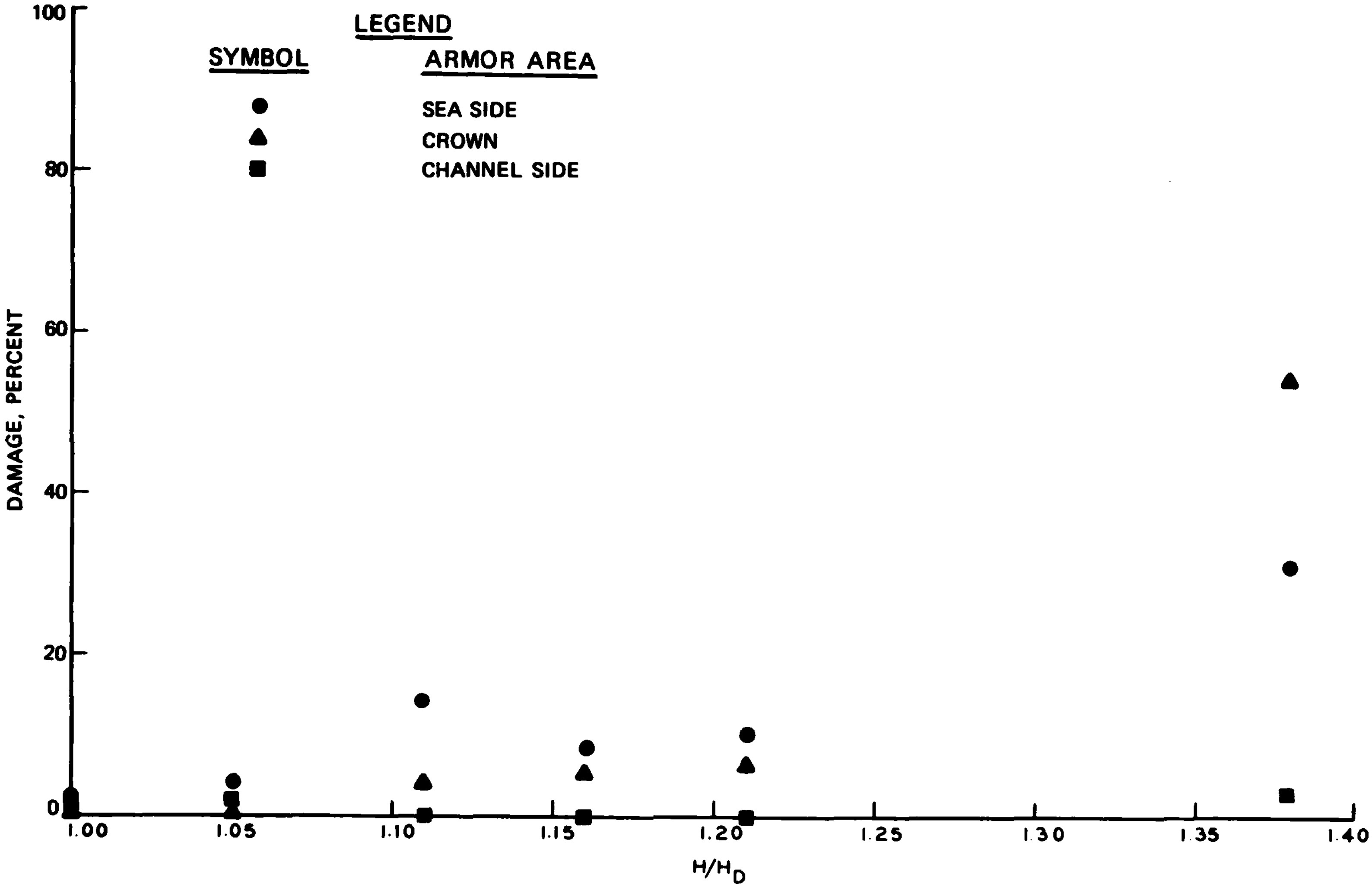

Figure 12. Damage as a function of H/H_D for Plan 10, sounding method

tons (Plan 10) would be stable for a design-wave height of 15.5 ft at an swl of +7.5 ft. Using these test results (K_D = 2.3 and 8.3 for plan 4D and Plan 10, respectively) in conjunction with the HSE, predicted stable armor weights for a design-wave height of 17.2 ft at the +9.5 ft swl are 30.5 and 12.5 tons for the stone and dolosse, respectively. Therefore, initial stability tests were conducted with 30.5-ton stone and 12.5-ton dolosse.

Plans tested and general results

47. Details of the plans tested and general results were as follows:

a. Plan 4E (Plate 27 and Photos 109 and 110) was constructed to a crown elevation of +14.5 and used armor slopes of 1V on 1.5H both sea side and channel side. Sea-side slope and toe and crown protection was afforded by 30.5-ton stone while the channel side of the structure was armored with 15-ton stone. Attack of 15-sec, 17.2-ft waves produced only minor damage. Photos 111 and 112 show the after-testing condition of the structure.

b. Plan 11 (Plate 28 and Photos 113 and 114) used 12.5-ton dolosse on the seaward slope and toe while the channelward slope was armored with 5-ton dolosse. Crown protection was provided by three rows of 30.5-ton stone. The breakwater was built to a crown elevation of +14.5 and armor slopes of 1V on 1.5H were used both sea side and channel side. As evidenced in Photos 115 and 116, attack of 15-sec, 17.2-ft waves produced only minor damage. Several sea-side armor units were displaced onto or over the crown. However, the structure did stabilize and the amount of movement experienced was judged to be acceptable.

48. The 2-ton, channel-side toe-protection stone used on both plans was stable. Each plan was exposed to wave attack until it stabilized and results for both plans were verified by one repeat test.

Summary of damage

49. Damage incurred by Plans 4E and 11 is presented in Table 9 for both the number and sounding methods. These data support the general test results discussed in paragraphs 47 and 48, i.e., both plans incurred only minor damage.

Development of Composite Damage Curves

50. Based on the data available from the 2-d tests, it was desired to develop a functional relation between total percent damage occurring on a given type structure (stone or dolosse) and wave heights expressed as exceedance of the selected design wave heights (H/H_D). In order to develop the data into the proper form, storm-surge hydrograph and percent damage data on individual test

plans from Tables 3 and 8 were reduced and combined in Table 10. The composite damage values presented in Table 10 were obtained by using the total armor area and total number of armor units (combination of sea side, crown, and beach side) as the base area and armor unit number and applying the sounding and number methods as described in PART II.

51. Plots of composite damage versus H/H_D are presented in Figures 13-16 for both damage methods and armor types. In general, these data show that overall damage to each type of base design increases as H/H_D increases, until some maximum value of H/H_D (which is dependent upon the combination of swl, wave condition, and structure crown elevation, geometry, and armor type) is reached and damage declines. Although there probably is some scatter in the data due to the inherent variation of stability test results when high damage values are considered, the data plots seem reasonable considering each base design crown elevation remained the same while being attacked by an increasing depth-limited breaking wave condition at each increasing depth of water. The data trend for each base design is the same regardless of the damage-evaluation method used, i.e. the sounding method and number method of evaluation tends to increase and decrease at the same values of H/H_D.

Correlation of Base Design Data with Hudson's Stability Equation

52. Since no formal stability tests have ever been conducted to check the validity of using HSE to predict stable armor for depth-limited breaking wave conditions on severely overtopped structures, the base design data experimentally determined at the +5.5, +7.5, and +9.5 ft swl's were used to investigate the viability of the equation. The HSE is expressed as follows:

$$W_a = \frac{\gamma_a H^3}{K_D (S_a - 1)^3 \cot \alpha} \qquad \text{(1 bis)}$$

and can be rearranged as

$$K_D = \frac{\gamma_a}{(S_a - 1)^3 \cot \alpha} \frac{H^3}{W_a} \qquad (2)$$

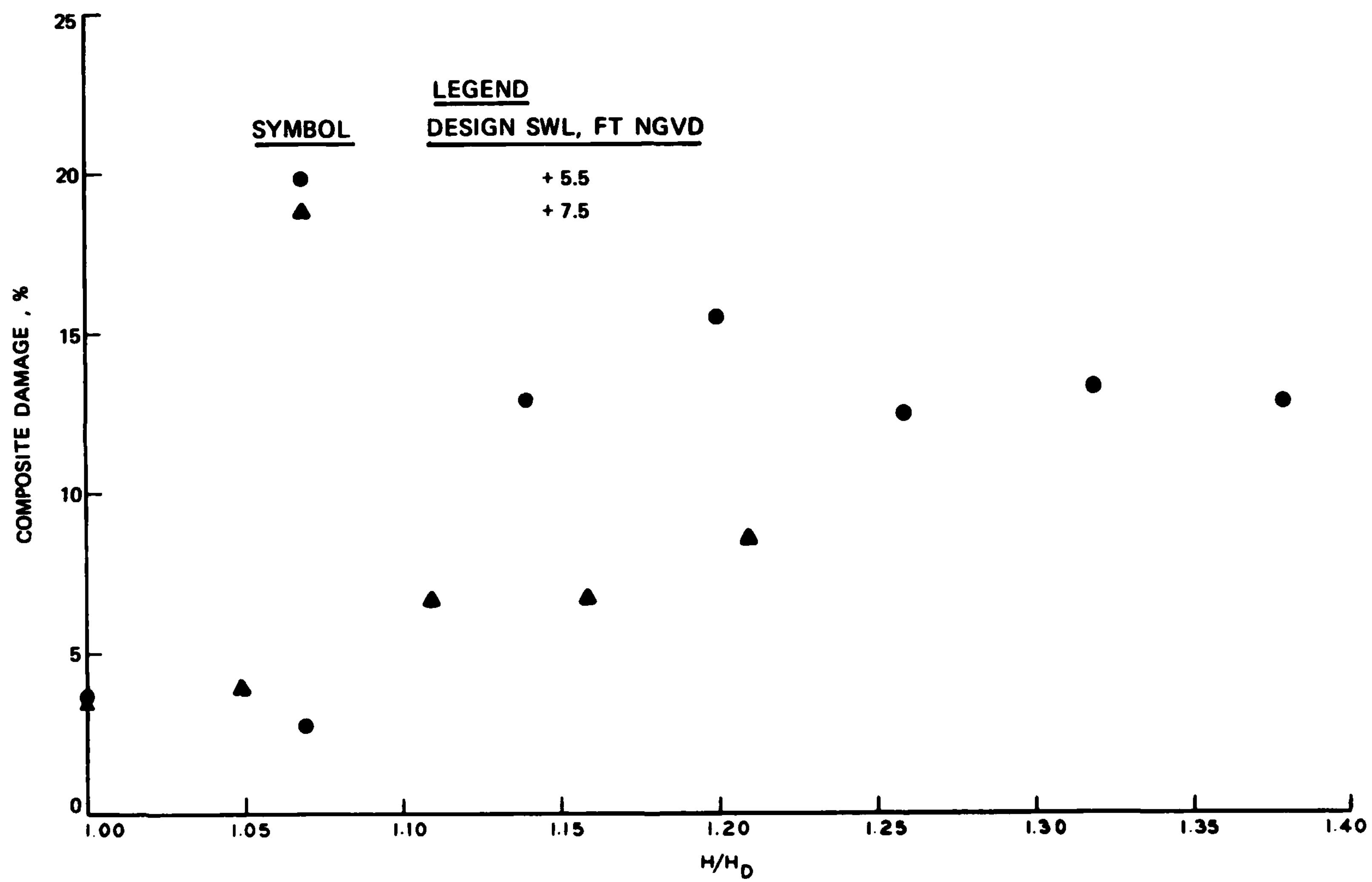

Figure 13. Composite damage as a function of H/H_D for armor stone, sounding method

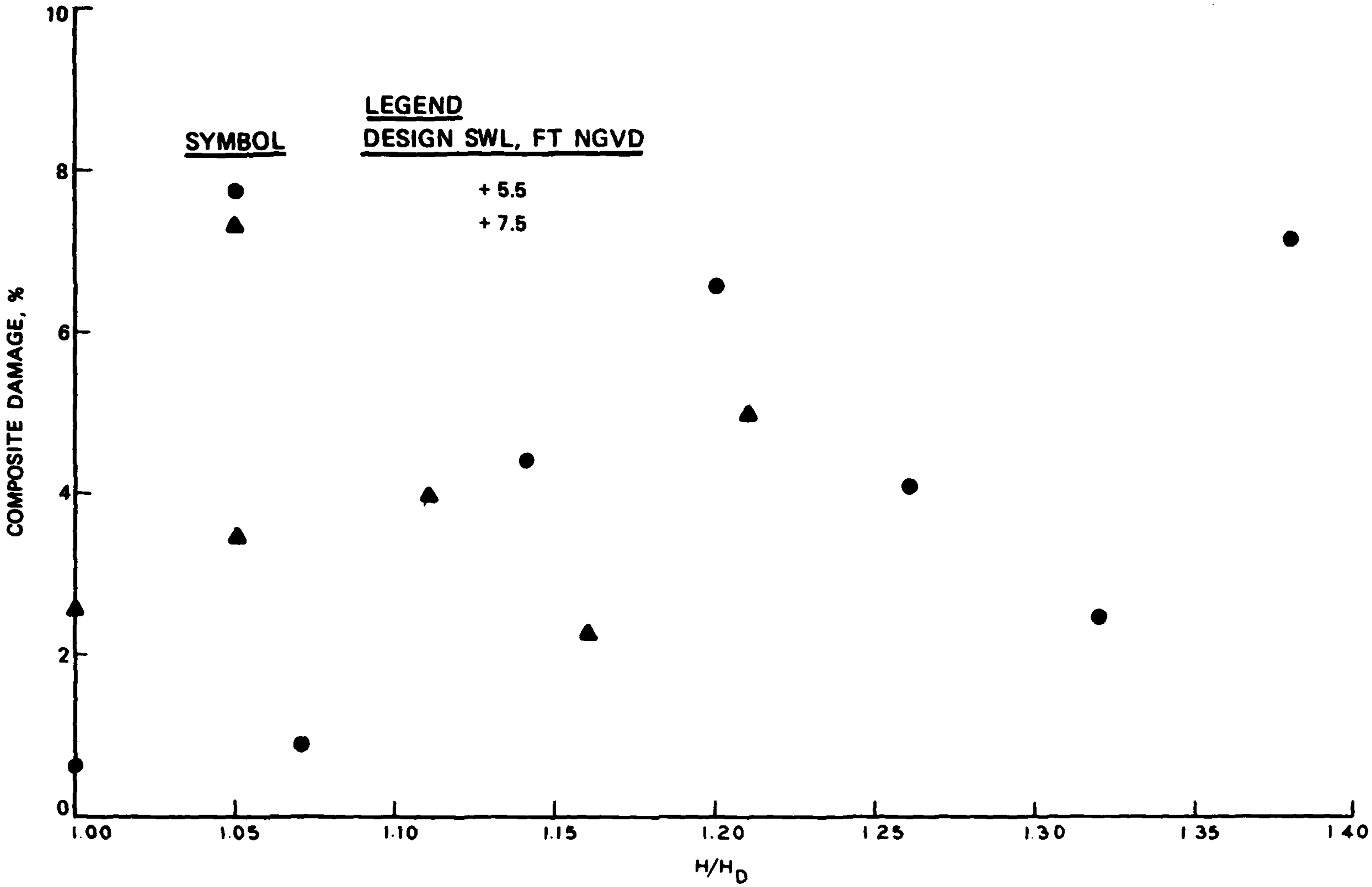

Figure 14. Composite damage as a function of H/H_D for armor stone, number method

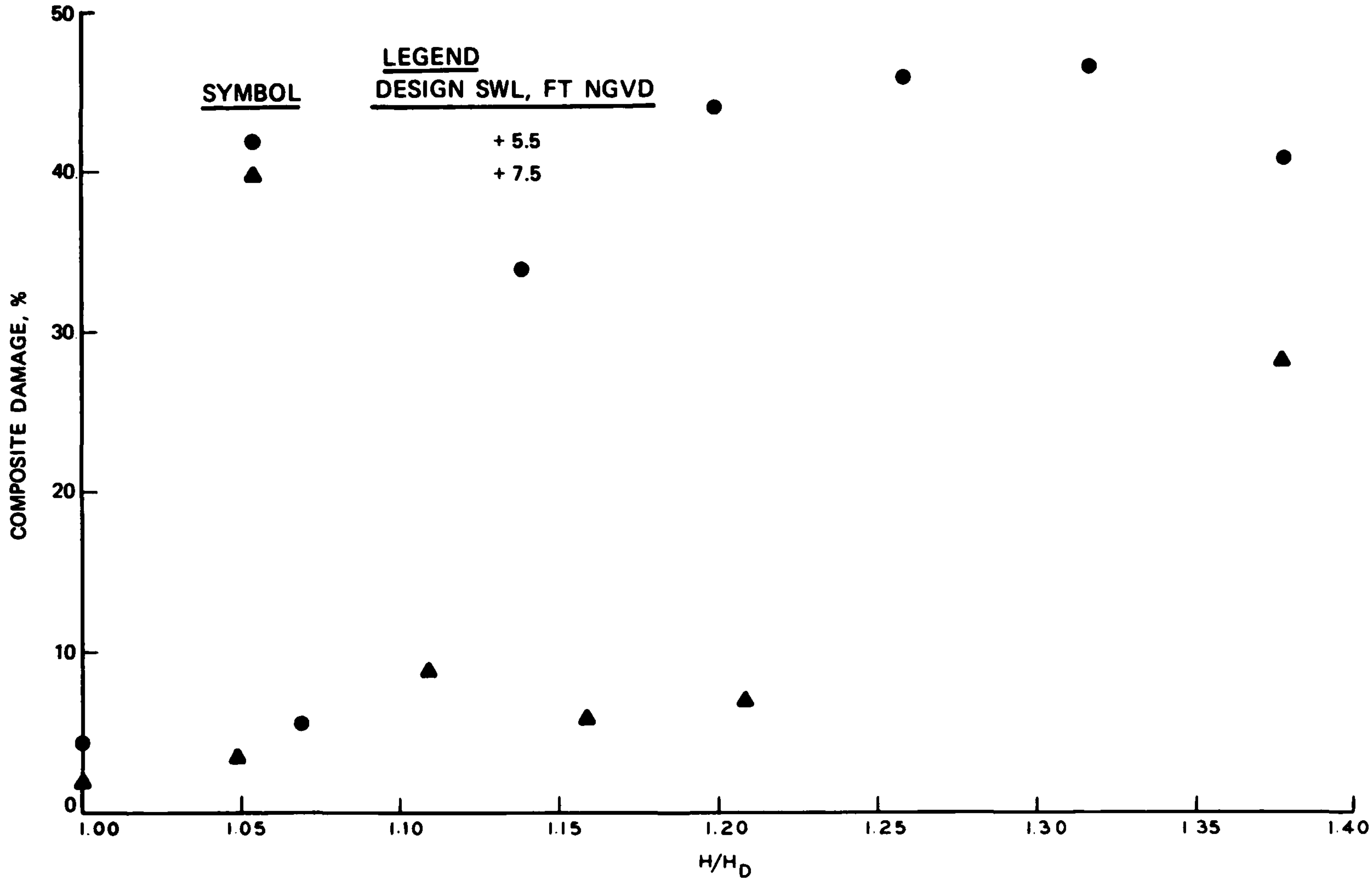

Figure 15. Composite damage as a function of H/H_D for dolos armor, sounding method

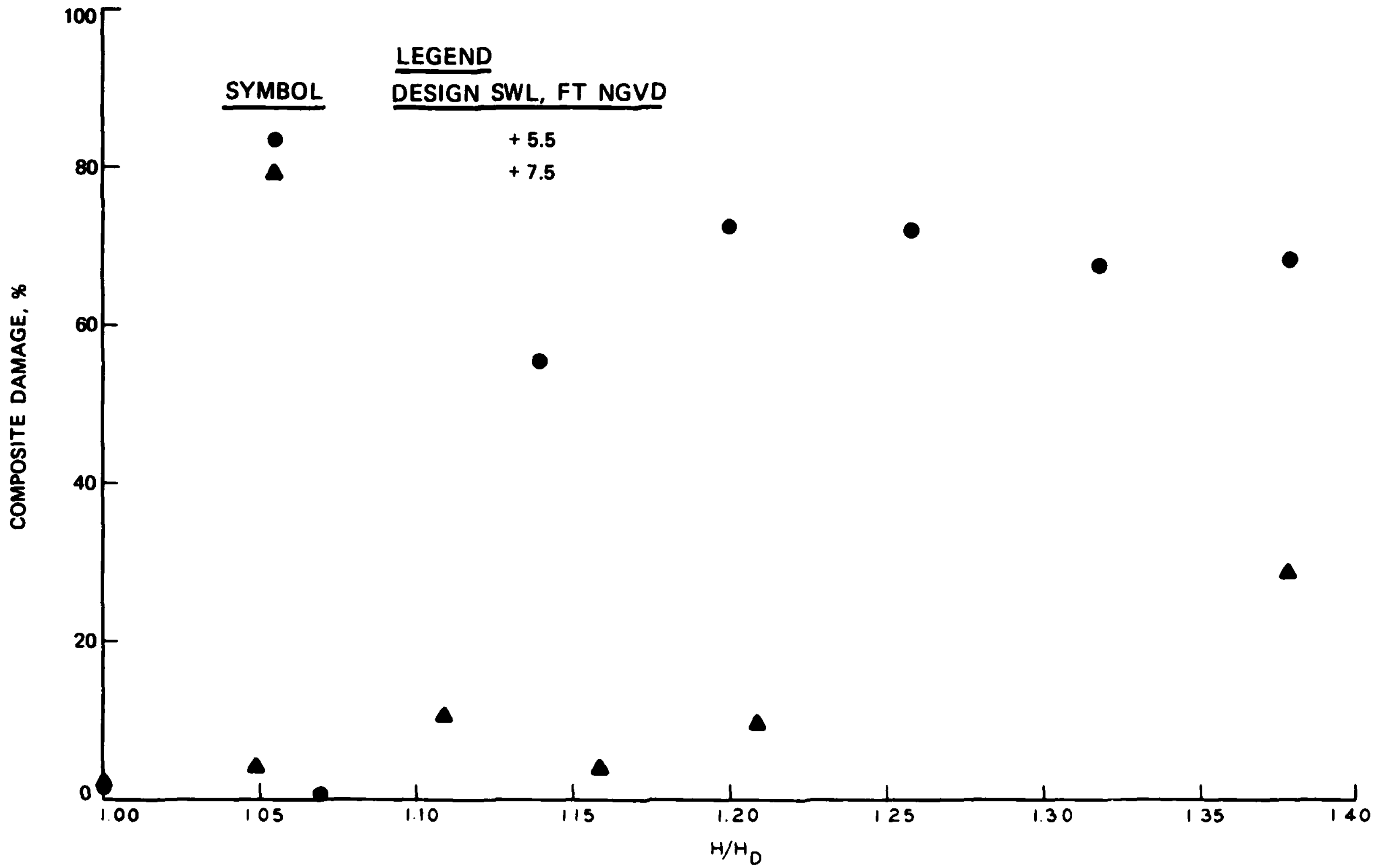

Figure 16. Composite damage as a function of H/H_D for dolos armor, number method

Recalling that the specific weights of the dolosse and stone were 150 and 165 pcf, respectively, and the sea-side slope of the structures was 1V on 1.5H the following constants may be introduced:

$$C_s = \frac{(\gamma_a)_s}{(S_s - 1)^3 \cot \alpha} \tag{3}$$

$$= \frac{165}{(165/64 - 1)^3 \; 1.5}$$

$$= 28.0 \text{ pcf}$$

$$C_d = \frac{(\gamma_a)_d}{(S_d - 1)^3 \cot \alpha} \tag{4}$$

$$= \frac{150}{(150/64 - 1)^3 \; 1.5}$$

$$= 41.2 \text{ pcf}$$

where the subscripts s and d signify stone and dolosse, respectively. Substituting Equations 3 and 4 in Equation 2 yields

$$K_{D_s} = \frac{C_s H^3}{W_s} \quad \text{and} \quad K_{D_d} = \frac{C_d H^3}{W_d}$$

53. Stable armor weights, design wave heights, and the products $C_s H^3$ and $C_d H^3$ for the base designs developed at the three design swl's are summarized below:

swl ft NGVD	Sea-side Armor* Weight, 10^3 lb Stone	Dolosse	Wave Height, ft	$C_s H^3$, 10^3 lb	$C_d H^3$, 10^3 lb
+5.5	30.0	6.5	13.6	70.4	103.6
+7.5	44.0	18.5	15.5	104.3	153.4
+9.5	61.0	25.0	17.2	142.5	209.6

* The correlation applied herein is applicable only to the sea-side armor.

If HSE is applicable to the above test results, plots of W_s versus C_sH^3 and W_d versus C_dH^3 should yield first-order curves that pass through the origin of the plots and the coefficients $(K_D)_s$ and $(K_D)_d$ will be equal to the reciprocal of the appropriate slope. As shown in Figure 17, a plot of W_s versus C_sH^3 gives a first-order curve that passes almost exactly through the origin and has a slope of 0.43 which yields a $(K_D)_s$ of 2.3. Figure 17 further shows that a similar plot of the initial dolos test results does not yield a first-order curve. Upon reviewing data from the +5.5, +7.5, and +9.5 ft swl's, it became apparent that the base dolos designs were not in complete concert, i.e., even though the 3.25-ton dolosse selected for the +5.5 ft swl were acceptable, their relative stability was less conservative than the +7.5 and +9.5 ft swl's. Using only the results from the +7.5 and +9.5 ft swl's, Figure 17 shows that a plot of W_d versus C_dH^3 is first order and passes through the origin of the plot. The slope of this curve is 0.12 and yields a $(K_D)_d$ of 8.3.

54. Based on the indications above, a check test of Plan 8 was conducted using 5-ton dolosse (Plan 8A). Results of this test (Photos 117 and 118) showed the 5-ton units to be a more reasonable choice for the +5.5 ft swl, i.e., although both the 3.25-ton dolosse and the 5-ton dolosse provided adequate protection at the end of their respective tests, the 5-ton dolosse did not require as much onslope movement or adjustment to maintain their stability as did the 3.25-ton units. If hindsight gained by the conclusion of the 2-d tests had been available when base designs were developed for the +5.5 ft swl, a dolos weight of at least 5 tons would probably have been selected. Adding the 5-ton dolos data point to Figure 17 shows that it is in reasonable agreement with the results predicted by the other two swl's. Based on these results, HSE can be used to predict valid armor weights for breaking wave conditions on overtopped structures, but one should be reminded that the correlation made above is applicable only to the sea side of the structure and is limited to the specific range of test conditions investigated herein.

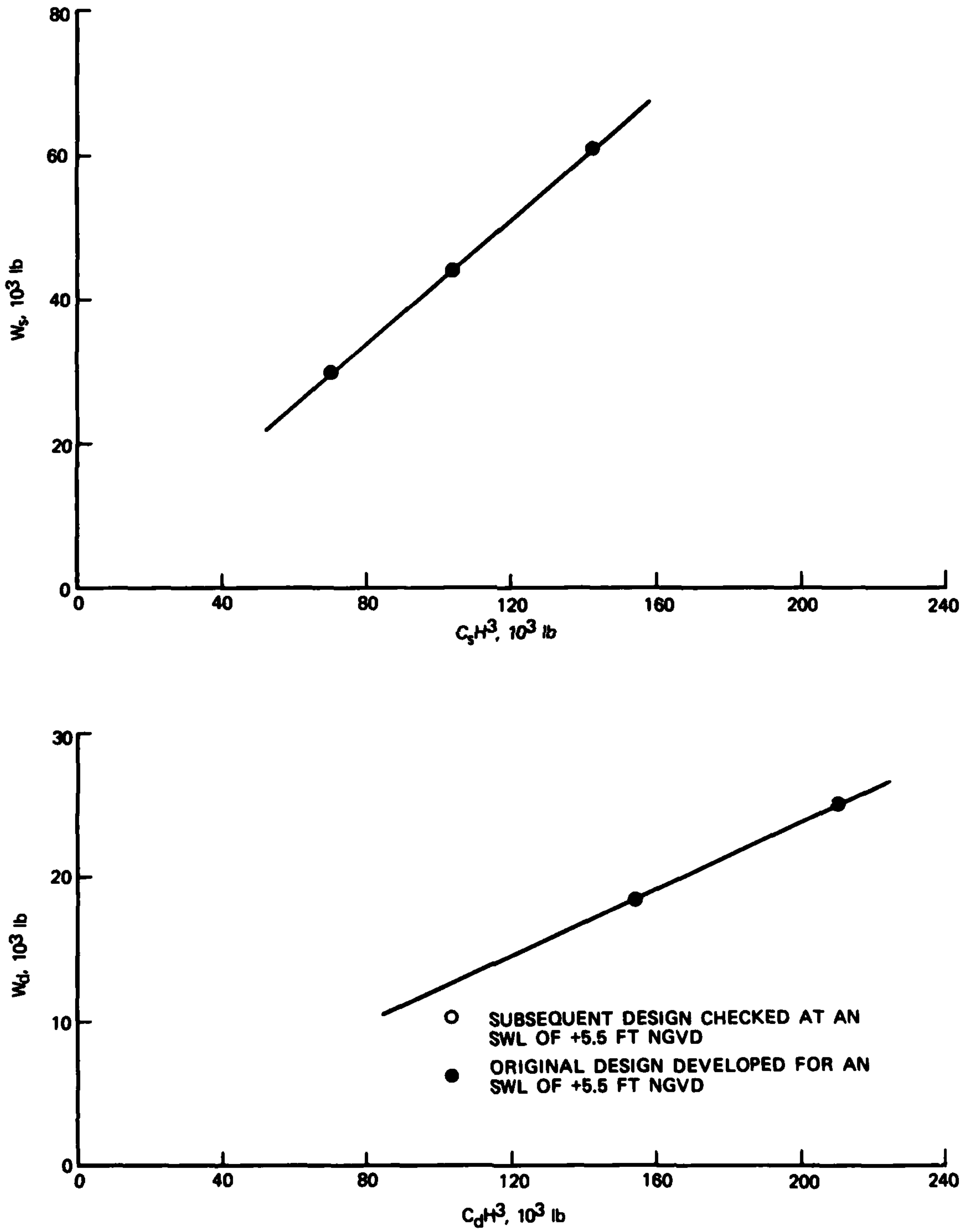

Figure 17. W_s as a function of C_sH^3 and W_d as a function of C_dH^3

PART IV: THREE-DIMENSIONAL STABILITY TESTS

Selection of Test Conditions

55. Using results from the previously described 2-d stability tests, an economic optimization of the stone and dolos armoring alternatives was conducted by SAW. This analysis yielded design swl's of +7.5 ft and +8.0 ft for stone and dolosse, respectively. Based on an extreme wave-height frequency analysis, design wave heights with return periods equal to those of the design swl's were determined to be 16.8 ft for stone and 17.6 ft for dolosse. The maximum wave period associated with the selected design swl's and wave heights was determined to be 15 sec.

56. Since the determined design conditions for the two types of armor were so similar, it was decided to test both structures with the conditions determined for the dolos armor, i.e., both structures were tested with 15-sec, 17.6-ft waves at an swl of +8.0 ft (thus inducing a small amount of conservatism in the stone design). The structures also were tested for 15-sec, 17.6-ft breaking waves since the 15-sec, 17.6-ft waves might occur at an swl sufficiently low to allow the waves to break. Model observations of swl's and wave-height combinations for Plans 3D-1 and 3D-2 showed that a severe depth-limited 15-sec, 17.6-ft breaking wave condition could be achieved at an swl of +1 ft.

57. Based on the proposed alignment of the jetties and the directional distribution of the local wave climate, it was decided to test the structures for angles of wave attack of 0, 22.5, 45, 67.5, and 90 deg relative to the center line of the jetty. Plate 29 shows test section orientation for a 45-deg angle of wave attack.

Development of Stable Sections for a 90-Deg Angle of Wave Attack

Description of plans tested

58. Four dolos alternatives (Plans 3D-1, 3D-1A, 3D-1B, and 3D-1C) and four stone alternatives (Plans 3D-2, 3D-2A, 3D-2B, and 3D-2C) were investigated before final designs were selected for the 90-deg angle of wave attack. Armor unit sizes of 14-ton dolosse and 30-ton stone were used throughout the jetty-head tests because 30-ton stone was about the largest prototype size suitable and reasonably transportable to the site and 14-ton dolosse was the

optimum-economical size dolosse considering the design wave conditions and placement density. Details of the plans tested were as follows:

a. Plan 3D-1 (Plates 30-32 and Photos 119-121) used two layers of 14-ton dolos armor on the slopes and toes and one layer of 30-ton stone armor on the crown. The trunk of the structure was built to a crown elevation of +14.2, while the head was built to a crown elevation of +18. Side-armor slopes of 1V on 1.5H and 1V on 3H were used on the trunk and head, respectively. The structure was symmetrical about its center line except the trunk used 25 ft of toe protection sea side and 40 ft of toe protection channel side. Trunk and head sections were joined by a 50-ft linear transition area.

b. Plan 3D-1A (Plates 30-32) was the same as Plan 3D-1 except that the marine-limestone bedding (W_4) was bonded to the bottom of the test section.

c. Plan 3D-1B (Plates 31-33 and Photos 122-124) was similar to Plan 3D-1A except that the first two rows of toe armor were placed with the vertical leg downslope and the transition length was increased to 100 ft.

d. Plan 3D-1C (Plates 31, 34, and 35 and Photos 125-127) was similar to Plan 3D-1A except that the head's toe protection width was increased to 52 ft and the transition length was increased to 150 ft.

e. Plan 3D-2 (Plates 36-38 and Photos 128-130) used 30-ton stone armoring: one layer on the toes, two layers on the slopes, one layer on the trunk's crown, and two layers on the head's crown. Side armor slopes of 1V on 1.5H and 1V on 3H were used on the trunk and head, respectively. The trunk of the structure was built to a crown elevation of +14.2, while the head was built to a crown elevation of +18. Trunk and head sections were joined by a 50-ft linear transition.

f. Plan 3D-2A (Plates 36-38) was the same as Plan 3D-2 except that the bedding (W_3) was bonded to the bottom of the test section.

g. Plan 3D-2B (Plates 37, 39, and 40 and Photos 131-133) was similar to Plan 3D-2A except that two layers of toe armor were used on the head and the transition length was increased to 100 ft.

h. Plan 3D-2C (Plates 37, 41, and 42 and Photos 134-136) was similar to Plan 3D-2B except that the head's toe protection width was increased to 60 ft and the transition length was increased to 150 ft.

Tests and Results

59. Initially, Plans 3D-1 and 3D-2 were simultaneously tested with 15-sec, 17.6-ft breaking waves at an swl of +1 ft. This wave condition produced significant damage to the sea-side toes of both plans; however, little or no movement was detectable on the channel side or crown of either structure. Upon completion of testing at the +1 ft swl, the water level was raised to +8 ft

and the test sections were subjected to 15-sec, 17.6-ft nonbreaking waves. Attack of the nonbreaking waves produced no further damage to either structure. Photos 137-142 depict the combined effects of wave attack of both the +1 and +8 ft swl's. For this and all other 3-d tests, the structures were surveyed for damage following the breaking and nonbreaking wave portions of the test.

60. In order to better quantify and describe changes that occurred during wave attack, each structure was divided into three segments (trunk, transition, and head), and each segment was divided into three armor areas (sea side, crown, and channel side), thus yielding a total of nine individual areas. Plate 43 shows locations of the various areas.

61. Test results for Plans 3D-1 and 3D-2 were verified by a complete reconstruction and retesting of the structures. For the selected design conditions (15-sec, 17.6-ft breaking waves at an swl of +1 ft and 15-sec, 17.6-ft nonbreaking waves at an swl of +8 ft), it is most probable that the structures will be first attacked by the 15-sec, 17.6-ft breaking waves; however, it is possible that storm conditions may be such that the structures will initially be attacked by 15-sec, 17.6-ft nonbreaking waves. Therefore, in the repeat tests, the model sections were first subjected to 15-sec, 17.6-ft nonbreaking waves at an swl of +8 ft.

62. Attack of the 15-sec, 17.6-ft nonbreaking waves produced damage in areas 2 and 3 of Plan 3D-1 and areas 1, 2, 3, and 9 of Plan 3D-2. Upon completion of testing of the +8 ft swl, the water level was lowered to +1 ft and the structures were subjected to 15-sec, 17.6-ft breaking waves. This test condition initiated damage in area 1 of Plan 3D-1 and also produced an increase in damage to areas 2 and 3 of Plan 3D-1 and areas 1, 2, 3, and 9 of Plan 3D-2. Photos 143-148 show the final stability condition of the structures.

63. Based on observations of Plans 3D-1 and 3D-2 under wave attack, it was felt that the instability observed in areas 1, 2, 3, and 9 might have been initiated by sliding of the marine-limestone bedding (W_4 of Plan 3D-1 and W_3 of Plan 3D-2). It was not deemed reasonable that toe slippage of this magnitude would occur in the prototype. Consequently, tests were conducted to evaluate armor stability in the absence of bedding slippage. To accomplish this objective, the bedding material of both plans was bonded to the molded concrete bottom, thus creating Plans 3D-1A and 3D-2A.

64. Plans 3D-1A and 3D-2A were initially tested with 15-sec, 17.6-ft breaking waves at an swl of +1 ft. Both plans were damaged in areas 1, 2, and

3 and Plan 3D-2A also was slightly damaged in area 9. Next, the water level was raised to +8 ft and the test sections were subjected to 15-sec, 17.6-ft nonbreaking waves. The higher swl initiated slight damage in area 9 of Plan 3D-1A and area 4 of Plan 3D-2A and also produced a small damage increase in area 3 of Plan 3D-2A. The after-testing condition of the structures is shown in Photos 149-154.

65. Both Plans 3D-1A and 3D-2A were reconstructed and retested, starting at the +8 ft swl and then proceeding to the +1 ft swl. During the repeat tests, movement of armor was experienced in areas 1, 2, and 3 of both plans and areas 4 and 9 of Plan 3D-2A. Photos 155-160 document the final condition of the sections.

66. Based on observation of Plans 3D-1A and 3D-2A under wave attack and the final stabilized condition of the structures, it was felt that much of the damage in armor areas 1, 2, and 3 was caused by sliding of the toe armor and too short a transition length. Therefore, in order to help isolate and identify the sources of instability, the transition length of both structures was increased to 100 ft, dolos toe units were pattern-placed, a second layer of armor stone was added to the toe of the stone structure, and the stone structure's toe was prevented from slipping with a wooden toe strip, thus creating Plans 3D-1B and 3D-2B.

67. Plans 3D-1B and 3D-2B were simultaneously tested with 15-sec, 17.6-ft breaking waves at an swl of +1 ft. This wave condition produced moderate damage in armor area 3 of Plan 3D-1B and minor damage in armor areas 1, 2, and 3 of Plan 3D-2B. Upon completion of testing at the +1 ft swl, the water level was raised to +8 ft and the test sections were subjected to 15-sec, 17.6-ft nonbreaking waves. Attack of the nonbreaking waves produced a slight increase in damage in armor area 3 of Plan 3D-1B; however, there was no detectable change in the stability condition of Plan 3D-2B. Photos 161-166 show the combined effects of wave attack at both the +1 and +8 ft swl's.

68. Test results of Plans 3D-1B and 3D-2B were verified by a complete reconstruction and retesting of the structures. Test sections were initially subjected to wave attack at the +8 ft swl in the repeat tests. Attack of 15-sec, 17.6-ft nonbreaking waves produced minor damage in areas 2 and 3 of Plan 3D-1B and areas 1 and 2 of Plan 3D-2B. Upon completion of testing at the +8 ft swl, the water level was lowered to +1 ft and the structures were subjected to 15-sec, 17.6-ft breaking waves. This test condition initiated

light damage in armor area 3 of Plan 3D-2B, produced a small increase in damage in armor area 1 of Plan 3D-2B, and caused a moderate increase in damage in armor area 3 of Plan 3D-1B. Photos 167-172 depict the combined effects of wave attack at both swl's.

69. The stability responses of Plans 3D-1B and 3D-2B demonstrated that a reduction in slippage of toe armor and an increase in the transition length served to improve the overall stability of both armoring schemes. Since it was not deemed reasonable to draw conclusions of prototype toe armor stability for the head and transition sections of Plan 3D-2B (toe-strip assumption) and SAW was not certain that they could achieve pattern placement of dolos toe units, it was decided to attempt to achieve an increase in toe stability by extending armor coverage to the -20 ft contour on the heads and increasing the transition lengths to 150 ft, thus creating Plans 3D-1C and 3D-2C.

70. Plans 3D-1C and 3D-2C were initially tested with 15-sec, 17.6-ft breaking waves at an swl of +1 ft. This wave condition produced minor damage in armor areas 1, 2, and 3 on both structures. Upon completion of testing at the +1 ft swl, the water level was raised to +8 ft and the test sections were subjected to 15-sec, 17.6-ft nonbreaking waves. Attack of the nonbreaking waves produced a slight increase in damage in armor areas 2 and 3 of both plans; however, the overall stability condition of the structures changed very little at this water level. Photos 173-178 depict the combined effects of wave attack at both the +1 and +8 ft swl's.

71. Test results of Plans 3D-1C and 3D-2C were verified by a complete reconstruction and retesting of the structures. In the repeat test, the sections were initially subjected to 15-sec, 17.6-ft nonbreaking waves at an swl of +8 ft. This test condition produced very minor damage in armor areas 2, 3, and 8 of Plan 3D-1C and armor areas 2 and 7 of Plan 3D-2C. After completion of testing at the +8 ft swl, the water level was lowered to +1 ft and the structures were subjected to 15-sec, 17.6-ft breaking waves. Attack of the breaking waves initiated minor damage in armor areas 1 and 9 of Plan 3D-1C, produced a small damage increase in armor area 3 of Plan 3D-1C, initiated damage in armor areas 3 and 4 of Plan 3D-2C, and caused a small damage increase in armor area 2 of Plan 3D-2C. Photos 179-184 show the final stability condition of the structures.

72. During both the initial and repeat testings of all plans, the structures were subjected to wave attack for 3 hr (prototype) at each swl. This

duration of wave attack allowed sufficient time for the structures to stabilize, i.e., time for all movement of armor material to abate.

73. Damage to the structures determined by the number method is presented in Tables 11 and 12. These data show that generally (a) movement was mostly confined to the seaward armor areas; (b) the +1 ft swl produced significantly more movement than the +8 ft swl; and (c) the final stability condition of the test section was essentially independent of the sequencing of the swl's.

74. Based on the tests and results described in this section, it was decided that Plans 3D-1C and 3D-2C were the best dolos and stone alternatives. Even though both plans experienced minor stabilized damage, it was shown that this movement was not extensive enough to alter the overall integrity of either section. Further, since the instability was always nearly instigated in the toe area, it was surmised that in the prototype the outer bedding layer and toe units would stabilize into the sand and defer any further deterioration of the armor.

Stability Tests of Plans 3D-1C and 3D-2C for Angles of Wave Attack of 0.0, 22.5, 45.0, and 67.5 Deg

75. Plans 3D-1C and 3D-2C also were tested for angles of wave attack of 0.0, 22.5, 45.0, and 67.5 deg. For each angle of wave attack tested, the structures were subjected to 15-sec, 17.6-ft breaking waves at an swl of +1 ft followed by 15-sec, 17.6-ft nonbreaking waves at an swl of +8 ft. Each test section was reconstructed after testing at each angle of wave attack. Also, test results of each wave direction were verified by a complete retesting of both plans. In the repeat tests, the sections were initially subjected to 15-sec, 17.6-ft nonbreaking waves at an swl of +8 ft followed by 15-sec, 17.6-ft breaking waves at an swl of +1 ft. Photos 185-200 show the after-testing condition of the structures for the various angles of wave attack. Some minor stabilized damage was observed for each wave direction; however, the damage was never extensive enough to alter the functional integrity of either plan.

76. During both the initial and repeat tests, the structures were subjected to wave attack for 3 hr (prototype) at each swl. This duration of wave attack allowed sufficient time for the structures to stabilize, i.e., time for all armor material movement to abate.

77. Damage to the structures, as determined by the number method, is presented in Tables 13-16. Also, Figures 18-21 present damage as a function of angle of wave attack for armor areas 2, 3, and 9 and total armor area. The data presented in Tables 13-16 and Figures 18-21 show that (a) most movement was confined to armor areas 2, 3, and 9; (b) the +1 ft swl produced significantly more movement than the +8 ft swl; (c) damage in armor area 2 decreased to zero, damage in armor area 3 generally decreased, and armor area 9 damage generally increased as the angle of wave attack was reduced from 90.0 to 0.0 deg; and (d) based on the total armor area, no particular angle of wave attack was significantly more damaging than the others for either plan.

Cumulative-Damage Tests of Plans 3D-1C and 3D-2C

78. Following completion of repeat tests at the 0.0-deg wave direction, it was decided to investigate the cumulative effects (i.e., test sections not rebuilt between wave directions) of wave attack for wave directions of 0.0, 45.0, and 90.0 deg. To accomplish this, toe armor displaced during the 0.0-deg test was removed from the model and the structures were carefully rotated to the 45.0-deg wave direction. Wave attack at this direction consisted of 15-sec, 17.6-ft nonbreaking waves at an swl of +8 ft followed by 15-sec, 17.6-ft breaking waves at an swl of +1 ft. The +8 ft swl produced a slight damage increase in armor areas 3 and 9 of Plan 3D-2C and initiated damage in armor area 3 of Plan 3D-1C. Damage increased in armor areas 3 and 9 of both plans and was initiated in armor area 2 of Plan 3D-2C during wave attack at the +1 ft swl.

79. Upon completion of wave attack at the 45.0-deg wave direction, the flume was again dewatered, displaced toe armor was removed, structures were rotated to the 90.0-deg direction, and wave attack was initiated with 15-sec, 17.6-ft nonbreaking waves at an swl of +8 ft. This wave condition produced a slight damage increase in armor areas 3 and 9 of both plans and armor area 2 of Plan 3D-2C. Minor damage was also initiated in armor area 1 of Plan 3D-1C. Finally, the water level was lowered to +1 ft and the structures were subjected to 15-sec, 17.6-ft breaking waves. This wave condition produced additional damage in armor areas 3 and 9 of both plans, armor area 1 of Plan 3D-1C, and armor area 2 of Plan 3D-2C. Damage was incurred in armor area 2 of Plan 3D-1C and armor areas 1 and 7 of Plan 3D-2C. Photos 201-204 show

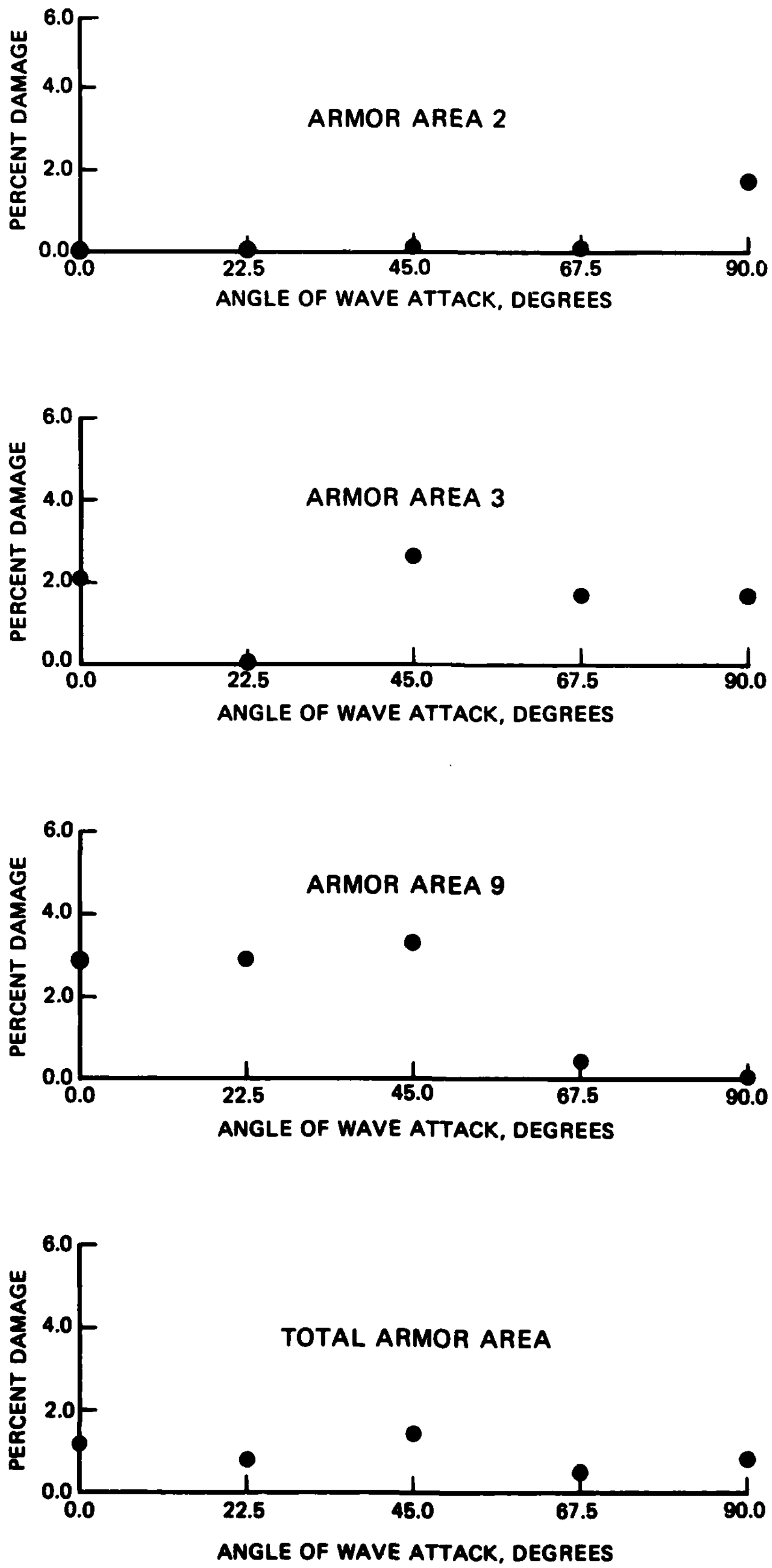

Figure 18. Percent damage as a function of angle of wave attack for Plan 3D-1C; +1 ft swl followed by +8 ft swl

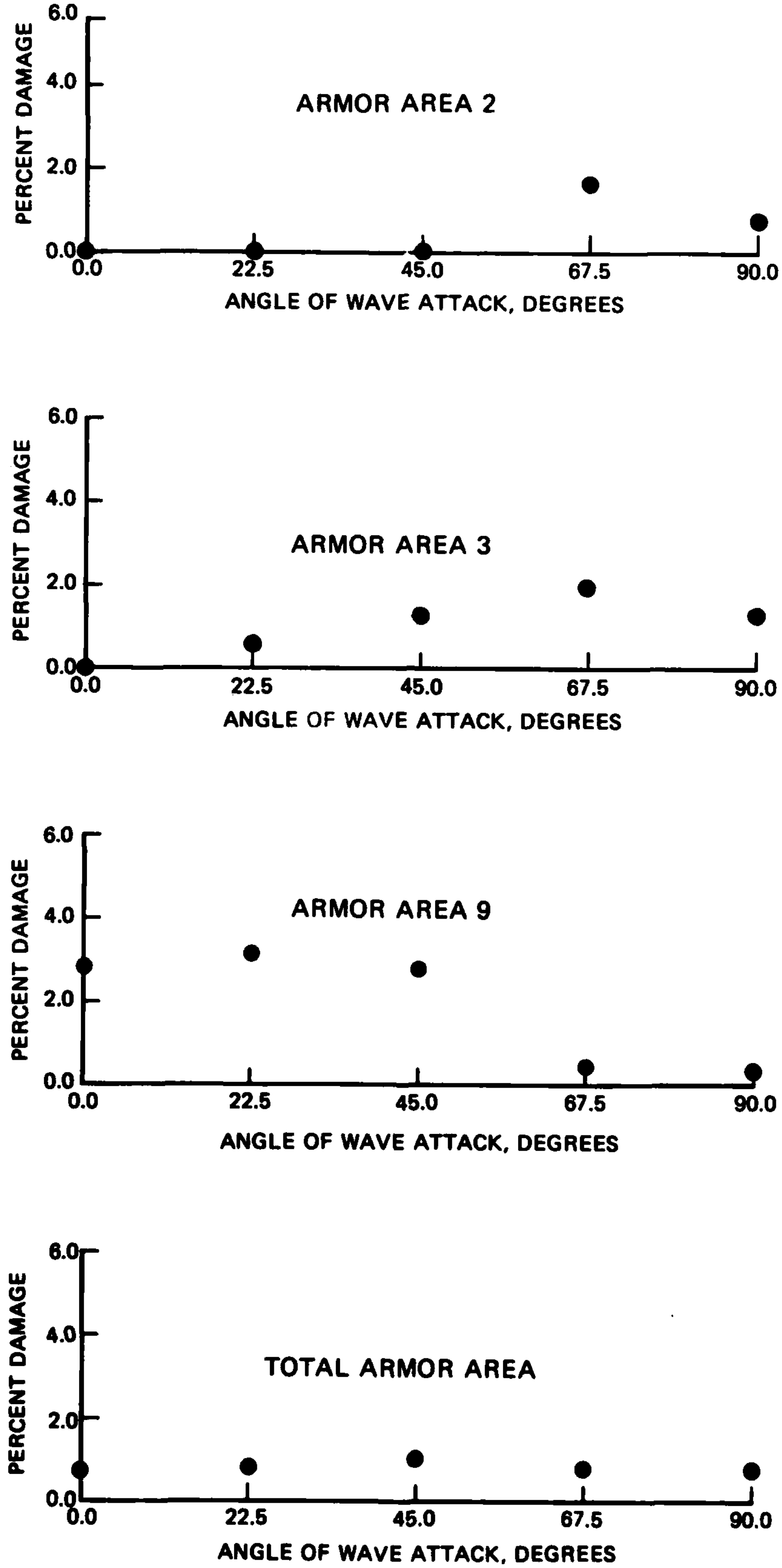

Figure 19. Percent damage as a function of angle of wave attack for Plan 3D-1C; +8 ft swl followed by +1 ft swl

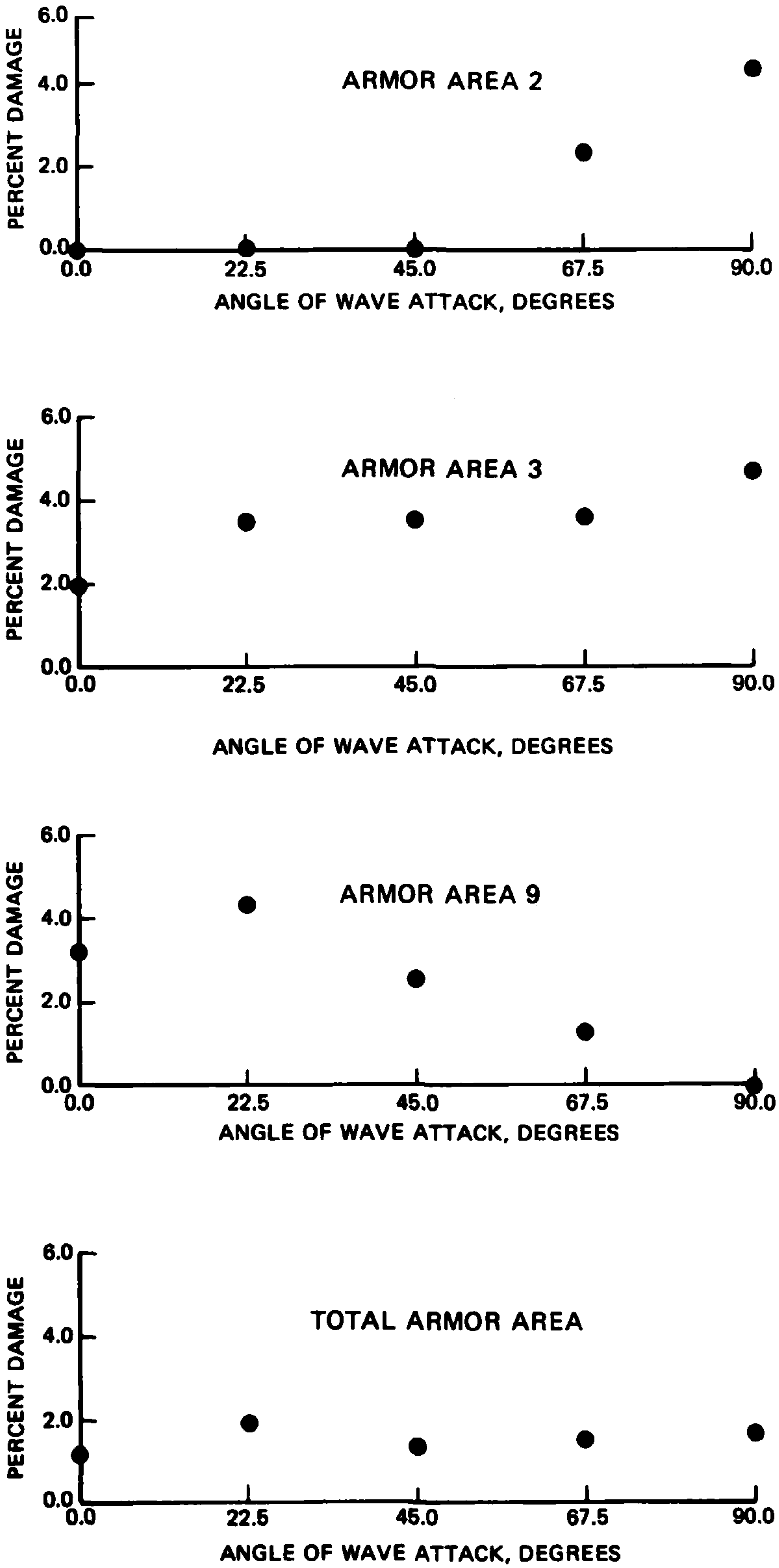

Figure 20. Percent damage as a function of angle of wave attack for Plan 3D-2C; +1 ft swl followed by +8 ft swl

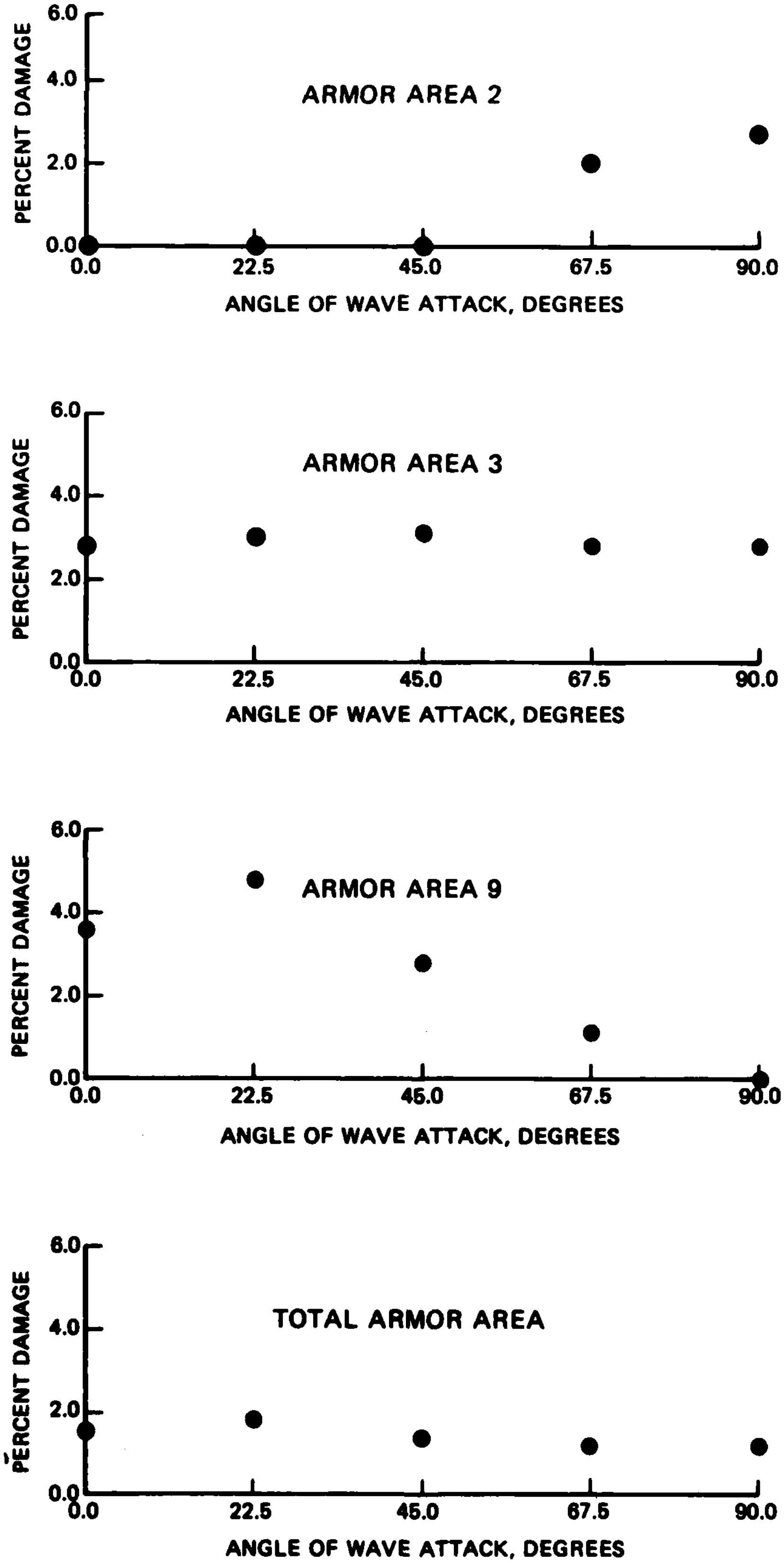

Figure 21. Percent damage as a function of angle of wave attack for Plan 3D-2C; +8 ft swl followed by +1 ft swl

the combined effects of wave attack at the 0.0, 45.0, and 90.0-deg wave direction. Examination of these photographs shows that neither structure experienced major deterioration; however, some concentrated toe armor damage can be observed.

80. Damage to the structures determined by the number method is presented in Table 17. These data show that the +1 ft swl produced substantially more movement than the +8 ft swl and most damage was confined to armor areas 2, 3, and 9.

81. Test sections were subjected to wave attack for 3 hr (prototype) at each swl and wave direction tested. This duration of wave attack allowed sufficient time for the structures to stabilize, i.e., time for all movement of armor material to abate.

Safety Factor Tests of Plans 3D-1C and 3D-2C

82. In designing rubble-mound jetties, as with any engineered structures, it is advantageous to determine what margin of safety is present in the selected designs. Consequently, it was decided to investigate the stability response of Plans 3D-1C and 3D-2C for wave heights in excess of the design height (H = 17.6 ft). A check of calibration data revealed that for the design wave period of 15 sec, capabilities of the wave generator were limited to maximum breaking and nonbreaking wave heights of 19.2 ft (swl = +3 ft) and 22 ft (swl = +8 ft), respectively. Even though the previously described tests of Plans 3D-1C and 3D-2C showed that for the 15-sec, 17.6-ft breaking and nonbreaking waves, no particular angle of wave attack between 0 and 90 deg was significantly more damaging than the others, tests conducted on dolosse by Willock (1977) suggest that an angle of attack around 45 deg may be most critical if the wave height is at or near the maximum that the armor can withstand. Therefore, safety factor tests were conducted with a 45-deg angle of wave attack using 15-sec, 19.2-ft breaking waves at an swl of +3 ft and 15-sec, 22-ft nonbreaking waves at an swl of +8 ft.

83. Plans 3D-1C and 3D-2C were initially tested with 15-sec, 19.2-ft breaking waves at an swl of +3 ft. As depicted in Photos 205-208, this wave condition produced minor to moderate damage in armor areas 2, 3, and 9 of both plans. Without rebuilding, the water level was raised to +8 ft and the test sections were subjected to 15-sec, 22-ft nonbreaking waves. Attack of the

nonbreaking waves produced a slight damage increase in armor areas 3 and 9 of both plans and armor area 2 of Plan 3D-2C. Photos 209-212 show the combined effects of wave attack of both the +3 and +8 ft swl's.

84. Damage to the structures determined by the number method is presented in Table 18. These data show that damage was confined to armor areas 2, 3, and 9. It also is interesting to note that the damages incurred are not a great deal larger than those incurred in the previously described tests with 15-sec, 17.6-ft breaking and nonbreaking waves.

85. Test sections were subjected to wave attack for 3 hr (prototype) at each swl. Again, this duration of wave attack allowed sufficient time for the structures to stabilize, i.e., time for all movement of armor material to abate.

PART V: CONCLUSIONS

86. Based on the assumptions, tests, and results reported herein, it is concluded from the 2-d tests that:

a. For a design swl of +5.5 ft:

(1) Plans 1, 2, 5, and 6 were not acceptable.

(2) Plan 3 was marginally acceptable.

(3) Plans 4, 4A, 4B, 7, and 8 were acceptable.

(4) Plan 4B exhibited the best stability response of all stone-armored structures.

(5) The slightly improved stability response of Plan 4B (relative to Plan 4A) is probably attributable to a back-pressure reduction achieved by using 18-ton capstone in place of the concrete crownwall.

(6) Plan 8 showed the best stability response of all dolos-armored structures initially tested (based on hindsight and subsequent check tests at the +5.5 ft swl reported in paragraphs 52-54, the 3.25-ton dolosse used in Plan 8 should probably have been increased to 5 tons).

(7) The improved stability response of Plan 8 (relative to Plan 7) is probably attributable to both increased crown elevation and back-pressure reduction.

(8) Plan 4B can withstand storm surges up to an swl of +11.5 ft without experiencing major deterioration.

(9) Plan 8 will be severely damaged by storm surges of +7.5 to +11.5 ft swl.

(10) If Plans 4B and 8 are attacked by two successive +7.5 ft swl hydrographs, Plan 4B will experience little further deterioration during the second hydrograph; however, Plan 8 will continue to deteriorate during the second hydrograph.

b. For a design swl of +7.5 ft:

(1) Plans 4C and 9 were not acceptable.

(2) Plans 4D and 10 were acceptable.

(3) Both Plans 4D and 10 can withstand storm surges up to +11.5 ft swl without experiencing major deterioration.

c. Plans 4E and 11 were acceptable designs for an swl of +9.5 ft.

d. Those portions of the jetty trunk not specifically modeled can be designed by the Hudson Stability Equation provided that:

(1) Stability coefficients of 2.3 and 8.3 are used for stone and dolosse, respectively.

(2) Armor slopes of 1V on 1.5H are used both sea side and channel side.

(3) The design wave height does not exceed 17.0 ft.

(4) The specific weight of the armor does not deviate by more than 5 percent from the prototype specific weights represented in the model tests.

(5) Toe and crown widths and the crown elevation relative to the swl are all approximately the same as those tested in the model study.

87. Results of the 3-d (head) tests substantiate the following conclusions:

a. For attack of 15-sec, 17.6-ft breaking waves at an swl of +1 ft and 15-sec, 17.6-ft nonbreaking waves at an swl of +8 ft with an angle of wave attack equal to 90 deg:

(1) Plans 3D-1, 3D-1A, 3D-2, and 3D-2A are not acceptable designs.

(2) Plan 3D-1B is an acceptable dolos design, provided that the first two rows of toe armor are placed with the vertical leg downslope and these two rows are made an integral part of the primary armor.

(3) Plan 3D-2B is an acceptable stone design, assuming toe slippage does not occur.

(4) Plan 3D-1C is an acceptable dolos design that allows complete random placement of the armor units.

(5) Plan 3D-2C is an acceptable stone-armored alternative.

b. Plans 3D-1C and 3D-2C are also stable for 15-sec, 17.6-ft breaking waves at an swl of +1 ft and 15-sec, 17.6-ft nonbreaking waves at an swl of +8 ft for angles of wave attack equal to 0.0, 22.5, 45.0, and 67.5 deg, and based on total armor area, no particular angle of wave attack is significantly more damaging than the others for either plan.

c. Plans 3D-1C and 3D-2C can withstand the cumulative effects (i.e., test sections not rebuilt between wave directions) of attack of 15-sec, 17.6-ft breaking waves at an swl of +1 ft and 15-sec, 17.6-ft nonbreaking waves at an swl of +8 ft for angles of wave attack equal to 0.0, 45.0, and 90.0 deg without experiencing major deterioration.

d. Safety factor tests show that Plans 3D-1C and 3D-2C can withstand attack of 15-sec, 19.2-ft breaking waves at an swl of +3 ft and 15-sec, 22-ft nonbreaking waves at an swl of +8 ft without experiencing a large increase in movement above that observed for the design condition (15-sec, 17.6-ft breaking and nonbreaking waves).

PART VI: PHASE II STABILITY TESTS

Design of Model

88. Tests were conducted at a geometrically undistorted linear scale of 1:31, model to prototype. Scale selection was determined by the absolute size of model breakwater sections necessary to ensure the preclusion of stability scale effects, capabilities of the available wave generator, and size of model armor units available compared with the estimated size of prototype armor units required for stability against wave attack. Based on Froude's model law and the linear scale of 1:31, the following model-prototype relations were derived. Dimensions are in terms of length (L) and time(T).

Characteristic	Dimension	Model:Prototype Scale Relation
Length	L	$L_r = 1:31$
Area	L^2	$A_r = L_r^2 = 1:961$
Volume	L^3	$V_r = L_r^3 = 1:29,791$
Time	T	$T_r = L_r^{1/2} = 1:5.57$

89. The specific weight of water used in the model was assumed to be 62.4 pcf and that of seawater is 64.0 pcf; specific weights of model breakwater construction materials were not always identical with their prototype counterparts. These variables were related using the following transference equation:

$$\frac{(W_a)_m}{(W_a)_p} = \frac{(\gamma_a)_m}{(\gamma_a)_p}\left(\frac{L_m}{L_p}\right)^3 \left[\frac{(S_a)_p - 1}{(S_a)_m - 1}\right]^3$$

where

subscripts m and p = model and prototype quantities, respectively

W_a = weight of an individual armor unit, lb

γ_a = specific weight of an individual armor unit, pcf

L_m/L_p = linear scale of the model

S_a = specific gravity of an individual armor unit relative to the water in which the breakwater is constructed, i.e., $S_a = \gamma_a/\gamma_w$, where γ_w is the specific weight of water, pcf

Test Equipment and Procedures

90. A concrete wave flume, 4 ft wide, 4 ft deep, and 119 ft long, was used for all tests. The flume is equipped with a vertical-displacement wave generator capable of producing sinusoidal waves of various periods and heights. Test waves of the required characteristics were generated by varying the frequency and amplitude of the plunger motion. Breakwater sections were installed in the flume about 85 ft from the wave generator. Local prototype bathymetry was represented by a 1V-on-20H slope seaward of the test sections.

Selection of Test Conditions

91. The stability response of all plans was investigated for 11-, 13-, and 15-sec waves at swl's of +4, +6, and +8 ft NGVD. Observations of the structures under wave attack indicated that the most critical breaking waves which could experimentally be made to attack the sections for the selected swl's and wave periods were as follows:

swl ft NGVD	Wave Period sec	Maximum Breaking Wave Height, ft
+4	11	10.9
+4	13	11.6
+4	15	12.4
+6	11	12.6
+6	13	13.5
+6	15	14.0
+8	11	14.2
+8	13	15.3
+8	15	16.0

92. It was anticipated that wave conditions associated with the +8 ft swl would probably have the greatest effect on stability. Therefore it was decided to initiate testing at this swl and, depending on results, either proceed to the lower water levels (acceptable stability response) or modify the test section (unacceptable stability response). All sections that exhibited

at least marginally acceptable stability after testing at the +8, +6, and +4 ft swl's were completely rebuilt and retested. The repeat tests were conducted with a reversed water level sequencing, i.e., wave attack was initiated at the +4 ft swl and then proceeded to higher levels.

Tests and Results

93. A total of five additional 2-d sections were tested. All structures used a bottom toe elevation of -9.0 and armor slopes of 1V on 2H both sea side and channel side. Armoring consisted of two layers of randomly placed dolosse or a combination of dolosse on the slopes and one layer of stone armor on the crown and/or toes. The number (N) of dolosse and stone per given area was equal to $0.83V^{-2/3}$ and $0.72V^{-2/3}$, respectively, where V is the volume of a single armor unit. In an effort to reduce permeability of the prototype jetties, a thin concrete core will be constructed along the center line up to an elevation of 0.0. Since the concrete core will not be exposed to wave attack, it was not deemed necessary to model its stability characteristics (weight and geometry). However, any effects on armor stability created by the core's reflection of incident wave energy were simulated by placing a thin sheet-metal barrier along the center line (below el 0.0) of the model structures. Individual characteristics and stability responses of plans investigated are described in the following paragraphs.

94. Plan 12 (Plate 44 and Photos 213-215) was constructed to a crown elevation of +7.6 and 10.5-ton, randomly placed dolosse were used to armor the slopes. Toe and crown protection was provided by 19- and 24-ton stone, respectively. As evidenced in Photos 216-218, Plan 12 withstood wave attack at the +8 ft swl without sustaining any significant damage. About 1.0 percent of the channel-side dolosse moved downslope and an equal portion of the sea-side armor units reoriented themselves along the seaward edge of the capstone. Occasional in-place rocking of an additional 2.0 percent of the dolosse was observed. A few 19-ton, toe-protection stones and 24-ton capstones shifted slightly as they sought a more stable orientation; however, none were displaced. In-place rocking 0.5 to 1.0 percent of the seaward dolosse was occasionally observed. All detected rocking motions were gentle and there was no armor displacement. Photos 219-221 show the section at the conclusion of testing. Comparisons of Photos 216-218 and 219-221 show that there were no

changes in the structure's appearance between the +8 and +4 ft swl's.

95. Plan 12 was completely rebuilt (Photos 222-224) and retested. The only effect of the +4 ft swl was minor, in-place rocking of 0.5 percent of the sea-side dolosse. The +6 ft swl reoriented 0.5 percent of the sea-side dolosse in the vicinity of the capstone and caused an additional 1.0 percent to occasionally rock in place. Photos 225-227 show Plan 12 after testing the +6 ft swl. Wave attack at the +8 ft swl displaced about 1.0 percent of the seaward dolosse upslope with one unit coming to rest partially on the capstone and an additional 1.0 to 2.0 percent exhibited in-place rocking. Minor, in-place rocking of 1.0 to 2.0 percent of the channel-side dolosse was observed; however, none were displaced. Slight shifting of a few 19- and 24-ton stones was also noted. Photos 228-230 show the structure at the conclusion of testing. The final stability condition of Plan 12 was acceptable and similar for both the initial and repeat tests (both swl sequences).

96. Plan 13 (Plate 45 and Photos 231-233) used randomly placed 10.5-ton dolosse on the slopes. The crown was constructed to an elevation of +7.0 and armored with 19-ton stone. Toe protection was provided by 14.5-ton stone. Wave attack at the +8 ft swl displaced 1.0 percent of the channel-side dolosse downslope with one armor unit coming to rest on the toe protection stone. Reorientation of 1.5 percent of the sea-side dolosse (along their interface with the capstone) was observed and one of these units was displaced onto the capstone. Occasional in-place rocking of an additional 2.0 percent of the seaward dolosse was observed. Rocking and reorientation of 4.0 to 5.0 percent of the 19-ton capstone were noted; however, none were displaced. The 14-ton, toe protection stone resisted displacement even though 6.0 to 8.0 percent of the sea-side units were reoriented. Photos 234-236 show the structure at the conclusion of the +8 ft swl. Occasional in-place rocking of 1.5 percent of the capstone and 1.0 percent of the sea-side dolosse was observed at the +6 ft swl while the only movement detected at the +4 ft swl was occasional in-place rocking of 0.5 percent of the sea-side dolosse. No armor displacement was observed at either swl. Comparisons of Photos 237 and 238 (taken at the conclusion of testing) with Photos 234-236 show there were no changes in the structure's appearance between the +8 and +4 ft swl's.

97. Plan 13 was completely rebuilt and Photos 239-241 show the structure prior to initiation of the repeat test. Occasional in-place rocking of 1.0 percent of the sea-side dolosse was the only movement observed at the +4 ft

swl. The +6 ft swl reoriented 1.0 percent of the sea-side dolosse in the vicinity of the capstone with one unit being pushed onto the seaward edge of the crown. An additional 1.5 percent of the sea-side dolosse occasionally rocked in place. Intermittent in-place rocking was observed for 1.0 and 1.5 percent of the channel-side dolosse and capstone, respectively. Also, 2.0 to 3.0 percent of the sea-side toe-protection stone was reoriented. Photos 242 and 243 show the section after testing the +6 ft swl. Wave attack at the +8 ft swl had a significant impact on stability. Reorientation of 3.0 percent of the sea-side dolosse (along their interface with the capstone) was observed and four of these units were displaced onto or over the capstone. An additional 2.5 percent of the seaward dolosse was observed to rock in place. The sea-side, toe-protection stone resisted displacement from its original area; however, about 8.0 percent of the units was reoriented with some of these tending to push slightly into the seaward dolosse. Rocking and reorientation of 6.0 percent of the 19-ton capstone were displayed while the only stability effect rendered to the channel-side dolosse was gentle in-place rocking of 1.0 percent of the units. Photos 244-246 show the final stability condition of the structure.

98. The stability response of Plan 13, especially in view of results of the second testing during which the swl's were sequenced from low to high, was marginal. It is felt that 14.5- and 19-ton stone are slightly too light in that excessive reorientation of these materials was observed. Also, the 10.5-ton dolosse are marginal when used in conjunction with the 14.5- and 19-ton stone.

99. Plan 14 (Plate 46 and Photos 247-249) was armored with randomly placed, 10.5-ton dolosse. The section used a crown elevation of +10.0 ft. Subjection to wave attack at the +8 ft swl caused about 7.0 percent of the dolosse comprising the seaward half of the crown to be reoriented, and four of these units were pushed onto the channel side of the crown. Intermittent in-place rocking was observed for 3.5 and 1.5 percent of the sea-side and channel-side onslope armor, respectively. Rocking and reorientation of 8.0 to 10.0 percent of the seaward toe armor were noted. No channel-side toe armor movement was detected. Photos 250 and 251 show the section at the conclusion of the +8 ft swl. Occasional in-place rocking of 1.5 percent of the sea-side onslope armor and minor reorientation of 1.0 to 2.0 percent of the seaward toe armor were observed at the +6 ft swl. The only movement detected at the +4 ft swl was gentle in-place rocking of 1.0 percent of the sea-side onslope

armor. Photos 252-254 show the structure at the completion of testing.

100. Plan 14 was completely rebuilt (Photos 255-257) and retested. Gentle in-place rocking of 1.5 percent of the sea-side onslope armor and 2.5 percent of the sea-side toe armor was the only effect recorded at the +4 ft swl. Wave attack at the +6 ft swl caused intermittent in-place rocking of 2.0 percent of the sea-side onslope armor and 1.0 percent of the channel-side onslope armor. Also, rocking and reorientation of 6.0 to 7.0 percent of the seaward toe armor were observed. Photos 258 to 259 show the cumulative effects of the +4 and +6 ft swl's. Wave attack at the +8 ft swl caused reorientation of about 3.0 percent of the dolosse comprising the seaward half of the crown and one of these units was pushed onto the channel side of the crown. Rocking and reorientation of 3.0 to 4.0 percent of the seaward toe armor were observed. Intermittent in-place rocking was recorded for 2.5 and 1.5 percent of the sea-side and channel-side onslope armor, respectively. No channel-side toe armor movement was noted. Photos 260-262 show the final stability condition of the structure. The stability response of Plan 14 was only marginally acceptable.

101. Plan 15 (Plate 47) was constructed to a crown elevation of +11.0 and armoring was provided by randomly placed, 14.0-ton dolosse. Wave attack at the +8 ft swl had little effect on stability. Intermittent in-place rocking was observed for 1.5 percent of the sea-side onslope armor and 1.0 percent of the channel-side onslope armor. Occasional in-place rocking of 1.0 percent of the dolosse comprising the seaward half of the crown was also noted. The only movement detected at the +6 ft swl was occasional in-place rocking of 0.5 percent of the sea-side onslope armor. No armor movement occurred at the +4 ft swl. All rocking motions were very gentle and no armor was displaced. Photos 263 and 264 show the structure at the conclusion of testing.

102. Plan 15 was completely rebuilt (Photos 265-267) and retested. No armor movement was detected at the +4 ft swl. Wave attack at the +6 ft swl caused intermittent in-place rocking of 1.0 percent of the sea-side onslope armor and 0.5 percent of the channel-side onslope armor. All rocking motions were very gentle and no armor displacement was observed. Photos 268 and 269 show the cumulative effects of the +4 and +6 ft swl's. Wave attack at the +8 ft swl produced occasional in-place rocking of 1.0 percent of the dolosse comprising the seaward half of the crown. Intermittent in-place rocking was recorded for 1.0 percent of both the sea-side and channel-side onslope armor.

Again, all rocking motions were very gentle and no armor was displaced. Photos 270-272 show the final stability condition of the structure. Plan 15 proved to be a conservatively stable design.

103. Plan 16 (Plate 48 and Photos 273-275) used randomly placed, 10.5-ton dolosse on the slopes and crown. Toe protection was provided by 19-ton stone. The section was constructed to a crown elevation of +10.0. Wave attack at the +8 ft swl reoriented about 3.0 percent of the dolosse comprising the seaward half of the crown and two of these units were pushed slightly channelward. Intermittent in-place rocking was observed for 2.0 percent of the sea-side onslope armor. One channel-side onslope armor unit was displaced onto the toe-protection stone and an additional 1.5 percent of the units exhibited occasional in-place rocking. No channel-side toe armor movement was detected; however, several sea-side toe-protection stones were reoriented. Photos 276-278 show the structure at the conclusion of the +8 ft swl. Occasional in-place rocking of 1.5 and 0.5 percent of the sea-side and channel-side onslope armor, respectively, was observed at the +6 ft swl. The only movement detected at the +4 ft swl was occasional in-place rocking of 0.5 percent of the sea-side onslope armor. Photos 279-281 show the structure at the completion of testing.

104. Plan 16 was completely rebuilt and Photos 282-284 show the section prior to initiation of wave attack. Occasional in-place rocking of 1.0 percent of the sea-side onslope armor was the only movement noted at the +4 ft swl. The +6 ft swl reoriented several sea-side toe-protection stones and occasional in-place rocking of 1.5 percent of the sea-side onslope armor was also observed. Photos 285-287 show the section after testing the +6 ft swl. Wave attack at the +8 ft swl reoriented 2.0 percent of the dolosse comprising the seaward half of the crown and one channel-side onslope armor unit was displaced downslope. Intermittent in-place rocking was observed for 1.0 and 2.0 percent of the channel-side and sea-side onslope armor, respectively. As evidenced in Photos 288-290, several additional sea-side toe-protection stones were reoriented. No channel-side toe armor movement was recorded. The stability response of Plan 16 was acceptable. It appears that 10.5-ton dolosse are an adequate armoring for the slopes and crown when used in conjunction with 19-ton, toe-protection stone.

105. For each combination of wave period and water level investigated, all plans were subjected to wave attack until stability was achieved, i.e., until significant movement of armor material had abated. It should be noted

that the +8 ft swl (and particularly the 15-sec, 16-ft waves observed at this water level) appeared to be the most severe condition investigated. Photo 291 shows a 15-sec, 16-ft wave inpinging on the seaward face of Plan 16 and Photo 292 shows the overtopping produced.

Conclusions

106. Based on tests, results, and assumptions described herein, it is concluded for the maximum breaking waves that may be expected to occur for 11- through 15-sec wave periods at swl's of +4, +6, and +8 ft that:

- a. Final stability conditions of individual plans are generally similar for both the initial (high to low water swl sequence) and repeat (low to high water swl sequence) tests.
- b. Plans 12 and 16 are stable designs.
- c. Plan 15 is a conservatively stable alternative.
- d. Plans 13 and 14 are marginally stable designs; however, they are acceptable provided that the probability of increased maintenance costs is accounted for.

REFERENCES

Carver, R. D., and Davidson, D. D. 1977 (Nov). "Dolos Armor Units Used on Rubble-Mound Breakwater Trunks Subjected to Nonbreaking Waves with No Overtopping," Technical Report H-77-19, U. S. Army Engineer Waterways Experiment Station, CE, Vicksburg, Miss.

Hudson, R. Y. 1958 (Jul). "Design of Quarry-Stone Cover Layers for Rubble-Mound Breakwaters," Research Report No. 2-2, U. S. Army Engineer Waterways Experiment Station, CE, Vicksburg, Miss.

__________. 1975 (Jun). "Reliability of Rubble-Mound Breakwater Stability Models; Hydraulic Model Investigation," Miscellaneous Paper H-75-5, U. S. Army Engineer Waterways Experiment Station, CE, Vicksburg, Miss.

Jackson, R. A. 1968 (Jun). "Design of Cover Layers for Rubble-Mound Breakwaters Subjected to Nonbreaking Waves," Research Report No. 2-11, U. S. Army Engineer Waterways Experiment Station, CE, Vicksburg, Miss.

Stevens, J. C., et al. 1942. "Hydraulic Models," Manuals on Engineering Practice No. 25, American Society of Civil Engineers, New York, N. Y.

Willock, A. F. 1977. "Stability of Dolos Blocks Under Oblique Wave Attack," Report No. IT 159, Hydraulics Research Station, Wallingford, England.

Table 1

Summary of Damage for Plans 2, 3, 4, 4A, 4B, 5, 6, 7, and 8; Design swl of +5.5 ft; T = 15 sec; H = 13.6 ft

Plan	Armor Area	Armor Type	Weight tons	Damage, percent Number Method	Sounding Method
2	Sea side	Stone	11.5	2.8	*
	Channel side	Stone	8.0	5.1	*
3	Sea side	Stone	11.5	2.5	21.2
	Channel side	Stone	11.5	2.8	8.3
4	Sea side	Stone	15.0	0.4	10.0
	Channel side	Stone	11.5	2.6	6.5
4A	Sea side	Stone	15.0	0.3	7.5
	Channel side	Stone	11.5	1.4	4.5
4B	Sea side	Stone	15.0	0.0	5.1
	Crown	Stone	18.0	0.0	2.7
	Channel side	Stone	11.5	1.4	1.8
5	Sea side	Dolosse	3.25	0.7	*
	Channel side	Dolosse	3.25	12.6	*
6	Sea side	Dolosse	3.25	0.7	12.0
	Channel side	Dolosse	3.25	5.4	*
7	Sea side	Dolosse	3.25	0.8	12.5
	Channel side	Dolosse	3.25	1.5	8.0
8	Sea side	Dolosse	3.25	1.6	8.4
	Crown	Stone	18.0	0.0	0.1
	Channel side	Dolosse	3.25	0.6	1.3

* Soundings not taken.

Table 2

Test Conditions for Storm-Surge Hydrographs of +6.5, +7.5, +8.5, +9.5, +10.5, and +11.5; Design swl of +5.5 ft

Step	swl ft NGVD	Step Length min	Wave Height ft
	Maximum Surge = +6.5		
1	+5.5	61	13.6
2	+6.5	103	14.5
3	+5.5	34	13.6
	Maximum Surge = +7.5		
1	+5.5	40	13.6
2	+6.5	88	14.5
3	+7.5	110	15.5
4	+6.5	48	14.5
5	+5.5	25	13.6
	Maximum Surge = +8.5		
1	+5.5	36	13.6
2	+6.5	72	14.5
3	+7.5	80	15.5
4	+8.5	97	16.3
5	+7.5	41	15.5
6	+6.5	38	14.5
7	+5.5	23	13.6
	Maximum Surge = +9.5		
1	+5.5	12	13.6
2	+6.5	22	14.5
3	+7.5	23	15.5
4	+8.5	51	16.3
5	+9.5	89	17.2
6	+8.5	44	16.3
7	+7.5	17	15.5
8	+6.5	14	14.5
9	+5.5	9	13.6

Step	swl ft NGVD	Step Length min	Wave Weight ft
	Maximum Surge = +10.5		
1	+5.5	11	13.6
2	+6.5	19	14.5
3	+7.5	15	15.5
4	+8.5	20	16.3
5	+9.5	50	17.2
6	+10.5	94	18.0
7	+9.5	41	17.2
8	+8.5	15	16.3
9	+7.5	12	15.5
10	+6.5	14	14.5
11	+5.5	7	13.6
	Maximum Surge = +11.5		
1	+5.5	11	13.6
2	+6.5	20	14.5
3	+7.5	16	15.5
4	+8.5	16	16.3
5	+9.5	19	17.2
6	+10.5	44	18.0
7	+11.5	89	18.8
8	+10.5	39	18.0
9	+9.5	22	17.2
10	+8.5	12	16.3
11	+7.5	13	15.5
12	+6.5	15	14.5
13	+5.5	9	13.6

Note: All tests conducted with 15-sec waves.

Table 3

Summary of Damage for Storm-Surge Hydrographs of +6.5, +7.5, +8.5, +9.5, +10.5, and +11.5; Design swl of +5.5 ft; Plans 4B and 8

Maximum swl ft NGVD	Maximum Wave Height ft	H/H_D	Damage, percent Number Method	Damage, percent Sounding Method	Maximum swl ft NGVD	Maximum Wave Height ft	H/H_D	Damage, percent Number Method	Damage, percent Sounding Method
Plan 4B; Sea-Side Armor					Plan 8; Sea-Side Armor				
+5.5	13.6	1.00	0.0	5.1	+5.5	13.6	1.00	1.6	8.4
+6.5	14.5	1.07	0.7	3.3	+6.5	14.5	1.07	0.4	8.4
+7.5	15.5	1.14	1.7	19.5	+7.5	15.5	1.14	79.7	54.8
+8.5	16.3	1.20	2.4	21.6	+8.5	16.3	1.20	98.0	57.5
+9.5	17.2	1.26	2.8	20.1	+9.5	17.2	1.26	98.2	58.5
+10.5	18.0	1.32	2.8	15.8	+10.5	18.0	1.32	94.2	59.6
+11.5	18.8	1.38	4.5	16.1	+11.5	18.8	1.38	87.1	41.9
Plan 4B; Crown Armor					Plan 8; Crown Armor				
+5.5	13.6	1.00	0.0	2.7	+5.5	13.6	1.00	0.0	0.1
+6.5	14.5	1.07	0.0	0.2	+6.5	14.5	1.07	0.0	1.5
+7.5	15.5	1.14	4.2	15.4	+7.5	15.5	1.14	45.9	37.6
+8.5	16.3	1.20	9.7	23.2	+8.5	16.3	1.20	79.6	81.8
+9.5	17.2	1.26	8.3	11.5	+9.5	17.2	1.26	82.7	89.8
+10.5	18.0	1.32	4.2	37.3	+10.5	18.0	1.32	72.4	86.3
+11.5	18.8	1.38	15.3	31.4	+11.5	18.8	1.38	75.5	93.7
Plan 4B; Channel-Side Armor					Plan 8; Channel-Side Armor				
+5.5	13.6	1.00	1.4	1.8	+5.5	13.6	1.00	0.6	1.3
+6.5	14.5	1.07	1.4	3.2	+6.5	14.5	1.07	0.9	3.7
+7.5	15.5	1.14	7.2	3.5	+7.5	15.5	1.14	20.9	0.0
+8.5	16.3	1.20	10.1	5.4	+8.5	16.3	1.20	32.8	0.0
+9.5	17.2	1.26	4.3	1.7	+9.5	17.2	1.26	31.0	0.0
+10.5	18.0	1.32	1.8	0.0	+10.5	18.0	1.32	26.3	0.0
+11.5	18.8	1.38	8.0	1.6	+11.5	18.8	1.38	37.9	3.7

Table 4

Test Conditions for Two Successive +7.5 Hydrographs;

Design swl of +5.5 ft

Step	swl ft NGVD	Step Length min	Wave Height ft
1	+5.5	40	13.6
2	+6.5	88	14.5
3	+7.5	110	15.5
4	+6.5	48	14.5
5	+5.5	25	13.6
6	+5.5	40	13.6
7	+6.5	88	14.5
8	+7.5	110	15.5
9	+6.5	48	14.5
10	+5.5	25	13.6

Note: All tests conducted with 15-sec waves.

Table 5

Summary of Damage for Two Successive +7.5 Hydrographs;

Design swl of +5.5 ft; Plans 4B and 8

Plan	Step	Armor Area	Damage, percent	
			Number Method	Sounding Method
4B	5	Sea side	2.4	21.6
		Crown	4.2	2.9
		Channel side	6.9	5.5
	10	Sea side	2.4	26.9
		Crown	6.9	26.1
		Channel side	8.0	7.3
8	5	Sea side	73.6	44.3
		Crown	49.0	17.9
		Channel side	13.1	0.0
	10	Sea side	94.8	45.7
		Crown	71.4	67.3
		Channel side	16.1	0.0

Table 6

Summary of Damage for Plans 4C, 4D, 9, and 10;

Design swl of +7.5 ft; T = 15 sec; H = 15.5 ft

Plan	Armor Area	Armor Type	Weight tons	Damage, percent Number Method	Sounding Method
4C	Sea side	Stone	22.0	0.3	28.3
	Crown	Stone	22.0	11.5	30.9
	Channel side	Stone	11.5	4.9	4.0
4D	Sea side	Stone	22.0	0.3	4.5
	Crown	Stone	22.0	0.0	3.5
	Channel side	Stone	11.5	4.6	2.1
9	Sea side	Dolosse	5.0	69.1	40.0
	Crown	Stone	22.0	42.1	2.9
	Channel side	Dolosse	5.0	4.6	0.0
10	Sea side	Dolosse	9.25	2.9	2.3
	Crown	Stone	22.0	0.0	0.0
	Channel side	Dolosse	5.0	2.0	1.6

Table 7

Test Conditions for Storm-Surge Hydrographs of +8.5, +9.5, +10.5, +11.5, and +14.5; Design swl of +7.5 ft

Step	swl ft NGVD	Step Length min	Wave Height ft	Step	swl ft NGVD	Step Length min	Wave Height ft
	Maximum Surge = +8.5				Maximum Surge = +14.5		
1	+7.5	48	15.5	1	+7.5	18	15.5
2	+8.5	97	16.3	2	+8.5	25	16.3
3	+7.5	24	15.5	3	+9.5	20	17.2
				4	+10.5	16	18.0
	Maximum Surge = +9.5			5	+11.5	16	18.8
1	+7.5	15	15.5	6	+12.5	19	19.7
2	+8.5	51	16.3	7	+13.5	44	20.6
3	+9.5	89	17.2	8	+14.5	89	21.4
4	+8.5	44	16.3	9	+13.5	39	20.6
5	+7.5	9	15.5	10	+12.5	22	19.7
	Maximum Surge = +10.5			11	+11.5	12	18.8
				12	+10.5	13	18.0
1	+7.5	8	15.5	13	+9.5	15	17.2
2	+8.5	20	16.3	14	+8.5	23	16.3
3	+9.5	50	17.2	15	+7.5	12	15.5
4	+10.5	94	18.0				
5	+9.5	41	17.2				
6	+8.5	15	16.3				
7	+7.5	5	15.5				
	Maximum Surge = +11.5						
1	+7.5	8	15.5				
2	+8.5	16	16.3				
3	+9.5	19	17.2				
4	+10.5	44	18.0				
5	+11.5	89	18.8				
6	+10.5	39	18.0				
7	+9.5	22	17.2				
8	+8.5	12	16.3				
9	+7.5	4	15.5				

Note: All tests conducted with 15-sec waves.

Table 8

Summary of Damage for Storm-Surge Hydrographs of +8.5, +9.5, +10.5, +11.5, and +14.5; Design swl of +7.5 ft

swl ft NGVD	Wave Height, ft	H/H_D	Number Method	Sounding Method
		Plan 4D; Sea-Side Armor		
+7.5	15.5	1.00	0.3	4.5
+8.5	16.3	1.05	1.4	4.0
+9.5	17.2	1.11	1.4	6.9
+10.5	18.0	1.16	0.9	7.9
+11.5	18.8	1.21	1.9	8.9
		Plan 4D; Crown Armor		
+7.5	15.5	1.00	0.0	3.5
+8.5	16.3	1.05	0.0	1.5
+9.5	17.2	1.11	0.0	1.7
+10.5	18.0	1.16	1.4	8.0
+11.5	18.8	1.21	7.1	10.8
		Plan 4D; Channel-Side Armor		
+7.5	15.5	1.00	4.6	2.1
+8.5	16.3	1.05	5.9	5.3
+9.5	17.2	1.11	6.9	8.6
+10.5	18.0	1.16	3.4	4.0
+11.5	18.8	1.21	6.9	7.4
		Plan 10; Sea-Side Armor		
+7.5	15.5	1.00	2.9	2.3
+8.5	16.3	1.05	6.7	4.0
+9.5	17.2	1.11	17.5	14.3
+10.5	18.0	1.16	5.7	8.8
+11.5	18.8	1.21	12.7	10.2
+14.5	21.4	1.38	35.2	31.0
		Plan 10; Crown Armor		
+7.5	15.5	1.00	0.0	0.0
+8.5	16.3	1.05	0.0	0.0
+9.5	17.2	1.11	10.5	4.4
+10.5	18.0	1.16	0.0	5.3
+11.5	18.8	1.21	10.5	6.4
+14.5	21.4	1.38	54.3	54.8
		Plan 10; Channel-Side Armor		
+7.5	15.5	1.00	2.0	1.6
+8.5	16.3	1.05	2.0	0.4
+9.5	17.2	1.11	2.6	0.0
+10.5	18.0	1.16	1.6	0.0
+11.5	18.8	1.21	4.9	0.0
+14.5	21.4	1.38	12.4	2.9

Table 9

Summary of Damage for Plans 4E and 11; Design swl of +9.5 ft;

T = 15 sec; H = 17.2 ft

Plan	Armor Area	Armor Type	Weight tons	Damage, percent Number Method	Sounding Method
4E	Sea side	Stone	30.5	0.3	4.8
	Crown	Stone	30.5	0.0	0.5
	Channel side	Stone	15.0	4.3	4.5
11	Sea side	Dolosse	12.5	2.1	3.5
	Crown	Stone	30.5	0.0	0.5
	Channel side	Dolosse	5.0	4.2	2.8

Table 10

Composite Damage as Determined by the Number and Sounding Methods; Plans 4B, 4D, 8, and 10

Maximum swl ft NGVD	Maximum Wave Height, ft	H/H_D	Composite Damage, percent Number Method	Composite Damage, percent Sounding Method
		Stone Armor; Plan 4B; Design swl of +5.5 ft		
+5.5	13.6	1.00	0.6	3.7
+6.5	14.5	1.07	0.9	2.8
+7.5	15.5	1.14	4.4	13.1
+8.5	16.3	1.20	6.6	15.4
+9.5	17.2	1.26	4.1	12.6
+10.5	18.0	1.32	2.5	13.4
+11.5	18.8	1.38	7.2	12.9
		Stone Armor; Plan 4D; Design swl of +7.5 ft		
+7.5	15.5	1.00	2.6	3.5
+8.5	16.3	1.05	3.5	4.1
+9.5	17.2	1.11	4.0	6.8
+10.5	18.0	1.16	2.3	6.7
+11.5	18.8	1.21	5.0	8.7
		Dolos Armor; Plan 8; Design swl of +5.5 ft		
+5.5	13.6	1.00	1.1	4.6
+6.5	14.5	1.07	0.5	5.6
+7.5	15.5	1.14	54.9	34.2
+8.5	16.3	1.20	72.6	44.1
+9.5	17.2	1.26	72.4	46.0
+10.5	18.0	1.32	67.4	46.5
+11.5	18.8	1.38	68.2	41.1
		Dolos Armor; Plan 10; Design swl of +7.5 ft		
+7.5	15.5	1.00	2.1	1.8
+8.5	16.3	1.05	3.8	3.3
+9.5	17.2	1.11	10.2	8.8
+10.5	18.0	1 16	3.2	5.8
+11.5	18.8	1.21	9.1	6.9
+14.5	21.4	1.38	28.0	28.3

Table 11

Number-Method Damage Summary of Plans 3D-1, 3D-1A, 3D-1B, 3D-1C, 3D-2, 3D-2A, 3D-2B, and 3D-2C; +1 ft swl Followed by +8 ft swl; Angle of Wave Attack = 90 Deg

Area	Percent Damage for Indicated Plan							
	3D-1	3D-1A	3D-1B	3D-1C	3D-2	3D-2A	3D-2B	3D-2C
	15-sec, 17.6-ft Breaking Waves; +1 ft swl							
1	6.9	1.1	0.0	2.1	7.0	8.5	0.9	0.7
2	13.2	3.4	0.0	1.0	9.8	18.8	1.1	4.0
3	8.2	4.9	4.5	1.5	9.5	5.2	0.8	4.3
4	0.0	0.0	0.0	0.0	0.0	0.0	0.0	0.0
5	0.0	0.0	0.0	0.0	0.0	0.0	0.0	0.0
6	0.0	0.0	0.0	0.0	0.0	0.0	0.0	0.0
7	0.0	0.0	0.0	0.0	0.0	0.0	0.0	0.0
8	0.0	0.0	0.0	0.0	0.0	0.0	0.0	0.0
9	0.0	0.0	0.0	0.0	2.1	0.3	0.0	0.0
Total	4.0	1.6	1.1	0.6	4.1	3.2	0.3	1.5
	15-sec, 17.6-ft Nonbreaking Waves; +8 ft swl							
1	6.9	1.1	0.0	2.1	7.0	8.5	0.9	0.7
2	13.2	3.4	0.0	1.7	9.8	18.8	1.1	4.3
3	8.2	4.9	5.1	1.7	9.5	5.8	0.8	4.7
4	0.0	0.0	0.0	0.0	0.0	1.3	0.0	0.0
5	0.0	0.0	0.0	0.0	0.0	0.0	0.0	0.0
6	0.0	0.0	0.0	0.0	0.0	0.0	0.0	0.0
7	0.0	0.0	0.0	0.0	0.0	0.0	0.0	0.0
8	0.0	0.0	0.4	0.0	0.0	0.0	0.0	0.0
9	0.0	0.2	0.0	0.0	2.1	0.3	0.0	0.0
Total	4.0	1.7	1.3	0.8	4.1	3.4	0.3	1.7

Table 12

Number-Method Damage Summary of Plans 3D-1, 3D-1A, 3D-1B, 3D-1C, 3D-2, 3D-2A, 3D-2B, and 3D-2C; +8 ft swl Followed by +1 ft swl; Angle of Wave Attack = 90 Deg

Area	Percent Damage for Indicated Plan							
	3D-1	3D-1A	3D-1B	3D-1C	3D-2	3D-2A	3D-2B	3D-2C
	15-sec, 17.6-ft Nonbreaking Waves; +8 ft swl							
1	0.0	0.0	0.0	0.0	7.6	4.1	0.9	0.0
2	5.3	4.5	1.4	0.7	11.5	0.0	1.1	0.3
3	0.7	0.4	0.2	0.4	6.0	0.3	0.0	0.0
4	0.0	0.0	0.0	0.0	0.0	2.5	0.0	0.0
5	0.0	0.0	0.0	0.0	0.0	0.0	0.0	0.0
6	0.0	0.0	0.0	0.0	0.0	0.0	0.0	0.0
7	0.0	0.0	0.0	0.0	0.0	0.0	0.0	1.5
8	0.0	0.0	0.0	0.3	0.0	0.0	0.0	0.0
9	0.0	0.0	0.0	0.0	2.9	0.3	0.0	0.0
Total	0.6	0.4	0.2	0.2	3.5	0.8	0.2	0.2
	15-sec, 17.6-ft Breaking Waves; +1 ft swl							
1	9.0	0.6	0.0	2.7	11.1	9.5	2.7	0.0
2	13.2	11.2	1.4	0.7	19.7	20.3	1.1	2.7
3	8.0	4.7	5.2	1.3	11.0	4.7	0.5	2.8
4	0.0	0.0	0.0	0.0	0.0	2.5	0.0	4.4
5	0.0	0.0	0.0	0.0	0.0	0.0	0.0	0.0
6	0.0	0.0	0.0	0.0	0.0	0.0	0.0	0.0
7	0.0	0.0	0.0	0.0	0.0	0.0	0.0	1.5
8	0.0	0.0	0.0	0.3	0.0	0.0	0.0	0.0
9	0.0	0.0	0.0	0.3	3.2	0.9	0.0	0.0
Total	4.1	1.9	1.5	0.7	5.6	3.5	0.4	1.2

Table 13

Number-Method Damage Summary of Plan 3D-1C for Angles of Wave Attack of 0.0, 22.5, 45.0, 67.5, and 90.0 Deg; +1 ft swl Followed by +8 ft swl

Area	Percent Damage for Indicated Angle of Wave Attack				
	0.0	22.5	45.0	67.5	90.0
	15-sec, 17.6-ft Breaking Waves; +1 ft swl				
1	0.0	0.0	0.0	0.0	2.1
2	0.0	0.0	0.0	0.0	1.0
3	2.1	0.0	2.6	1.7	1.5
4	0.0	0.0	0.0	0.0	0.0
5	0.0	0.0	0.0	0.0	0.0
6	0.0	0.0	0.0	0.0	0.0
7	0.0	0.0	0.0	0.0	0.0
8	0.0	0.0	0.0	0.0	0.0
9	2.6	2.7	3.3	0.5	0.0
Total	1.1	0.7	1.4	0.5	0.6
	15-sec, 17.6-ft Nonbreaking Waves; +8 ft swl				
1	0.0	0.0	0.0	0.0	2.1
2	0.0	0.0	0.0	0.0	1.7
3	2.1	0.0	2.6	1.7	1.7
4	0.0	0.0	0.0	0.0	0.0
5	0.0	0.0	0.0	0.0	0.0
6	0.0	0.0	0.0	0.0	0.0
7	0.0	0.0	0.0	0.0	0.0
8	0.0	0.0	0.0	0.0	0.0
9	2.9	2.9	3.3	0.5	0.0
Total	1.2	0.8	1.4	0.5	0.8

Table 14

Number-Method Damage Summary of Plan 3D-1C for Angles of Wave Attack of 0.0, 22.5, 45.0, 67.5, and 90.0 Deg; +8 ft swl Followed by +1 ft swl

Area	Percent Damage for Indicated Angle of Wave Attack				
	0.0	22.5	45.0	67.5	90.0
	15-sec, 17.6-ft Nonbreaking Waves; +8 ft swl				
1	0.0	0.0	0.0	0.0	0.0
2	0.0	0.0	0.0	0.3	0.7
3	0.0	0.2	0.2	0.0	0.4
4	0.0	0.0	0.0	0.0	0.0
5	0.0	0.0	0.0	0.0	0.0
6	0.0	0.0	0.0	0.0	0.0
7	0.0	0.0	0.0	0.0	0.0
8	0.0	0.0	0.0	0.0	0.3
9	0.0	0.3	0.2	0.2	0.0
Total	0.0	0.1	0.1	0.1	0.2
	15-sec, 17.6-ft Breaking Waves; +1 ft swl				
1	0.0	0.0	0.0	0.0	2.7
2	0.0	0.0	0.0	1.7	0.7
3	0.0	0.6	1.3	1.9	1.3
4	0.0	0.0	0.0	0.0	0.0
5	0.0	0.0	0.0	0.0	0.0
6	0.0	0.0	0.0	0.0	0.0
7	0.0	0.0	0.0	0.0	0.0
8	0.0	0.0	0.0	0.0	0.3
9	2.9	3.1	2.8	0.5	0.3
Total	0.7	0.9	1.0	0.8	0.7

Table 15

Number-Method Damage Summary of Plan 3D-2C for Angles of Wave Attack of 0.0, 22.5, 45.0, 67.5, and 90.0 Deg; +1 ft swl Followed by +8 ft swl

Area	Percent Damage for Indicated Angle of Wave Attack				
	0.0	22.5	45.0	67.5	90.0
	15-sec, 17.6-ft Breaking Waves; +1 ft swl				
1	0.0	0.0	0.0	0.0	0.7
2	0.0	0.0	0.0	2.3	4.0
3	2.0	3.1	3.5	3.7	4.3
4	0.0	0.0	0.0	0.0	0.0
5	0.0	0.0	0.0	0.0	0.0
6	0.0	0.0	0.0	0.0	0.0
7	0.0	0.0	0.0	0.0	0.0
8	0.0	0.0	0.0	0.0	0.0
9	2.8	4.1	2.6	0.9	0.0
Total	1.1	1.7	1.4	1.4	1.5
	15-sec, 17.6-ft Nonbreaking Waves; +8 ft swl				
1	0.0	0.0	0.0	0.0	0.7
2	0.0	0.0	0.0	2.3	4.3
3	2.0	3.5	3.5	3.7	4.7
4	0.0	0.0	0.0	0.0	0.0
5	0.0	0.0	0.0	0.0	0.0
6	0.0	0.0	0.0	0.0	0.0
7	0.0	0.0	0.0	0.0	0.0
8	0.0	0.0	0.0	0.0	0.0
9	3.3	4.4	2.6	1.3	0.0
Total	1.2	1.9	1.4	1.5	1.7

Table 16

Number-Method Damage Summary of Plan 3D-2C for Angles of Wave Attack of 0.0, 22.5, 45.0, 67.5, and 90.0 Deg; +8 ft swl Followed by +1 ft swl

Area	Percent Damage for Indicated Angle of Wave Attack 0.0	22.5	45.0	67.5	90.0
	15-sec, 17.6-ft Nonbreaking Waves; +8 ft swl				
1	0.0	0.0	0.0	0.0	0.0
2	0.0	0.0	0.0	1.6	0.3
3	0.0	0.2	0.4	0.0	0.0
4	0.0	0.0	0.0	0.0	0.0
5	0.0	0.0	0.0	0.0	0.0
6	0.0	0.0	0.0	0.0	0.0
7	0.0	0.0	0.0	0.0	1.5
8	0.0	0.0	0.0	0.0	0.0
9	0.0	1.3	0.2	0.6	0.0
Total	0.0	0.4	0.1	0.4	0.2
	15-sec, 17.6-ft Breaking Waves; +1 ft swl				
1	0.0	0.0	0.0	0.0	0.0
2	0.0	0.0	0.0	2.0	2.7
3	2.8	3.0	3.1	2.8	2.8
4	0.0	0.0	0.0	0.0	4.4
5	0.0	0.0	0.0	0.0	0.0
6	0.0	0.0	0.0	0.0	0.0
7	0.0	0.0	0.0	0.0	1.5
8	0.0	0.0	0.0	0.0	0.0
9	3.5	4.8	2.8	1.1	0.0
Total	1.5	1.8	1.4	1.2	1.2

Table 17

Number-Method Damage Summary of Plans 3D-1C and 3D-2C; Cumulative Damage Tests Using 15-sec, 17.6-ft Nonbreaking Waves at an swl of +8 ft Followed by 15-sec, 17.6-ft Breaking Waves at an swl of +1 ft; Angles of Wave Attack = 0.0, 45.0, and 90.0 Deg

Plan	Percent Damage for Area									
	1	2	3	4	5	6	7	8	9	Total
Angle of Wave Attack = 0.0 Deg; +8 ft swl										
3D-1C	0.0	0.0	0.0	0.0	0.0	0.0	0.0	0.0	0.0	0.0
3D-2C	0.0	0.0	0.0	0.0	0.0	0.0	0.0	0.0	0.0	0.0
Angle of Wave Attack = 0.0 Deg; +1 ft swl										
3D-1C	0.0	0.0	0.0	0.0	0.0	0.0	0.0	0.0	2.9	0.7
3D-2C	0.0	0.0	2.8	0.0	0.0	0.0	0.0	0.0	3.5	1.5
Angle of Wave Attack = 45.0 Deg; +8 ft swl										
3D-1C	0.0	0.0	0.4	0.0	0.0	0.0	0.0	0.0	2.9	0.8
3D-2C	0.0	0.0	3.0	0.0	0.0	0.0	0.0	0.0	3.7	1.6
Angle of Wave Attack = 45.0 Deg; +1 ft swl										
3D-1C	0.0	0.0	1.1	0.0	0.0	0.0	0.0	0.0	5.6	1.7
3D-2C	0.0	0.3	6.5	0.0	0.0	0.0	0.0	0.0	6.5	3.1
Angle of Wave Attack = 90.0 Deg; +8 ft swl										
3D-1C	0.5	0.0	1.3	0.0	0.0	0.0	0.0	0.0	6.0	1.9
3D-2C	0.0	0.7	6.7	0.0	0.0	0.0	0.0	0.0	6.8	3.2
Angle of Wave Attack = 90.0 Deg; +1 ft swl										
3D-1C	3.0	1.0	5.6	0.0	0.0	0.0	0.0	0.0	6.7	3.3
3D-2C	1.3	4.3	11.8	0.0	0.0	0.0	1.0	0.0	7.2	5.2

Table 18

Safety-Factor Tests of Plans 3D-1C and 3D-2C; Number-Method Damage Summary for Attack of 15-sec, 19.2-ft Breaking Waves at an swl of +3 ft Followed by 15-sec, 22-ft Nonbreaking Waves at an swl of +8 ft; Angle of Wave Attack = 45 Deg

Plan	Percent Damage for Area 1	2	3	4	5	6	7	8	9	Total
				15-sec, 19.2-ft Breaking Waves; +3 ft swl						
3D-1C	0.0	1.0	3.8	0.0	0.0	0.0	0.0	0.0	3.1	1.8
3D-2C	0.0	3.0	4.7	0.0	0.0	0.0	0.0	0.0	2.4	2.0
				15-sec, 22-ft Nonbreaking Waves; +8 ft swl						
3D-1C	0.0	1.0	4.5	0.0	0.0	0.0	0.0	0.0	3.9	2.2
3D-2C	0.0	3.9	5.9	0.0	0.0	0.0	0.0	0.0	3.0	2.5

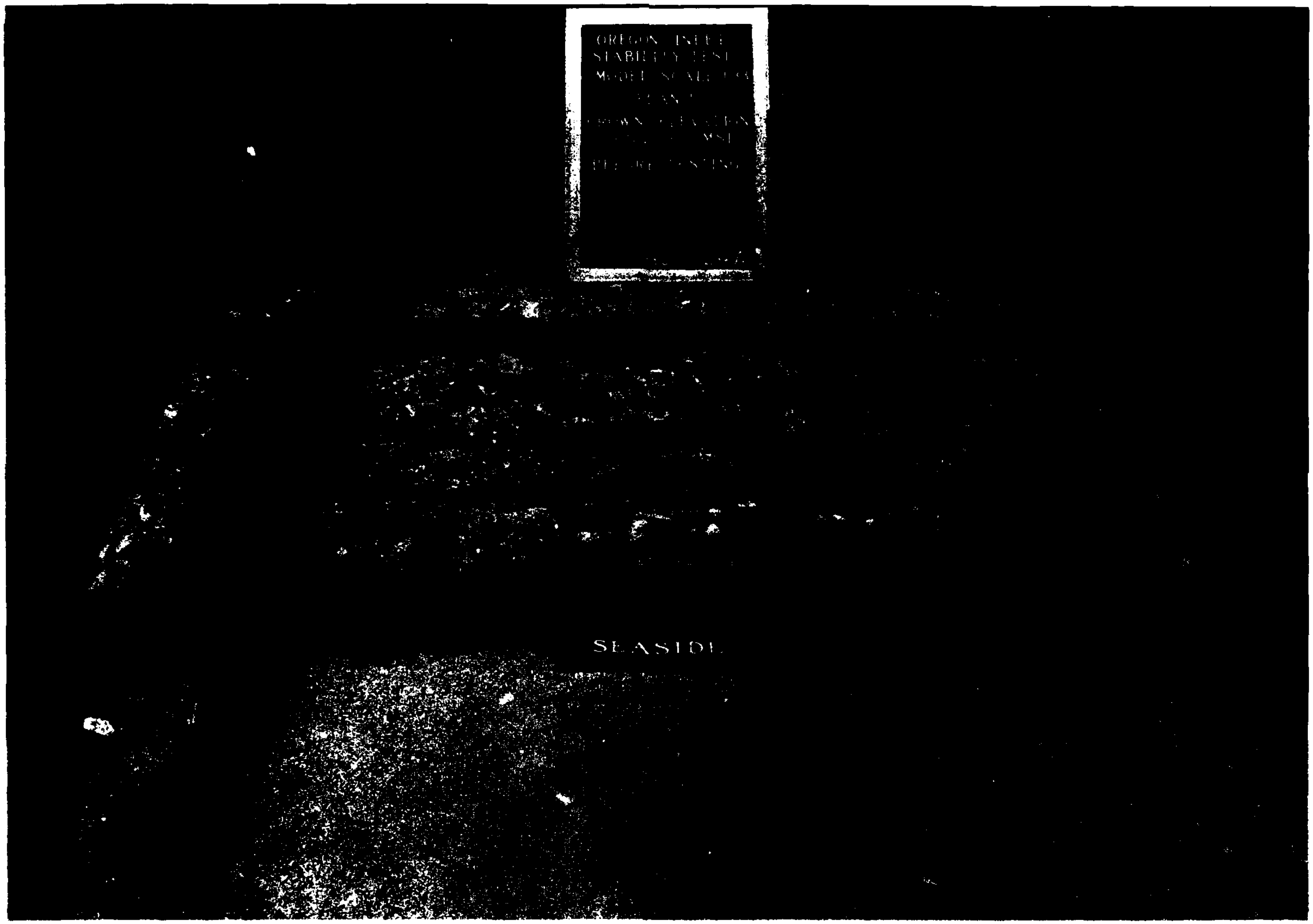

Photo 1. Sea-side view of Plan 1 before wave attack

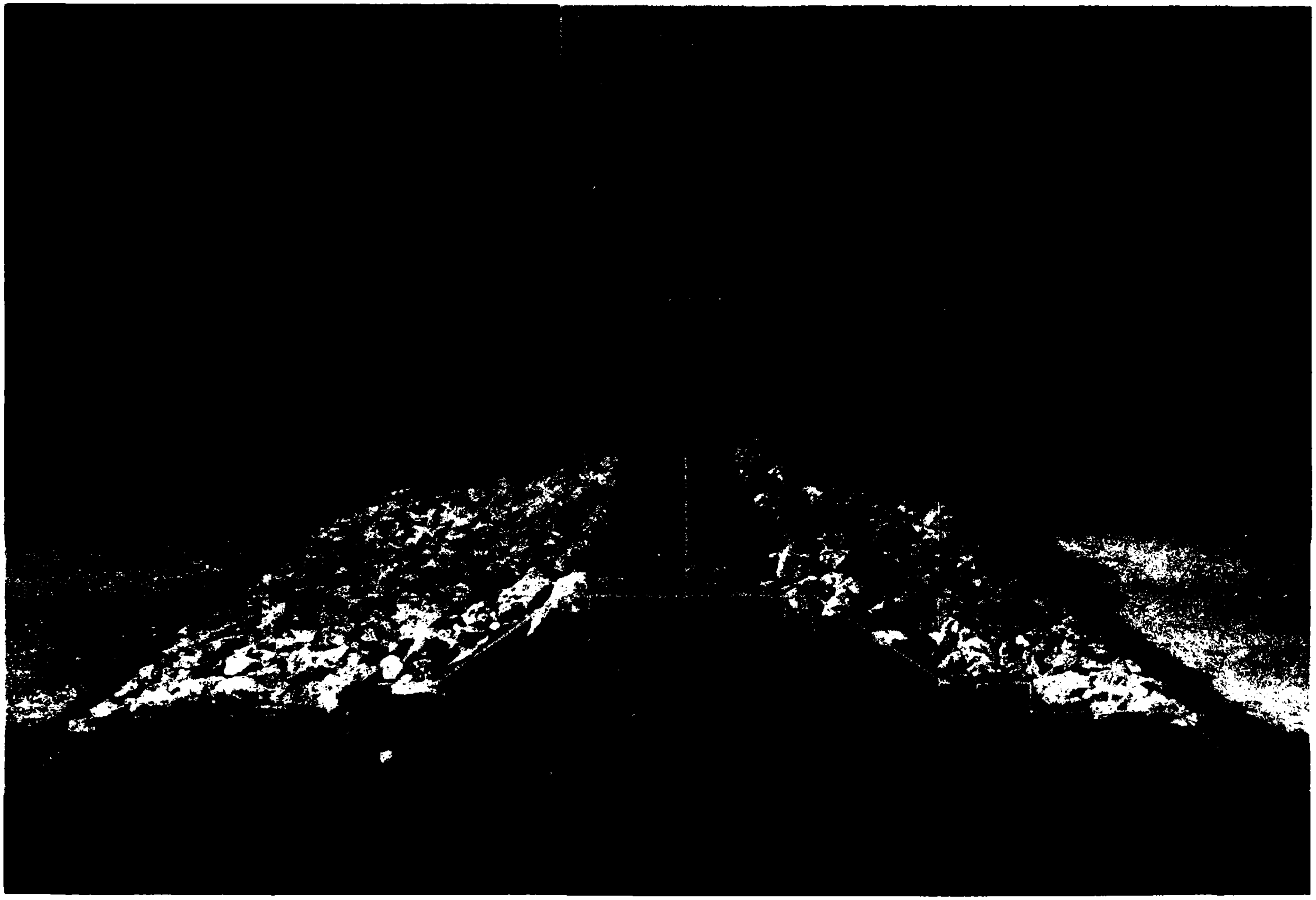

Photo 2. End view of Plan 1 before wave attack

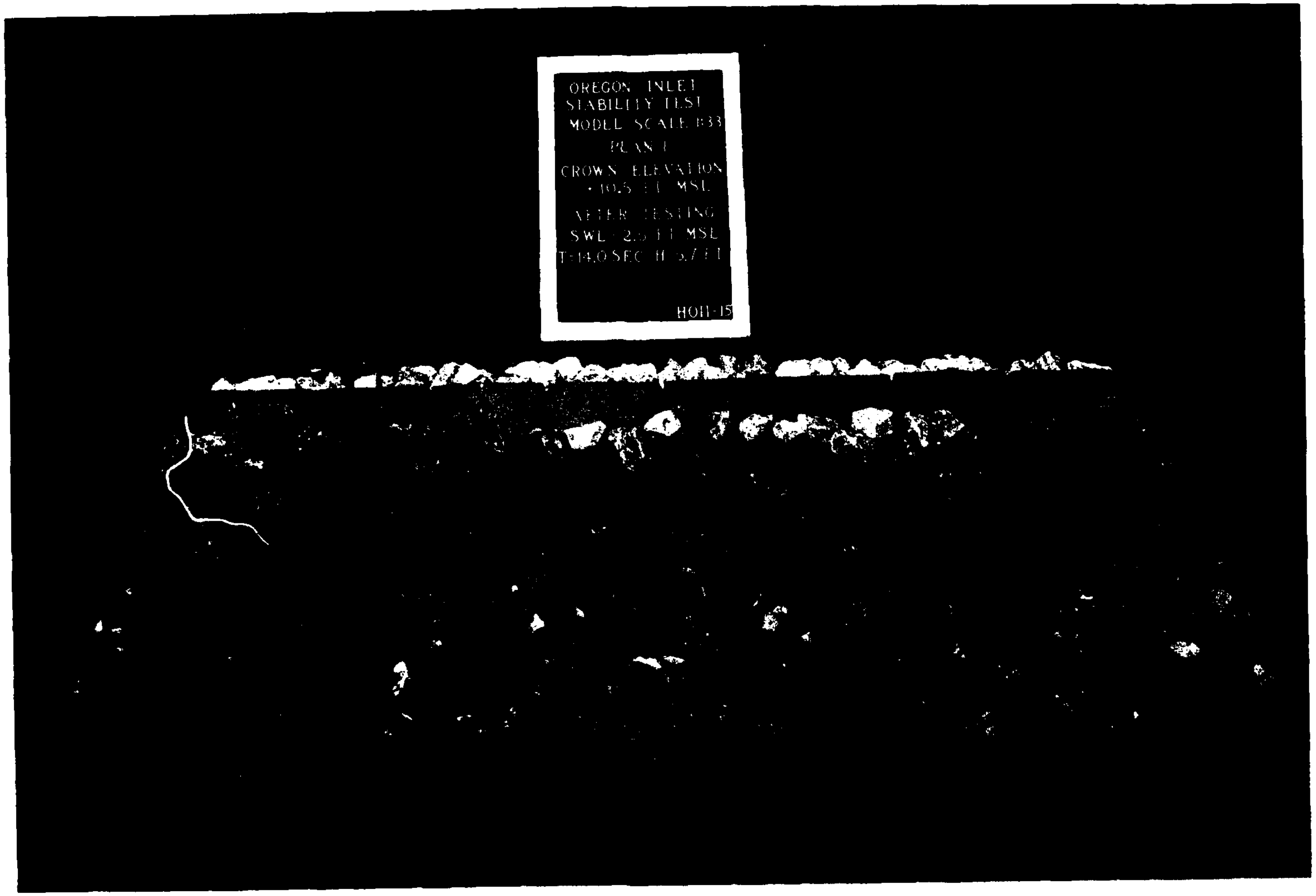

Photo 3. Sea-side view of Plan 1 after attack of 14-sec, 5.7-ft waves at an swl of -2.5 ft NGVD

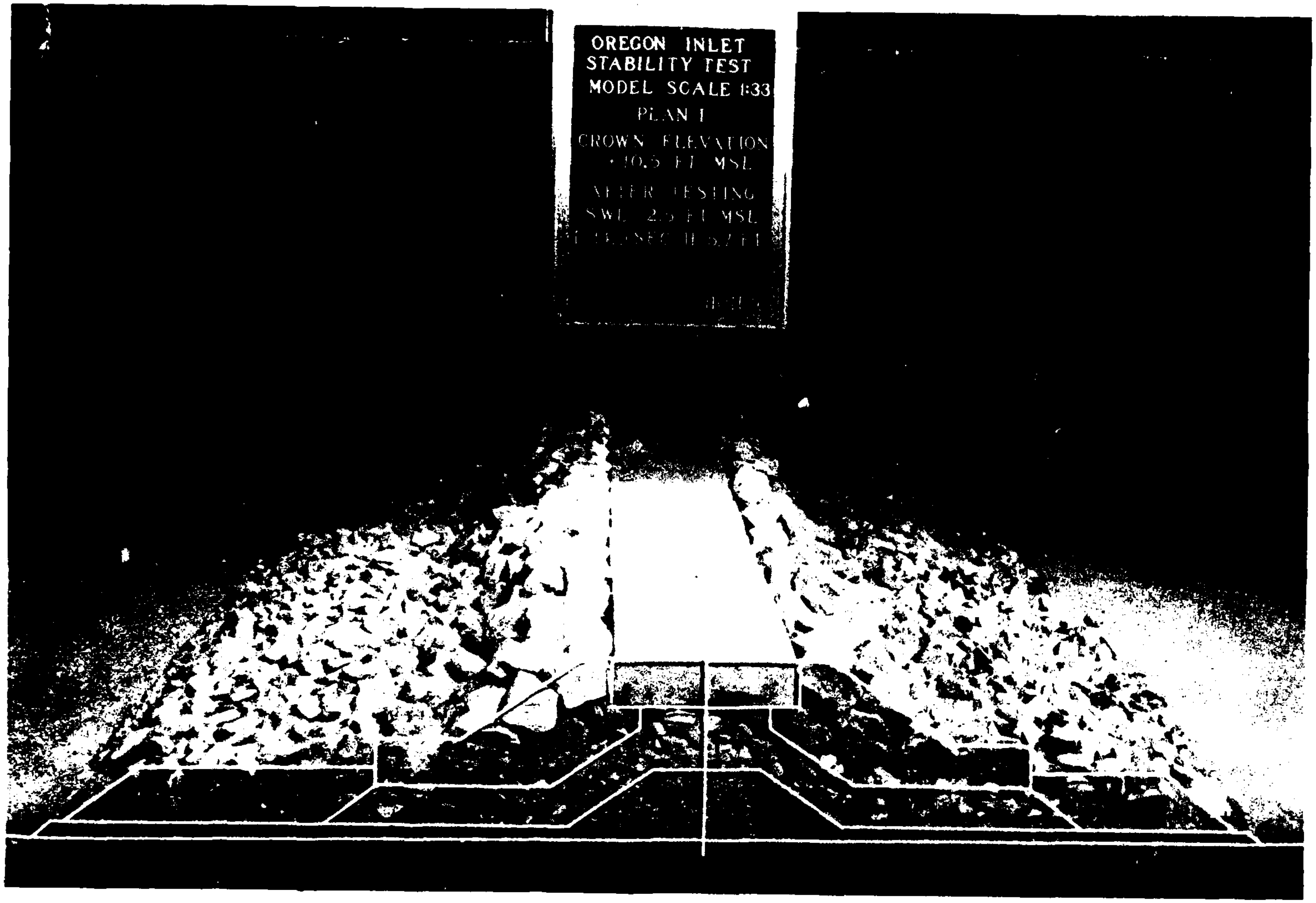

Photo 4. End view of Plan 1 after attack of 14-sec, 5.7-ft waves at an swl of -2.5 ft NGVD

AD-A136 610 JETTY STABILITY STUDY OREGON INLET NORTH CAROLINA 2/5
HYDRAULIC MODEL INVESTIGATION(U) COASTAL ENGINEERING
RESEARCH CENTER VICKSBURG MS R D CARVER ET AL. SEP 83
UNCLASSIFIED CERC-TR-83-3 F/G 13/2 NL

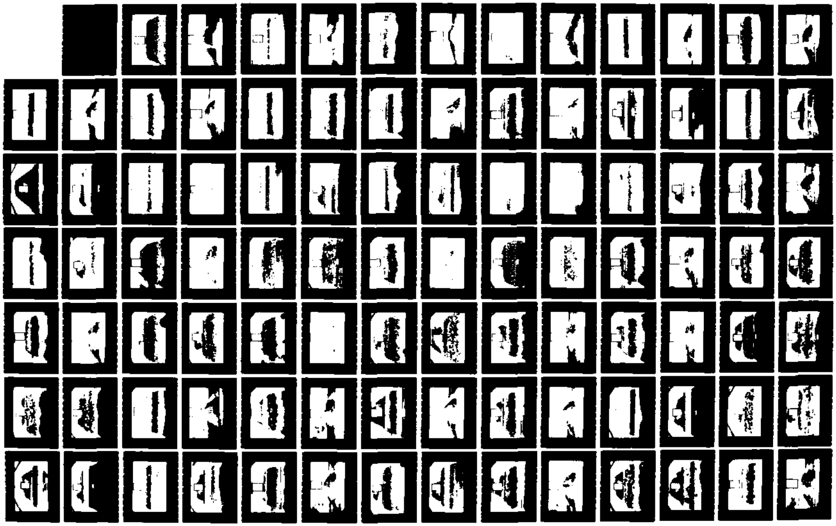

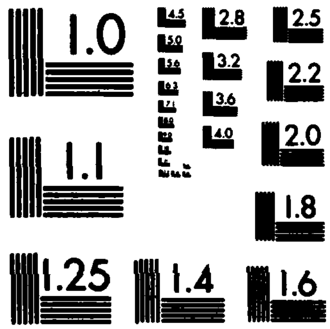

MICROCOPY RESOLUTION TEST CHART
NATIONAL BUREAU OF STANDARDS-1963-A

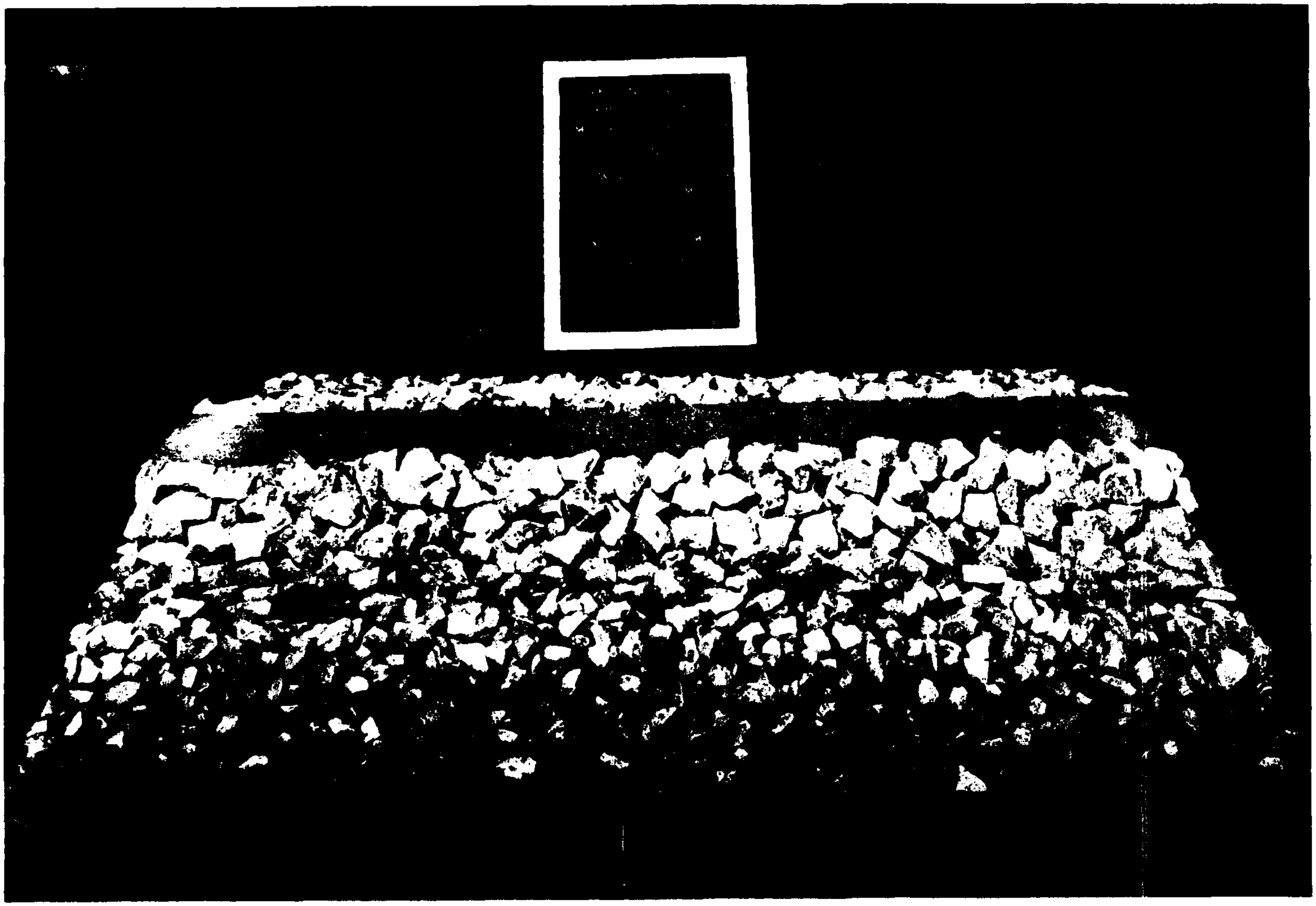

Photo 5. Sea-side view of Plan 1 after attack of 14-sec, 6.3-ft waves at an swl of -1.6 ft NGVD

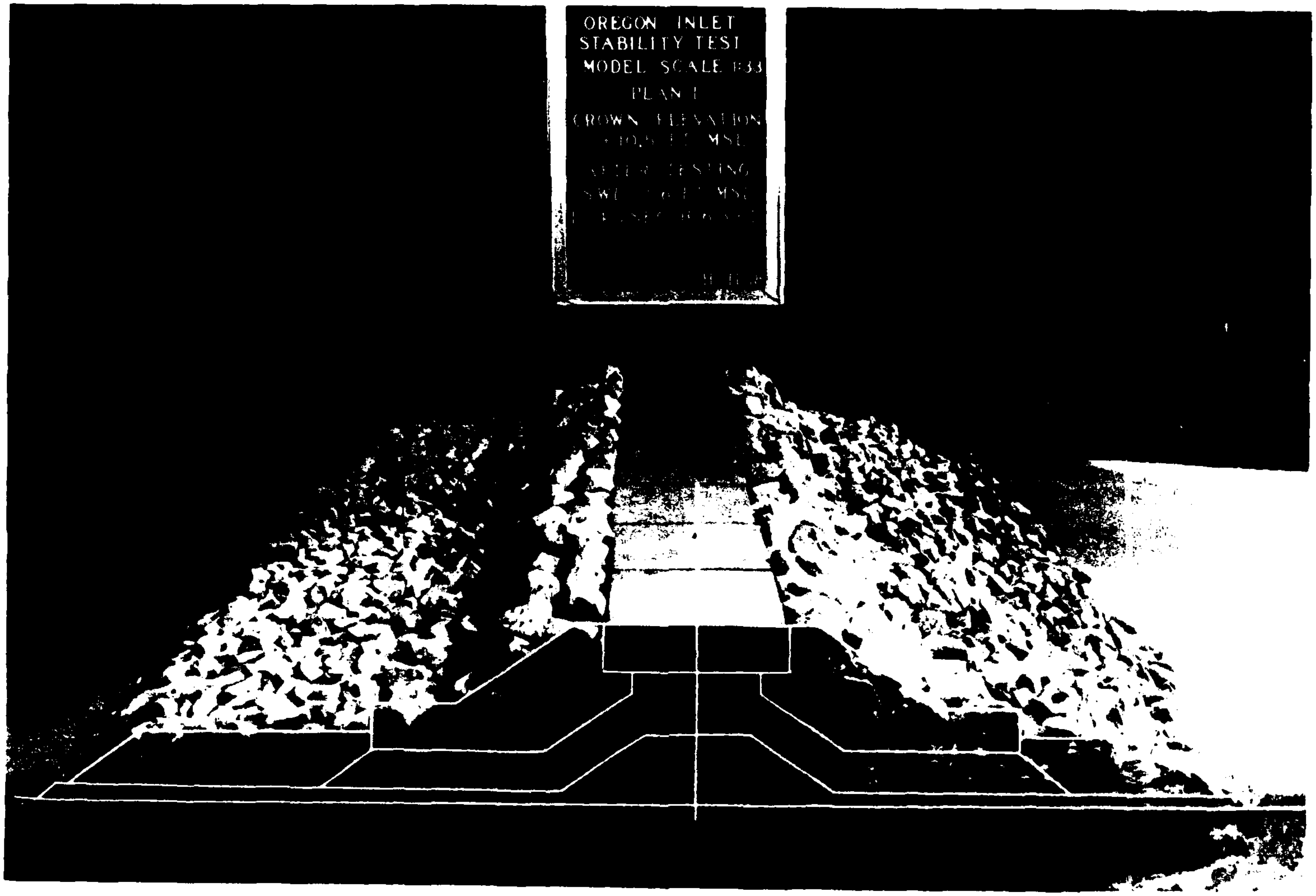

Photo 6. End view of Plan 1 after attack of 14-sec, 6.3-ft waves at an swl of -1.6 ft NGVD

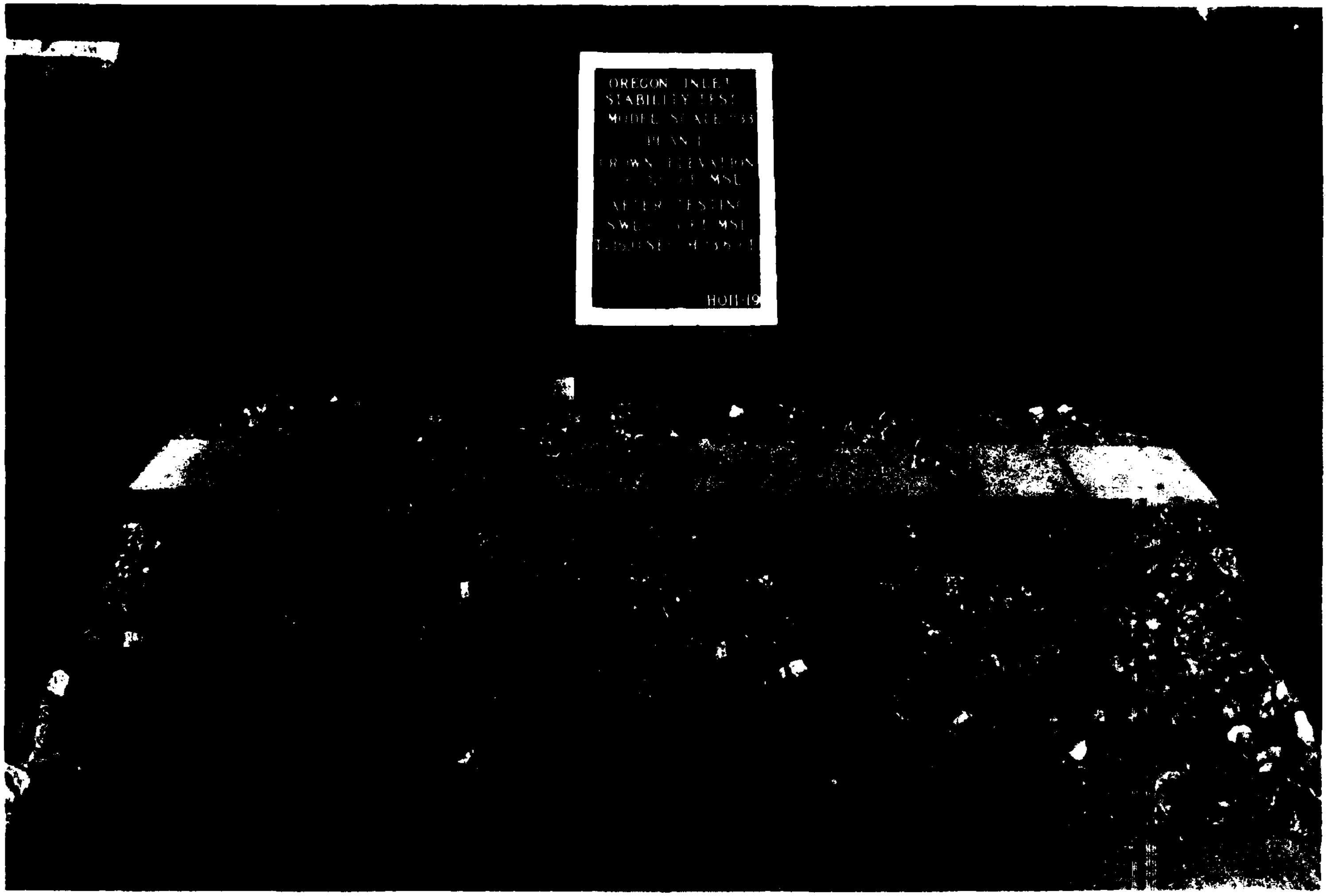

Photo 7. Sea-side view of Plan 1 after attack of 15-sec, 13.6-ft waves at an swl of +5.5 ft NGVD

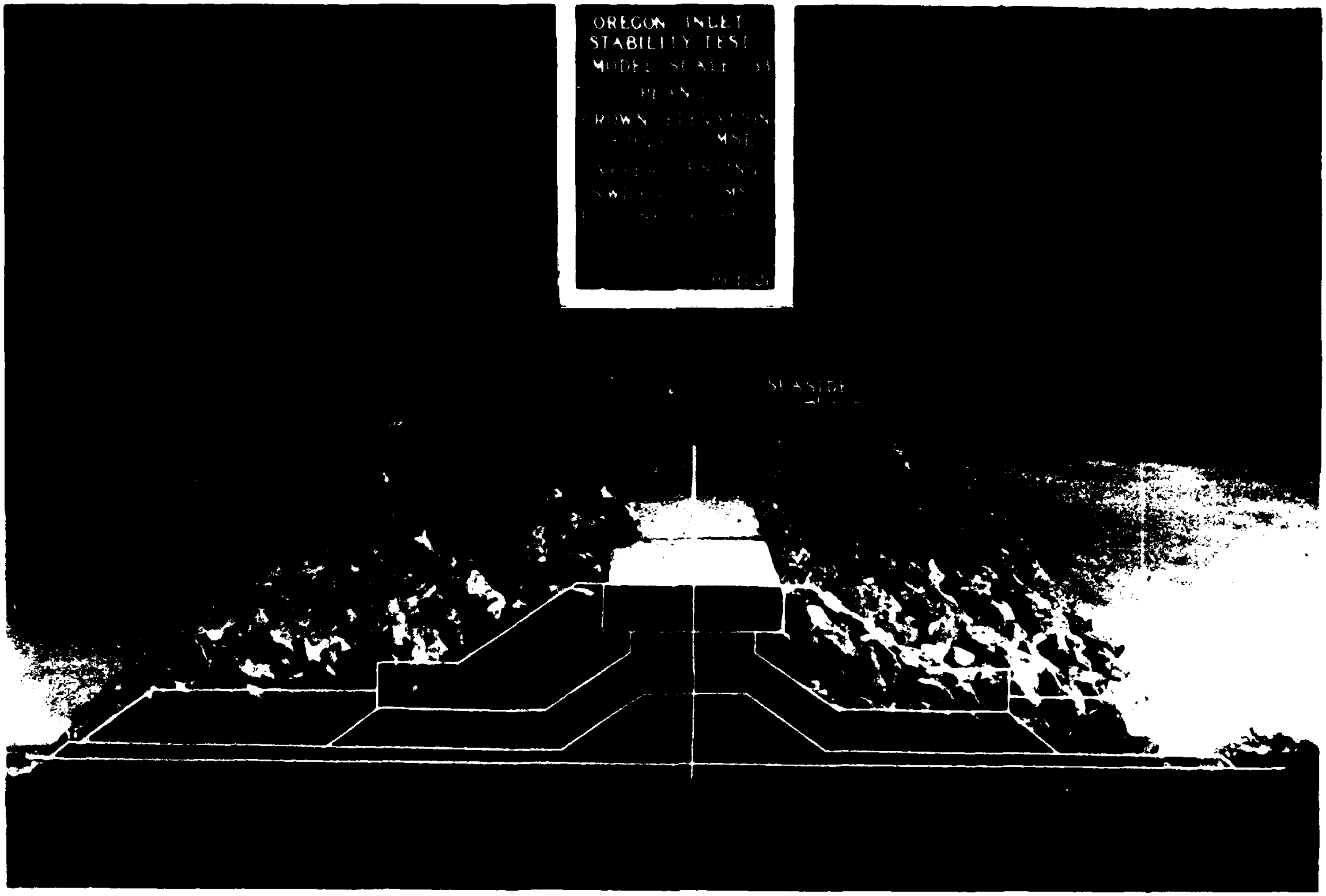

Photo 8. End view of Plan 1 after attack of 15-sec, 13.6-ft waves at an swl of +5.5 ft NGVD

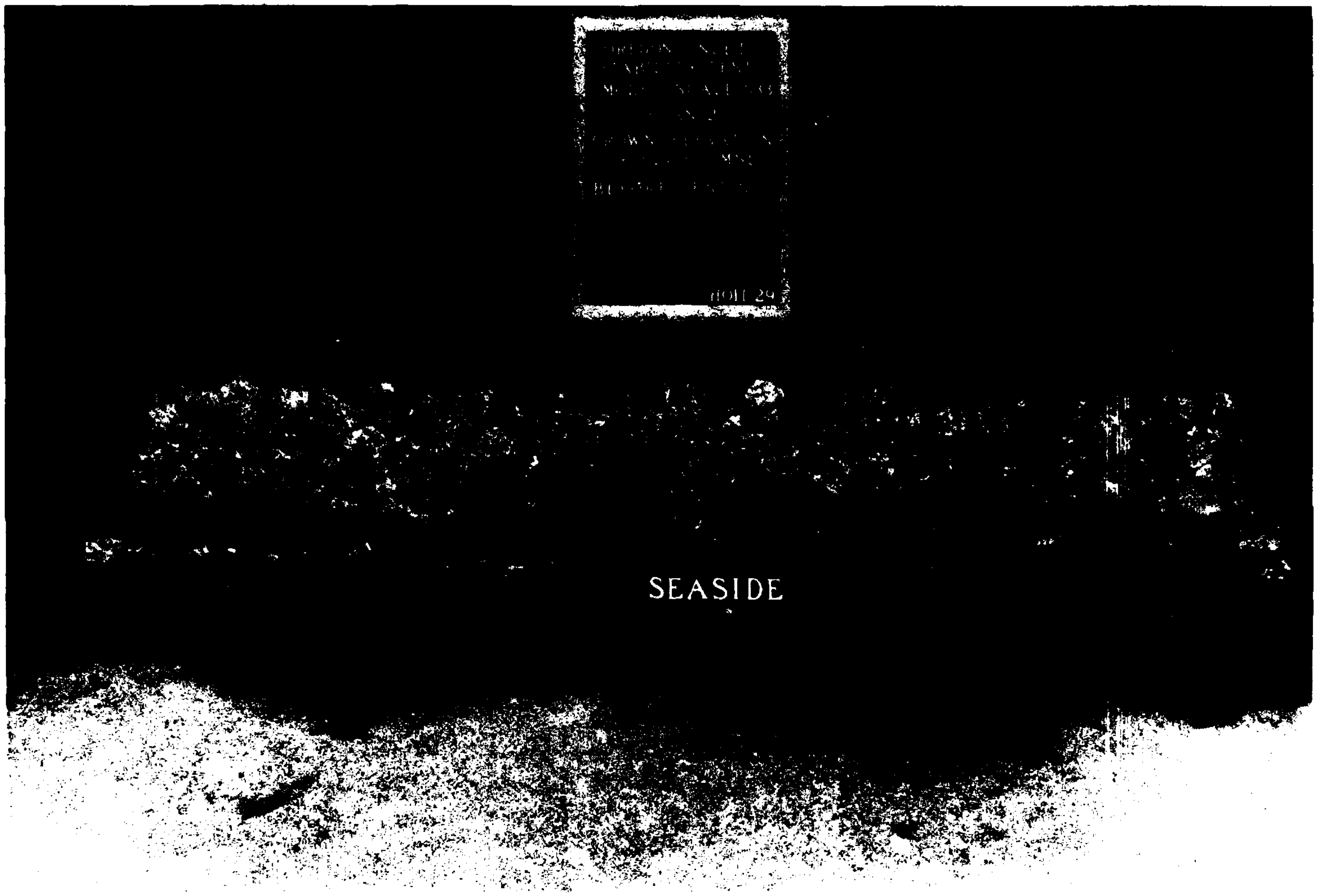

Photo 9. Sea-side view of Plan 2 before wave attack

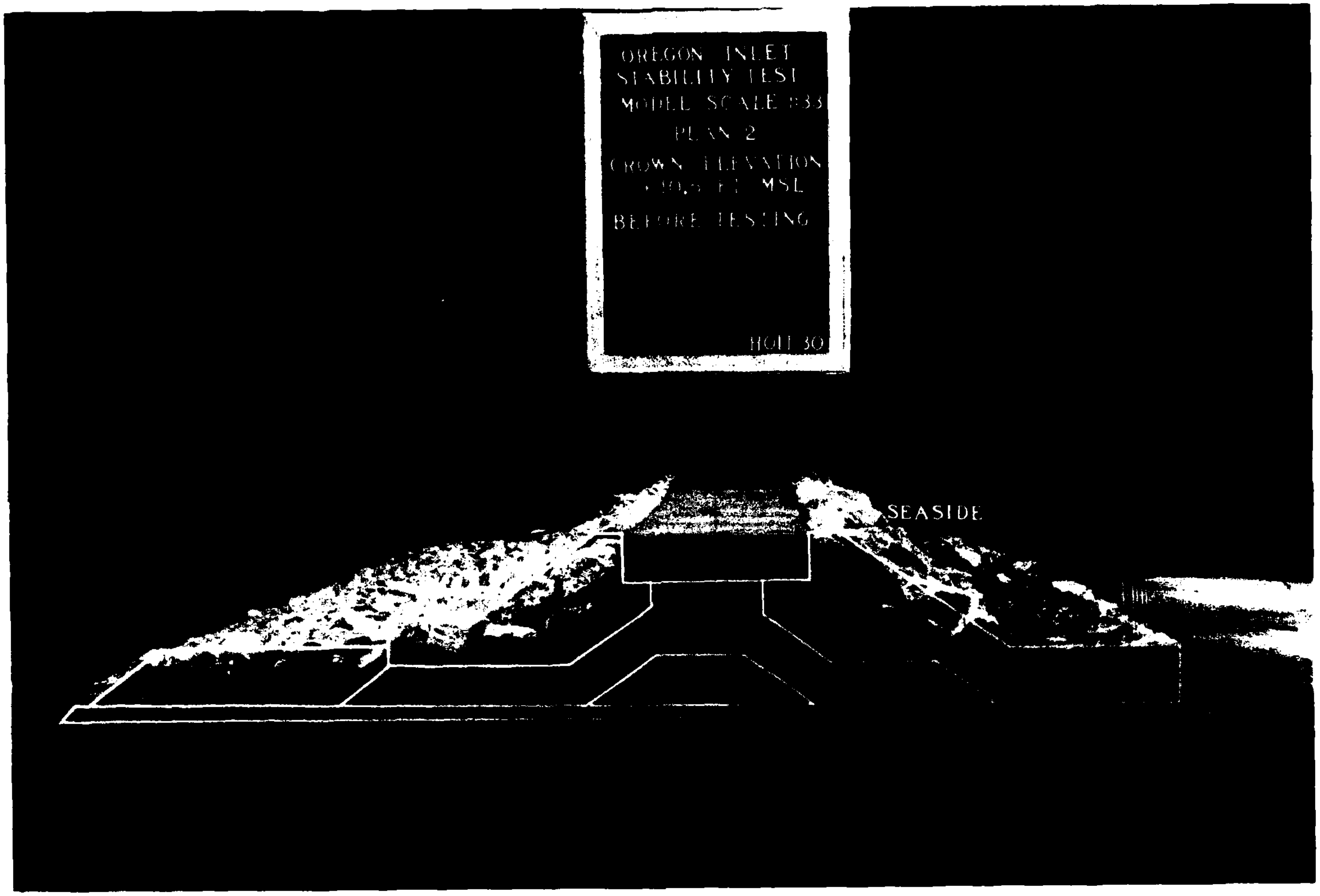

Photo 10. End view of Plan 2 before wave attack

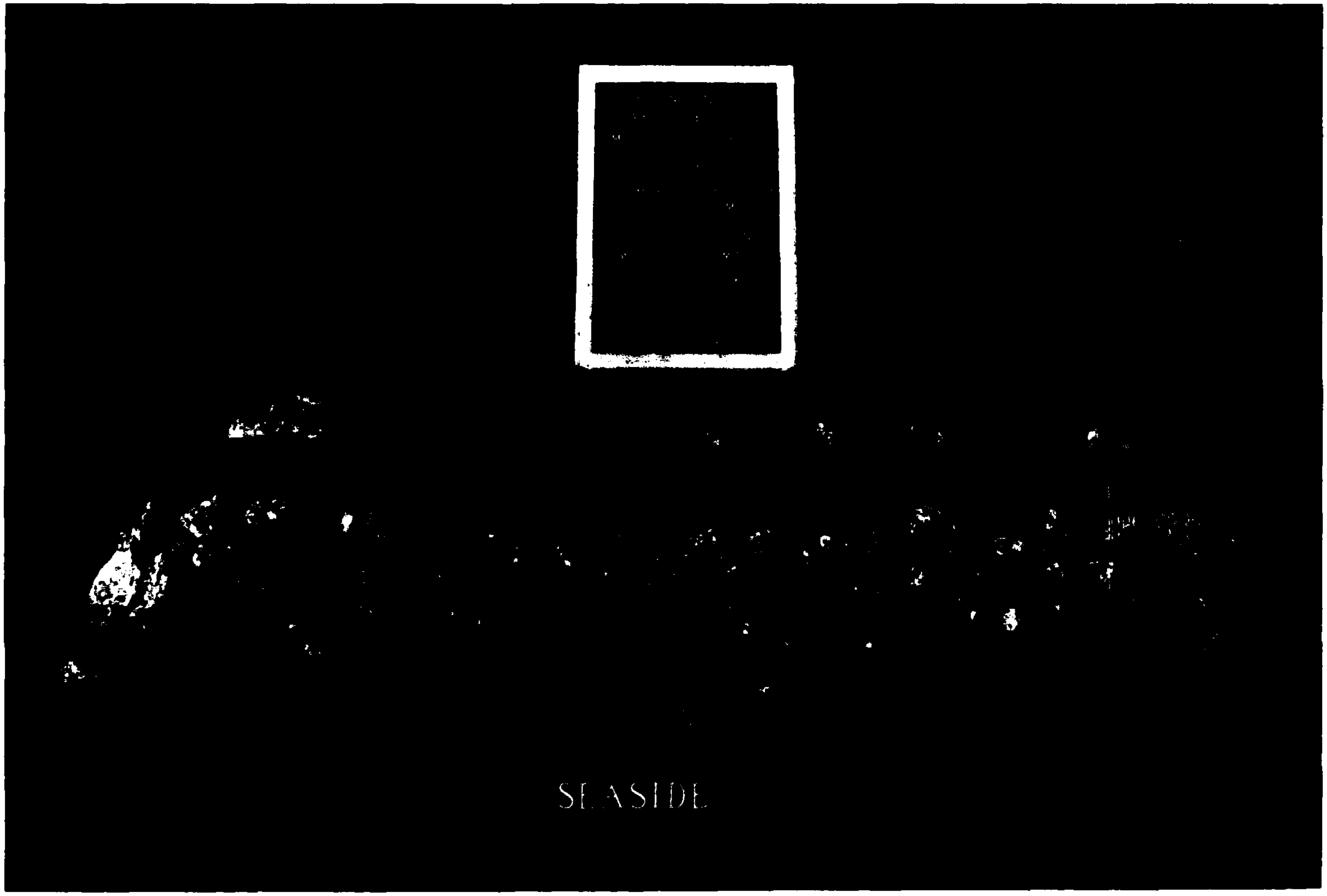

Photo 11. Sea-side view of Plan 2 after attack of 15-sec, 13.6-ft waves at an swl of +5.5 ft NGVD

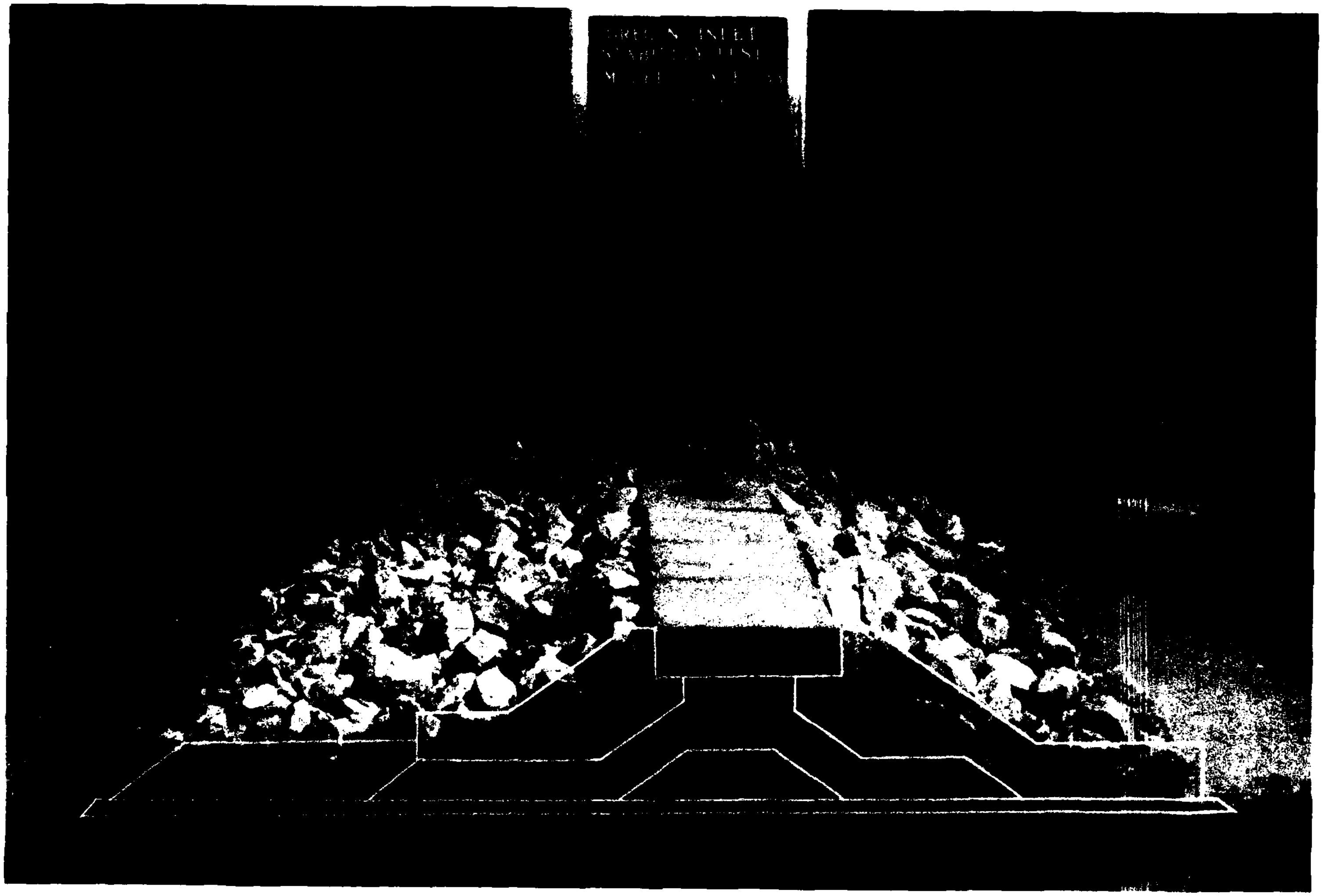

Photo 12. End view of Plan 2 after attack of 15-sec, 13.6-ft waves at an swl of +5.5 ft NGVD

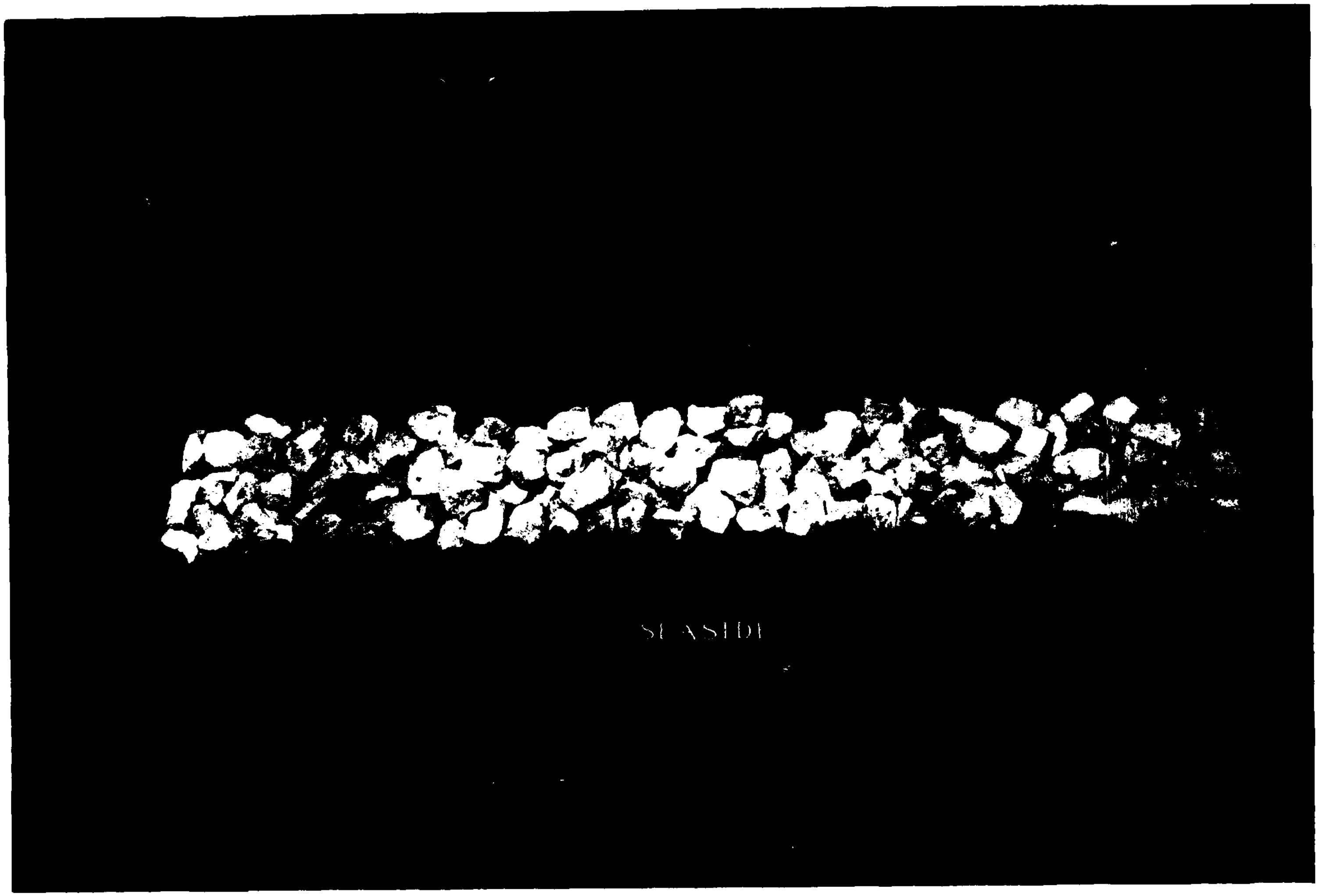

Photo 13. Sea-side view of Plan 3 before wave attack

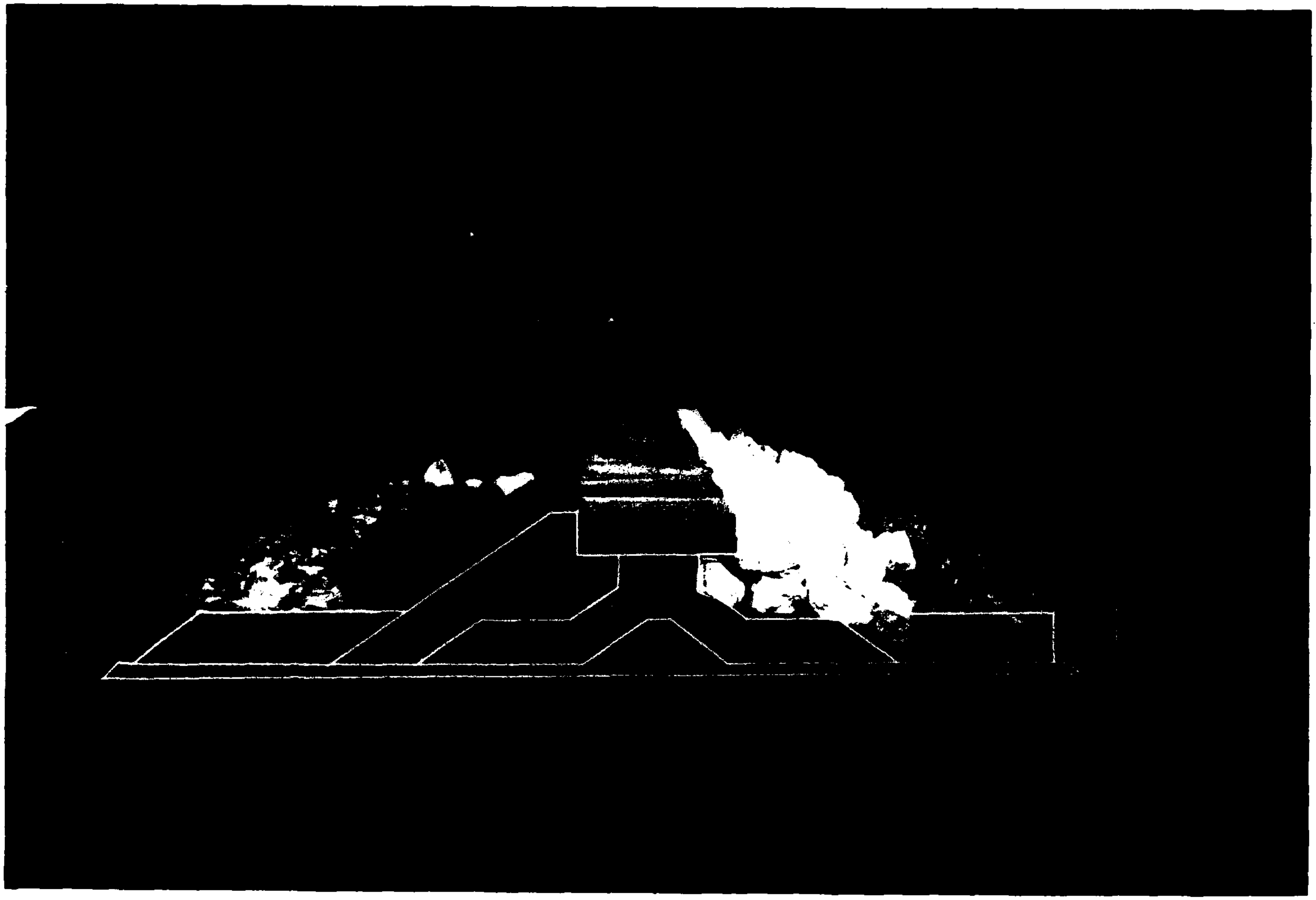

Photo 14. End view of Plan 3 before wave attack

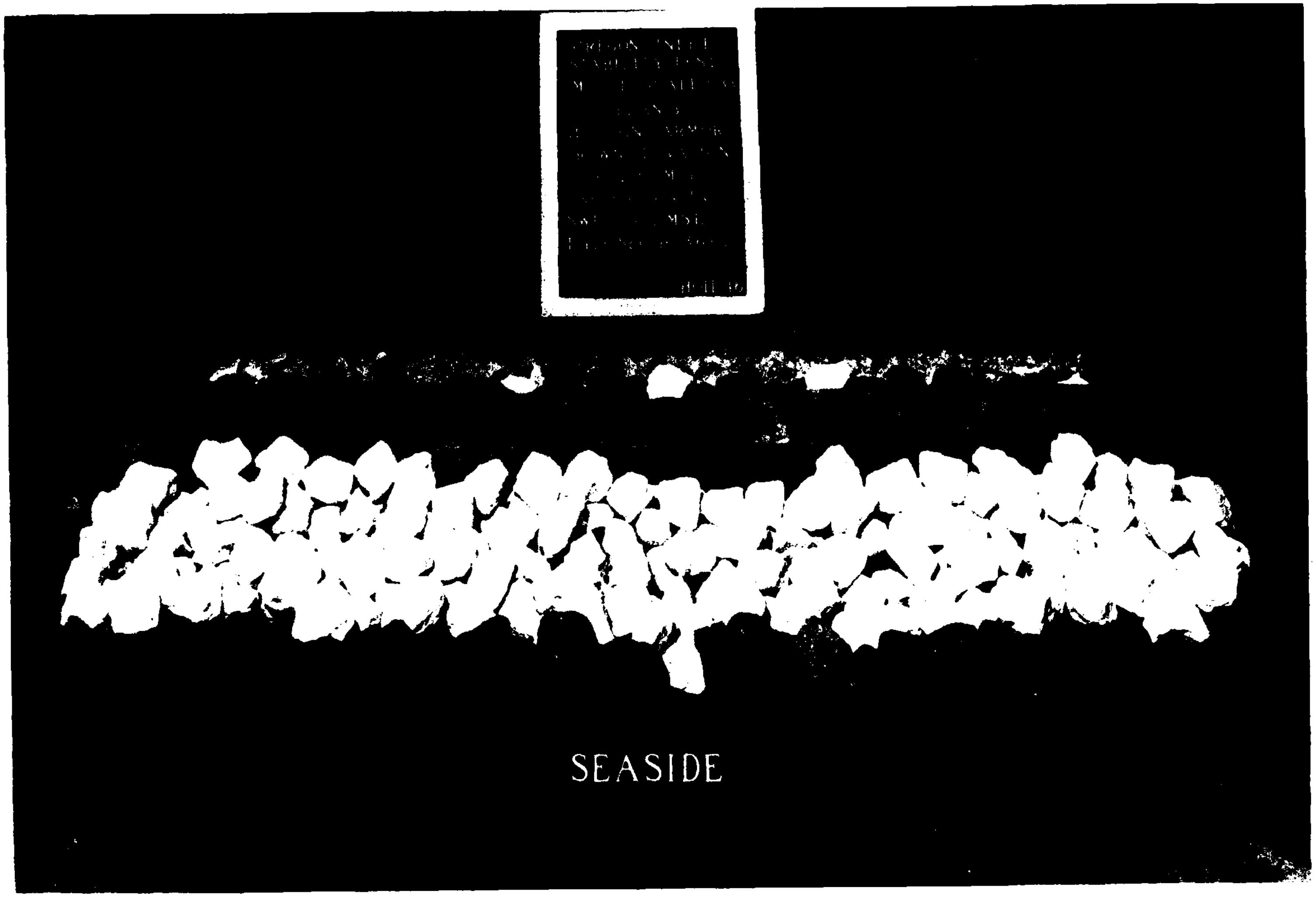

Photo 15. Sea-side view of Plan 3 after attack of 15-sec, 13.6-ft waves at an swl of +5.5 ft NGVD

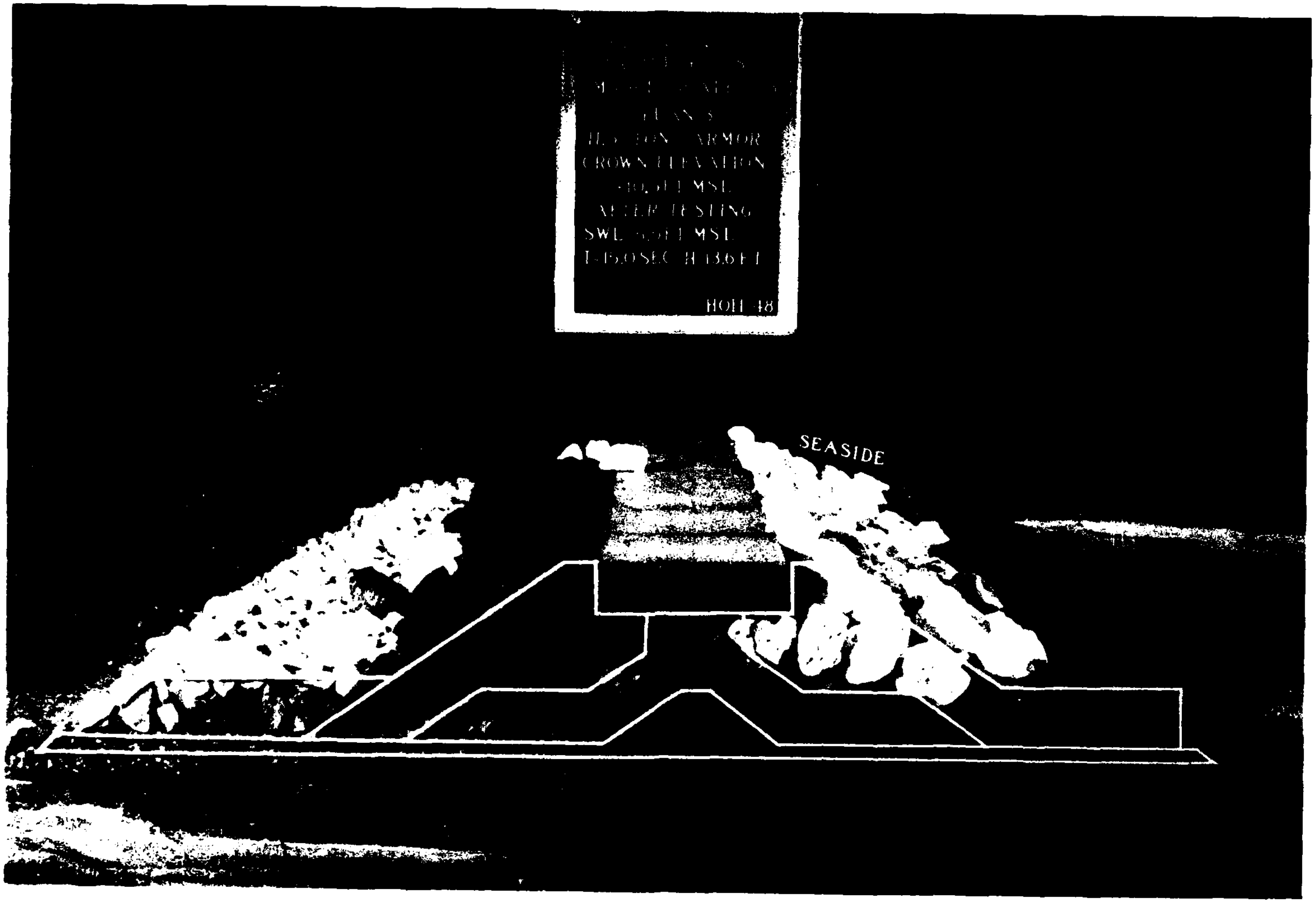

Photo 16. End view of Plan 3 after attack of 15-sec, 13.6-ft waves at an swl of +5.5 ft NGVD

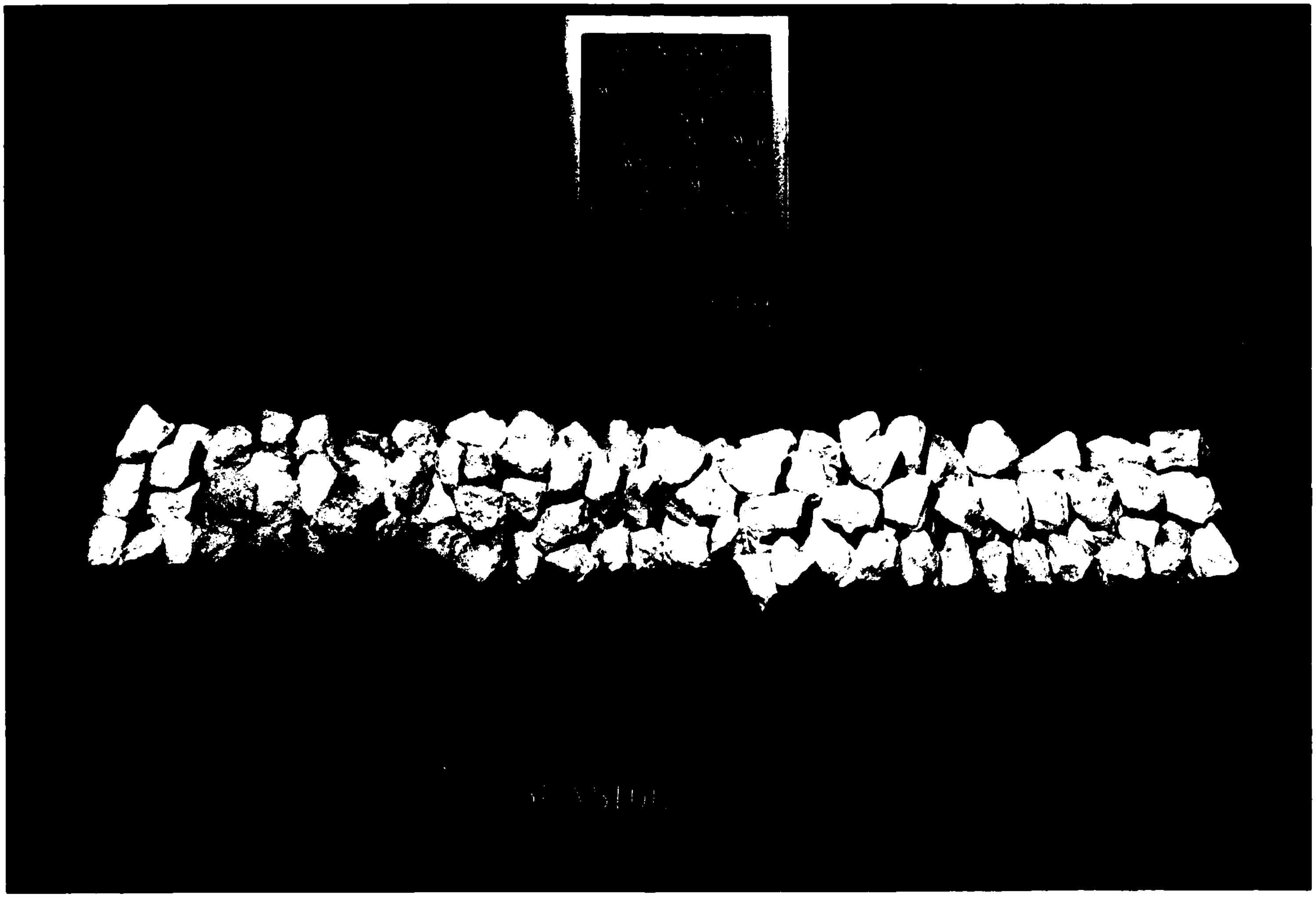

Photo 17. Sea-side view of Plan 4 before wave attack

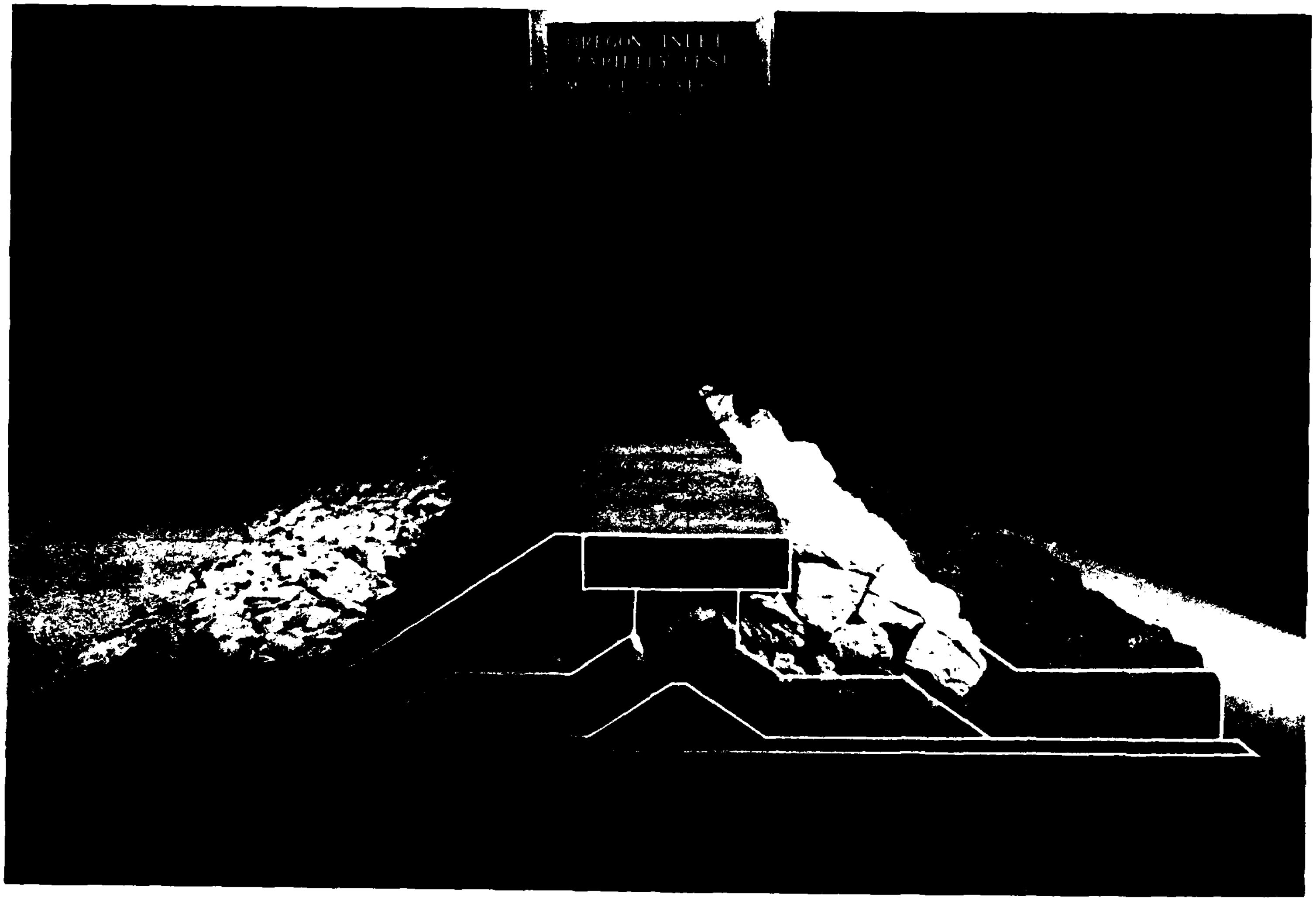

Photo 18. End view of Plan 4 before wave attack

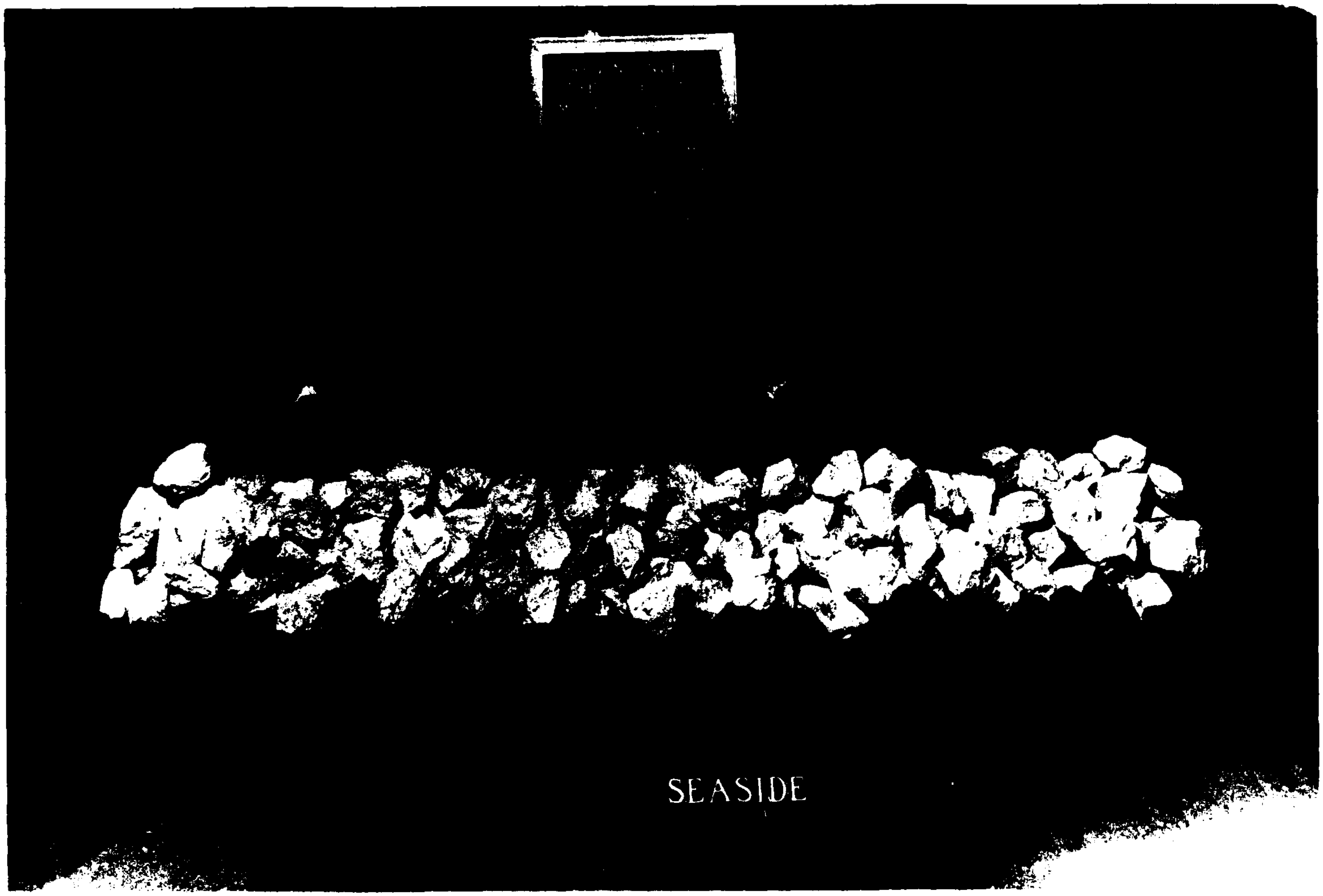

Photo 19. Sea-side view of Plan 4 after attack of 15-sec, 13.6-ft waves at an swl of +5.5 ft NGVD

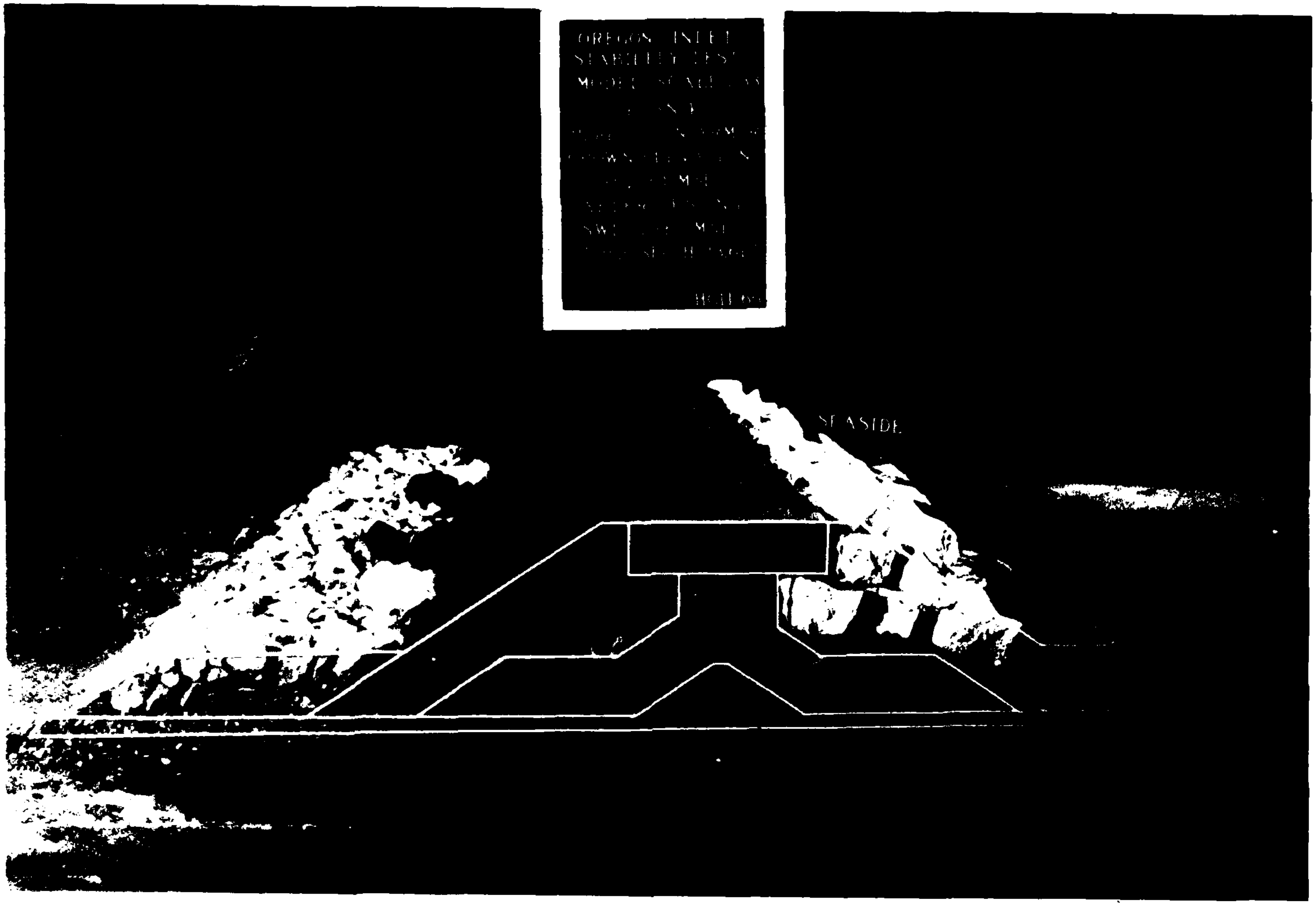

Photo 20. End view of Plan 4 after attack of 15-sec, 13.6-ft waves at an swl of +5.5 ft NGVD

Photo 21. Sea-side view of Plan 4A before wave attack

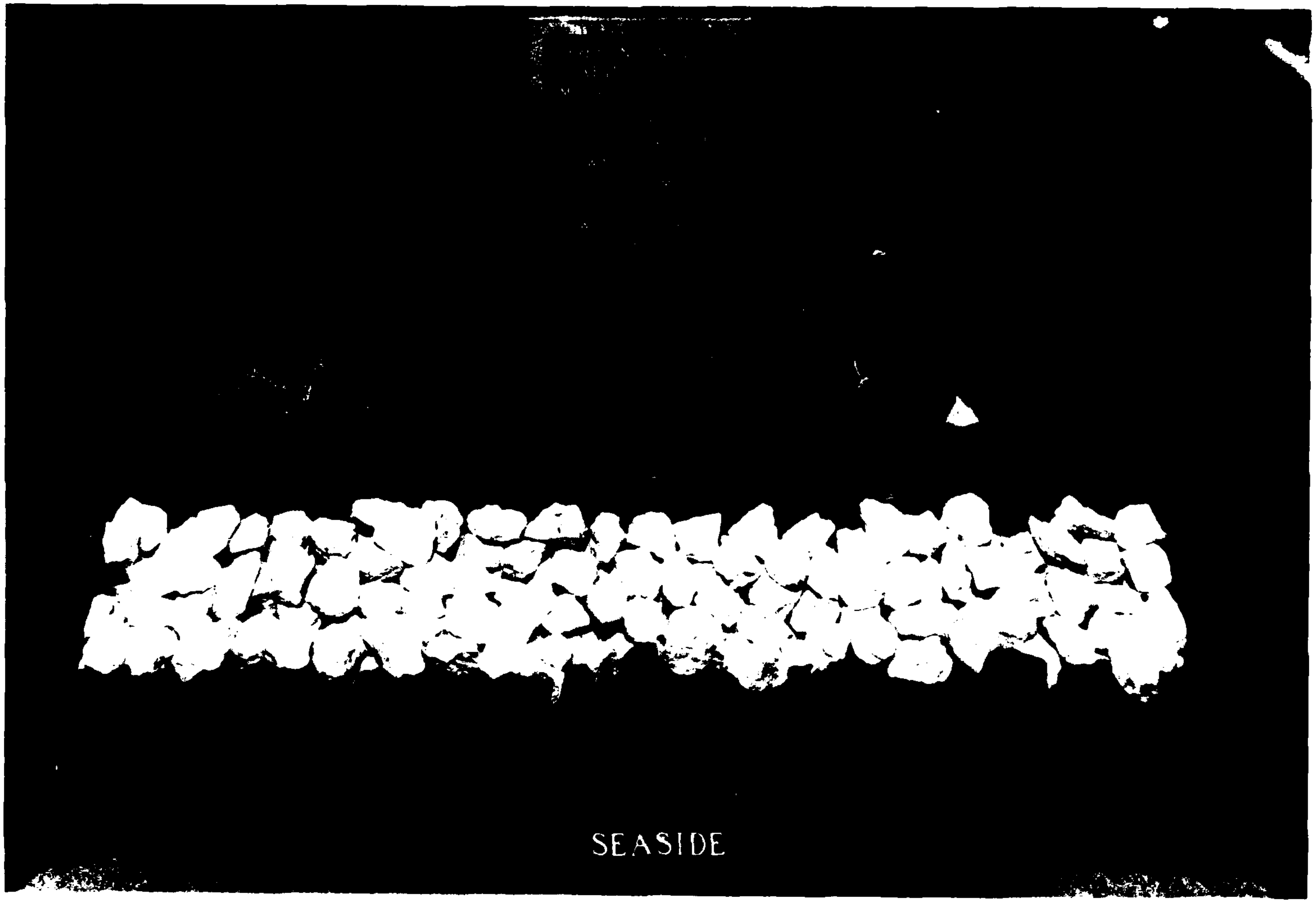

Photo 22. Sea-side view of Plan 4A after attack of 15-sec, 13.6-ft waves at an swl of +5.5 ft NGVD

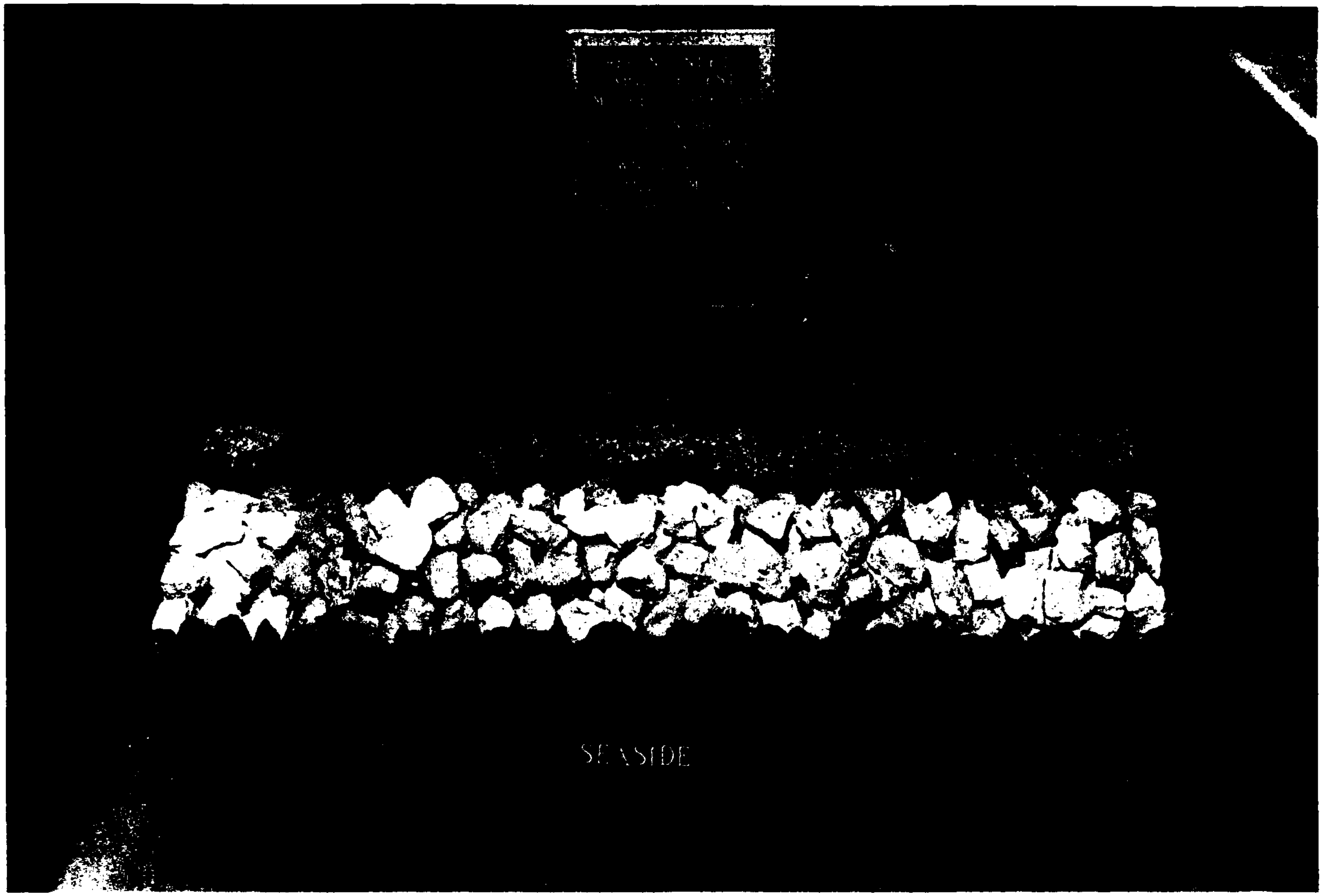

Photo 23. Sea-side view of Plan 4B before wave attack

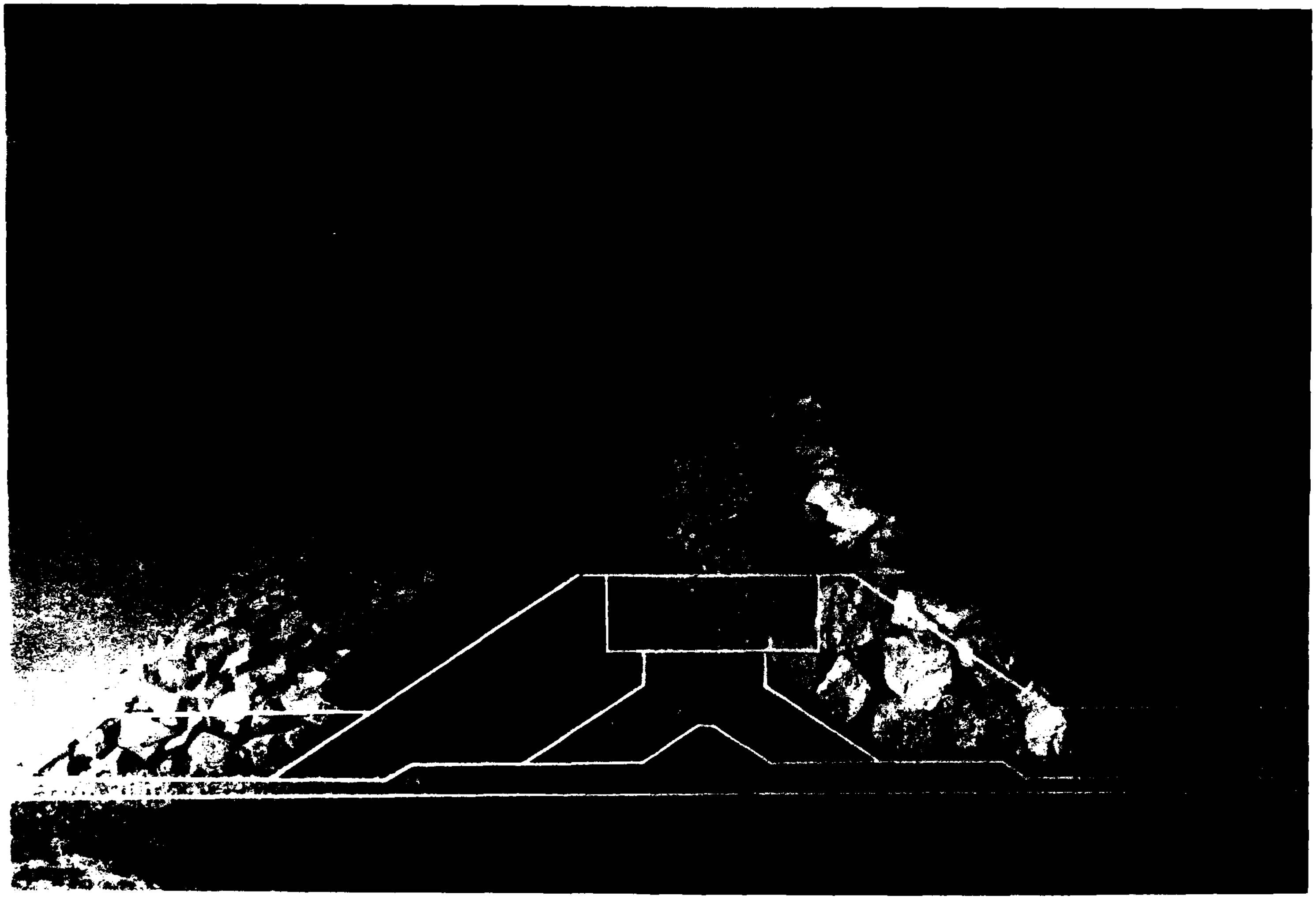

Photo 24. End view of Plan 4B before wave attack

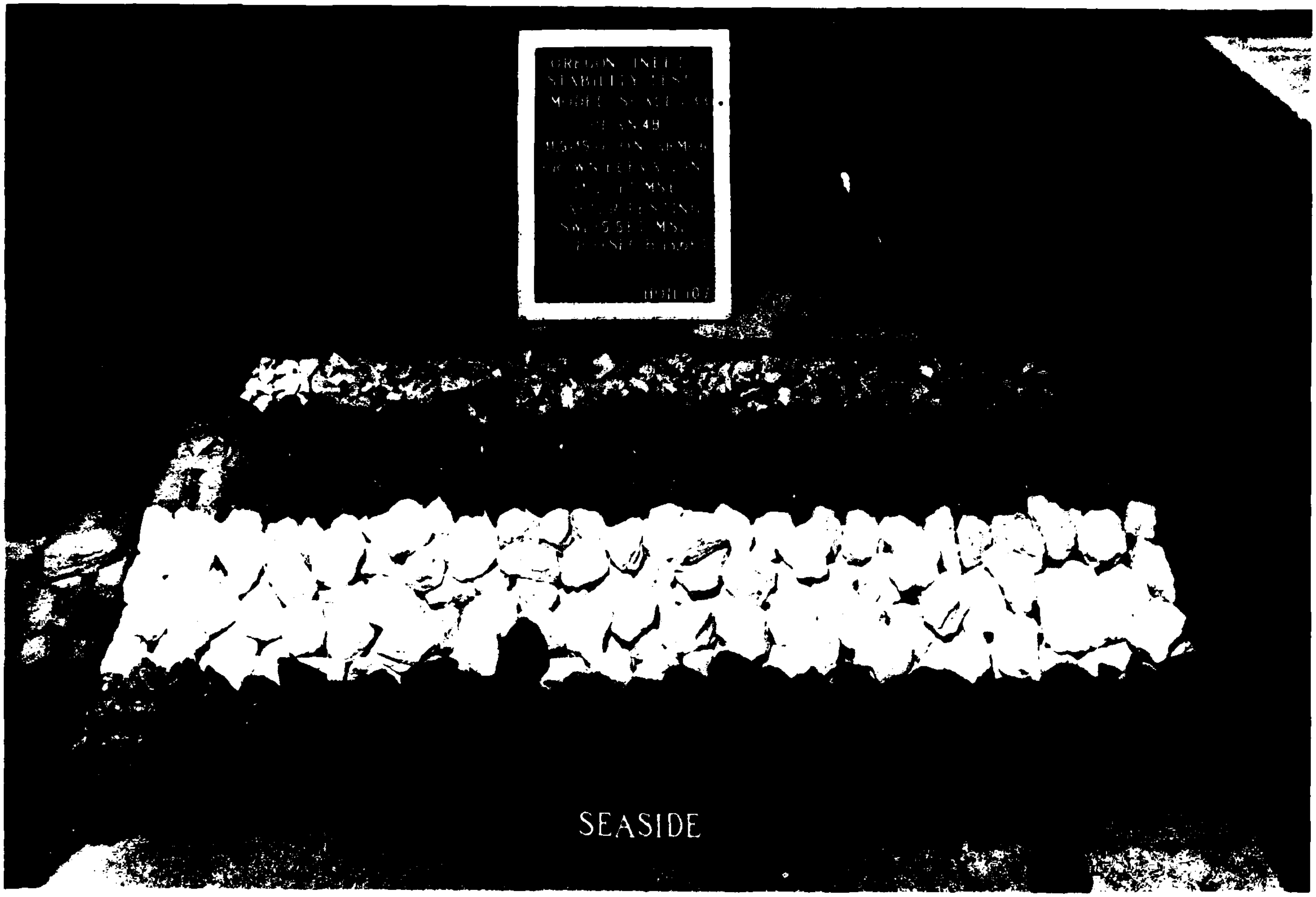

Photo 25. Sea-side view of Plan 4B after attack of 15-sec, 13.6-ft waves at an swl of +5.5 ft NGVD

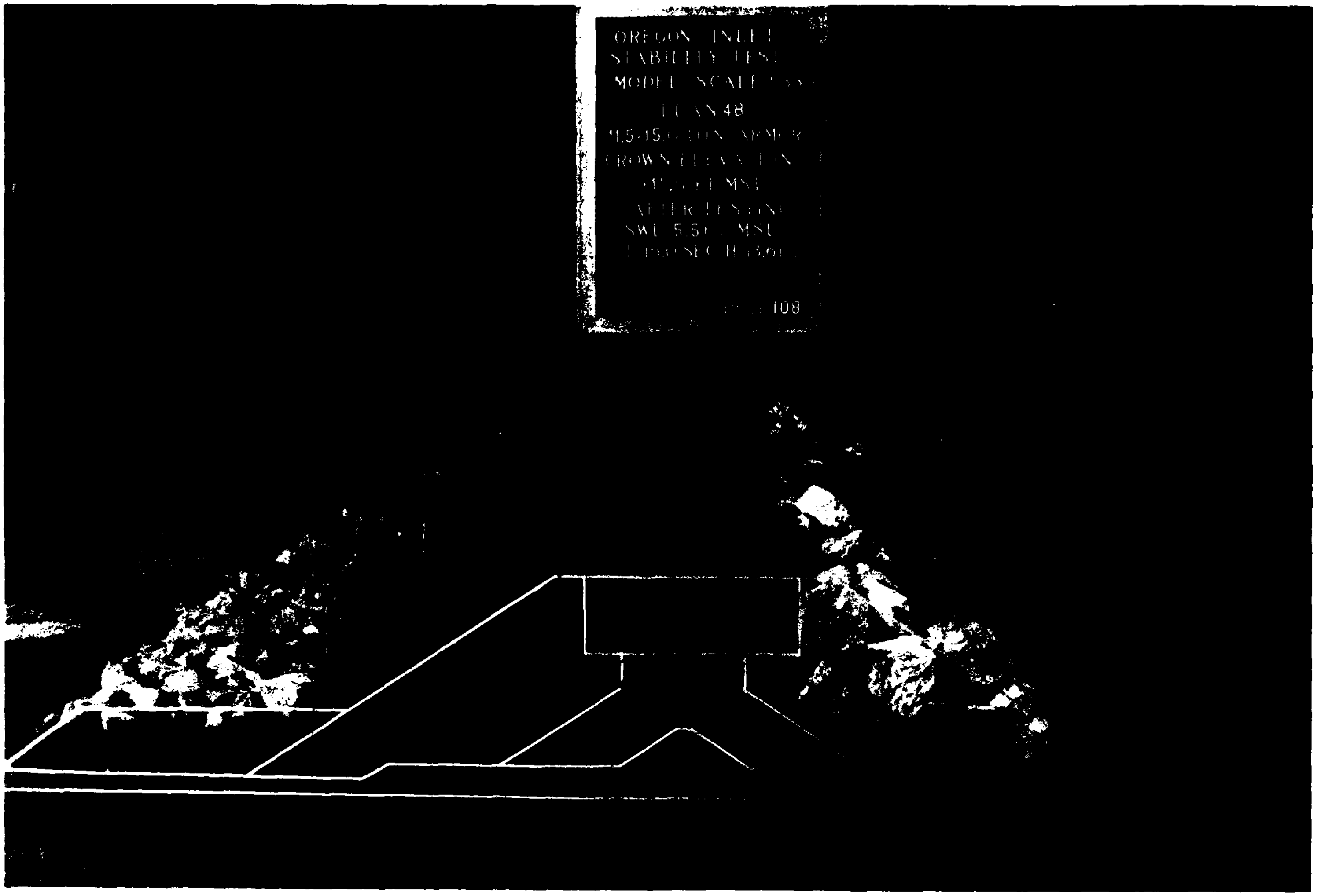

Photo 26. End view of Plan 4B after attack of 15-sec, 13.6-ft waves at an swl of +5.5 ft NGVD

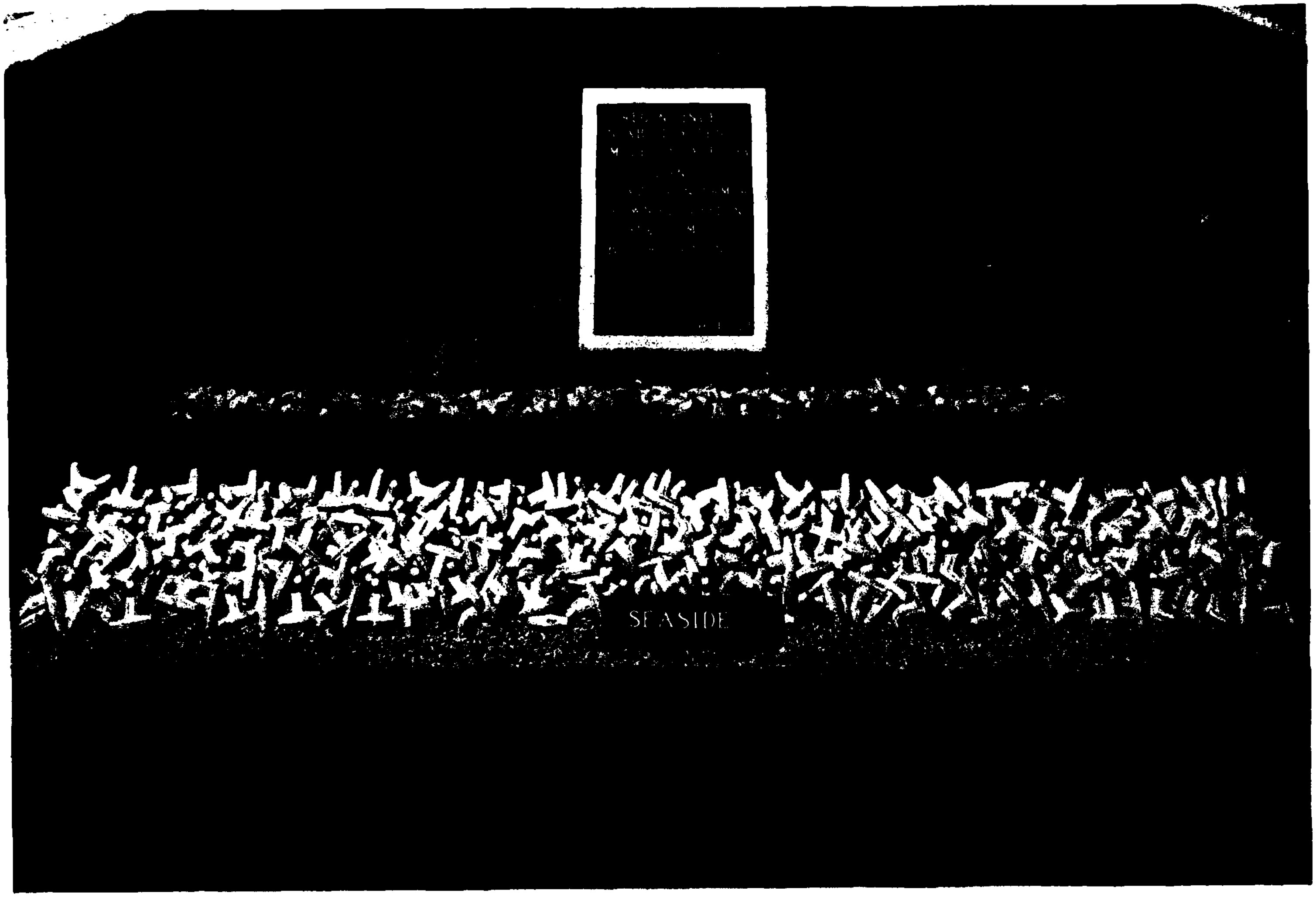

Photo 27. Sea-side view of Plan 5 before wave attack

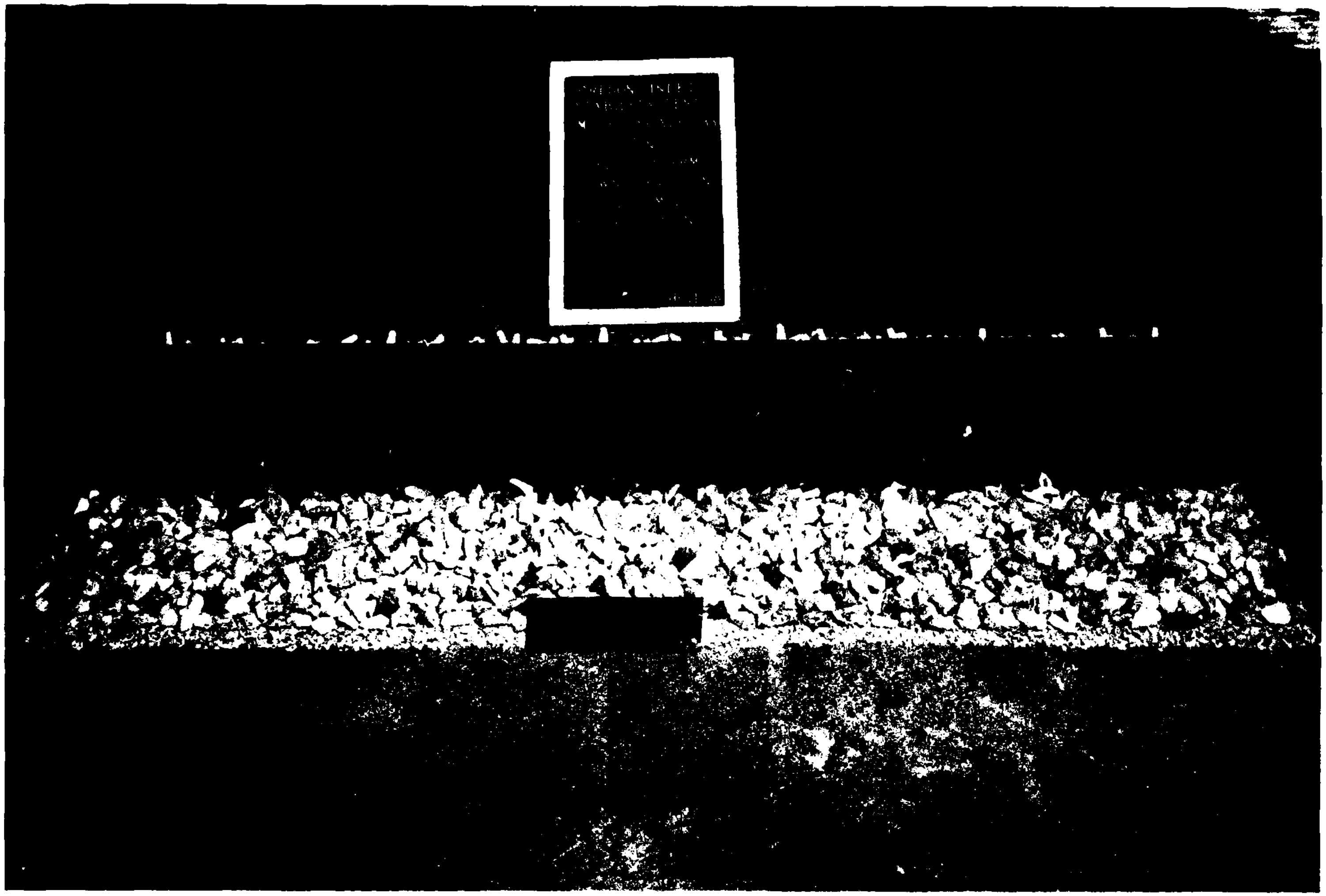

Photo 28. Channel-side view of Plan 5 before wave attack

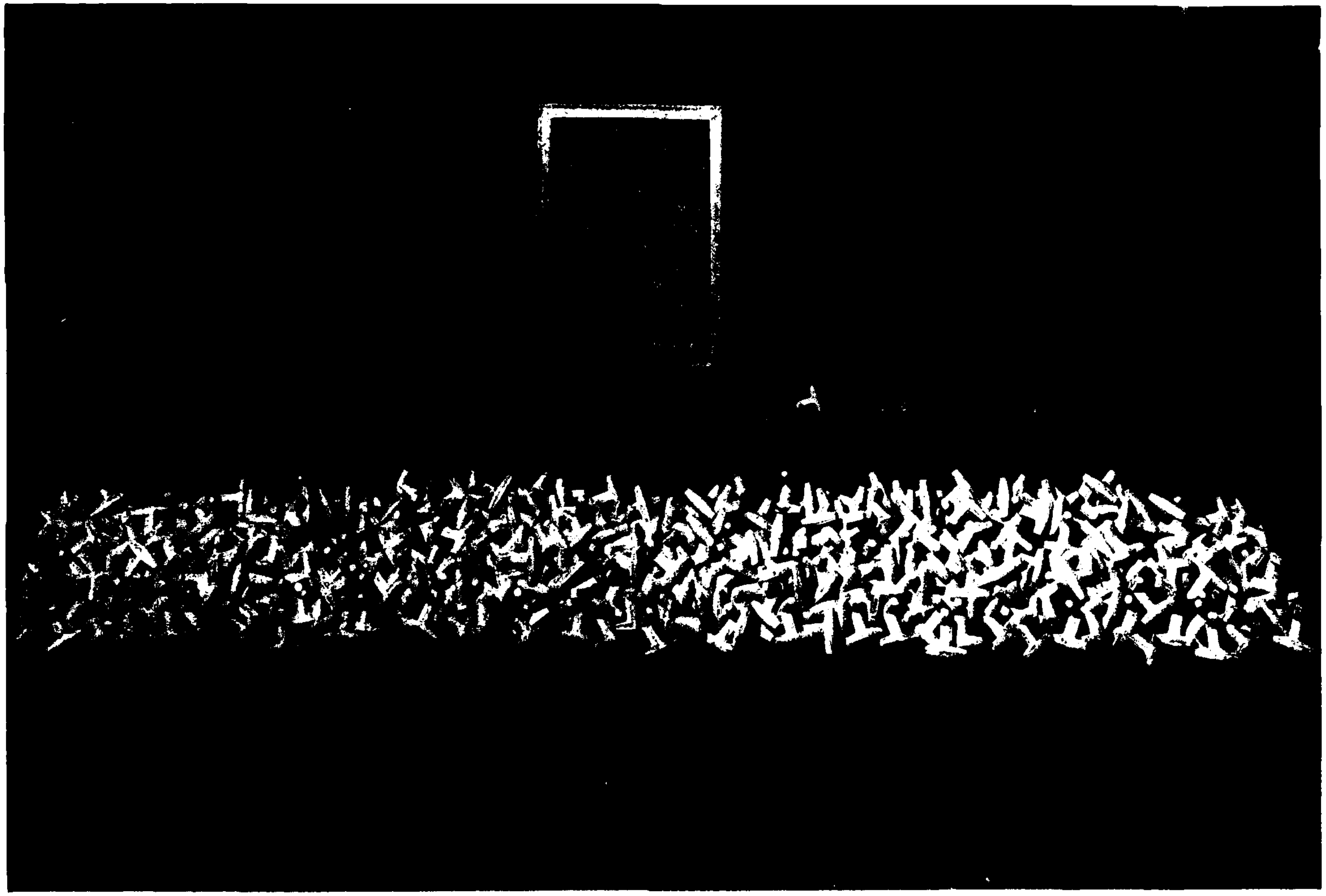

Photo 29. Sea-side view of Plan 5 after attack of 15-sec, 13.6-ft waves at an swl of +5.5 ft NGVD

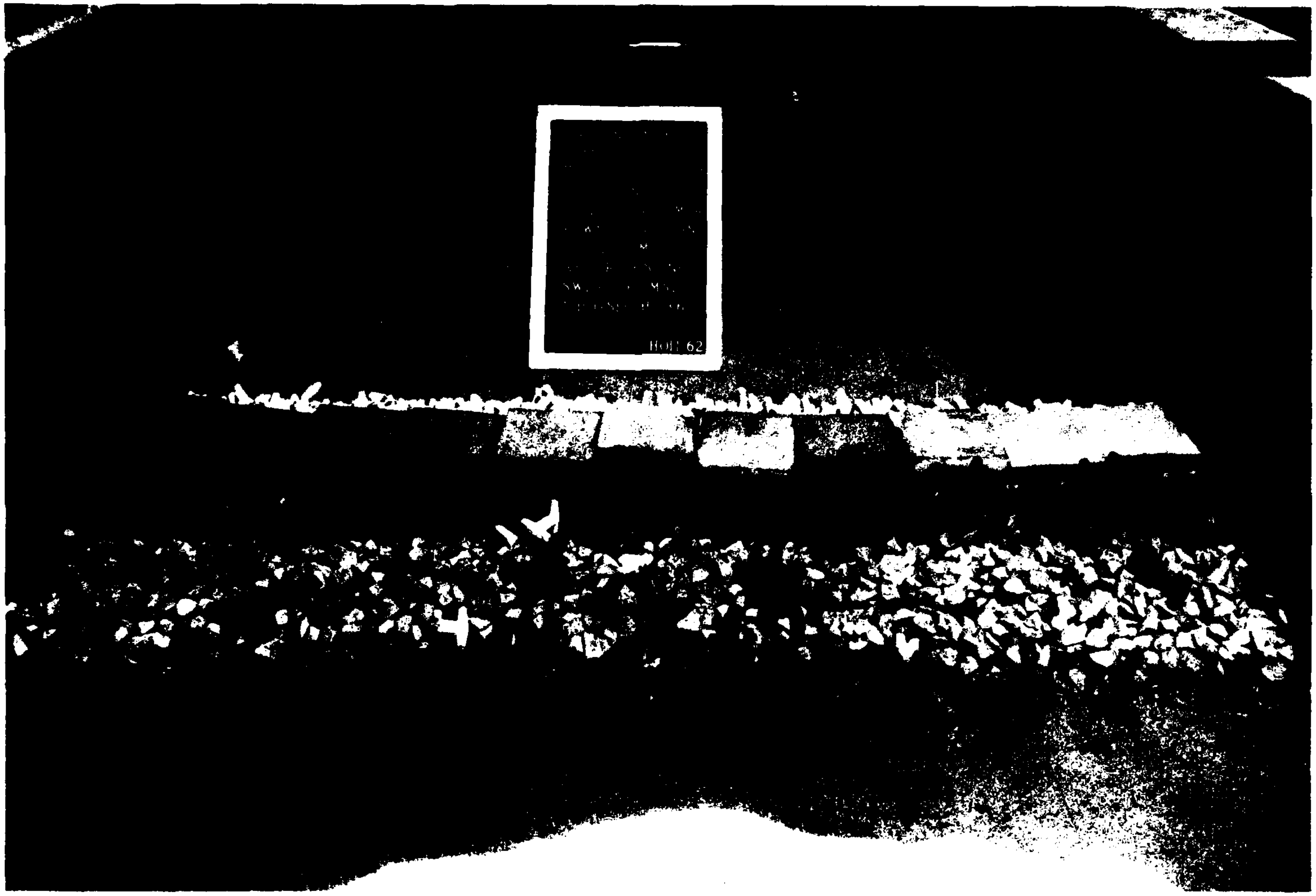

Photo 30. Channel-side view of Plan 5 after attack of 15-sec, 13.6-ft waves at an swl of +5.5 ft NGVD

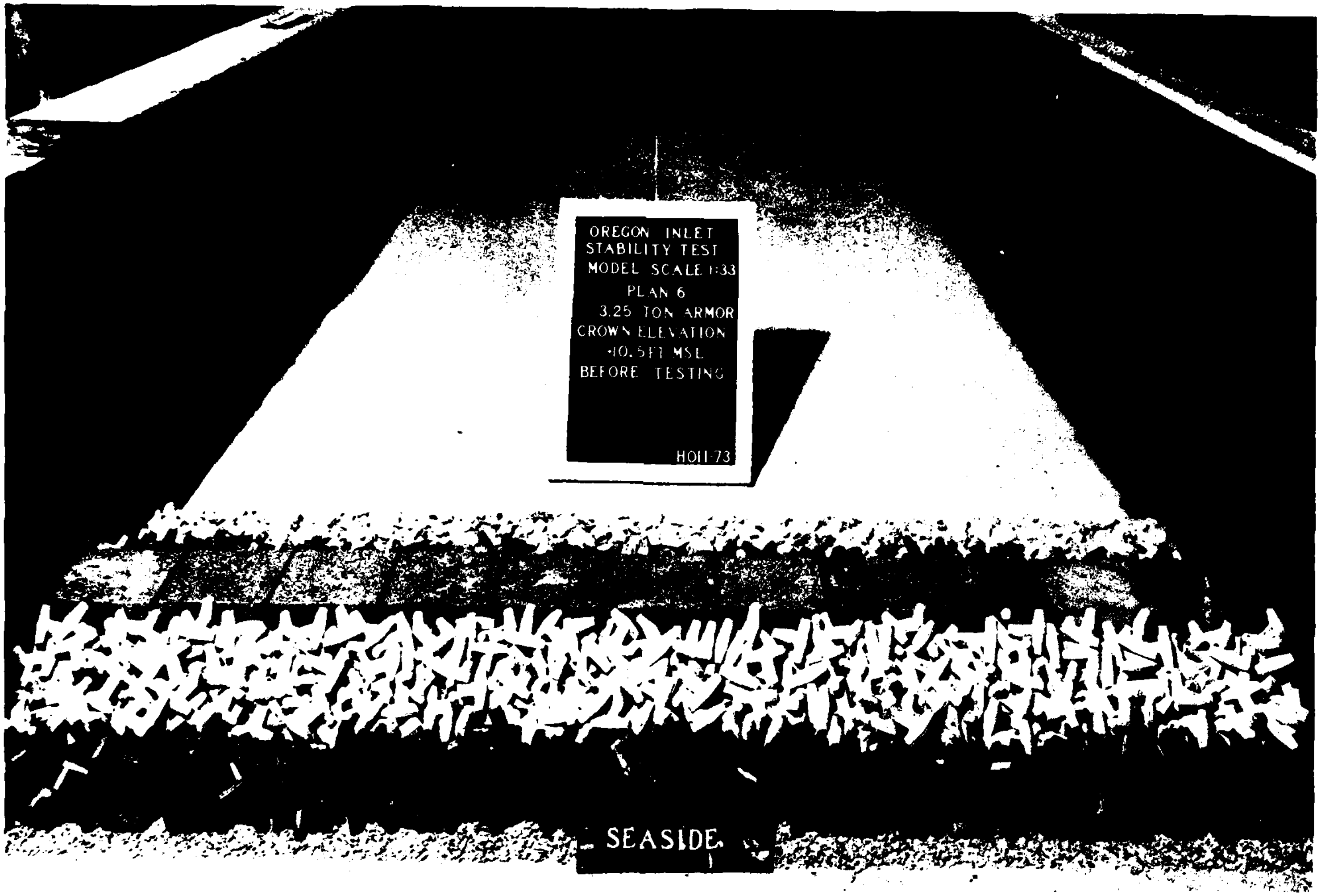

Photo 31. Sea-side view of Plan 6 before wave attack

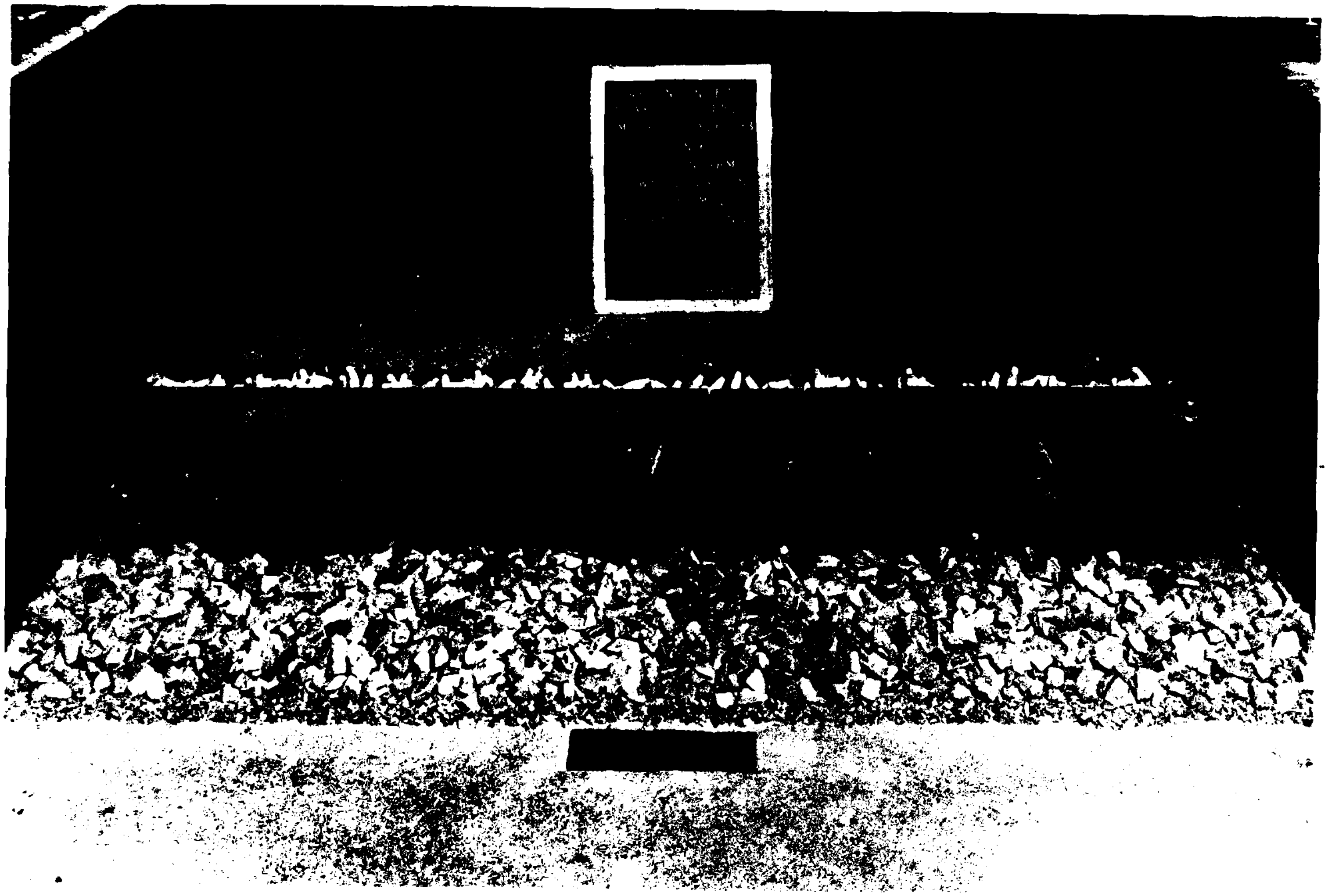

Photo 32. Channel-side view of Plan 6 before wave attack

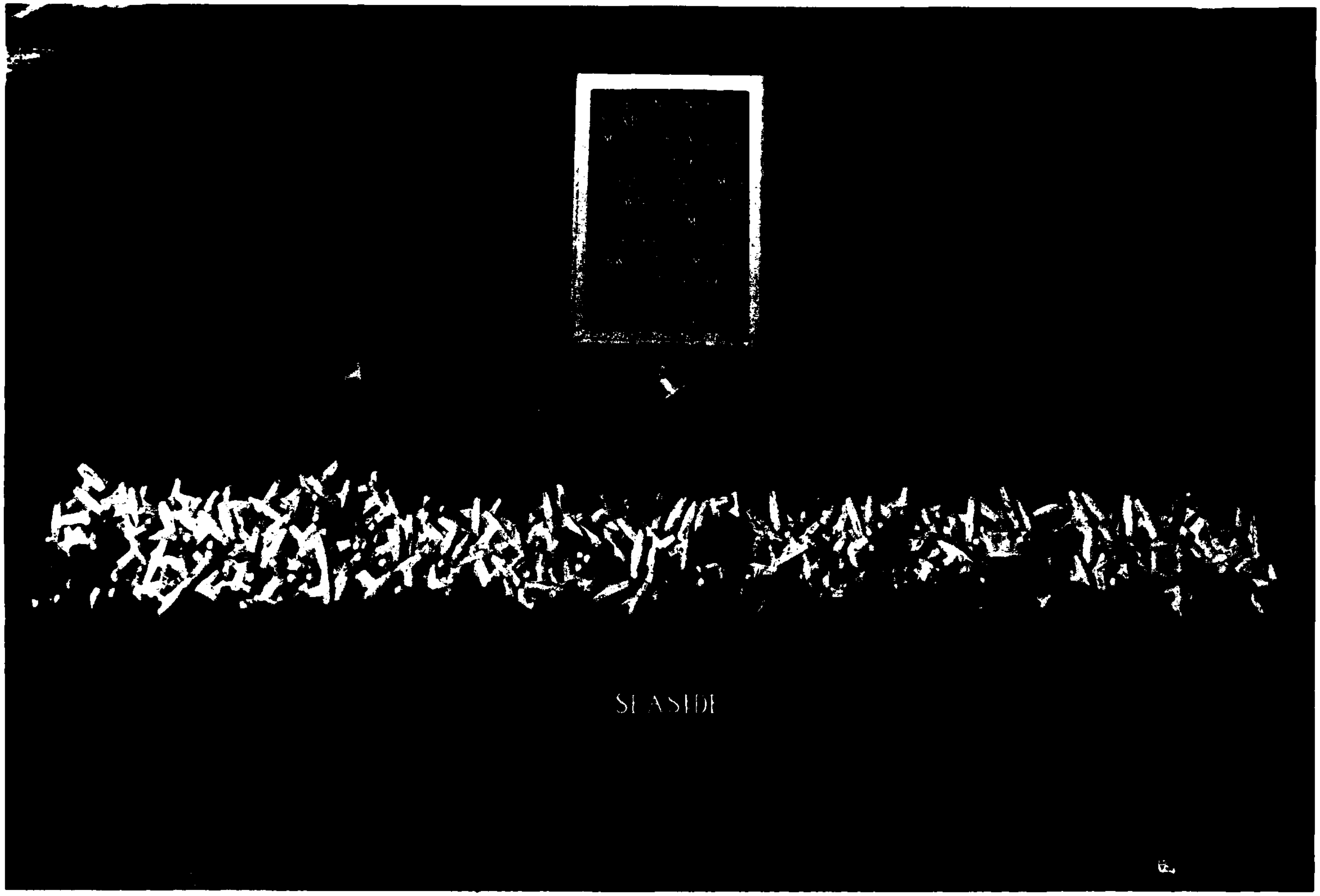

Photo 33. Sea-side view of Plan 6 after attack of 15-sec, 13.6-ft waves at an swl of +5.5 ft NGVD

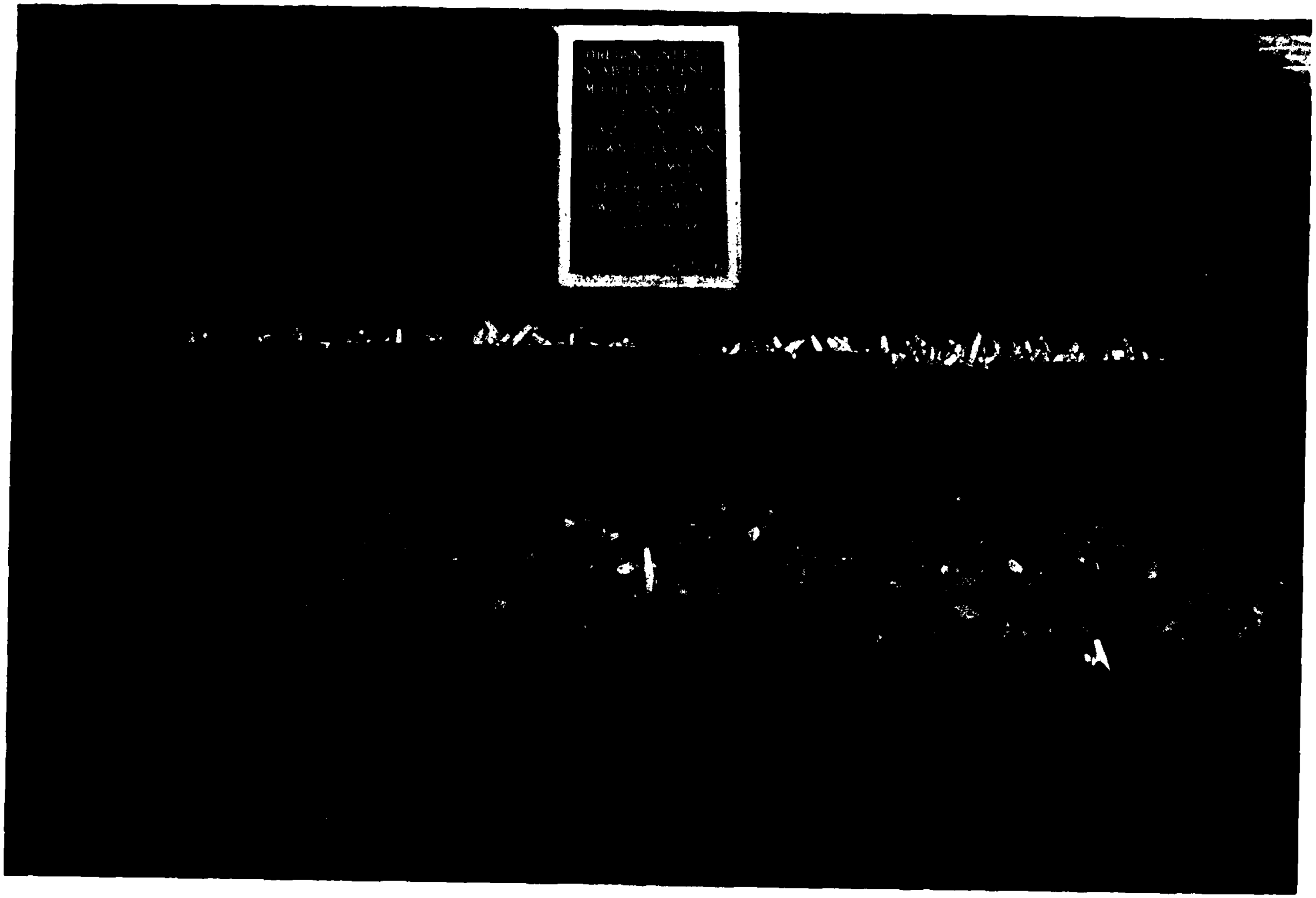

Photo 34. Channel-side view of Plan 6 after attack of 15-sec, 13.6-ft waves at an swl of +5.5 ft NGVD

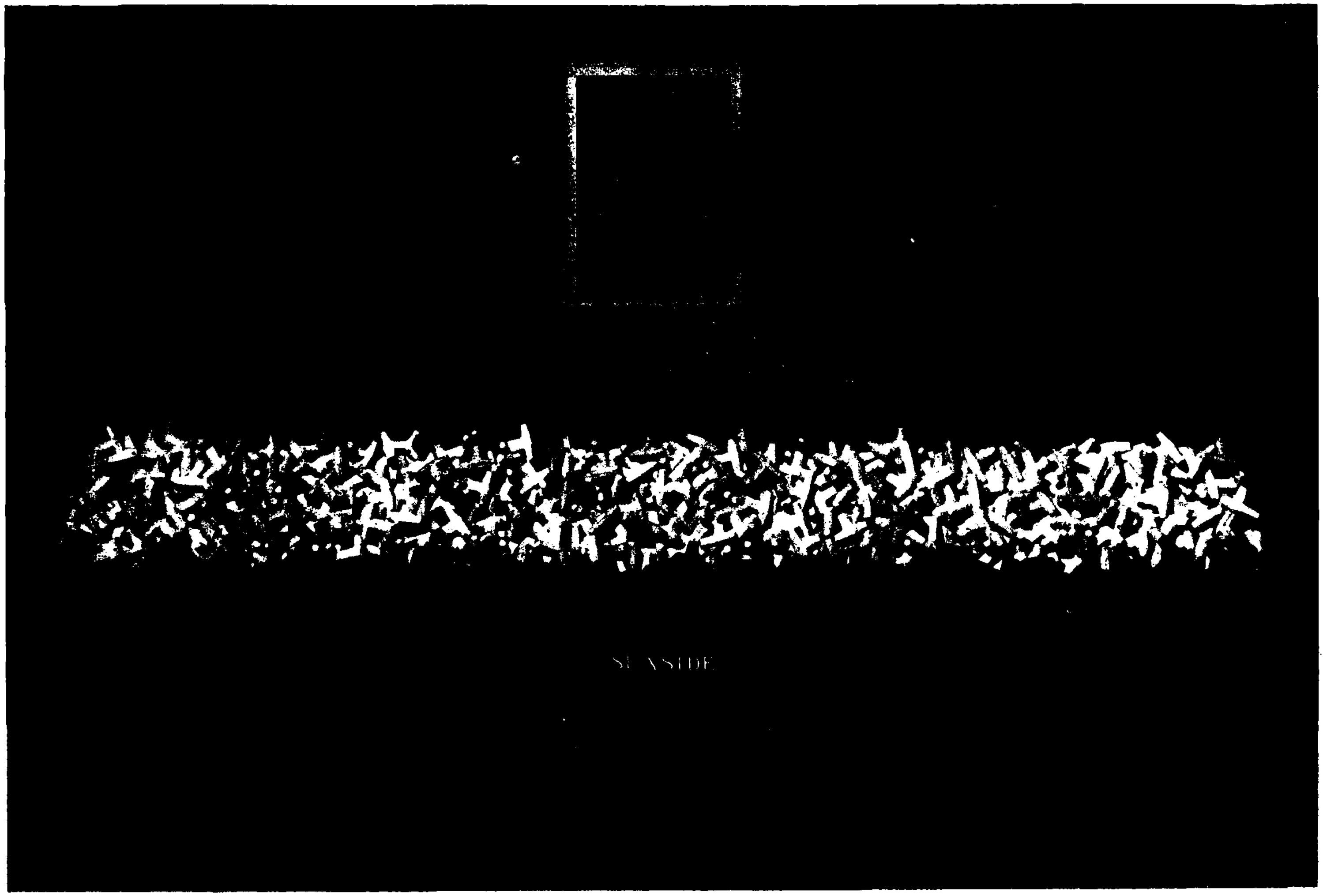

Photo 35. Sea-side view of Plan 7 before wave attack

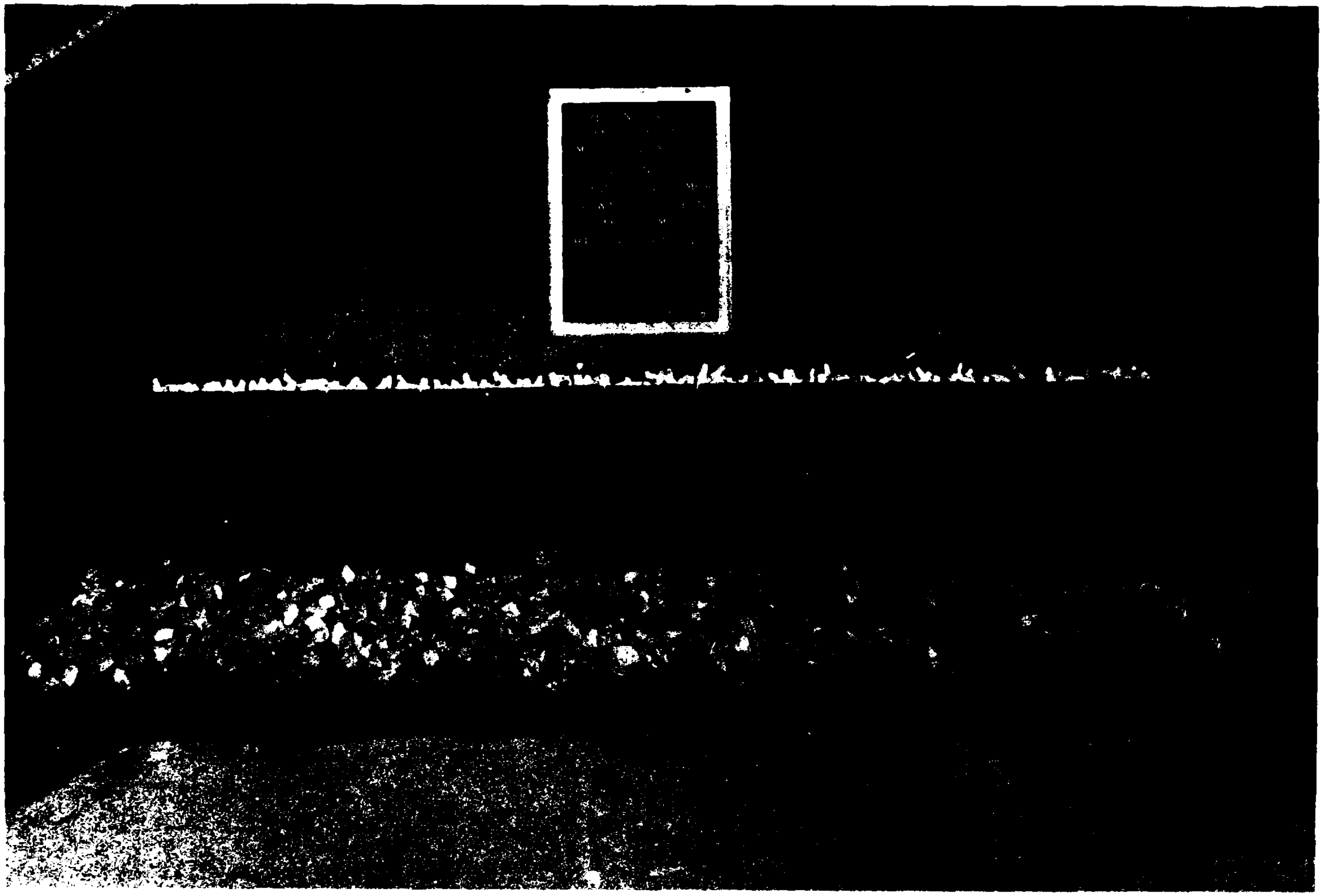

Photo 36. Channel-side view of Plan 7 before wave attack

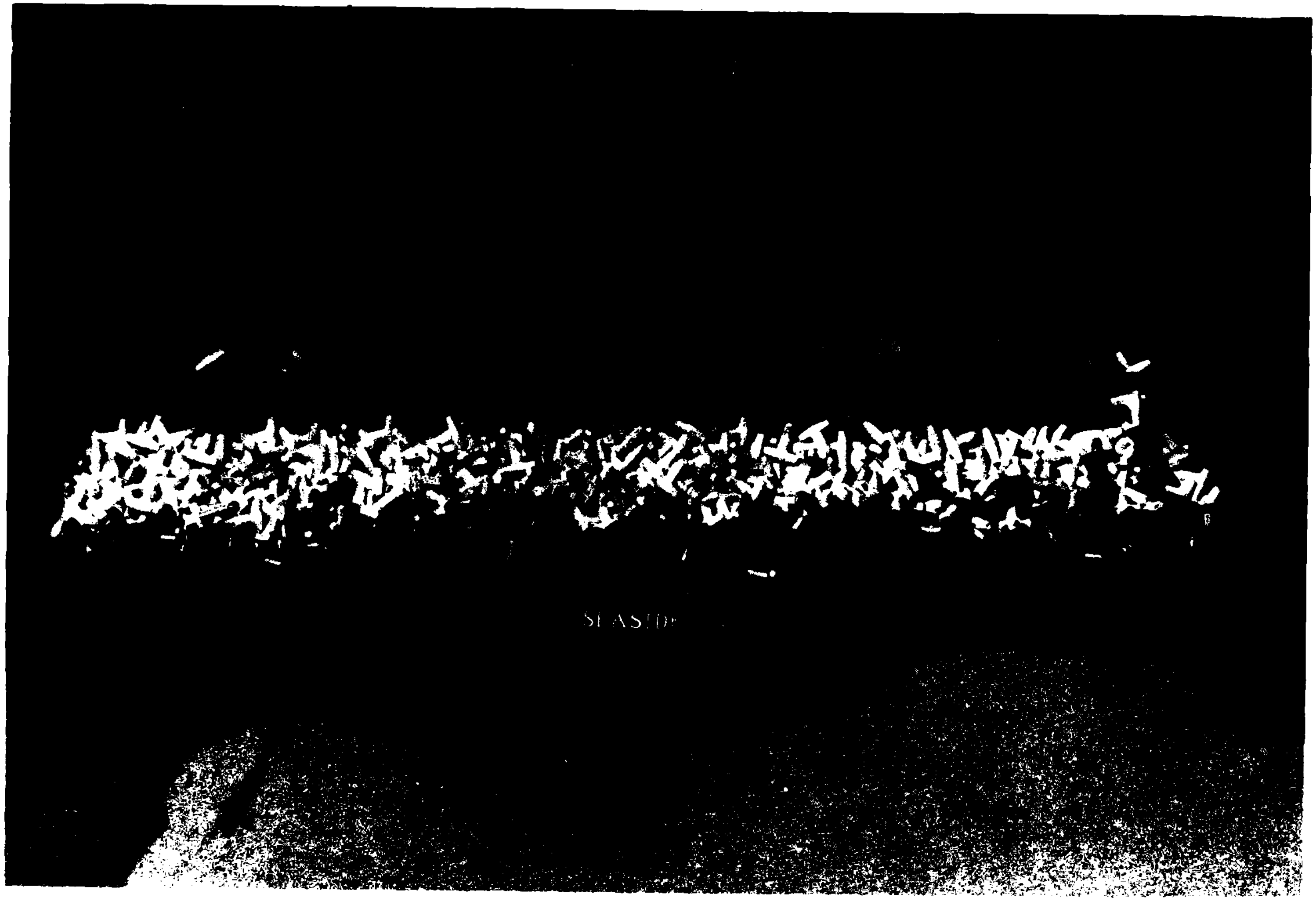

Photo 37. Sea-side view of Plan 7 after attack of 15-sec, 13.6-ft waves at an swl of +5.5 ft NGVD

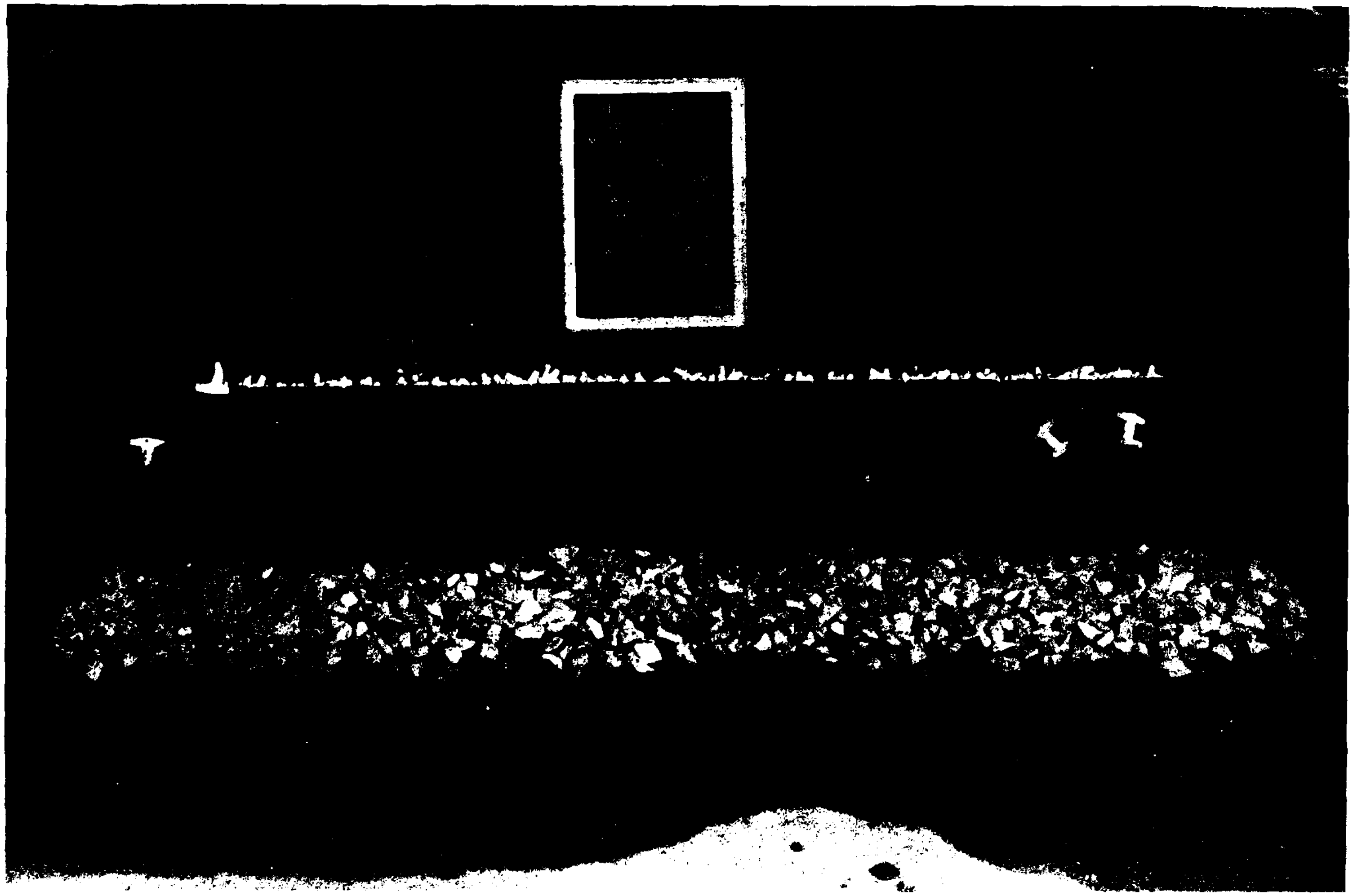

Photo 38. Channel-side view of Plan 7 after attack of 15-sec, 13.6-ft waves at an swl of +5.5 ft NGVD

Photo 39. Sea-side view of Plan 8 before wave attack

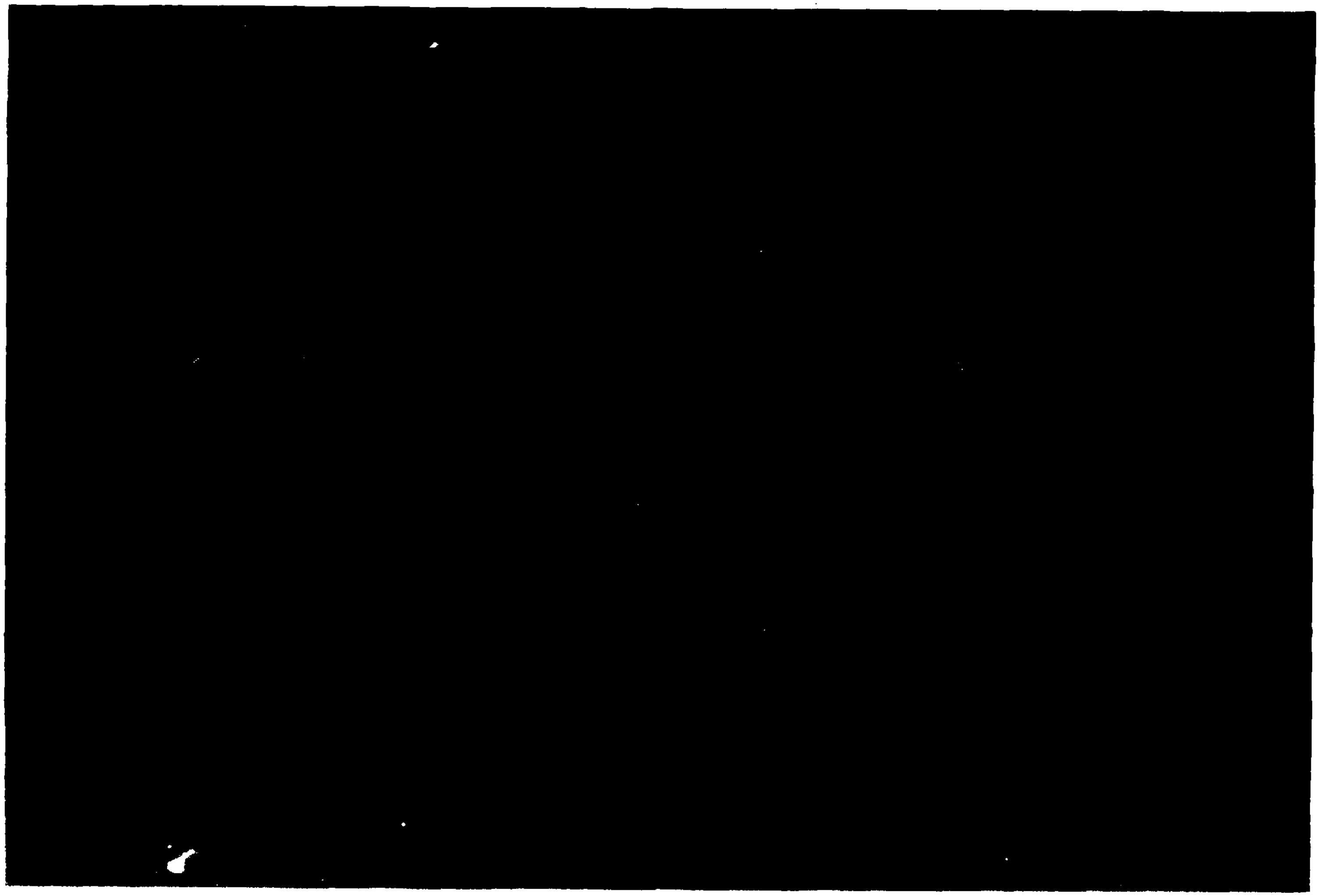

Photo 40. Channel-side view of Plan 8 before wave attack

Photo 41. Sea-side view of Plan 8 after attack of 15-sec, 13.6-ft waves at an swl of +5.5 ft NGVD

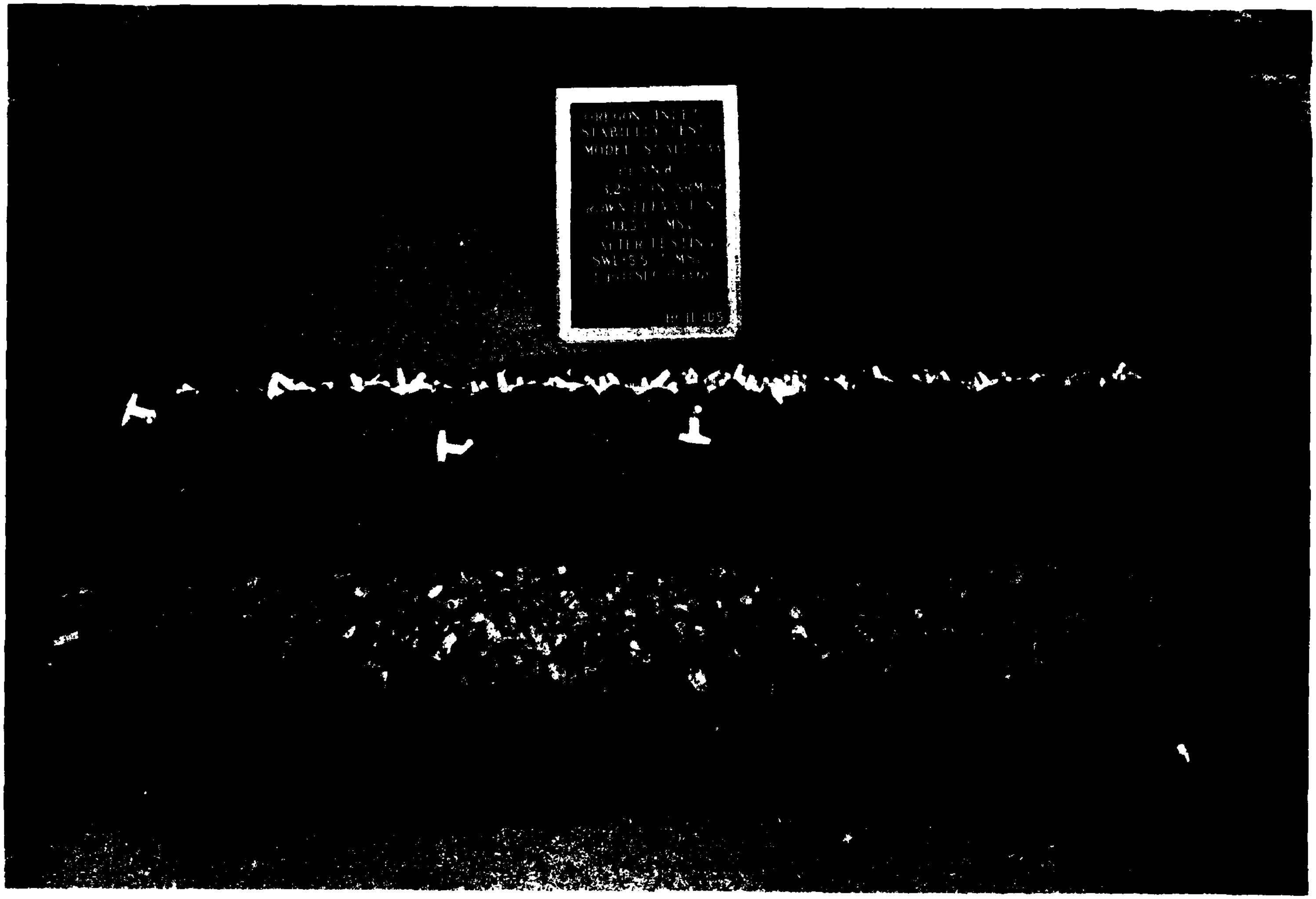

Photo 42. Channel-side view of Plan 8 after attack of 15-sec, 13.6-ft waves at an swl of +5.5 ft NGVD

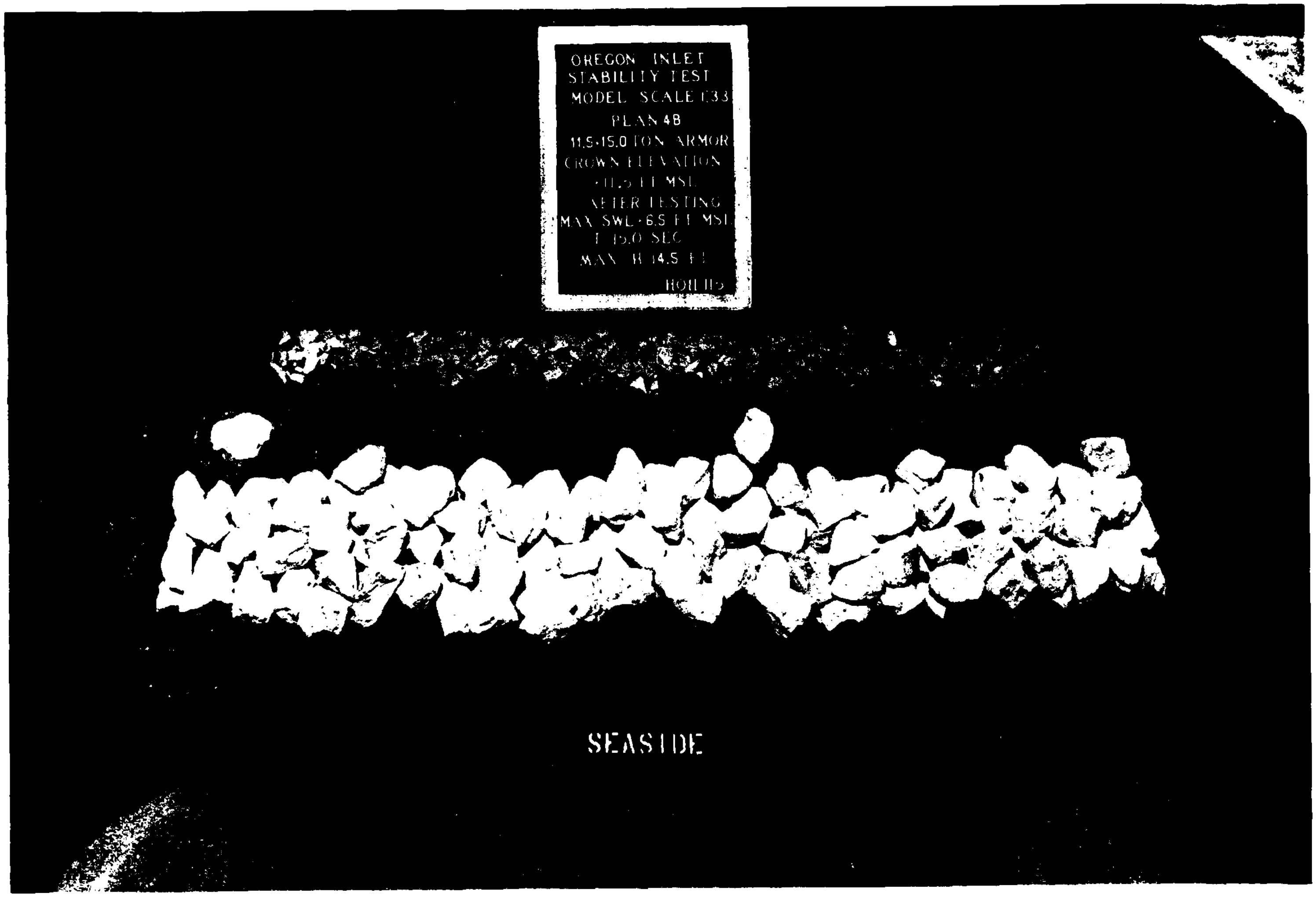

Photo 43. Sea-side view of Plan 4B after testing step 3 of the +6.5 ft NGVD hydrograph

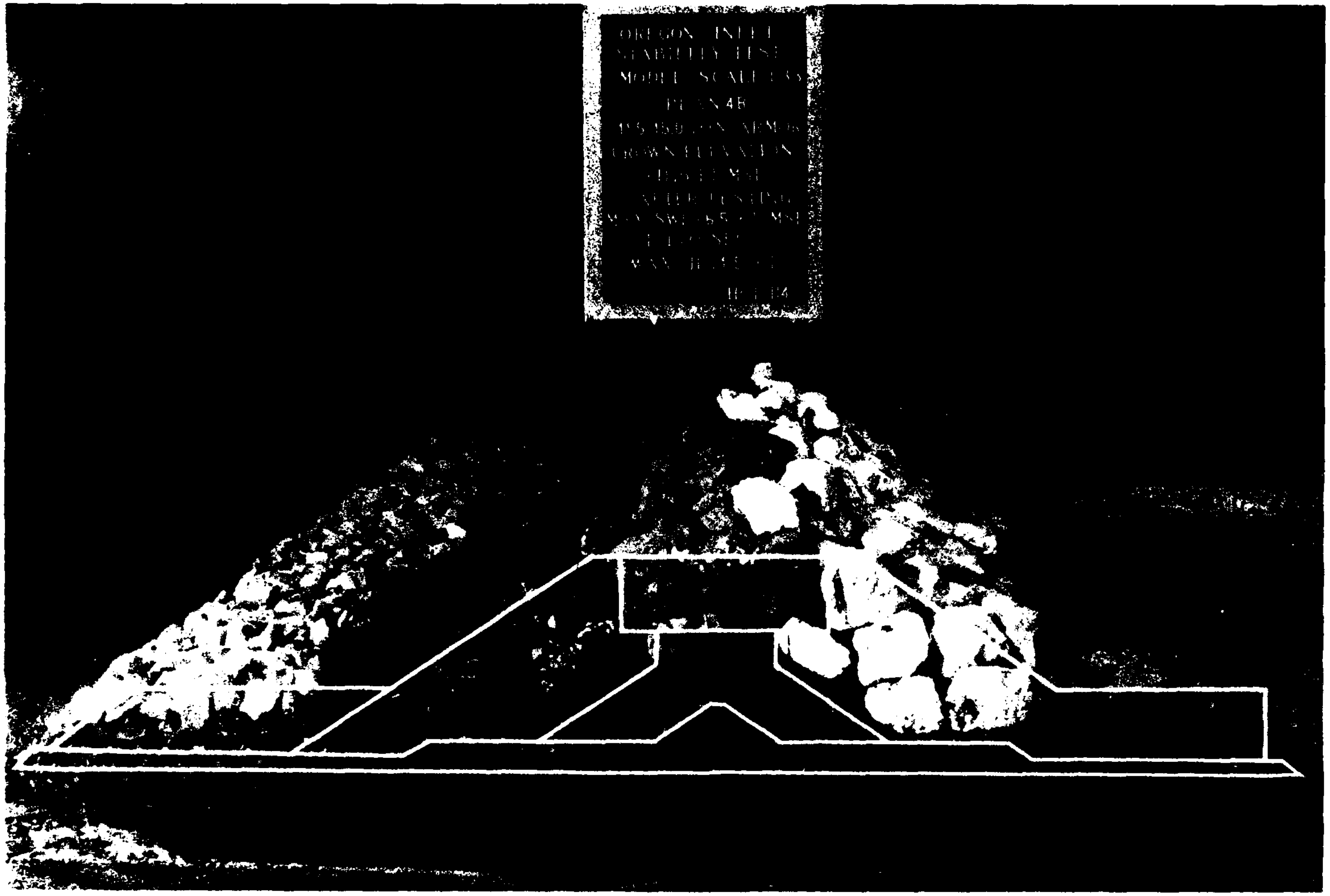

Photo 44. End view of Plan 4B after testing step 3 of the +6.5 ft NGVD hydrograph

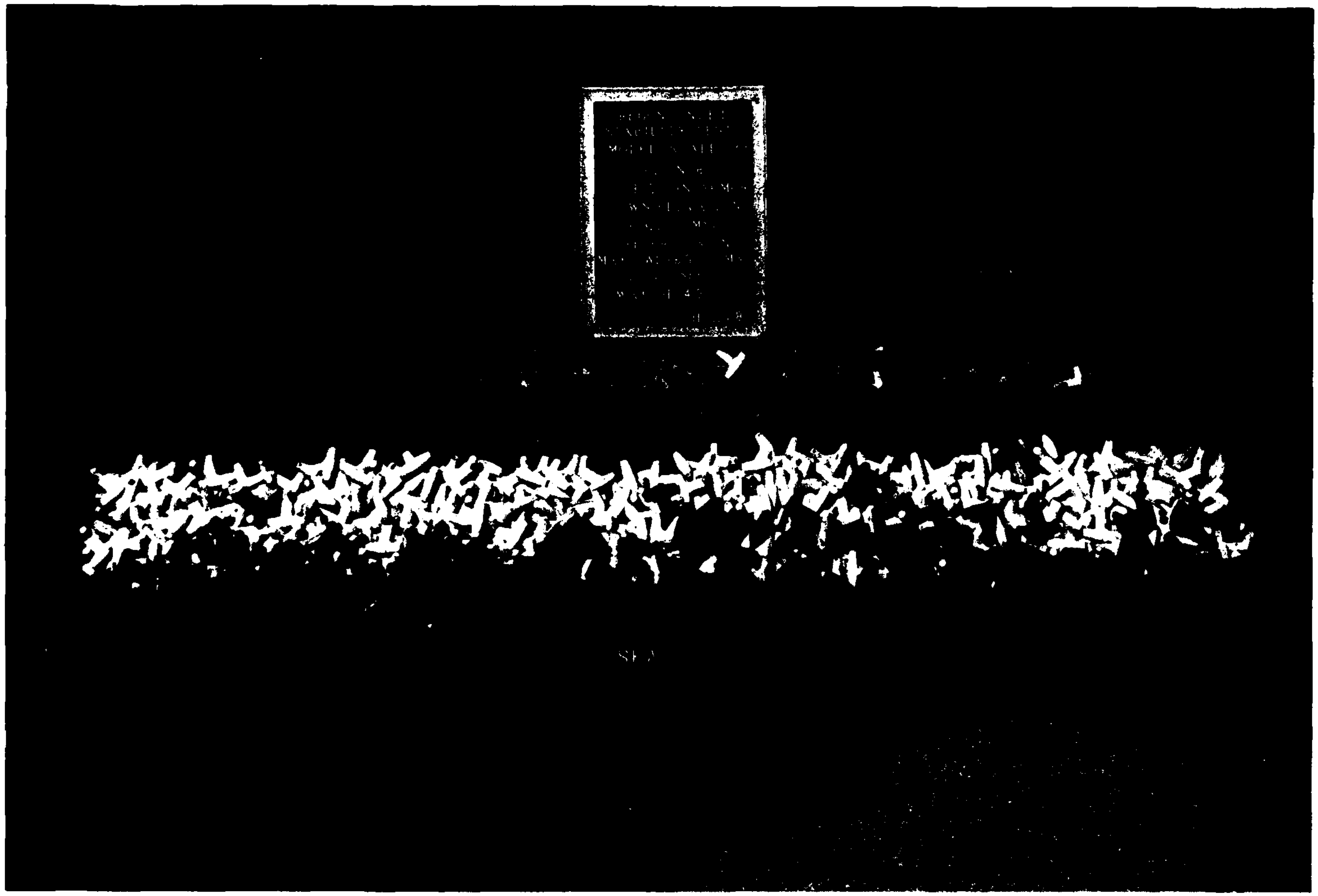

Photo 45. Sea-side view of Plan 8 after testing step 3 of the +6.5 ft NGVD hydrograph

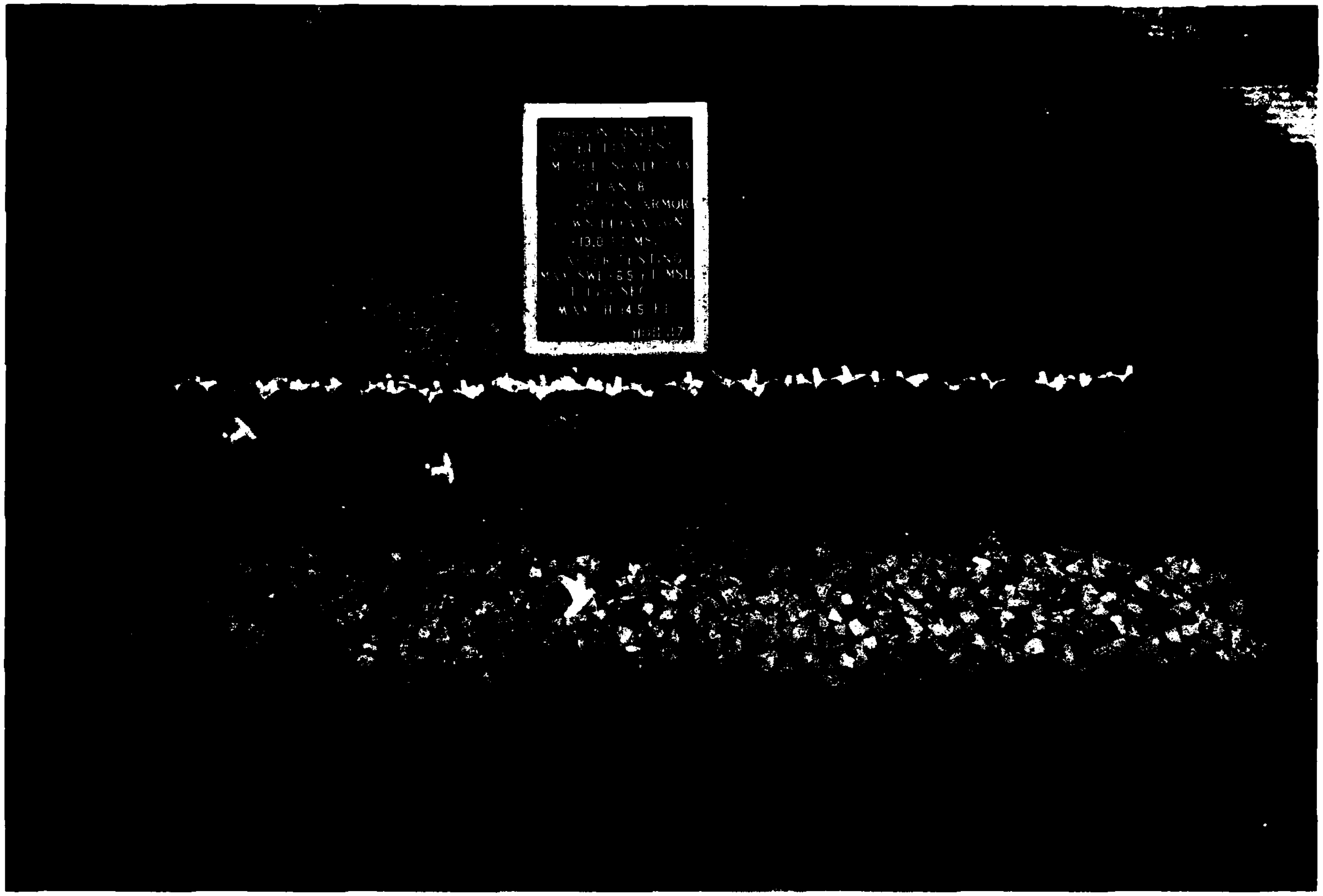

Photo 46. Channel-side view of Plan 8 after testing step 3 of the +6.5 ft NGVD hydrograph

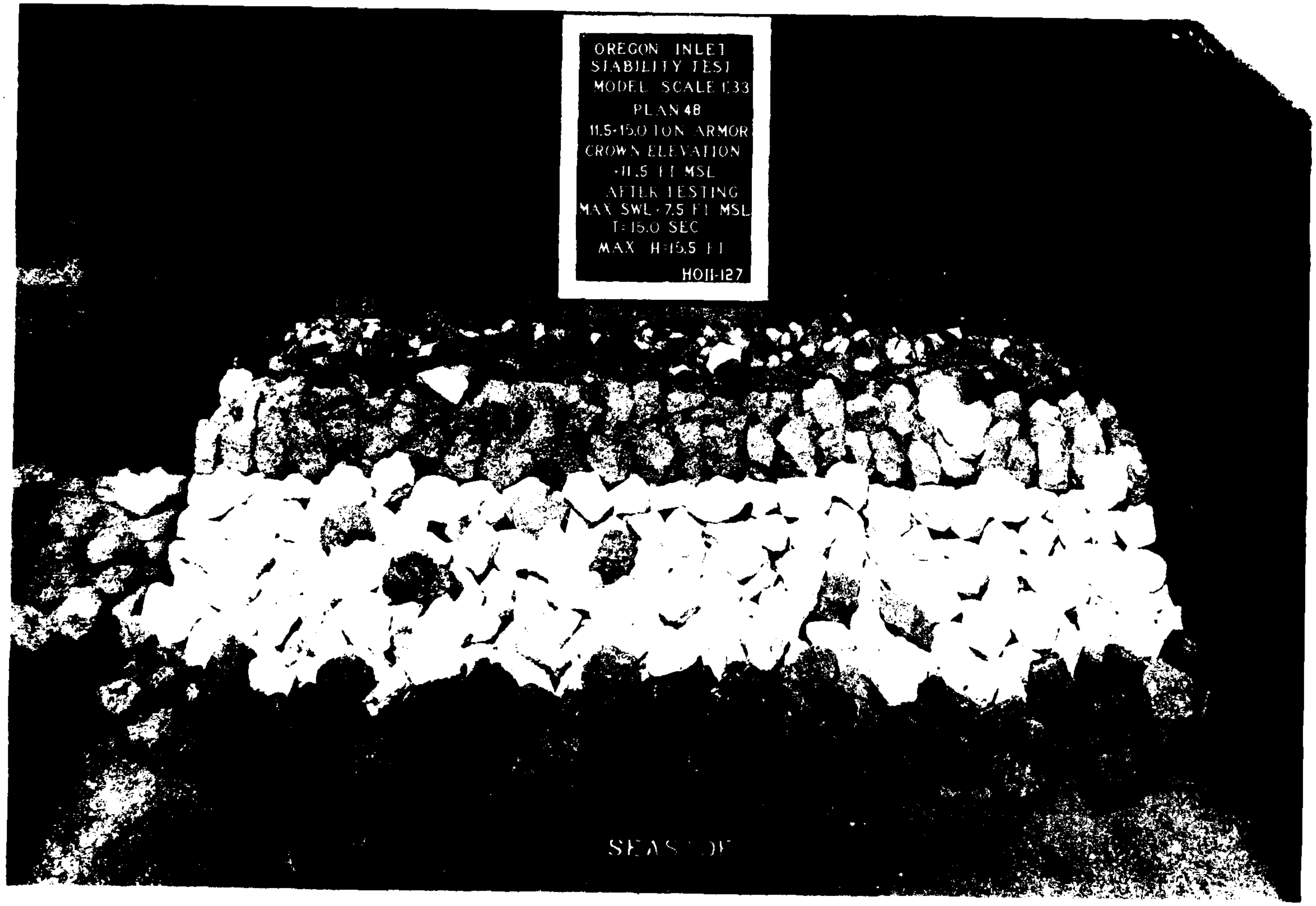

Photo 47. Sea-side view of Plan 4B after testing step 5 of the +7.5 ft NGVD hydrograph

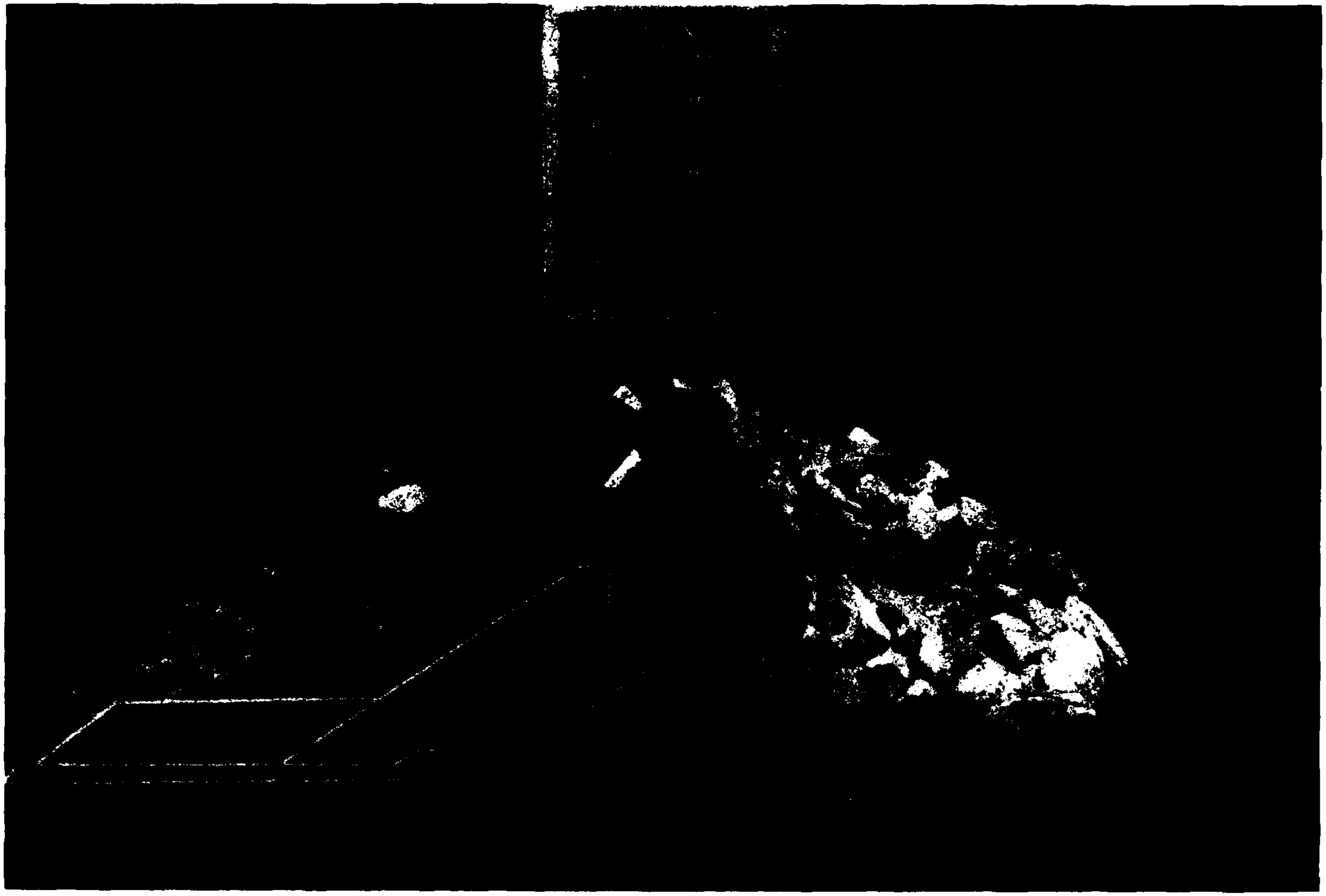

Photo 48. End view of Plan 4B after testing step 5 of the +7.5 ft NGVD hydrograph

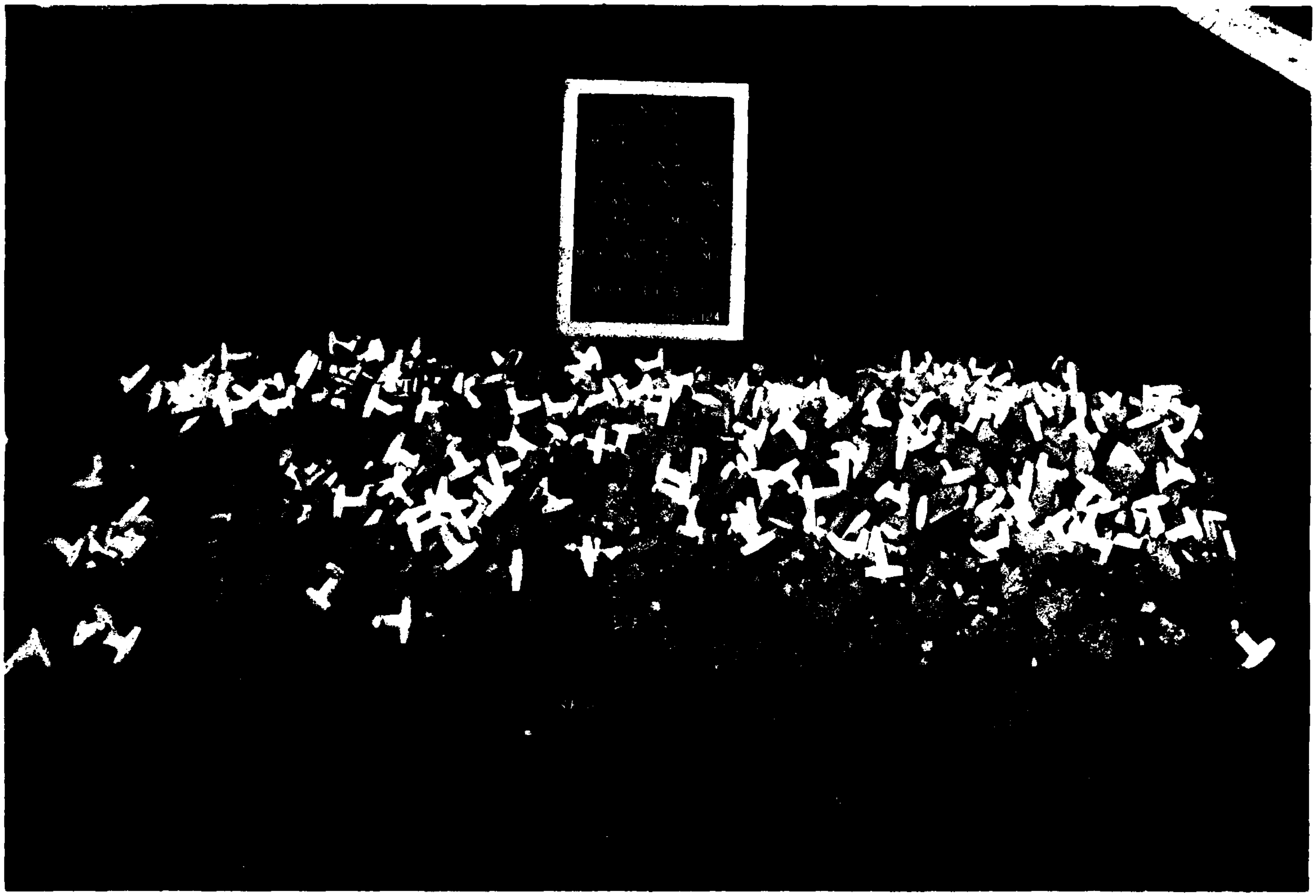

Photo 49. Sea-side view of Plan 8 after testing step 5 of the +7.5 ft NGVD hydrograph

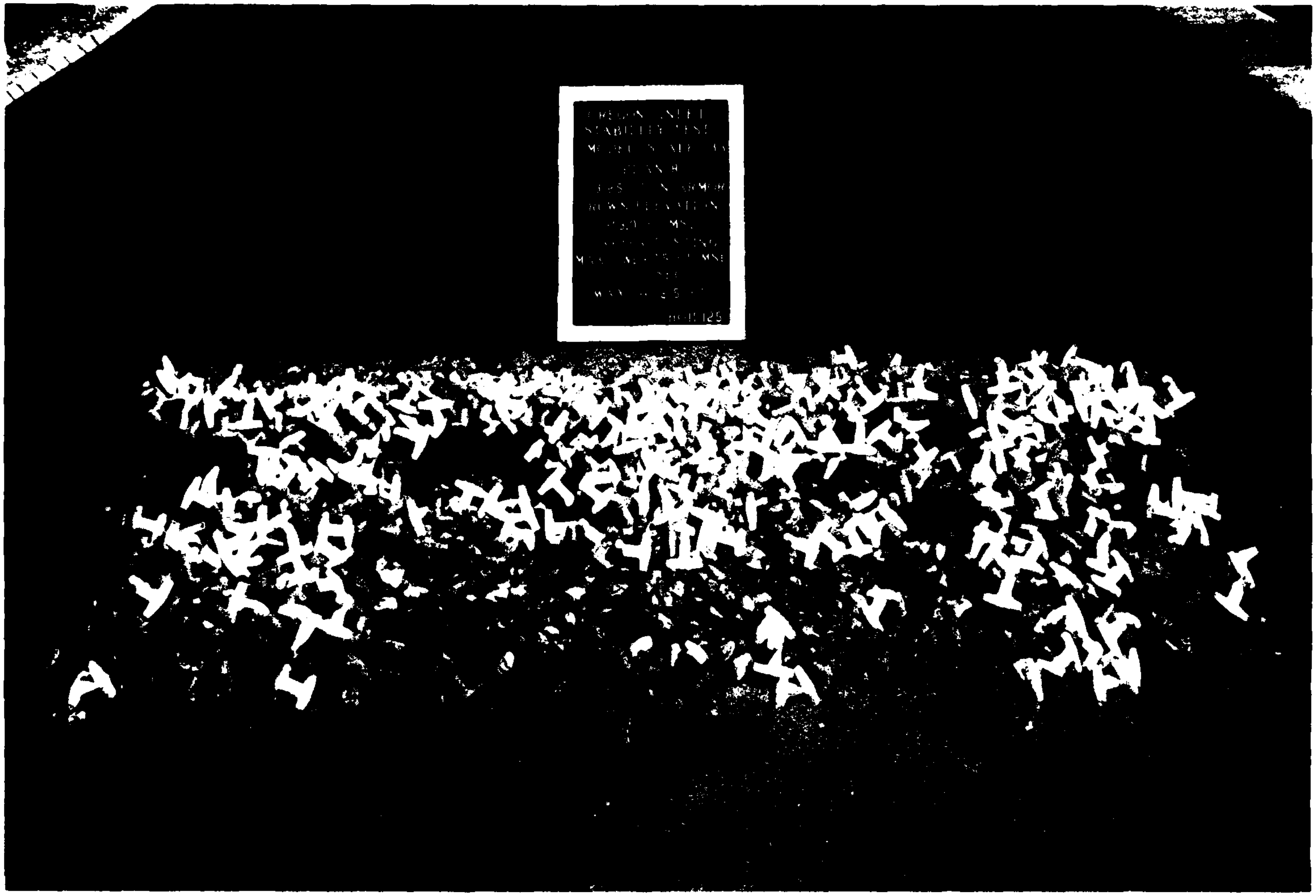

Photo 50. Channel-side view of Plan 8 after testing step 5 of the +7.5 ft NGVD hydrograph

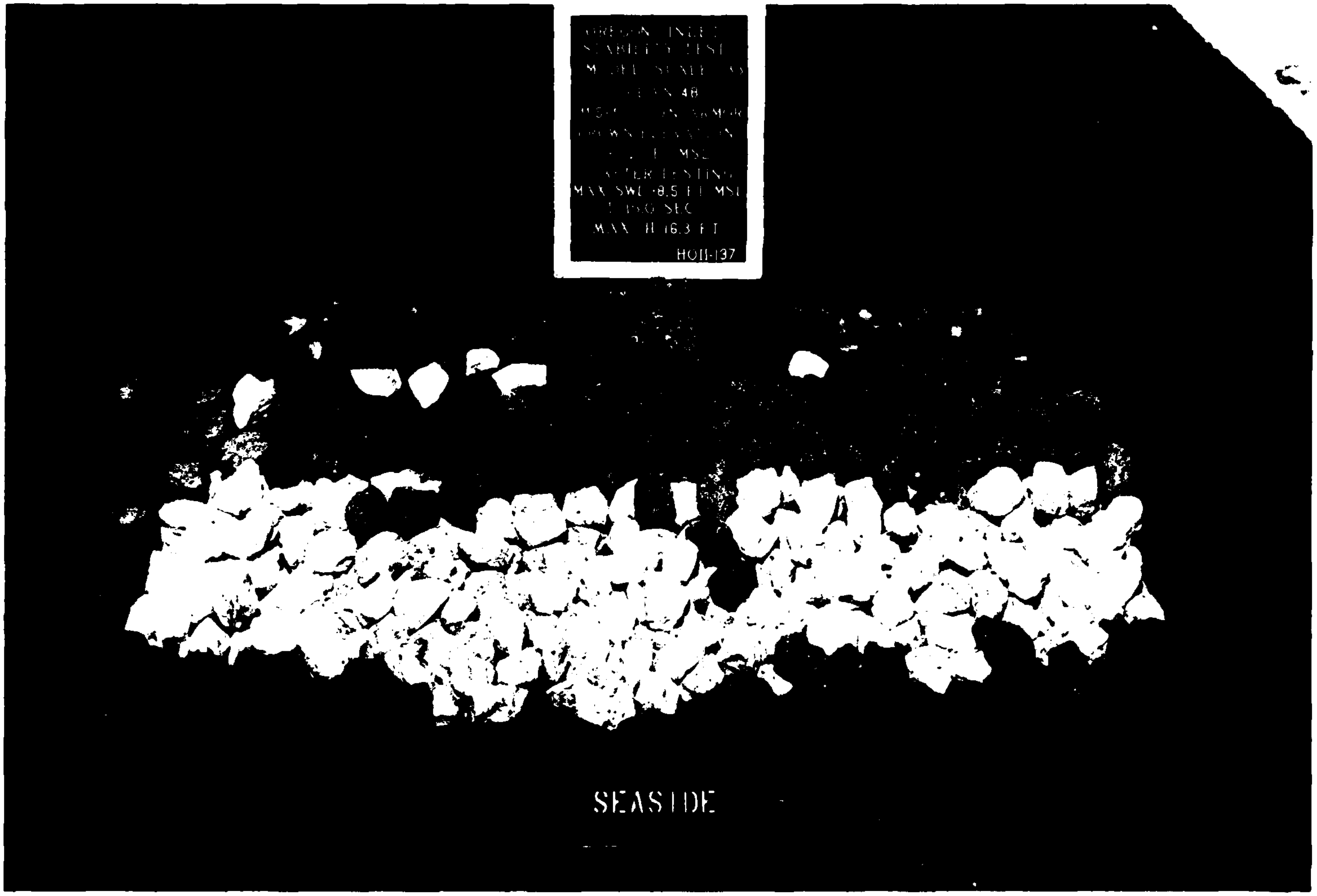

Photo 51. Sea-side view of Plan 4B after testing step 7 of the +8.5 ft NGVD hydrograph

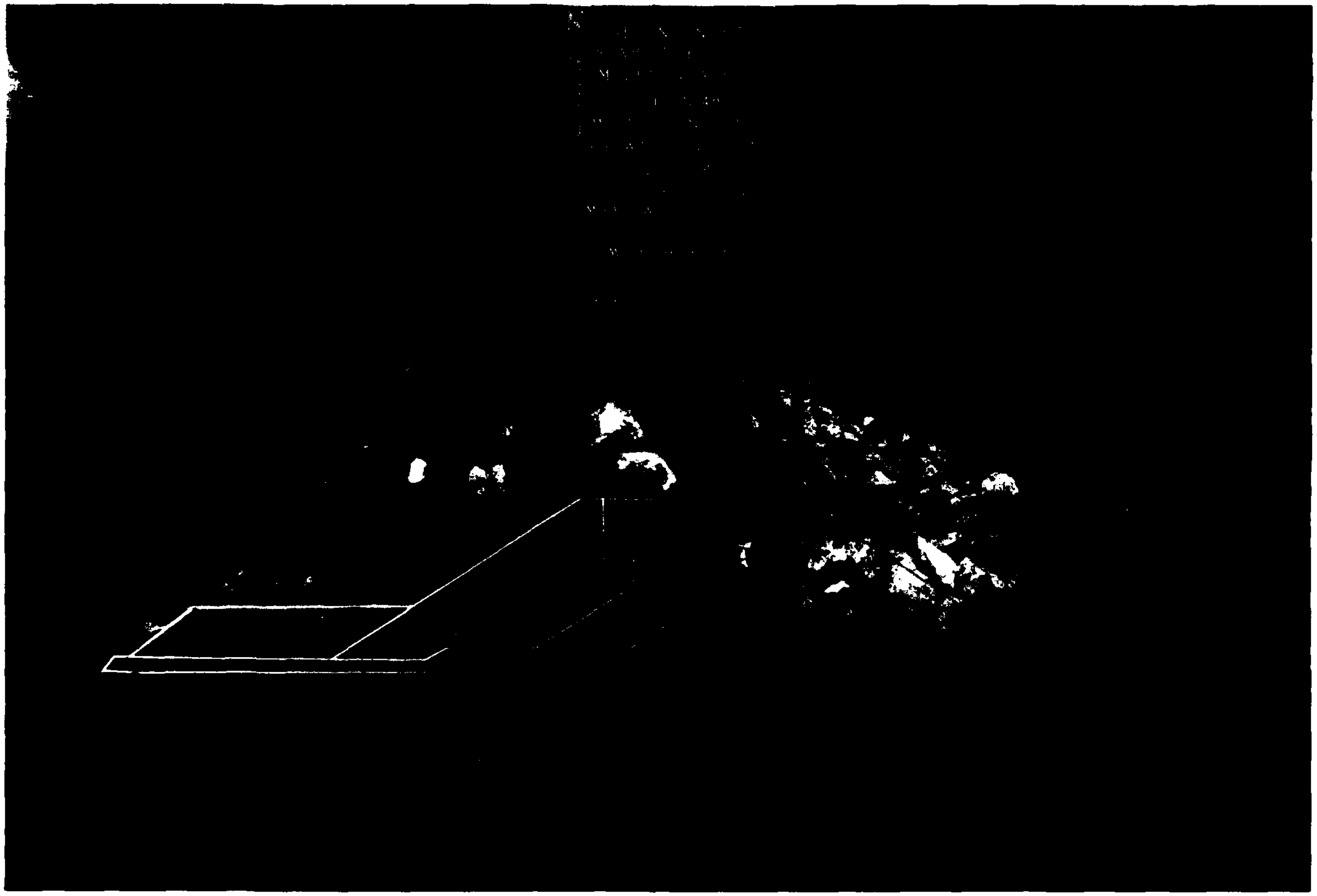

Photo 52. End view of Plan 4B after testing step 7 of the +8.5 ft NGVD hydrograph

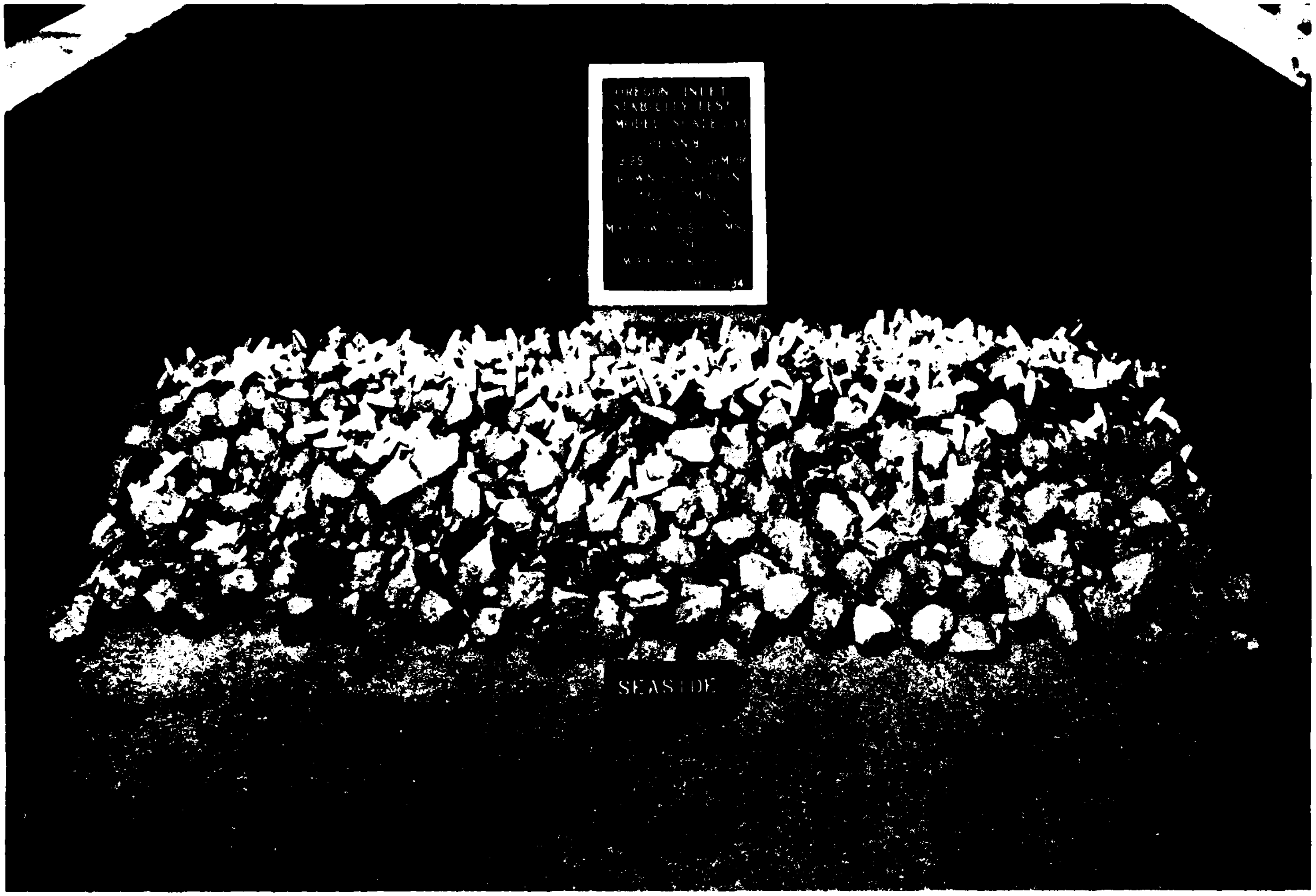

Photo 53. Sea-side view of Plan 8 after testing step 7 of the +8.5 ft NGVD hydrograph

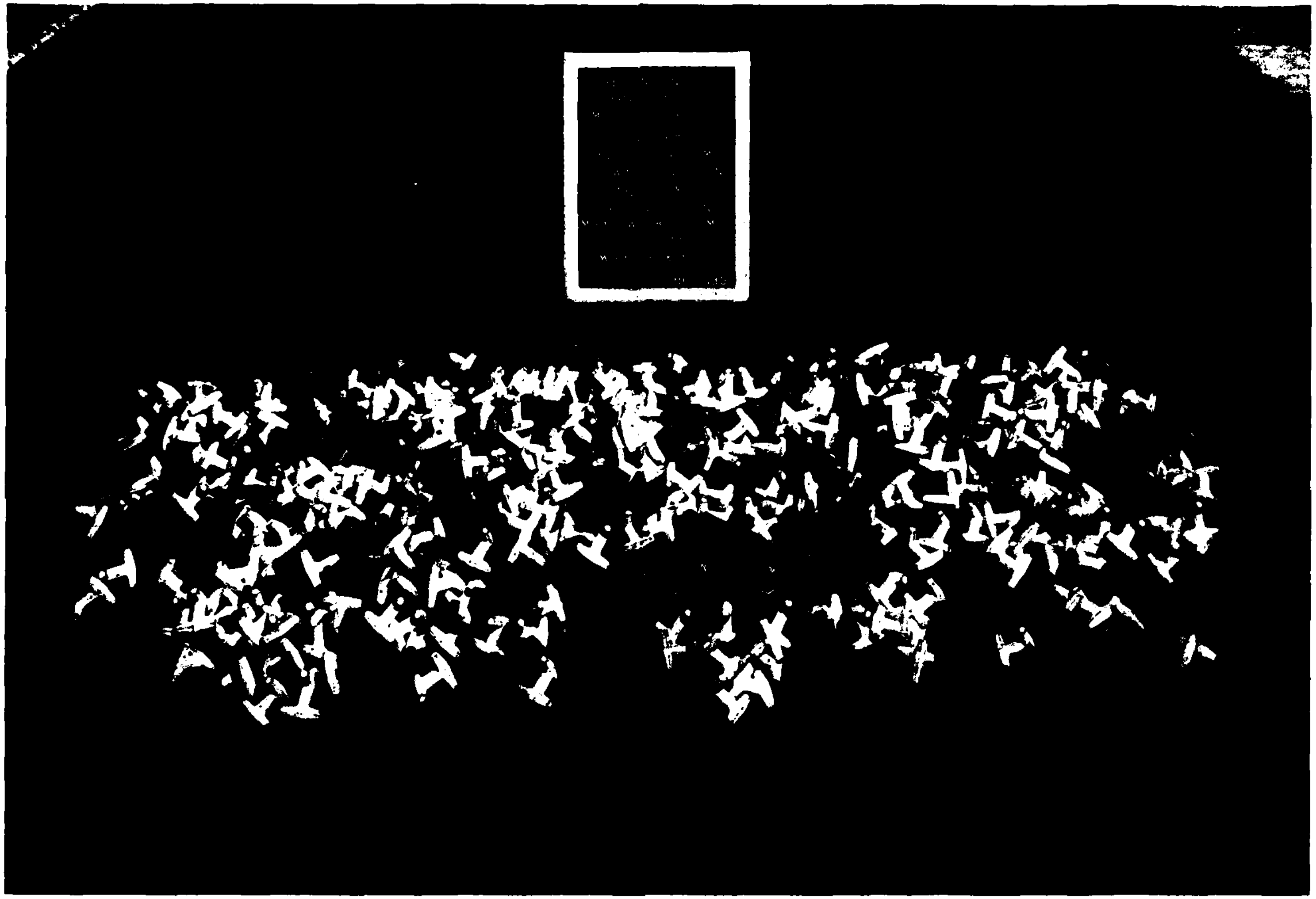

Photo 54. Channel-side view of Plan 8 after testing step 7 of the +8.5 ft NGVD hydrograph

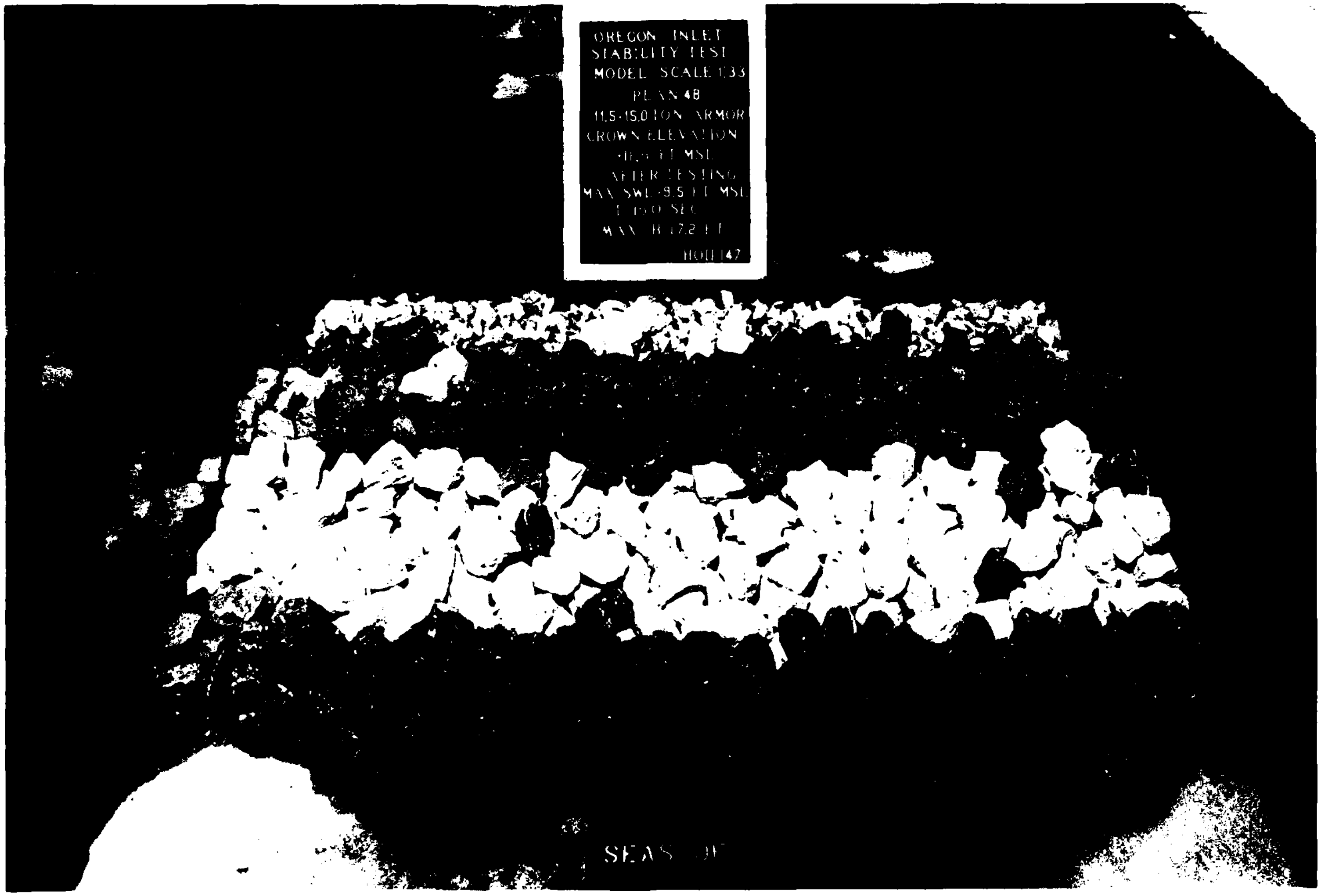

Photo 55. Sea-side view of Plan 4B after testing step 9 of the +9.5 ft NGVD hydrograph

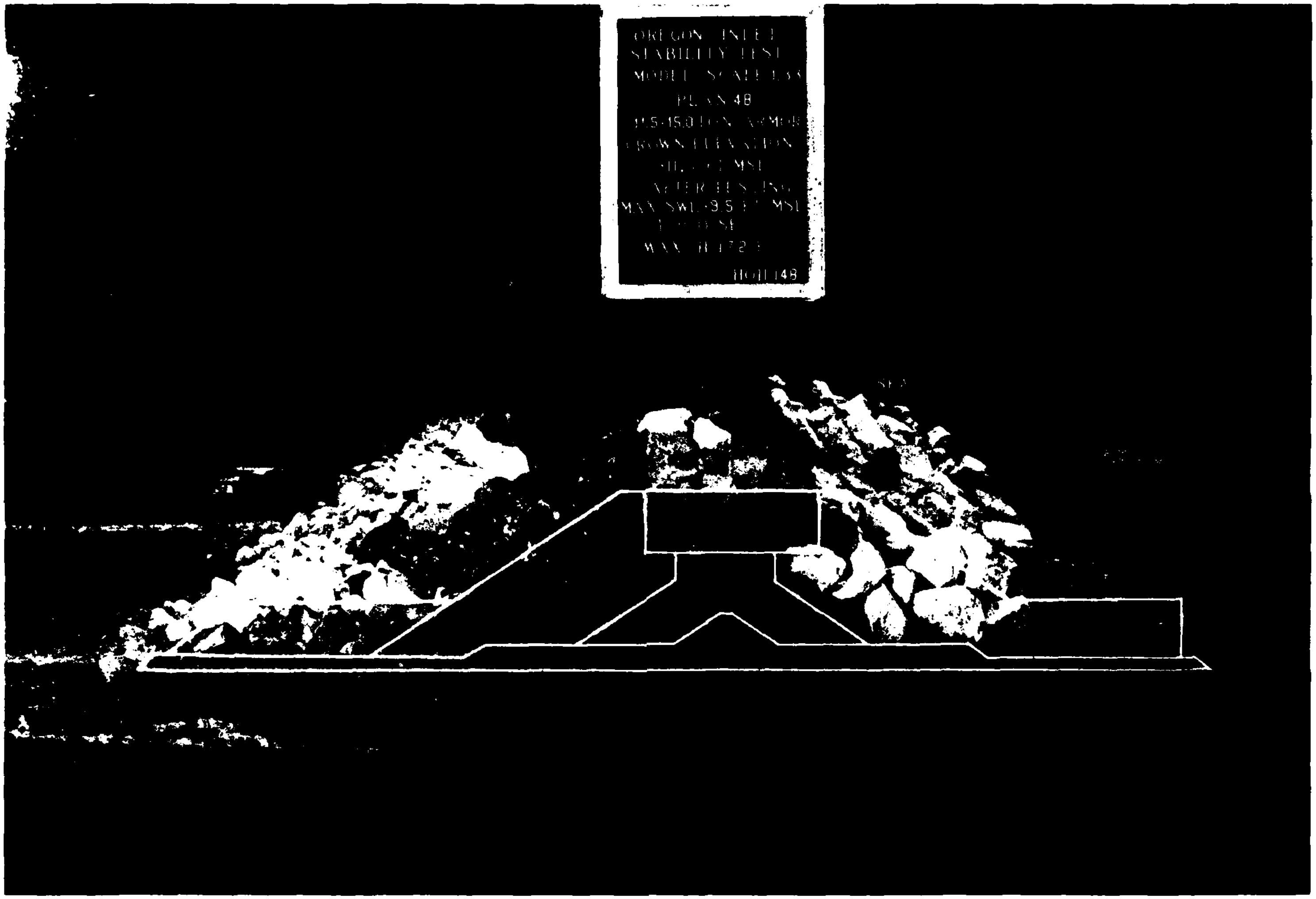

Photo 56. End view of Plan 4B after testing step 9 of the +9.5 ft NGVD hydrograph

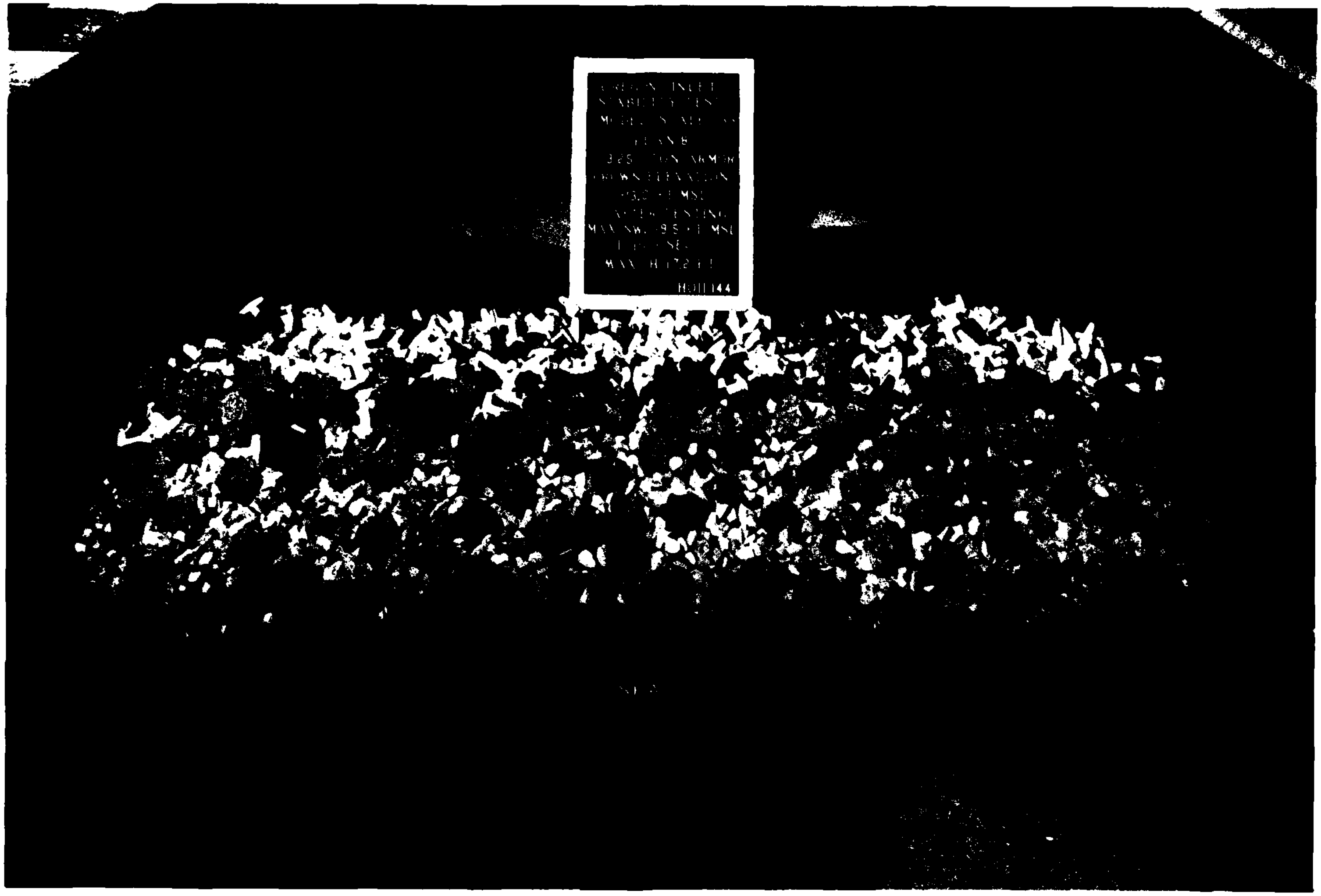

Photo 57. Sea-side view of Plan 8 after testing step 9 of the +9.5 ft NGVD hydrograph

Photo 58. Channel-side view of Plan 8 after testing step 9 of the +9.5 ft NGVD hydrograph

Photo 59. Sea-side view of Plan 4B after testing step 11 of the +10.5 ft NGVD hydrograph

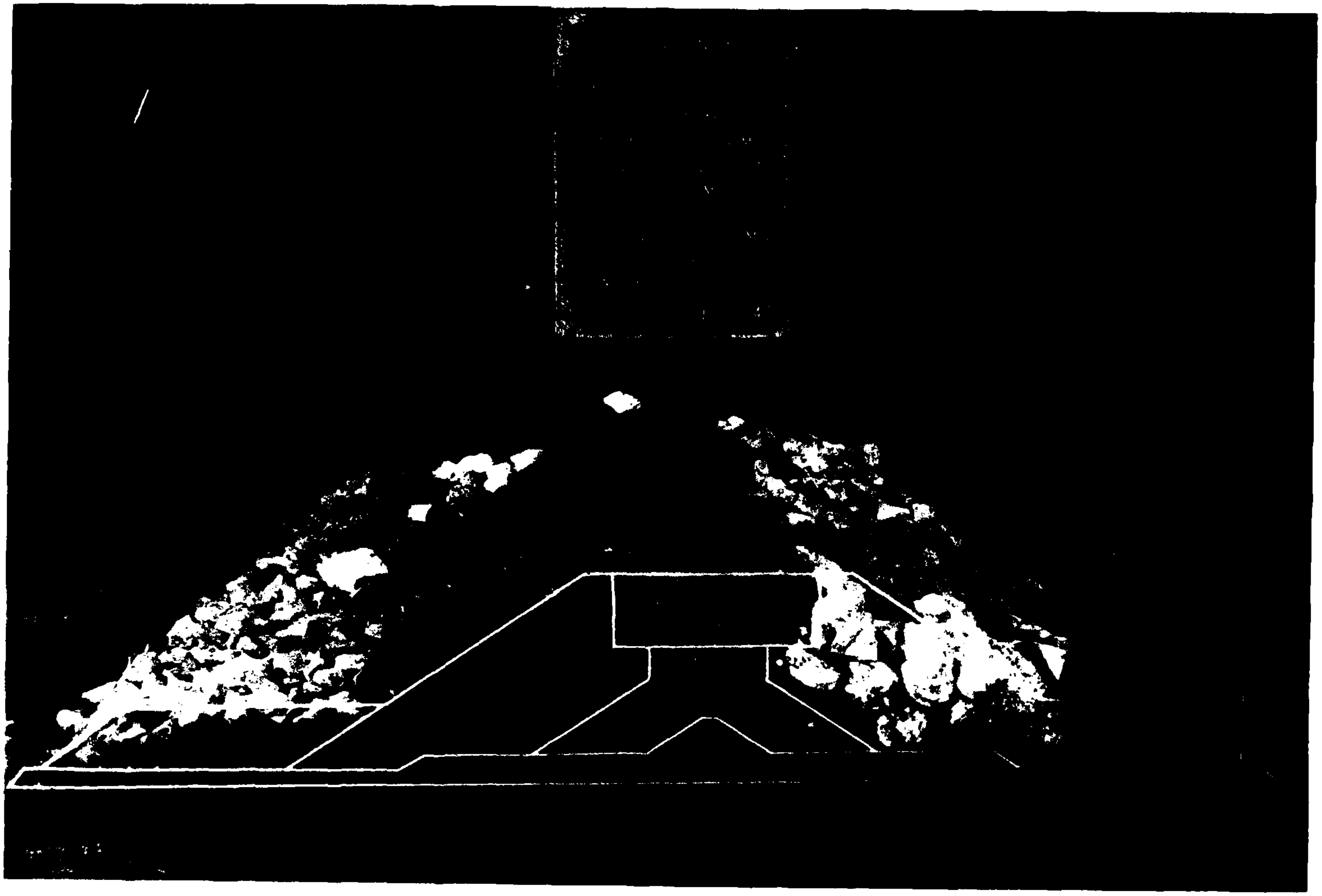

Photo 60. End view of Plan 4B after testing step 11 of the +10.5 ft NGVD hydrograph

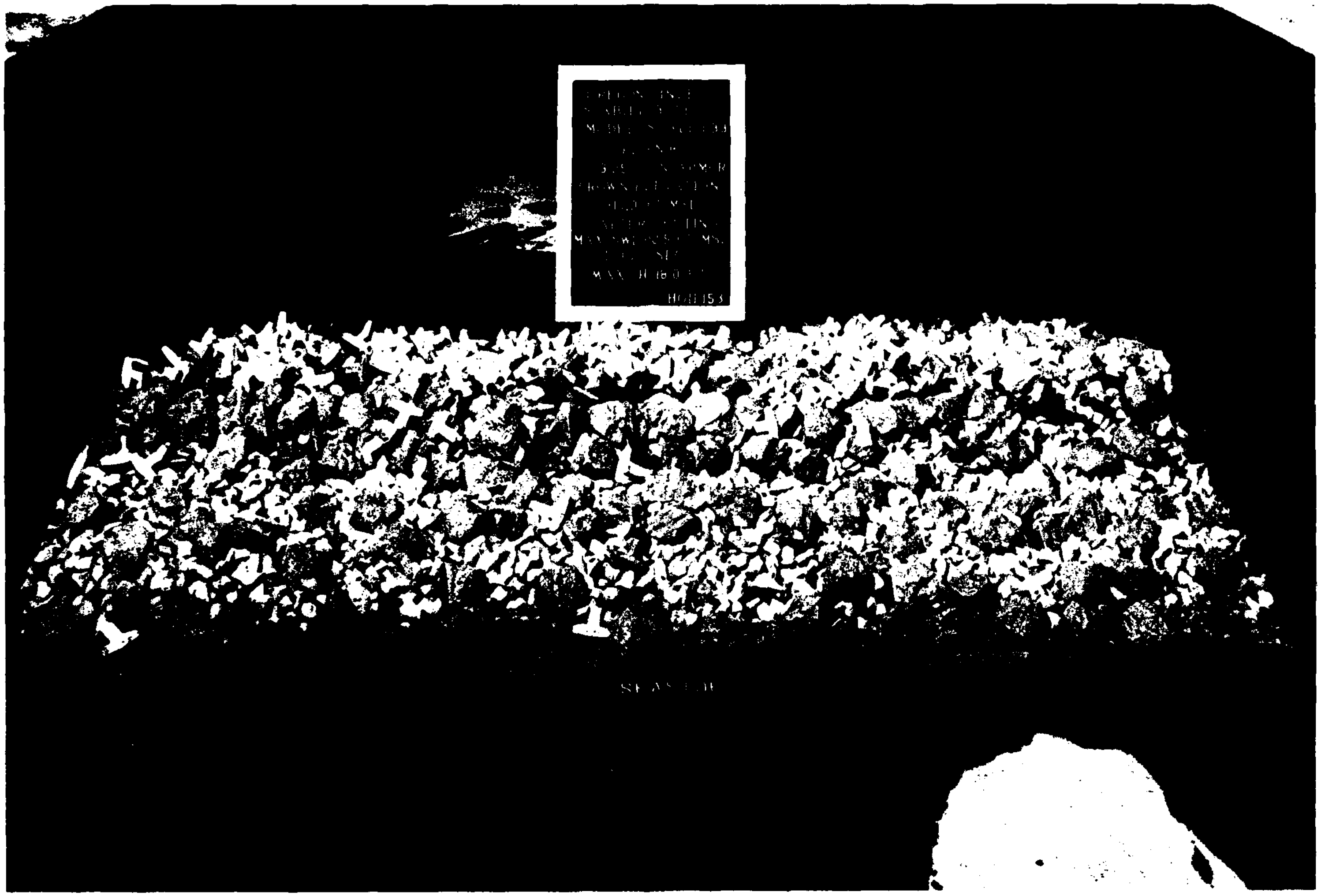

Photo 61. Sea-side view of Plan 8 after testing step 11 of the +10.5 ft NGVD hydrograph

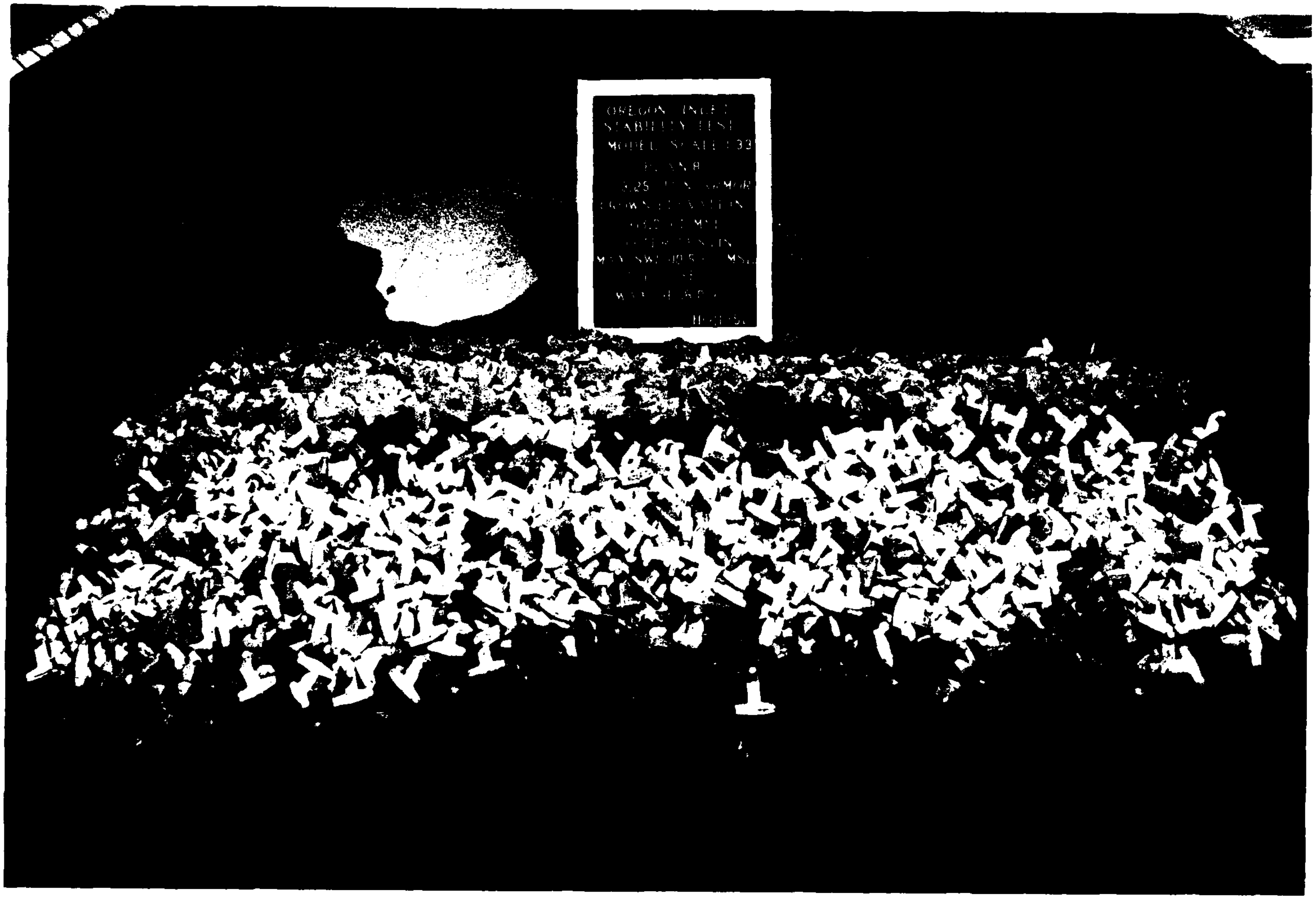

Photo 62. Channel-side view of Plan 8 after testing step 11 of the +10.5 ft NGVD hydrograph

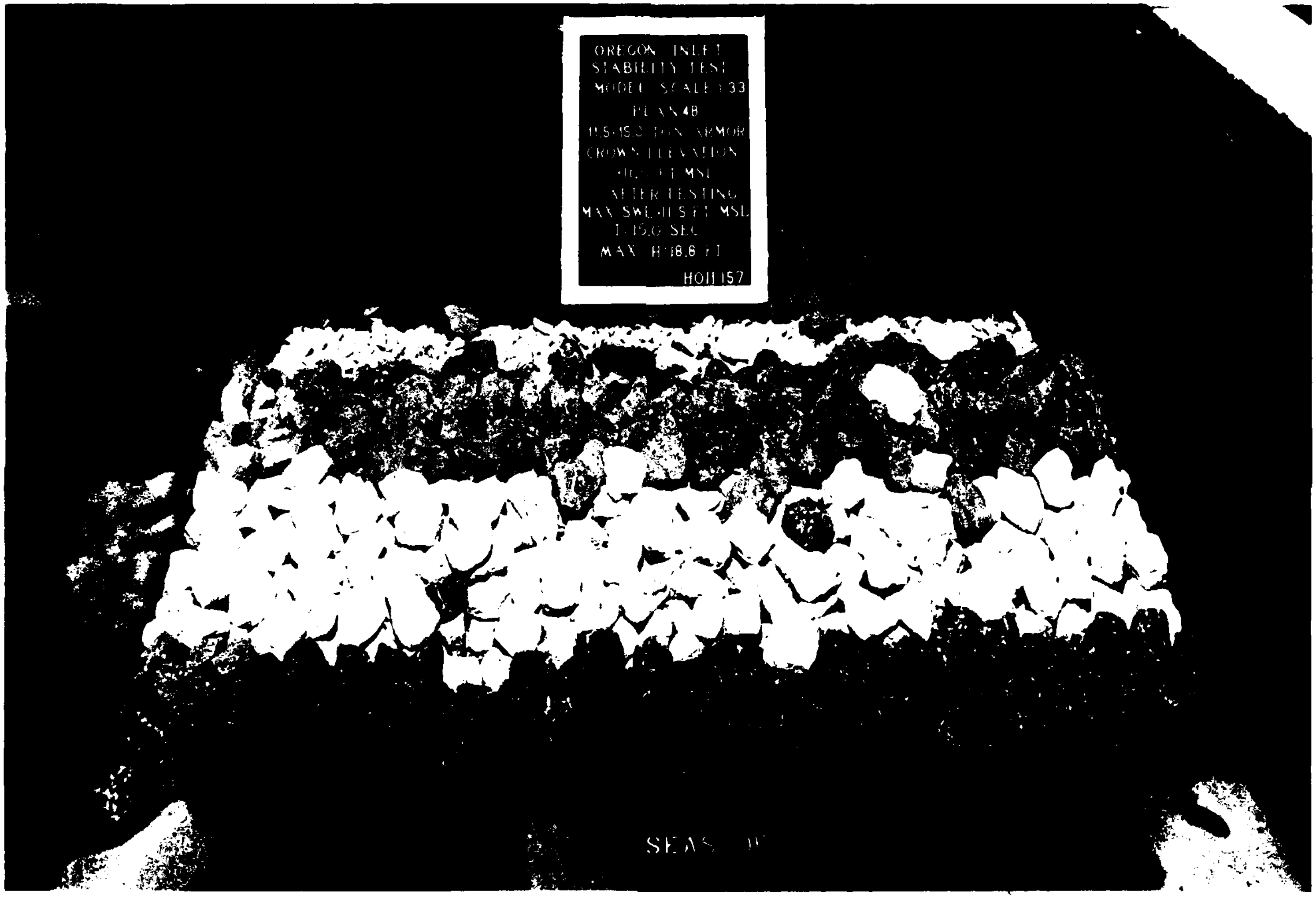

Photo 63. Sea-side view of Plan 4B after testing step 13 of the +11.5 ft NGVD hydrograph

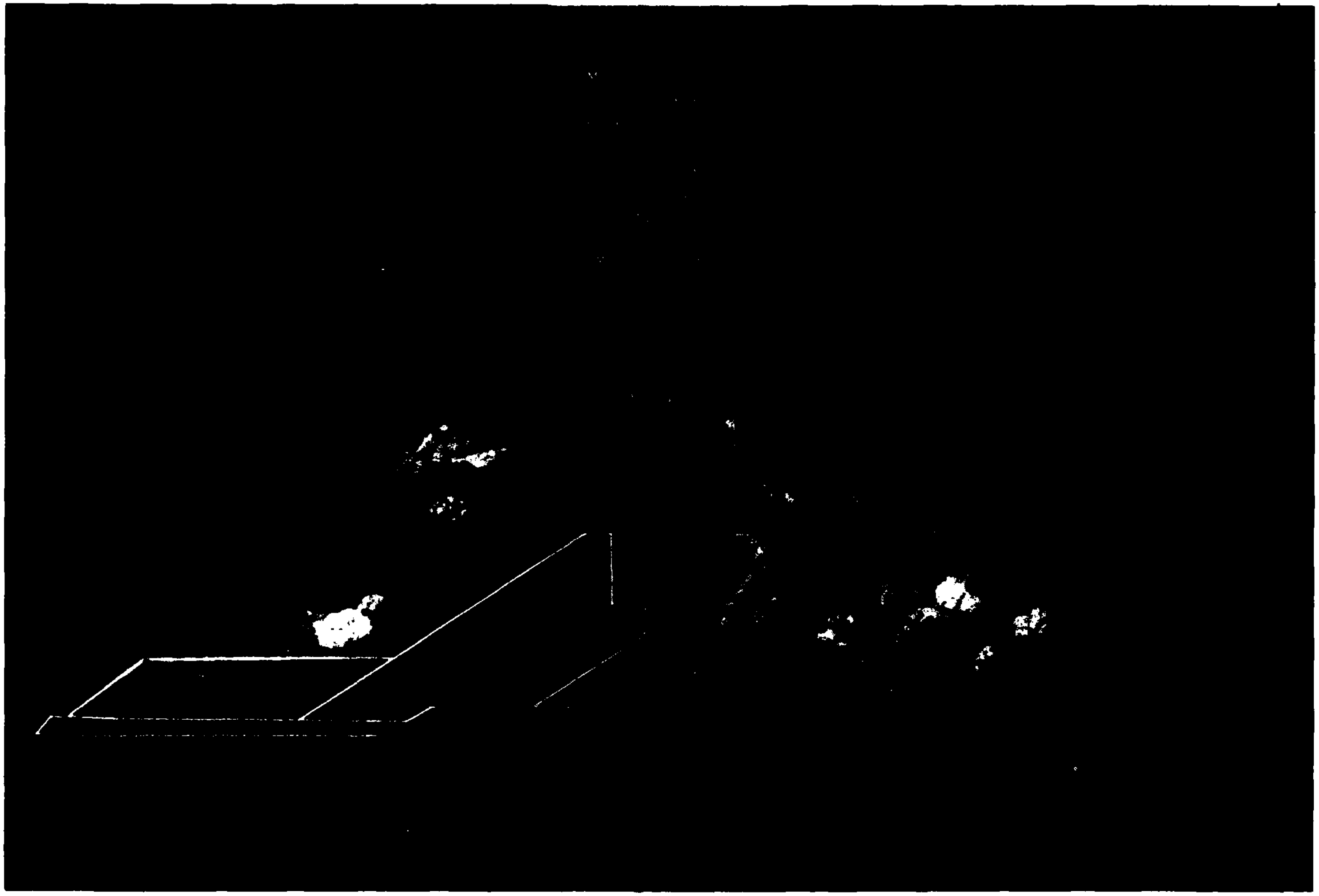

Photo 64. End view of Plan 4B after testing step 13 of the +11.5 ft NGVD hydrograph

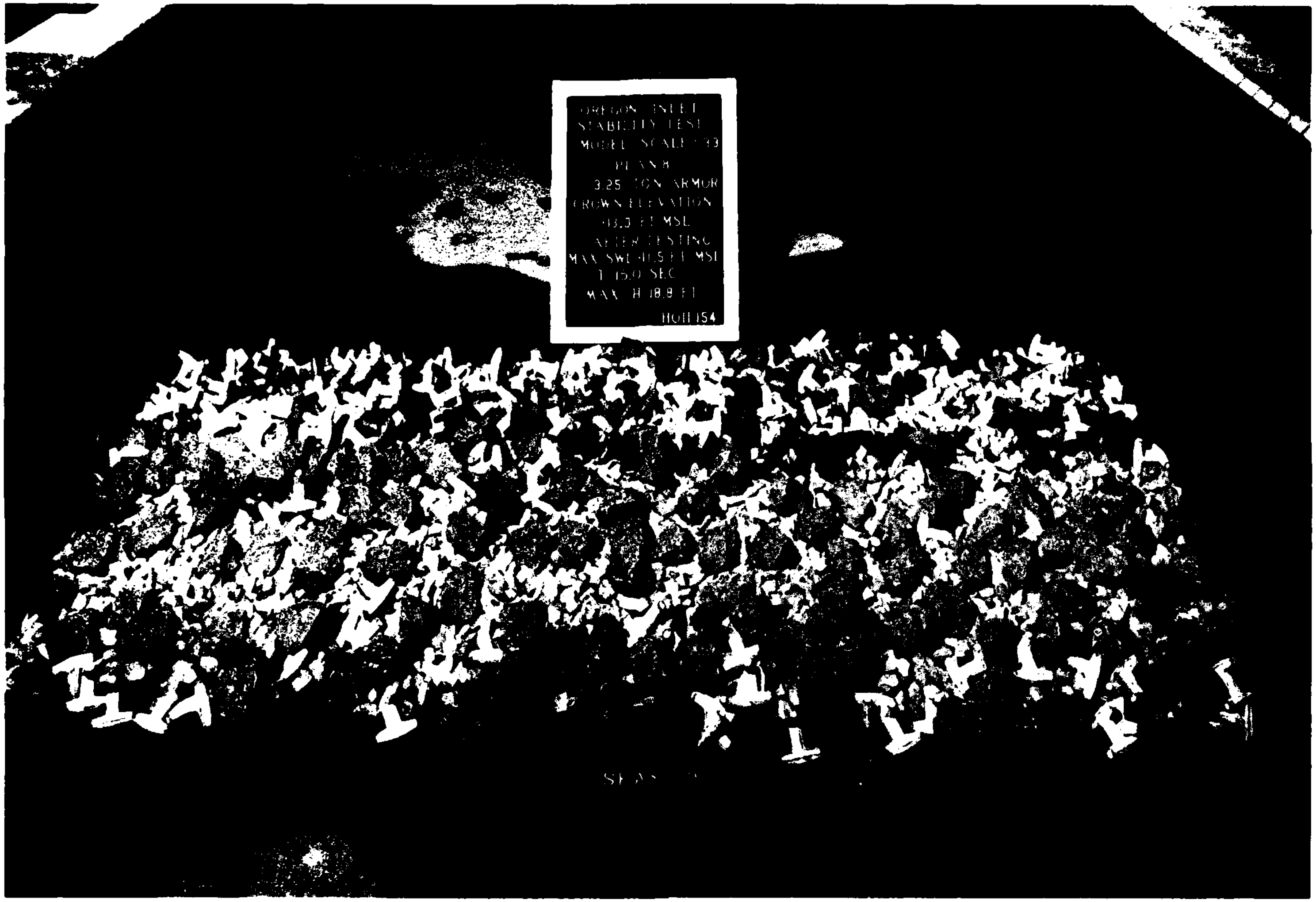

Photo 65. Sea-side view of Plan 8 after testing step 13 of the +11.5 ft NGVD hydrograph

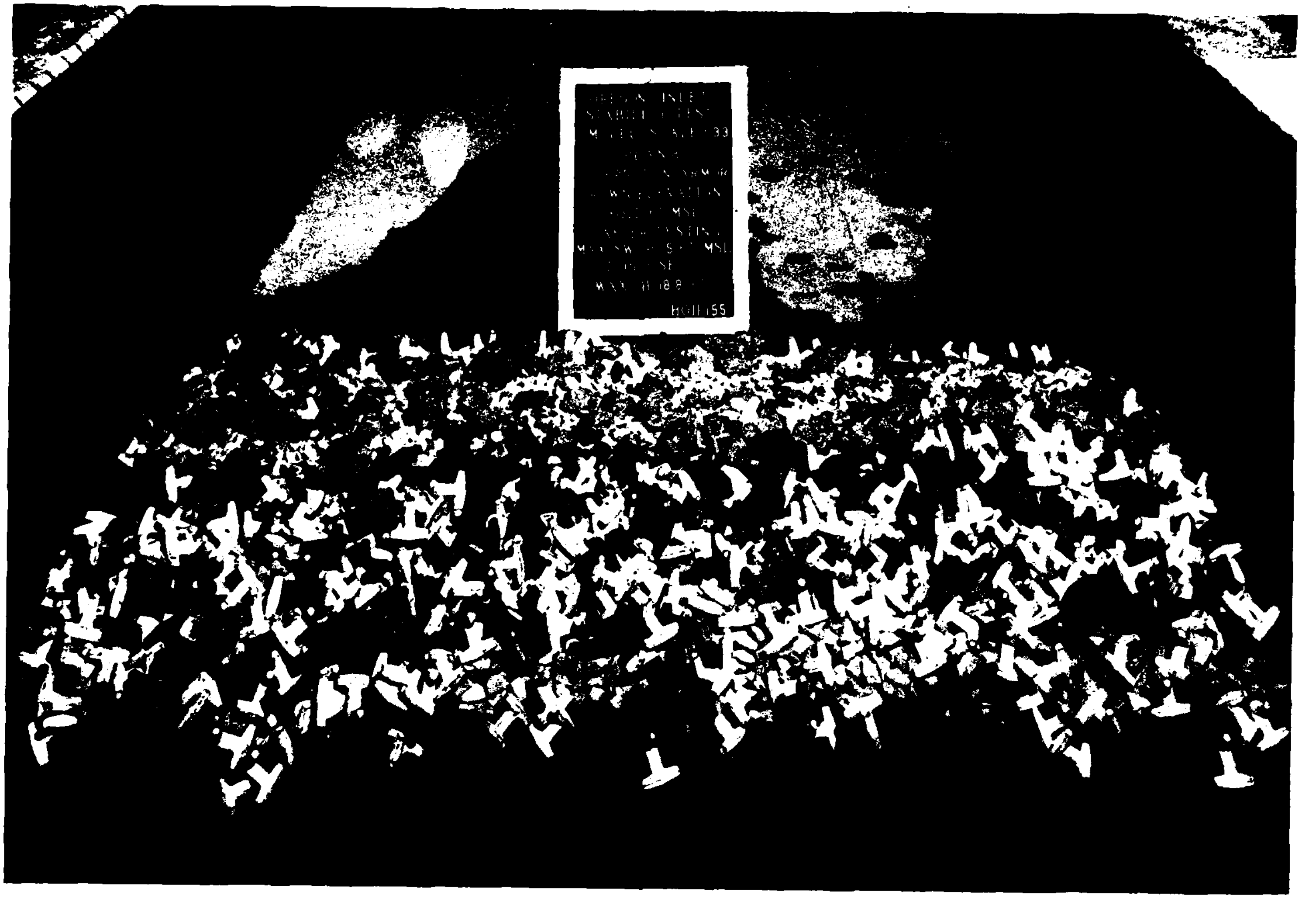

Photo 66. Channel-side view of Plan 8 after testing step 13 of the +11.5 ft NGVD hydrograph

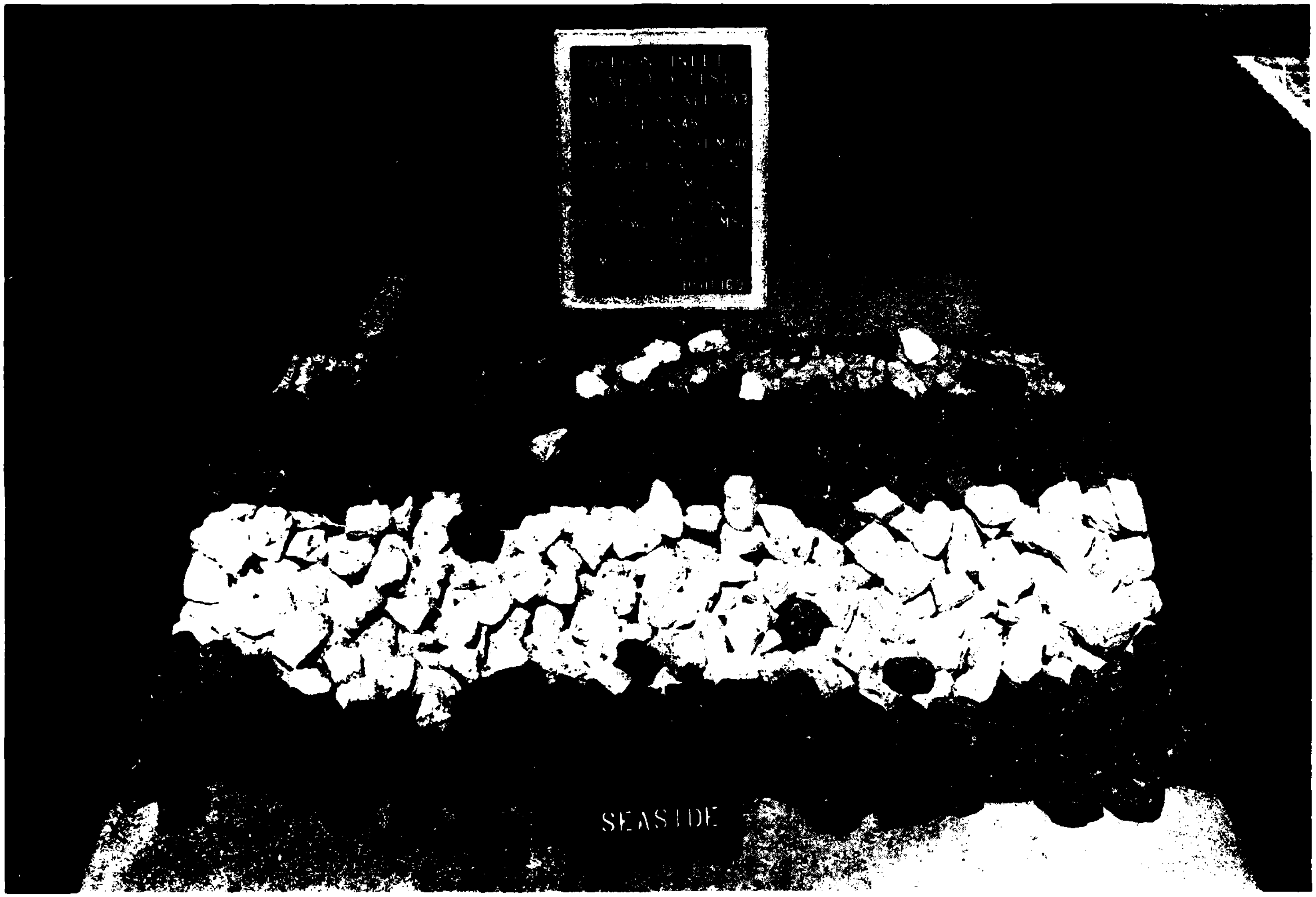

Photo 67. Sea-side view of Plan 4B after testing step 5 of two successive +7.5 ft NGVD hydrographs

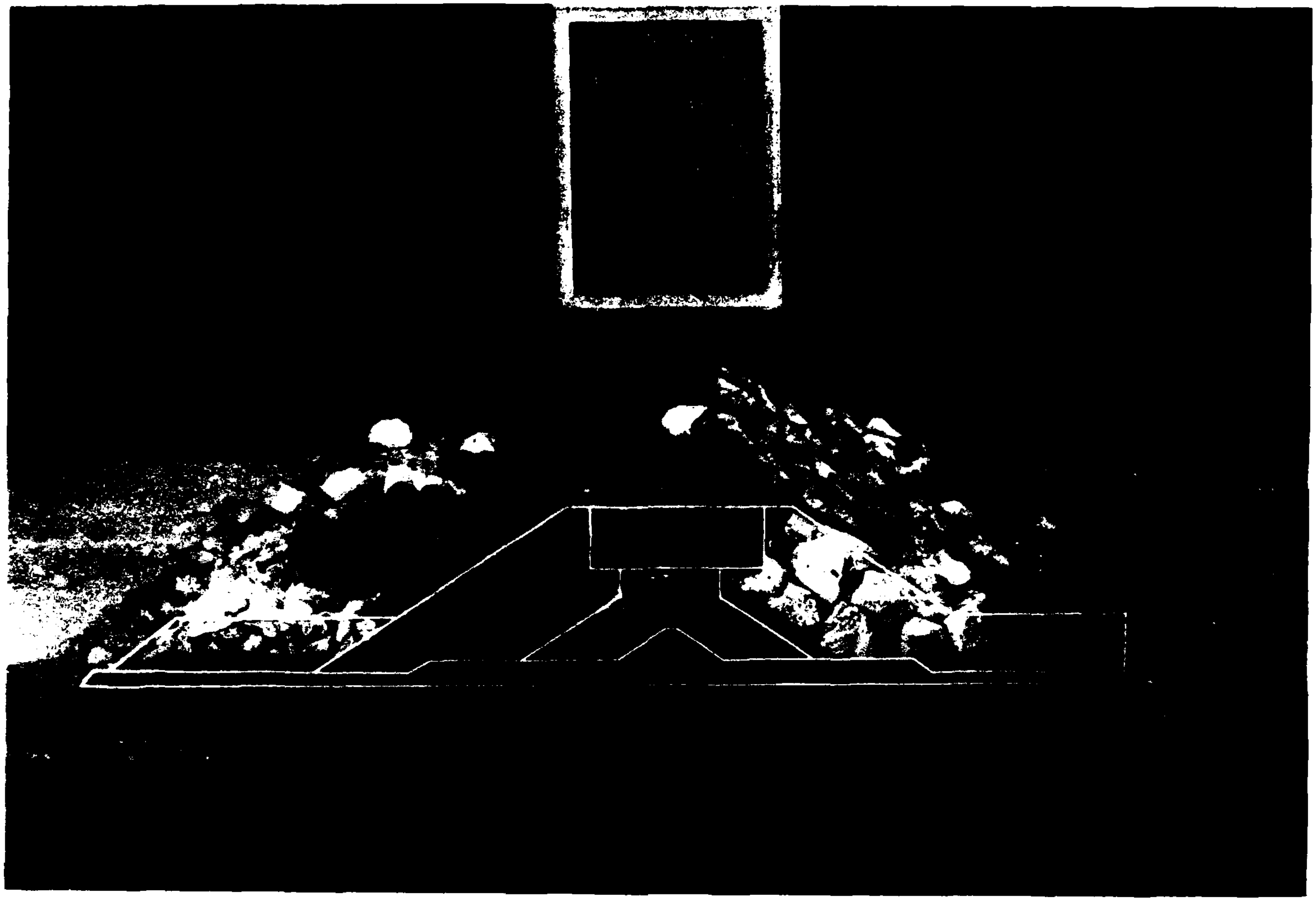

Photo 68. End view of Plan 4B after testing step 5 of two successive +7.5 ft NGVD hydrographs

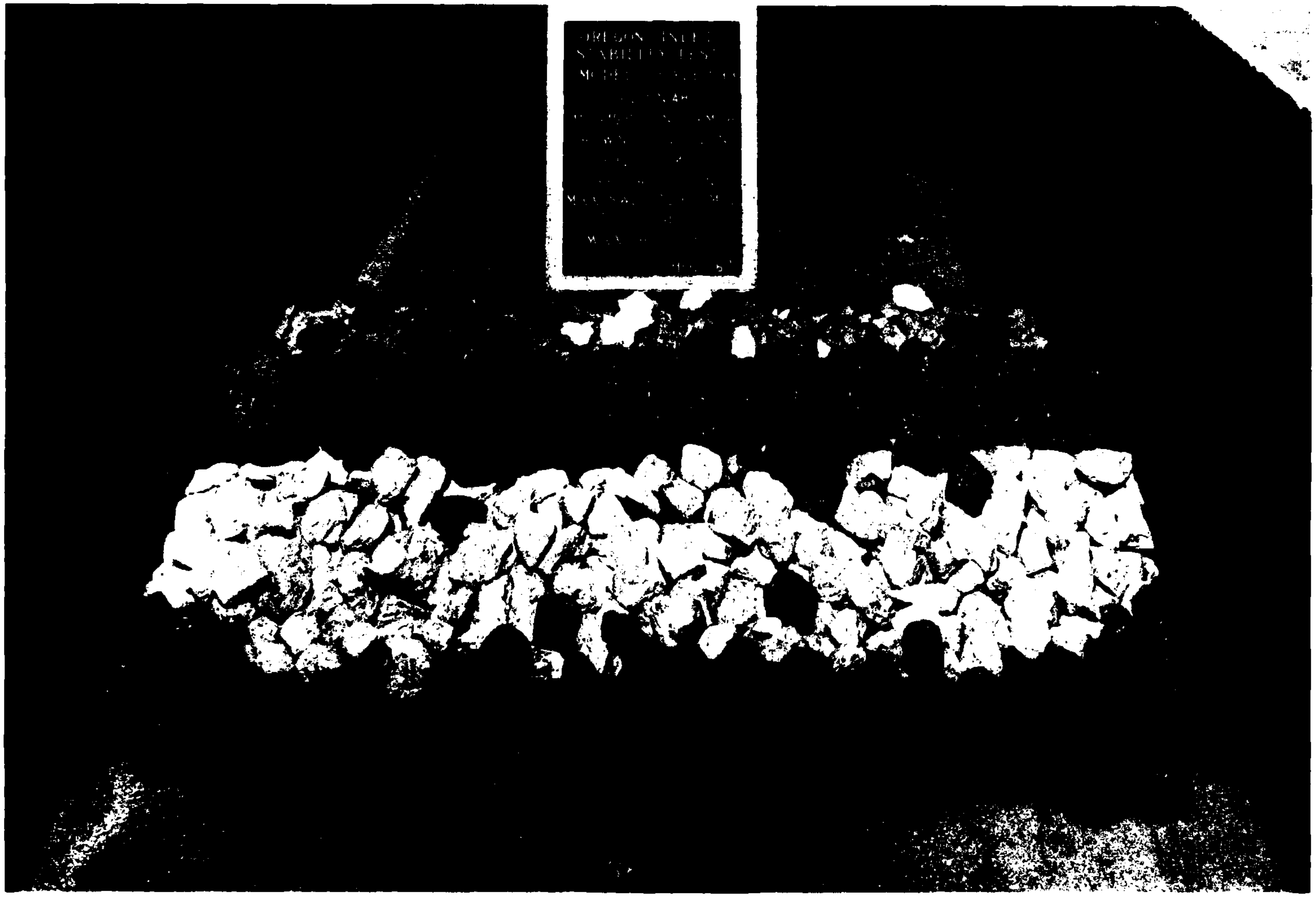

Photo 69. Sea-side view of Plan 4B after testing step 10 of two successive +7.5 ft NGVD hydrographs

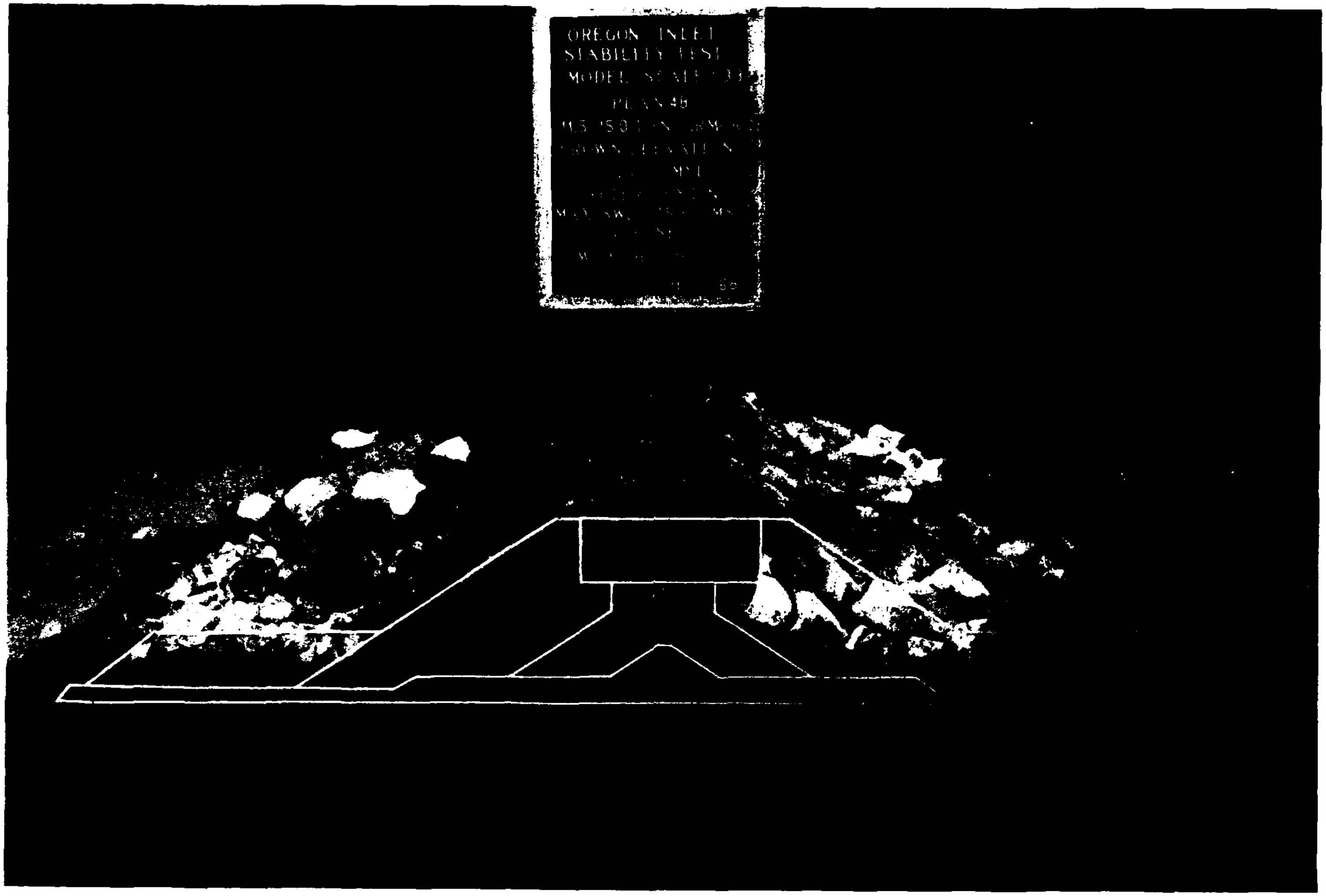

Photo 70. End view of Plan 4B after testing step 10 of two successive +7.5 ft NGVD hydrographs

Photo 71. Sea-side view of Plan 8 after testing step 5 of two successive +7.5 ft NGVD hydrographs

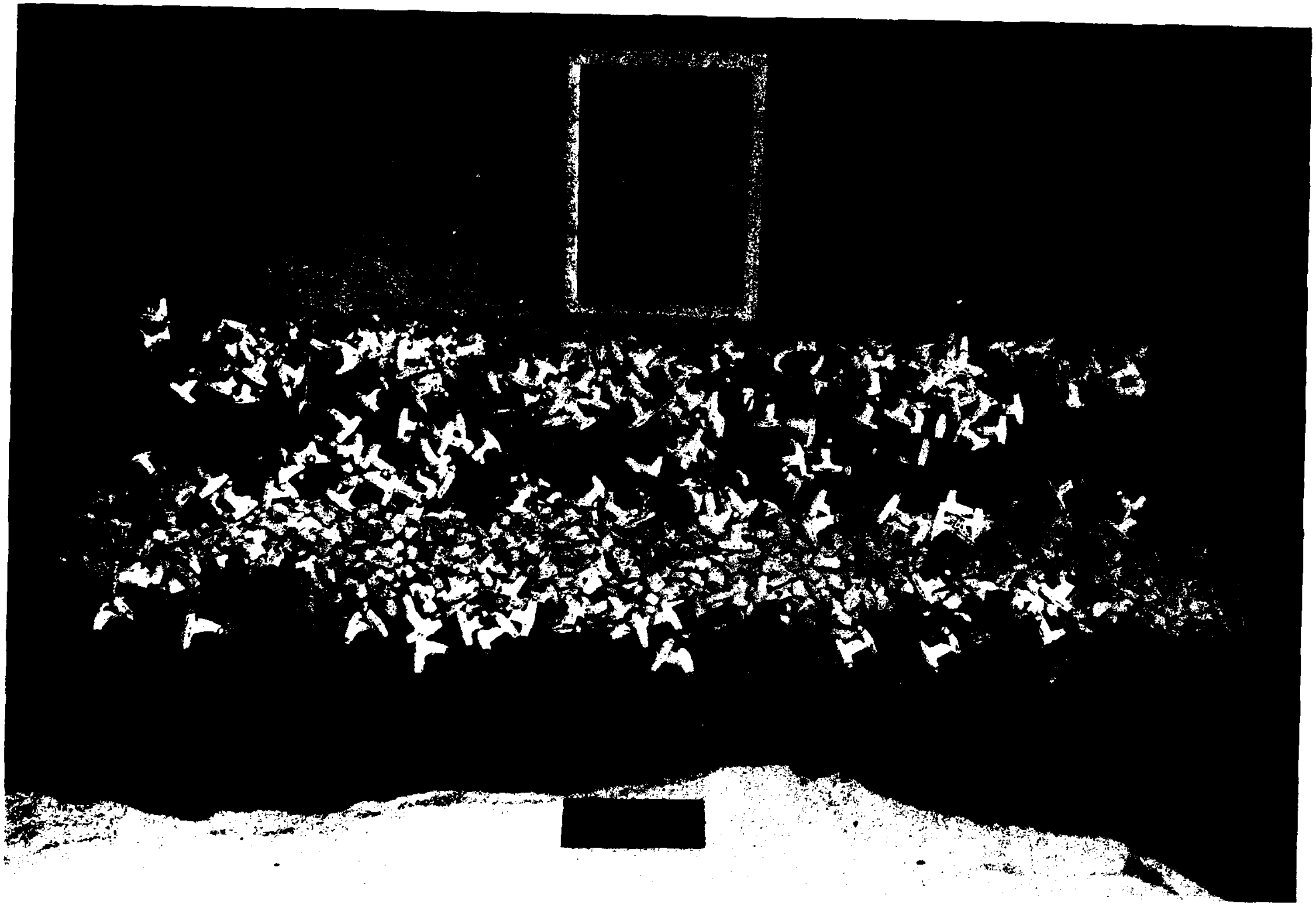

Photo 72. Channel-side view of Plan 8 after testing step 5 of two successive +7.5 ft NGVD hydrographs

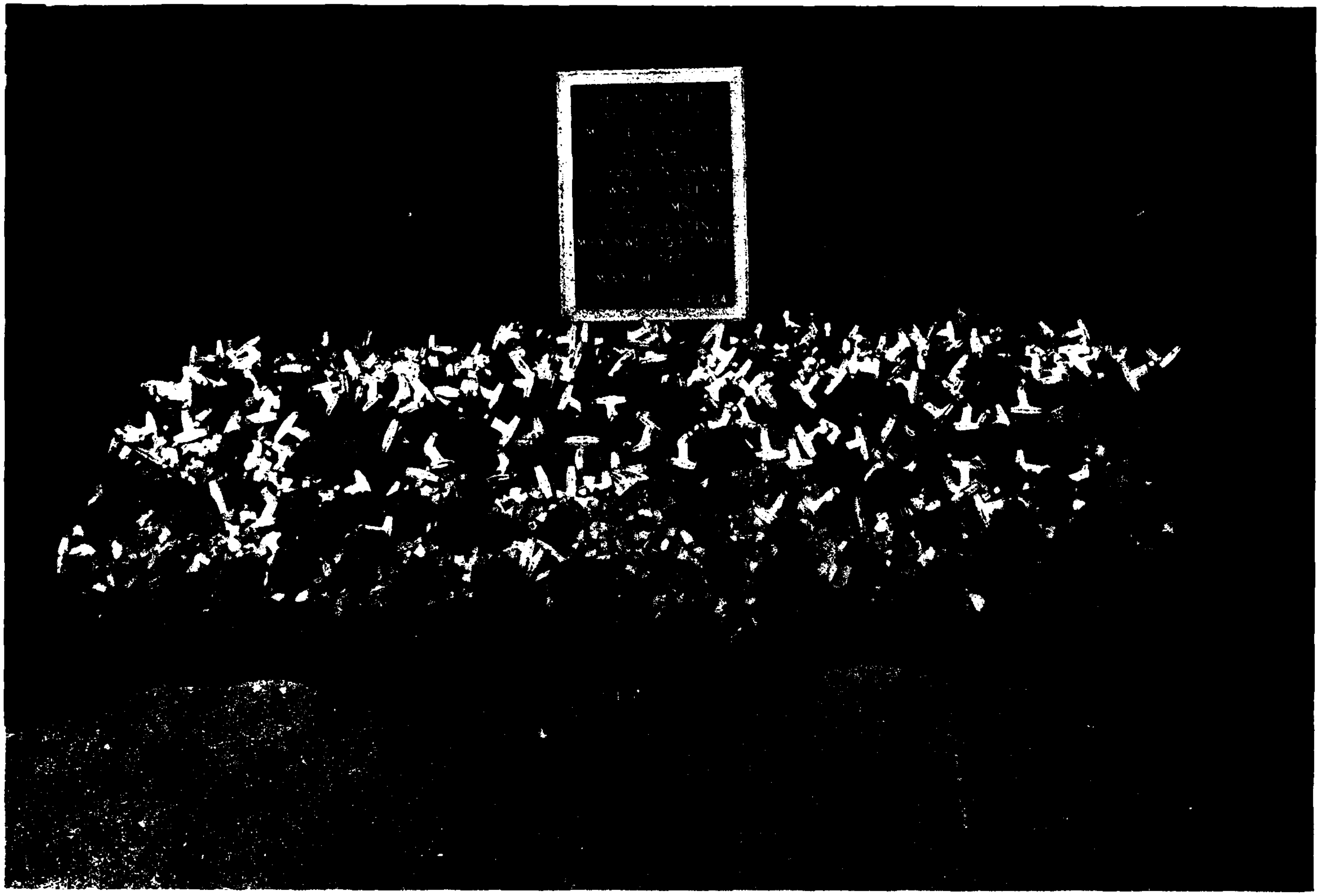

Photo 73. Sea-side view of Plan 8 after testing step 10 of two successive +7.5 ft NGVD hydrographs

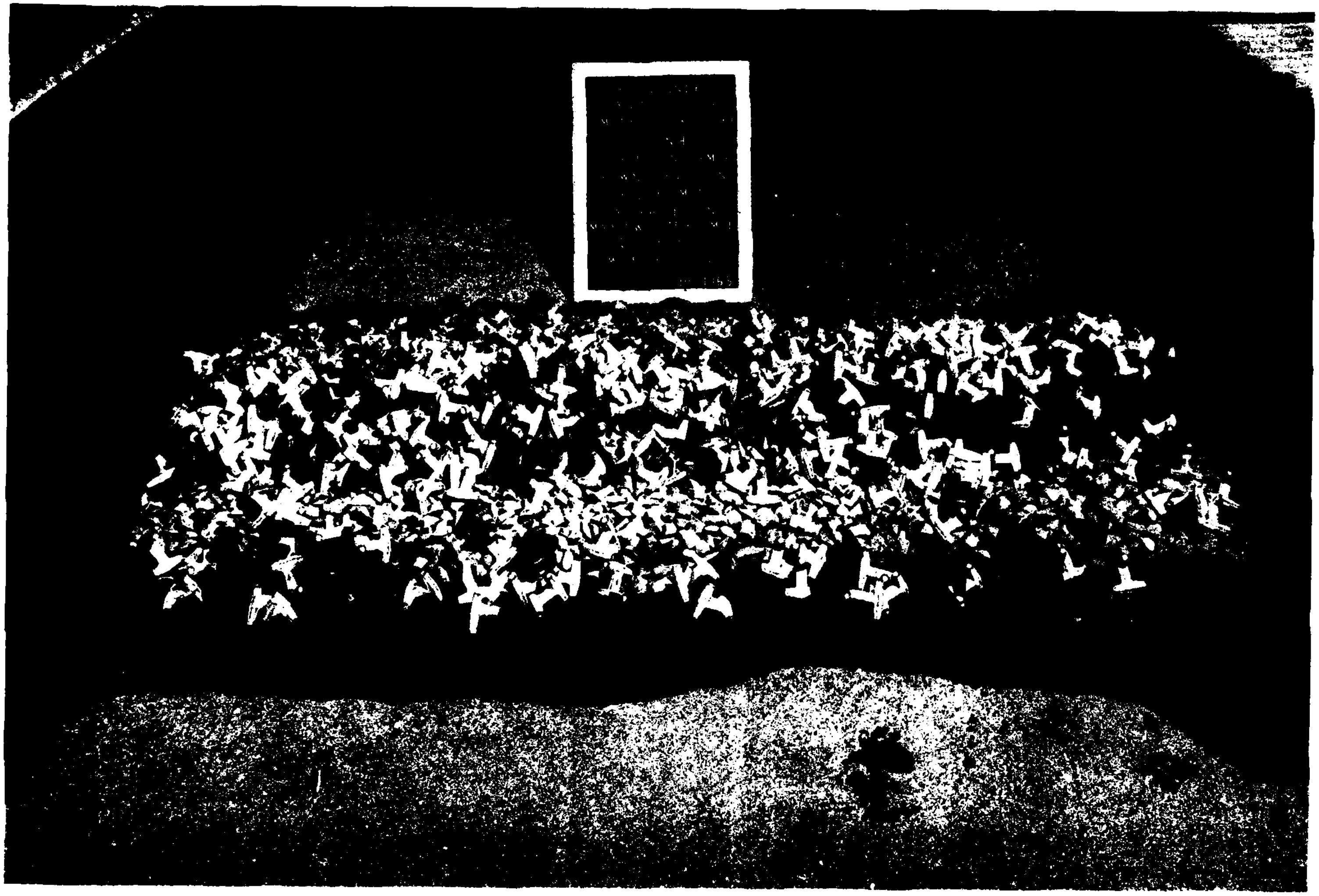

Photo 74. Channel-side view of Plan 8 after testing step 10 of two successive +7.5 ft NGVD hydrographs

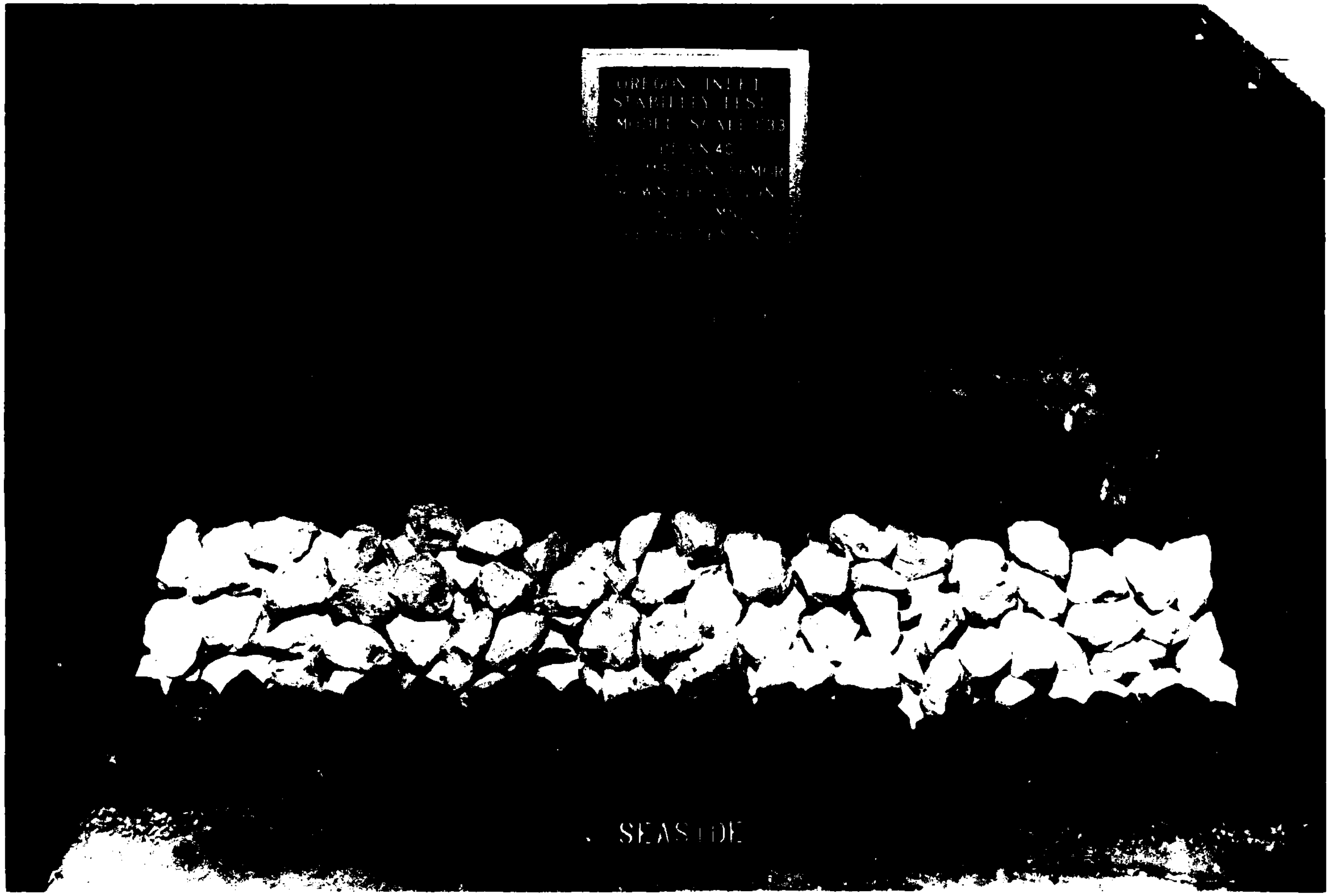

Photo 75. Sea-side view of Plan 4C before wave attack

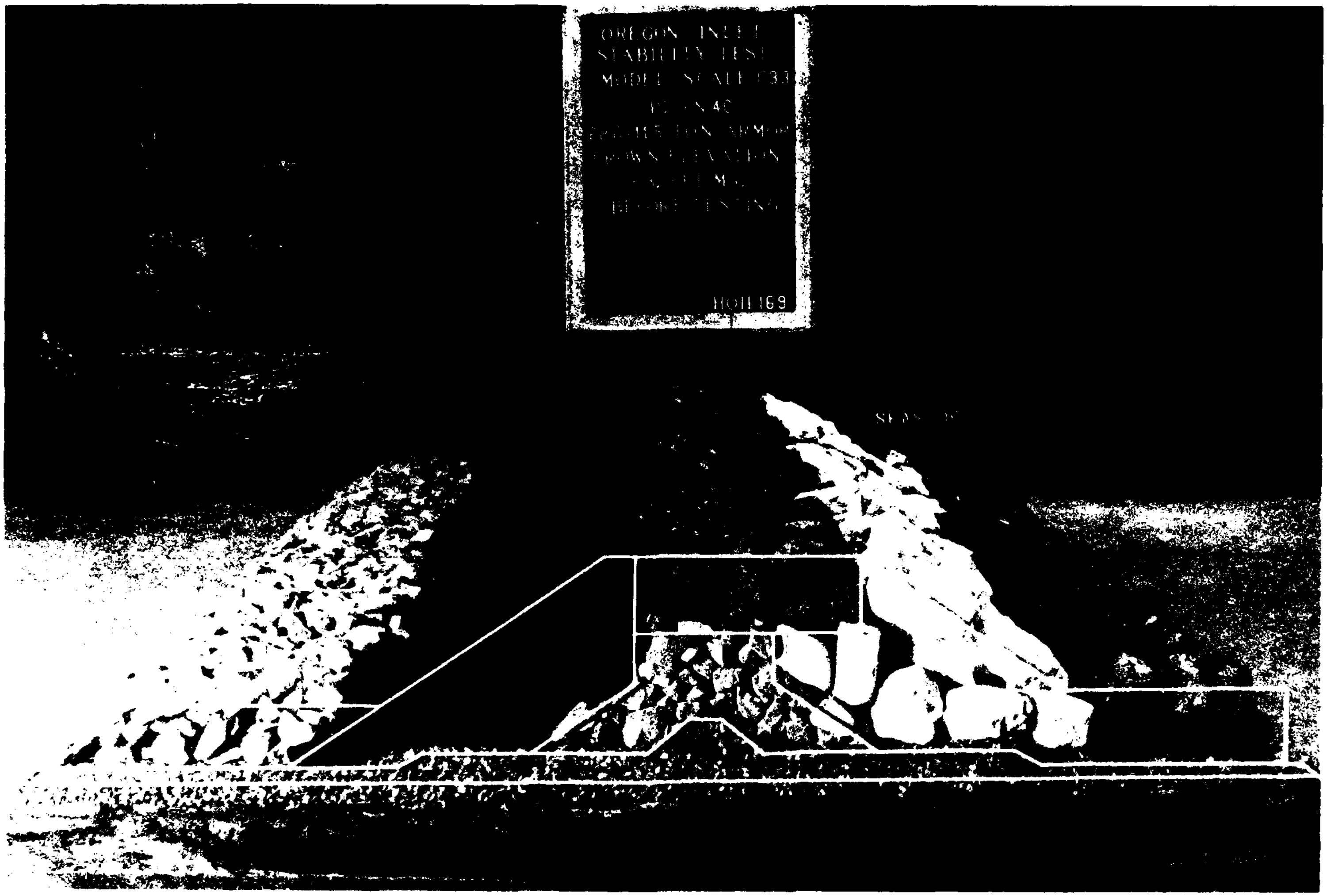

Photo 76. End view of Plan 4C before wave attack

Photo 77. Sea-side view of Plan 4C after attack of 15-sec, 15.5-ft waves at an swl of +7.5 ft NGVD

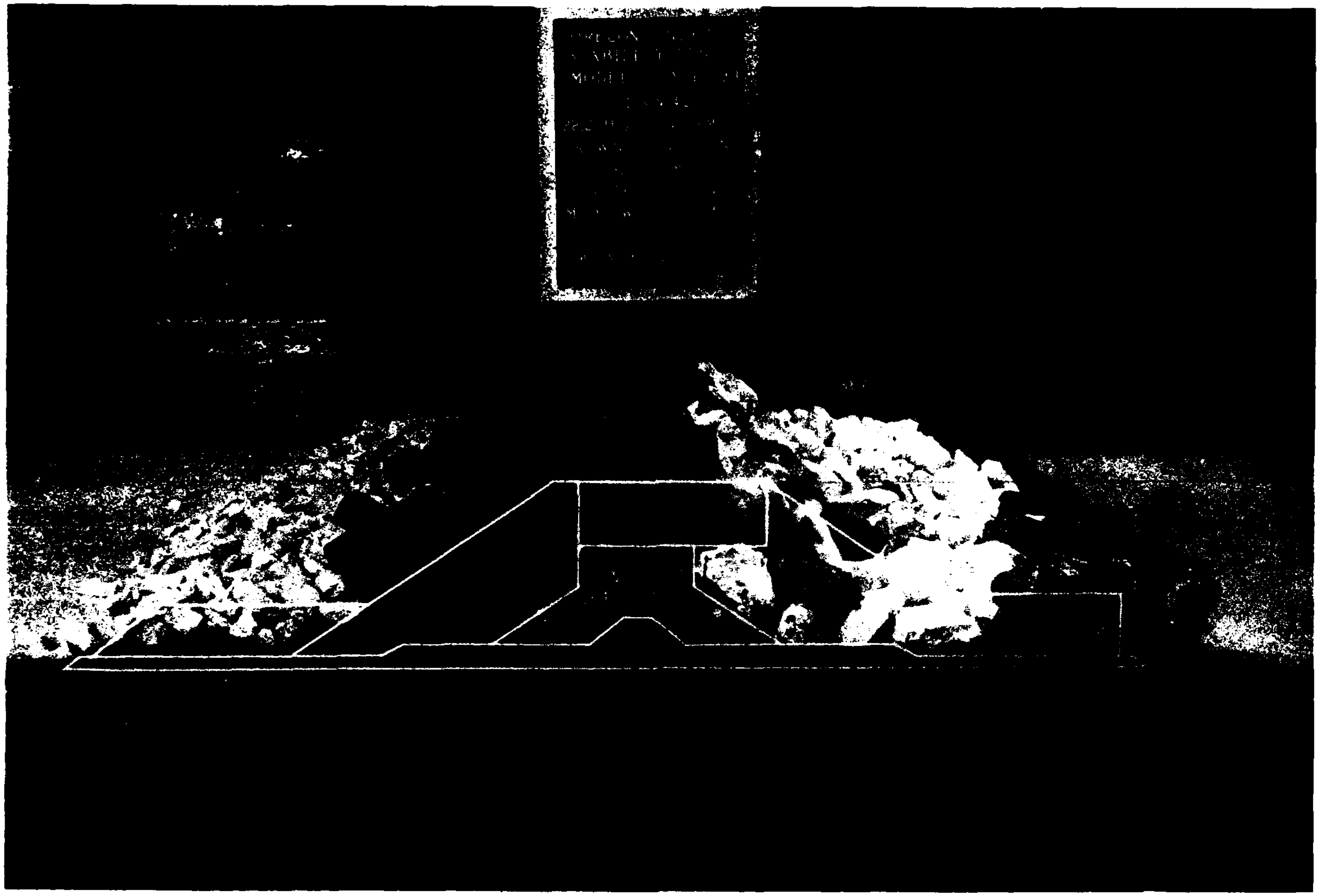

Photo 78. End view of Plan 4C after attack of 15-sec, 15.5-ft waves at an swl of +7.5 ft NGVD

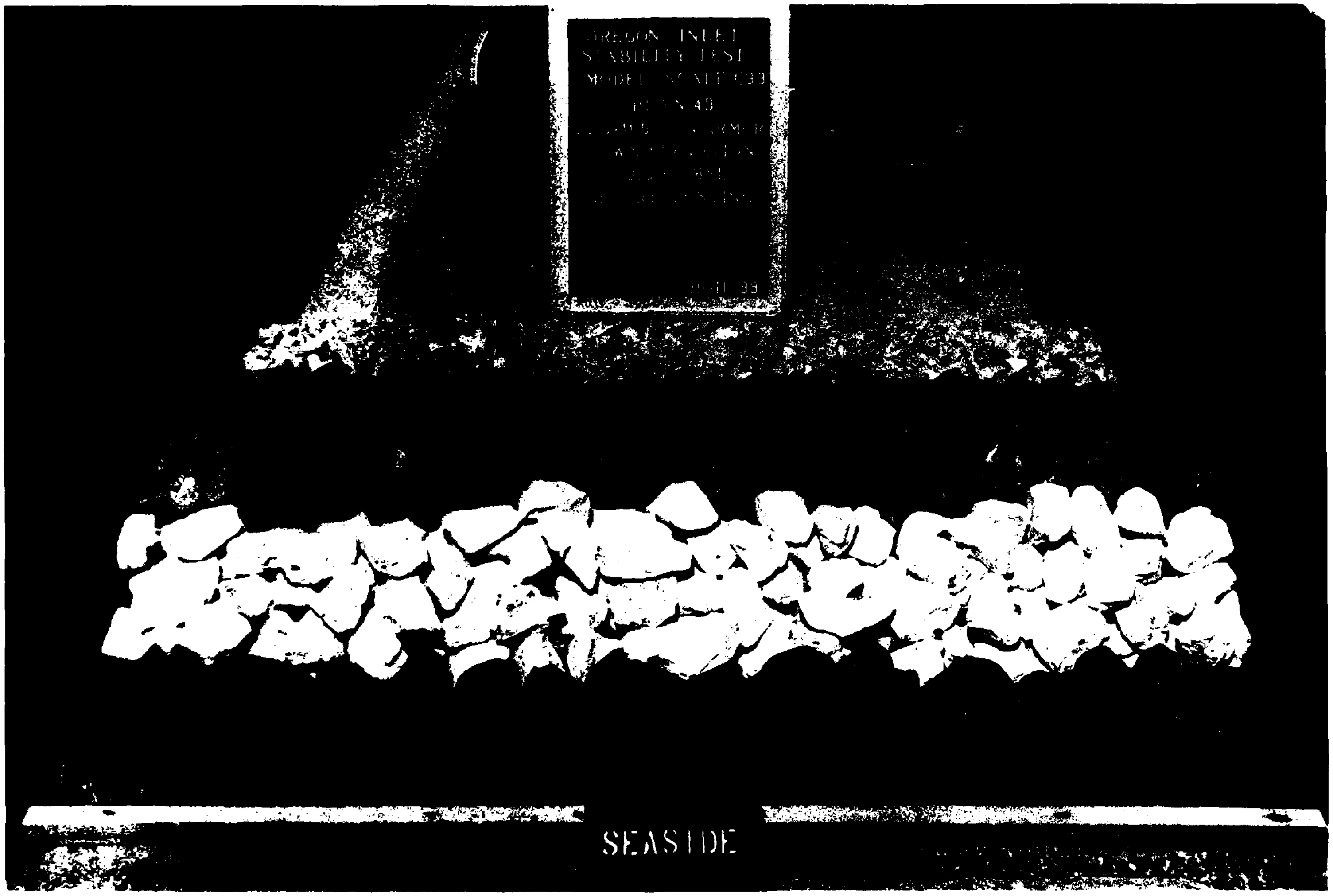

Photo 79. Sea-side view of Plan 4D before wave attack

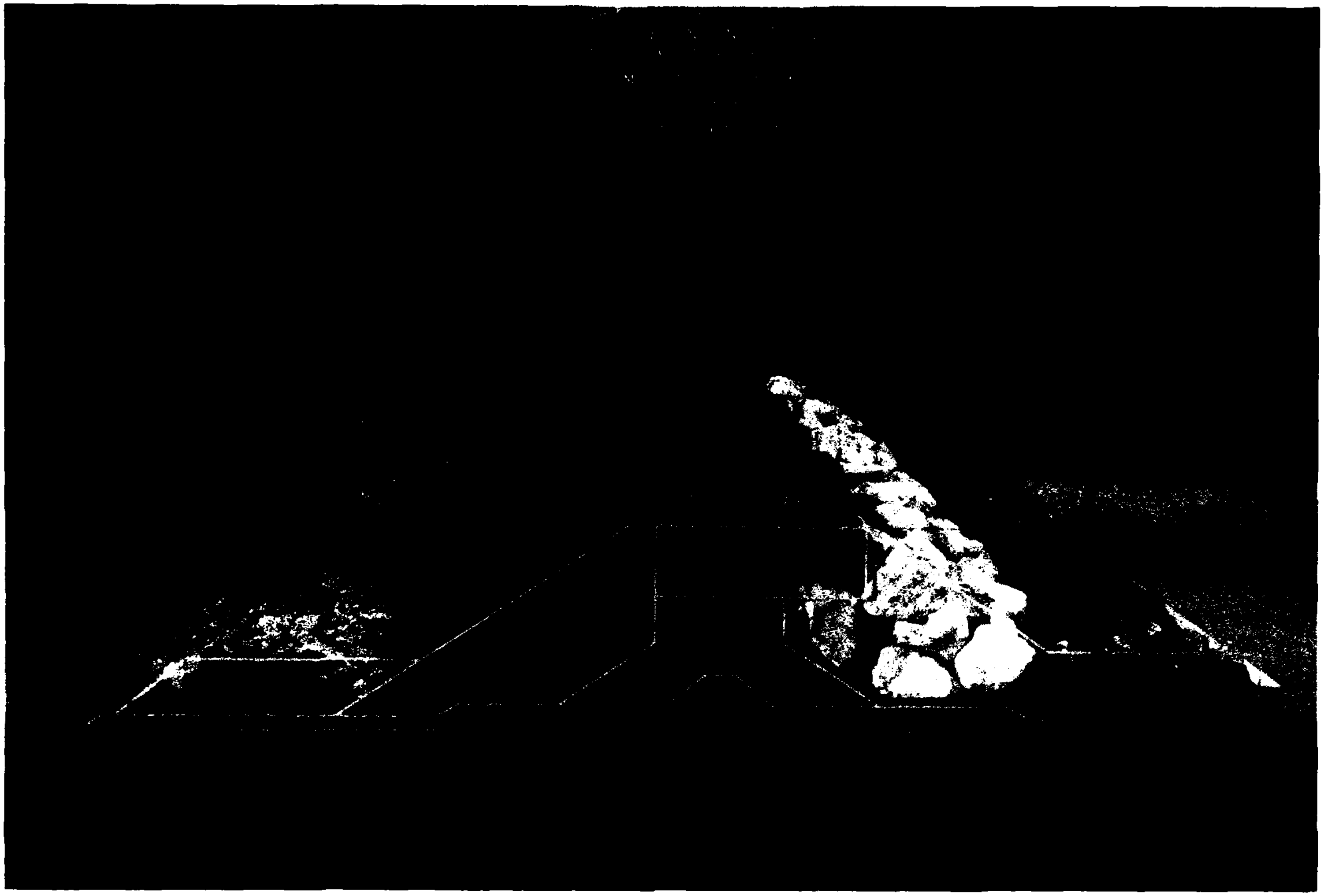

Photo 80. End view of Plan 4D before wave attack

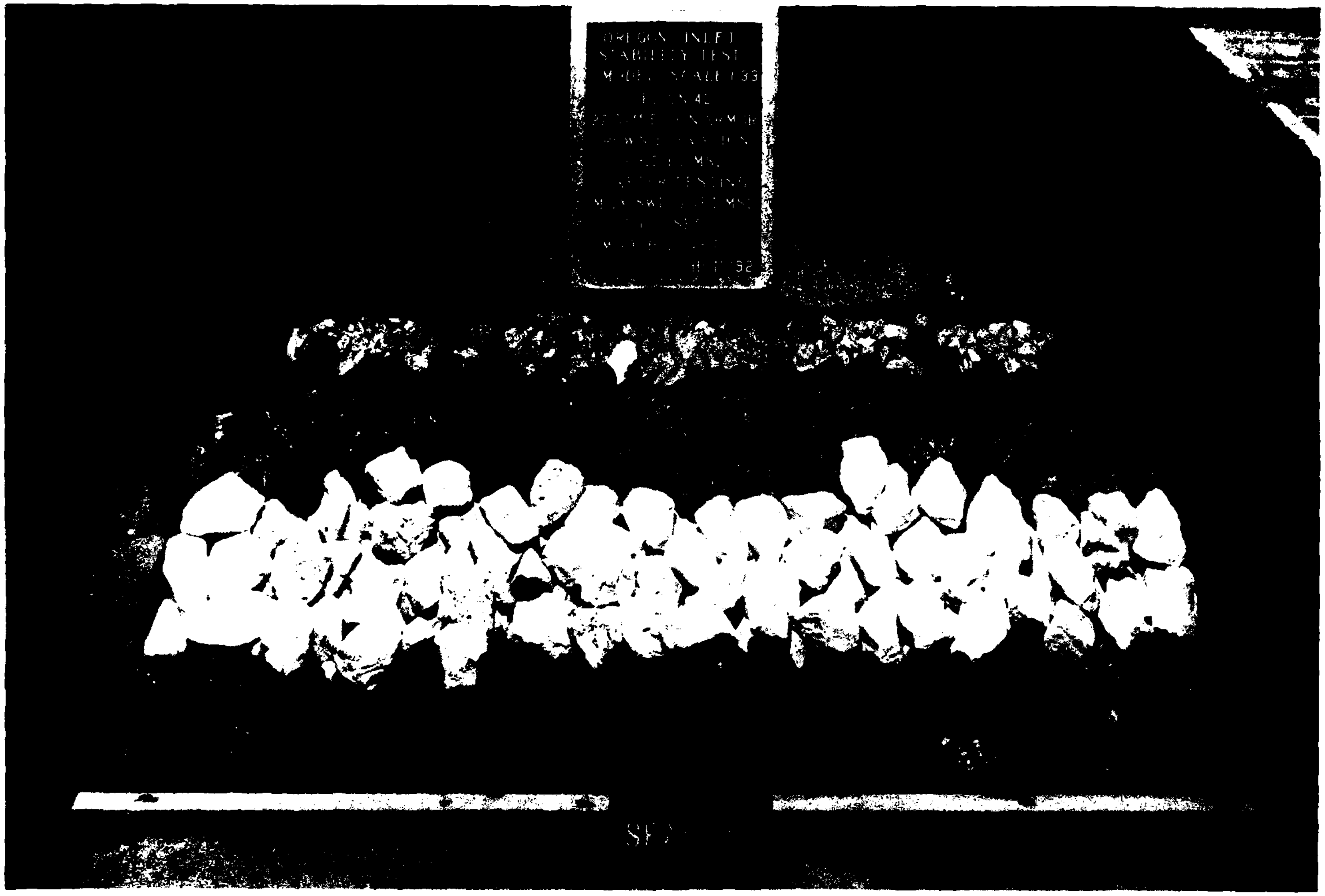

Photo 81. Sea-side view of Plan 4D after attack of 15-sec, 15.5-ft waves at an swl of +7.5 ft NGVD

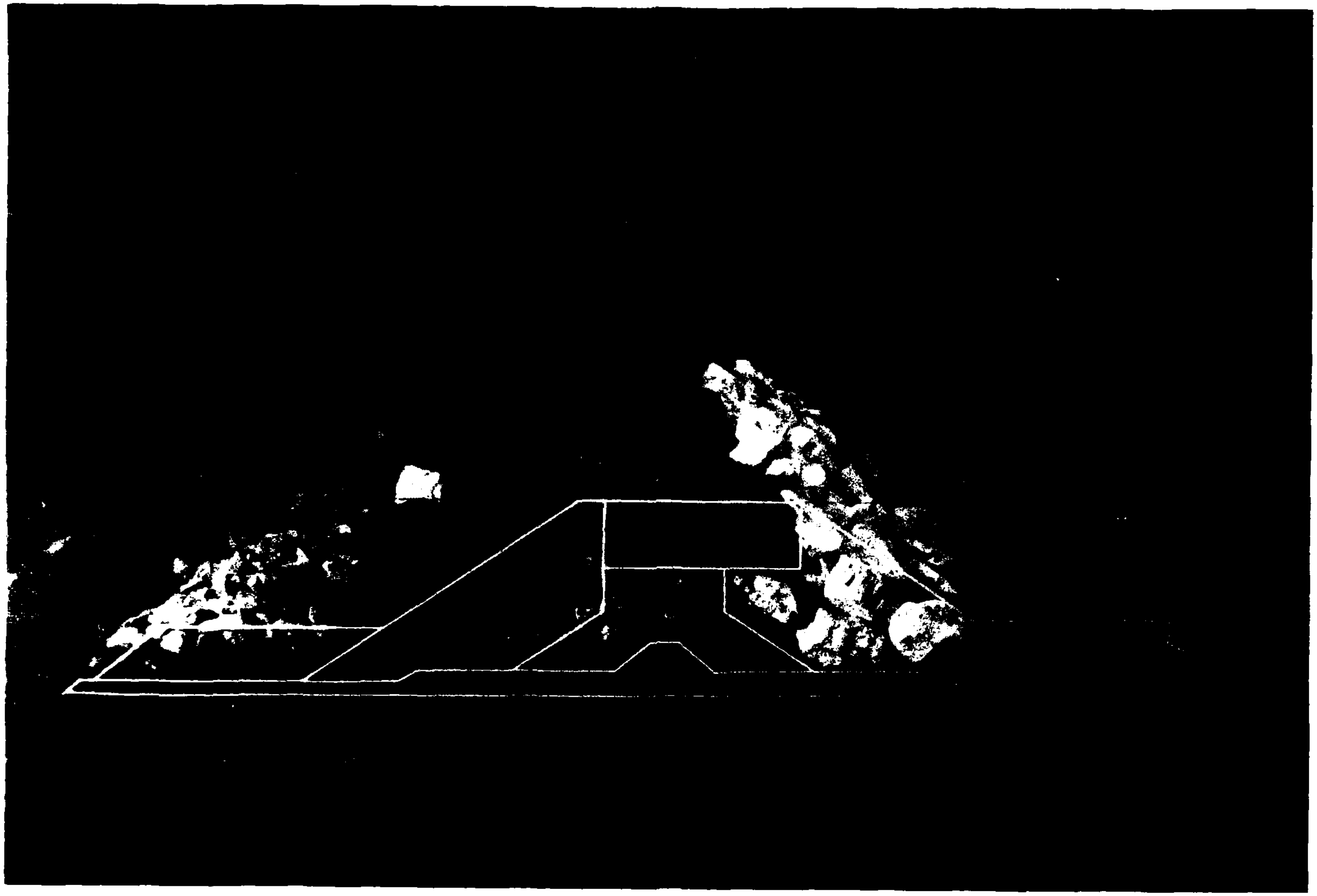

Photo 82. End view of Plan 4D after attack of 15-sec, 15.5-ft waves at an swl of +7.5 ft NGVD

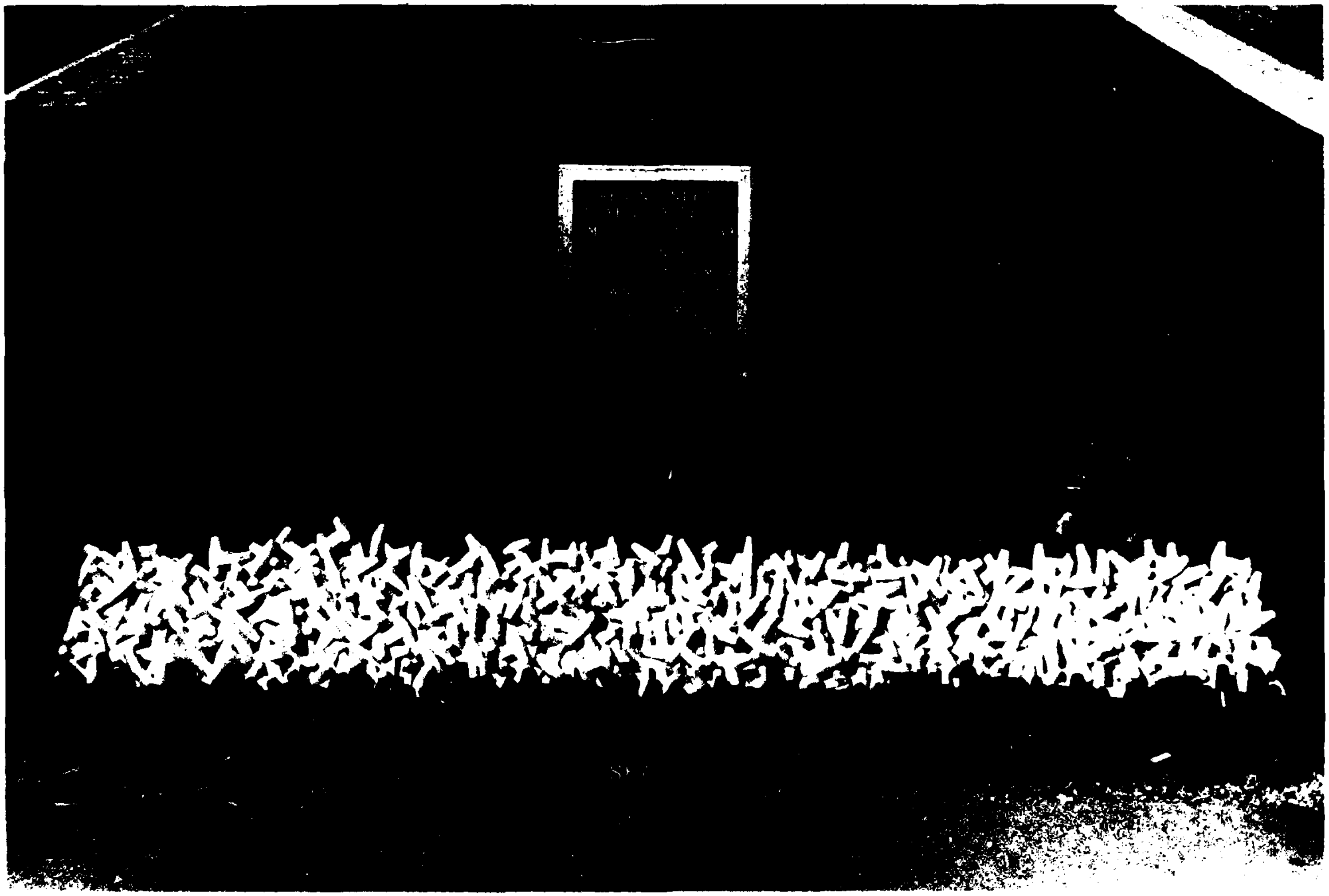

Photo 83. Sea-side view of Plan 9 before wave attack

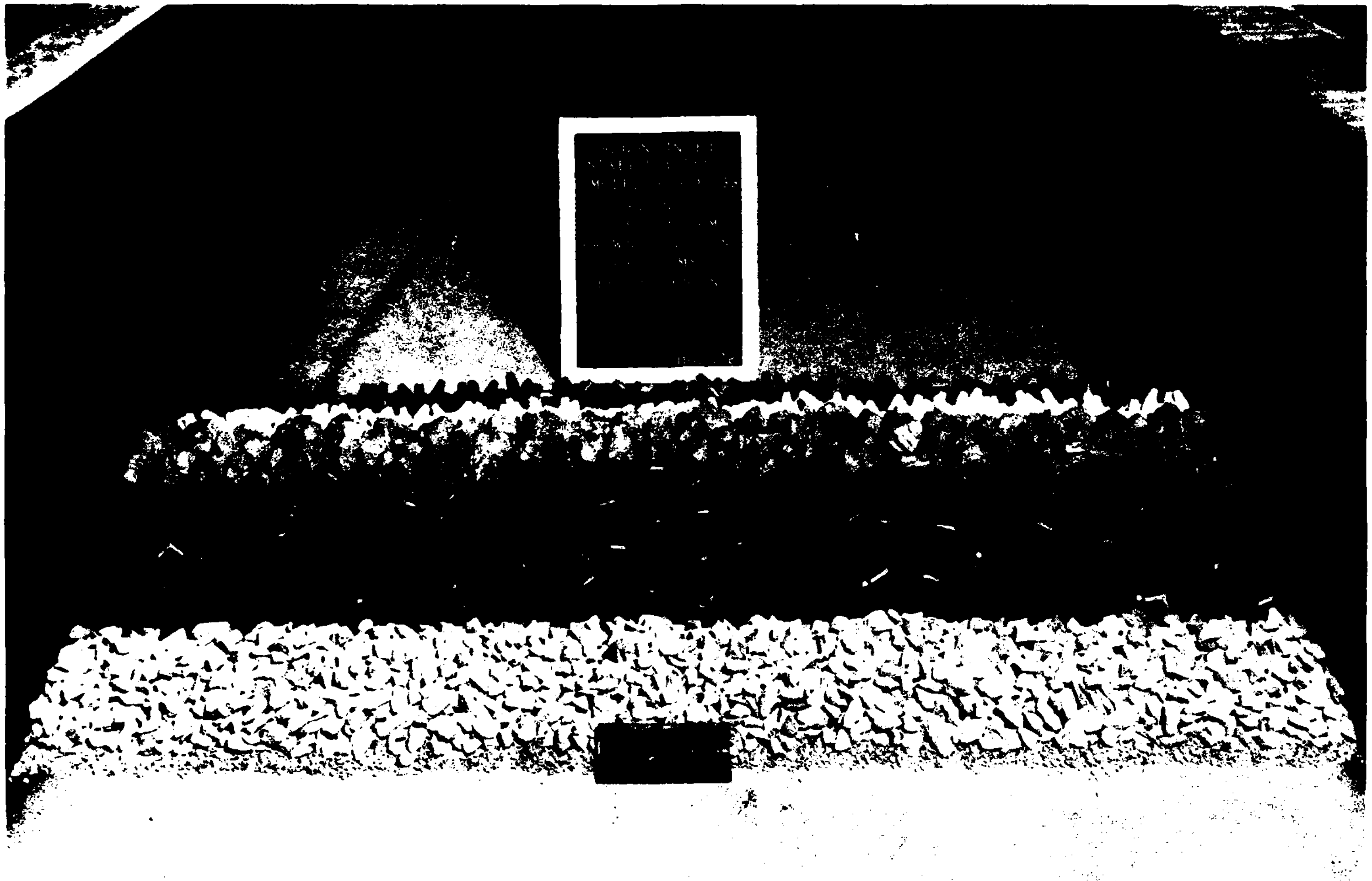

Photo 84. Channel-side view of Plan 9 before wave attack

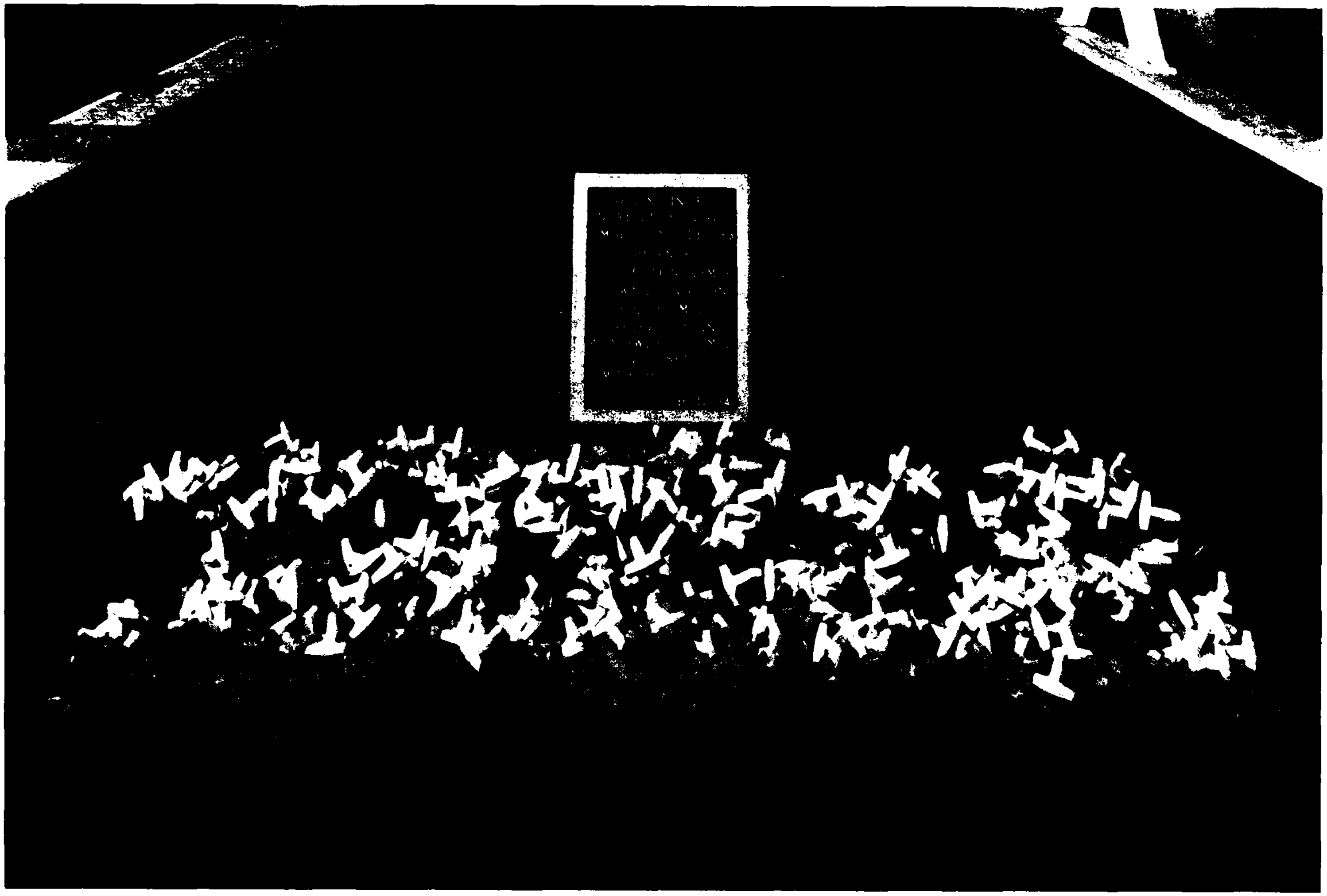

Photo 85. Sea-side view of Plan 9 after attack of 15-sec, 15.5-ft waves at an swl of +7.5 ft NGVD

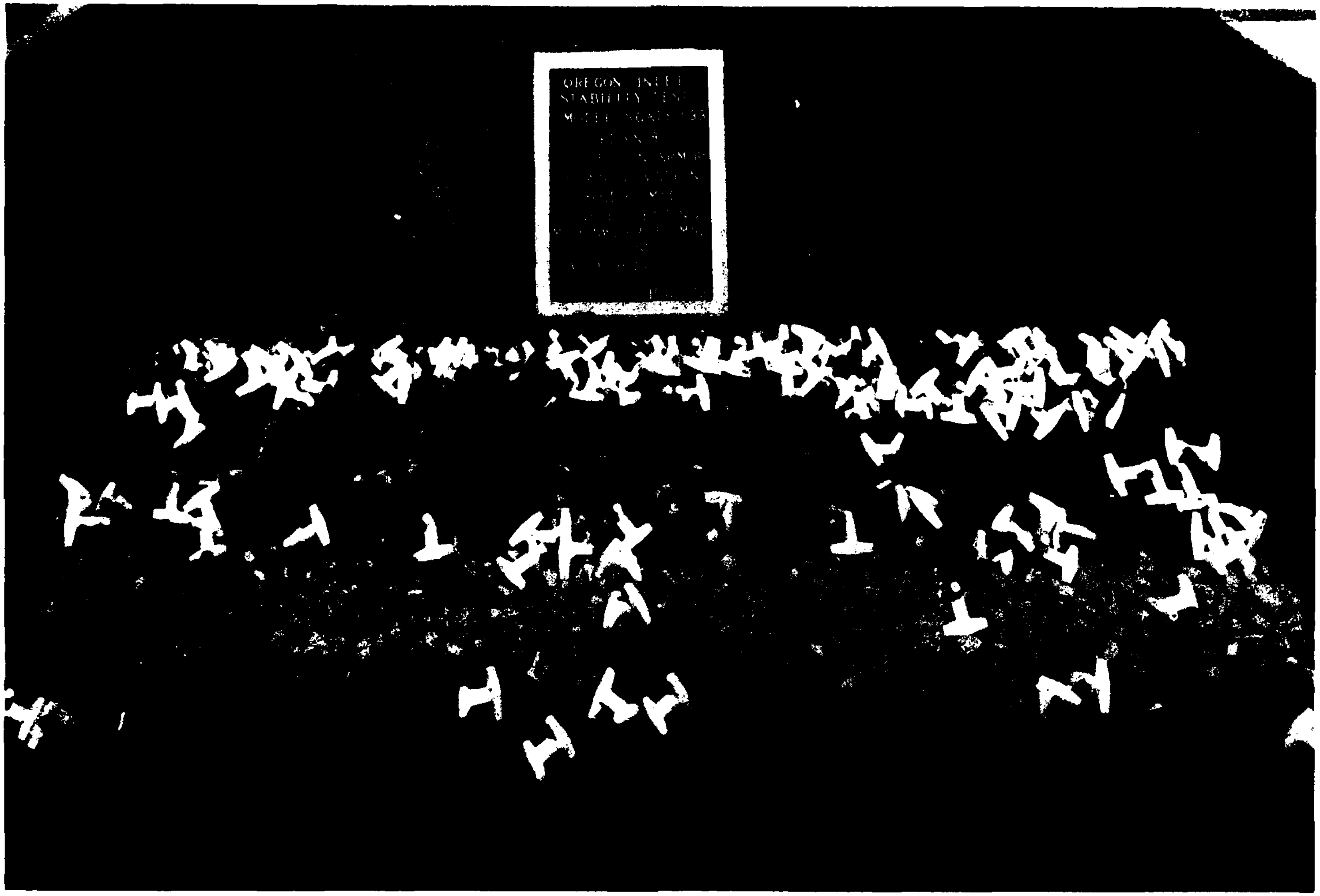

Photo 86. Channel-side view of Plan 9 after attack of 15-sec, 15.5-ft waves at an swl of +7.5 ft NGVD

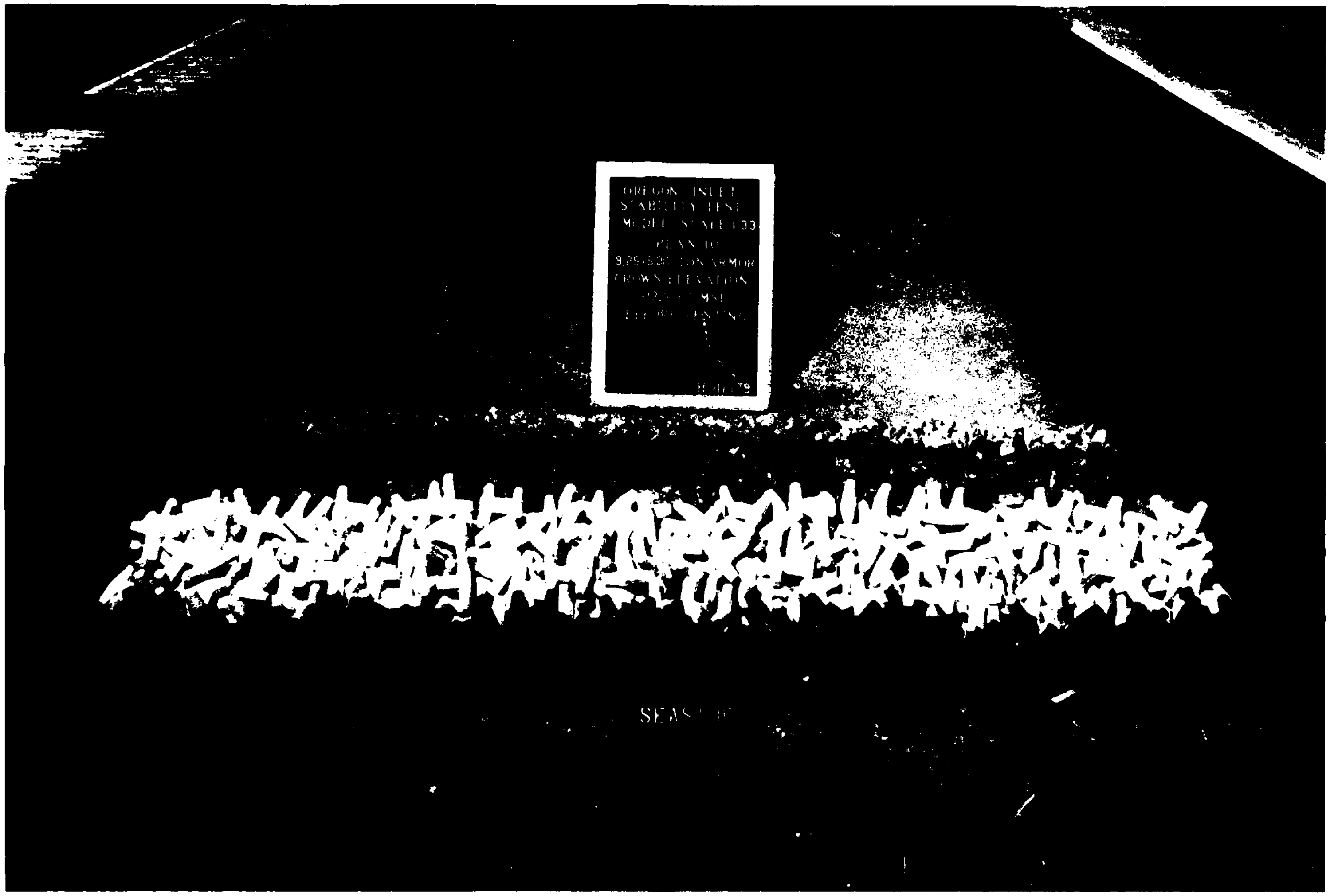

Photo 87. Sea-side view of Plan 10 before wave attack

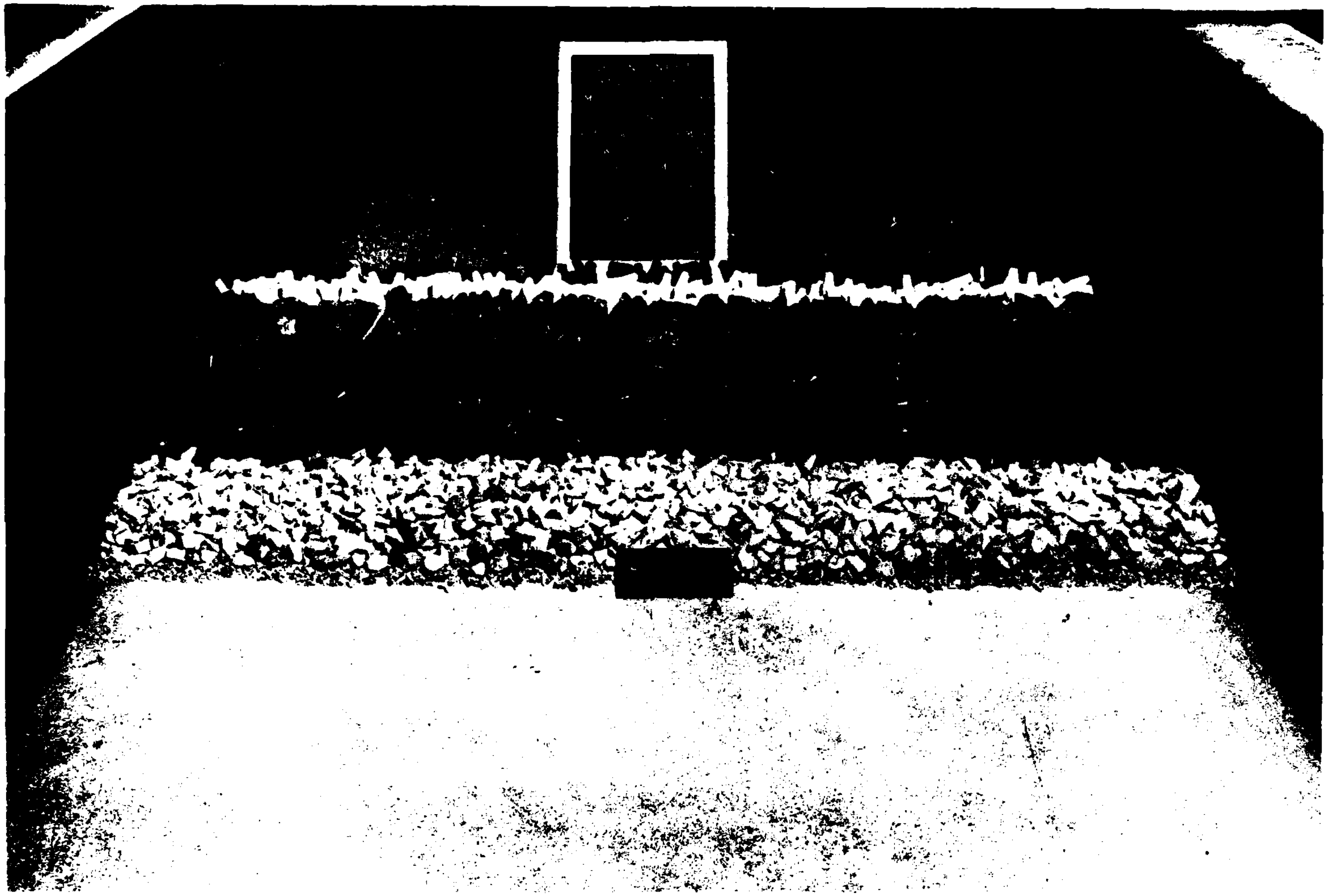

Photo 88. Channel-side view of Plan 10 before wave attack

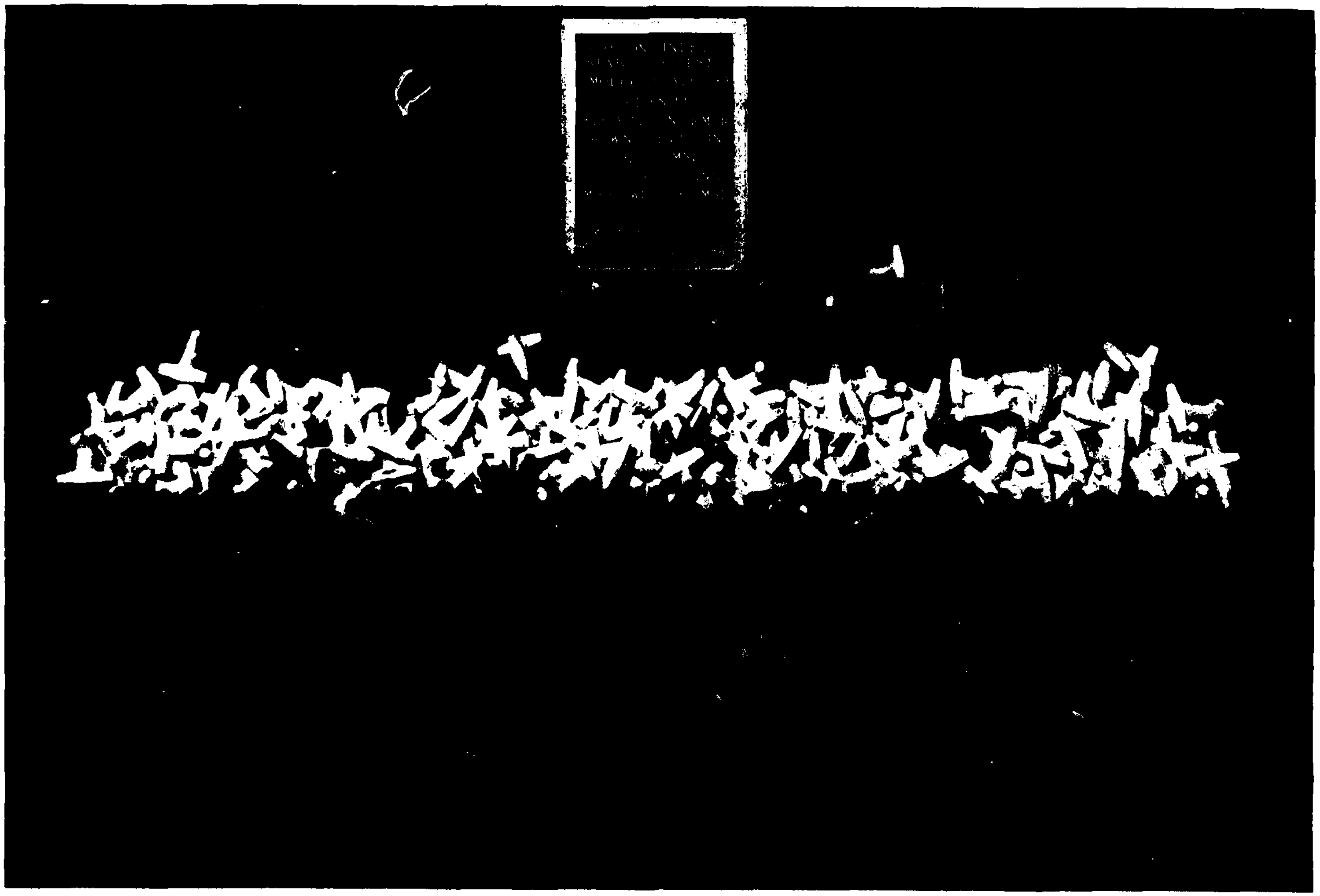

Photo 89. Sea-side view of Plan 10 after attack of 15-sec, 15.5-ft waves at an swl of +7.5 ft NGVD

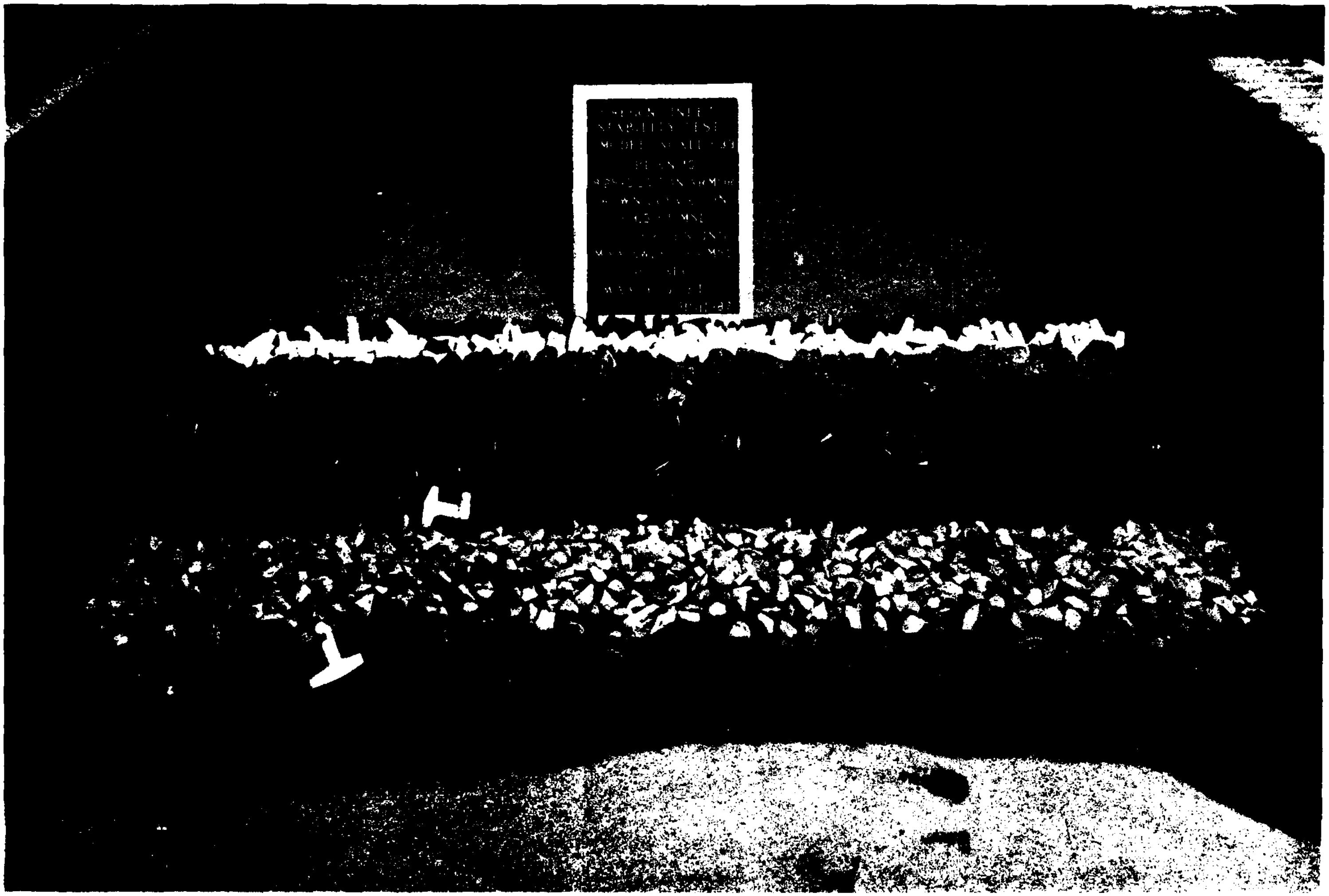

Photo 90. Channel-side view of Plan 10 after attack of 15-sec, 15.5-ft waves at an swl of +7.5 ft NGVD

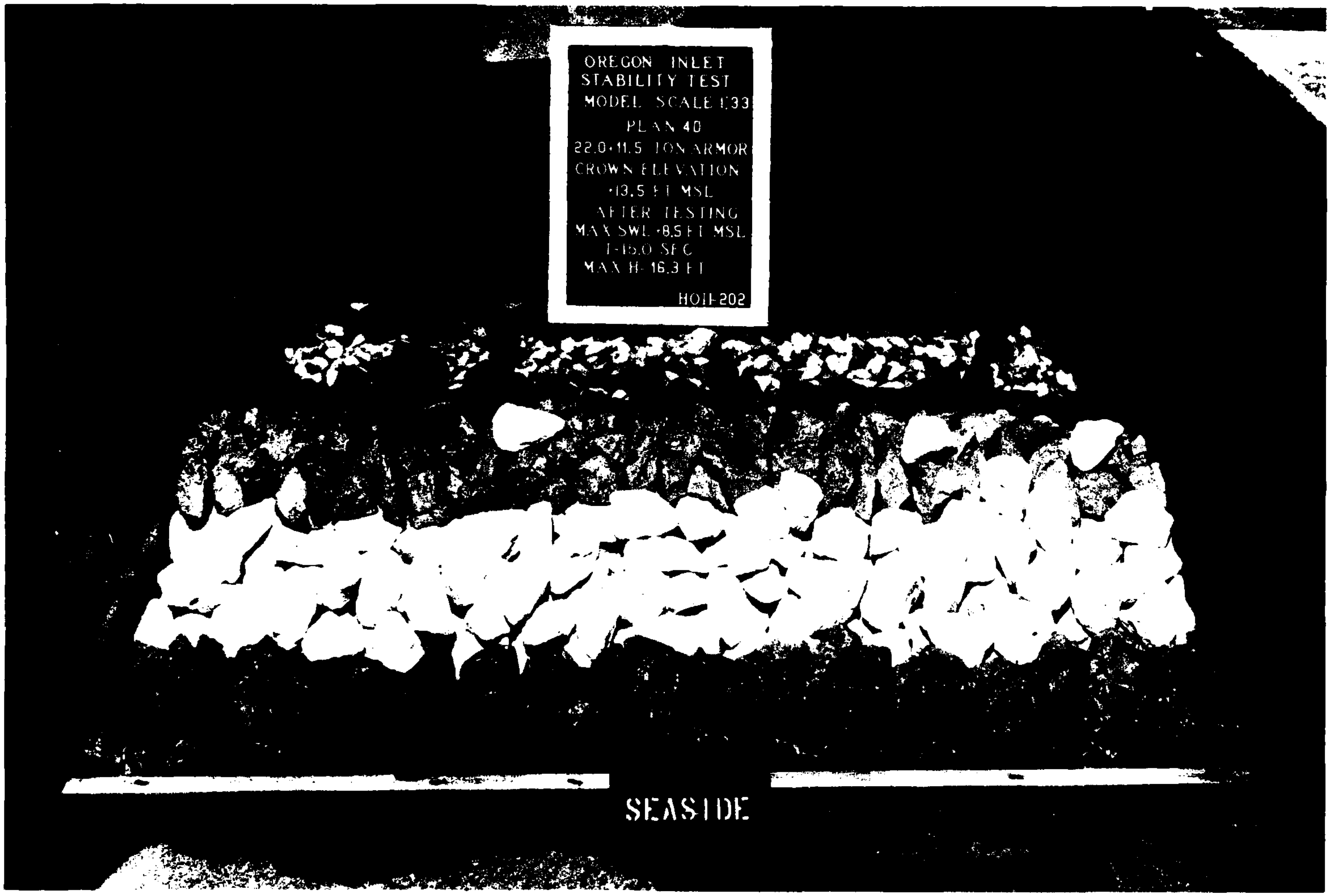

Photo 91. Sea-side view of Plan 4D after testing step 3 of the +8.5 ft NGVD hydrograph

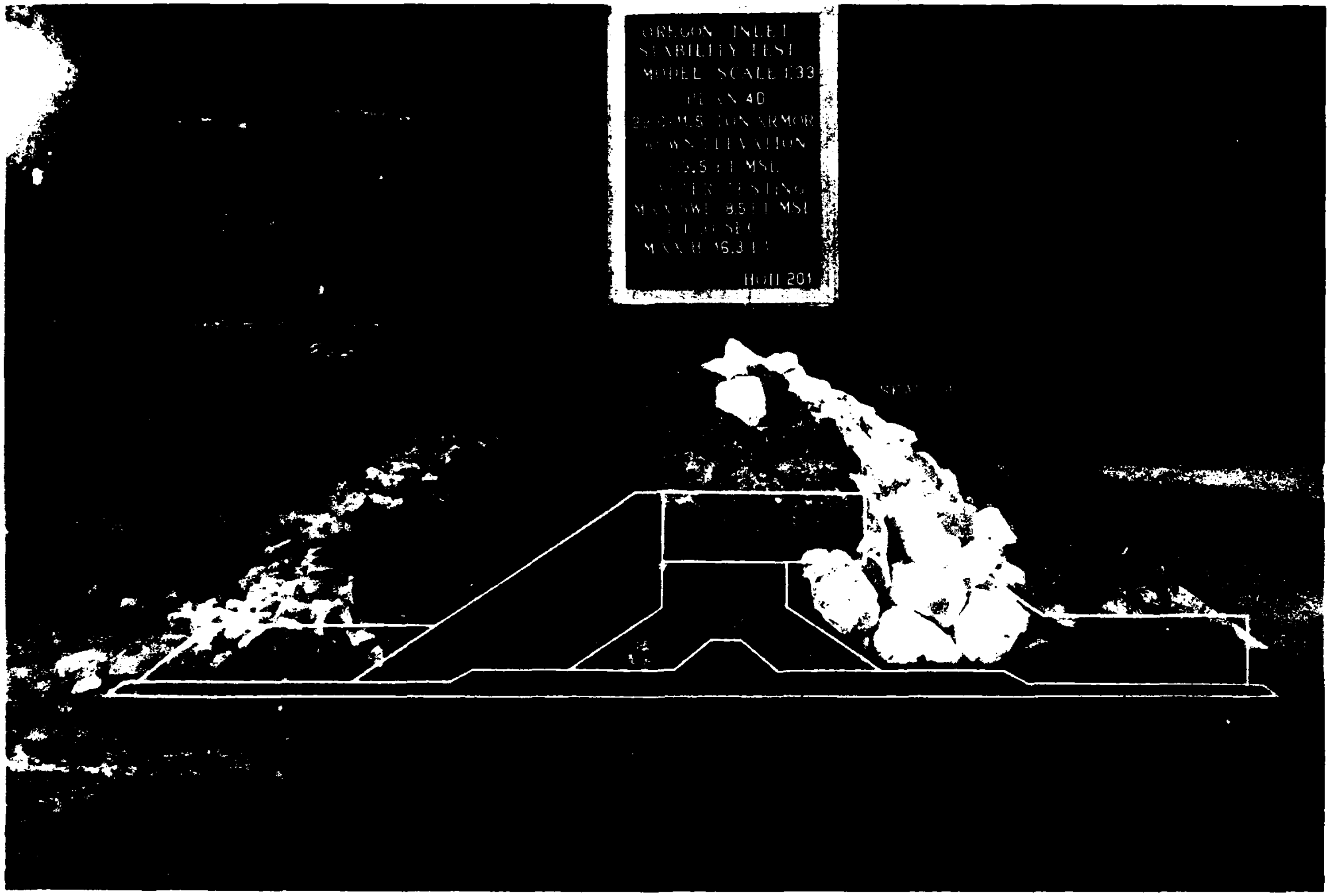

Photo 92. End view of Plan 4D after testing step 3 of the +8.5 ft NGVD hydrograph

Photo 93. Sea-side view of Plan 10 after testing step 3 of the +8.5 ft NGVD hydrograph

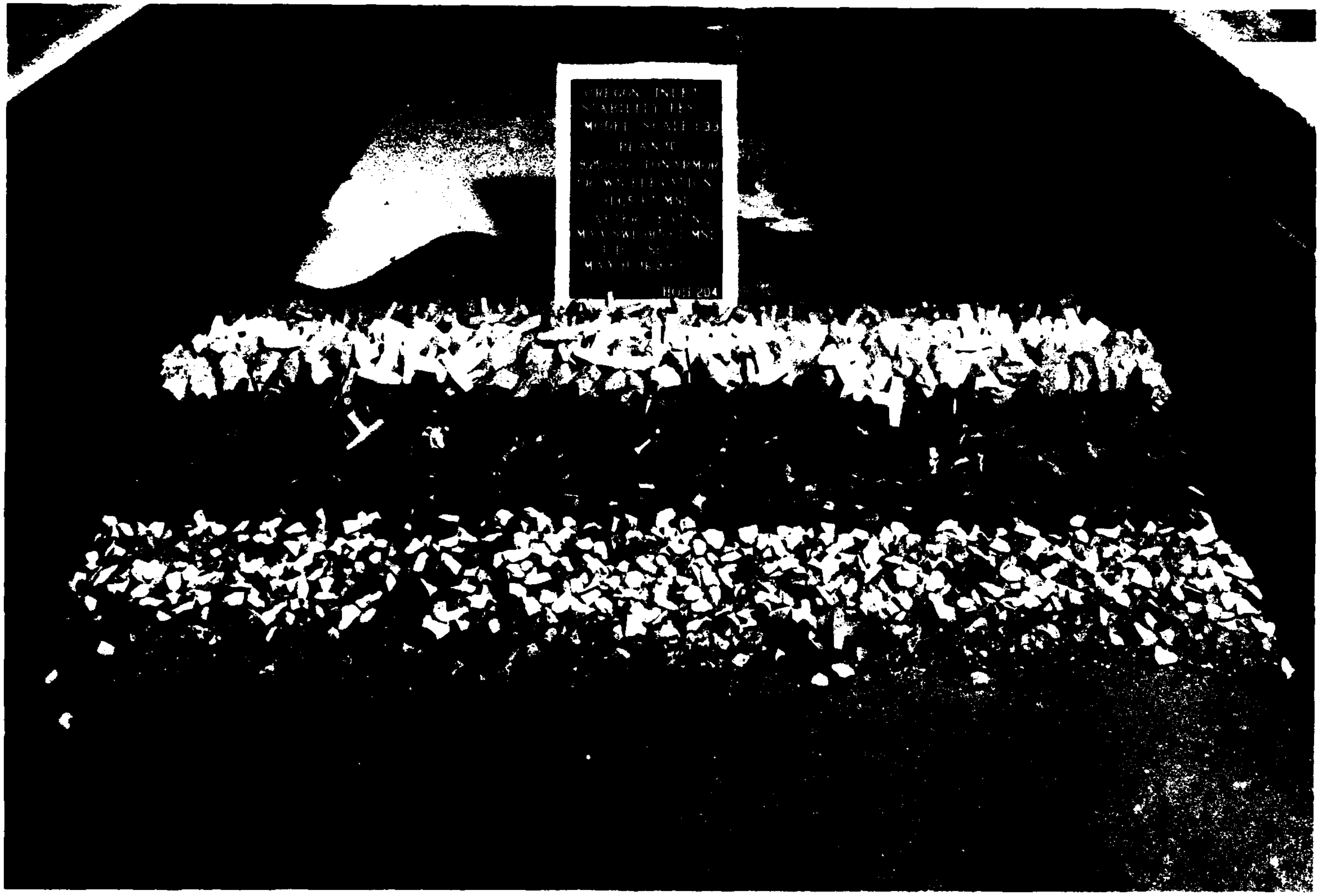

Photo 94. Channel-side view of Plan 10 after testing step 3 of the +8.5 ft NGVD hydrograph

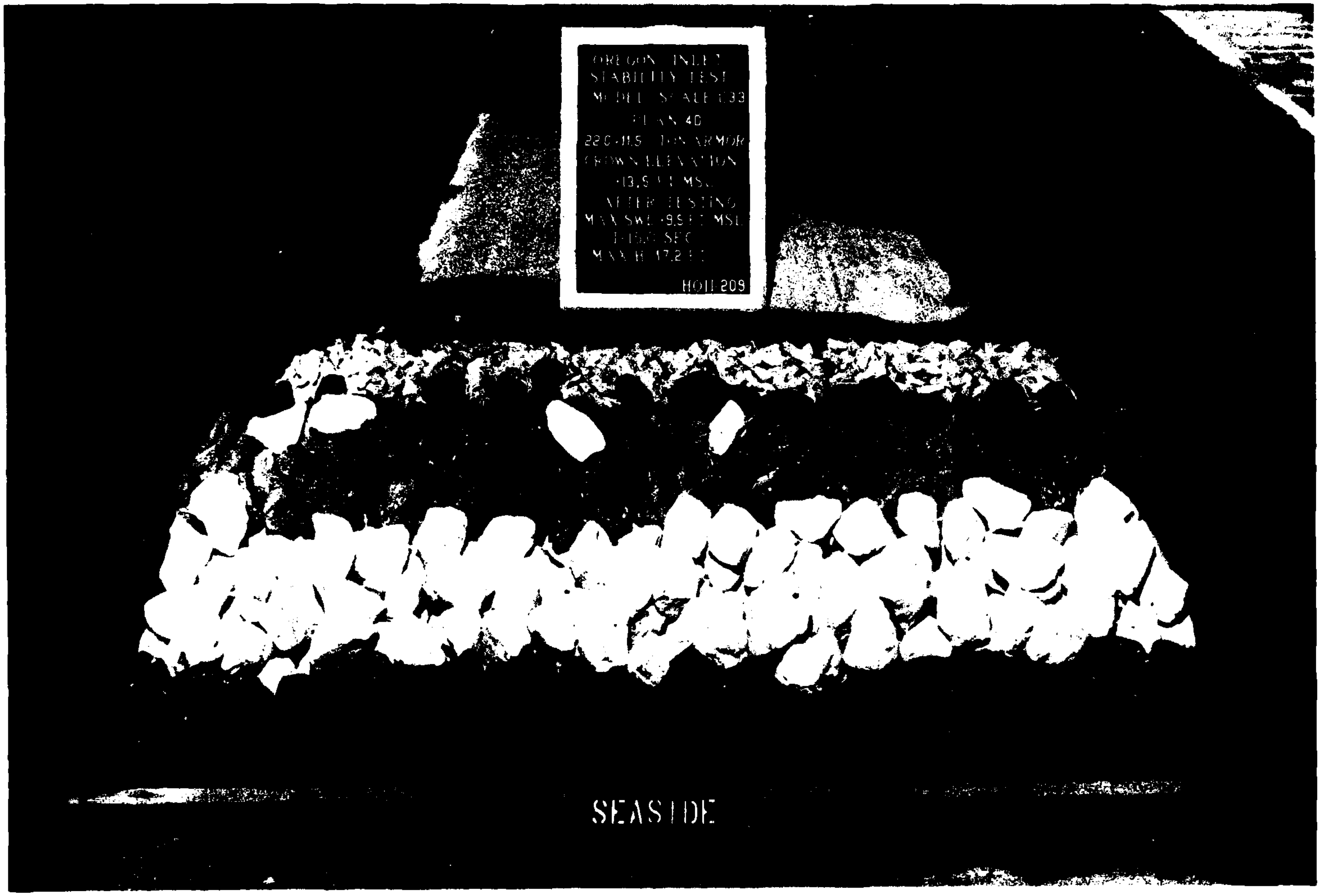

Photo 95. Sea-side view of Plan 4D after testing step 5 of the +9.5 ft NGVD hydrograph

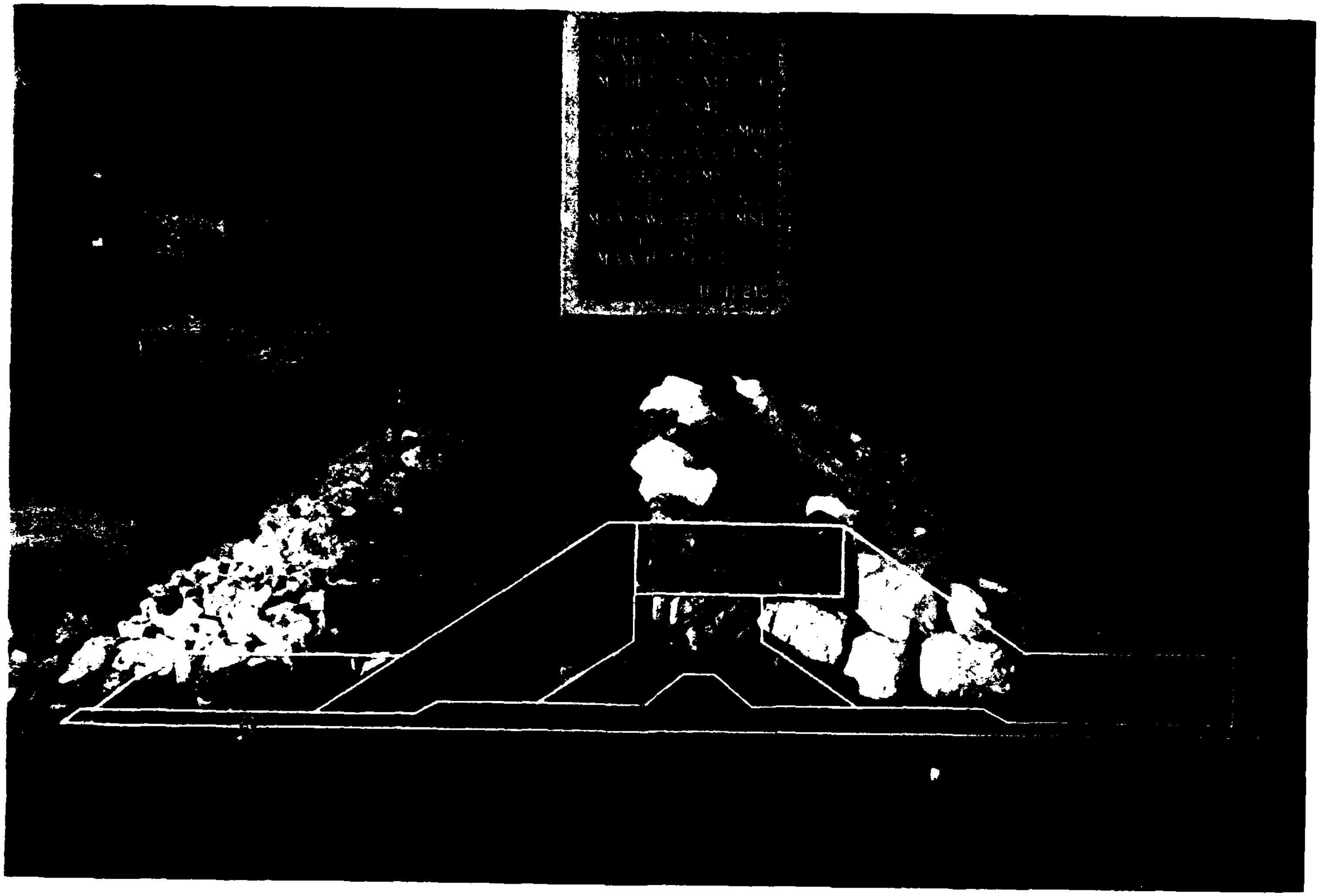

Photo 96. End view of Plan 4D after testing step 5 of the +9.5 ft NGVD hydrograph

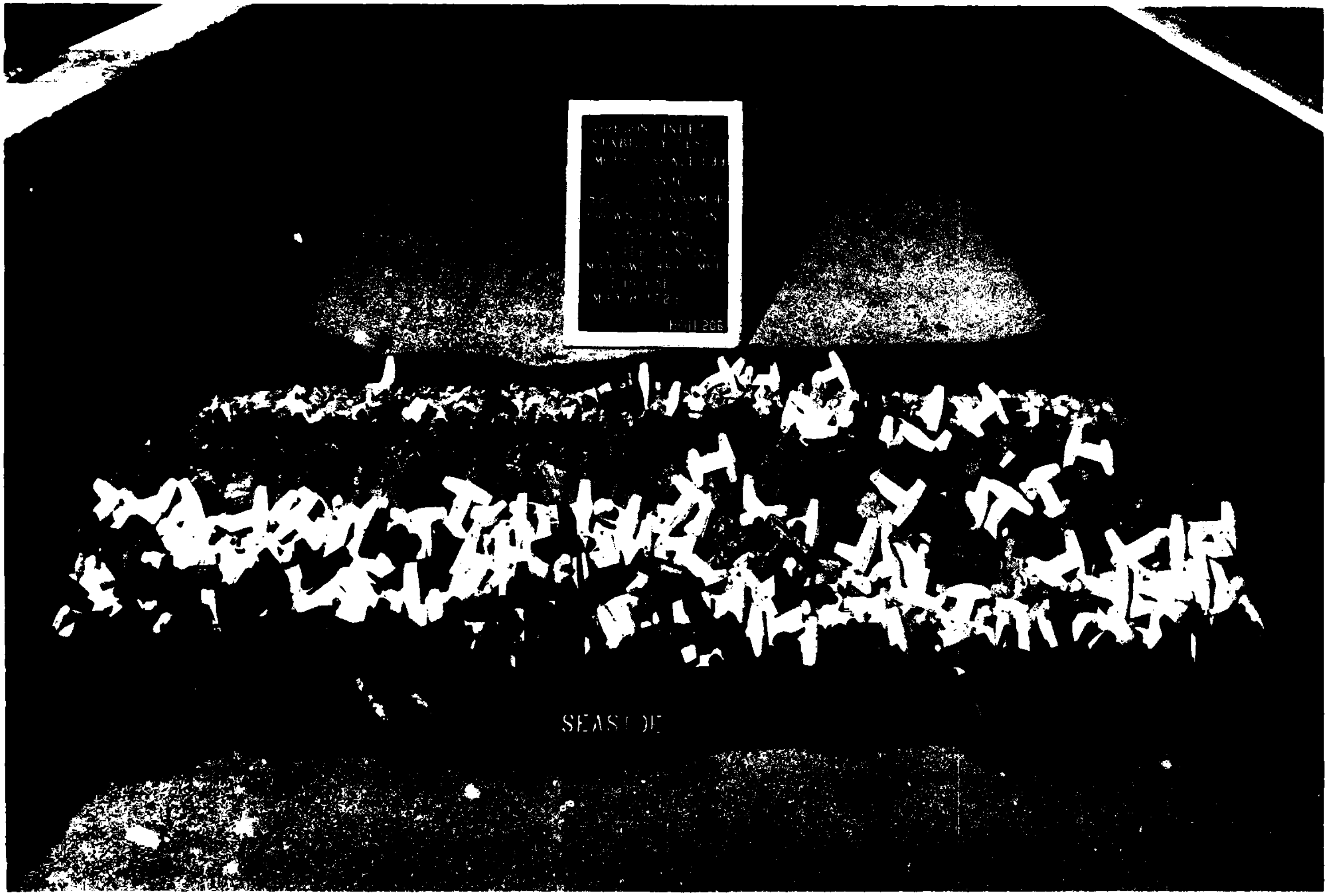

Photo 97. Sea-side view of Plan 10 after testing step 5 of the +9.5 ft NGVD hydrograph

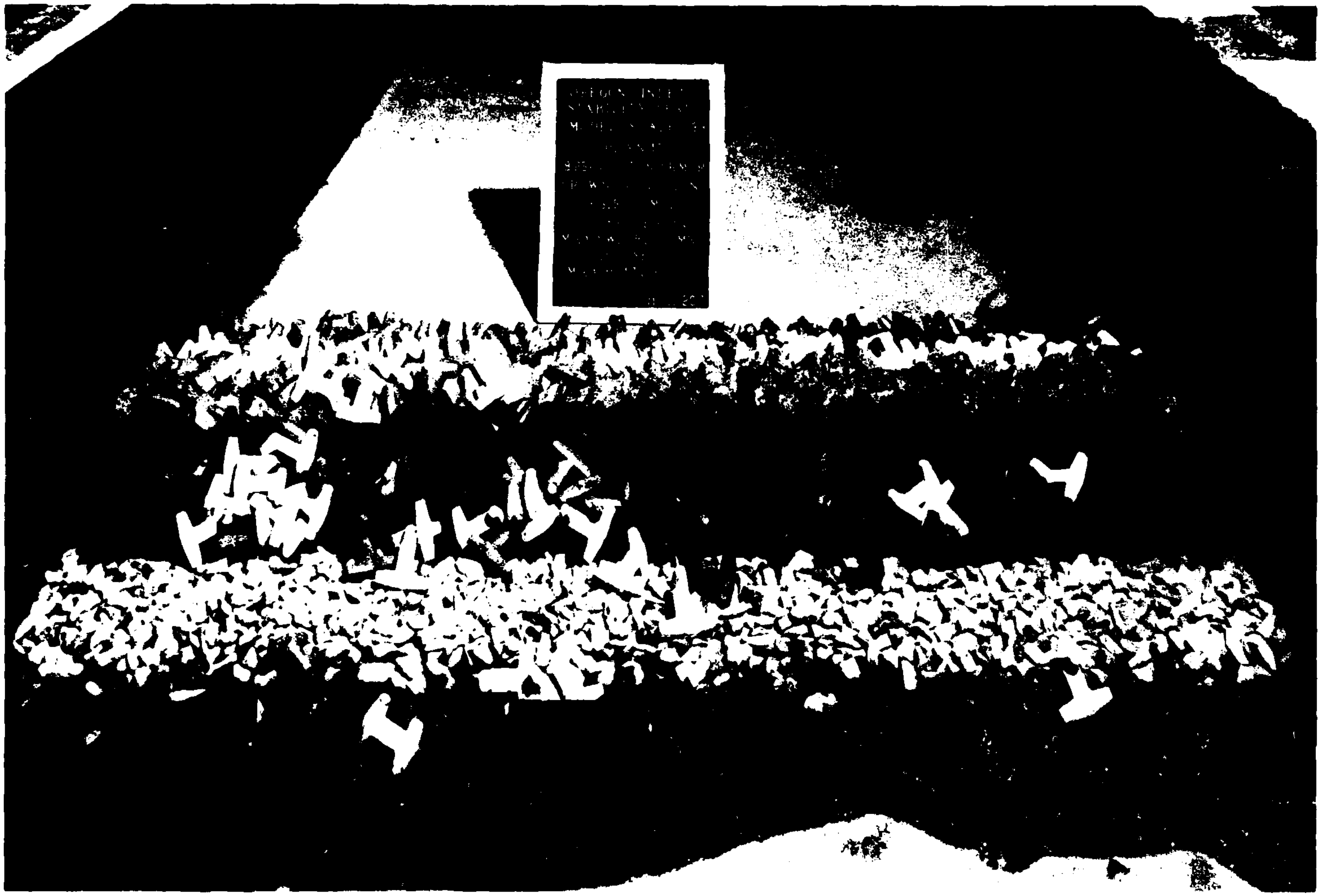

Photo 98. Channel-side view of Plan 10 after testing step 5 of the +9.5 ft NGVD hydrograph

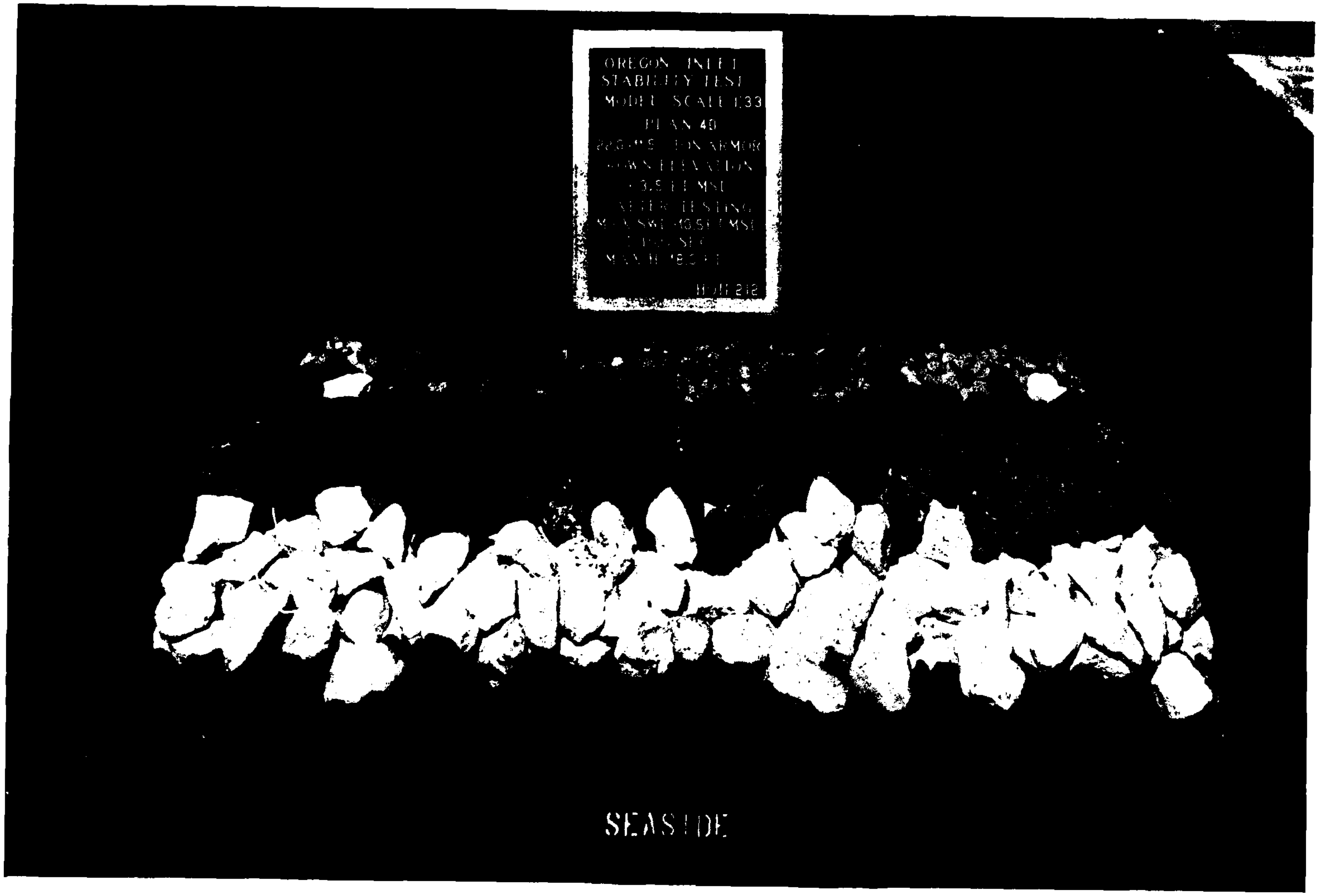

Photo 99. Sea-side view of Plan 4D after testing step 7 of the +10.5 ft NGVD hydrograph

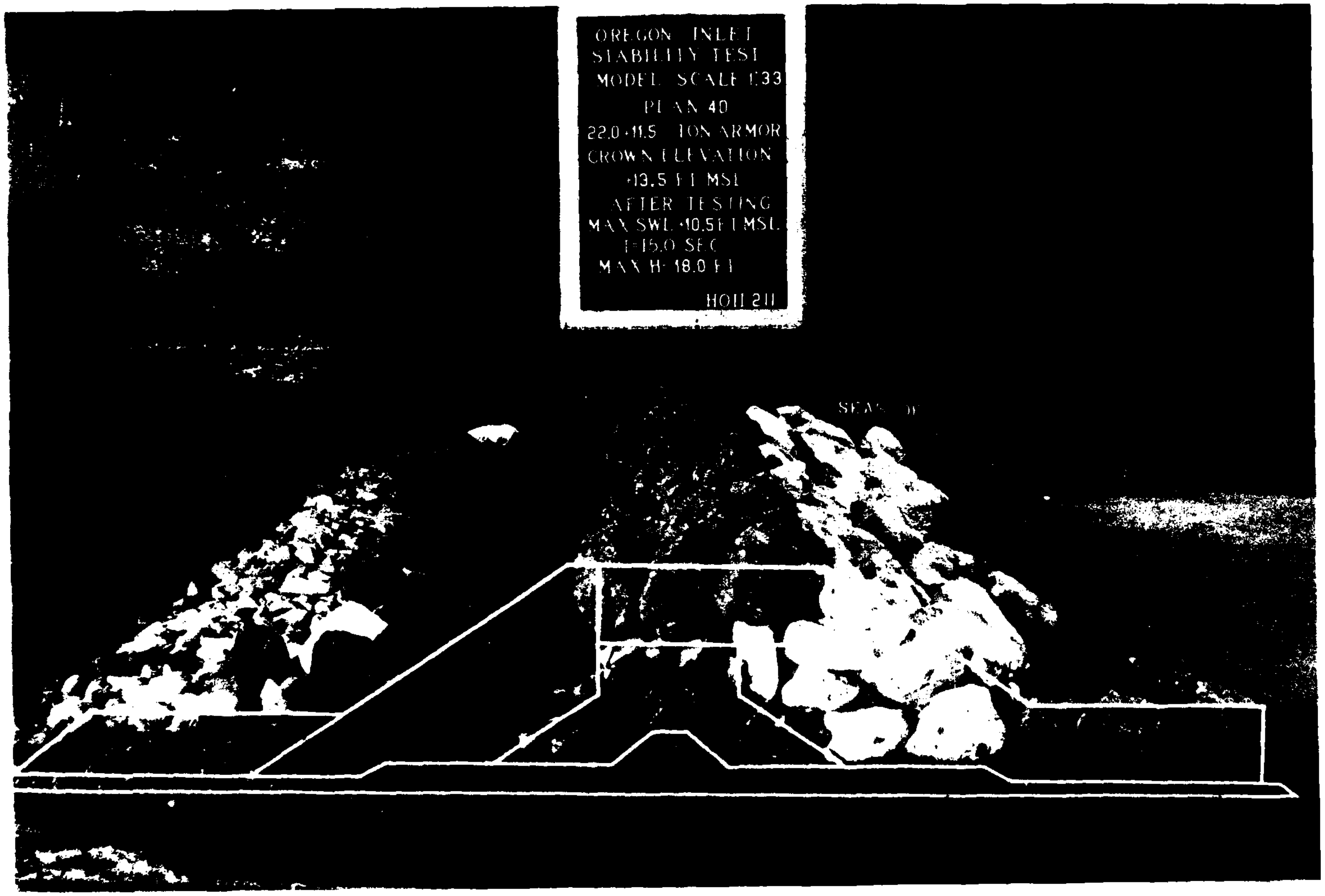

Photo 100. End view of Plan 4D after testing step 7 of the +10.5 ft NGVD hydrograph

AD-A136 610 JETTY STABILITY STUDY OREGON INLET NORTH CAROLINA HYDRAULIC MODEL INVESTIGATION(U) COASTAL ENGINEERING RESEARCH CENTER VICKSBURG MS R D CARVER ET AL. SEP 83 3/5

UNCLASSIFIED CERC-TR-83-3 F/G 13/2 NL

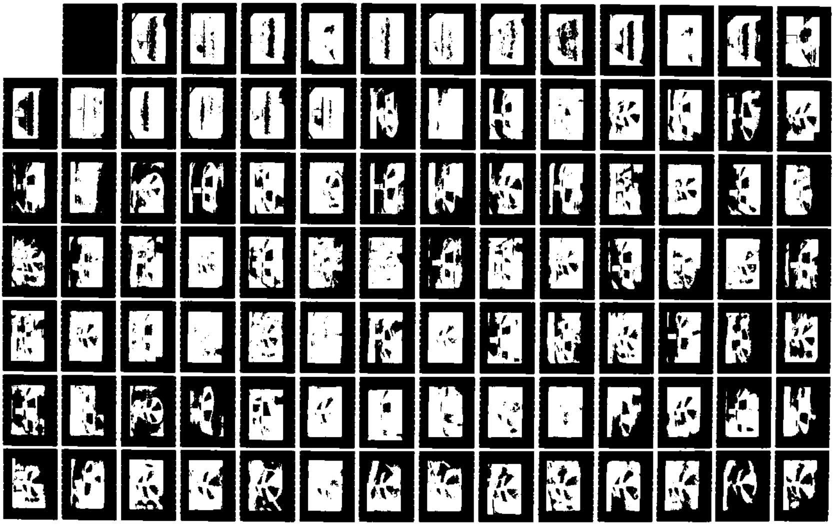

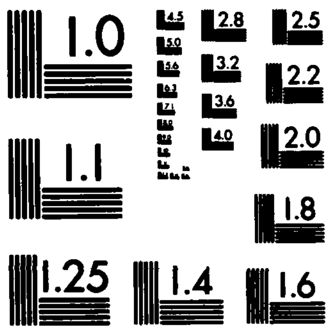

MICROCOPY RESOLUTION TEST CHART
NATIONAL BUREAU OF STANDARDS-1963-A

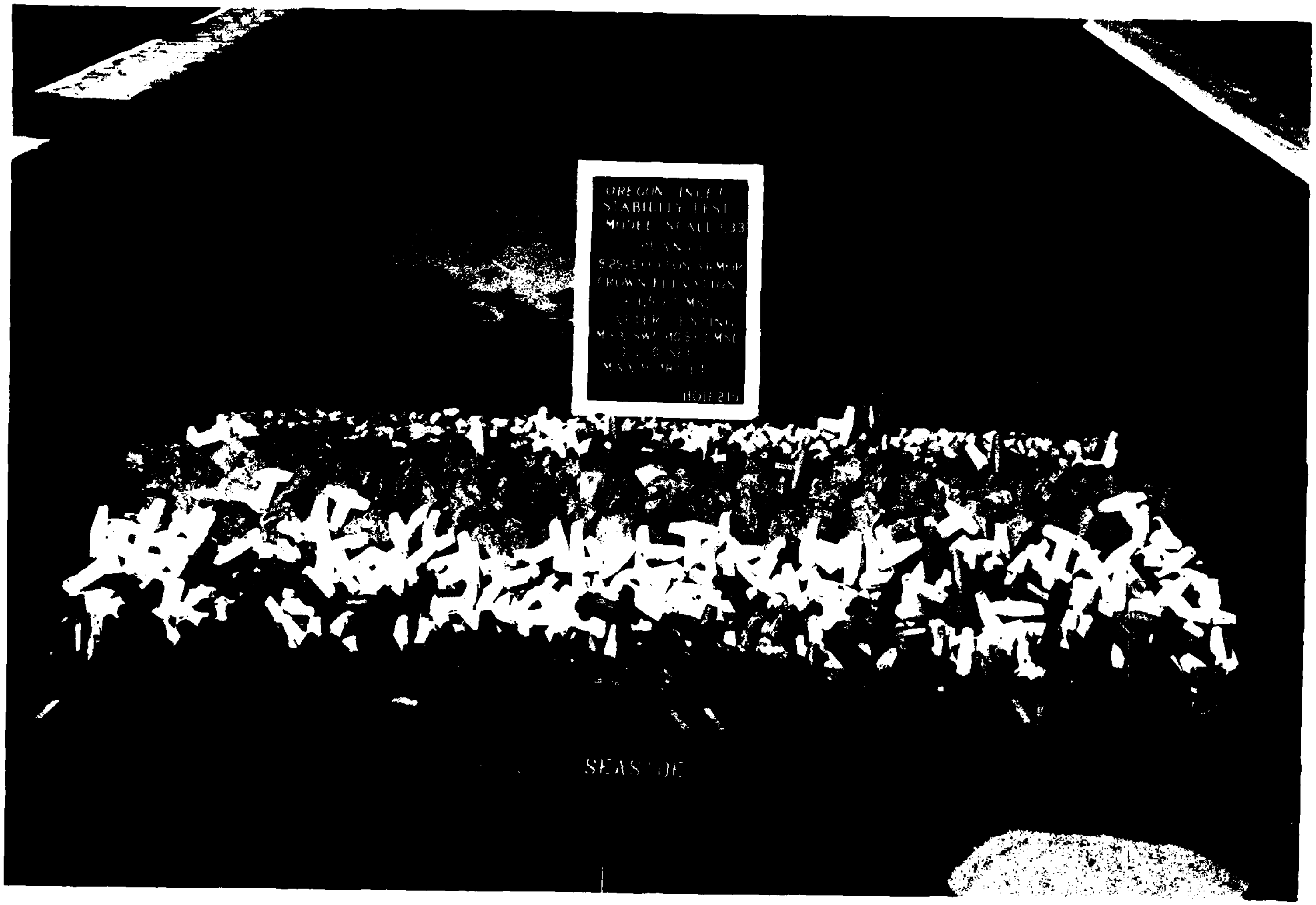

Photo 101. Sea-side view of Plan 10 after testing step 7 of the +10.5 ft NGVD hydrograph

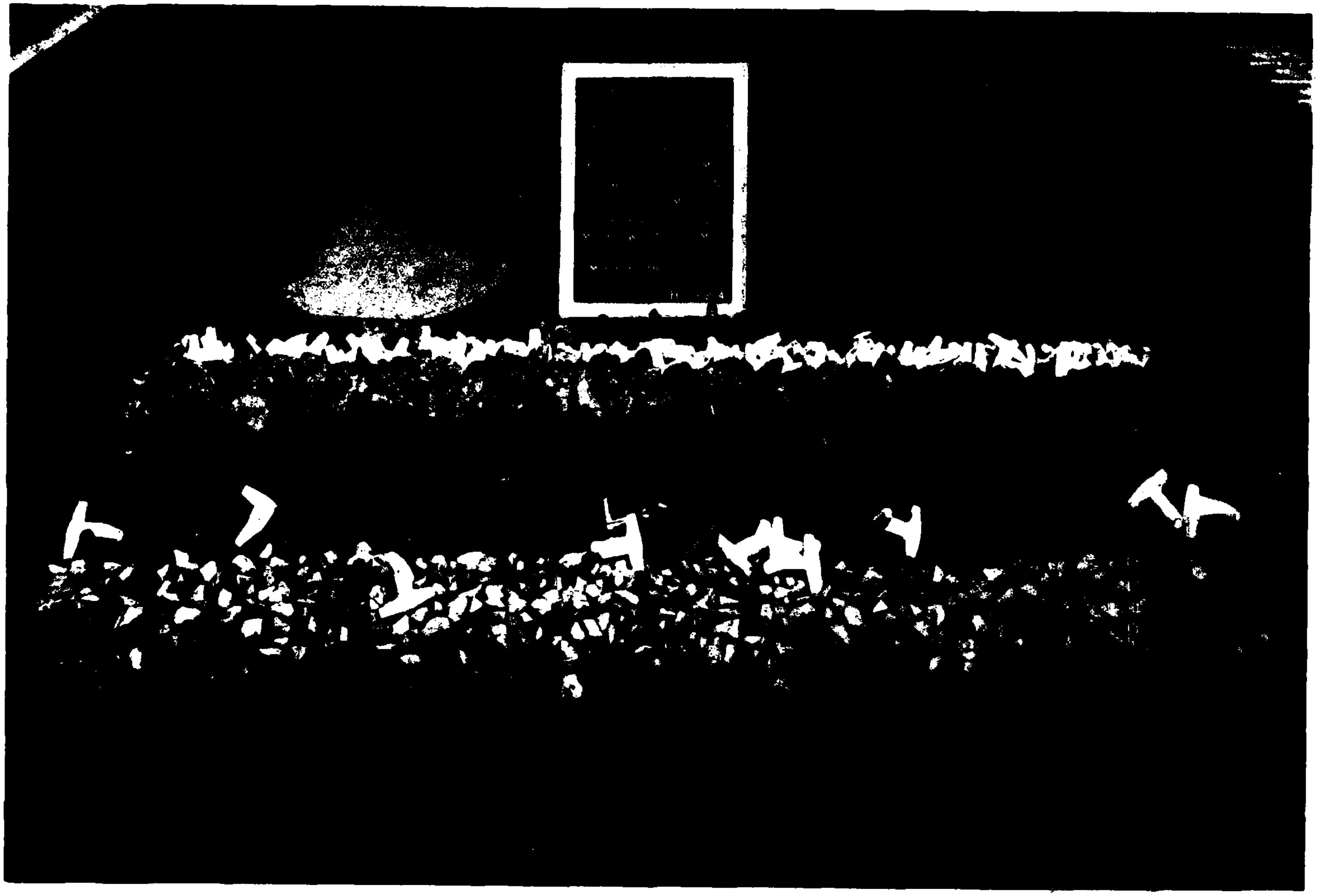

Photo 102. Channel-side view of Plan 10 after testing step 7 of the +10.5 ft NGVD hydrograph

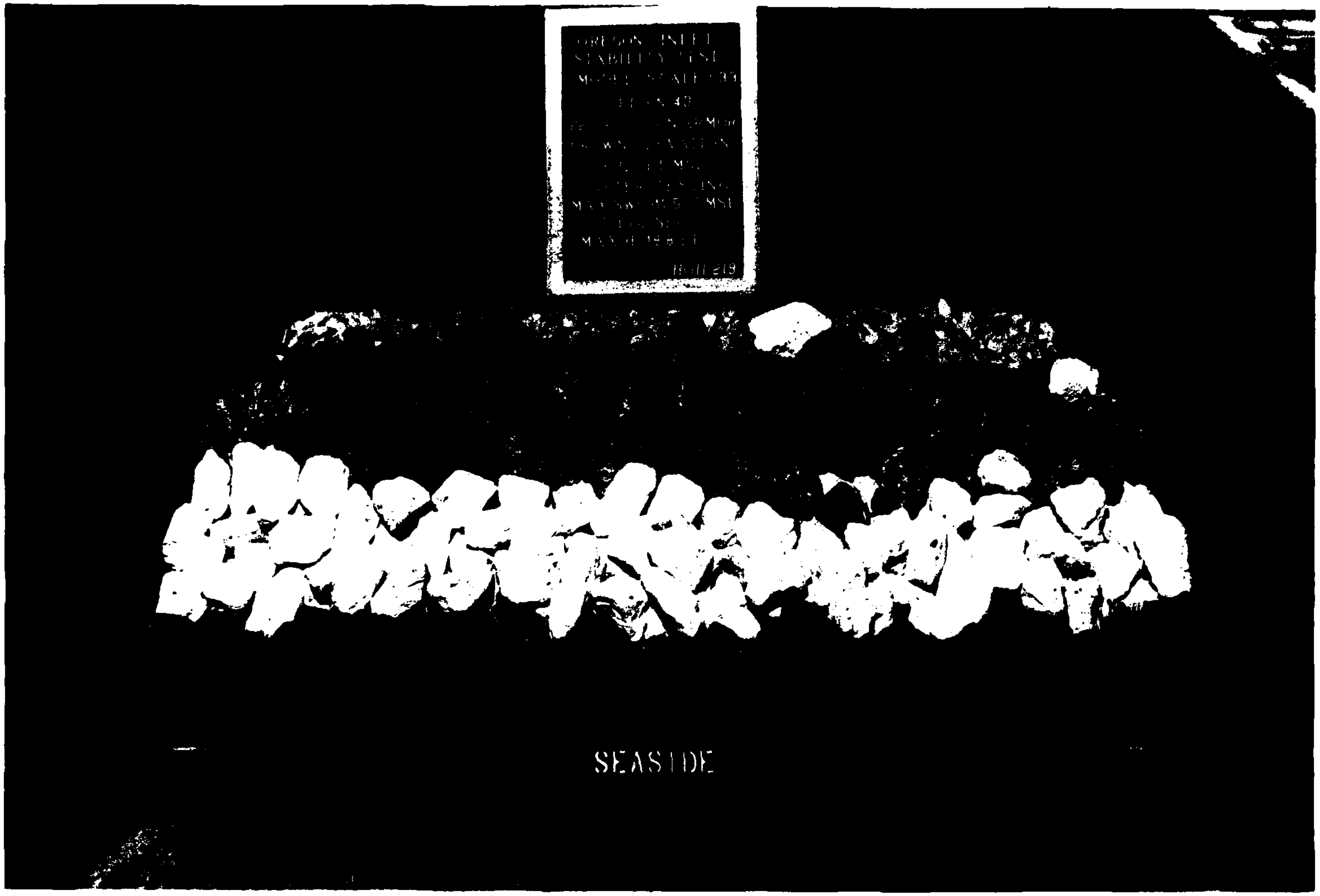

Photo 103. Sea-side view of Plan 4D after testing step 9 of the +11.5 ft NGVD hydrograph

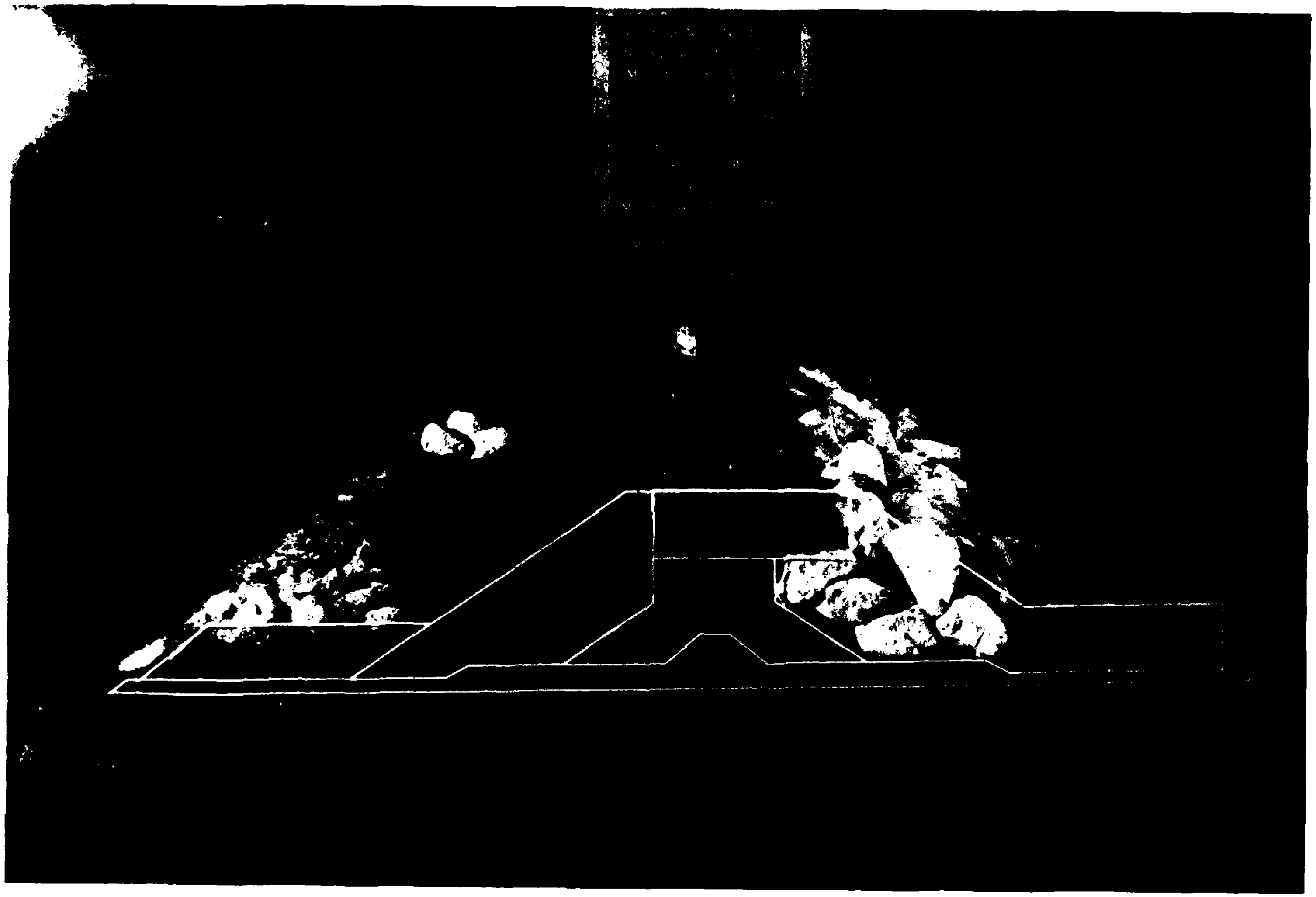

Photo 104. End view of Plan 4D after testing step 9 of the +11.5 ft NGVD hydrograph

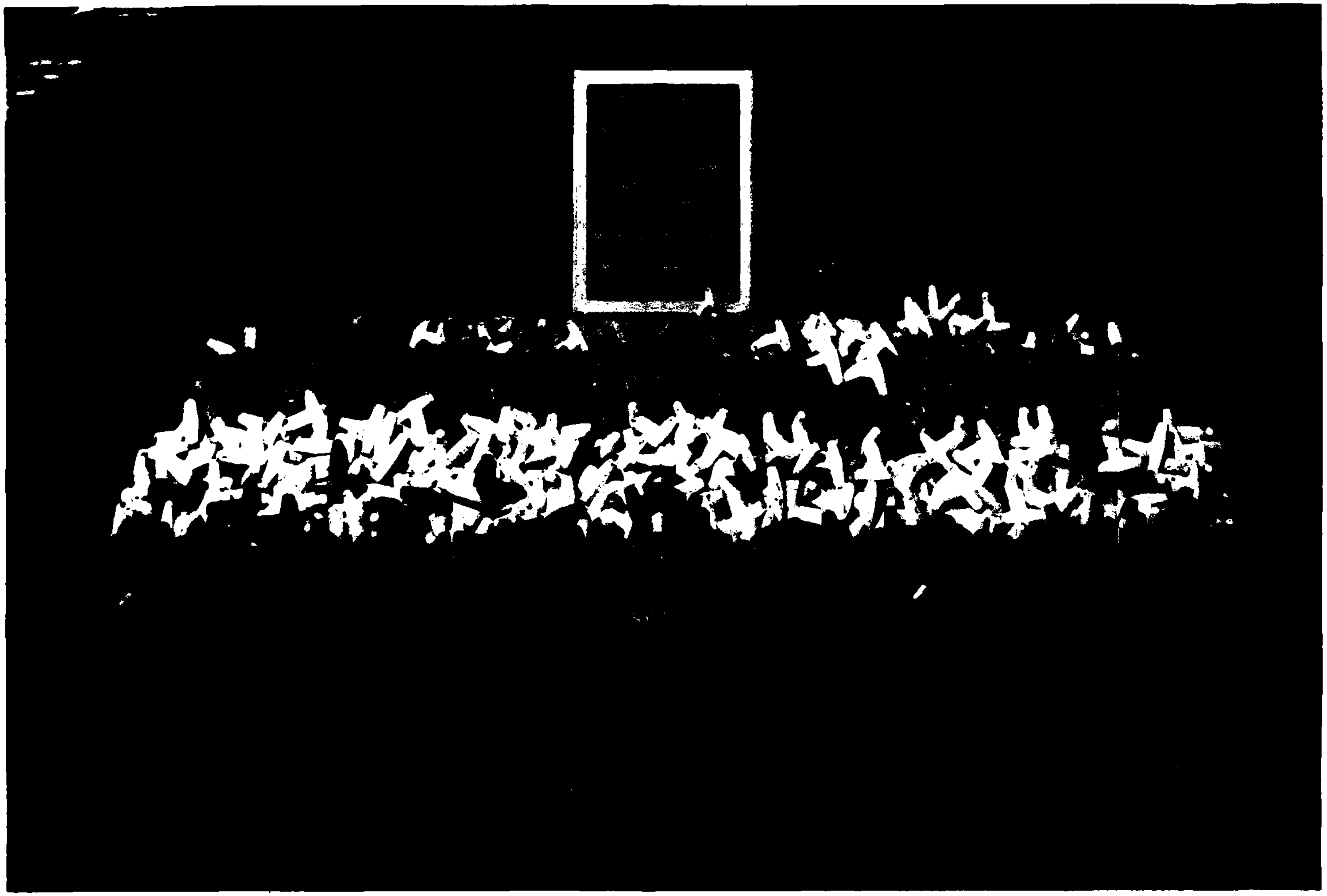

Photo 105. Sea-side view of Plan 10 after testing step 9 of the +11.5 ft NGVD hydrograph

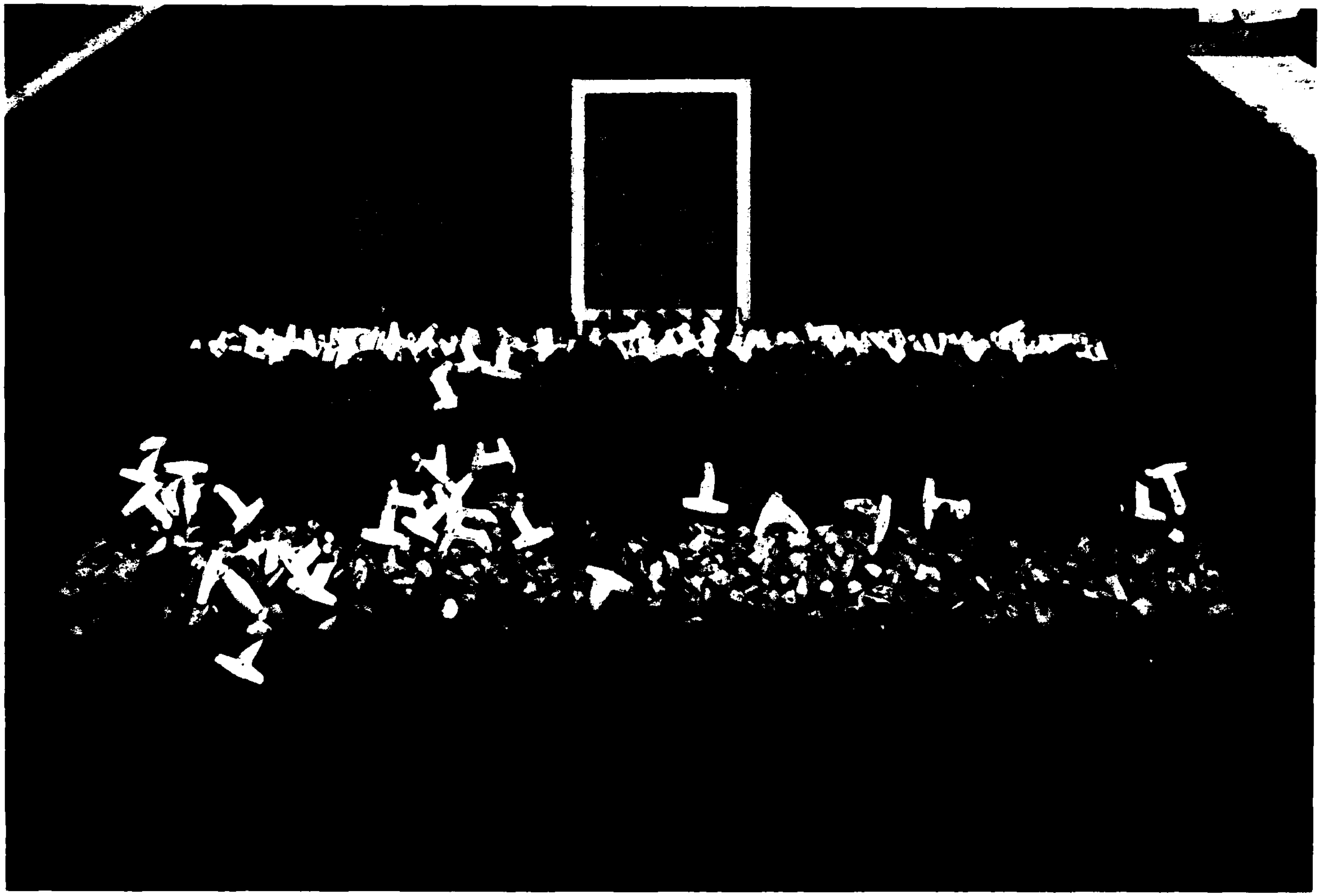

Photo 106. Channel-side view of Plan 10 after testing step 9 of the +11.5 ft NGVD hydrograph

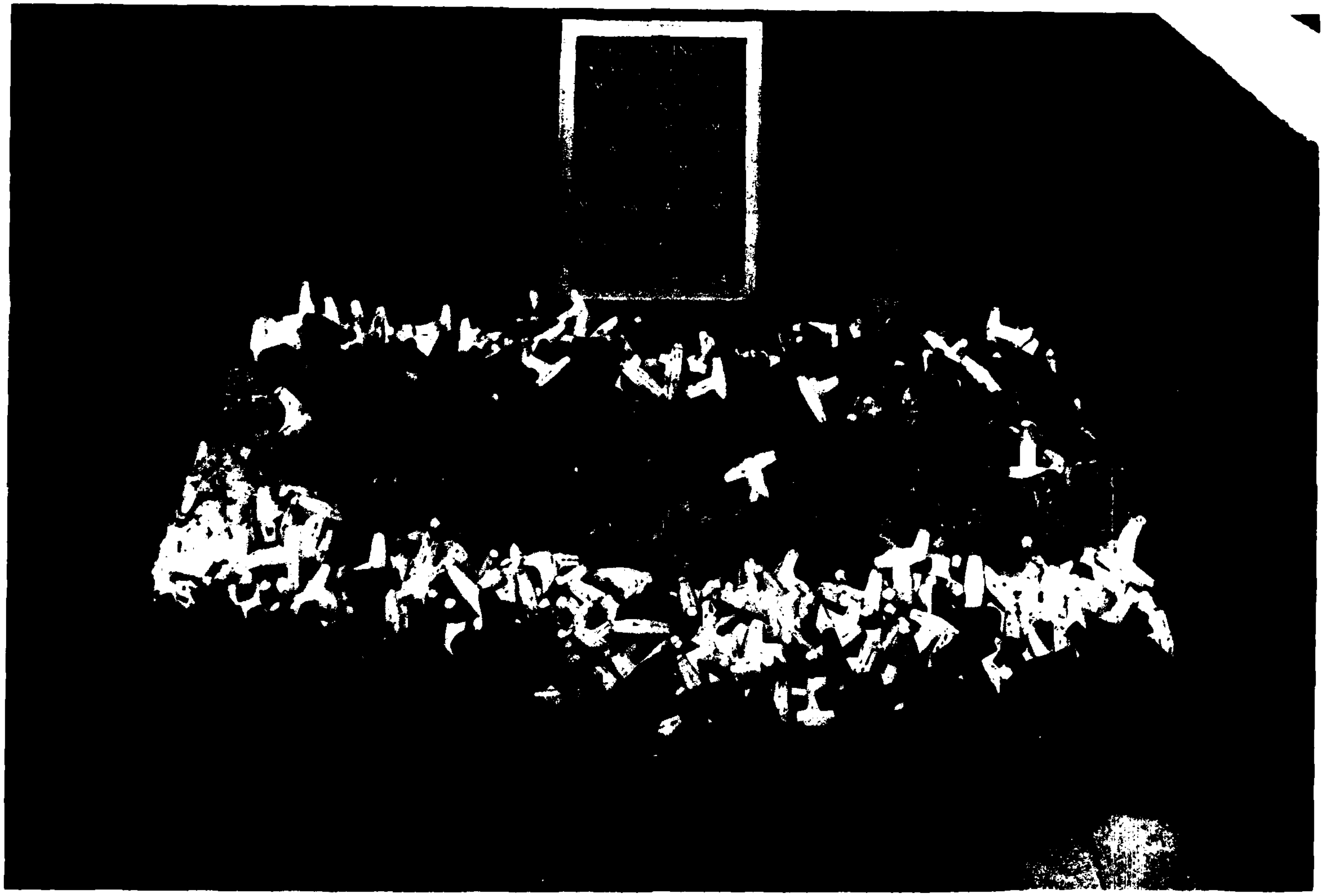

Photo 107. Sea-side view of Plan 10 after testing step 15 of the +14.5 ft NGVD hydrograph

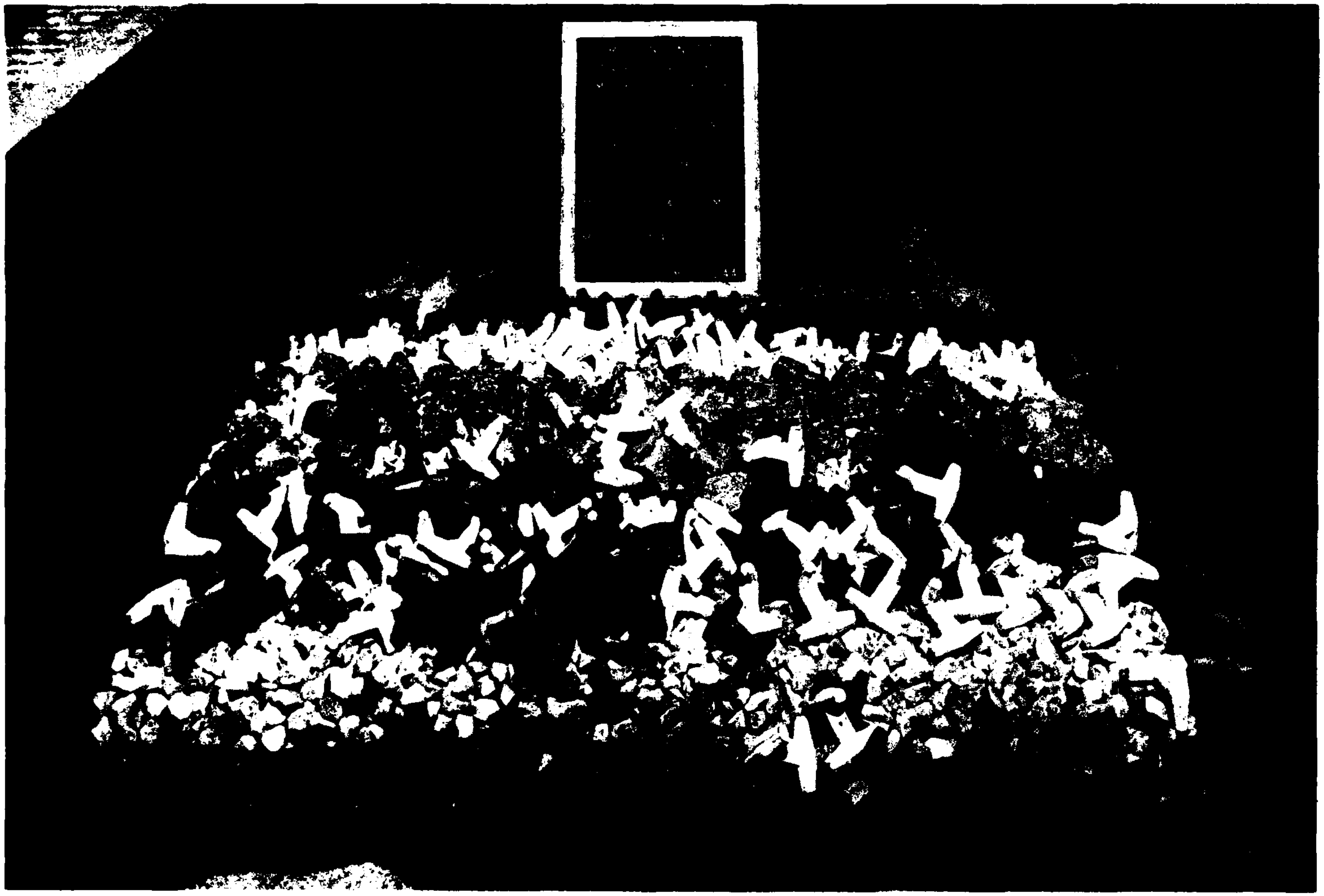

Photo 108. Channel-side view of Plan 10 after testing step 15 of the +14.5 ft NGVD hydrograph

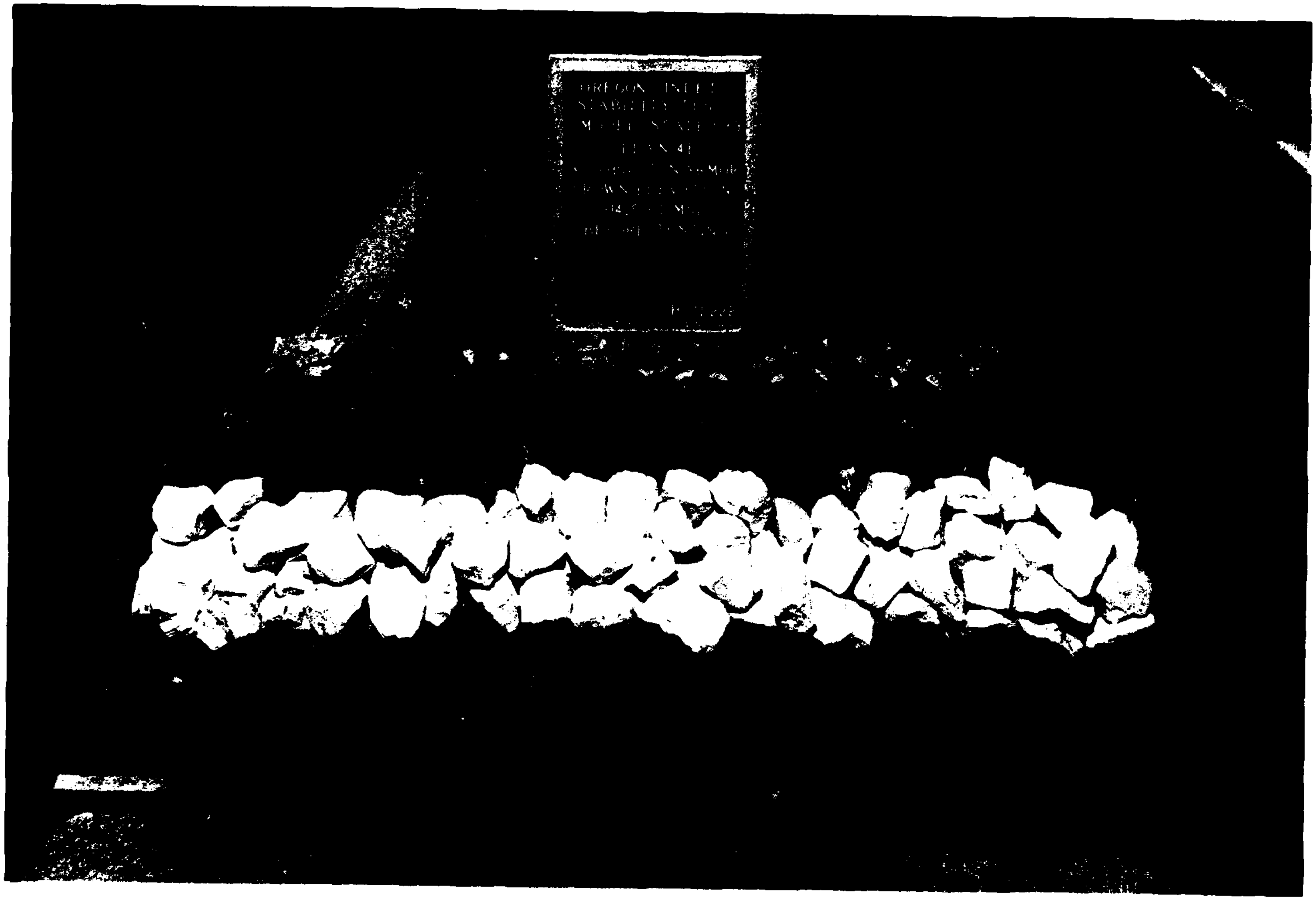

Photo 109. Sea-side view of Plan 4E before wave attack

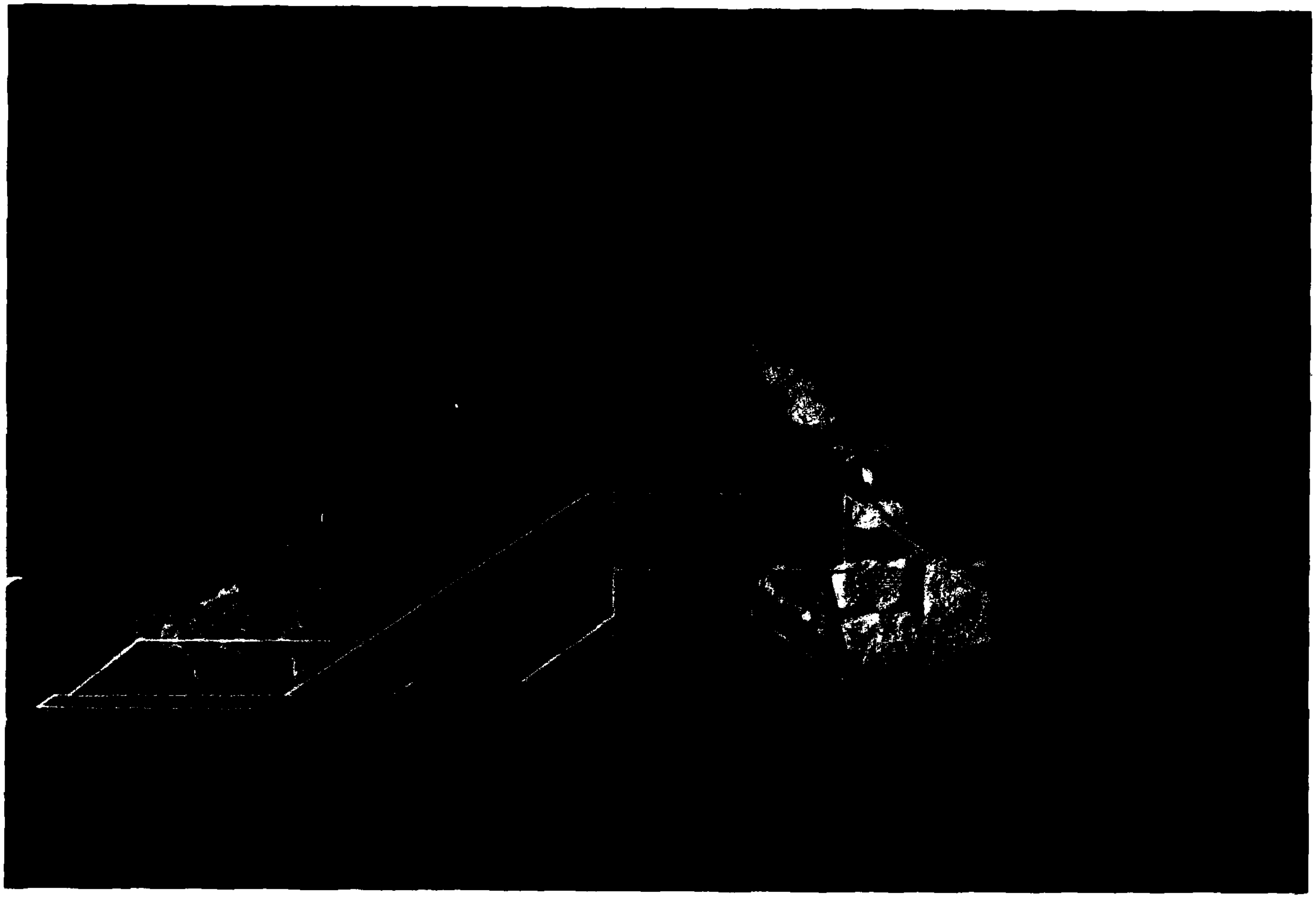

Photo 110. End view of Plan 4E before wave attack

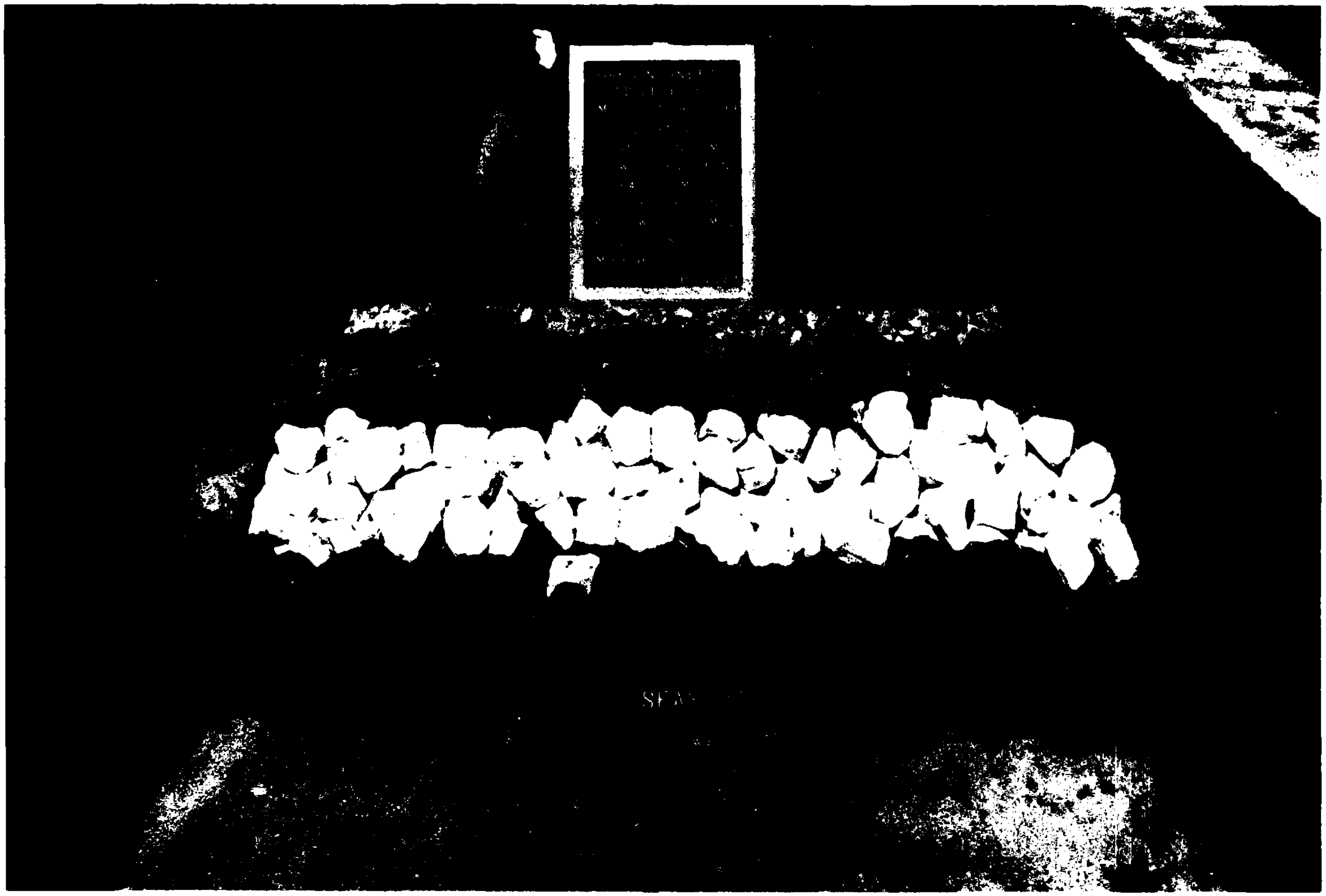

Photo 111. Sea-side view of Plan 4E after attack of 15-sec, 17.2-ft waves at an swl of +9.5 ft NGVD

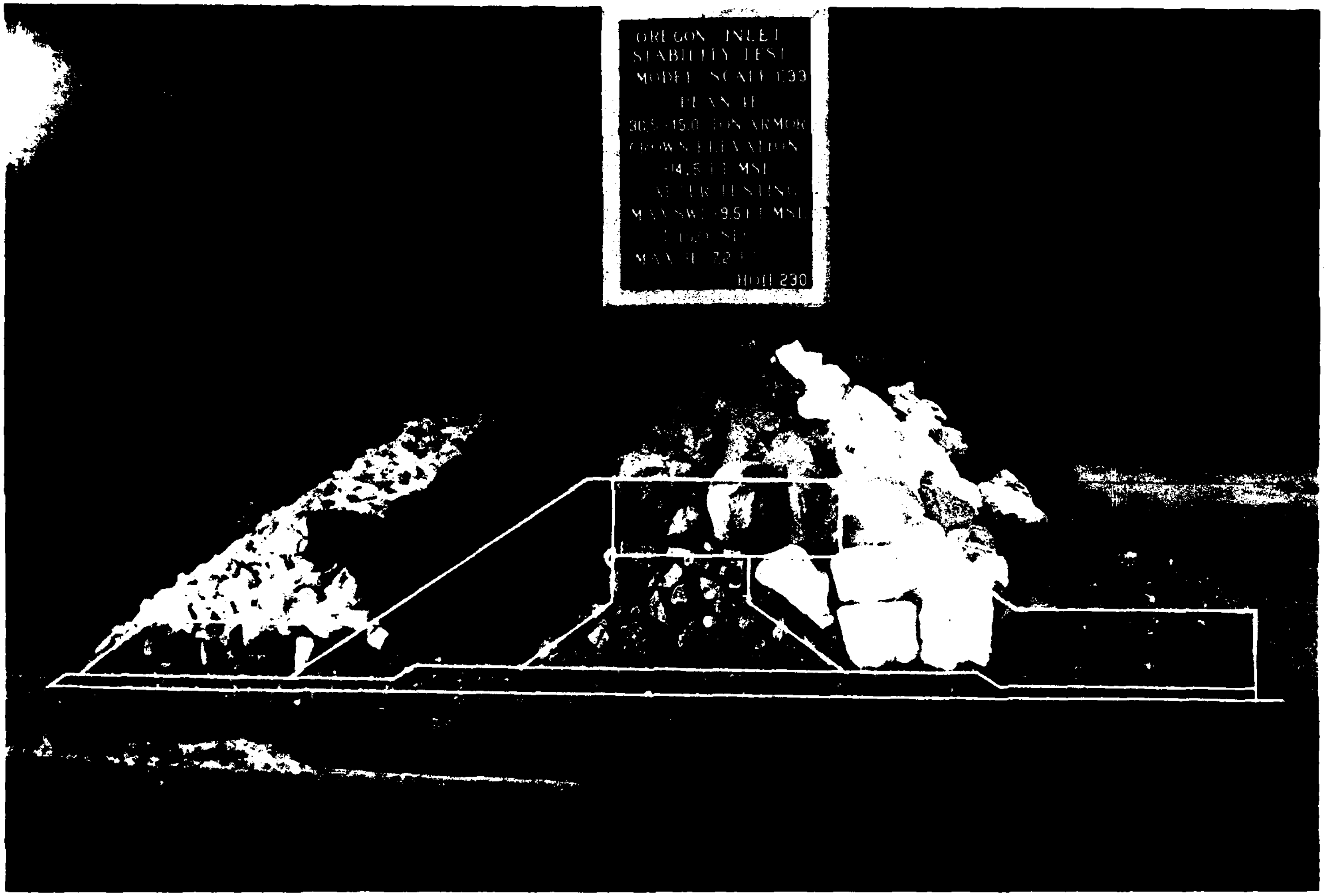

Photo 112. End view of Plan 4E after attack of 15-sec, 17.2-ft waves at an swl of +9.5 ft NGVD

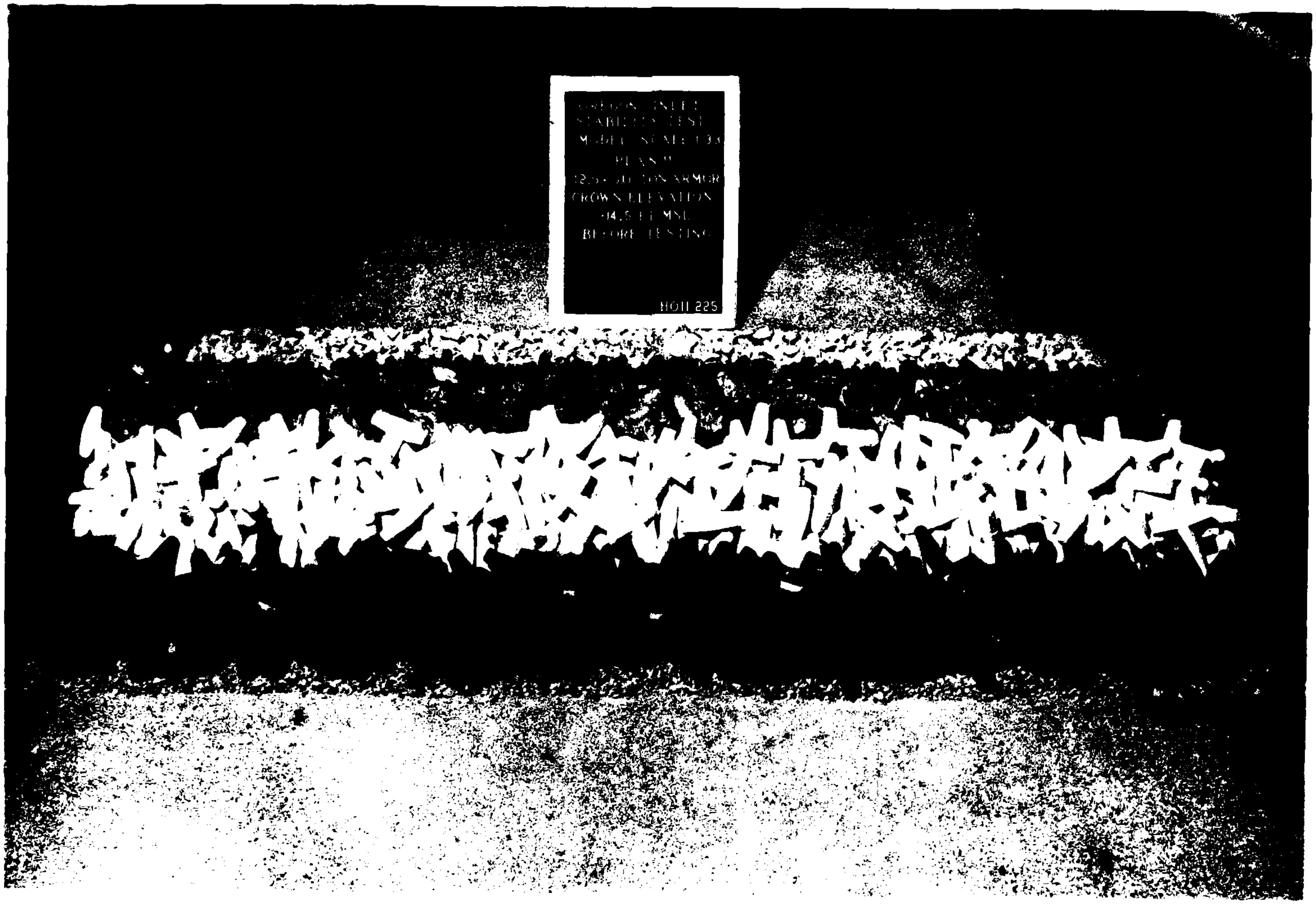

Photo 113. Sea-side view of Plan 11 before wave attack

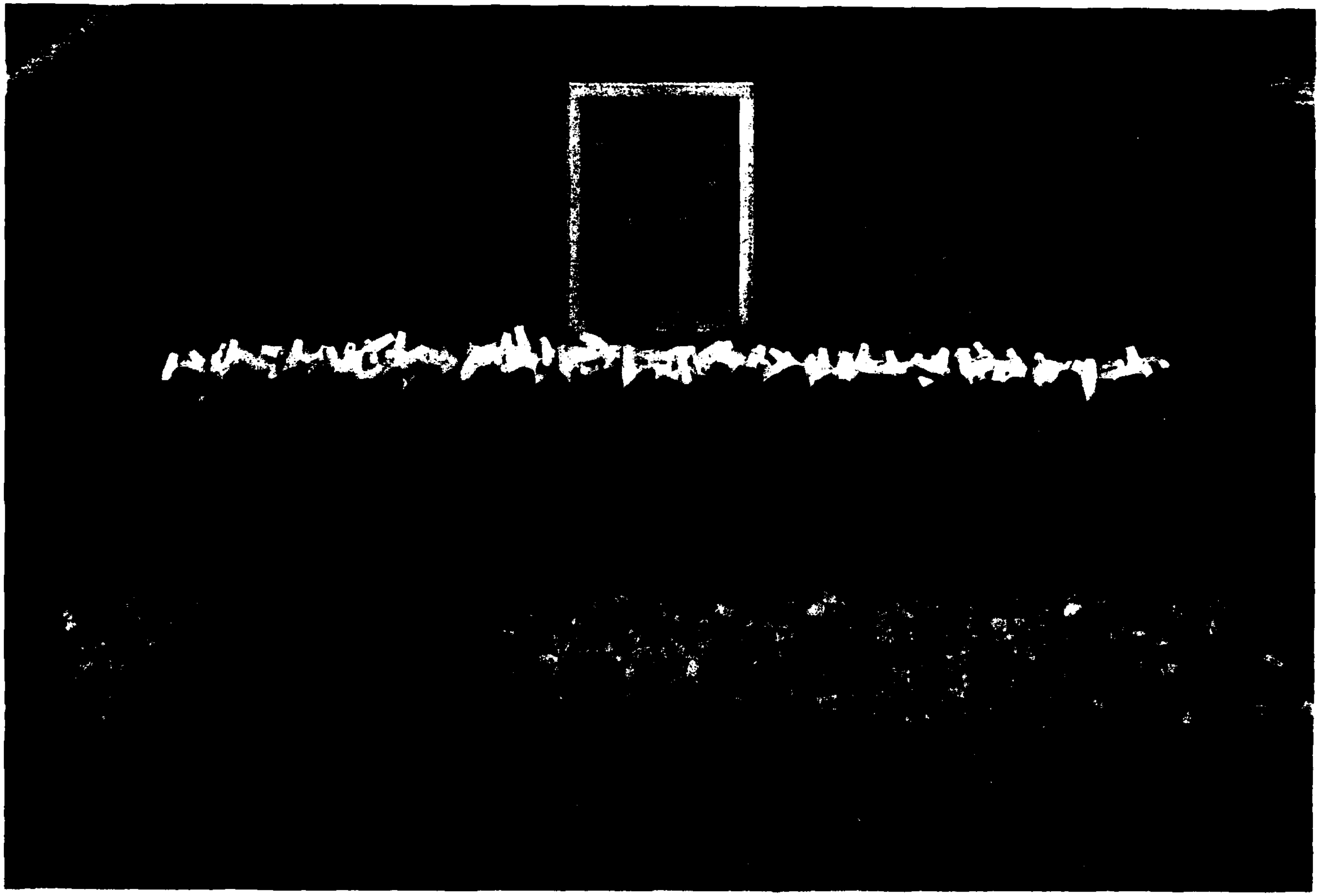

Photo 114. Channel-side view of Plan 11 before wave attack

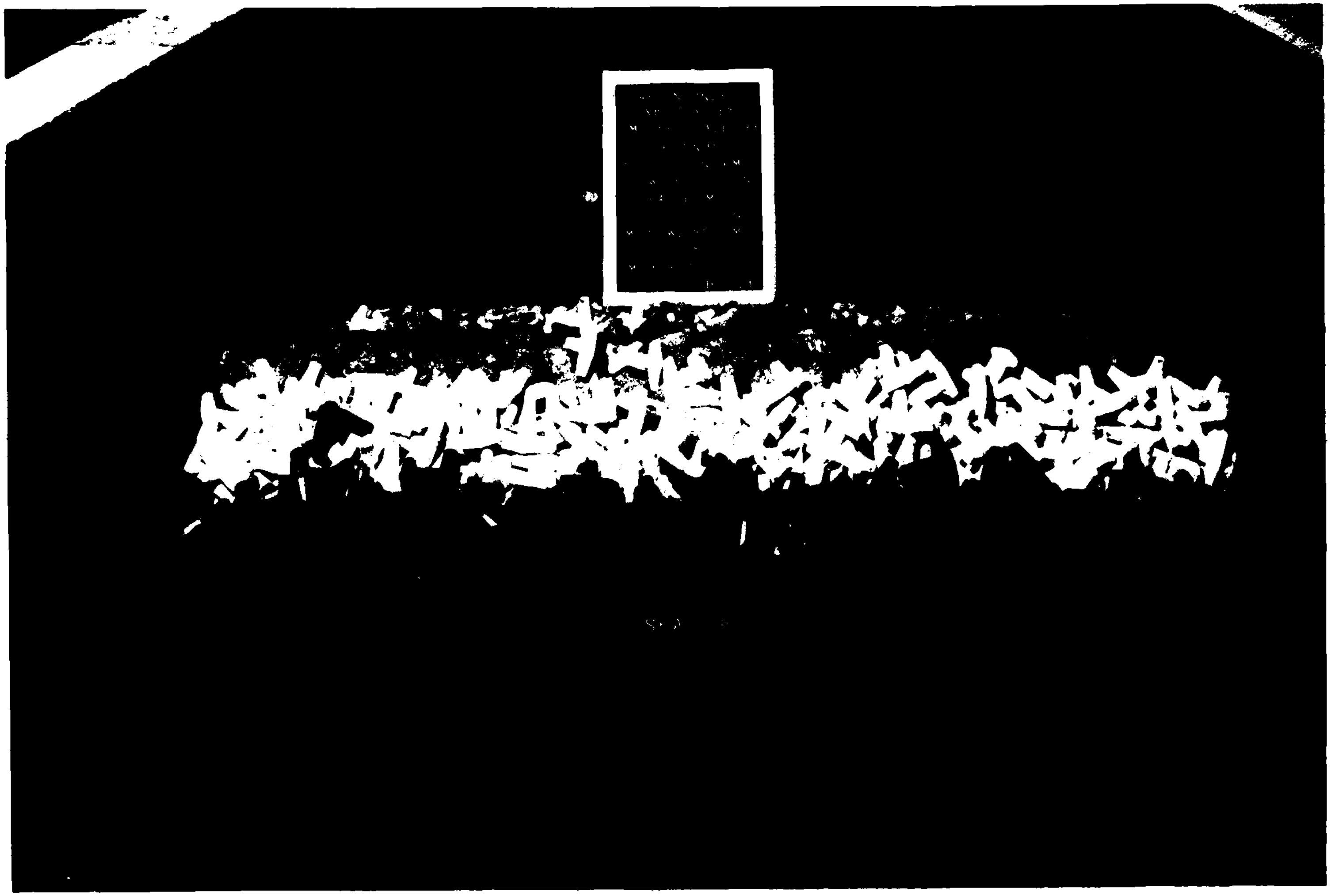

Photo 115. Sea-side view of Plan 11 after attack of 15-sec, 17.2-ft waves at an swl of +9.5 ft NGVD

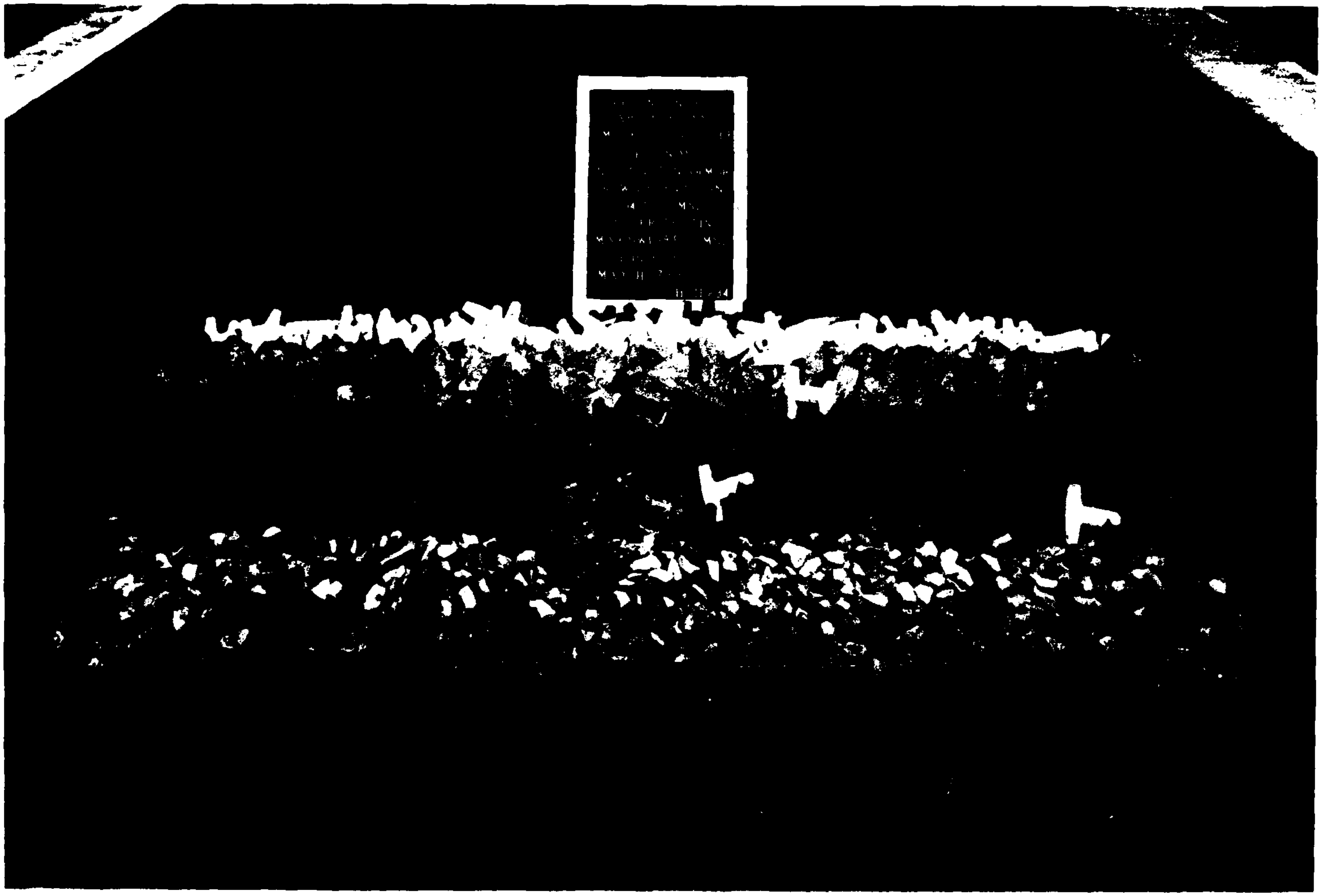

Photo 116. Channel-side view of Plan 11 after attack of 15-sec, 17.2-ft waves at an swl of +9.5 ft NGVD

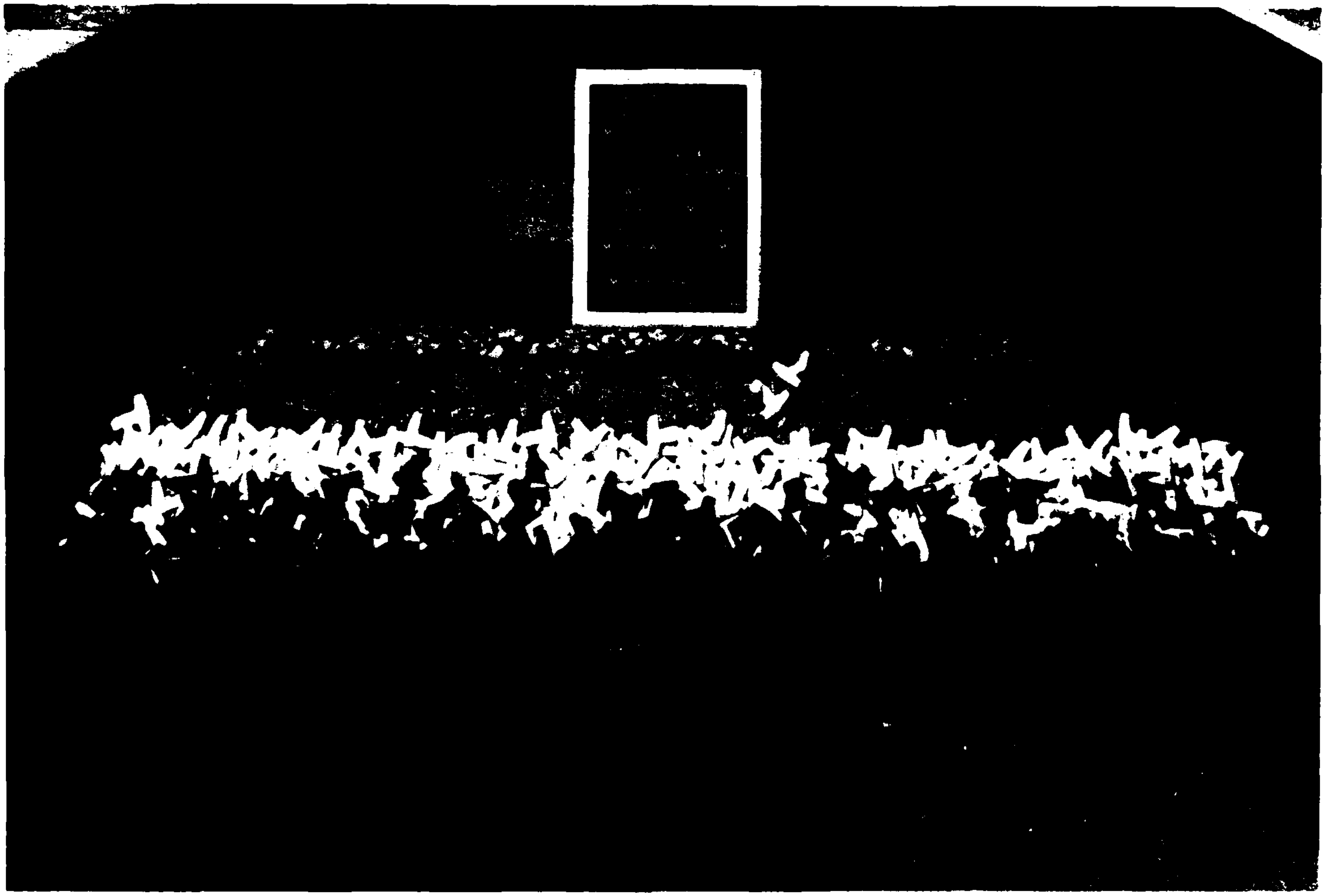

Photo 117. Sea-side view of Plan 8A after attack of 15-sec, 13.6-ft waves at an swl of +5.5 ft NGVD

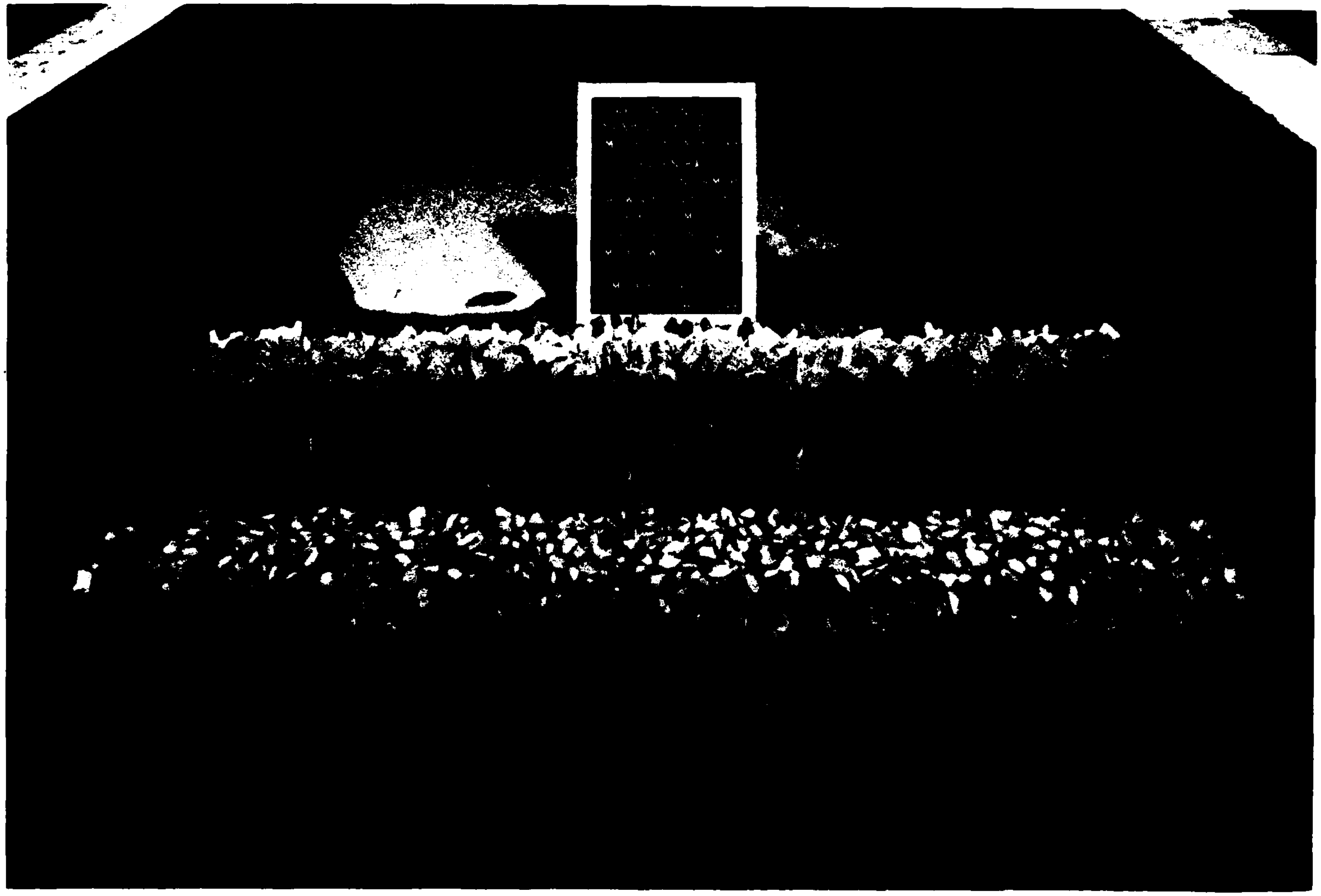

Photo 118. Channel-side view of Plan 8A after attack of 15-sec, 13.6-ft waves at an swl of +5.5 ft NGVD

Photo 119. Sea-side view of Plan 3D-1 before wave attack

Photo 120. End view of Plan 3D-1 before wave attack

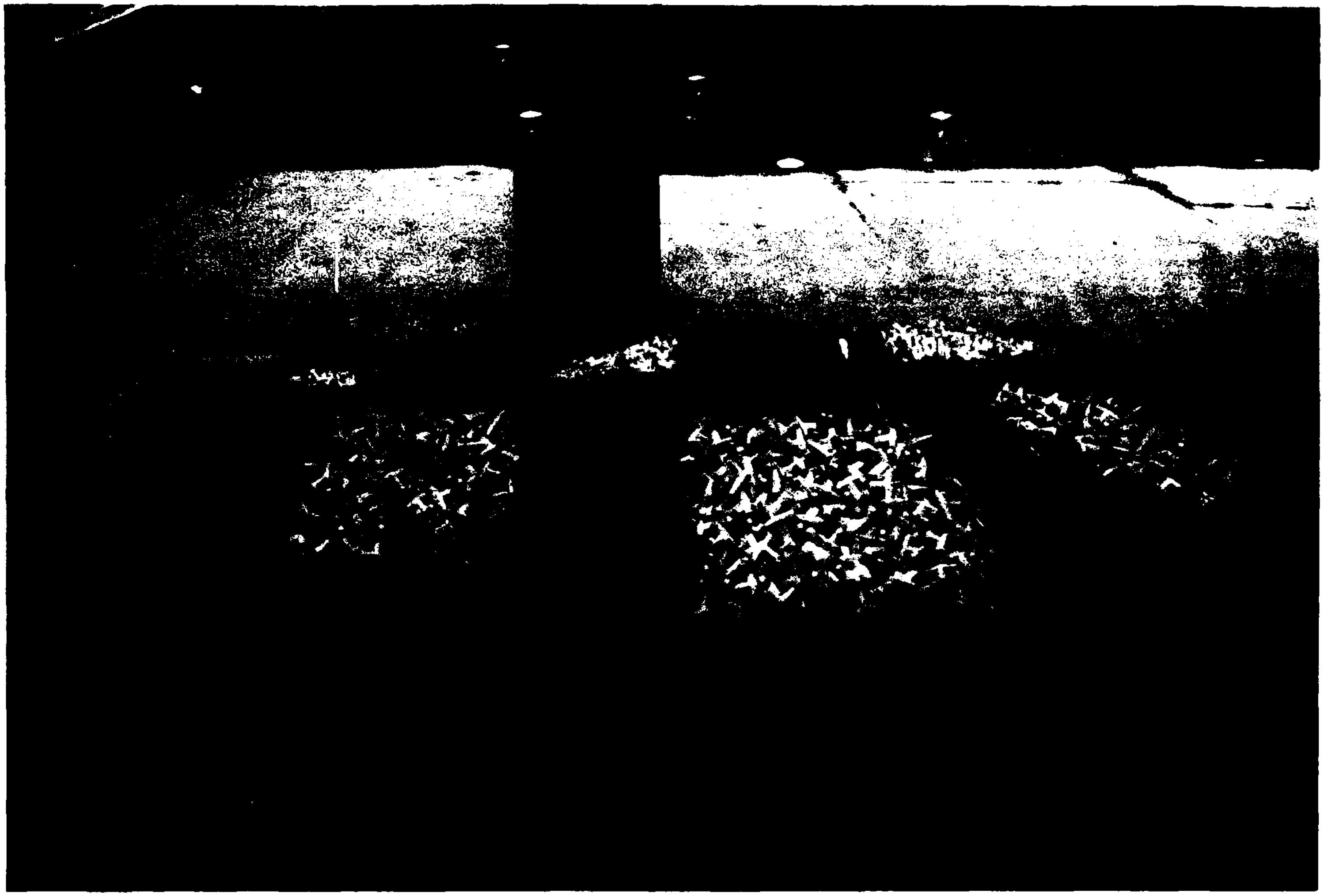

Photo 121. Channel-side view of Plan 3D-1 before wave attack

Photo 122. Sea-side view of Plan 3D-1B before wave attack

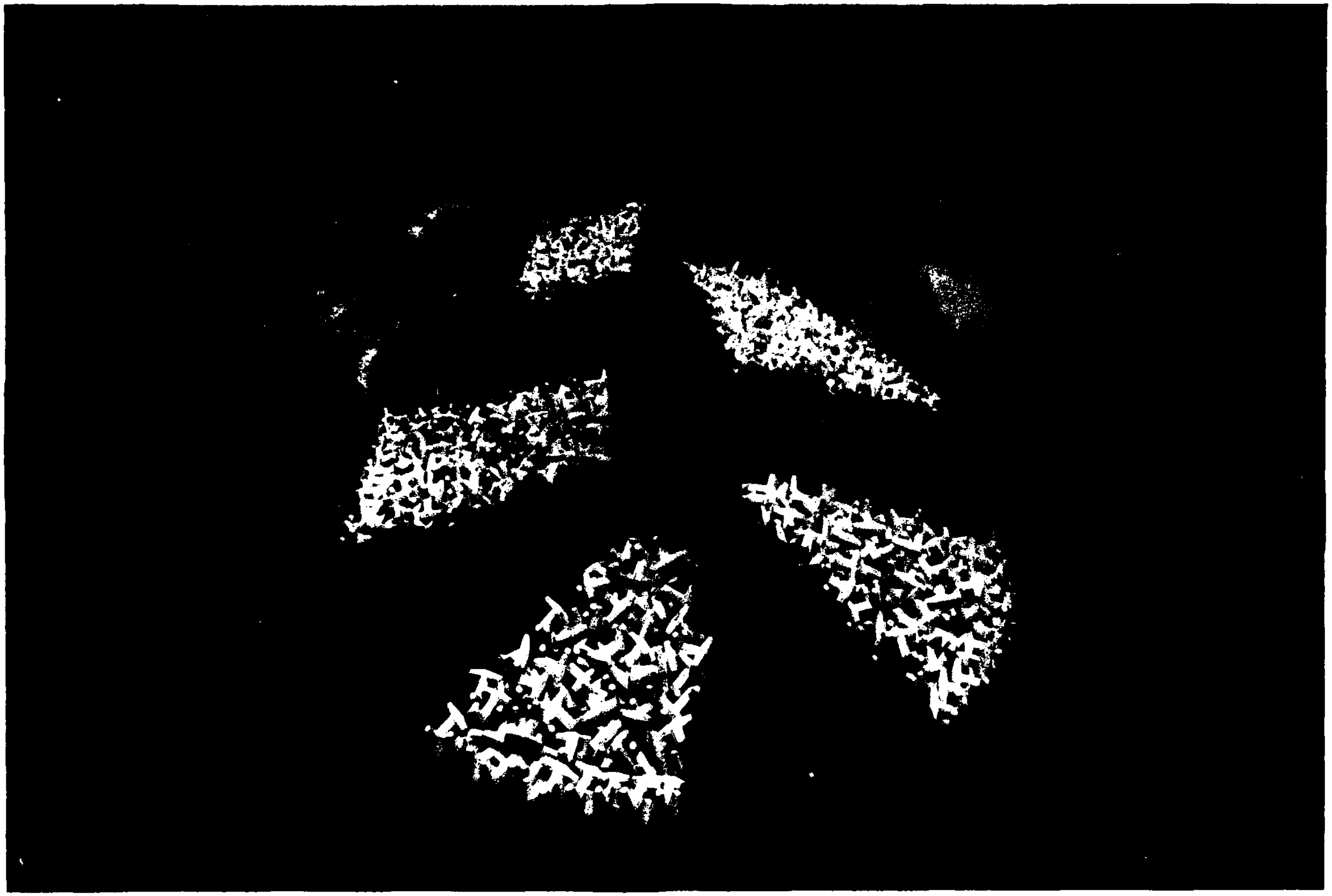

Photo 123. End view of Plan 3D-1B before wave attack

Photo 124. Channel-side view of Plan 3D-1B before wave attack

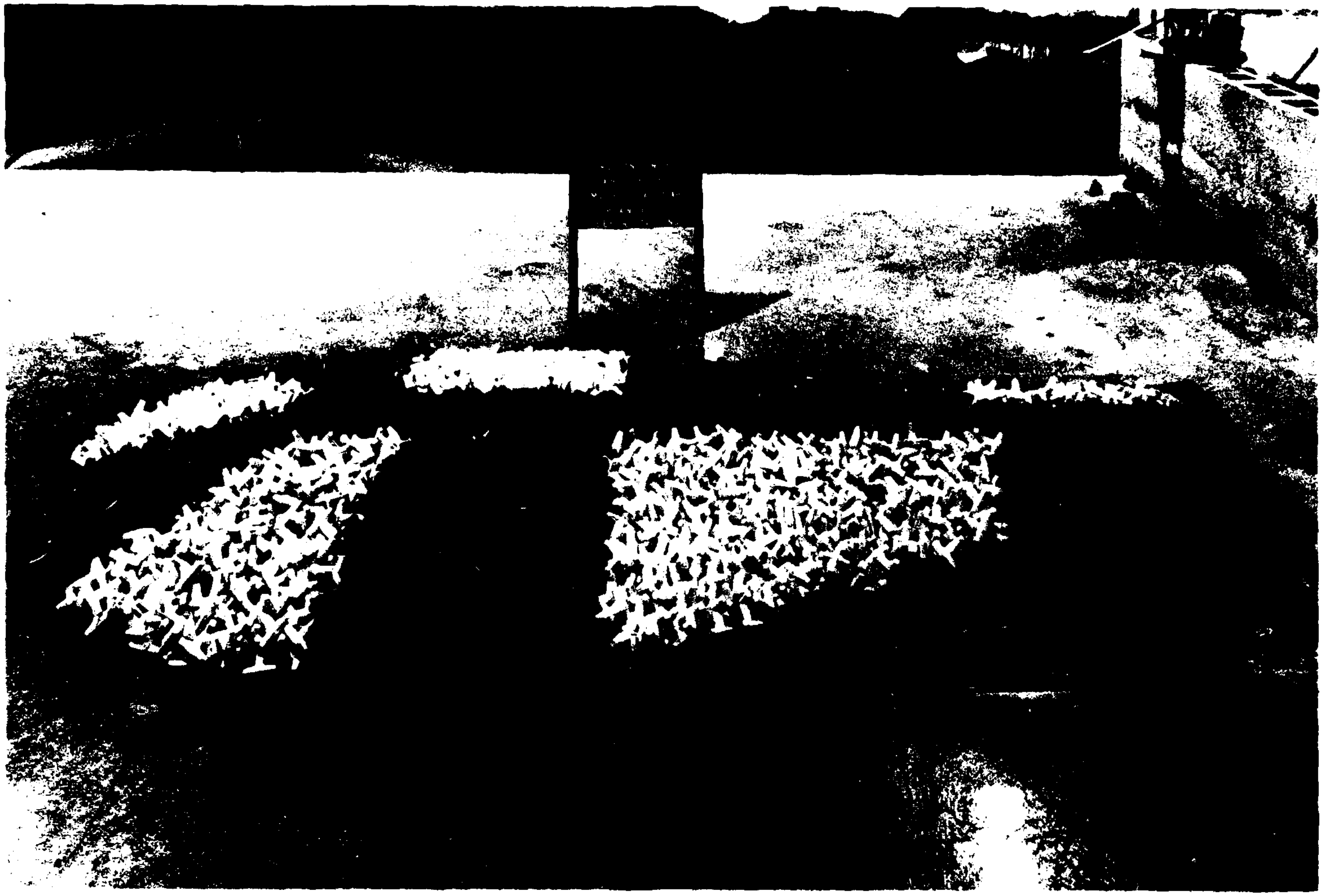

Photo 125. Sea-side view of Plan 3D-1C before wave attack

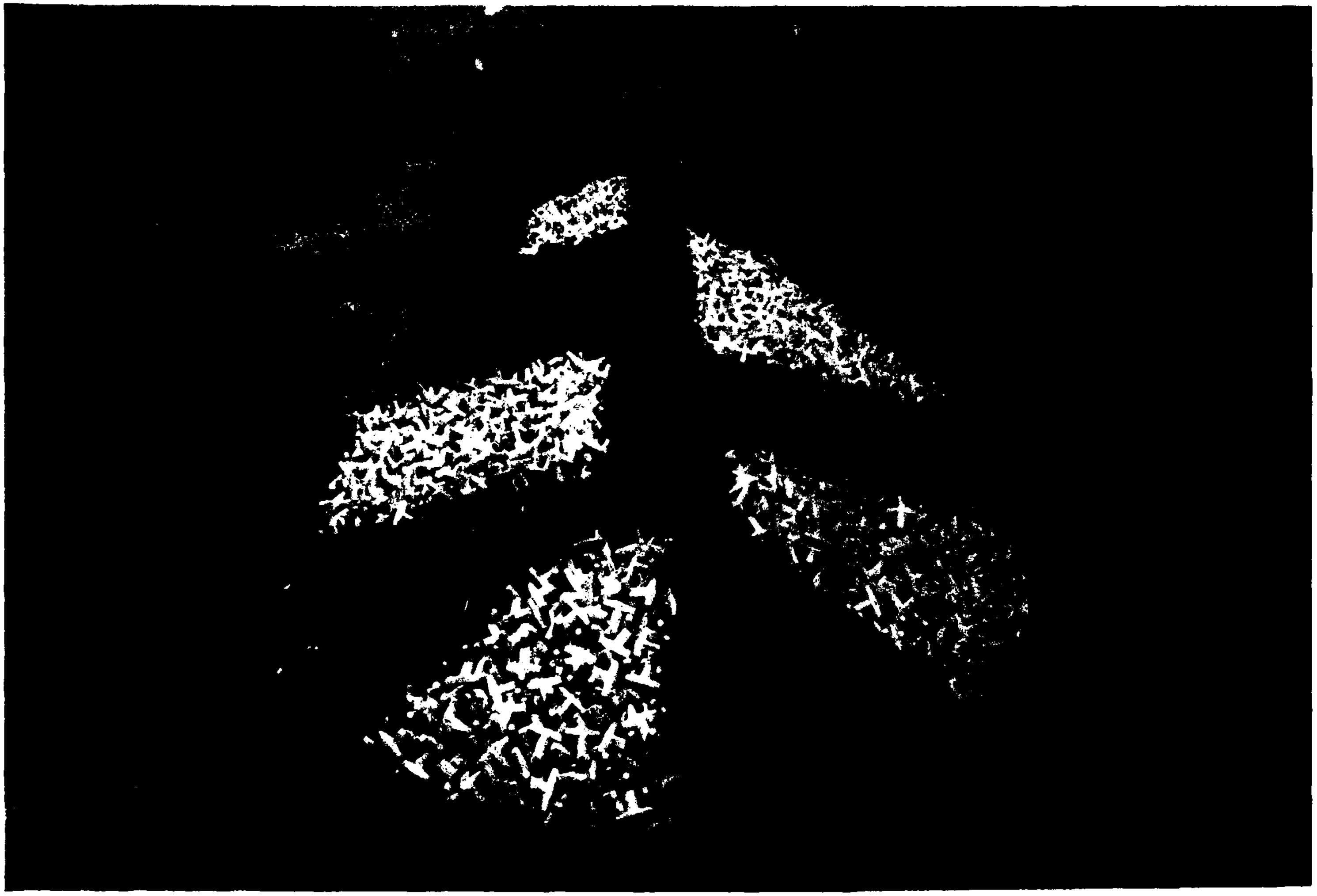

Photo 126. End view of Plan 3D-1C before wave attack

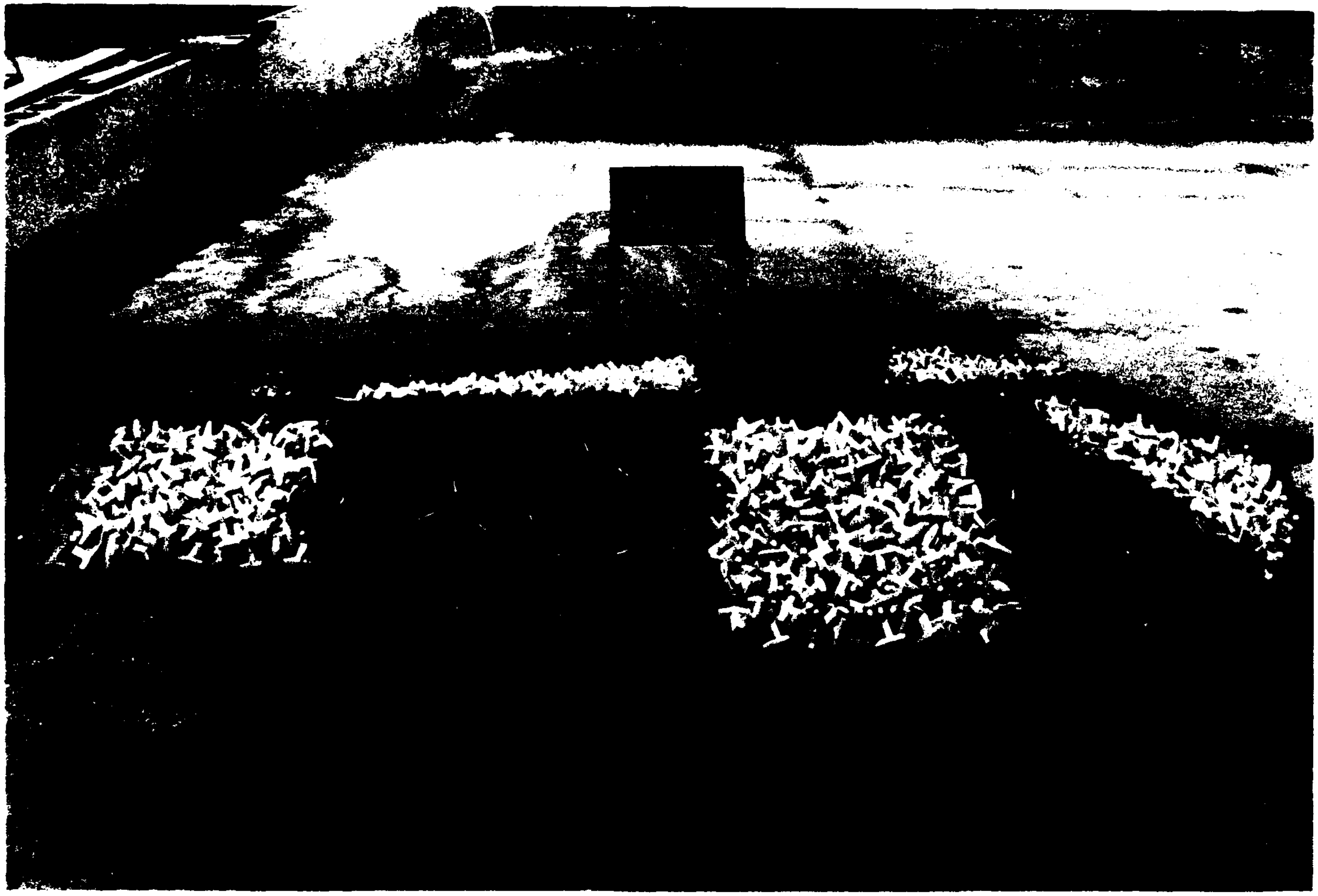

Photo 127. Channel-side view of Plan 3D-1C before wave attack

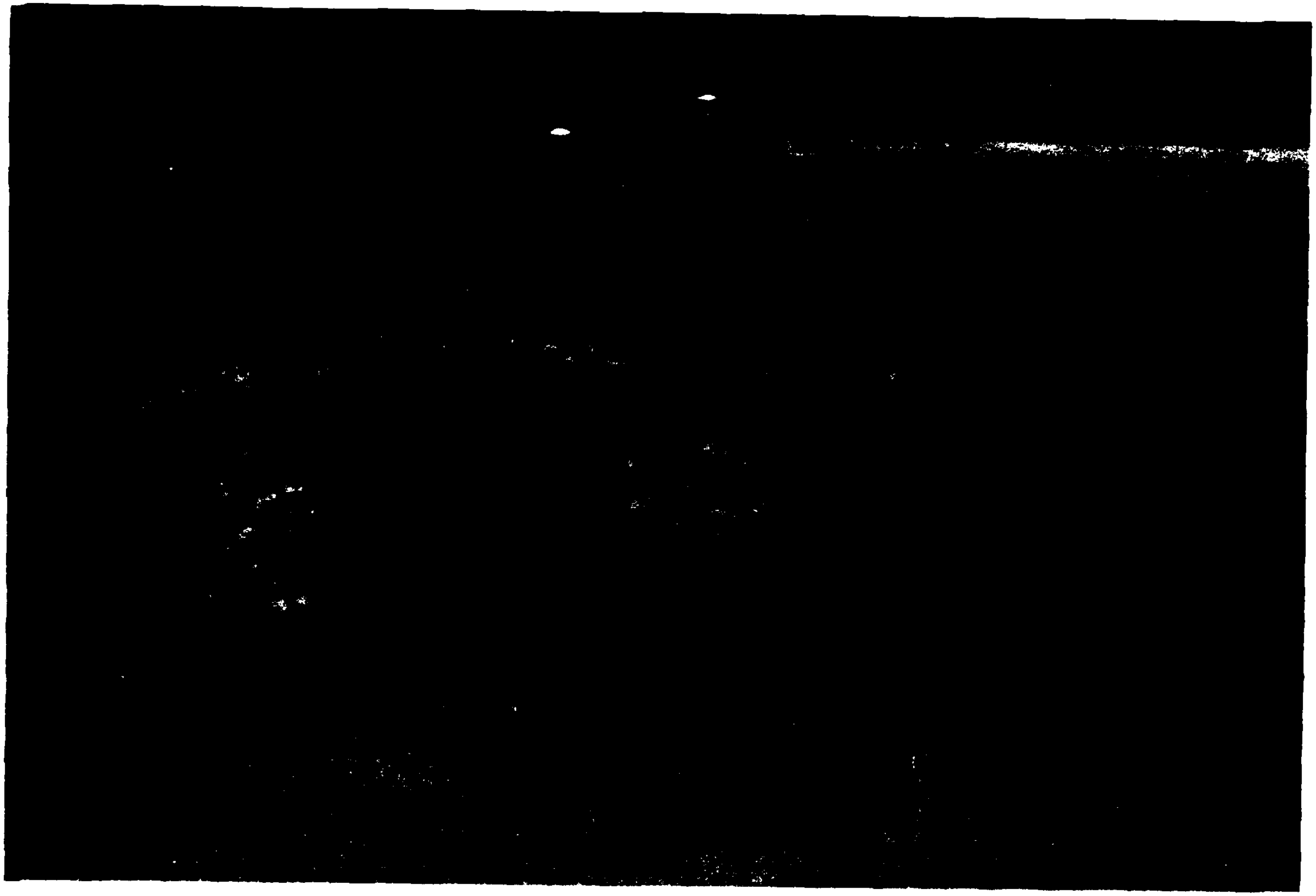

Photo 128. Sea-side view of Plan 3D-2 before wave attack

Photo 129. End view of Plan 3D-2 before wave attack

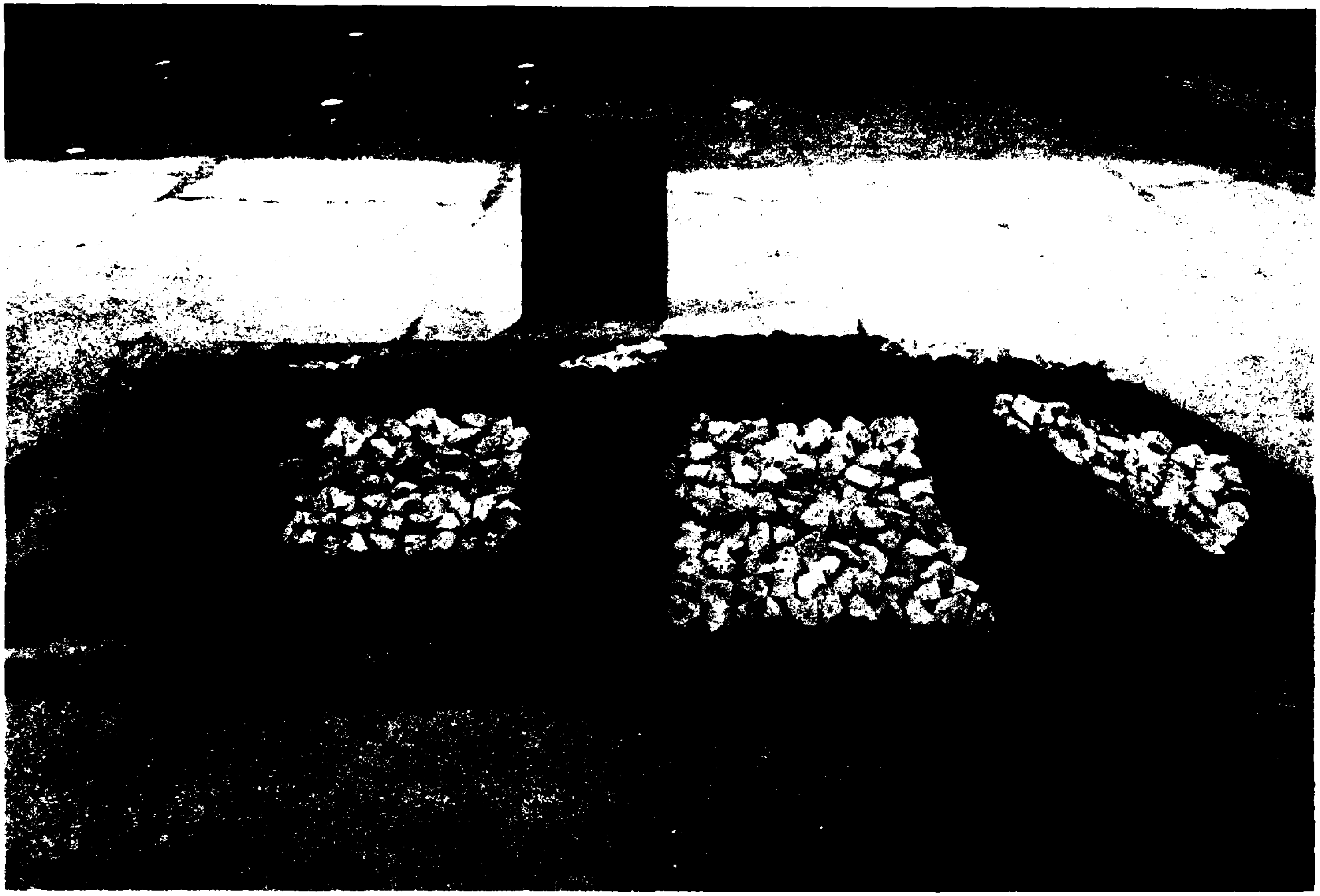

Photo 130. Channel-side view of Plan 3D-2 before wave attack

Photo 131. Sea-side view of Plan 3D-2B before wave attack

Photo 132. End view of Plan 3D-2B before wave attack

Photo 133. Channel-side view of Plan 3D-2B before wave attack

Photo 134. Sea-side view of Plan 3D-2C before wave attack

Photo 135. End view of Plan 3D-2C before wave attack

Photo 136. Channel-side view of Plan 3D-2C before wave attack

Photo 137. Sea-side view of Plan 3D-1 after attack of 15-sec, 17.6-ft breaking waves at an swl of +1 ft NGVD followed by 15-sec, 17.6-ft nonbreaking waves at an swl of +8 ft NGVD; angle of wave attack = 90 deg

Photo 138. End view of Plan 3D-1 after attack of 15-sec, 17.6-ft breaking waves at an swl of +1 ft NGVD followed by 15-sec, 17.6-ft nonbreaking waves at an swl of +8 ft NGVD; angle of wave attack = 90 deg

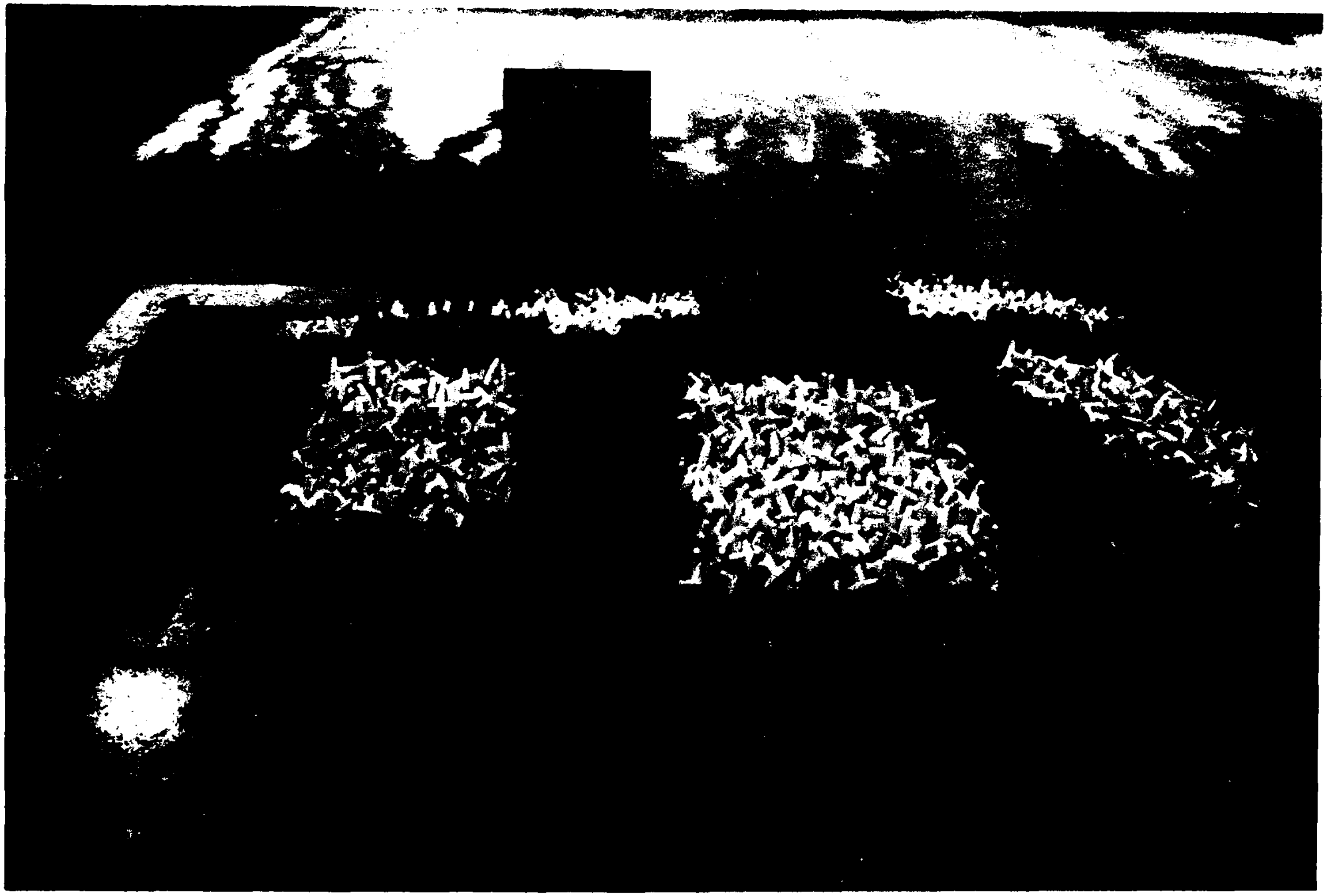

Photo 139. Channel-side view of Plan 3D-1 after attack of 15-sec, 17.6-ft breaking waves at an swl of +1 ft NGVD followed by 15-sec, 17.6-ft nonbreaking waves at an swl of +8 ft NGVD; angle of wave attack = 90 deg

Photo 140. Sea-side view of Plan 3D-2 after attack of 15-sec, 17.6-ft breaking waves at an swl of +1 ft NGVD followed by 15-sec, 17.6-ft nonbreaking waves at an swl of +8 ft NGVD; angle of wave attack = 90 deg

Photo 141. End view of Plan 3D-2 after attack of 15-sec, 17.6-ft breaking waves at an swl of +1 ft NGVD followed by 15-sec, 17.6-ft nonbreaking waves at an swl of +8 ft NGVD; angle of wave attack = 90 deg

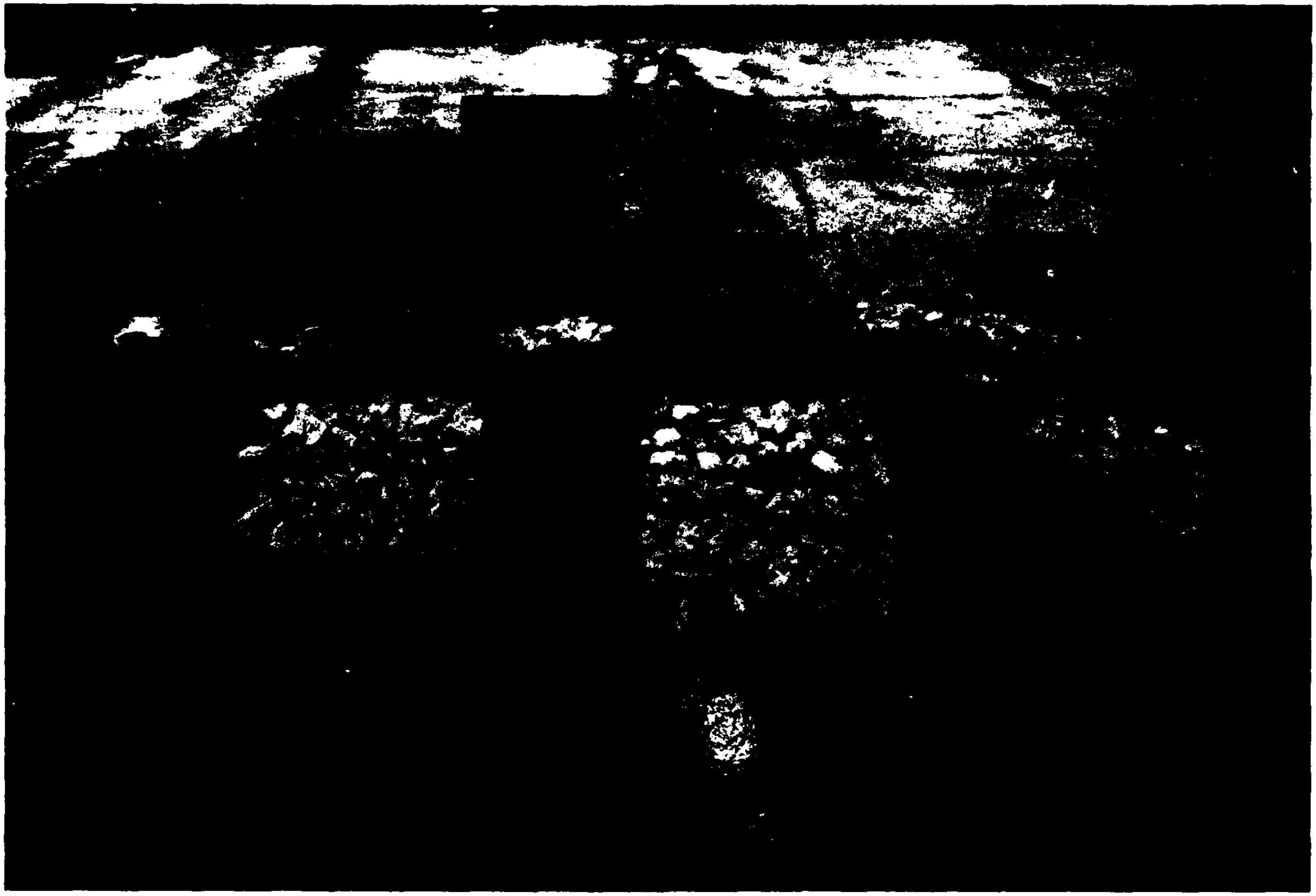

Photo 142. Channel-side view of Plan 3D-2 after attack of 15-sec, 17.6-ft breaking waves at an swl of +1 ft NGVD followed by 15-sec, 17.6-ft nonbreaking waves at an swl of +8 ft NGVD; angle of wave attack = 90 deg

Photo 143. Repeat test of Plan 3D-1; sea-side view after attack of 15-sec, 17.6-ft nonbreaking waves at an swl of +8 ft NGVD followed by 15-sec, 17.6-ft breaking waves at an swl of +1 ft NGVD; angle of wave attack = 90 deg

Photo 144. Repeat test of Plan 3D-1; end view after attack of 15-sec, 17.6-ft nonbreaking waves at an swl of +8 ft NGVD followed by 15-sec, 17.6-ft breaking waves at an swl of +1 ft NGVD; angle of wave attack = 90 deg

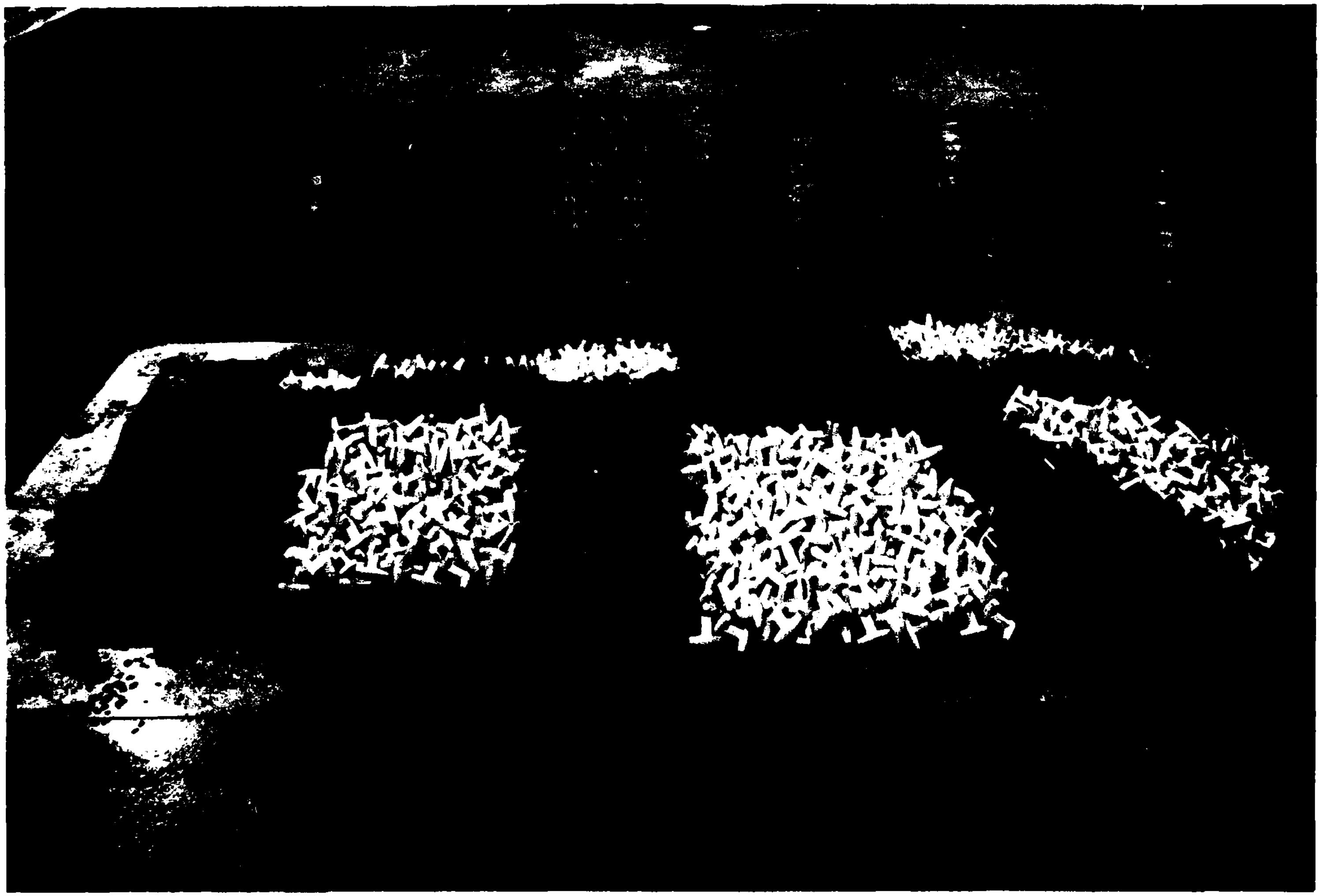

Photo 145. Repeat test of Plan 3D-1; channel-side view after attack of 15-sec, 17.6-ft nonbreaking waves at an swl of +8 ft NGVD followed by 15-sec, 17.6-ft breaking waves at an swl of +1 ft NGVD; angle of wave attack = 90 deg

Photo 146. Repeat test of Plan 3D-2; sea-side view after attack of 15-sec, 17.6-ft nonbreaking waves at an swl of +8 ft NGVD followed by 15-sec, 17.6-ft breaking waves at an swl of +1 ft NGVD; angle of wave attack = 90 deg

Photo 147. Repeat test of Plan 3D-2; end view after attack of 15-sec, 17.6-ft nonbreaking waves at an swl of +8 ft NGVD followed by 15-sec, 17.6-ft breaking waves at an swl of +1 ft NGVD; angle of wave attack = 90 deg

Photo 148. Repeat test of Plan 3D-2; channel-side view after attack of 15-sec, 17.6-ft nonbreaking waves at an swl of +8 ft NGVD followed by 15-sec, 17.6-ft breaking waves at an swl of +1 ft NGVD; angle of wave attack = 90 deg

Photo 149. Sea-side view of Plan 3D-1A after attack of 15-sec, 17.6-ft breaking waves at an swl of +1 ft NGVD followed by 15-sec, 17.6-ft nonbreaking waves at an swl of +8 ft NGVD; angle of wave attack = 90 deg

Photo 150. End view of Plan 3D-1A after attack of 15-sec, 17.6-ft breaking waves at an swl of +1 ft NGVD followed by 15-sec, 17.6-ft nonbreaking waves at an swl of +8 ft NGVD; angle of wave attack = 90 deg

Photo 151. Channel-side view of Plan 3D-1A after attack of 15-sec, 17.6-ft breaking waves at an swl of +1 ft NGVD followed by 15-sec, 17.6-ft nonbreaking waves at an swl of +8 ft NGVD; angle of wave attack = 90 deg

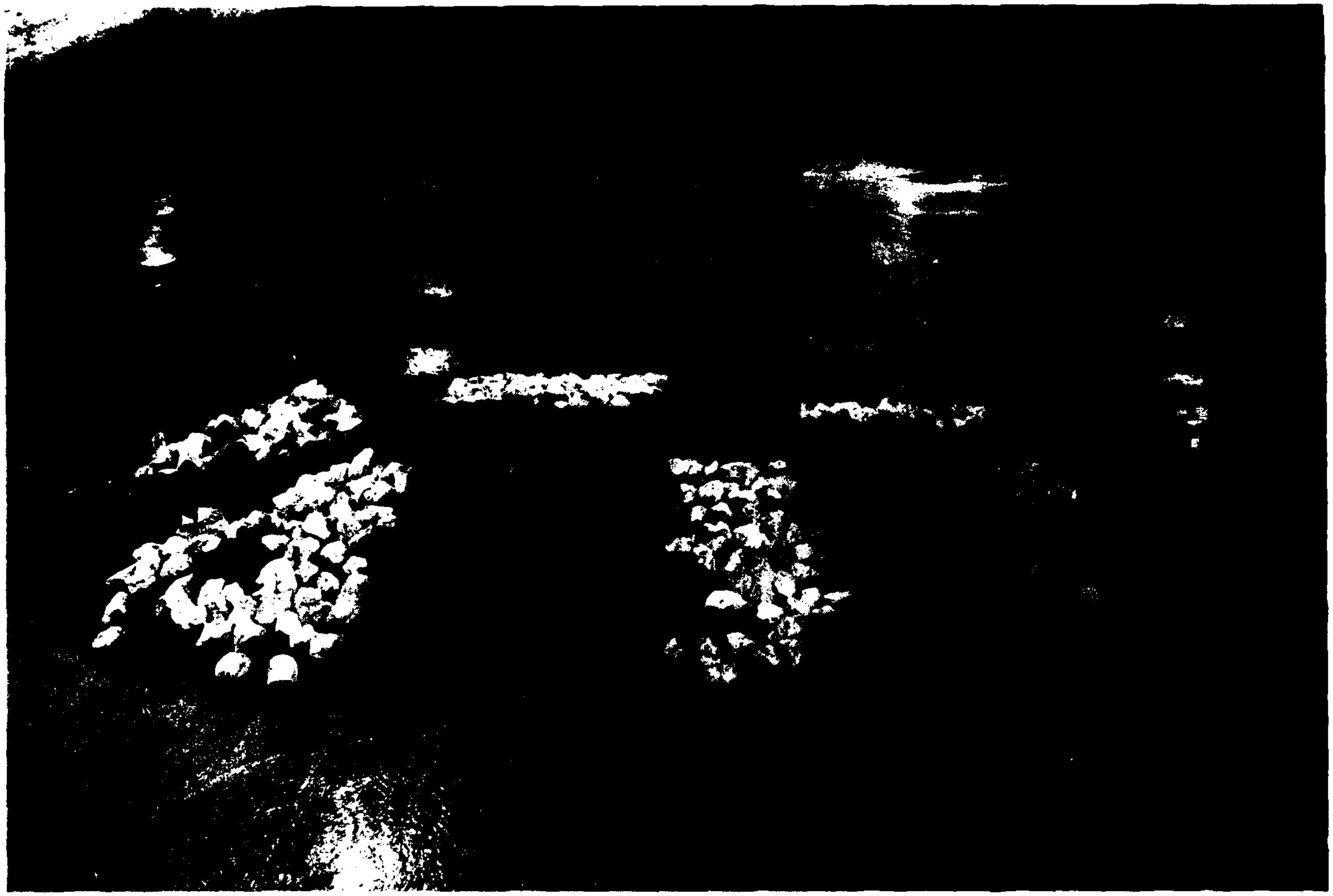

Photo 152. Sea-side view of Plan 3D-2A after attack of 15-sec, 17.6-ft breaking waves at an swl of +1 ft NGVD followed by 15-sec, 17.6-ft nonbreaking waves at an swl of +8 ft NGVD; angle of wave attack = 90 deg

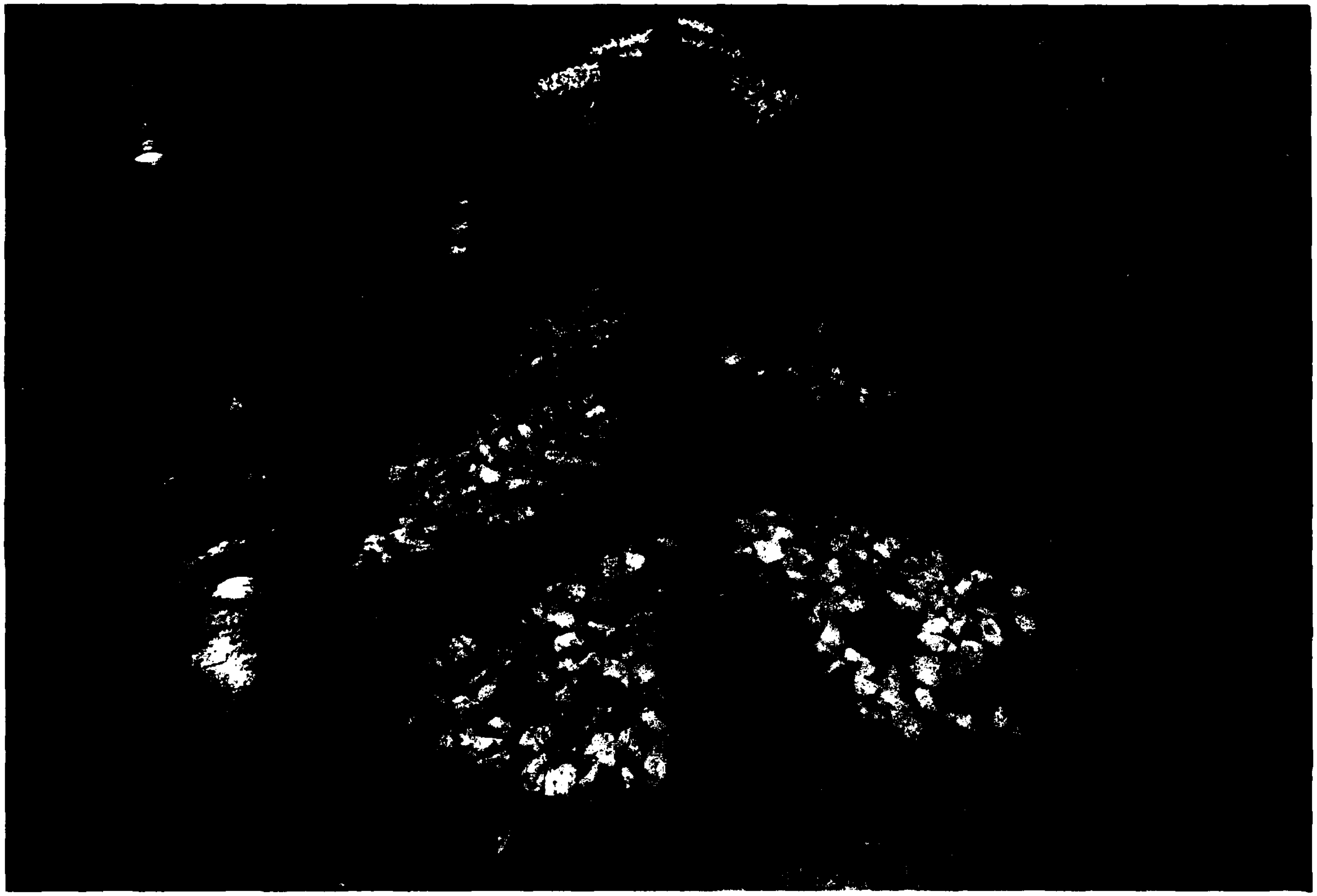

Photo 153. End view of Plan 3D-2A after attack of 15-sec, 17.6-ft breaking waves at an swl of +1 ft NGVD followed by 15-sec, 17.6-ft nonbreaking waves at an swl of +8 ft NGVD; angle of wave attack = 90 deg

Photo 154. Channel-side view of Plan 3D-2A after attack of 15-sec, 17.6-ft breaking waves at an swl of +1 ft NGVD followed by 15-sec, 17.6-ft nonbreaking waves at an swl of +8 ft NGVD; angle of wave attack = 90 deg

Photo 155. Repeat test of Plan 3D-1A; sea-side view after attack of 15-sec, 17.6-ft nonbreaking waves at an swl of +8 ft NGVD followed by 15-sec, 17.6-ft breaking waves at an swl of +1 ft NGVD; angle of wave attack = 90 deg

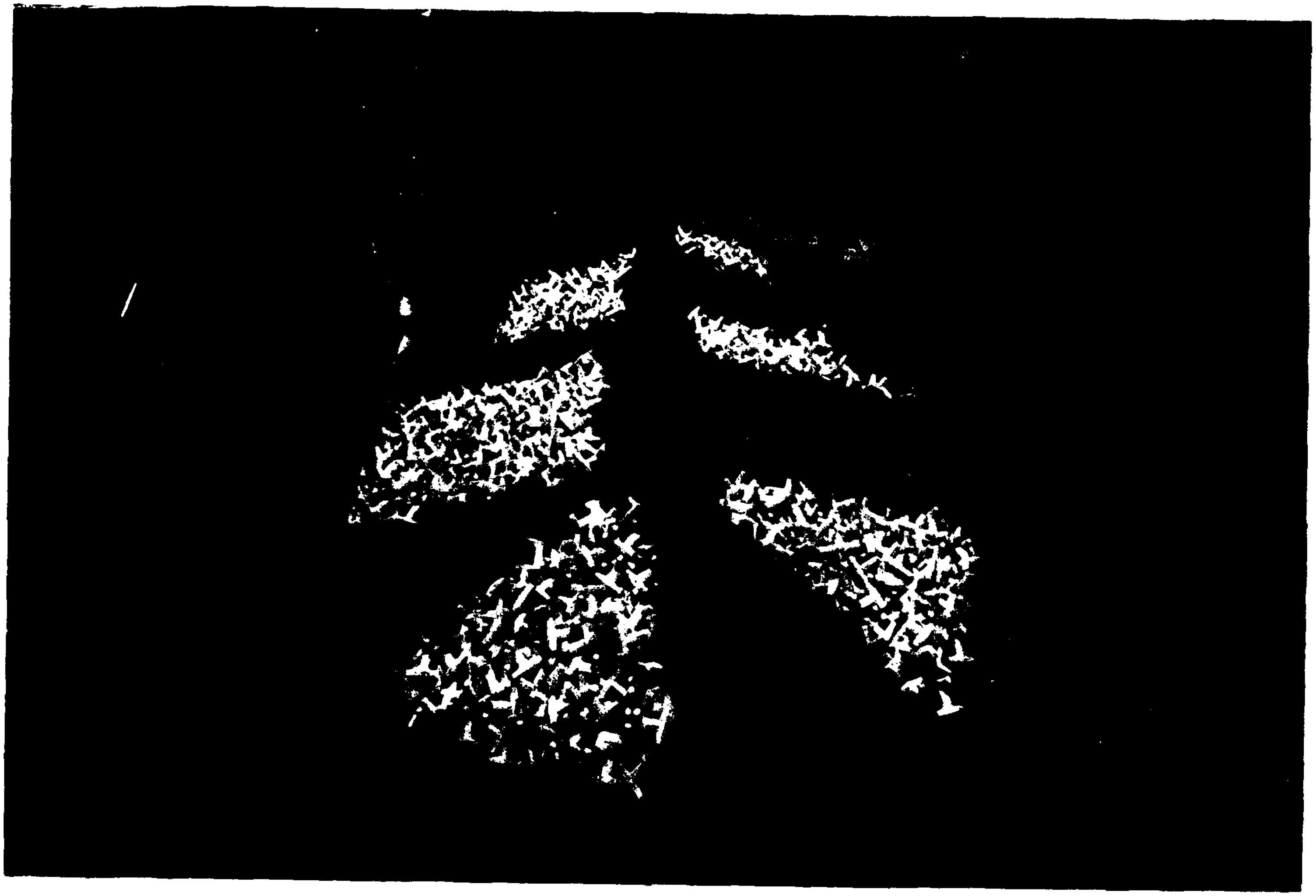

Photo 156. Repeat test of Plan 3D-1A; end view after attack of 15-sec, 17.6-ft nonbreaking waves at an swl of +8 ft NGVD followed by 15-sec, 17.6-ft breaking waves at an swl of +1 ft NGVD; angle of wave attack = 90 deg

Photo 157. Repeat test of Plan 3D-1A; channel-side view after attack of 15-sec, 17.6-ft nonbreaking waves at an swl of +8 ft NGVD followed by 15-sec, 17.6-ft breaking waves at an swl of +1 ft NGVD; angle of wave attack = 90 deg

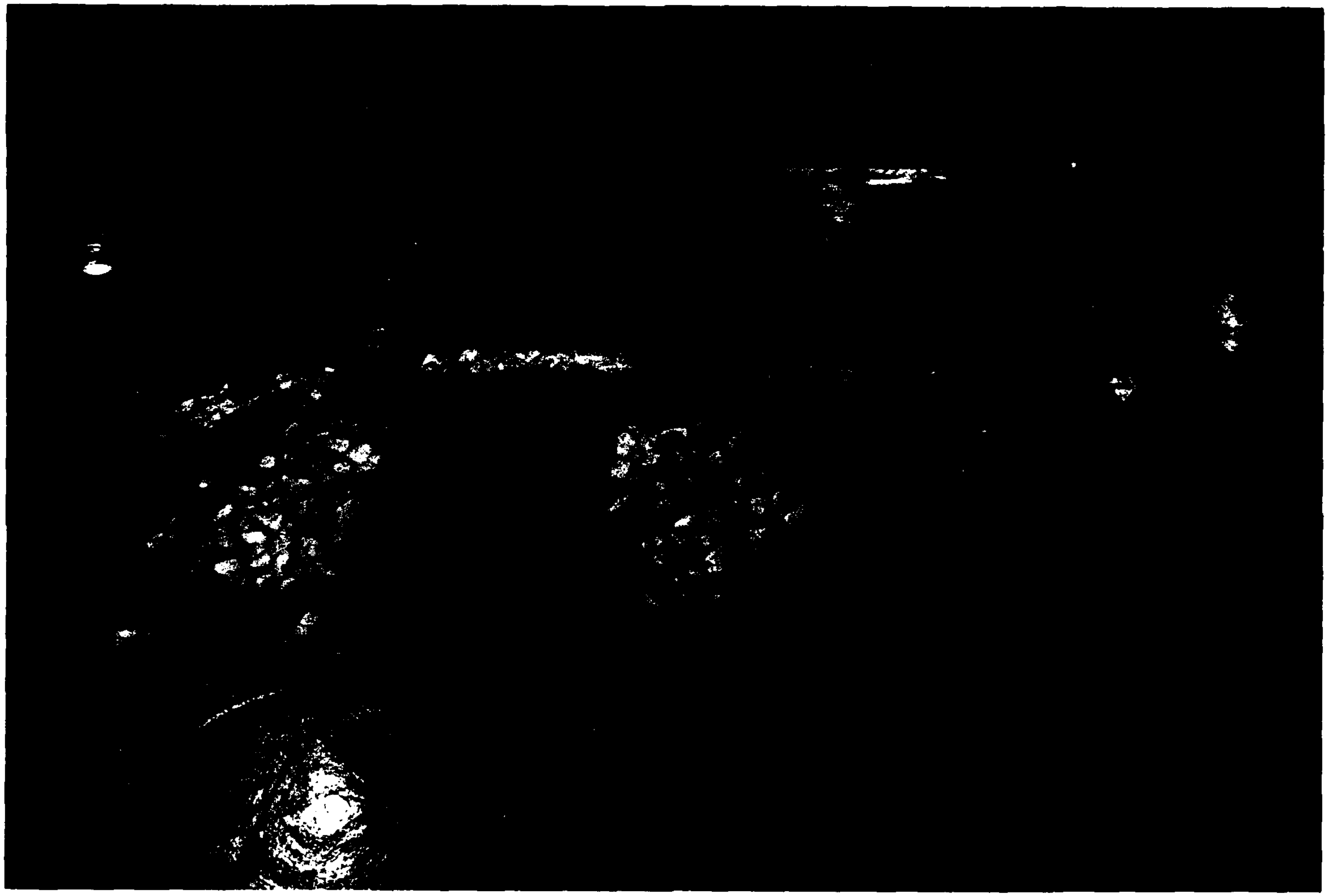

Photo 158. Repeat test of Plan 3D-2A; sea-side view after attack of 15-sec, 17.6-ft nonbreaking waves at an swl of +8 ft NGVD followed by 15-sec, 17.6-ft breaking waves at an swl of +1 ft NGVD; angle of wave attack = 90 deg

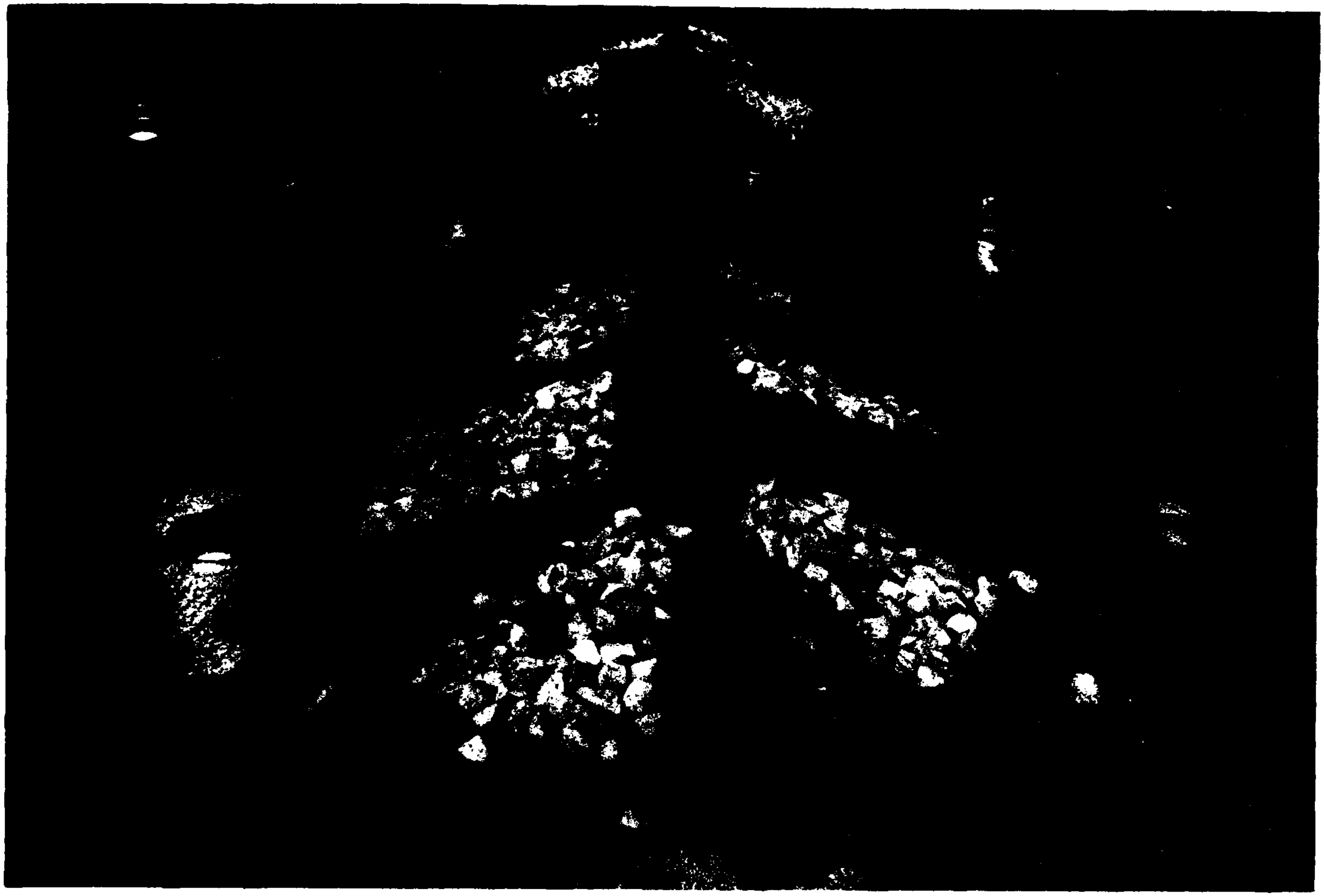

Photo 159. Repeat test of Plan 3D-2A; end view after attack of 15-sec, 17.6-ft nonbreaking waves at an swl of +8 ft NGVD followed by 15-sec, 17.6-ft breaking waves at an swl of +1 ft NGVD; angle of wave attack = 90 deg

Photo 160. Repeat test of Plan 3D-2A; channel-side view after attack of 15-sec, 17.6-ft nonbreaking waves at an swl of +8 ft NGVD followed by 15-sec, 17.6-ft breaking waves at an swl of +1 ft NGVD; angle of wave attack = 90 deg

Photo 161. Sea-side view of Plan 3D-1B after attack of 15-sec, 17.6-ft breaking waves at an swl of +1 ft NGVD followed by 15-sec, 17.6-ft nonbreaking waves at an swl of +8 ft NGVD; angle of wave attack = 90 deg

Photo 162. End view of Plan 3D-1B after attack of 15-sec, 17.6-ft breaking waves at an swl of +1 ft NGVD followed by 15-sec, 17.6-ft nonbreaking waves at an swl of +8 ft NGVD; angle of wave attack = 90 deg

Photo 163. Channel-side view of Plan 3D-1B after attack of 15-sec, 17.6-ft breaking waves at an swl of +1 ft NGVD followed by 15-sec, 17.6-ft nonbreaking waves at an swl of +8 ft NGVD; angle of wave attack = 90 deg

Photo 164. Sea-side view of Plan 3D-2B after attack of 15-sec, 17.6-ft breaking waves at an swl of +1 ft NGVD followed by 15-sec, 17.6-ft nonbreaking waves at an swl of +8 ft NGVD; angle of wave attack = 90 deg

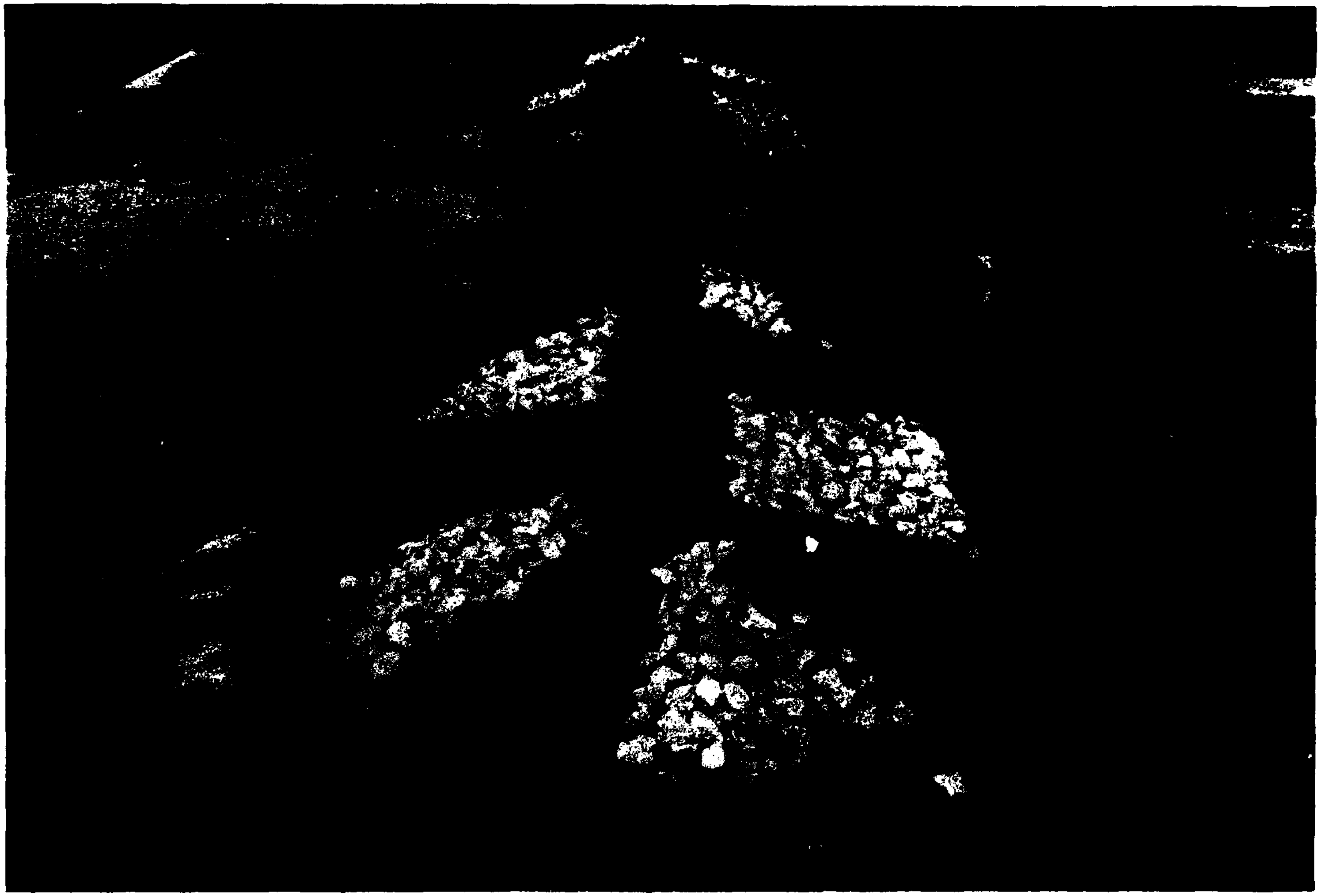

Photo 165. End view of Plan 3D-2B after attack of 15-sec, 17.6-ft breaking waves at an swl of +1 ft NGVD followed by 15-sec, 17.6-ft nonbreaking waves at an swl of +8 ft NGVD; angle of wave attack = 90 deg

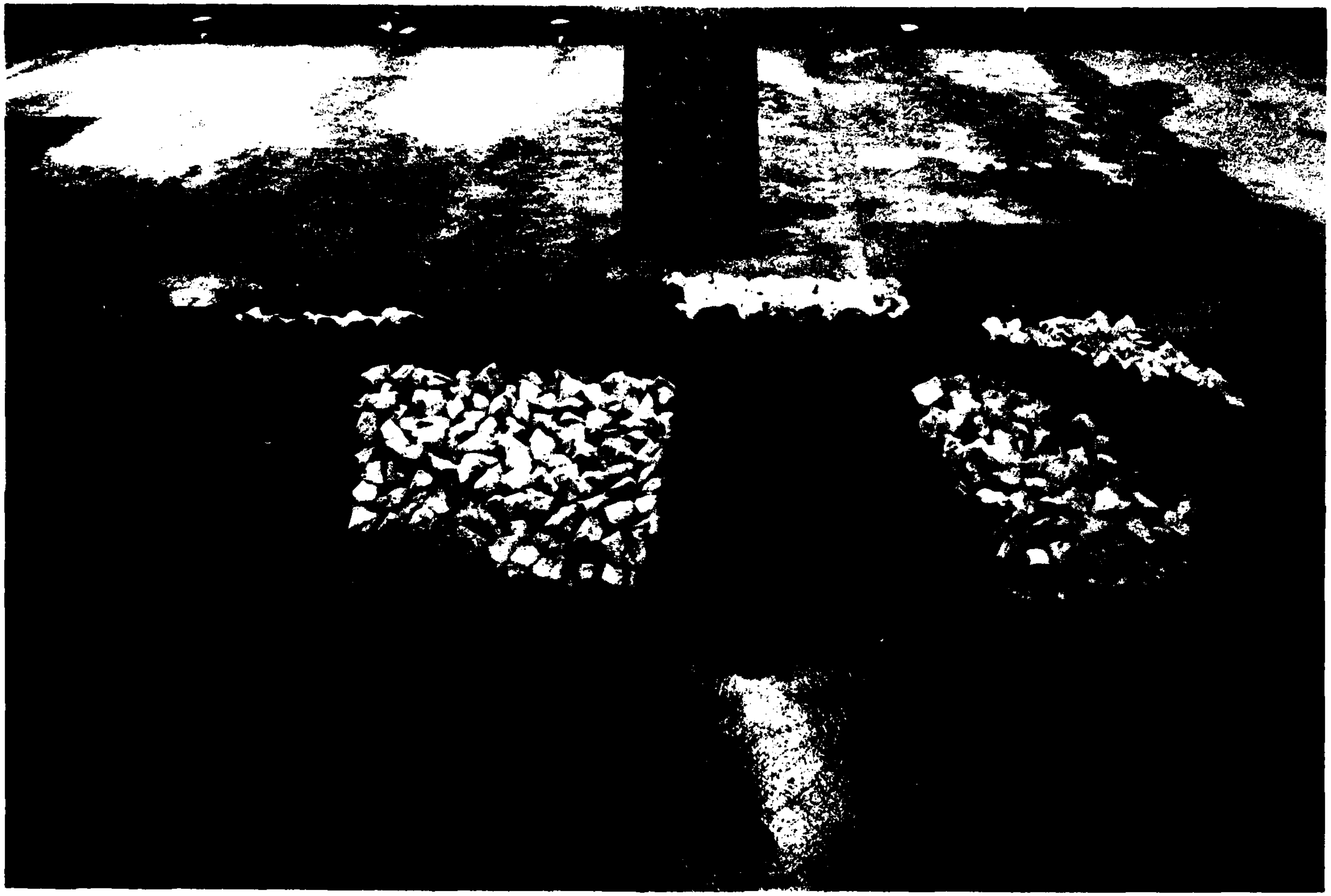

Photo 166. Channel-side view of Plan 3D-2B after attack of 15-sec, 17.6-ft breaking waves at an swl of +1 ft NGVD followed by 15-sec, 17.6-ft nonbreaking waves at an swl of +8 ft NGVD; angle of wave attack = 90 deg

Photo 167. Repeat test of Plan 3D-1B; sea-side view after attack of 15-sec, 17.6-ft nonbreaking waves at an swl of +8 ft NGVD followed by 15-sec, 17.6-ft breaking waves at an swl of +1 ft NGVD; angle of wave attack = 90 deg

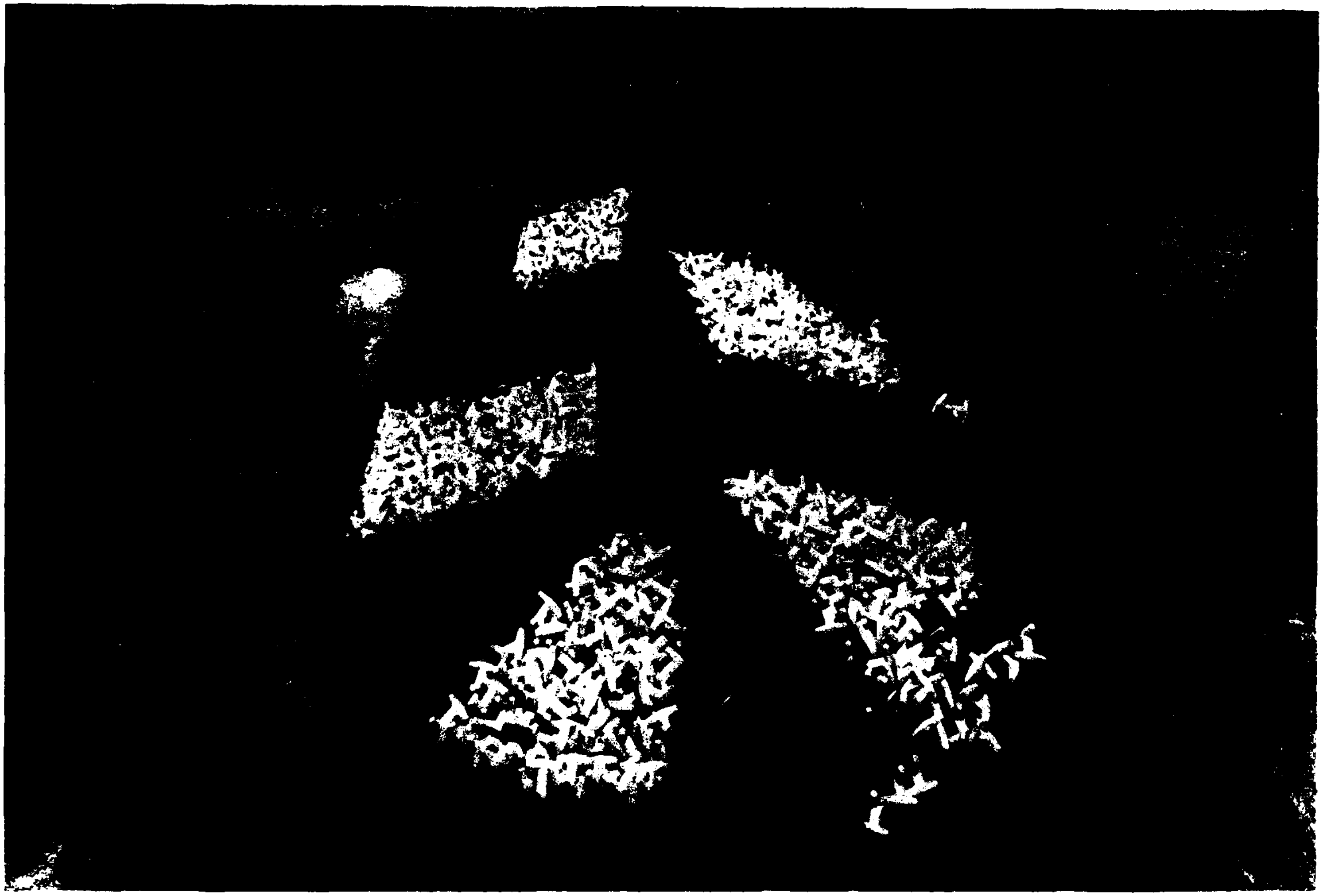

Photo 168. Repeat test of Plan 3D-1B; end view after attack of 15-sec, 17.6-ft nonbreaking waves at an swl of +8 ft NGVD followed by 15-sec, 17.6-ft breaking waves at an swl of +1 ft NGVD; angle of wave attack = 90 deg

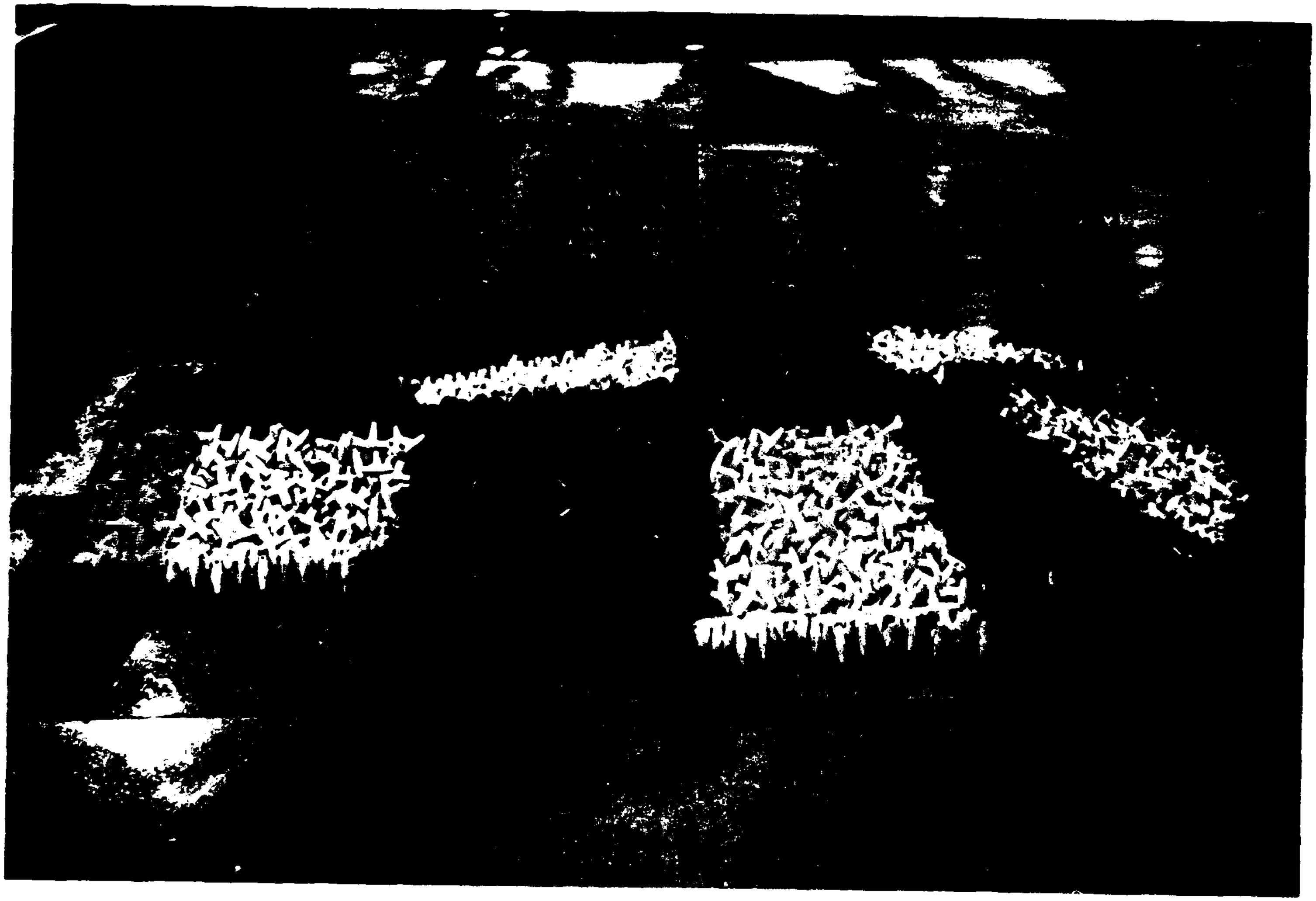

Photo 169. Repeat test of Plan 3D-1B; channel-side view after attack of 15-sec, 17.6-ft nonbreaking waves at an swl of +8 ft NGVD followed by 15-sec, 17.6-ft breaking waves at an swl of +1 ft NGVD; angle of wave attack = 90 deg

Photo 170. Repeat test of Plan 3D-2B; sea-side view after attack of 15-sec, 17.6-ft nonbreaking waves at an swl of +8 ft NGVD followed by 15-sec, 17.6-ft breaking waves at an swl of +1 ft NGVD; angle of wave attack = 90 deg

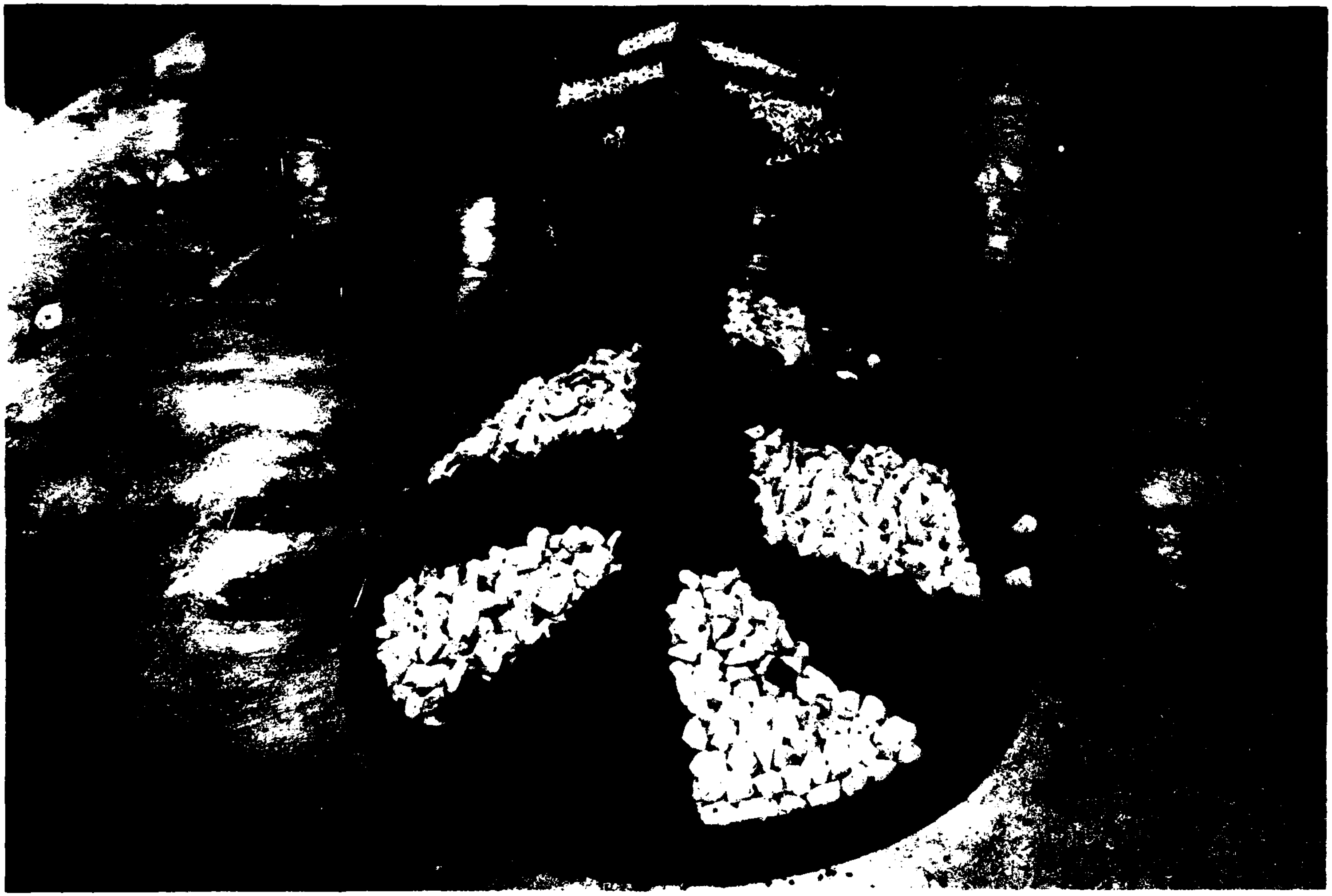

Photo 171. Repeat test of Plan 3D-2B; end view after attack of 15-sec, 17.6-ft nonbreaking waves at an swl of +8 ft NGVD followed by 15-sec, 17.6-ft breaking waves at an swl of +1 ft NGVD; angle of wave attack = 90 deg

Photo 172. Repeat test of Plan 3D-2B; channel-side view after attack of 15-sec, 17.6-ft nonbreaking waves at an swl of +8 ft NGVD followed by 15-sec, 17.6-ft breaking waves at an swl of +1 ft NGVD; angle of wave attack = 90 deg

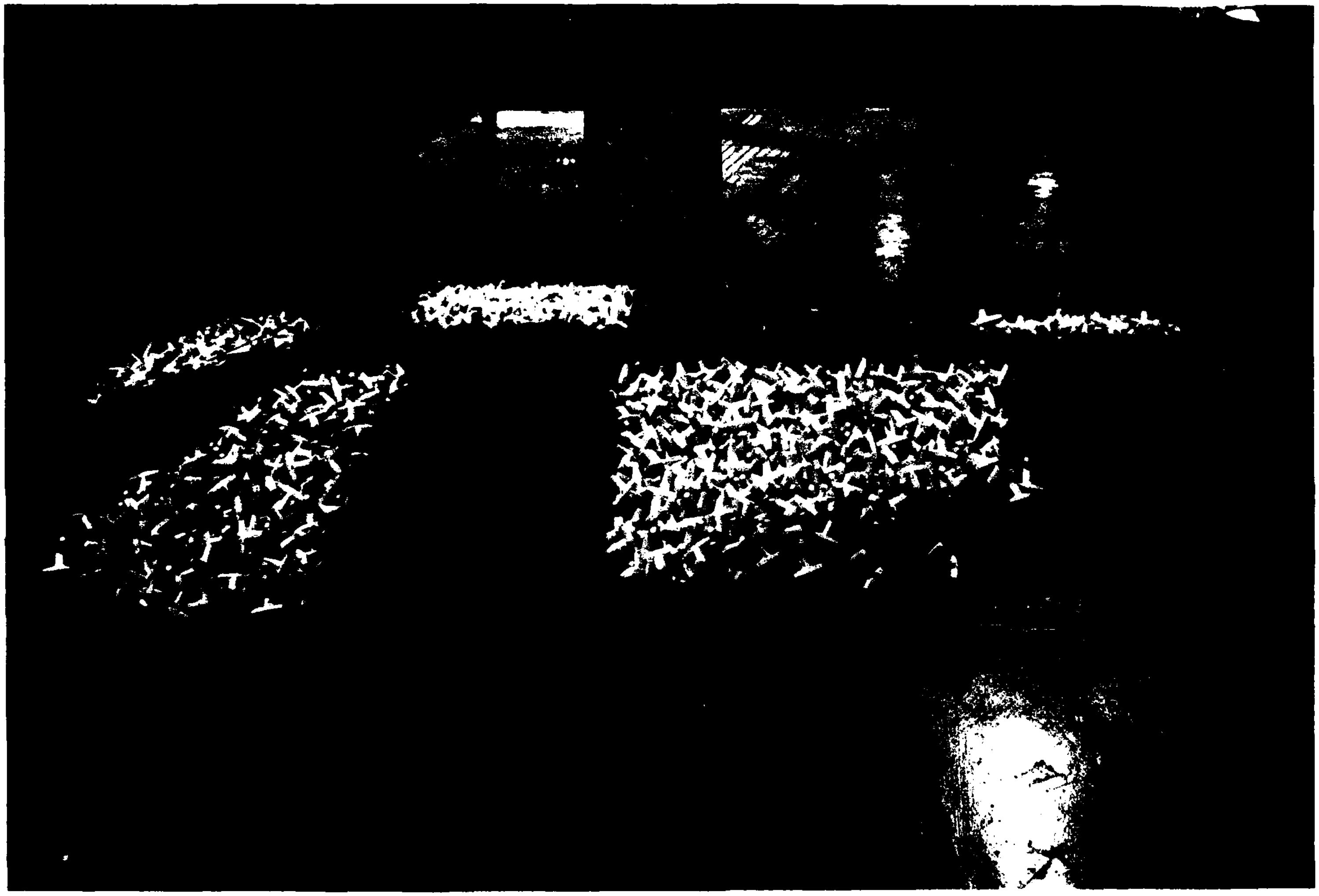

Photo 173. Sea-side view of Plan 3D-1C after attack of 15-sec, 17.6-ft breaking waves at an swl of +1 ft NGVD followed by 15-sec, 17.6-ft nonbreaking waves at an swl of +8 ft NGVD; angle of wave attack = 90 deg

Photo 174. End view of Plan 3D-1C after attack of 15-sec, 17.6-ft breaking waves at an swl of +1 ft NGVD followed by 15-sec, 17.6-ft nonbreaking waves at an swl of +8 ft NGVD; angle of wave attack = 90 deg

Photo 175. Channel-side view of Plan 3D-1C after attack of 15-sec, 17.6-ft breaking waves at an swl of +1 ft NGVD followed by 15-sec, 17.6-ft nonbreaking waves at an swl of +8 ft NGVD; angle of wave attack = 90 deg

Photo 176. Sea-side view of Plan 3D-2C after attack of 15-sec, 17.6-ft breaking waves at an swl of +1 ft NGVD followed by 15-sec, 17.6-ft nonbreaking waves at an swl of +8 ft NGVD; angle of wave attack = 90 deg

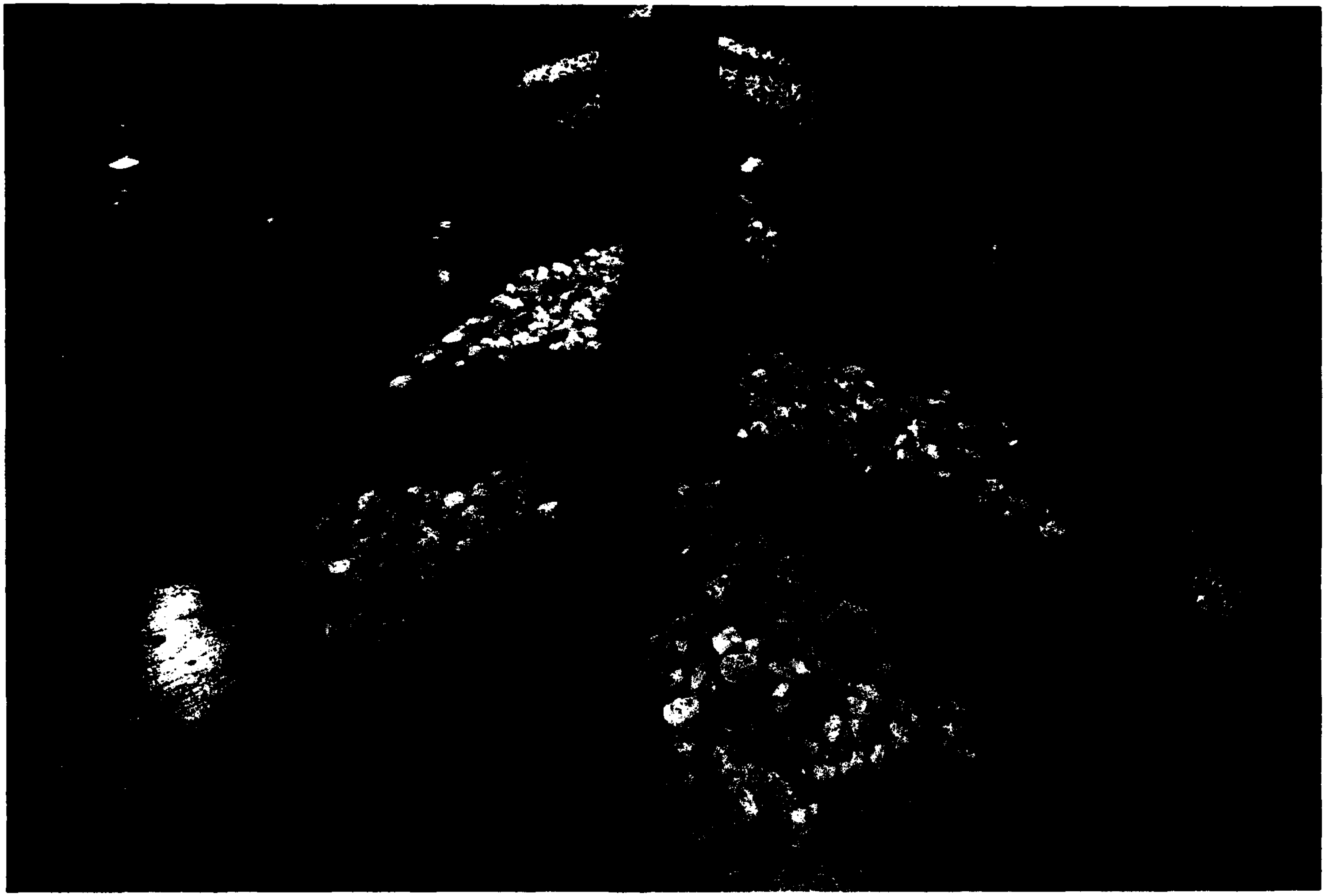

Photo 177. End view of Plan 3D-2C after attack of 15-sec, 17.6-ft breaking waves at an swl of +1 ft NGVD followed by 15-sec, 17.6-ft nonbreaking waves at an swl of +8 ft NGVD; angle of wave attack = 90 deg

Photo 178. Channel-side view of Plan 3D-2C after attack of 15-sec, 17.6-ft breaking waves at an swl of +1 ft NGVD followed by 15-sec, 17.6-ft nonbreaking waves at an swl of +8 ft NGVD; angle of wave attack = 90 deg

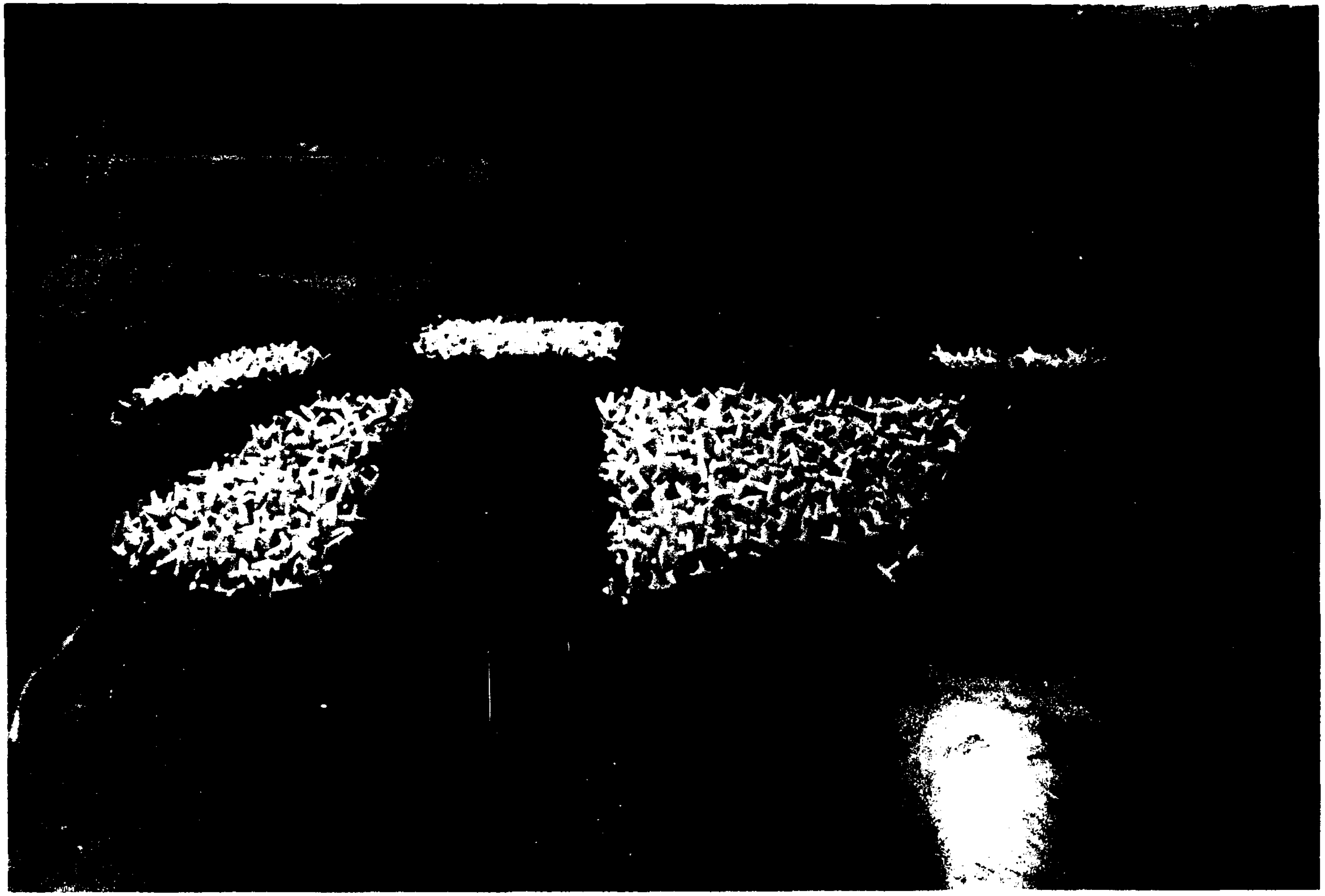

Photo 179. Repeat test of Plan 3D-1C; sea-side view after attack of 15-sec, 17.6-ft nonbreaking waves at an swl of +8 ft NGVD followed by 15-sec, 17.6-ft breaking waves at an swl of +1 ft NGVD; angle of wave attack = 90 deg

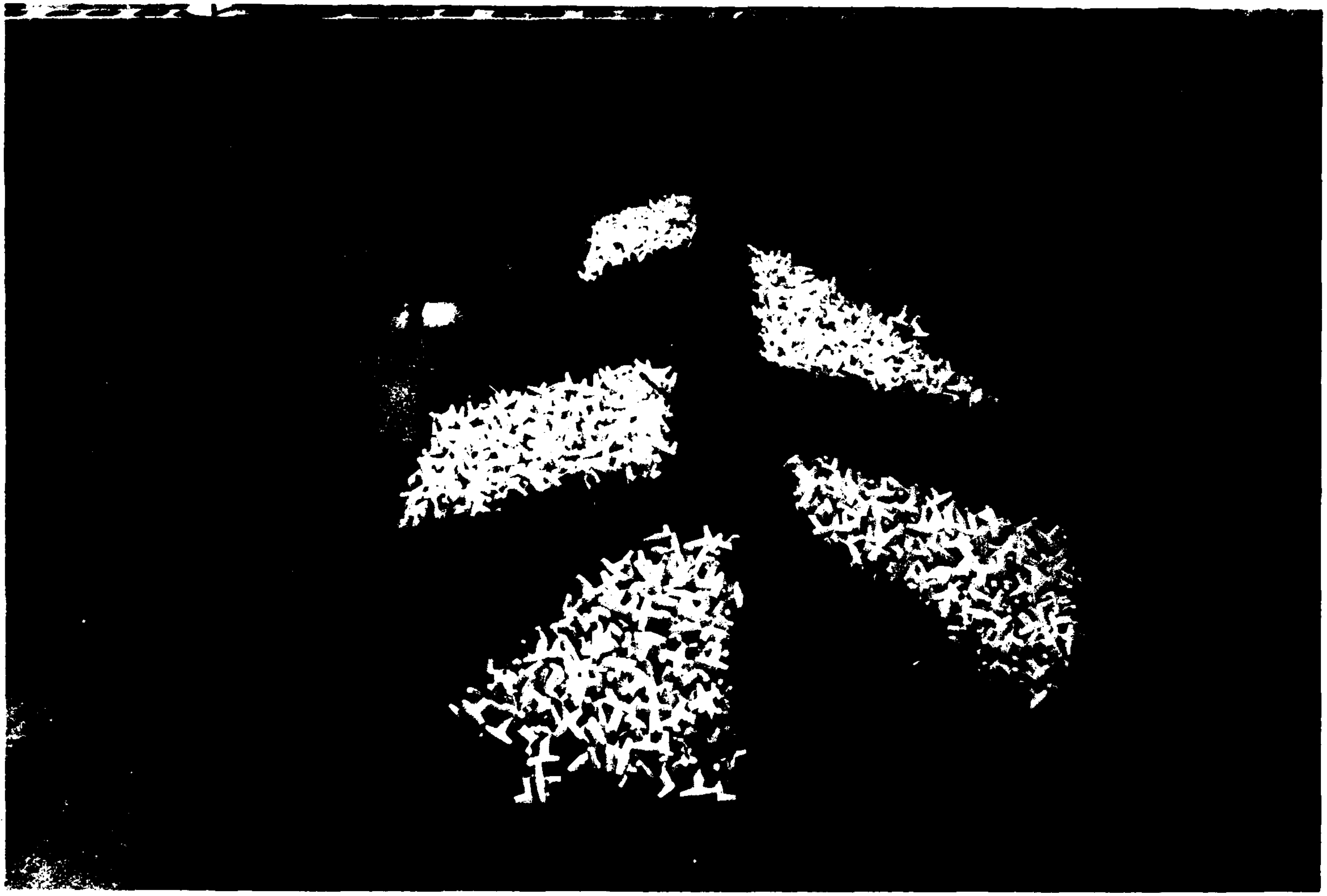

Photo 180. Repeat test of Plan 3D-1C; end view after attack of 15-sec, 17.6-ft nonbreaking waves at an swl of +8 ft NGVD followed by 15-sec, 17.6-ft breaking waves at an swl of +1 ft NGVD; angle of wave attack = 90 deg

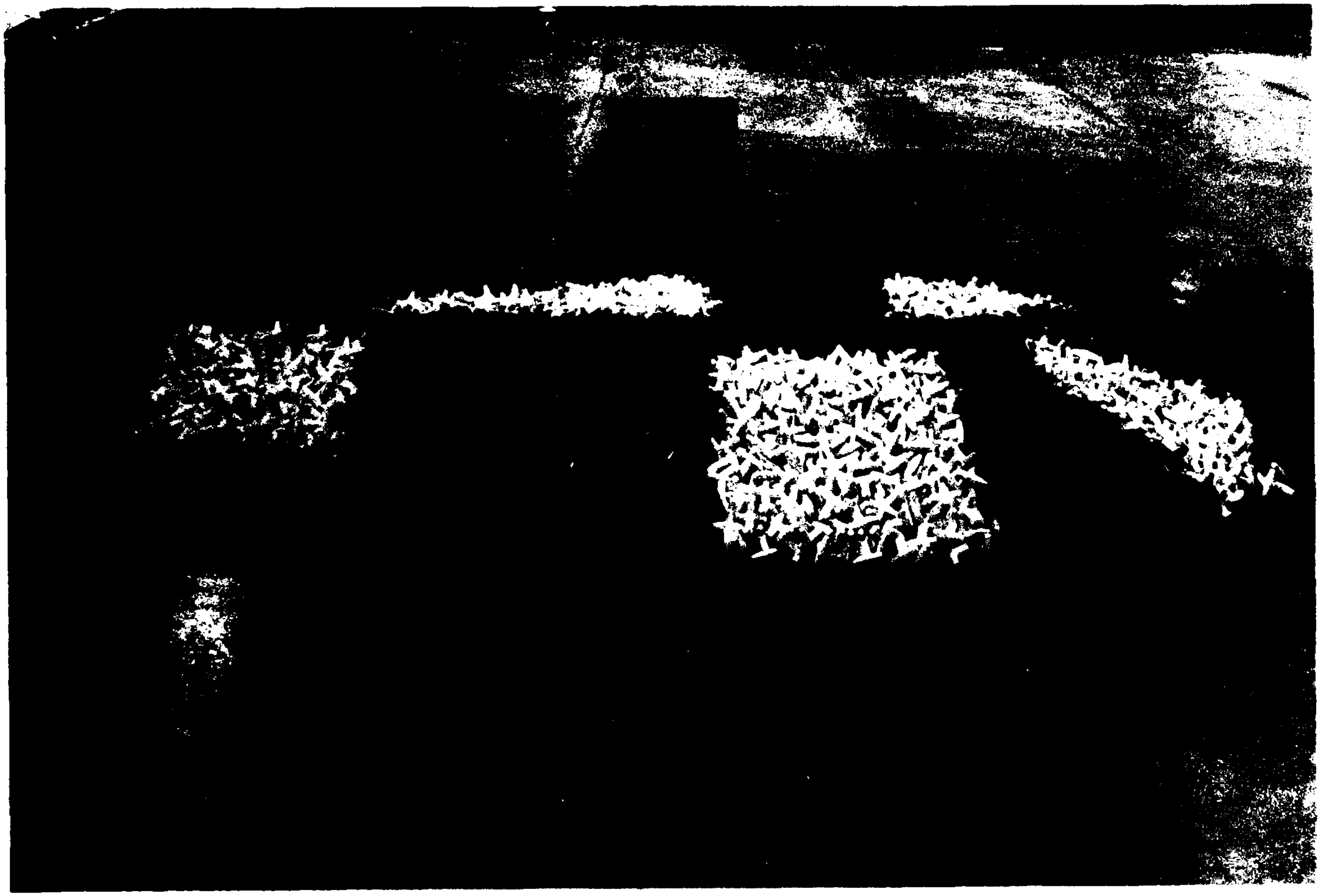

Photo 181. Repeat test of Plan 3D-1C; channel-side view after attack of 15-sec, 17.6-ft nonbreaking waves at an swl of +8 ft NGVD followed by 15-sec, 17.6-ft breaking waves at an swl of +1 ft NGVD; angle of wave attack = 90 deg

Photo 182. Repeat test of Plan 3D-2C; sea-side view after attack of 15-sec, 17.6-ft nonbreaking waves at an swl of +8 ft NGVD followed by 15-sec, 17.6-ft breaking waves at an swl of +1 ft NGVD; angle of wave attack = 90 deg

Photo 183. Repeat test of Plan 3D-2C; end view after attack of 15-sec, 17.6-ft nonbreaking waves at an swl of +8 ft NGVD followed by 15-sec, 17.6-ft breaking waves at an swl of +1 ft NGVD; angle of wave attack = 90 deg

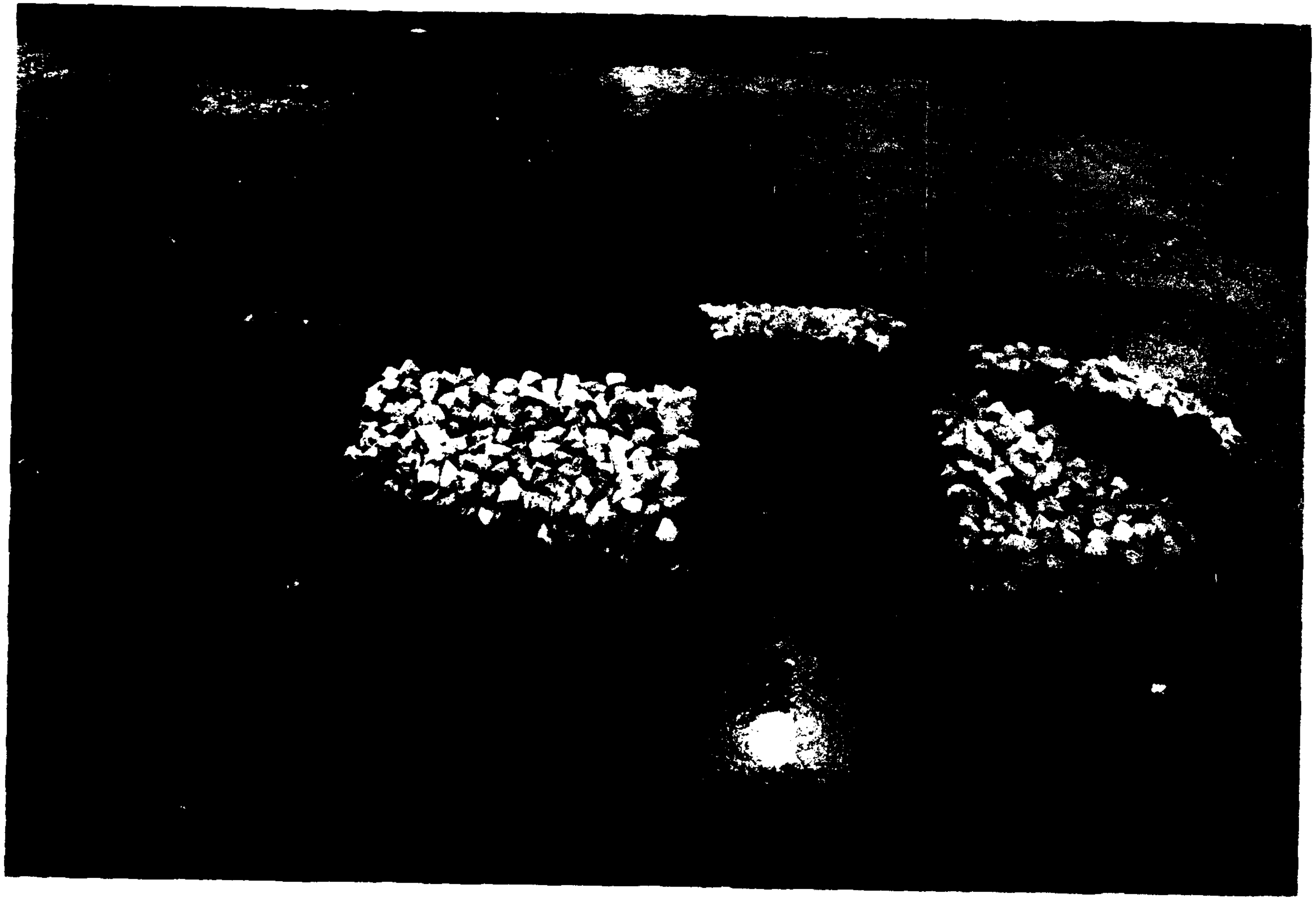

Photo 184. Repeat test of Plan 3D-2C; channel-side view after attack of 15-sec, 17.6-ft nonbreaking waves at an swl of +8 ft NGVD followed by 15-sec, 17.6-ft breaking waves at an swl of +1 ft NGVD; angle of wave attack = 90 deg

Photo 185. End view of Plan 3D-1C after attack of 15-sec, 17.6-ft breaking waves at an swl of +1 ft NGVD followed by 15-sec, 17.6-ft nonbreaking waves at an swl of +8 ft NGVD; angle of wave attack = 67.5 deg

Photo 186. End view of Plan 3D-2C after attack of 15-sec, 17.6-ft breaking waves at an swl of +1 ft NGVD followed by 15-sec, 17.6-ft nonbreaking waves at an swl of +8 ft NGVD; angle of wave attack = 67.5 deg

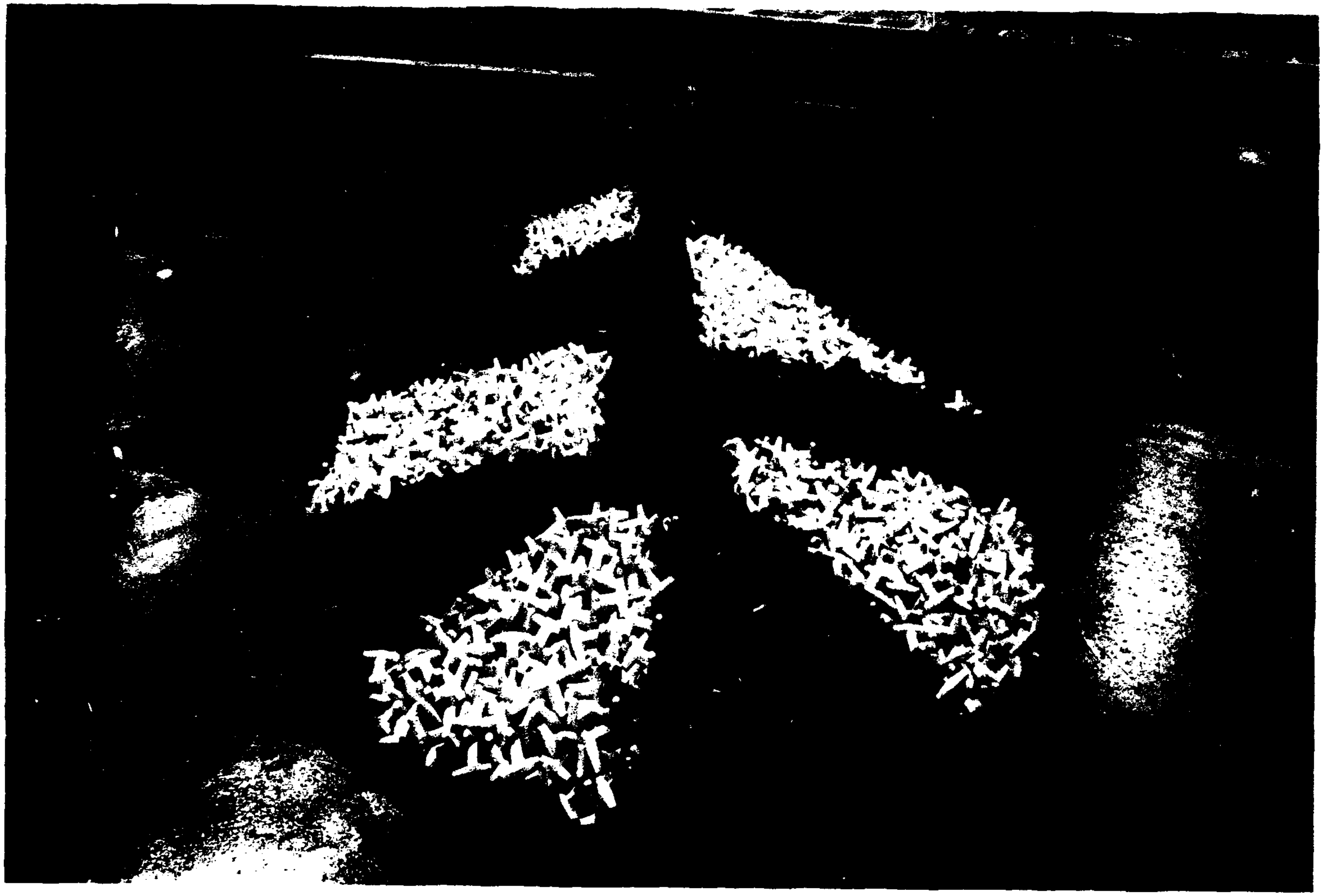

Photo 187. Repeat test of Plan 3D-1C; end view after attack of 15-sec, 17.6-ft nonbreaking waves at an swl of +8 ft NGVD followed by 15-sec, 17.6-ft breaking waves at an swl of +1 ft NGVD; angle of wave attack = 67.5 deg

Photo 188. Repeat test of Plan 3D-2C; end view after attack of 15-sec, 17.6-ft nonbreaking waves at an swl of +8 ft NGVD followed by 15-sec, 17.6-ft breaking waves at an swl of +1 ft NGVD; angle of wave attack = 67.5 deg

Photo 189. End view of Plan 3D-1C after attack of 15-sec, 17.6-ft breaking waves at an swl of +1 ft NGVD followed by 15-sec, 17.6-ft nonbreaking waves at an swl of +8 ft NGVD; angle of wave attack = 45 deg

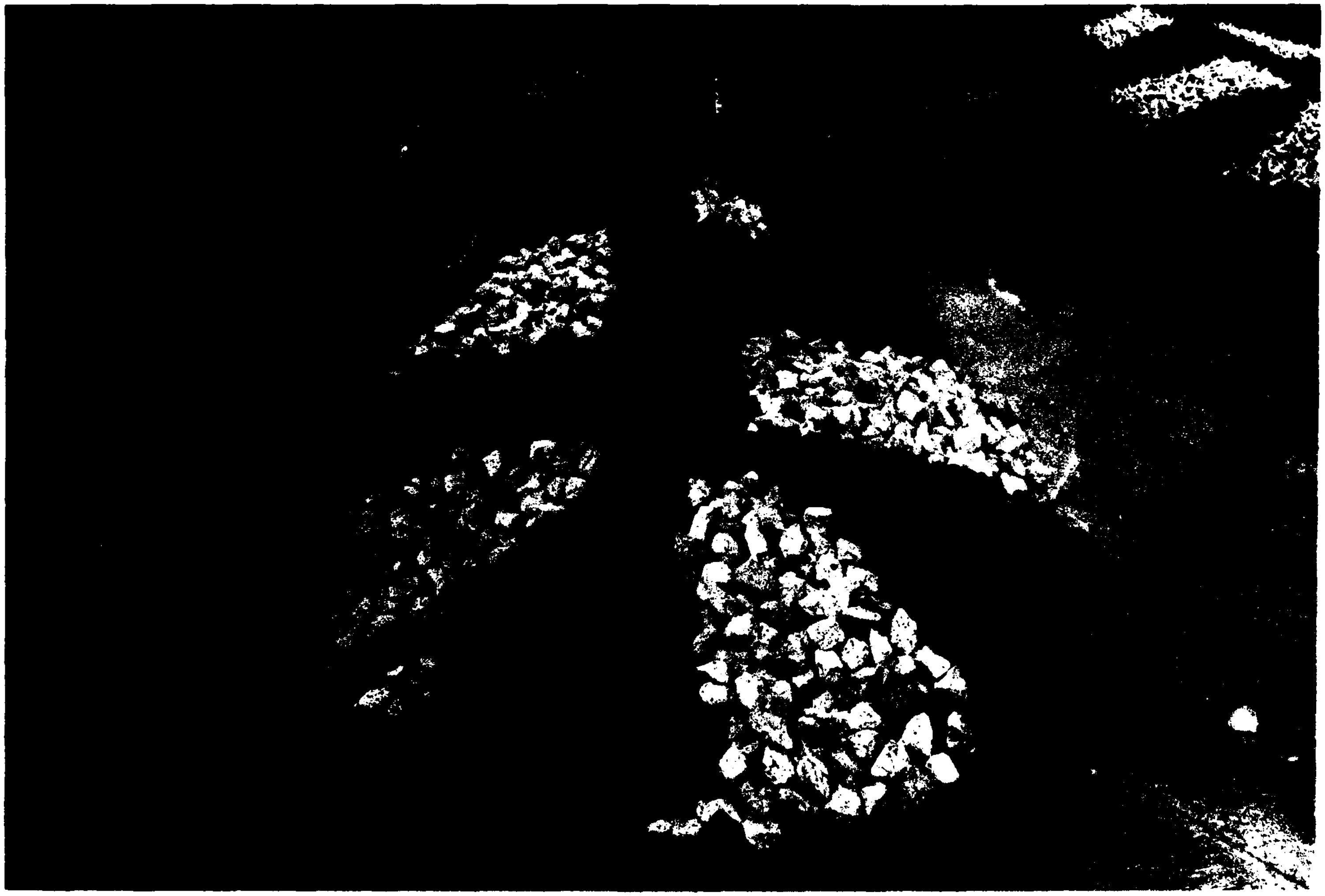

Photo 190. End view of Plan 3D-2C after attack of 15-sec, 17.6-ft breaking waves at an swl of +1 ft NGVD followed by 15-sec, 17.6-ft nonbreaking waves at an swl of +8 ft NGVD; angle of wave attack = 45 deg

Photo 191. Repeat test of Plan 3D-1C; end view after attack of 15-sec, 17.6-ft nonbreaking waves at an swl of +8 ft NGVD followed by 15-sec, 17.6-ft breaking waves at an swl of +1 ft NGVD; angle of wave attack = 45 deg

Photo 192. Repeat test of Plan 3D-2C; end view after attack of 15-sec, 17.6-ft nonbreaking waves at an swl of +8 ft NGVD followed by 15-sec, 17.6-ft breaking waves at an swl of +1 ft NGVD; angle of wave attack = 45 deg

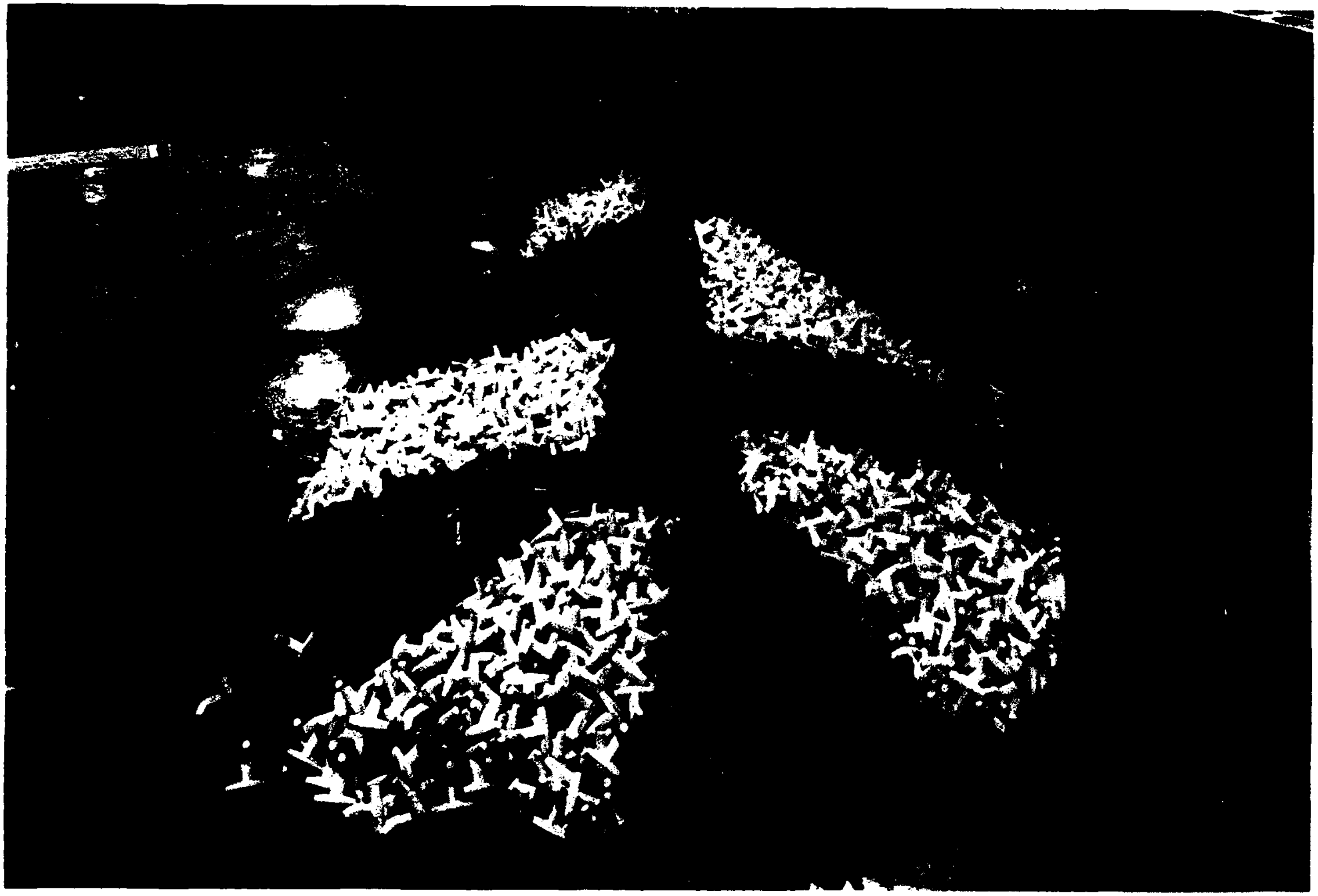

Photo 193. End view of Plan 3D-1C after attack of 15-sec, 17.6-ft breaking waves at an swl of +1 ft NGVD followed by 15-sec, 17.6-ft nonbreaking waves at an swl of +8 ft NGVD; angle of wave attack = 22.5 deg

Photo 194. End view of Plan 3D-2C after attack of 15-sec, 17.6-ft breaking waves at an swl of +1 ft NGVD followed by 15-sec, 17.6-ft nonbreaking waves at an swl of +8 ft NGVD; angle of wave attack = 22.5 deg

Photo 195. Repeat test of Plan 3D-1C; end view after attack of 15-sec, 17.6-ft nonbreaking waves at an swl of +8 ft NGVD followed by 15-sec, 17.6-ft breaking waves at an swl of +1 ft NGVD; angle of wave attack = 22.5 deg

Photo 196. Repeat test of Plan 3D-2C; end view after attack of 15-sec, 17.6-ft nonbreaking waves at an swl of +8 ft NGVD followed by 15-sec, 17.6-ft breaking waves at an swl of +1 ft NGVD; angle of wave attack = 22.5 deg

AD-A136 610 JETTY STABILITY STUDY OREGON INLET NORTH CAROLINA 4/5
HYDRAULIC MODEL INVESTIGATION(U) COASTAL ENGINEERING
RESEARCH CENTER VICKSBURG MS R D CARVER ET AL. SEP 83
UNCLASSIFIED CERC-TR-83-3 F/G 13/2 NL

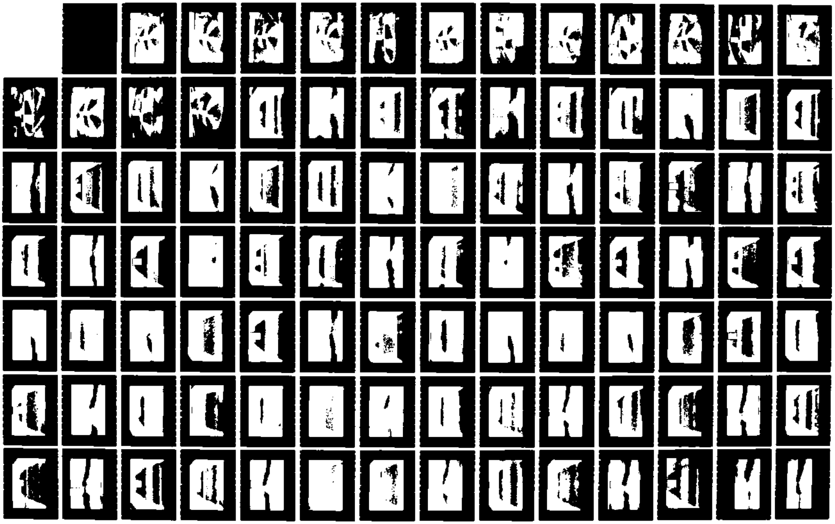

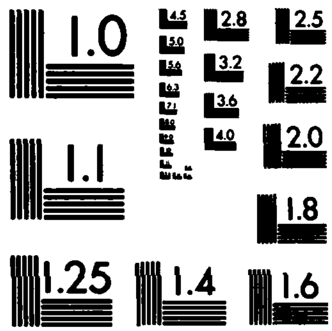

MICROCOPY RESOLUTION TEST CHART
NATIONAL BUREAU OF STANDARDS-1963-A

Photo 197. End view of Plan 3D-1C after attack of 15-sec, 17.6-ft breaking waves at an swl of +1 ft NGVD followed by 15-sec, 17.6-ft nonbreaking waves at an swl of +8 ft NGVD; angle of wave attack = 0.0 deg

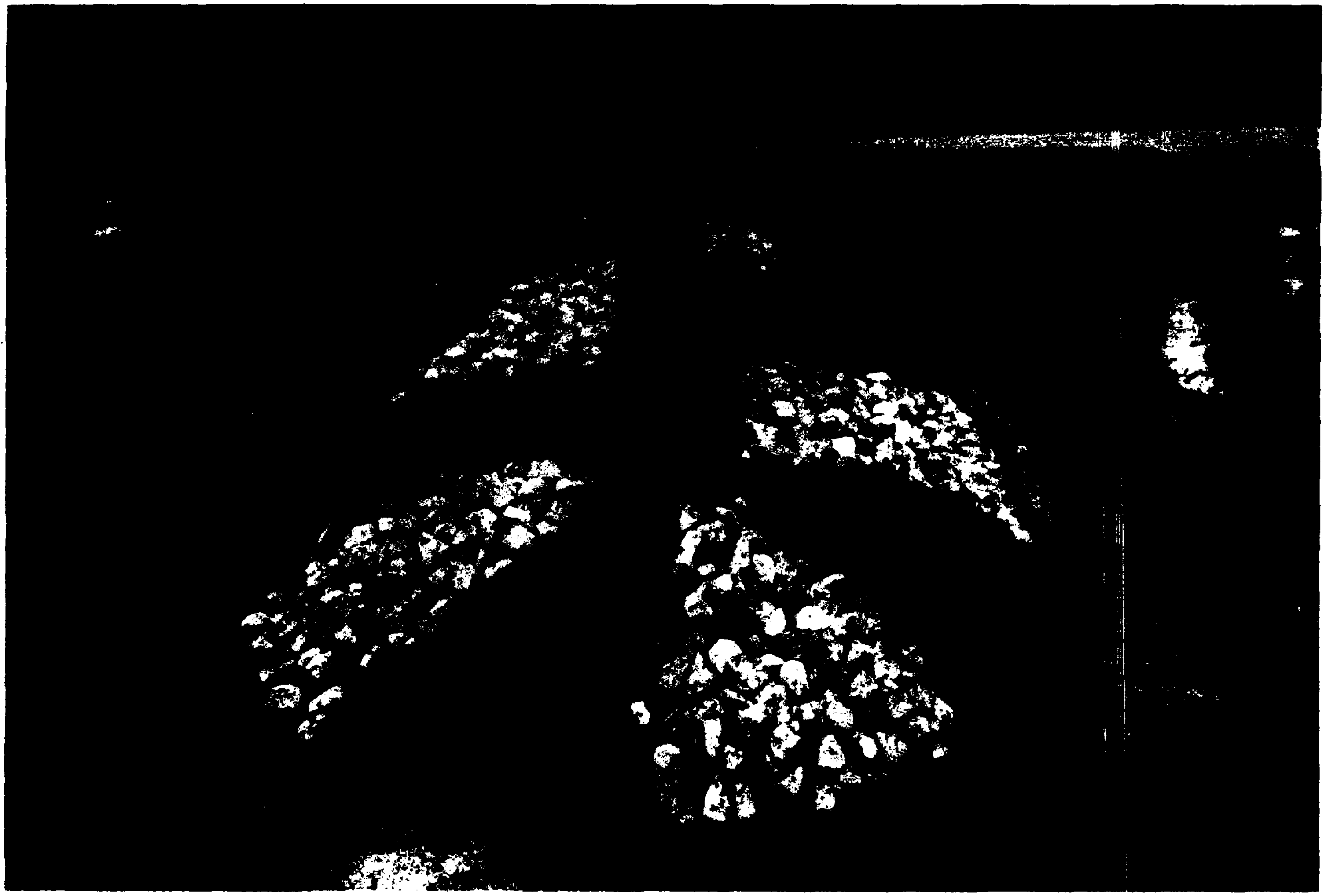

Photo 198. End view of Plan 3D-2C after attack of 15-sec, 17.6-ft breaking waves at an swl of +1 ft NGVD followed by 15-sec, 17.6-ft nonbreaking waves at an swl of +8 ft NGVD; angle of wave attack = 0.0 deg

Photo 199. Repeat test of Plan 3D-1C; end view after attack of 15-sec, 17.6-ft nonbreaking waves at an swl of +8 ft NGVD followed by 15-sec, 17.6-ft breaking waves at an swl of +1 ft NGVD; angle of wave attack = 0.0 deg

Photo 200. Repeat test of Plan 3D-2C; end view after attack of 15-sec, 17.6-ft nonbreaking waves at an swl of +8 ft NGVD followed by 15-sec, 17.6-ft breaking waves at an swl of +1 ft NGVD; angle of wave attack = 0.0 deg

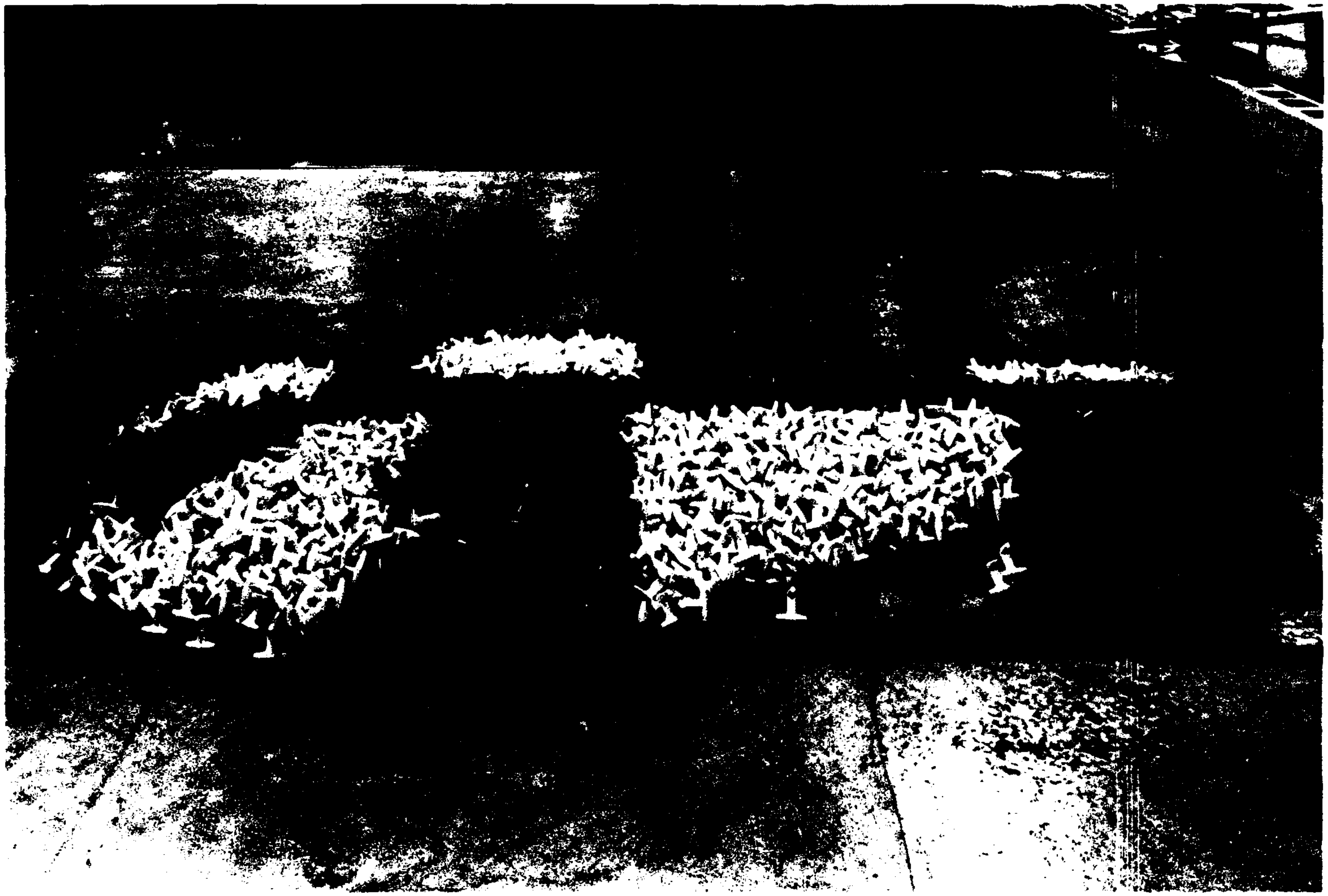

Photo 201. Cumulative damage test of Plan 3D-1C; sea-side view after attack of 15-sec, 17.6-ft nonbreaking waves at an swl of +8 ft NGVD followed by 15-sec, 17.6-ft breaking waves at an swl of +1 ft NGVD; angles of wave attack = 0.0, 45.0, and 90.0 deg

Photo 202. Cumulative damage test of Plan 3D-1C; end view after attack of 15-sec, 17.6-ft nonbreaking waves at an swl of +8 ft NGVD followed by 15-sec, 17.6-ft breaking waves at an swl of +1 ft NGVD; angles of wave attack = 0.0, 45.0, and 90.0 deg

Photo 203. Cumulative damage test of Plan 3D-2C; sea-side view after attack of 15-sec, 17.6-ft nonbreaking waves at an swl of +8 ft NGVD followed by 15-sec, 17.6-ft breaking waves at an swl of +1 ft NGVD; angles of wave attack = 0.0, 45.0, and 90.0 deg

Photo 204. Cumulative damage test of Plan 3D-2C; end view after attack of 15-sec, 17.6-ft nonbreaking waves at an swl of +8 ft NGVD followed by 15-sec, 17.6-ft breaking waves at an swl of +1 ft NGVD; angles of wave attack = 0.0, 45.0, and 90.0 deg

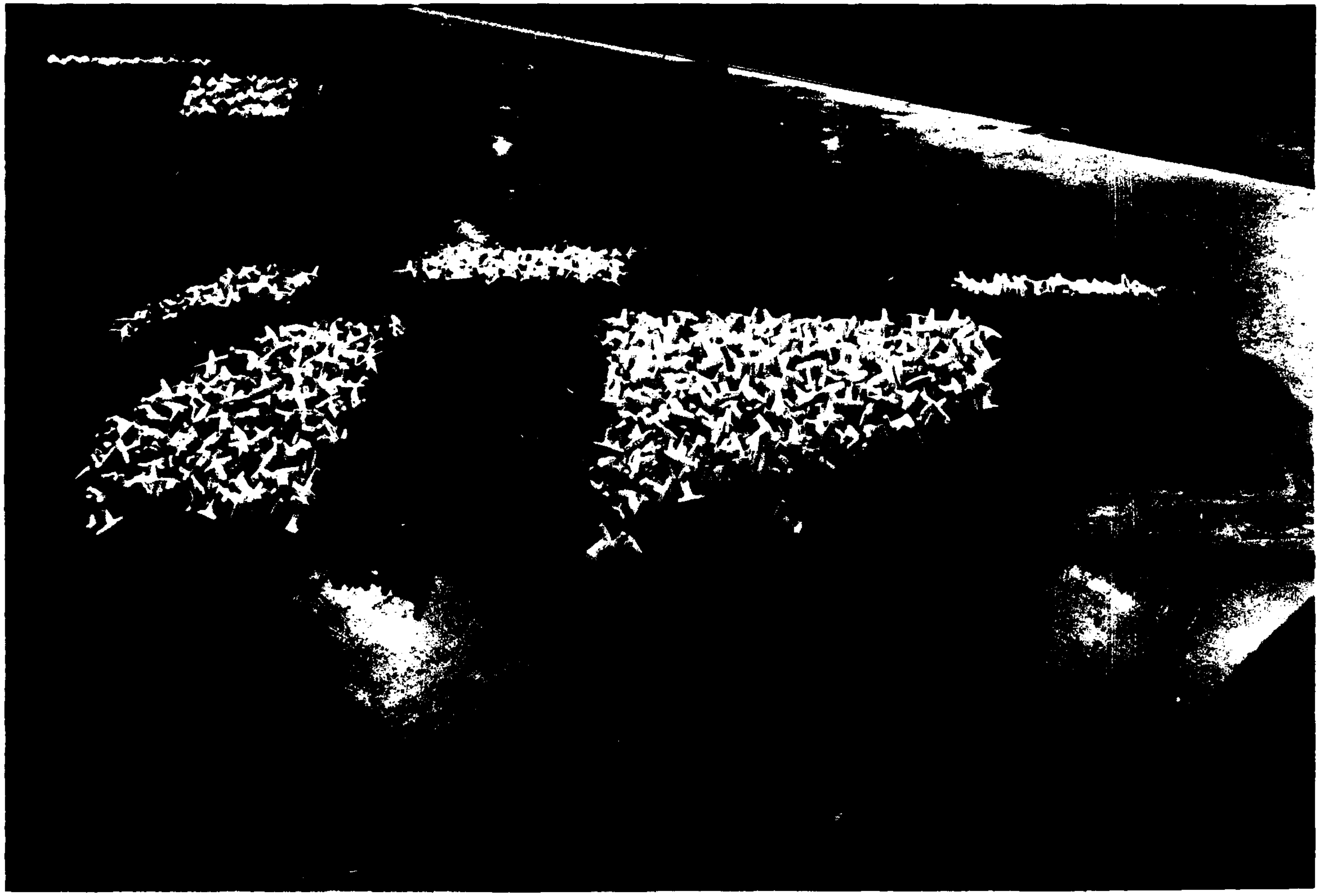

Photo 205. Safety-factor test of Plan 3D-1C; sea-side view after attack of 15-sec, 19.2-ft breaking waves at an swl of +3 ft NGVD; angle of wave attack = 45 deg

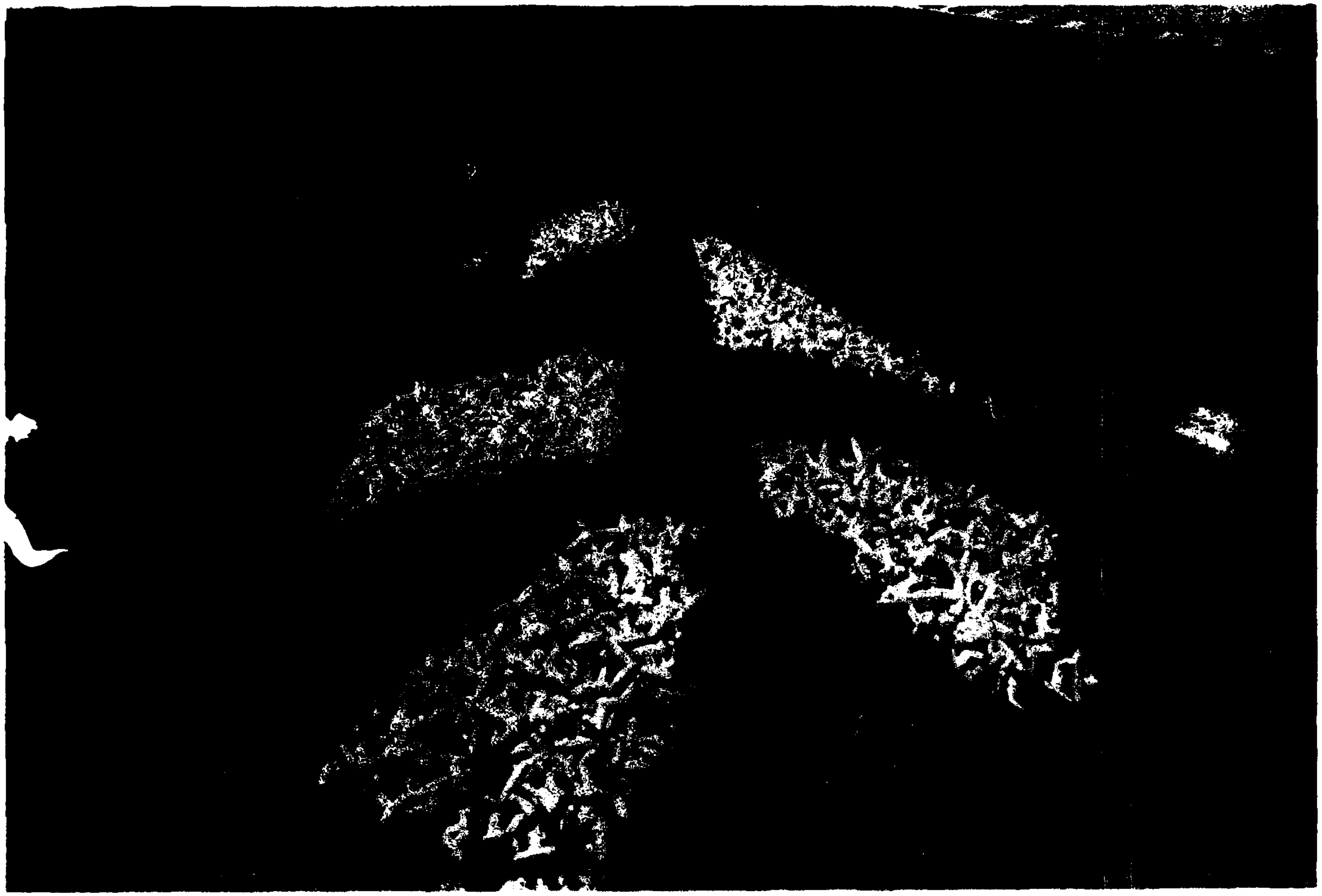

Photo 206. Safety-factor test of Plan 3D-1C; end view after attack of 15-sec, 19.2-ft breaking waves at an swl of +3 ft NGVD; angle of wave attack = 45 deg

Photo 207. Safety-factor test of Plan 3D-2C; sea-side view after attack of 15-sec, 19.2-ft breaking waves at an swl of +3 ft NGVD; angle of wave attack = 45 deg

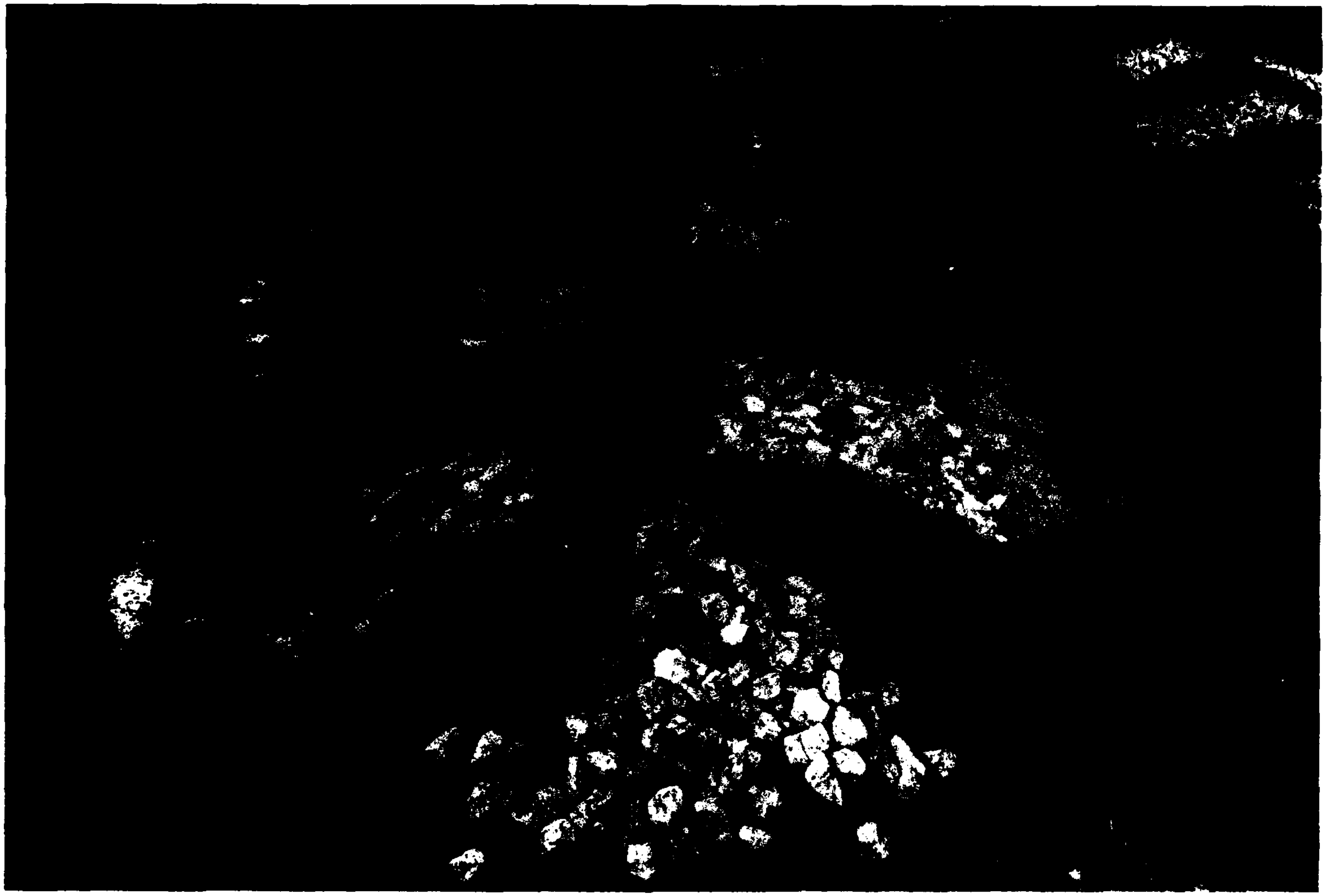

Photo 208. Safety-factor test of Plan 3D-2C; end view after attack of 15-sec, 19.2-ft breaking waves at an swl of +3 ft NGVD; angle of wave attack = 45 deg

Photo 209. Safety-factor test of Plan 3D-1C; sea-side view after attack of 15-sec, 19.2-ft breaking waves at an swl of +3 ft NGVD followed by 15-sec, 22-ft nonbreaking waves at an swl of +8 ft NGVD; angle of wave attack = 45 deg

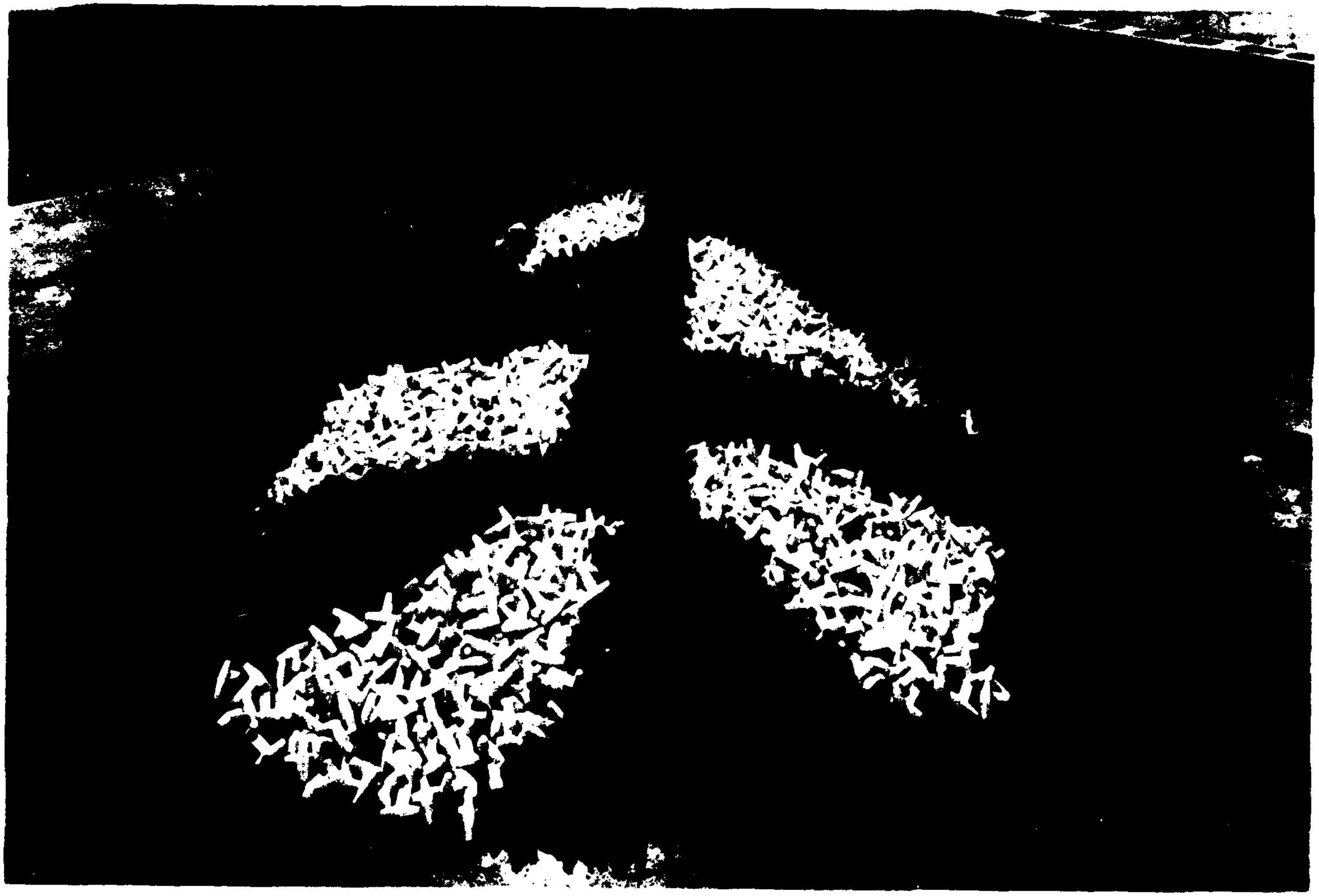

Photo 210. Safety-factor test of Plan 3D-1C; end view after attack of 15-sec, 19.2-ft breaking waves at an swl of +3 ft NGVD followed by 15-sec, 22-ft nonbreaking waves at an swl of +8 ft NGVD; angle of wave attack = 45 deg

Photo 211. Safety-factor test of Plan 3D-2C; sea-side view after attack of 15-sec, 19.2-ft breaking waves at an swl of +3 ft NGVD followed by 15-sec, 22-ft nonbreaking waves at an swl of +8 ft NGVD; angle of wave attack = 45 deg

Photo 212. Safety-factor test of Plan 3D-2C; end view after attack of 15-sec, 19.2-ft breaking waves at an swl of +3 ft NGVD followed by 15-sec, 22-ft nonbreaking waves at an swl of +8 ft NGVD; angle of wave attack = 45 deg

Photo 213. Sea-side view of Plan 12 before wave attack

Photo 214. End view of Plan 12 before wave attack

Photo 215. Channel-side view of Plan 12 before wave attack

Photo 216. Sea-side view of Plan 12 after testing at an swl of +8 ft NGVD; maximum wave height = 16.0 ft

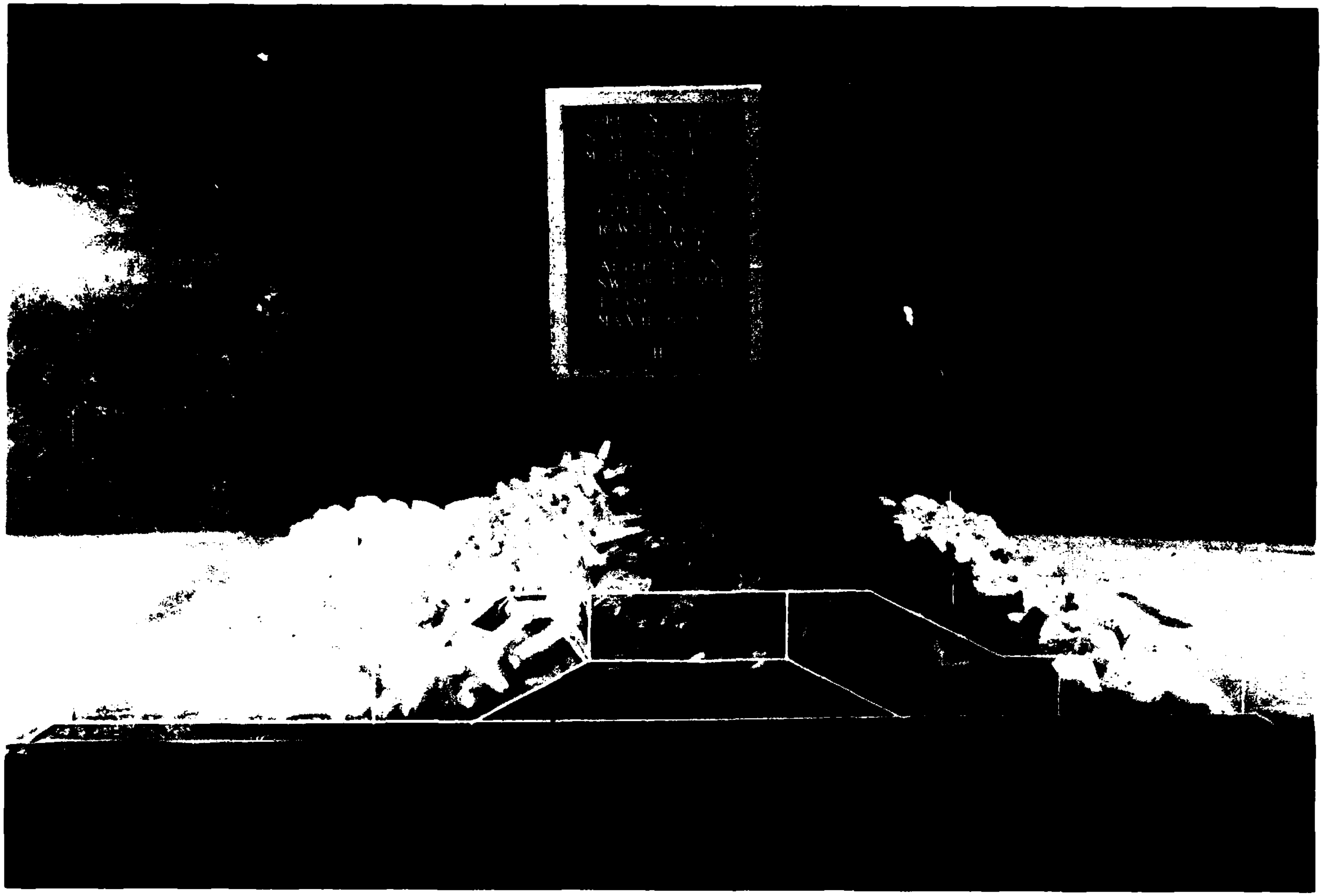

Photo 217. End view of Plan 12 after testing at an swl of +8 ft NGVD; maximum wave height = 16.0 ft

Photo 218. Channel-side view of Plan 12 after testing at an swl of +8 ft NGVD; maximum wave height = 16.0 ft

Photo 219. Sea-side view of Plan 12 after testing at swl's of +8, +6, and +4 ft NGVD; maximum wave heights = 16.0, 14.0, and 12.4 ft, respectively

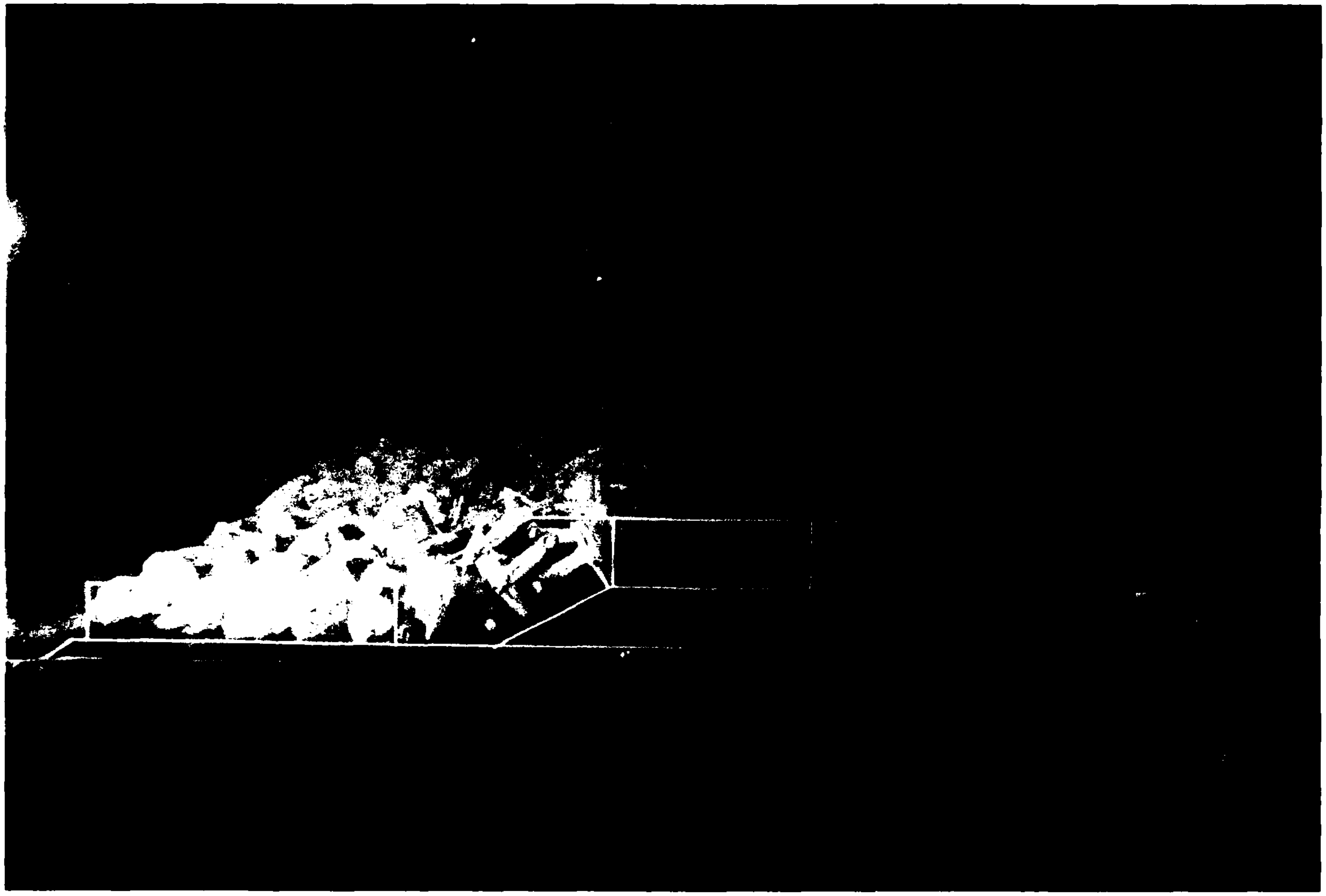

Photo 220. End view of Plan 12 after testing at swl's of +8, +6, and +4 ft NGVD; maximum wave heights = 16.0, 14.0, and 12.4 ft, respectively

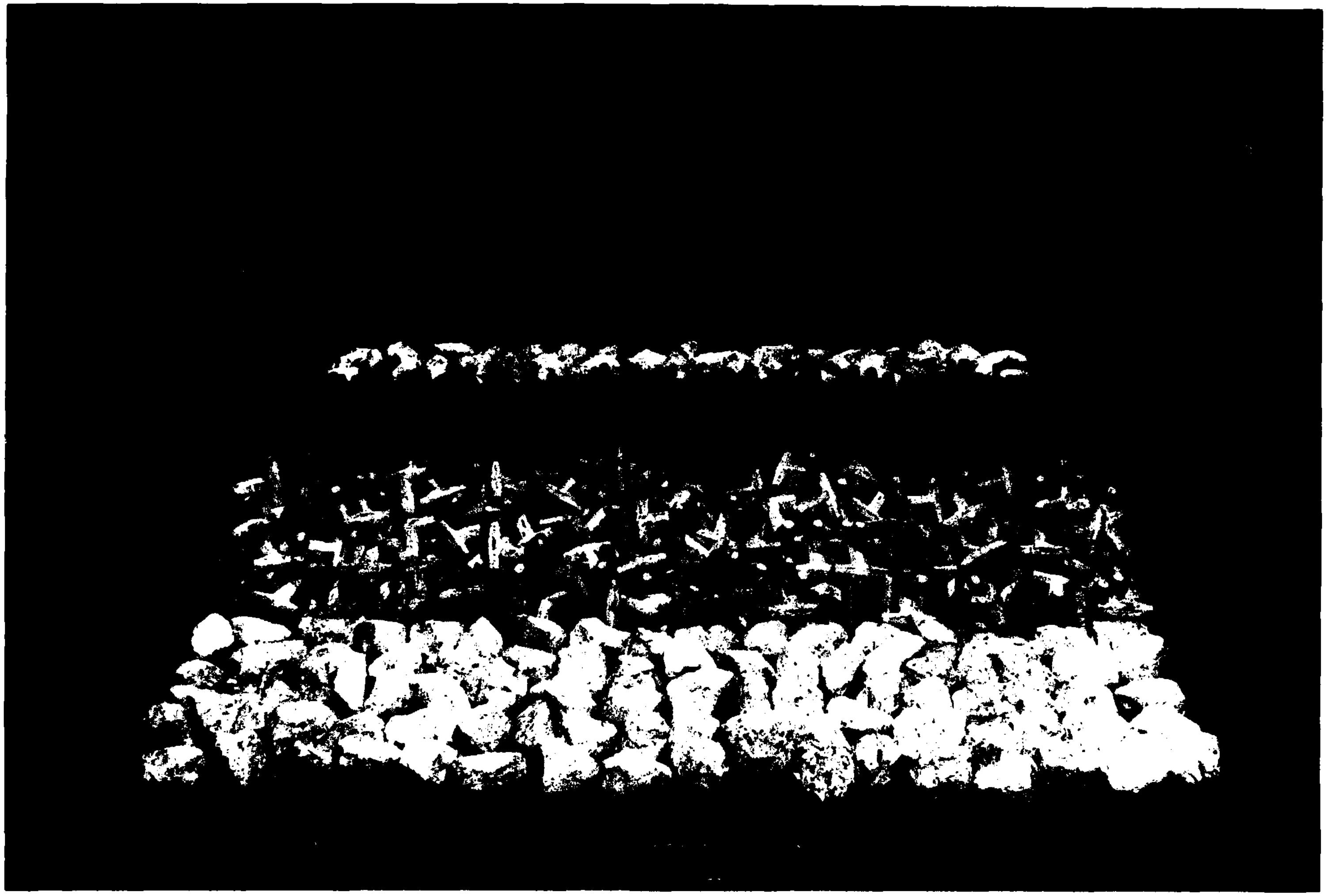

Photo 221. Channel-side view of Plan 12 after testing at swl's of +8, +6, and +4 ft NGVD; maximum wave heights = 16.0, 14.0, and 12.4 ft, respectively

Photo 222. Repeat test of Plan 12; sea-side view before wave attack

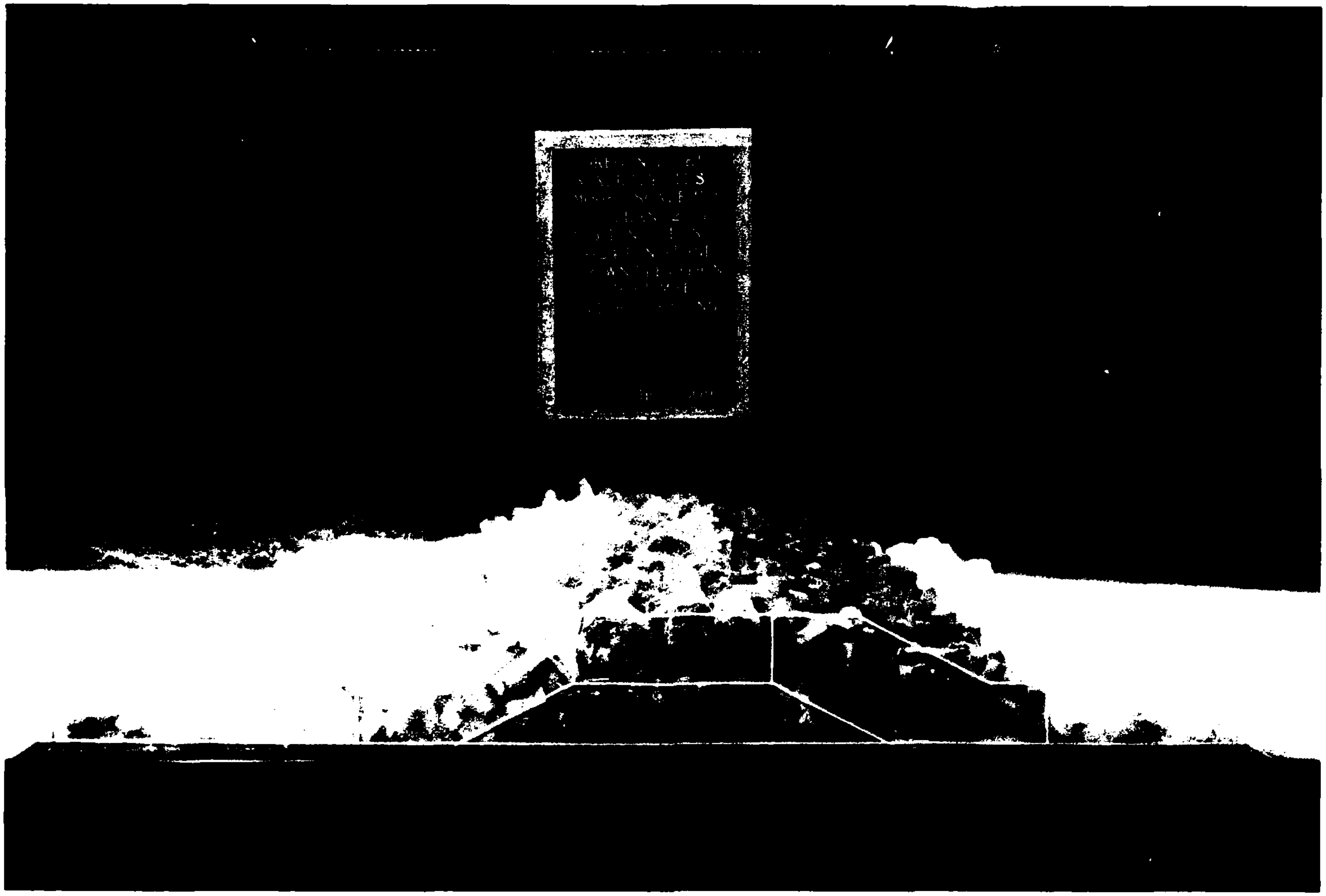

Photo 223. Repeat test of Plan 12; end view before wave attack

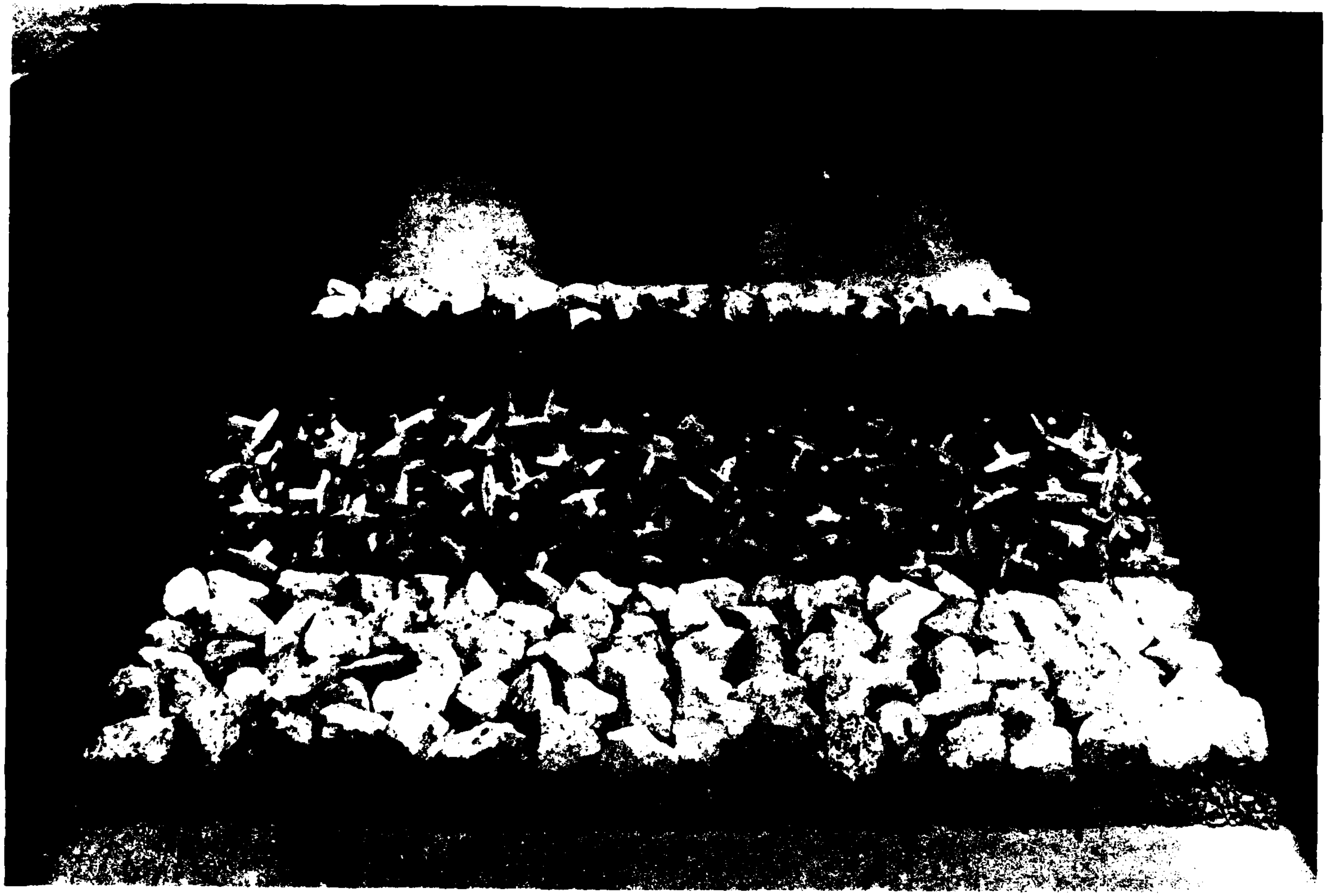

Photo 224. Repeat test of Plan 12; channel-side view before wave attack

Photo 225. Repeat test of Plan 12; sea-side view after testing at swl's of +4 and +6 ft NGVD; maximum wave heights = 12.4 and 14.0 ft, respectively

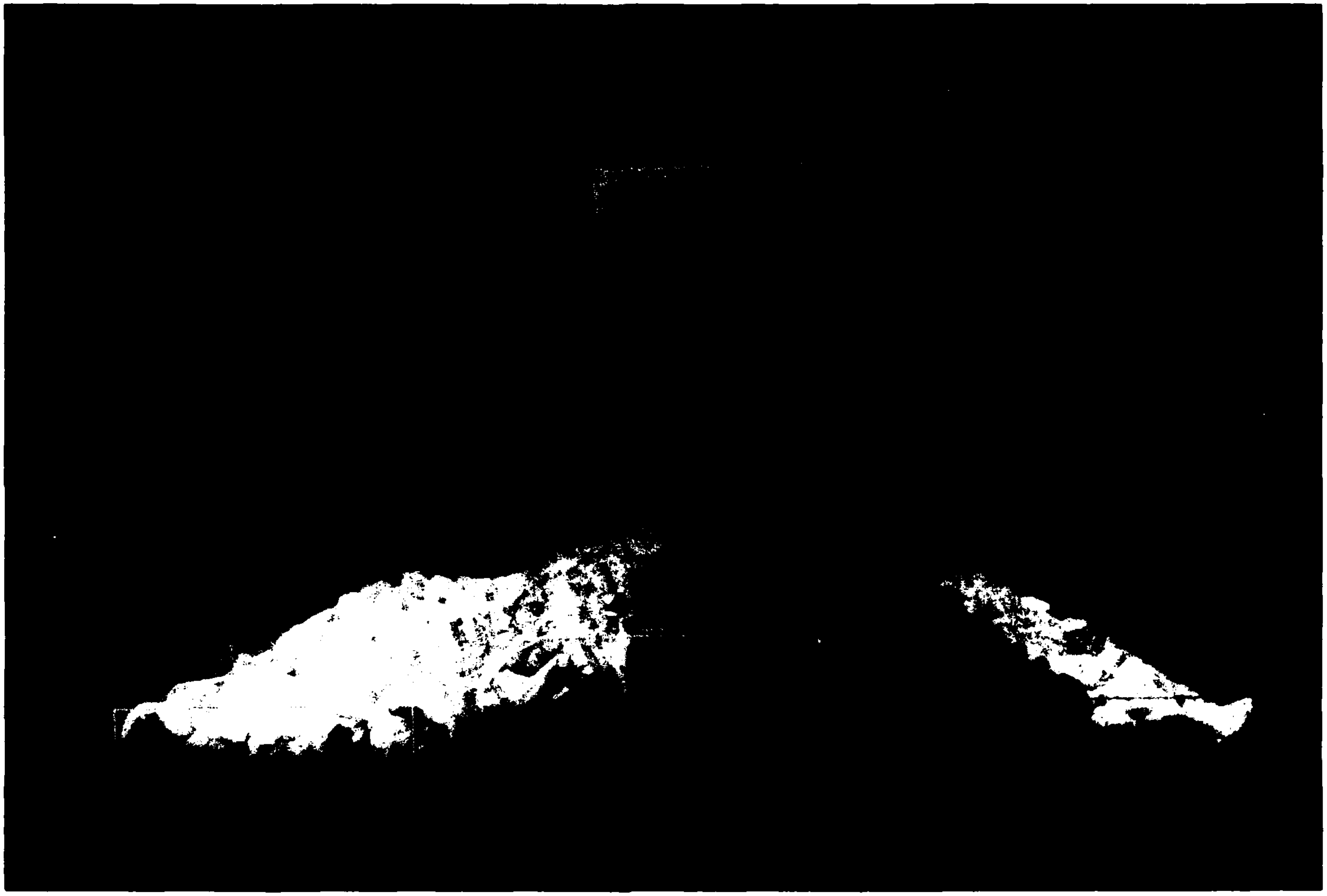

Photo 226. Repeat test of Plan 12; end view after testing at swl's of +4 and +6 ft NGVD; maximum wave heights = 12.4 and 14.0 ft, respectively

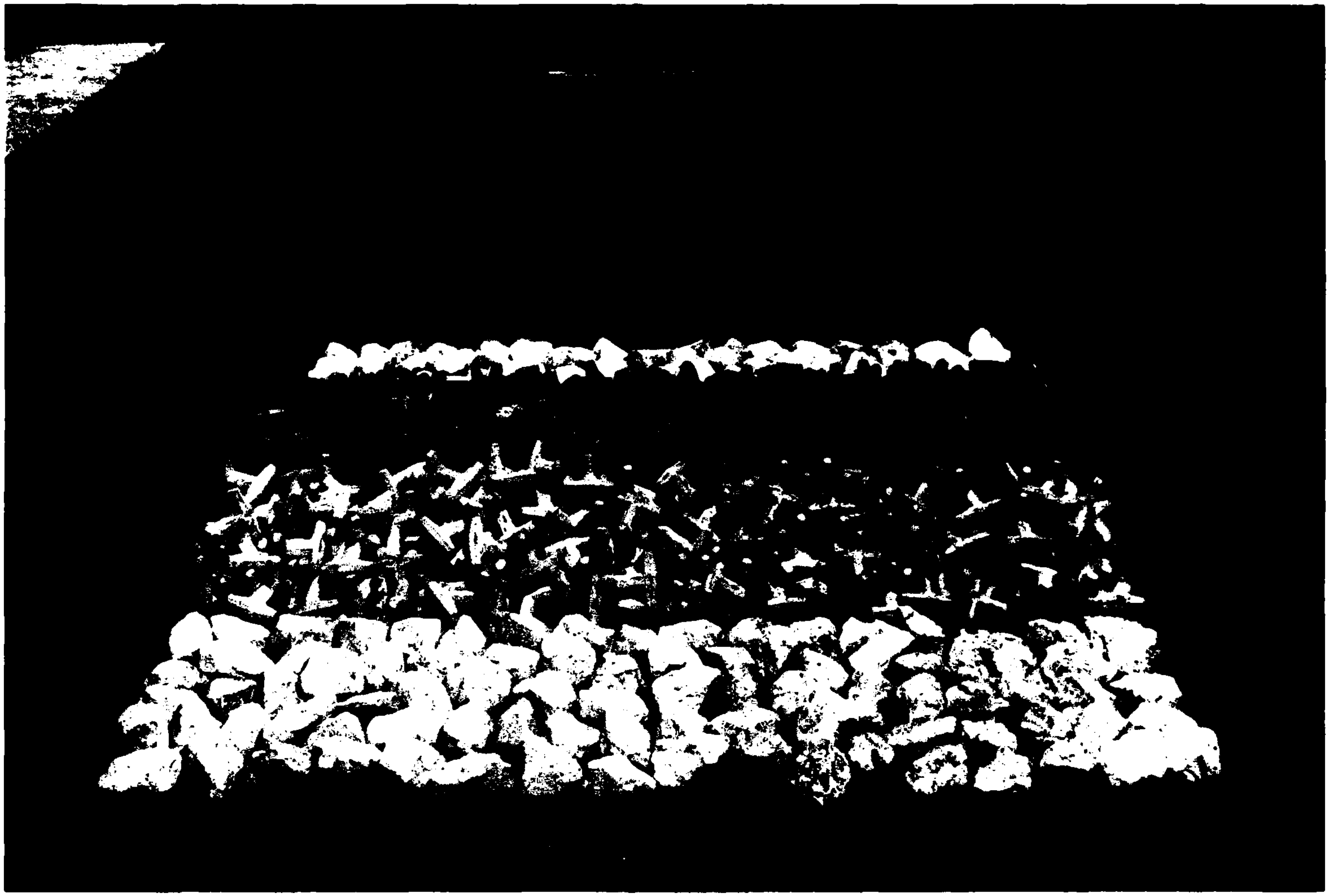

Photo 227. Repeat test of Plan 12; channel-side view after testing at swl's of +4 and +6 ft NGVD; maximum wave heights = 12.4 and 14.0 ft, respectively

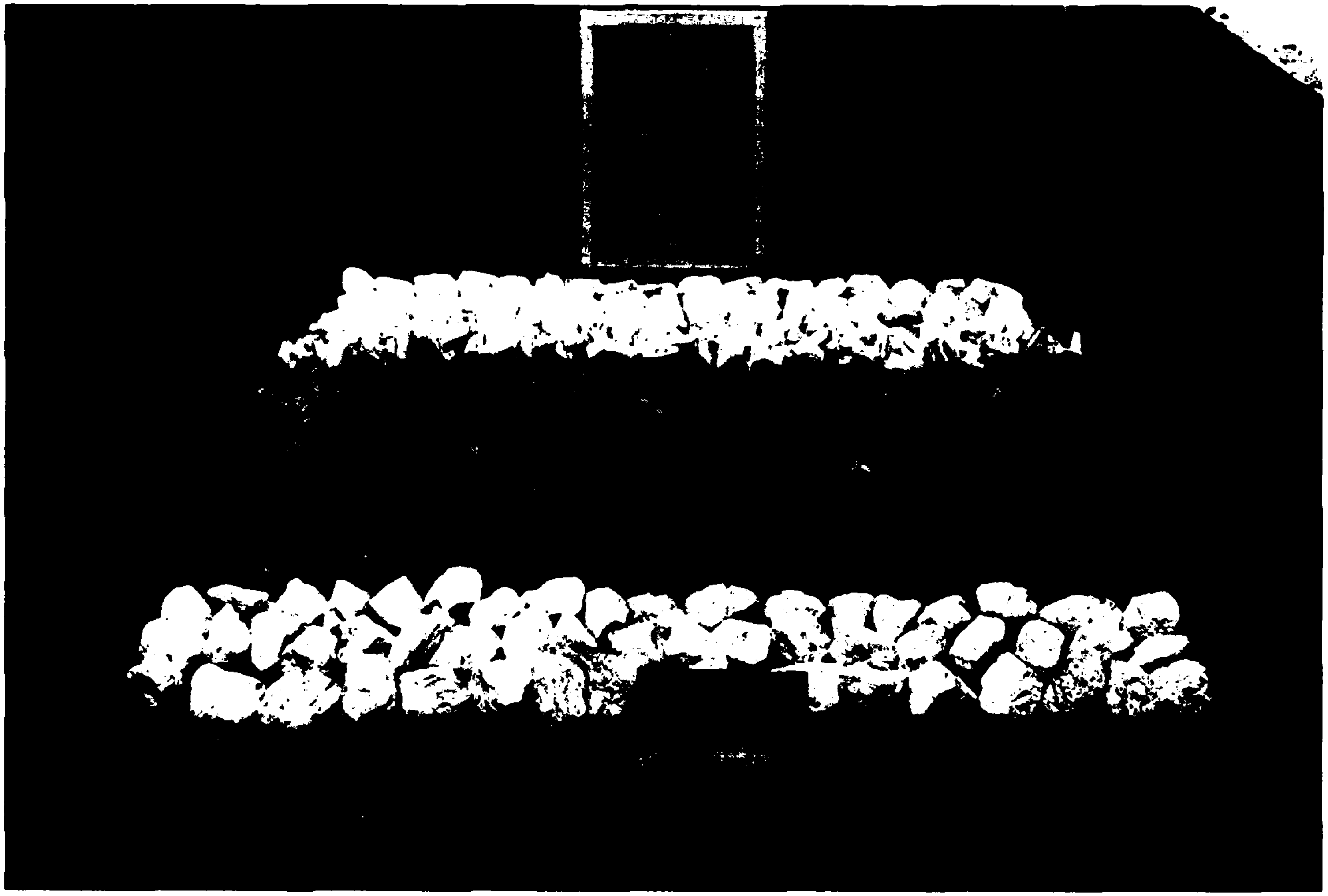

Photo 228. Repeat test of Plan 12; sea-side view after testing at swl's of +4, +6, and +8 ft NGVD; maximum wave heights = 12.4, 14.0, and 16.0 ft, respectively

Photo 229. Repeat test of Plan 12; end view after testing at swl's of +4, +6, and +8 ft NGVD; maximum wave heights = 12.4, 14.0, and 16.0 ft, respectively

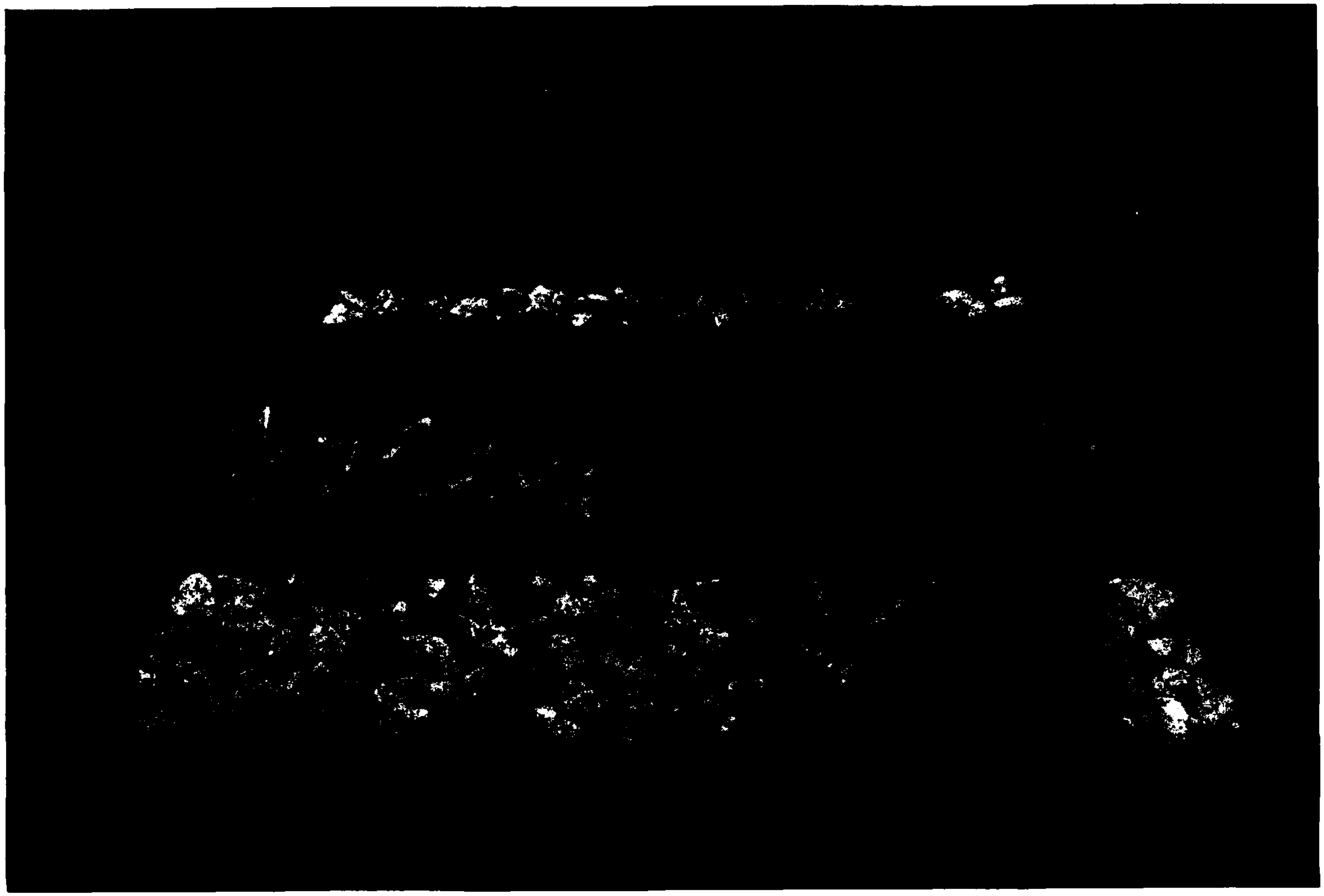

Photo 230. Repeat test of Plan 12; channel-side view after testing at swl's of +4, +6, and +8 ft NGVD; maximum wave heights = 12.4, 14.0, and 16.0 ft, respectively

Photo 231. Sea-side view of Plan 13 before wave attack

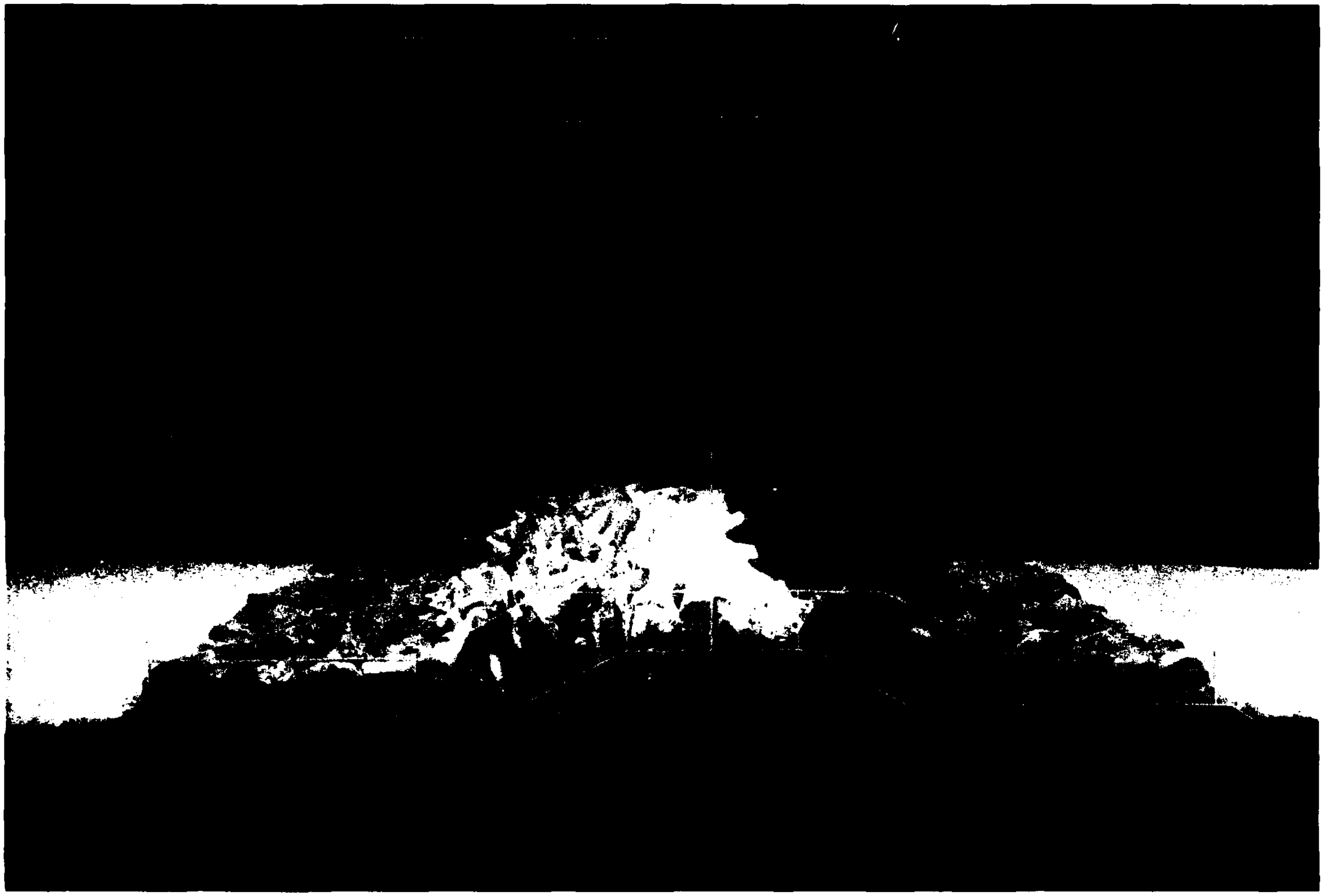

Photo 232. End view of Plan 13 before wave attack

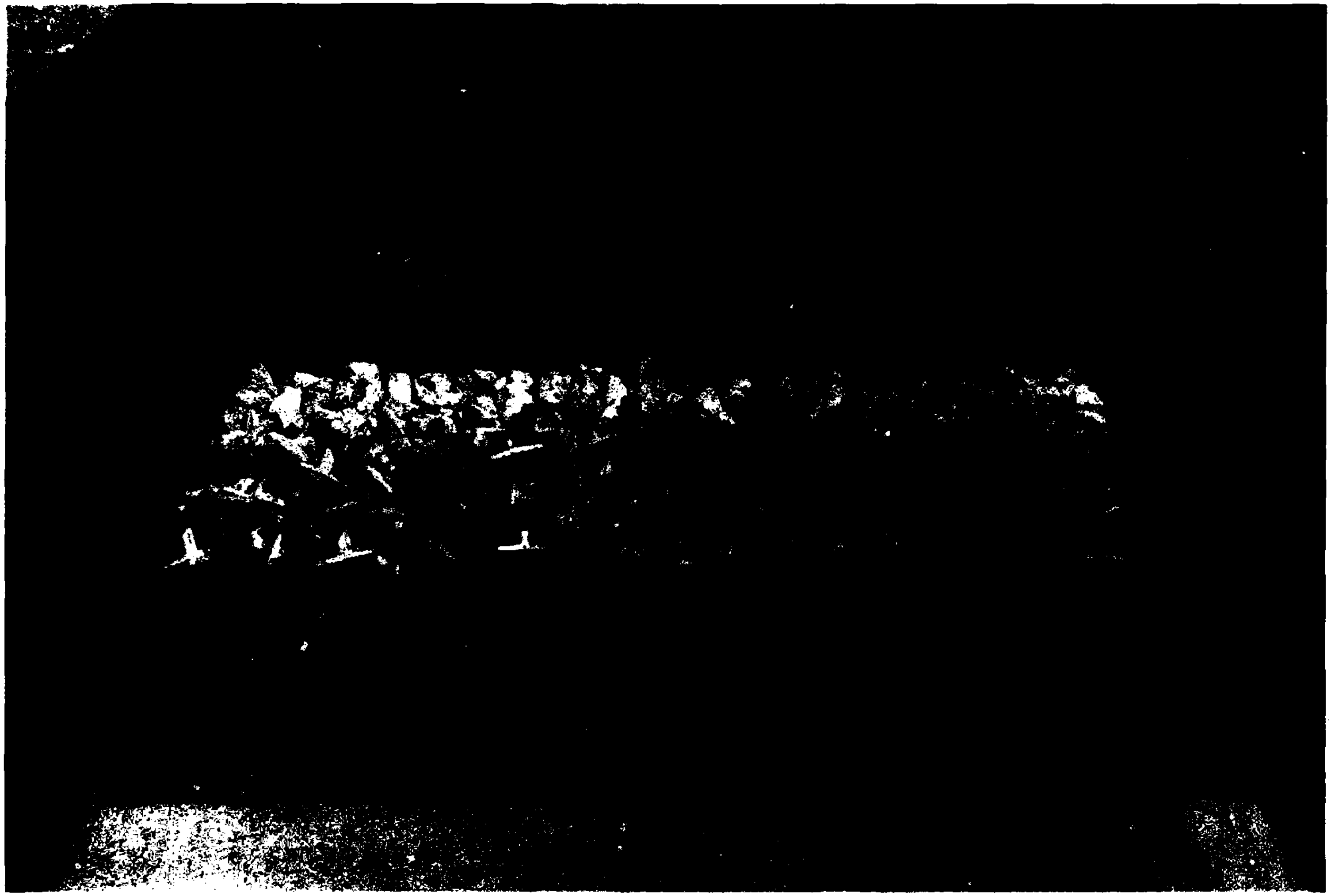

Photo 233. Channel-side view of Plan 13 before wave attack

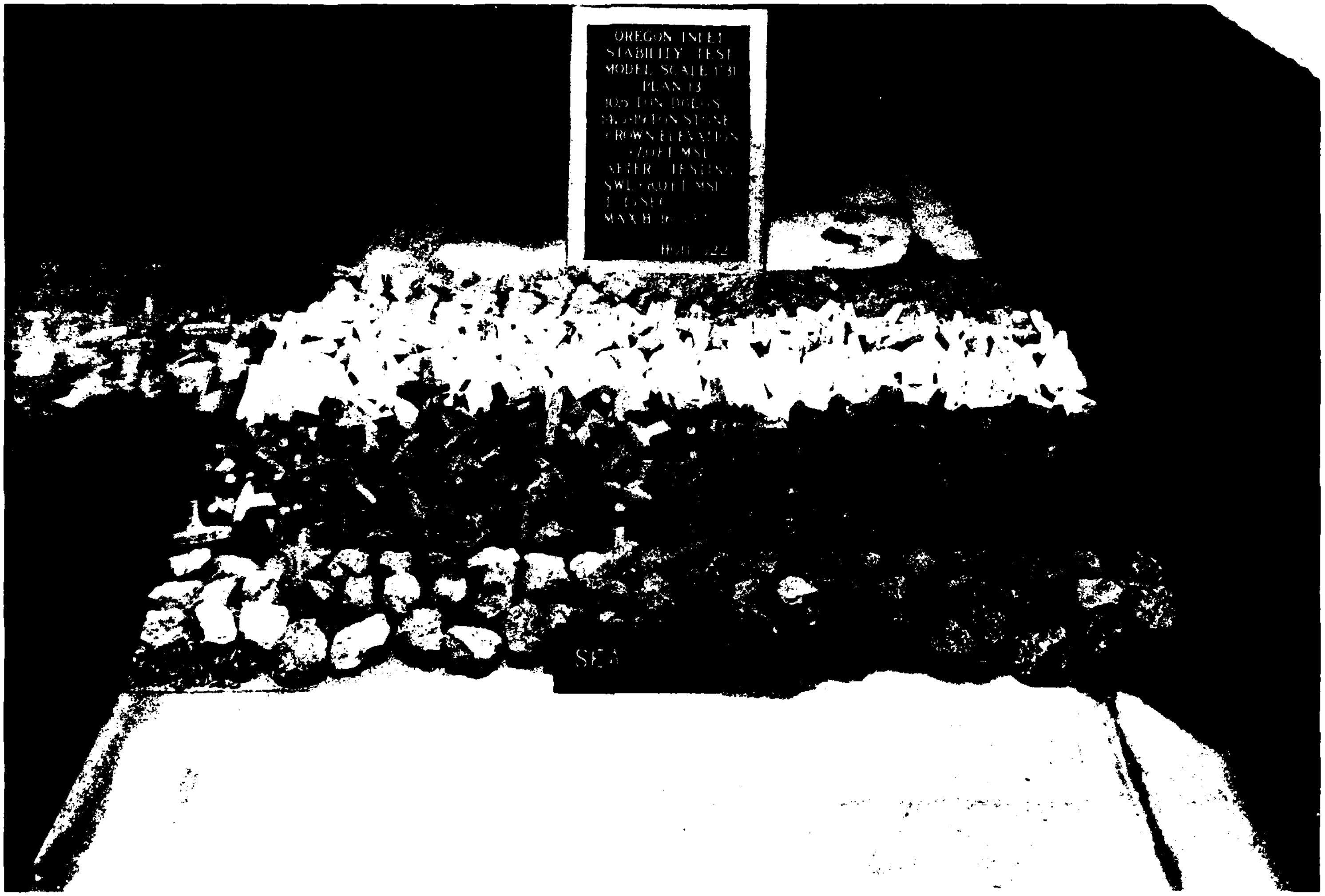

Photo 234. Sea-side view of Plan 13 after testing at an swl of +8 ft NGVD; maximum wave height = 16.0 ft

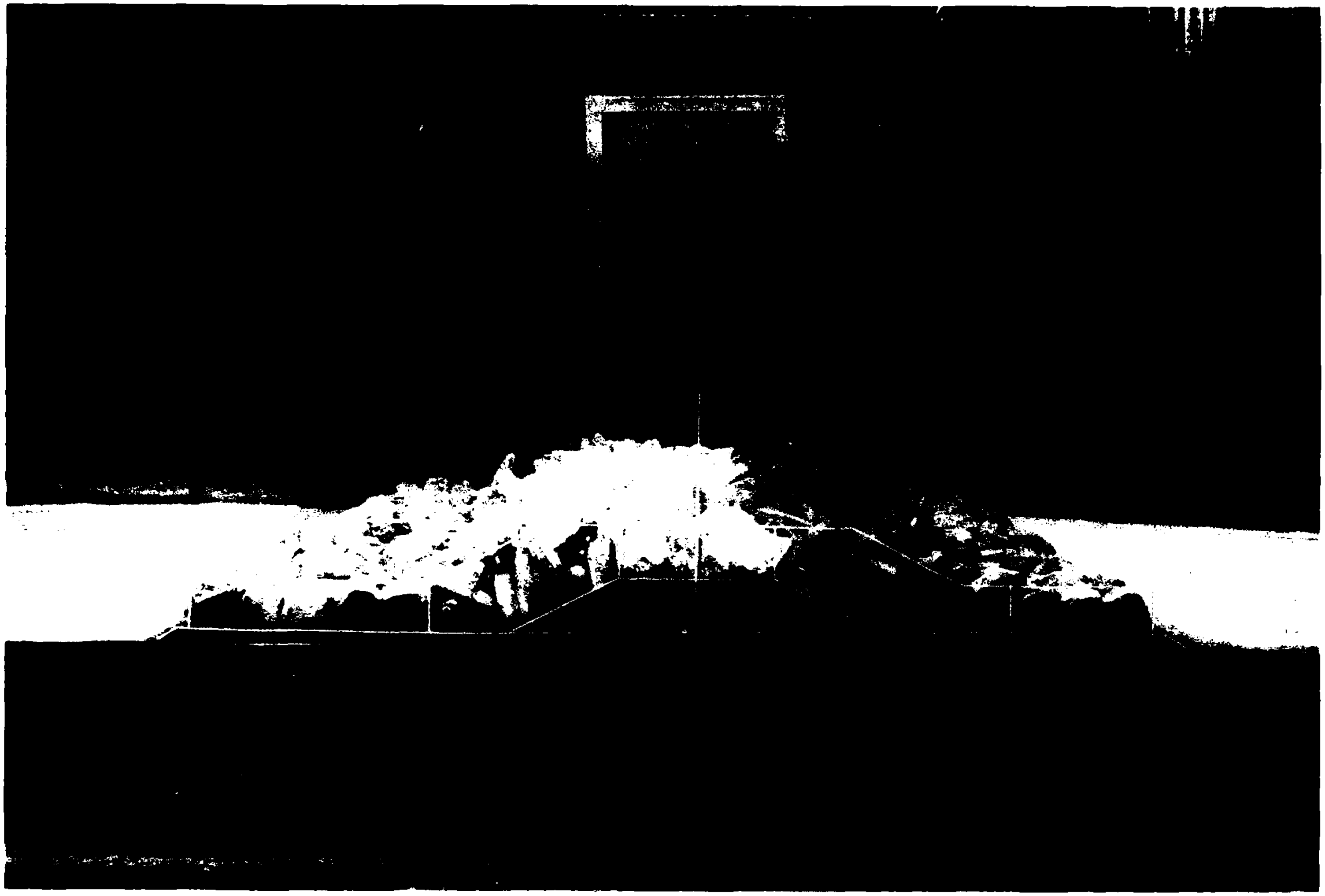

Photo 235. End view of Plan 13 after testing at an swl of +8 ft NGVD; maximum wave height = 16.0 ft

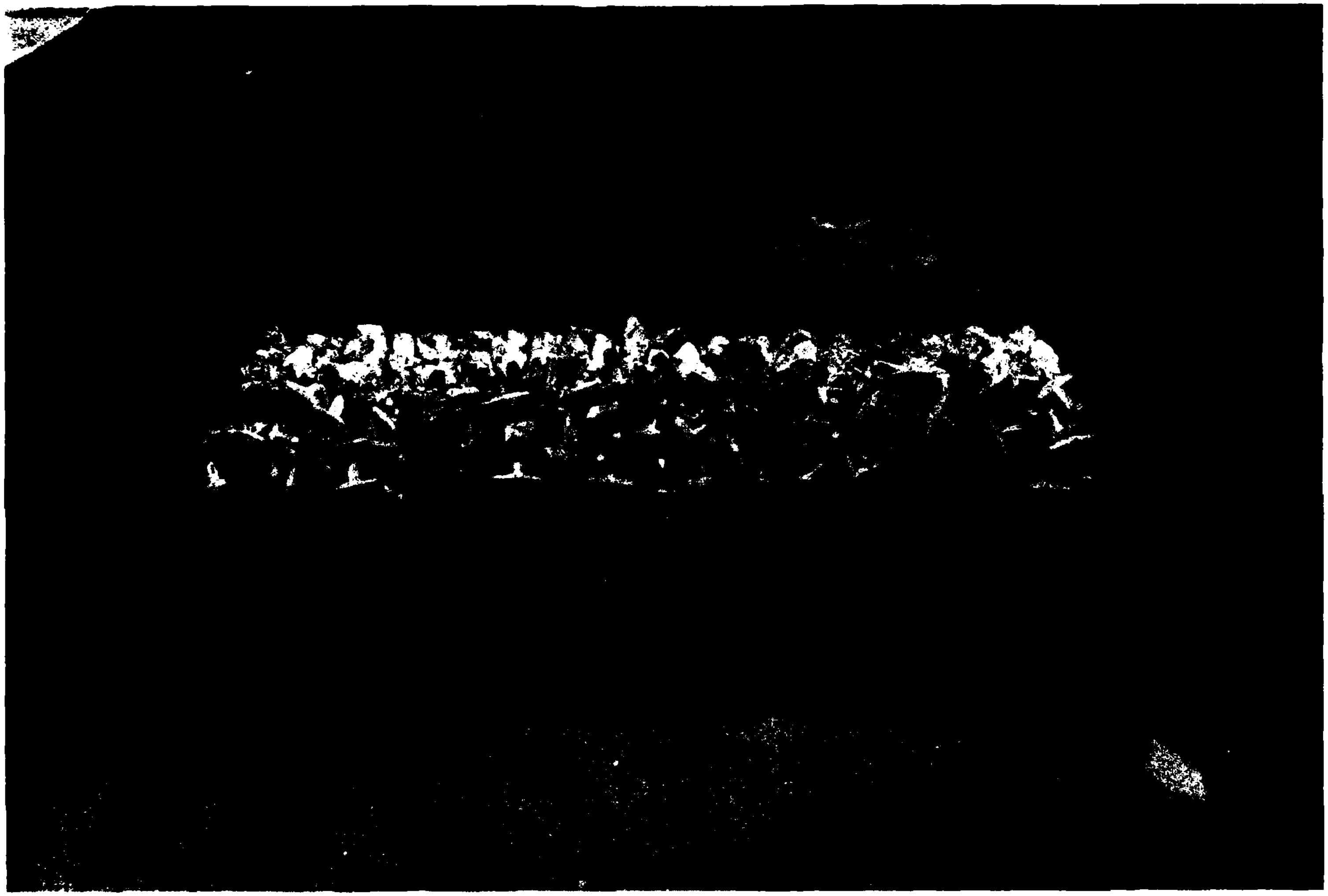

Photo 236. Channel-side view of Plan 13 after testing at an swl of +8 ft NGVD; maximum wave height = 16.0 ft

Photo 237. Sea-side view of Plan 13 after testing at swl's of +8, +6, and +4 ft NGVD; maximum wave heights = 16.0, 14.0, and 12.4 ft, respectively

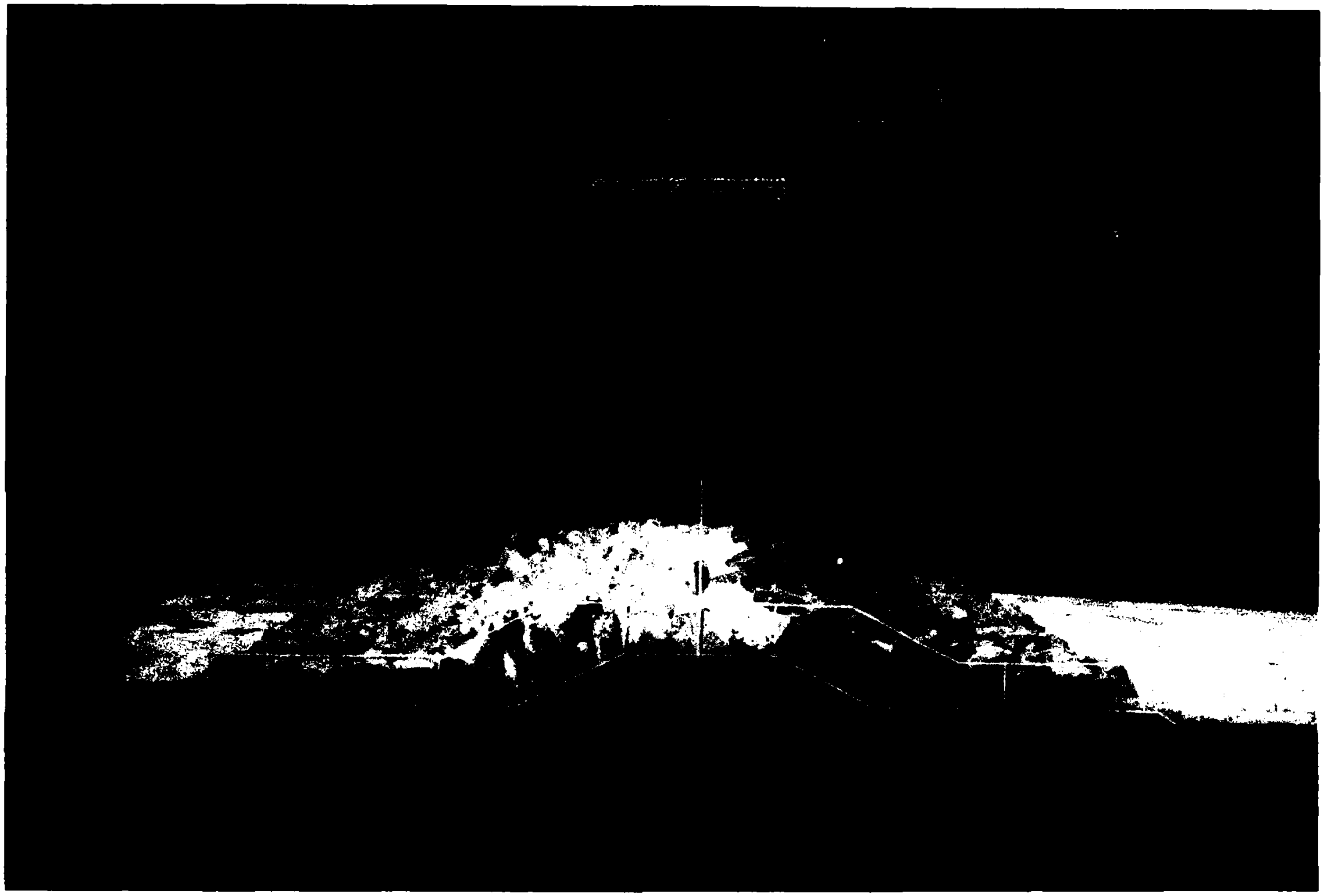

Photo 238. End view of Plan 13 after testing at swl's of +8, +6, and +4 ft NGVD; maximum wave heights = 16.0, 14.0, and 12.4 ft, respectively

Photo 239. Repeat test of Plan 13; sea-side view before wave attack

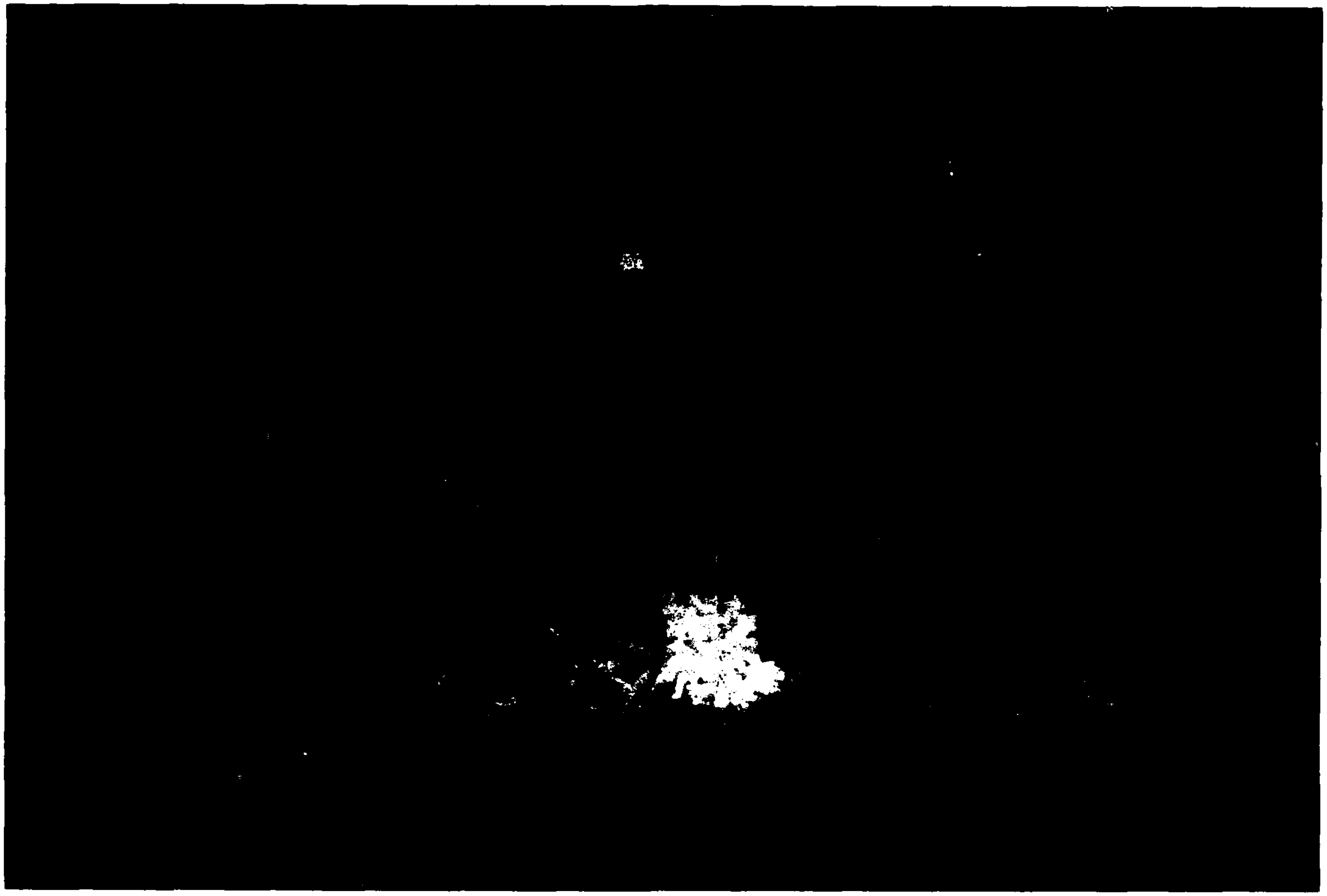

Photo 240. Repeat test of Plan 13; end view before wave attack

Photo 241. Repeat test of Plan 13; channel-side view before wave attack

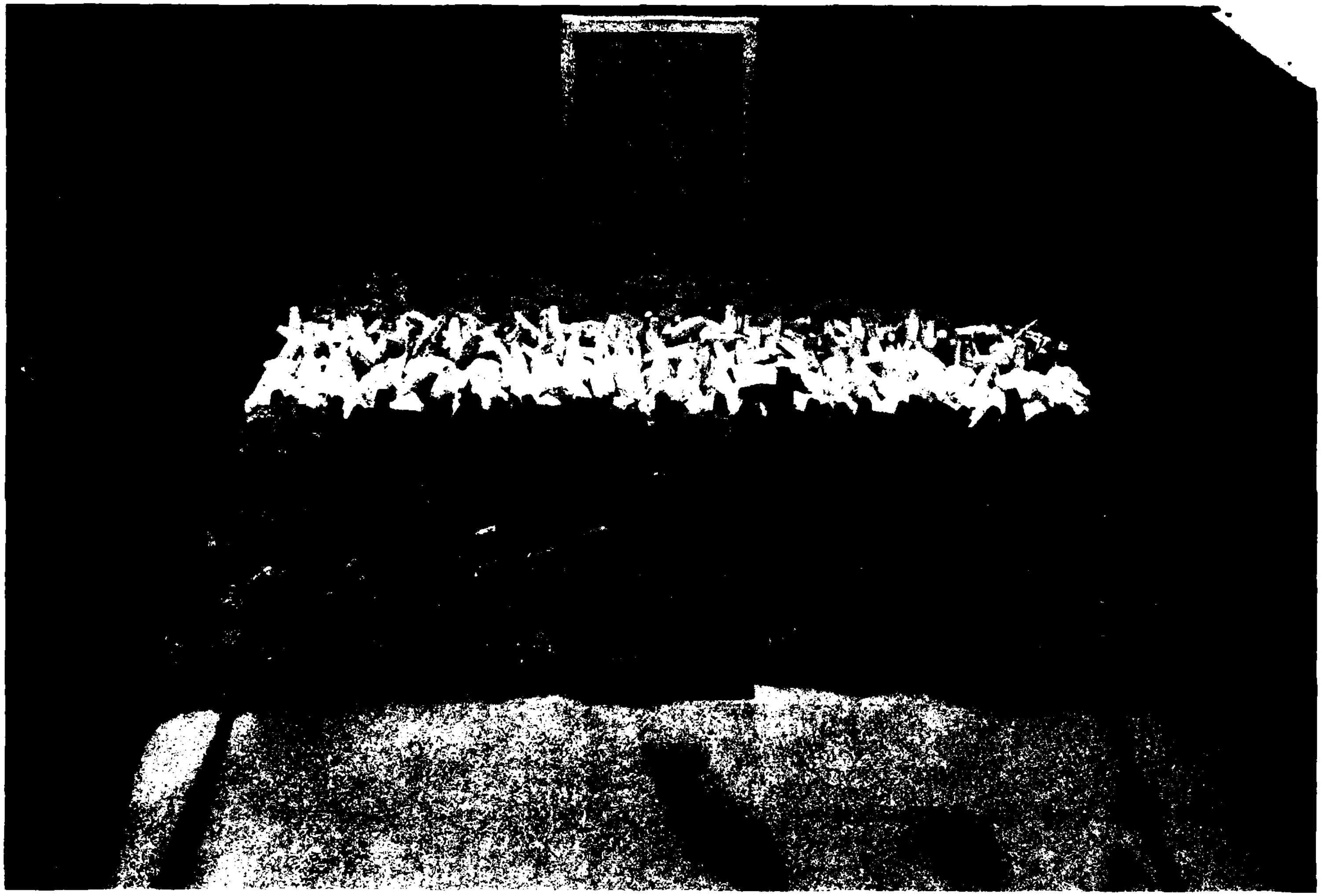

Photo 242. Repeat test of Plan 13; sea-side view after testing at swl's of +4 and +6 ft NGVD; maximum wave heights = 12.4 and 14.0 ft, respectively

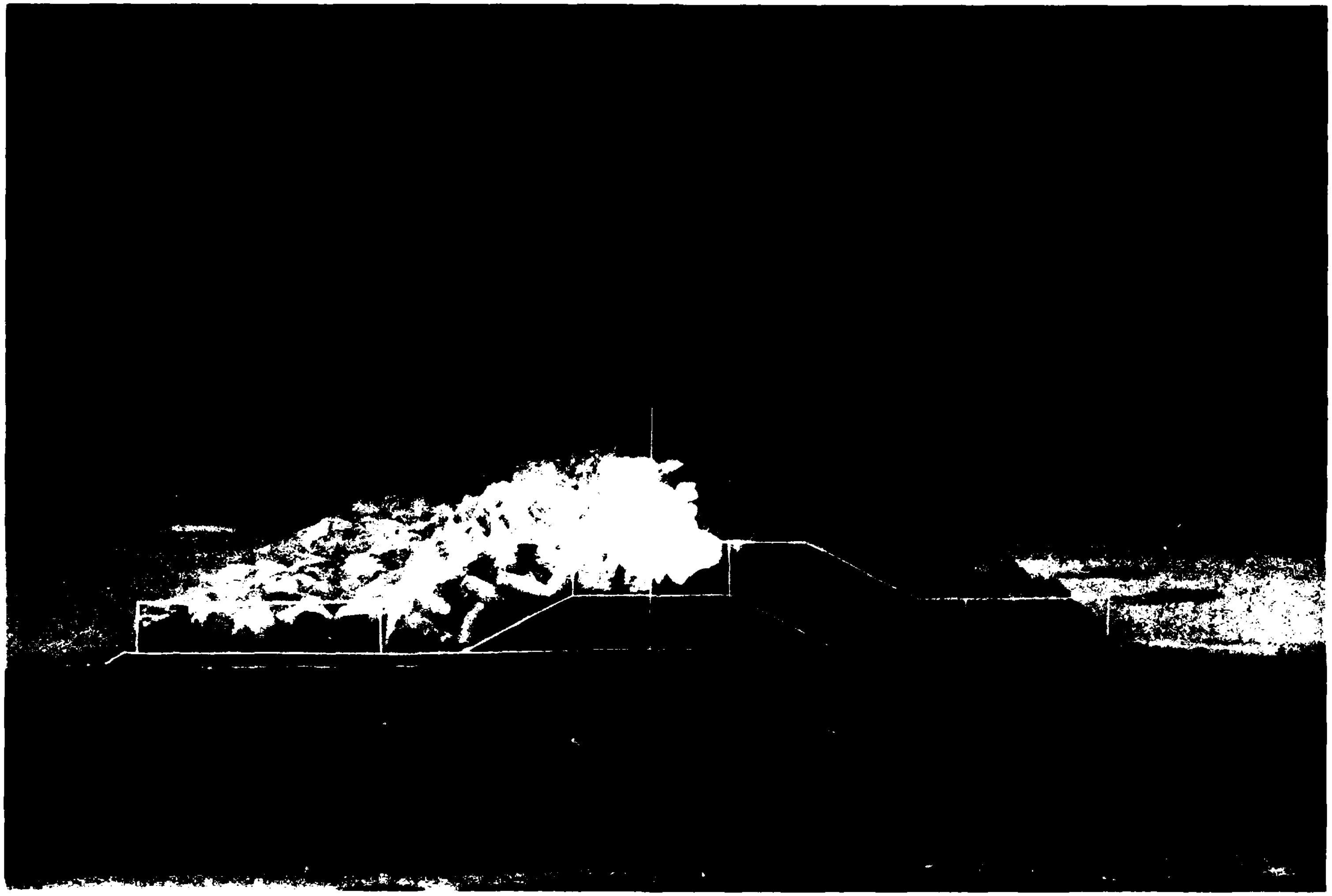

Photo 243. Repeat test of Plan 13; end view after testing at swl's of +4 and +6 ft NGVD; maximum wave heights = 12.4 and 14.0 ft, respectively

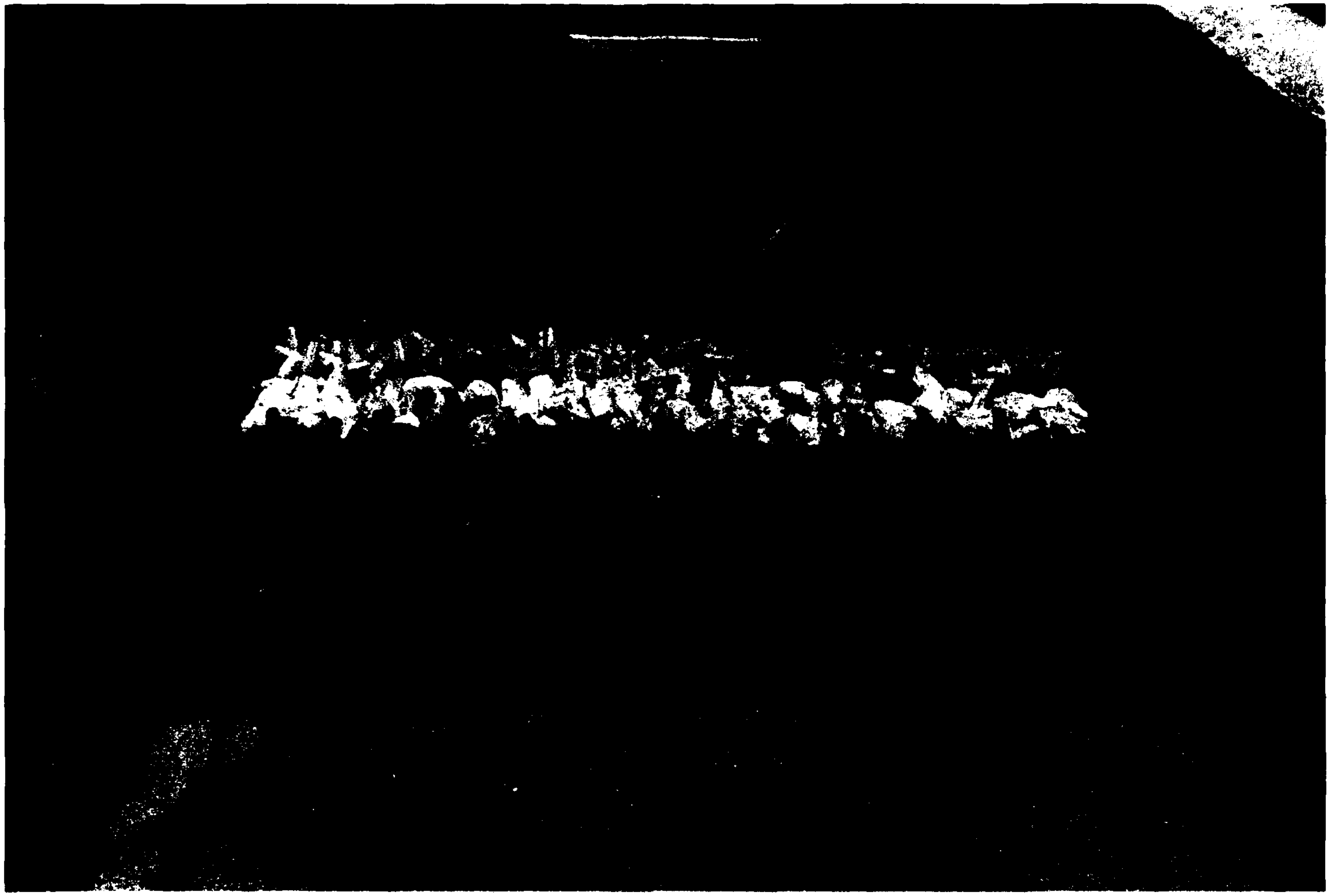

Photo 244. Repeat test of Plan 13; sea-side view after testing at swl's of +4, +6, and +8 ft NGVD; maximum wave heights = 12.4, 14.0, and 16.0 ft, respectively

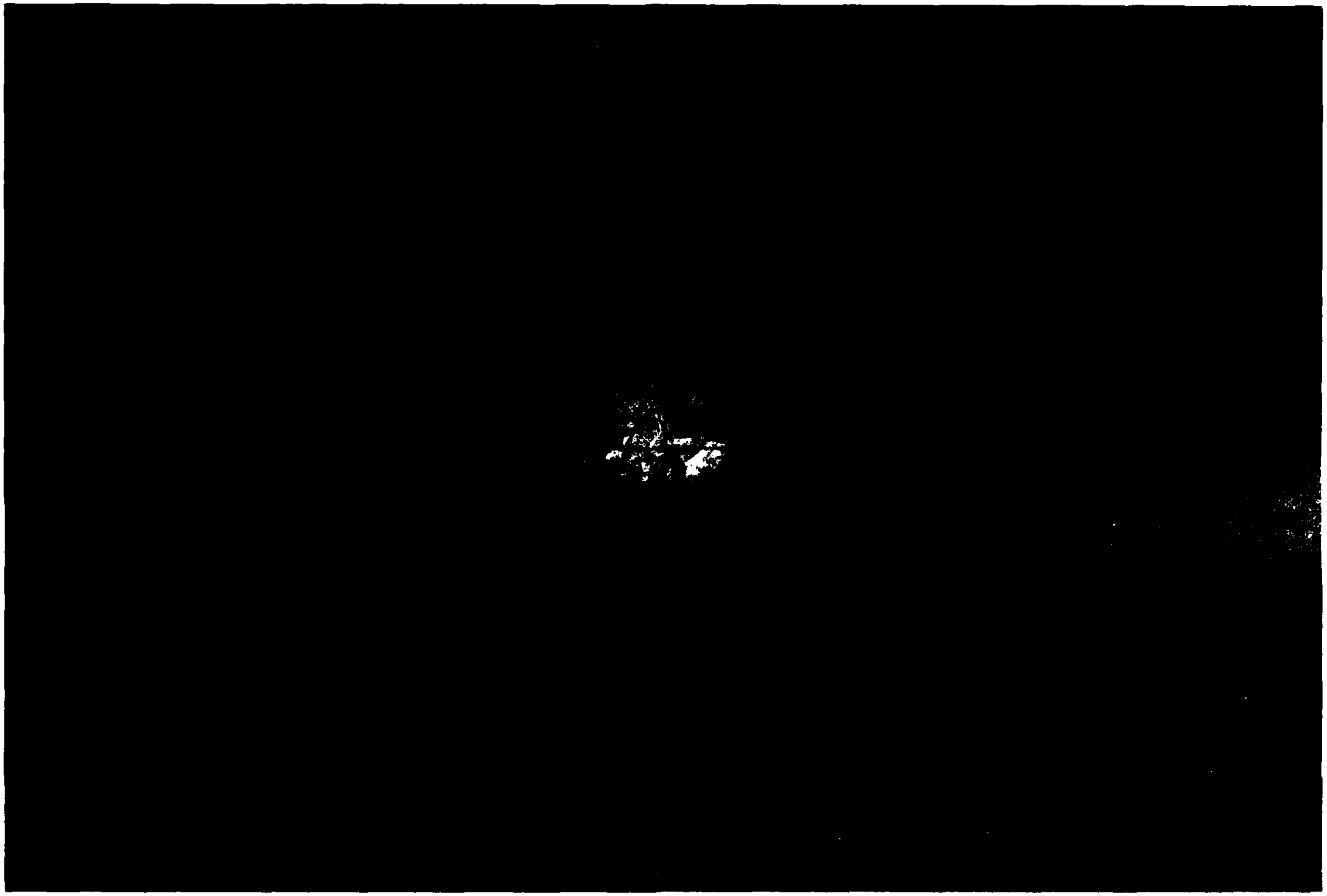

Photo 245. Repeat test of Plan 13; end view after testing at swl's of +4, +6, and +8 ft NGVD; maximum wave heights = 12.4, 14.0, and 16.0 ft, respectively

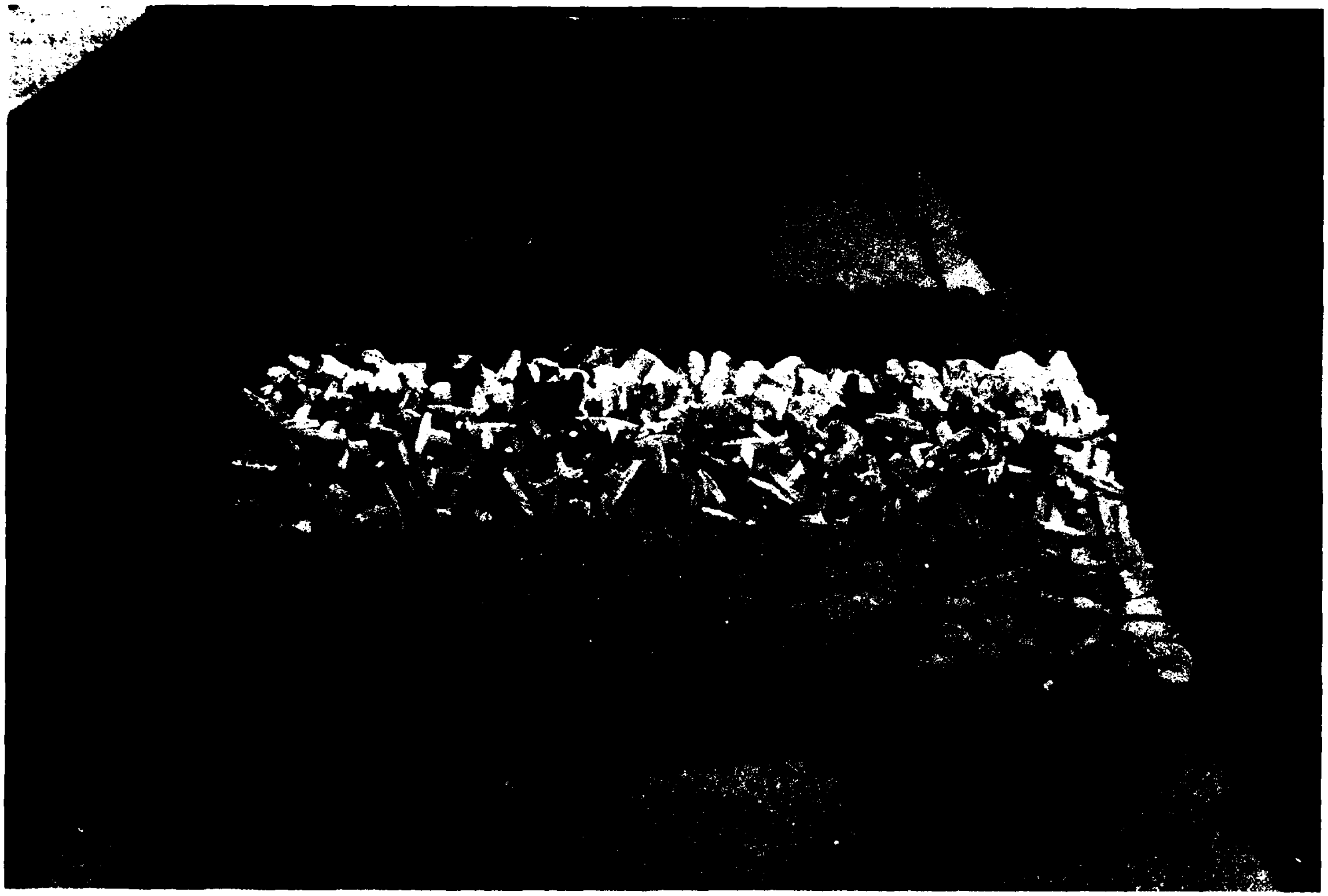

Photo 246. Repeat test of Plan 13; channel-side view after testing at swl's of +4, +6, and +8 ft NGVD; maximum wave heights = 12.4, 14.0, and 16.0 ft, respectively

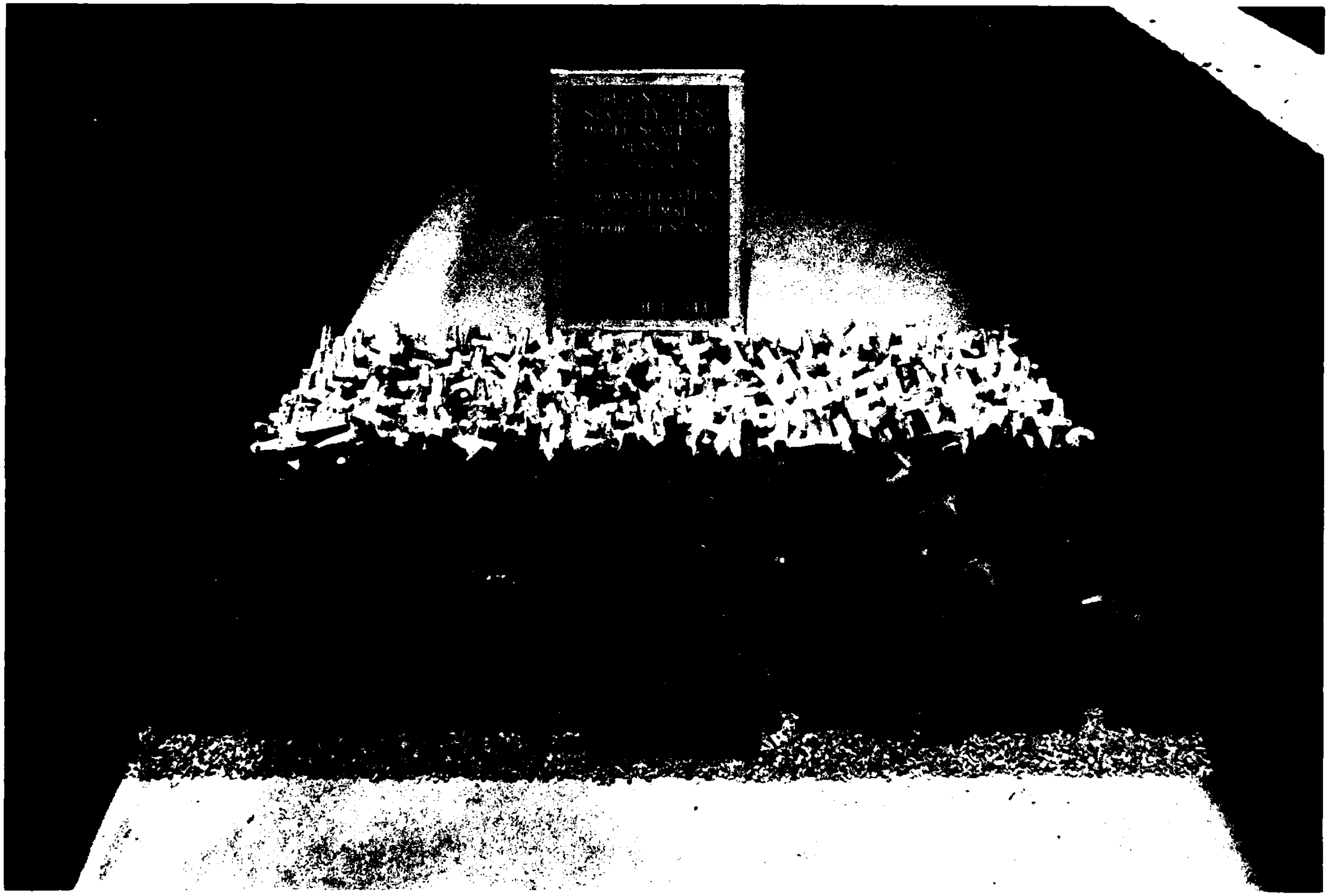

Photo 247. Sea-side view of Plan 14 before wave attack

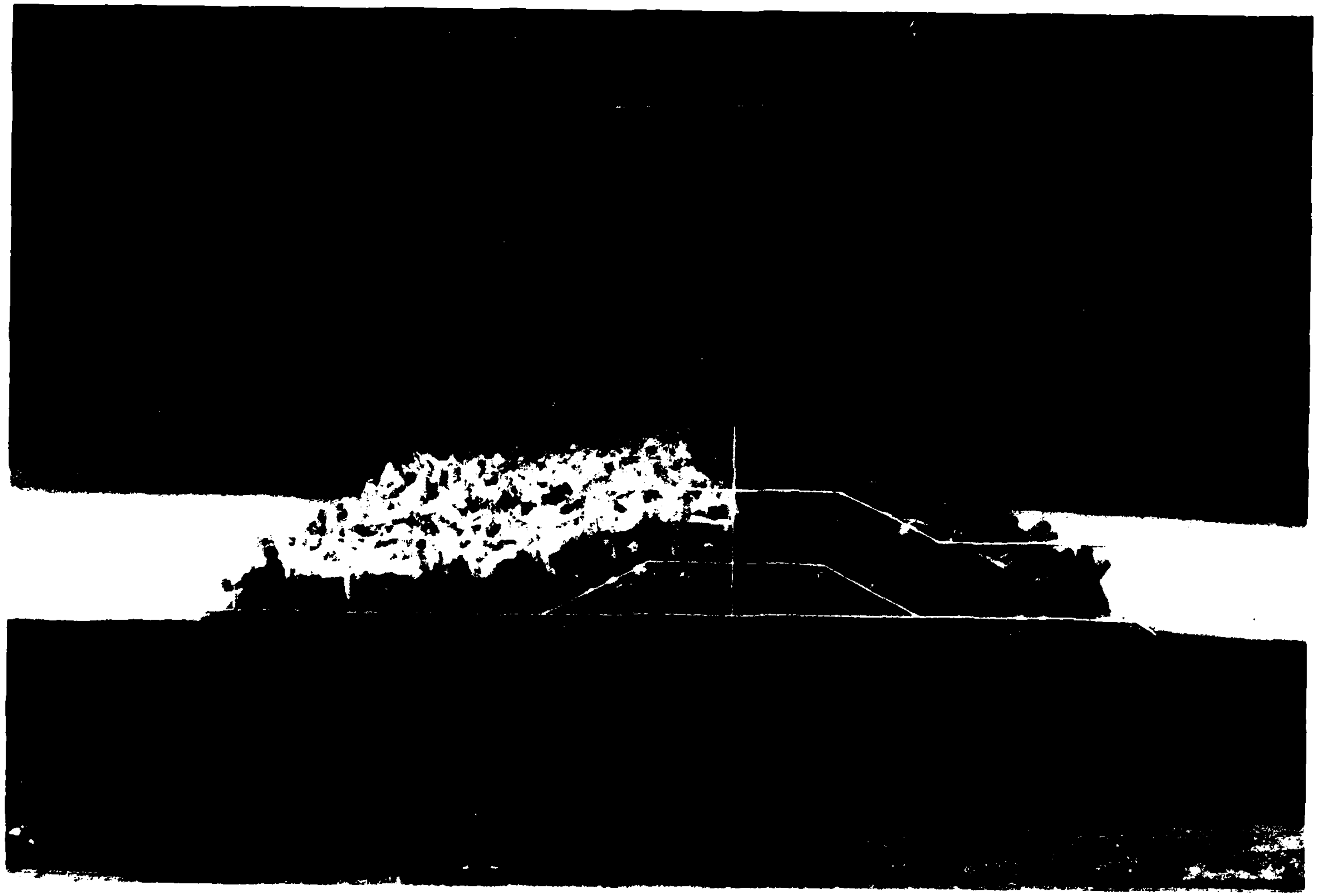

Photo 248. End view of Plan 14 before wave attack

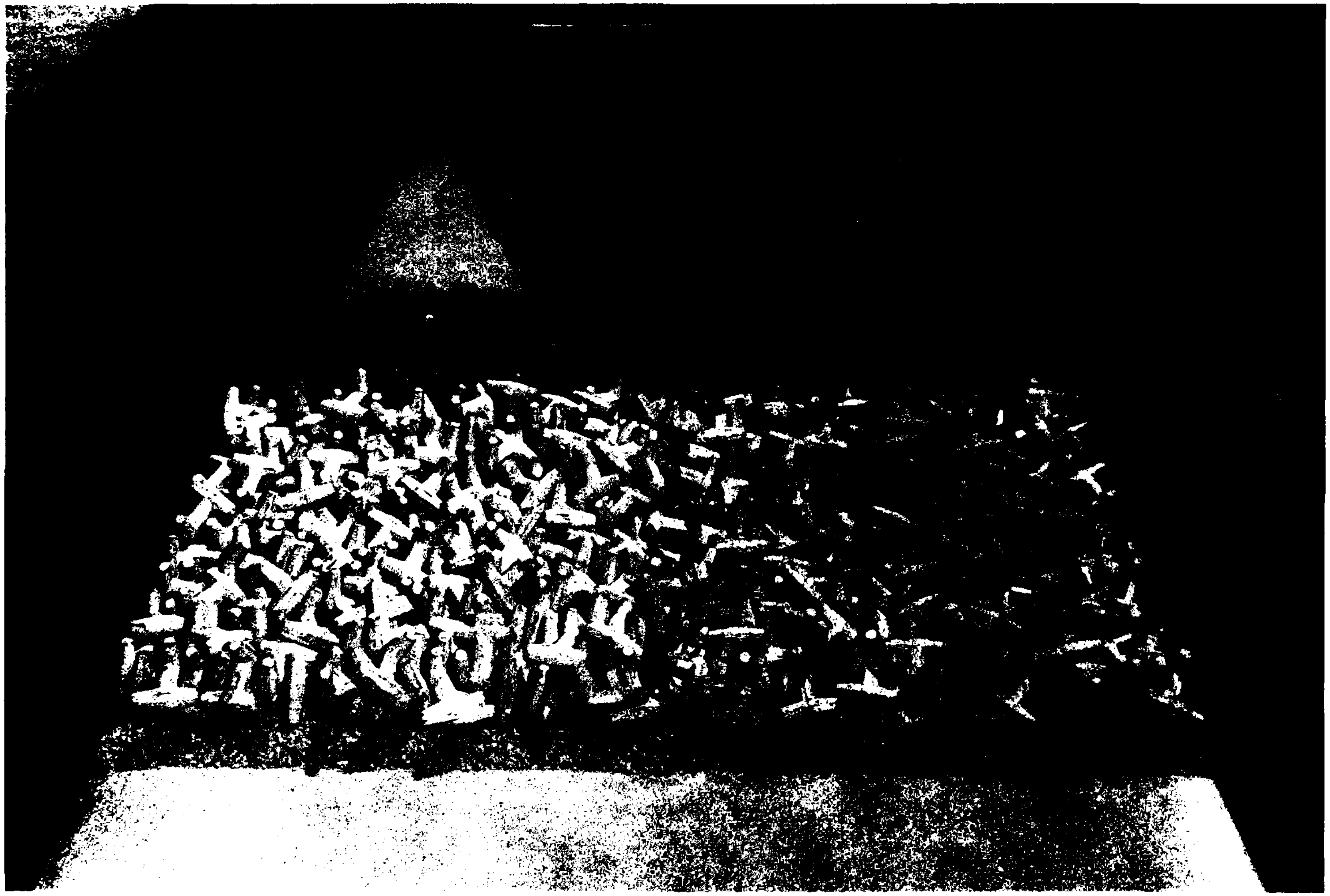

Photo 249. Channel-side view of Plan 14 before wave attack

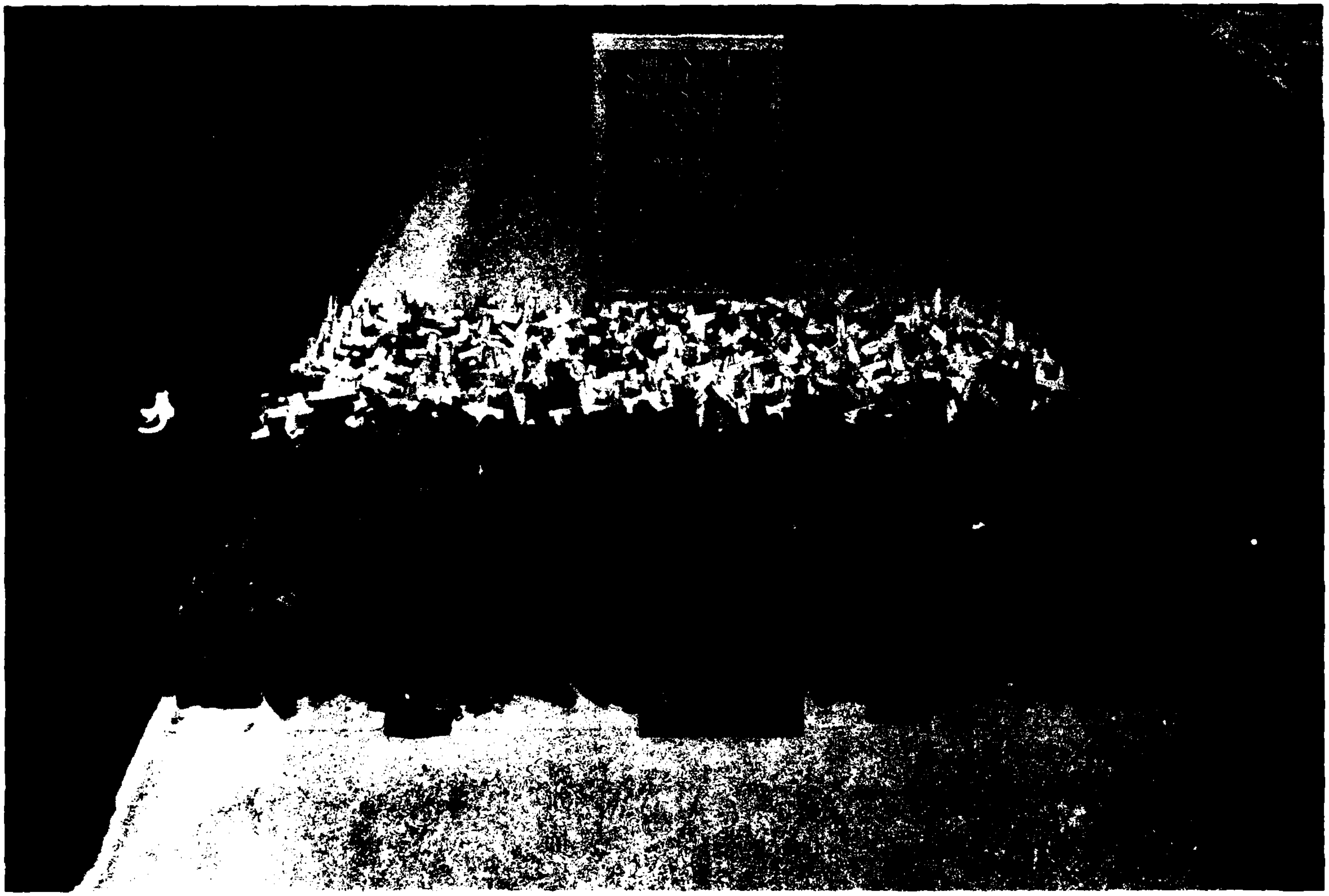

Photo 250. Sea-side view of Plan 14 after testing at an swl of +8 ft NGVD; maximum wave height = 16.0 ft

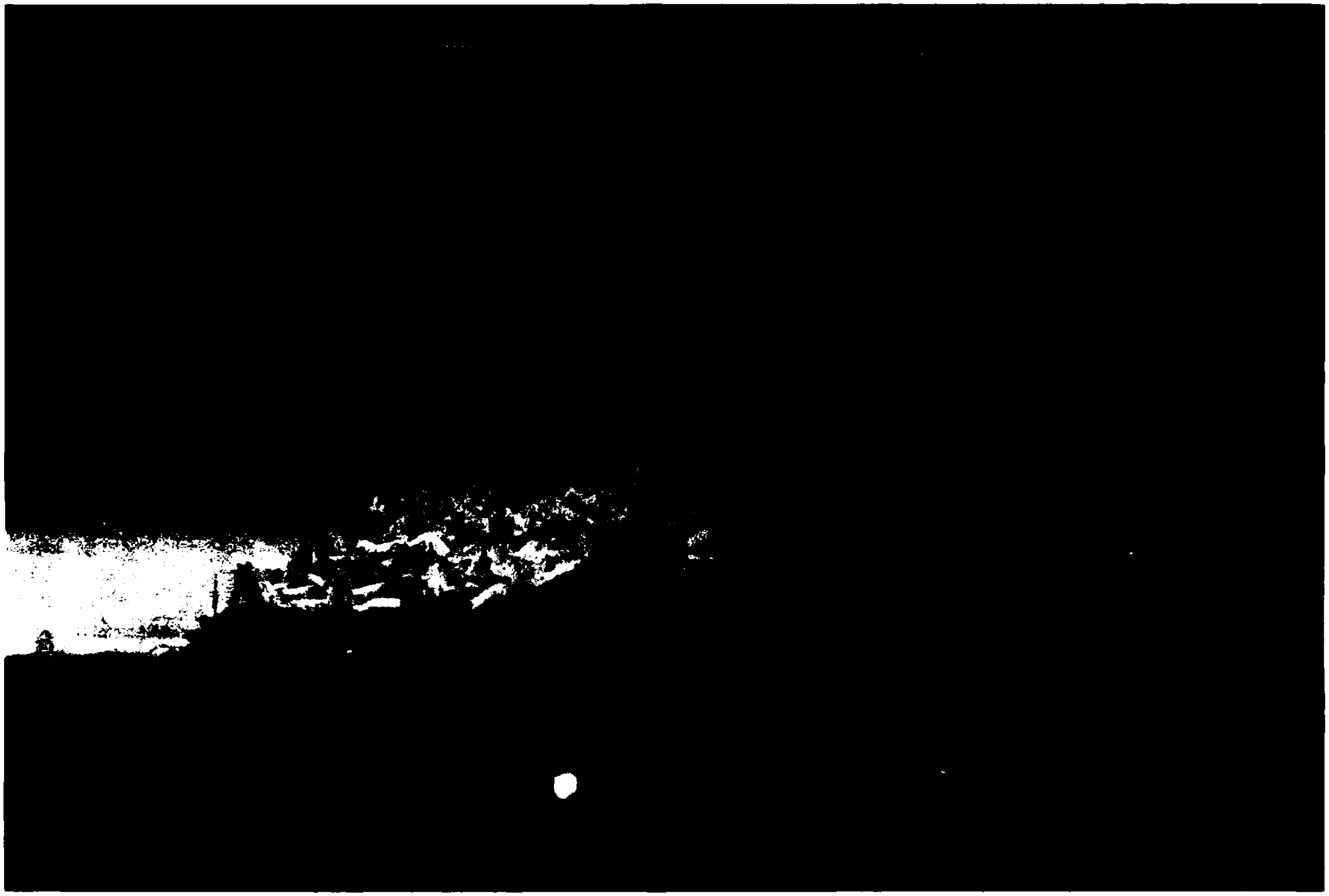

Photo 251. End view of Plan 14 after testing at an swl of +8 ft NGVD; maximum wave height = 16.0 ft

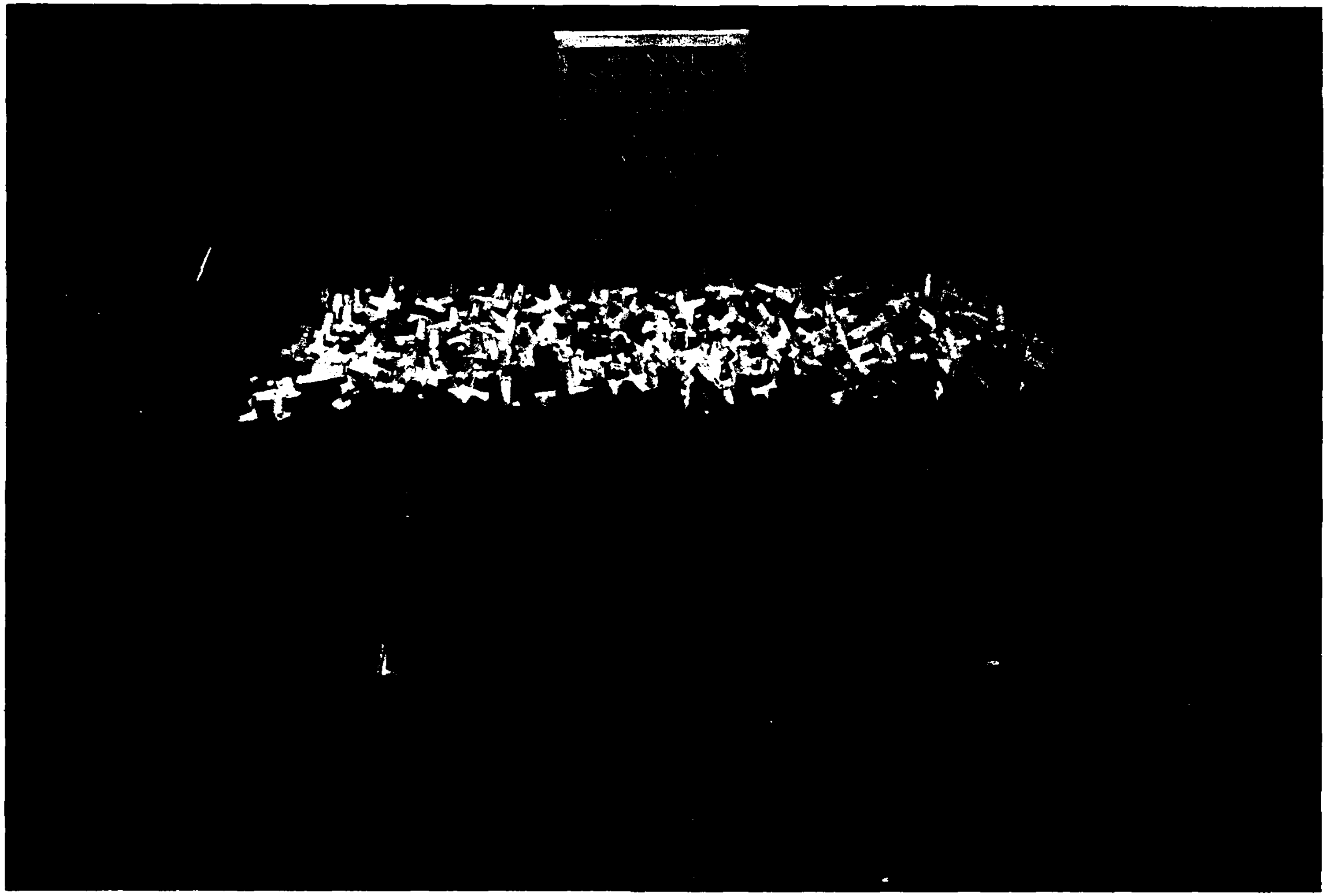

Photo 252. Sea-side view of Plan 14 after testing at swl's of +8, +6, and +4 ft NGVD; maximum wave heights = 16.0, 14.0, and 12.4 ft, respectively

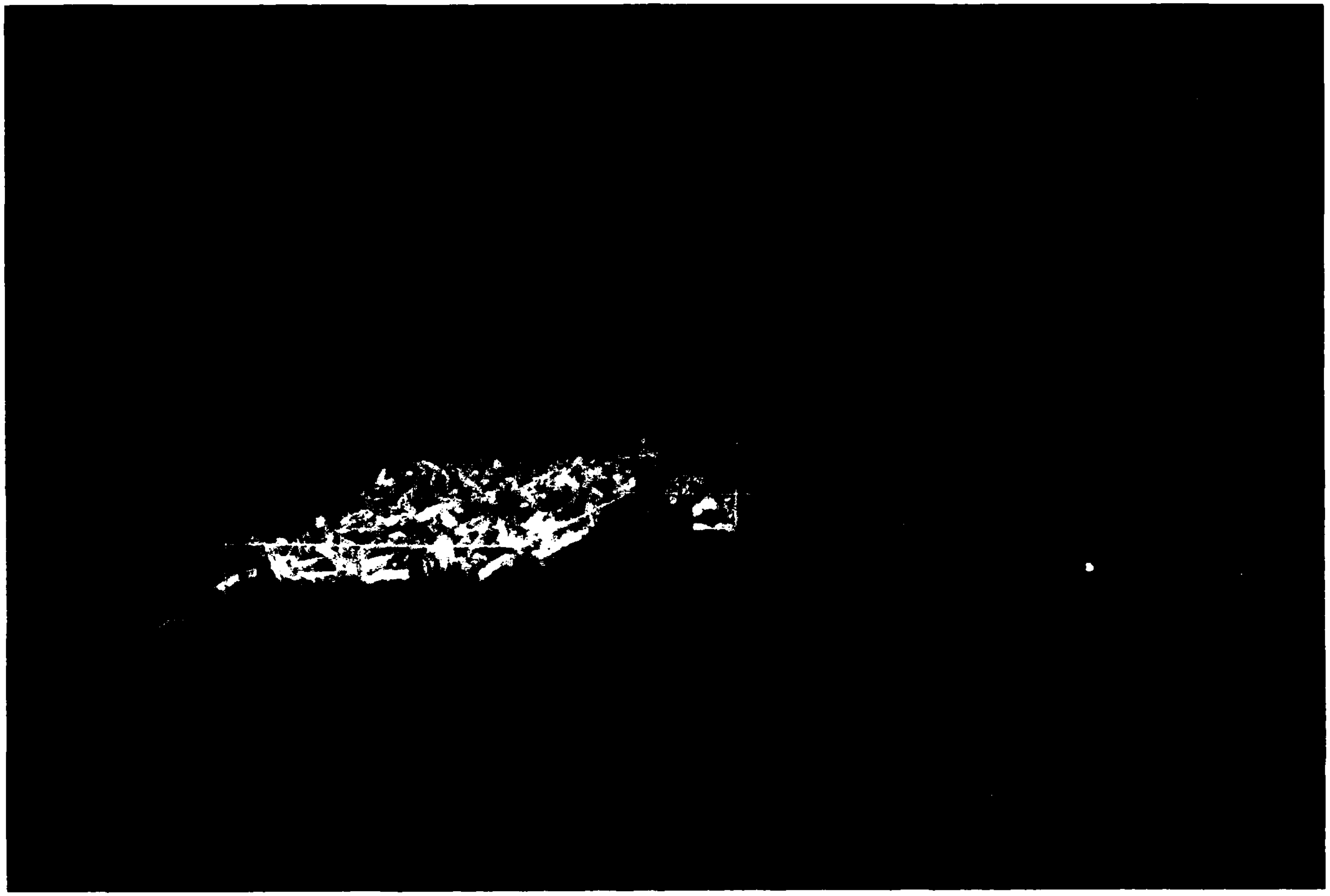

Photo 253. End view of Plan 14 after testing at swl's of +8, +6, and +4 ft NGVD; maximum wave heights = 16.0, 14.0, and 12.4 ft, respectively

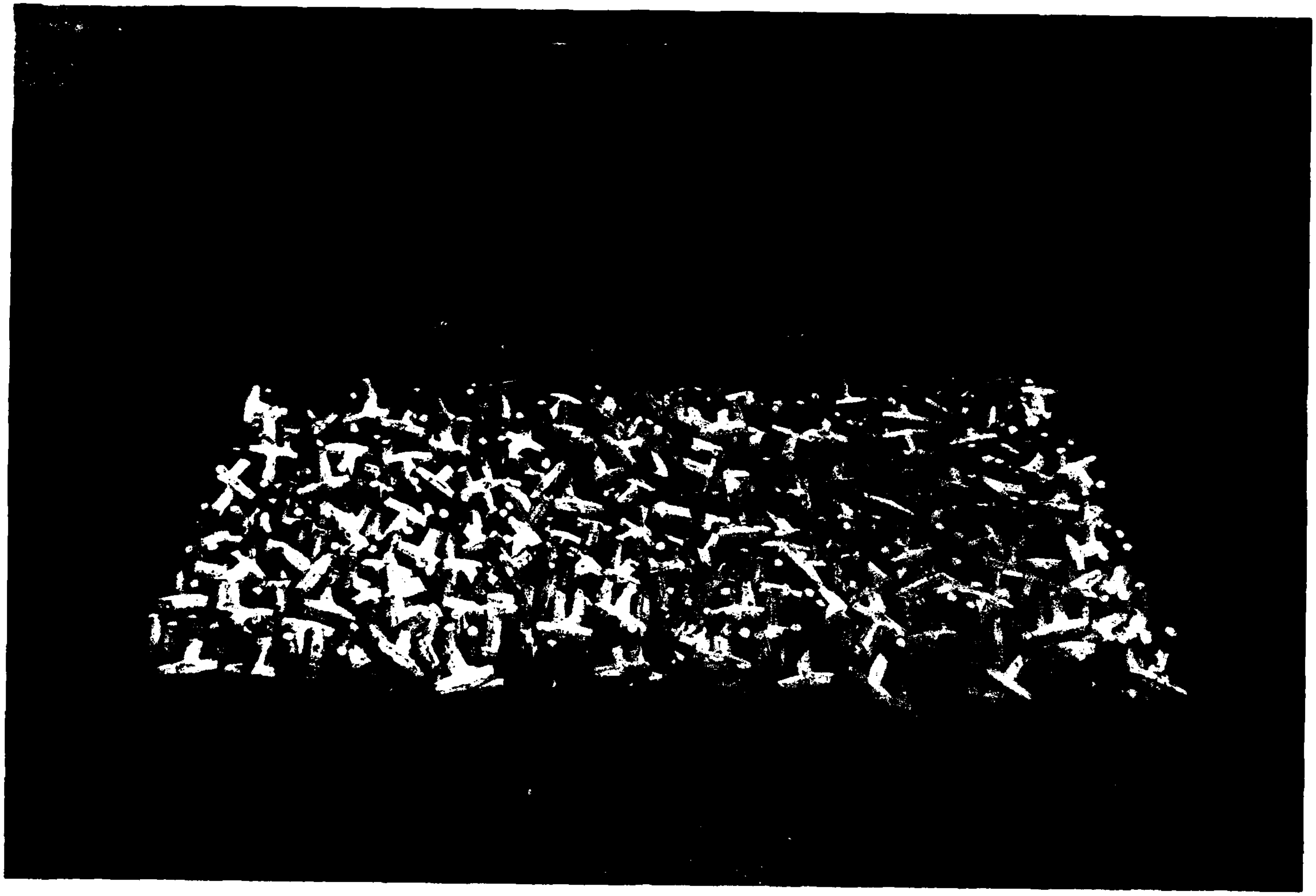

Photo 254. Channel-side view of Plan 14 after testing at swl's of +8, +6, and +4 ft NGVD; maximum wave heights = 16.0, 14.0, and 12.4 ft, respectively

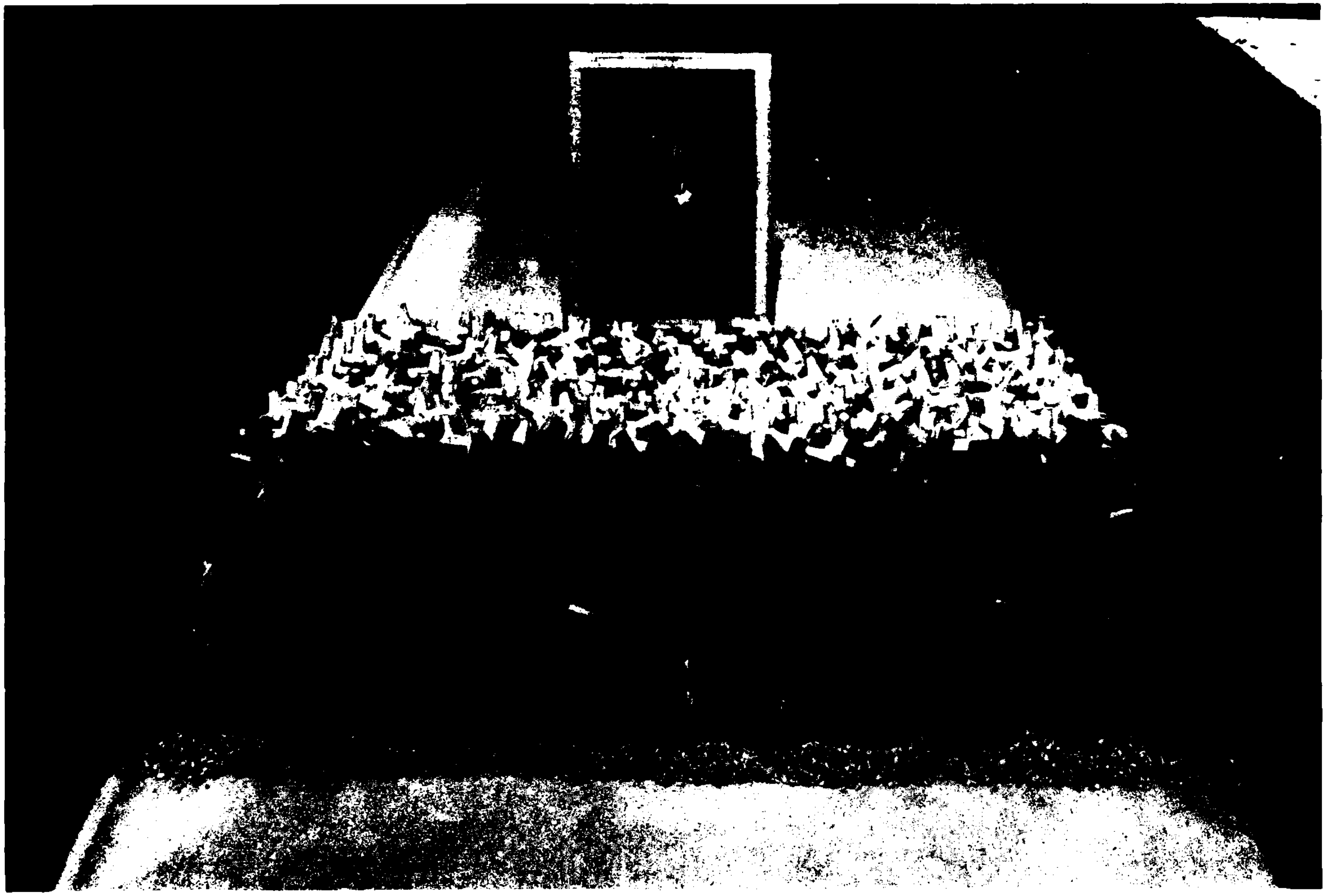

Photo 255. Repeat test of Plan 14; sea-side view before wave attack

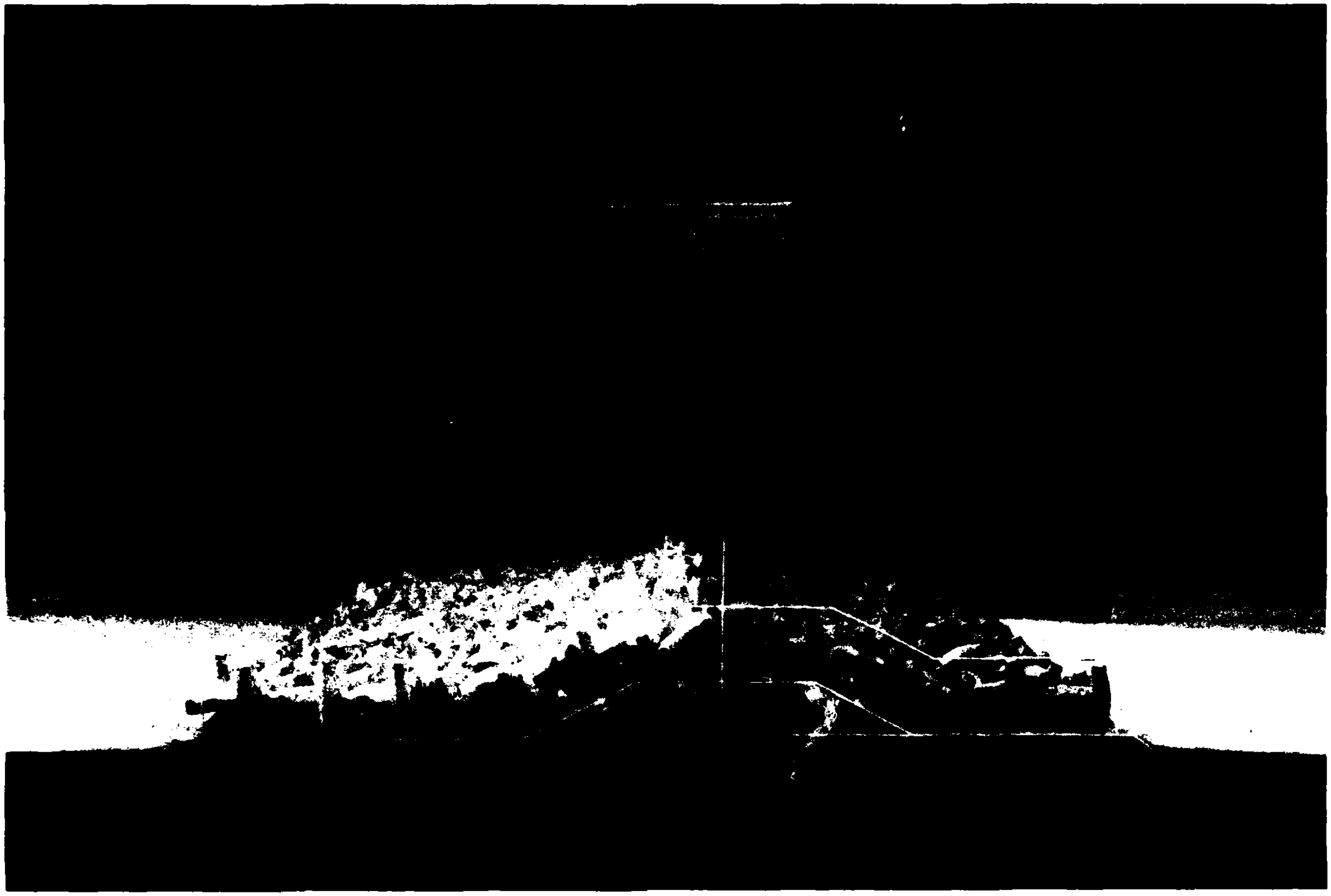

Photo 256. Repeat test of Plan 14; end view before wave attack

Photo 257. Repeat test of Plan 14; channel-side view before wave attack

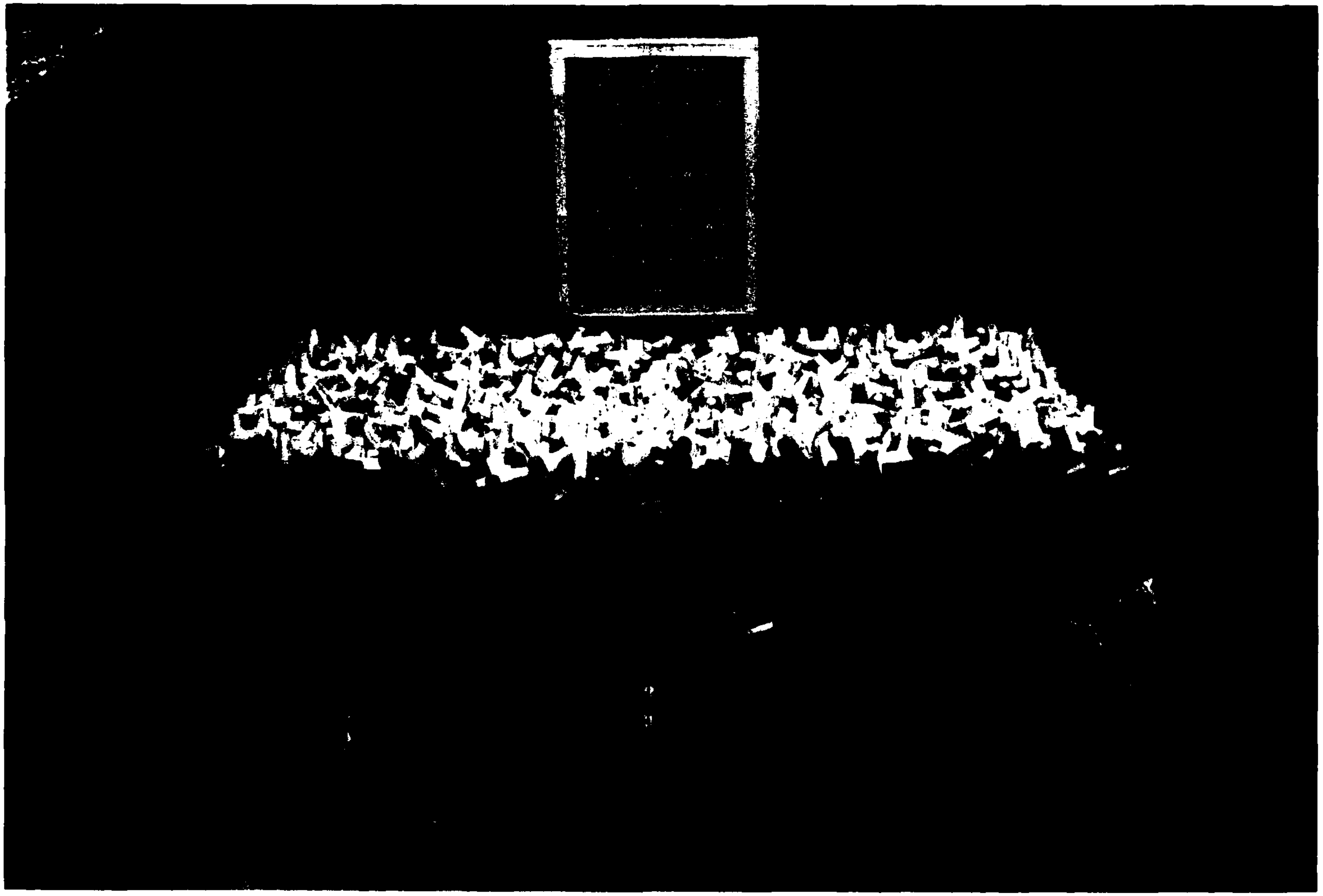

Photo 258. Repeat test of Plan 14; sea-side view after testing at swl's of +4 and +6 ft NGVD; maximum wave heights = 12.4 and 14.0 ft, respectively

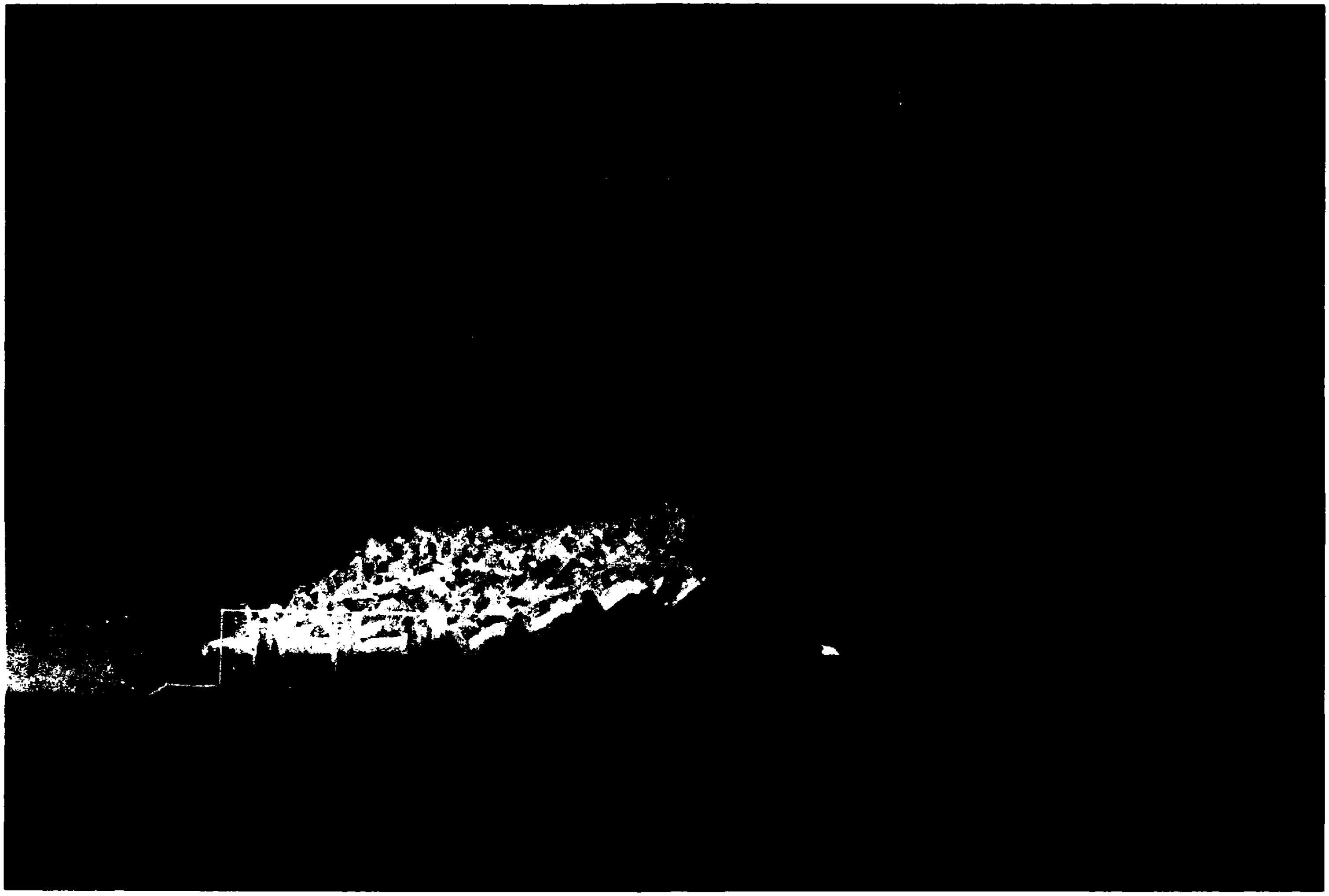

Photo 259. Repeat test of Plan 14; end view after testing at swl's of +4 and +6 ft NGVD; maximum wave heights = 12.4 and 14.0 ft, respectively

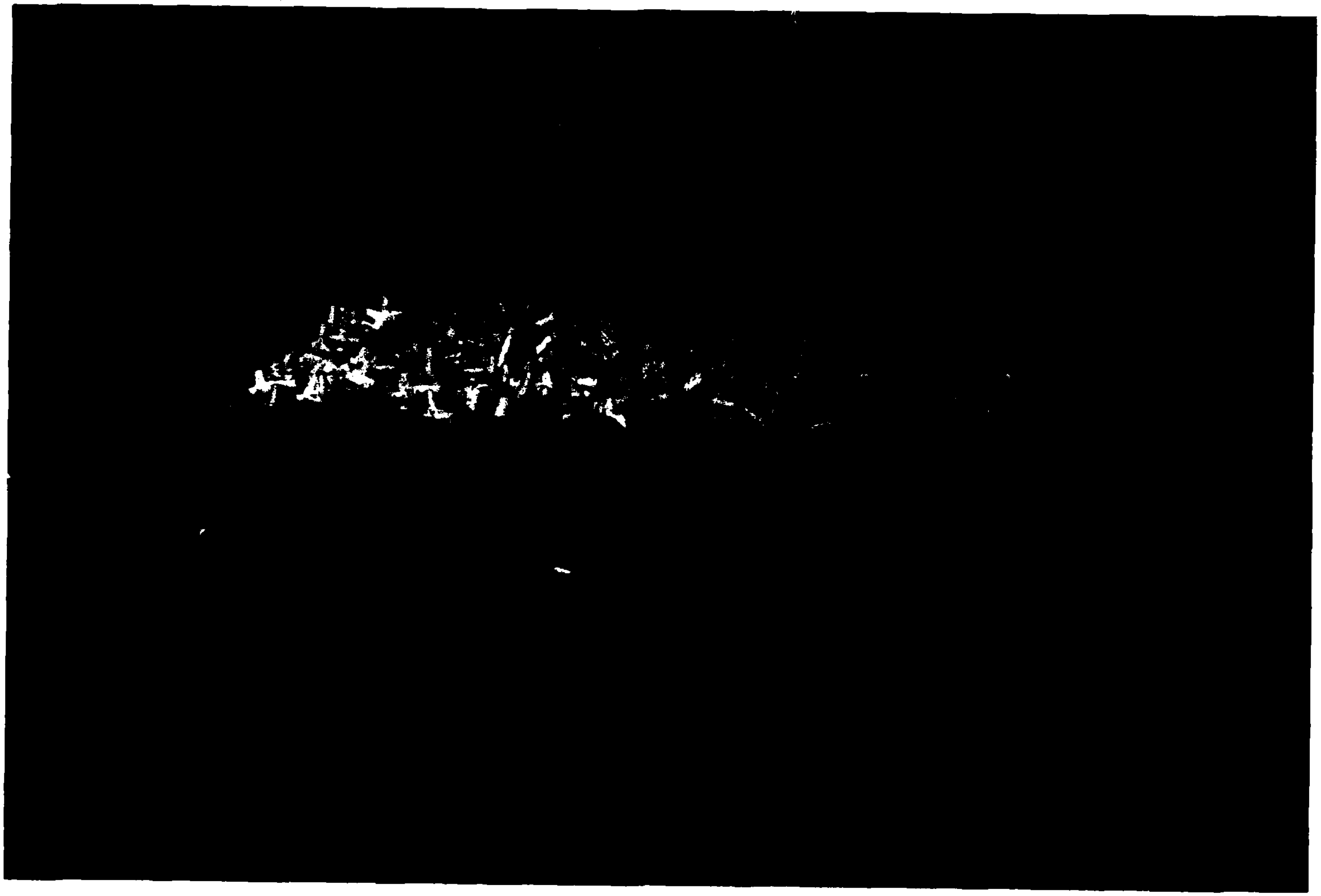

Photo 260. Repeat test of Plan 14; sea-side view after testing at swl's of +4, +6, and +8 ft NGVD; maximum wave heights = 12.4, 14.0, and 16.0 ft, respectively

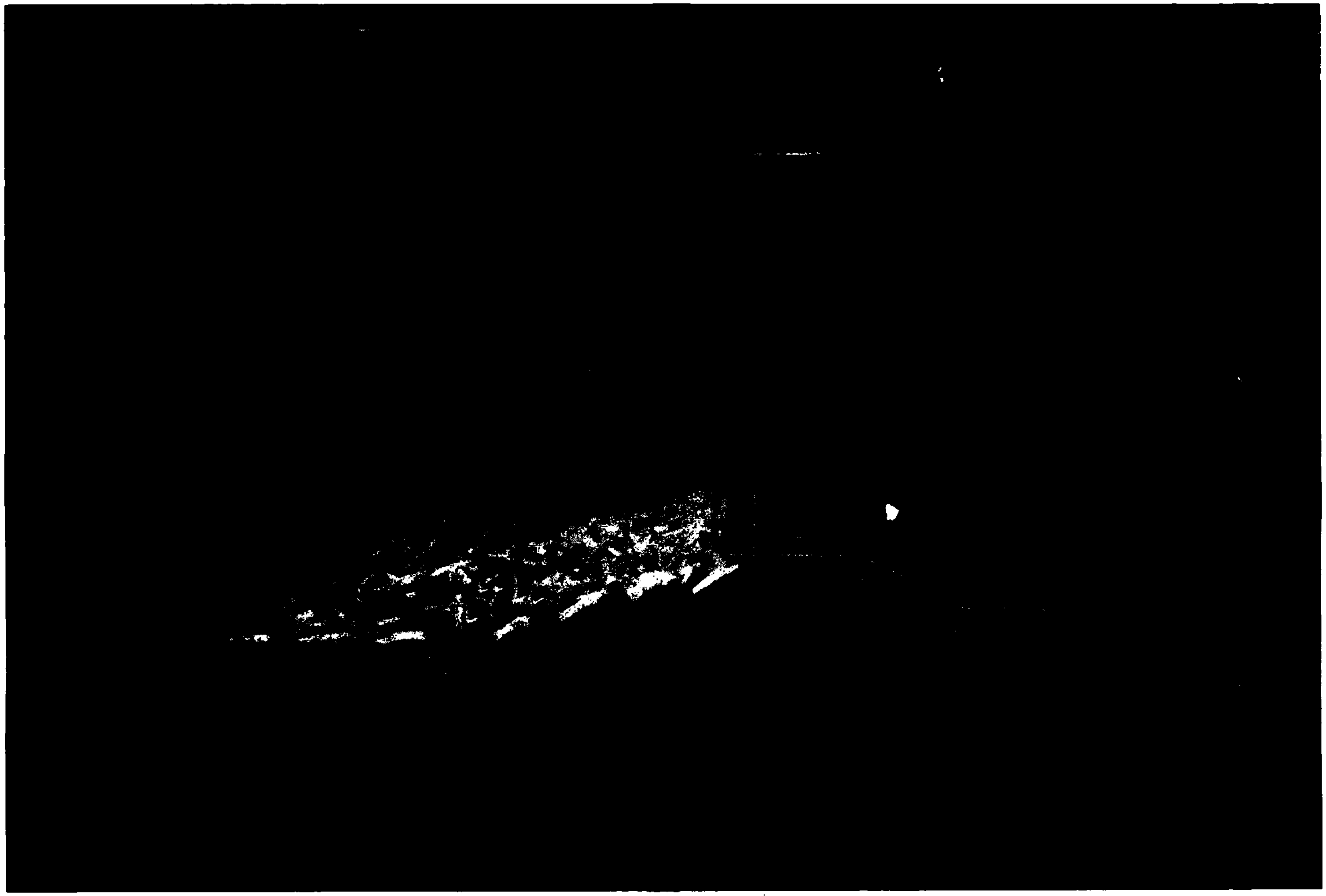

Photo 261. Repeat test of Plan 14; end view after testing at swl's of +4, +6, and +8 ft NGVD; maximum wave heights = 12.4, 14.0, and 16.0 ft, respectively

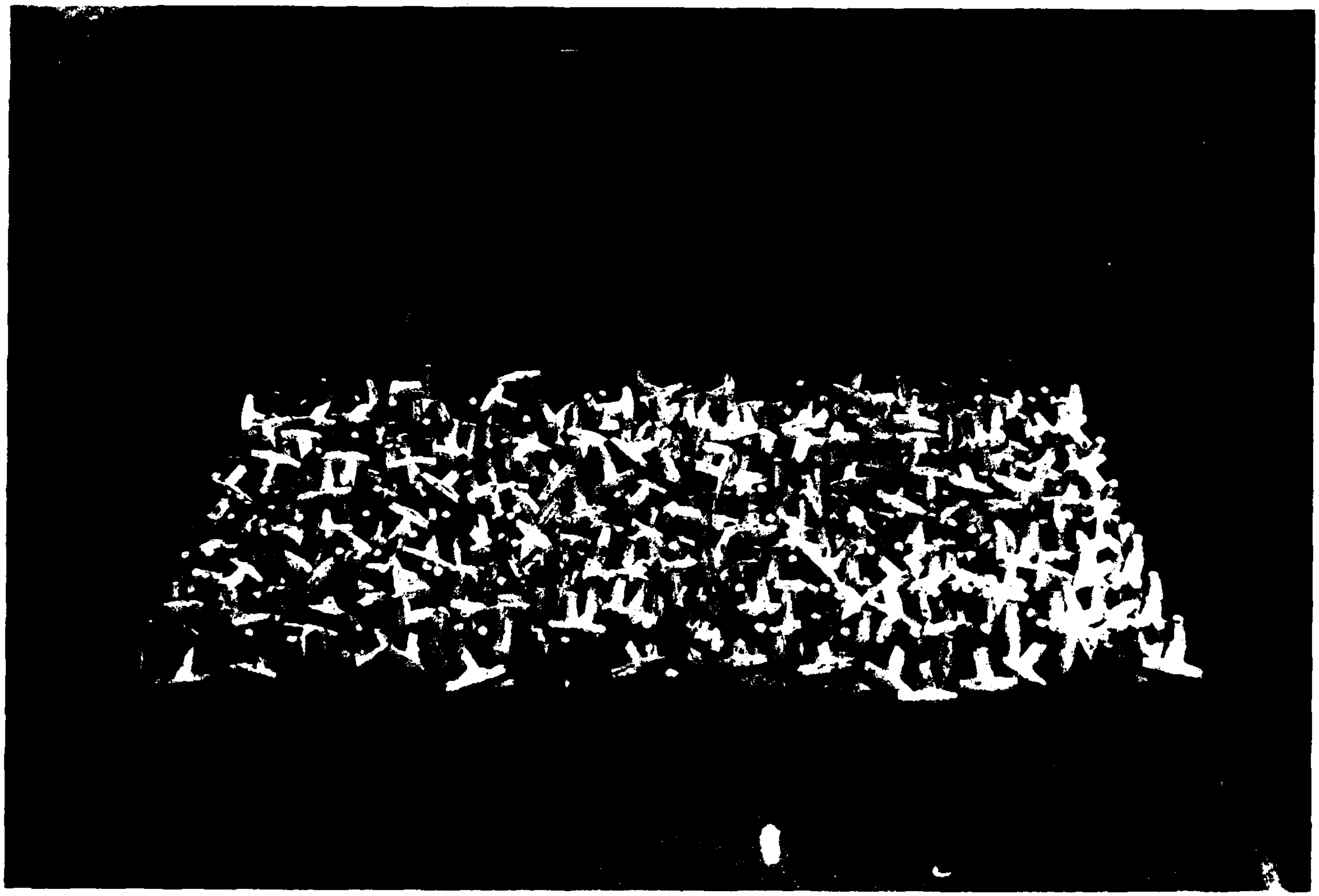

Photo 262. Repeat test of Plan 14; channel-side view after testing at swl's of +4, +6, and +8 ft NGVD; maximum wave heights = 12.4, 14.0, and 16.0 ft, respectively

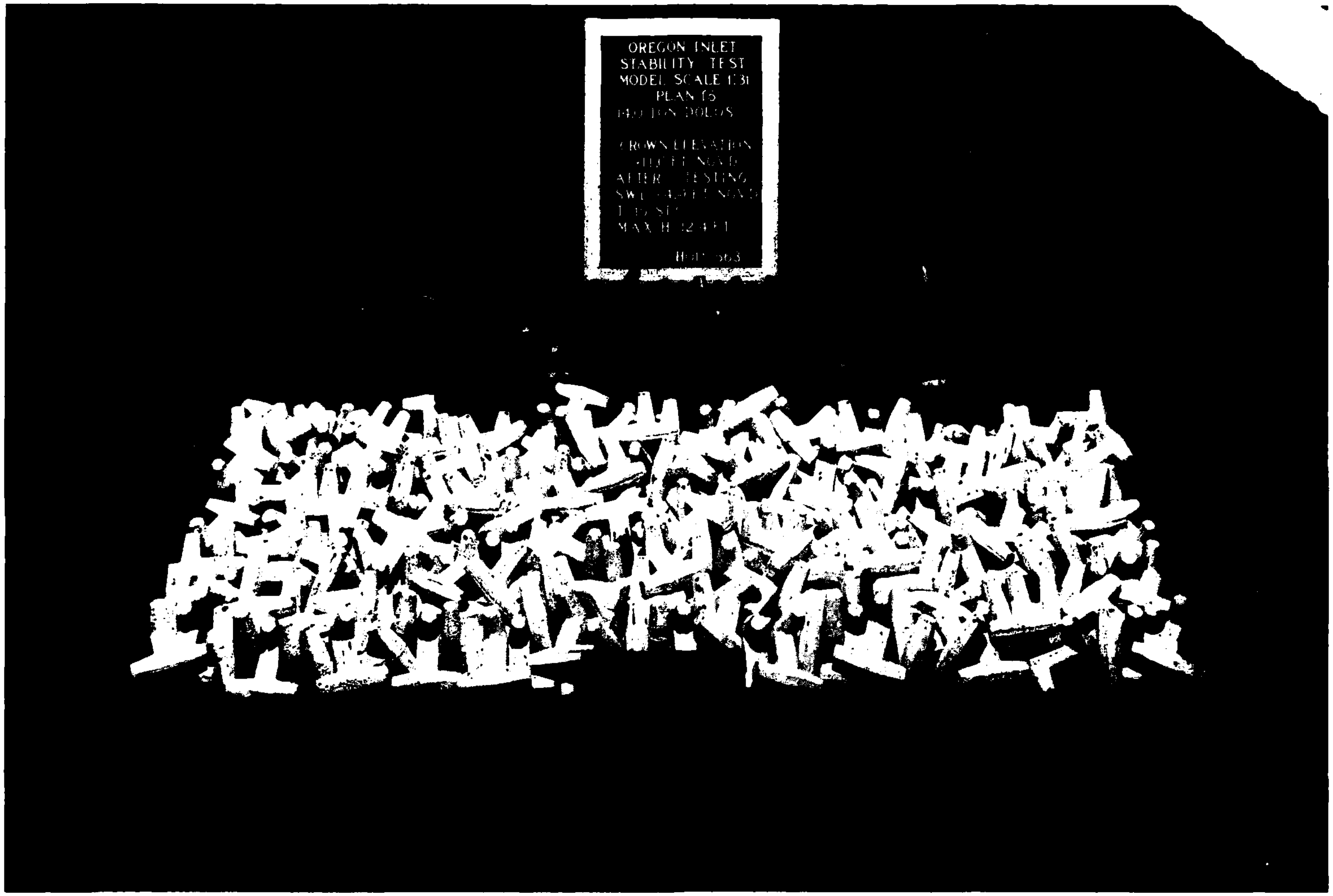

Photo 263. Sea-side view of Plan 15 after testing at swl's of +8, +6, and +4 ft NGVD; maximum wave heights = 16.0, 14.0, and 12.4 ft, respectively

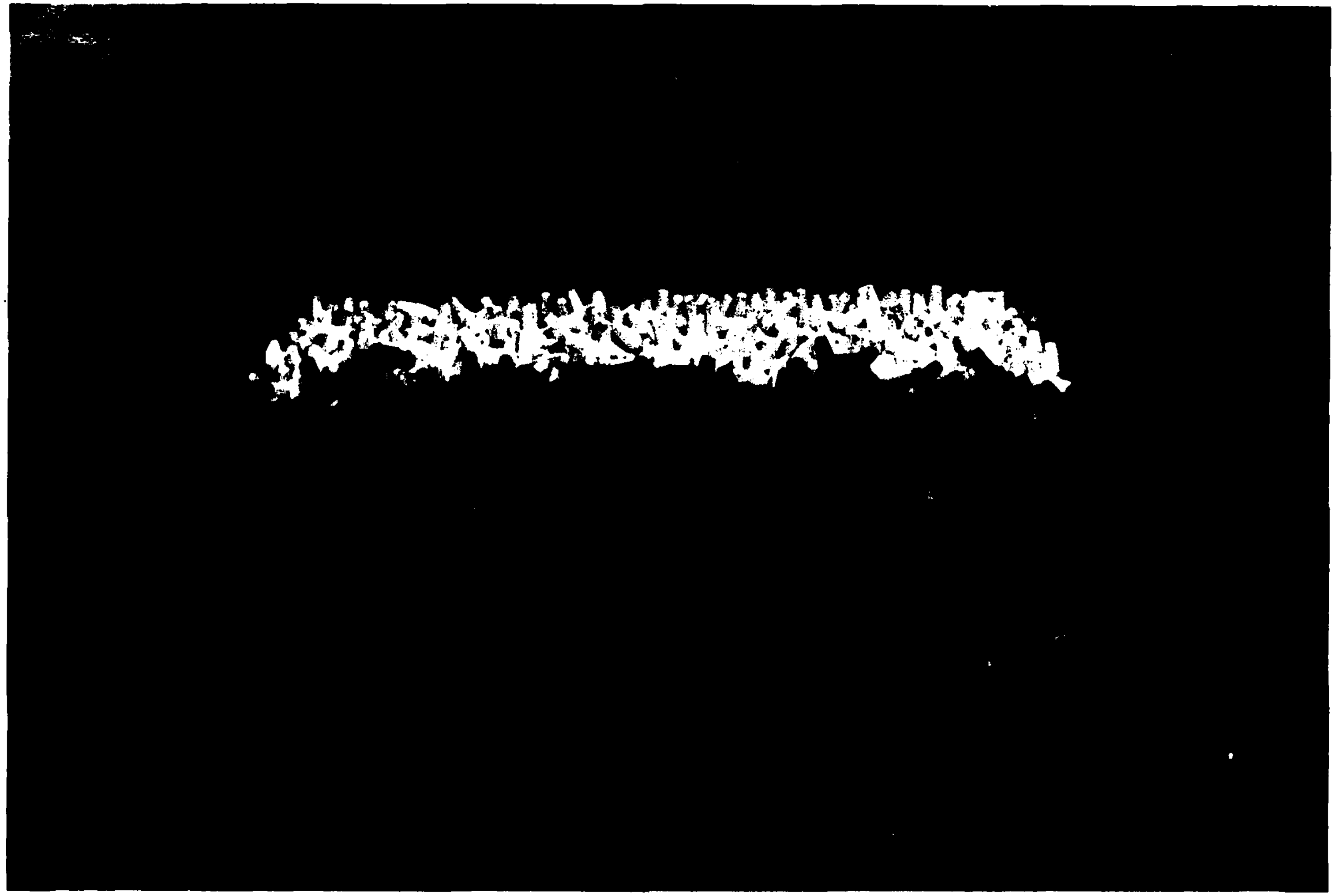

Photo 264. Channel-side view of Plan 15 after testing at swl's of +8, +6, and +4 ft NGVD; maximum wave heights = 16.0, 14.0, and 12.4 ft, respectively

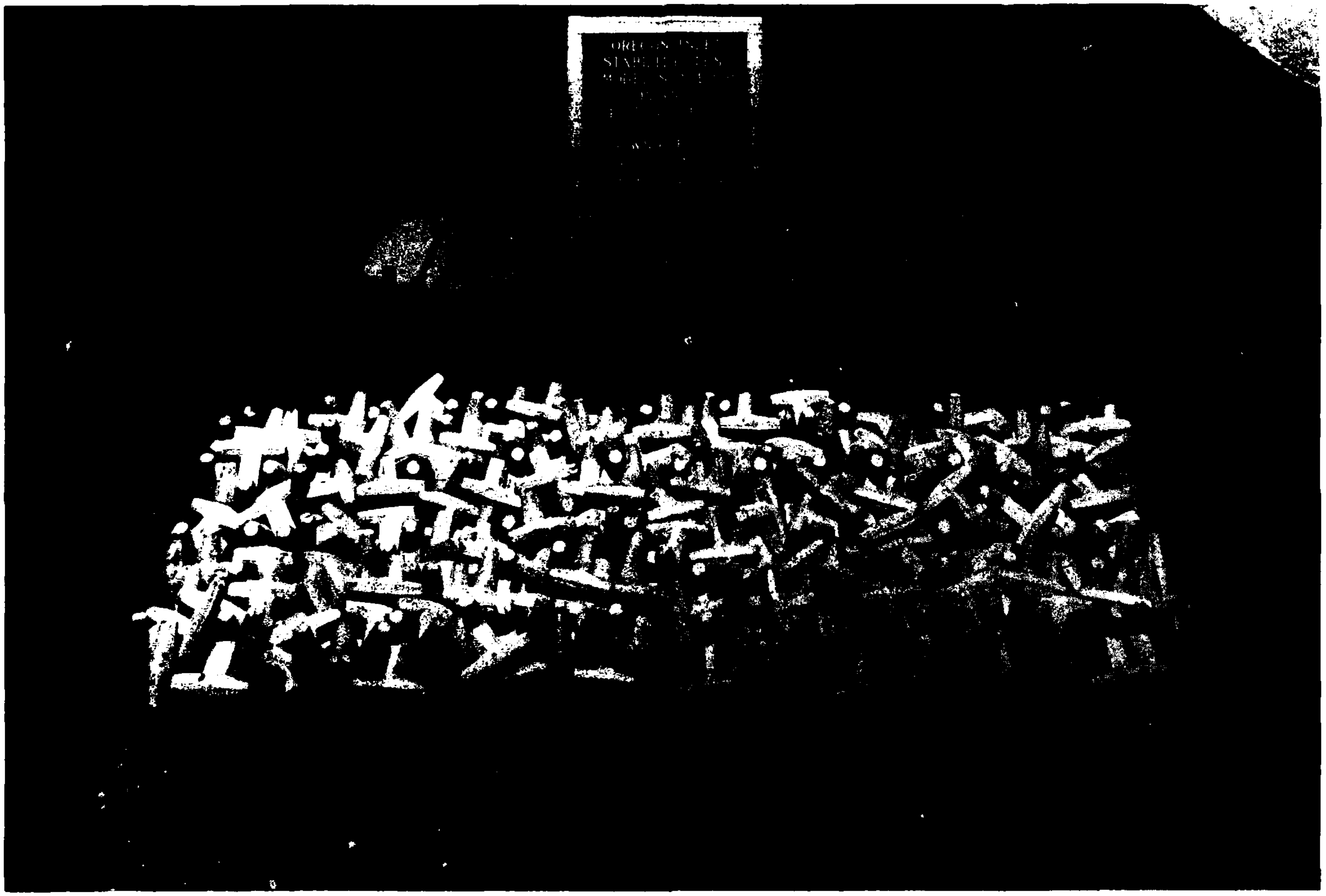

Photo 265. Repeat test of Plan 15; sea-side view before wave attack

Photo 266. Repeat test of Plan 15; end view before wave attack

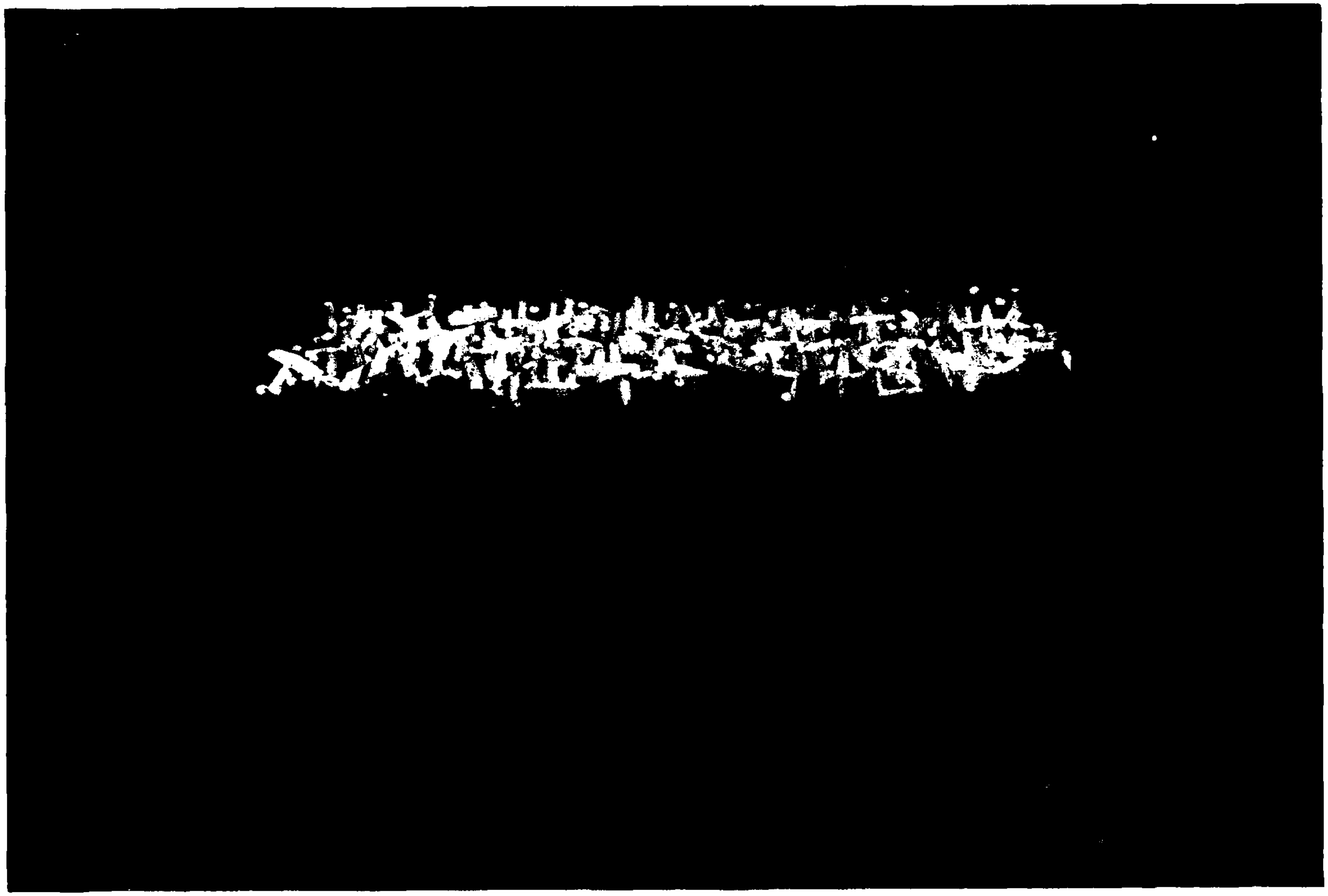

Photo 267. Repeat test of Plan 15; channel-side view before wave attack

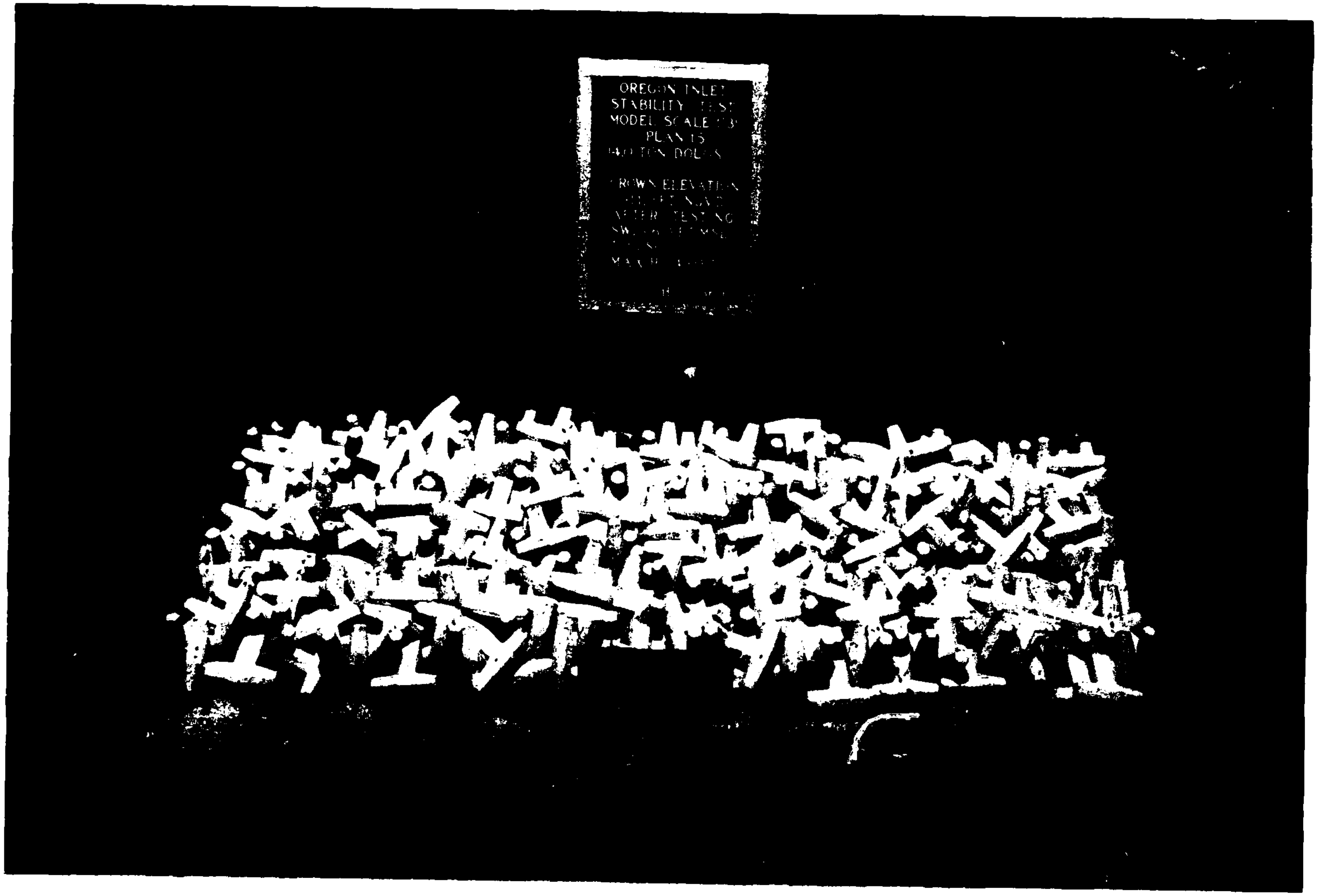

Photo 268. Repeat test of Plan 15; sea-side view after testing at swl's of +4 and +6 ft NGVD; maximum wave heights = 12.4 and 14.0 ft, respectively

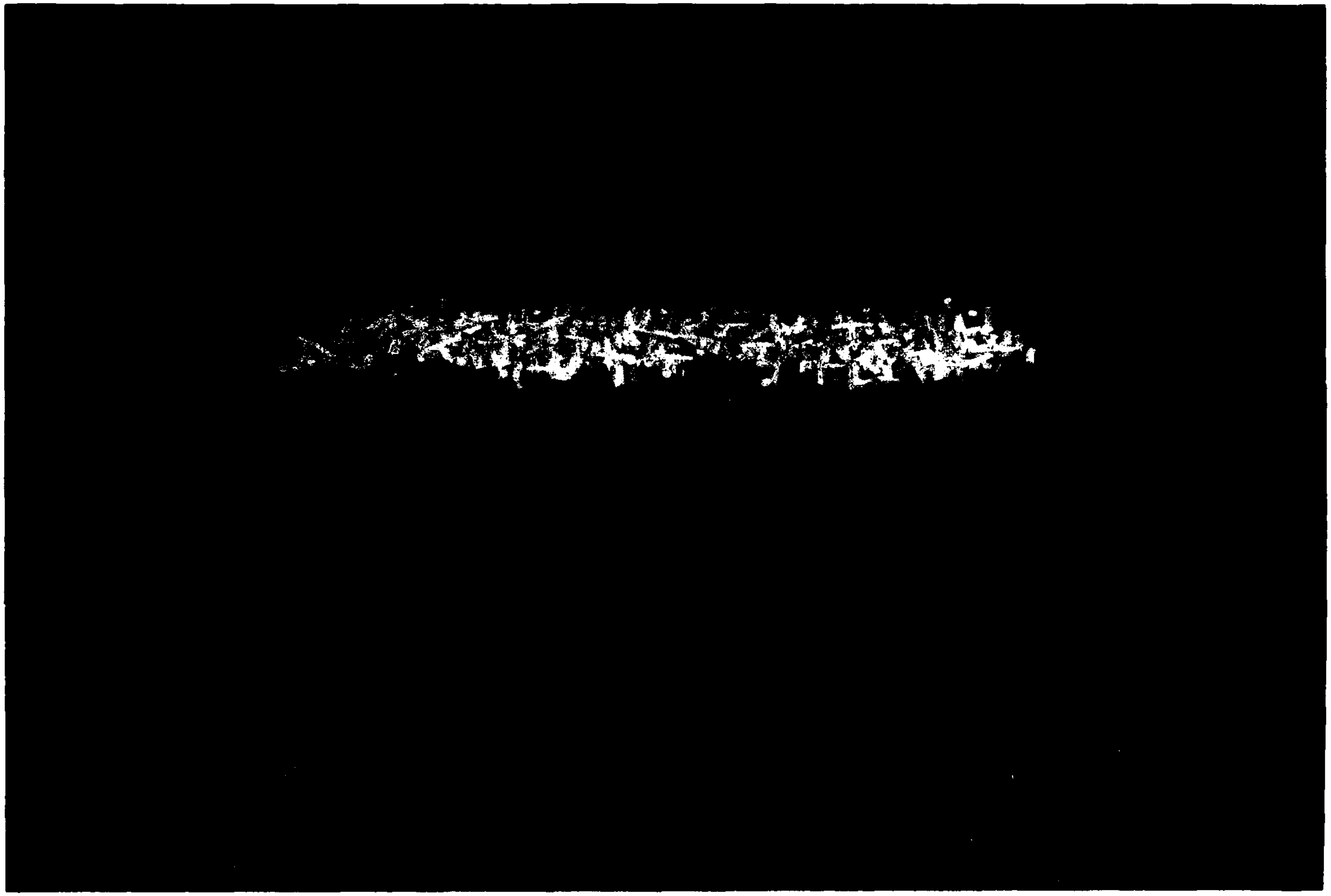

Photo 269. Repeat test of Plan 15; channel-side view after testing at swl's of +4 and +6 ft NGVD; maximum wave heights = 12.4 and 14.0 ft, respectively

Photo 270. Repeat test of Plan 15; sea-side view after testing at swl's of +4, +6, and +8 ft NGVD; maximum wave heights = 12.4, 14.0, and 16.0 ft, respectively

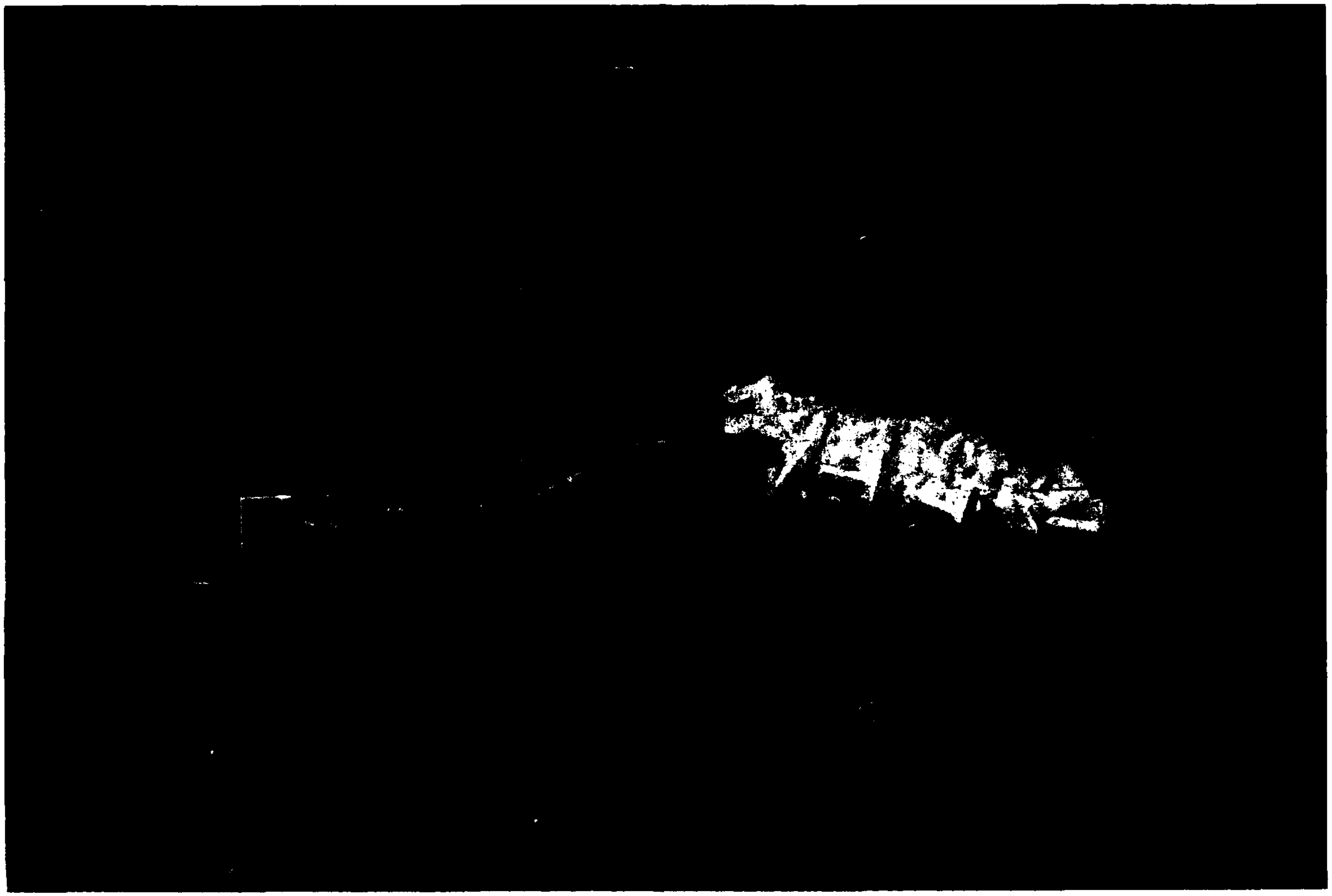

Photo 271. Repeat test of Plan 15; end view after testing at swl's of +4, +6, and +8 ft NGVD; maximum wave heights = 12.4, 14.0, and 16.0 ft, respectively

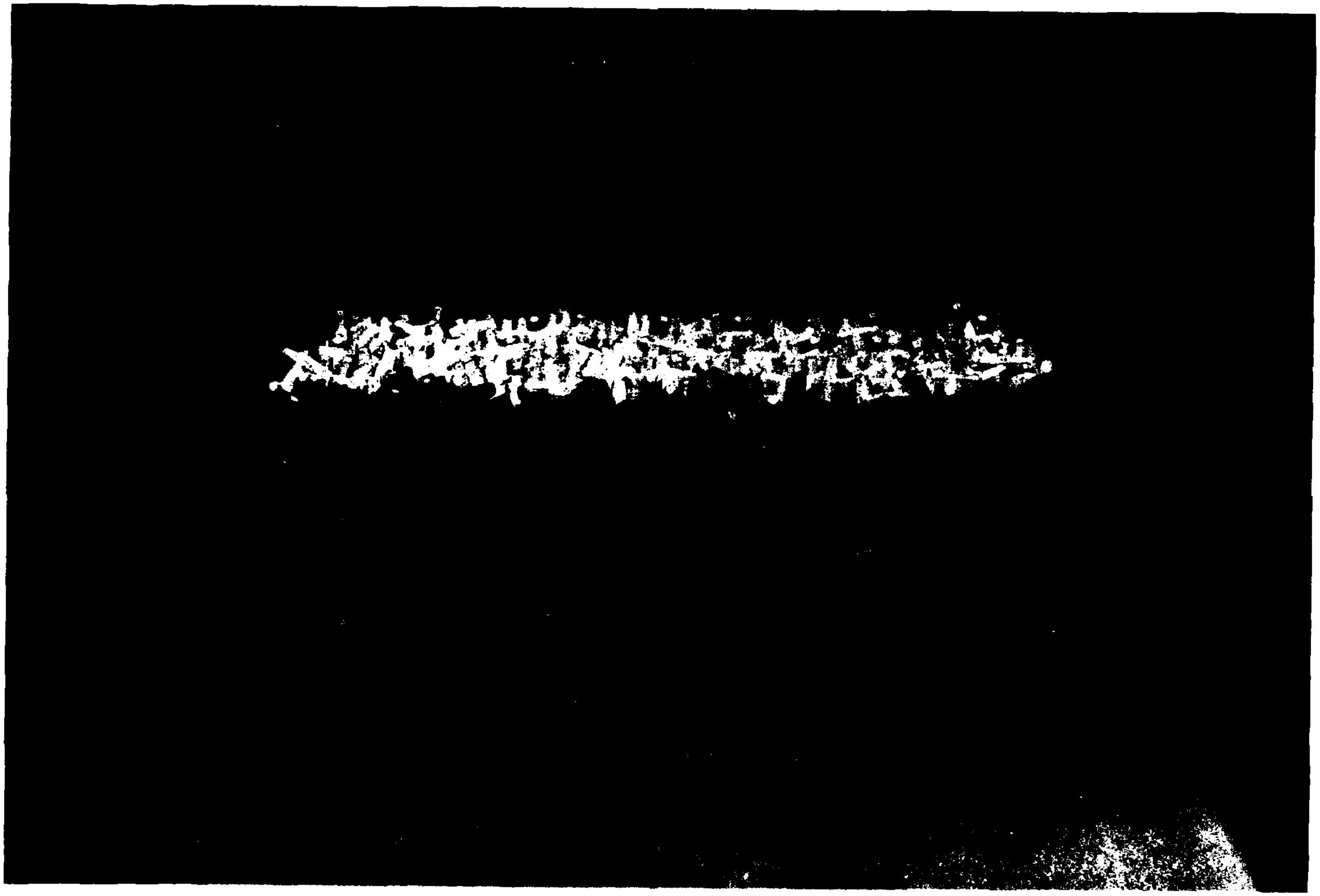

Photo 272. Repeat test of Plan 15; channel-side view after testing at swl's of +4, +6, and +8 ft NGVD; maximum wave heights = 12.4, 14.0, and 16.0 ft, respectively

Photo 273. Sea-side view of Plan 16 before wave attack

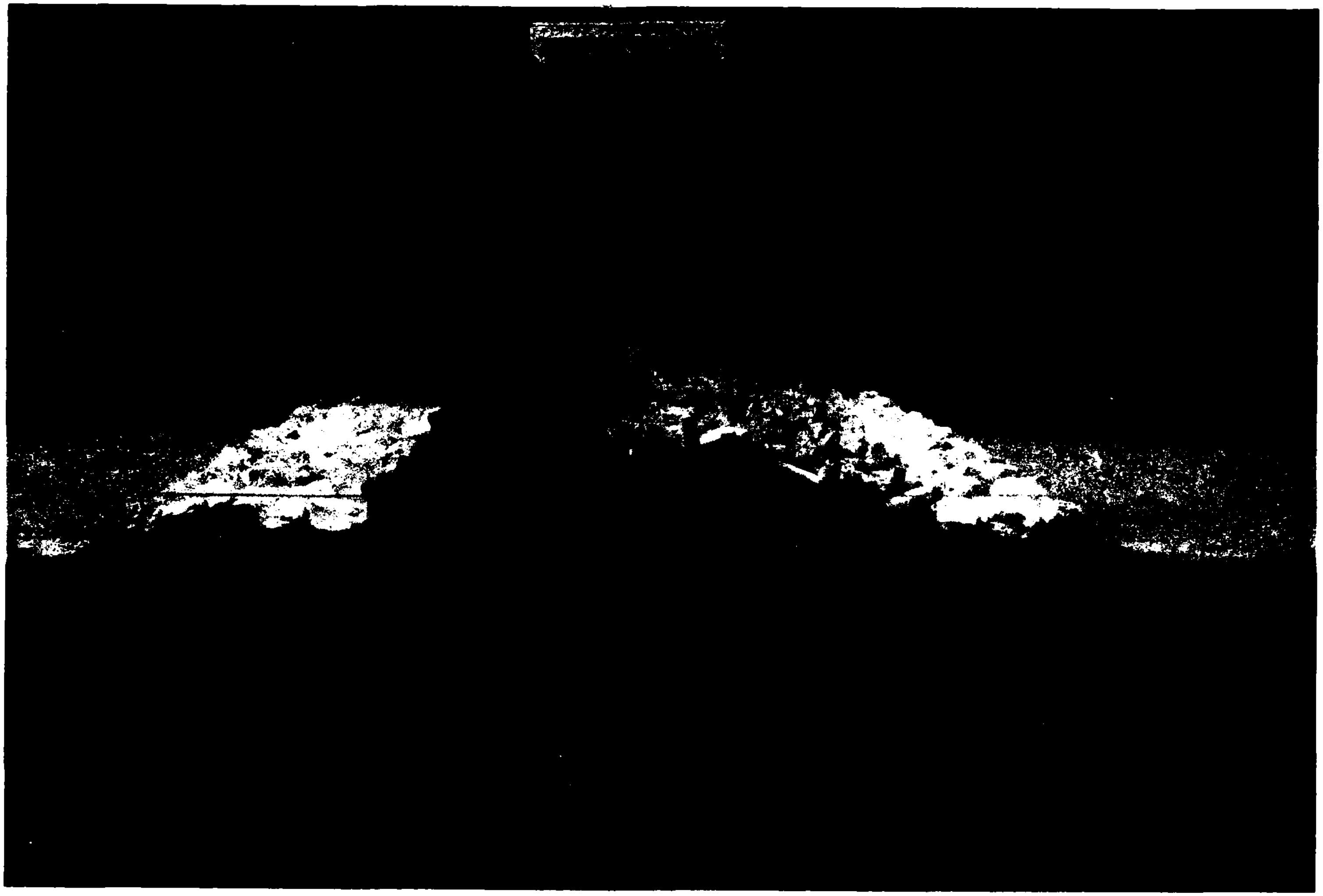

Photo 274. End view of Plan 16 before wave attack

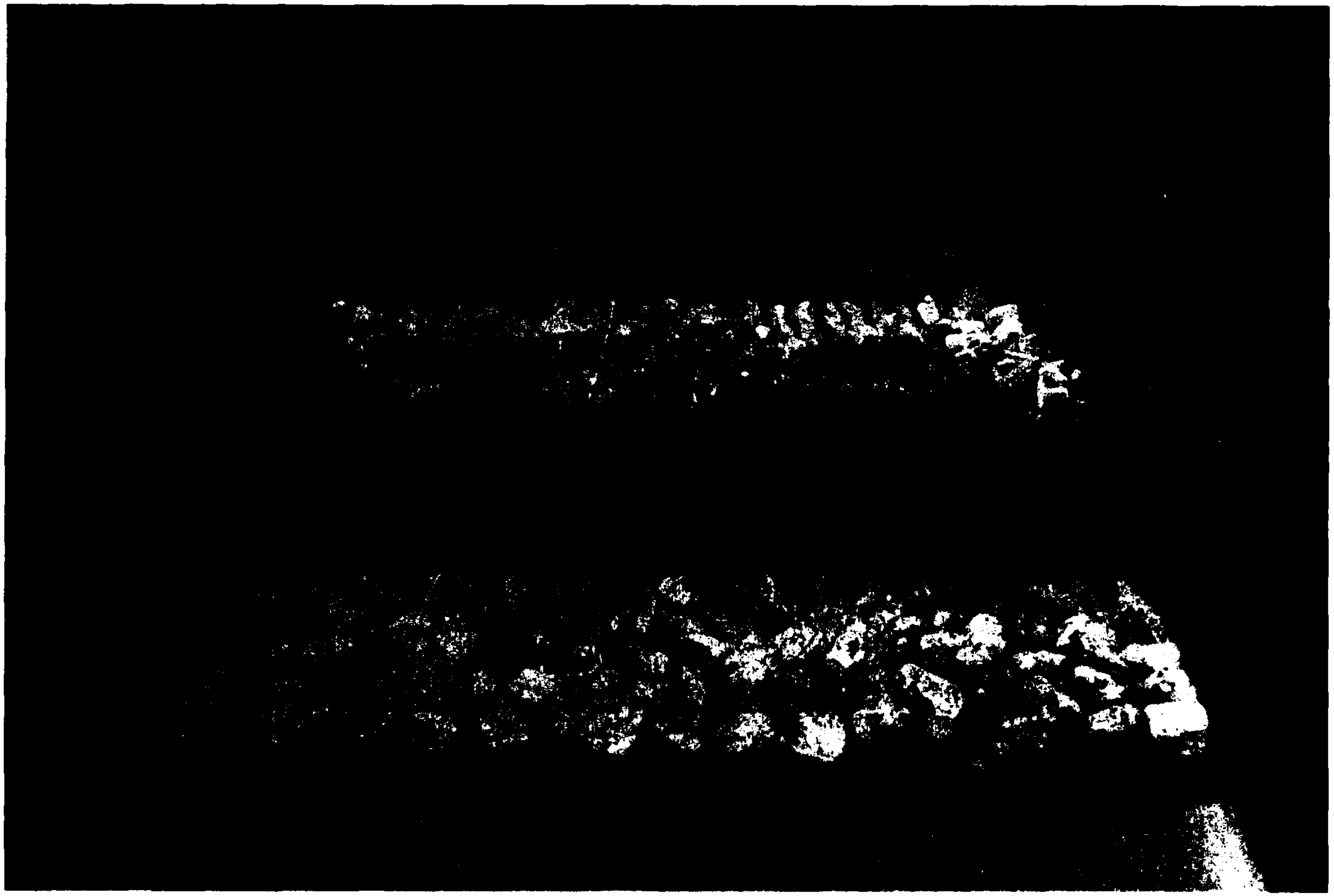

Photo 275. Channel-side view of Plan 16 before wave attack

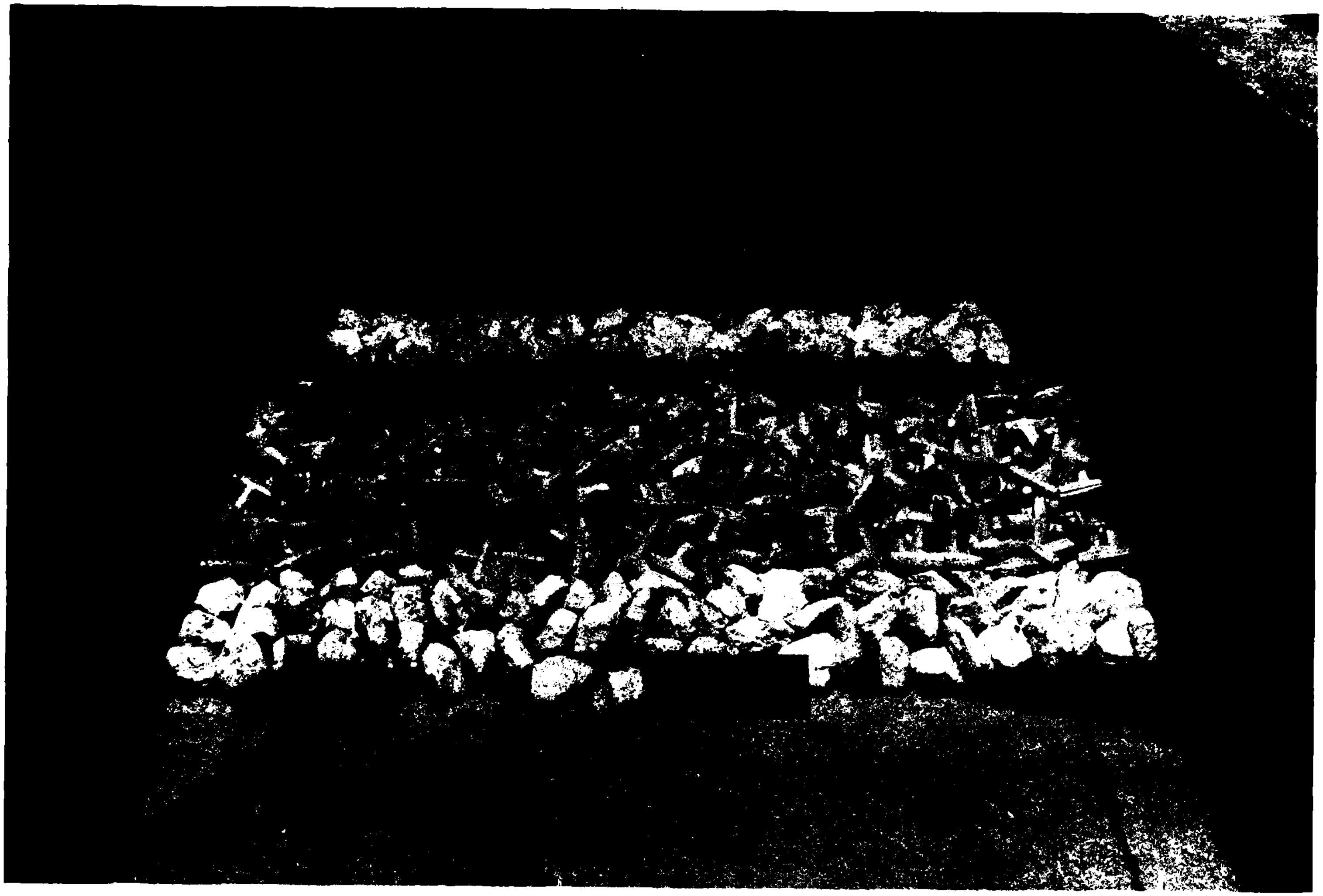

Photo 276. Sea-side view of Plan 16 after testing at an swl of +8 ft NGVD; maximum wave height = 16.0 ft

Photo 277. End view of Plan 16 after testing at an swl of +8 ft NGVD; maximum wave height = 16.0 ft

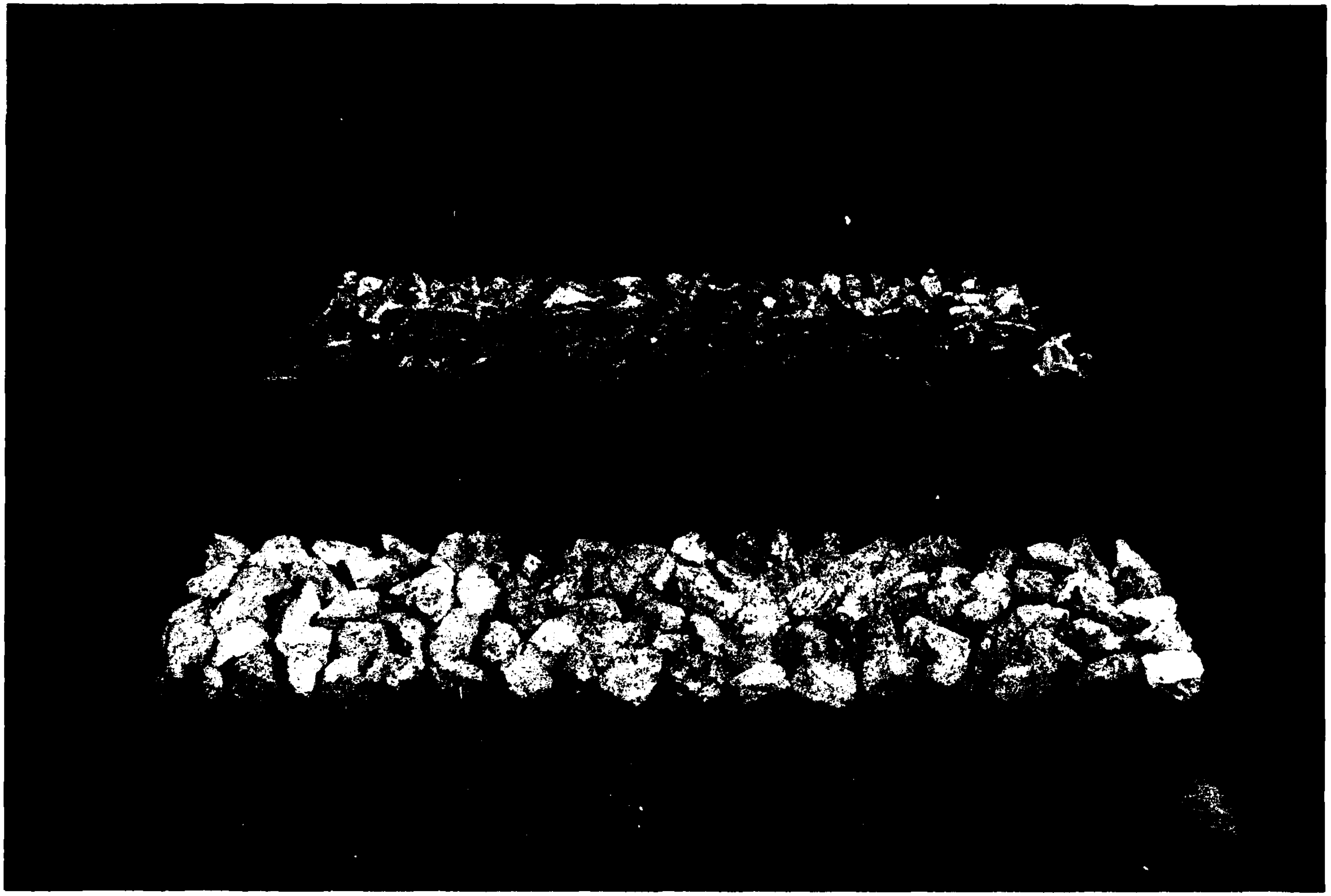

Photo 278. Channel-side view of Plan 16 after testing at an swl of +8 ft NGVD; maximum wave height = 16.0 ft

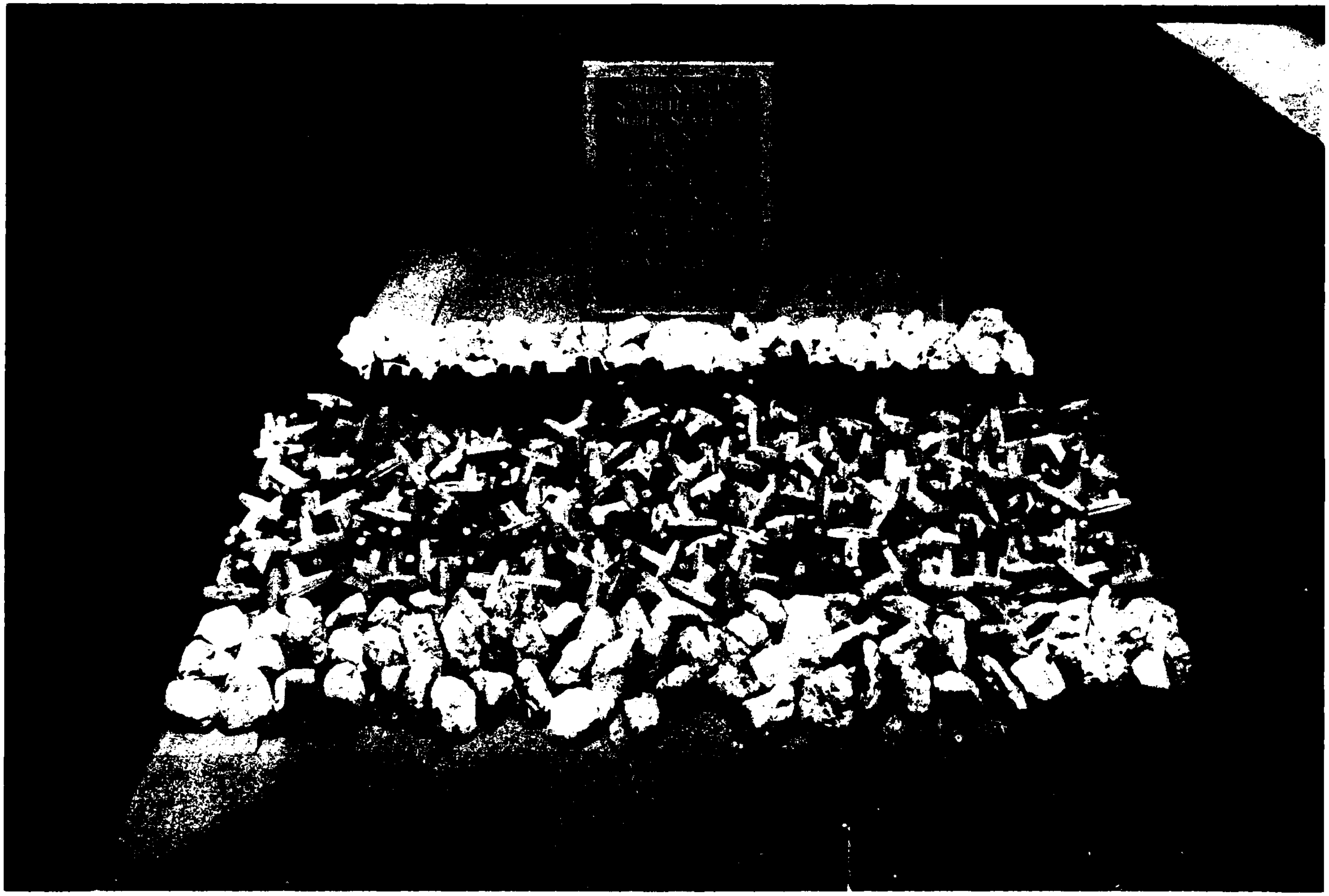

Photo 279. Sea-side view of Plan 16 after testing at swl's of +8, +6, and +4 ft NGVD; maximum wave heights = 16.0, 14.0, and 12.4 ft, respectively

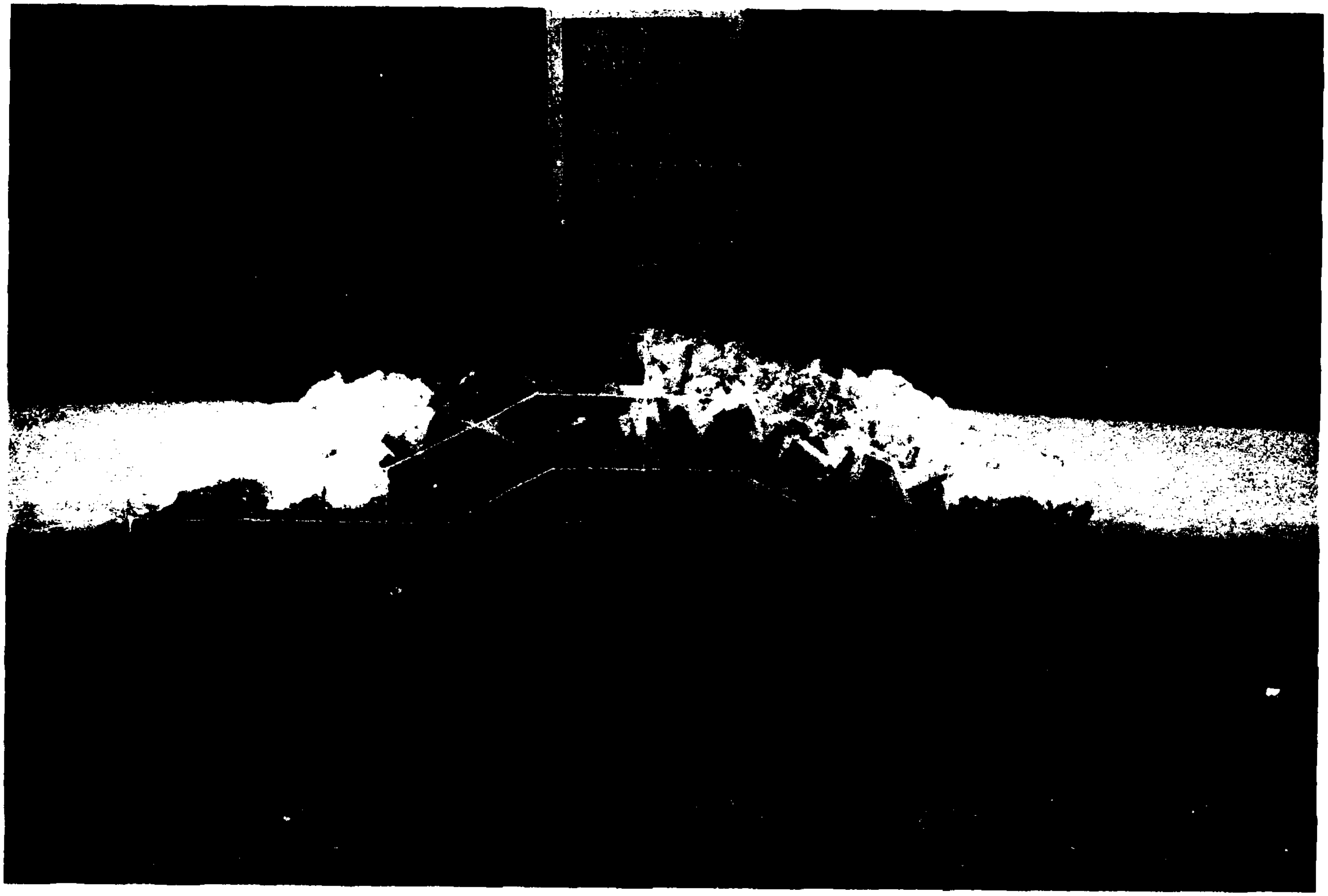

Photo 280. End view of Plan 16 after testing at swl's of +8, +6, and +4 ft NGVD; maximum wave heights = 16.0, 14.0, and 12.4 ft, respectively

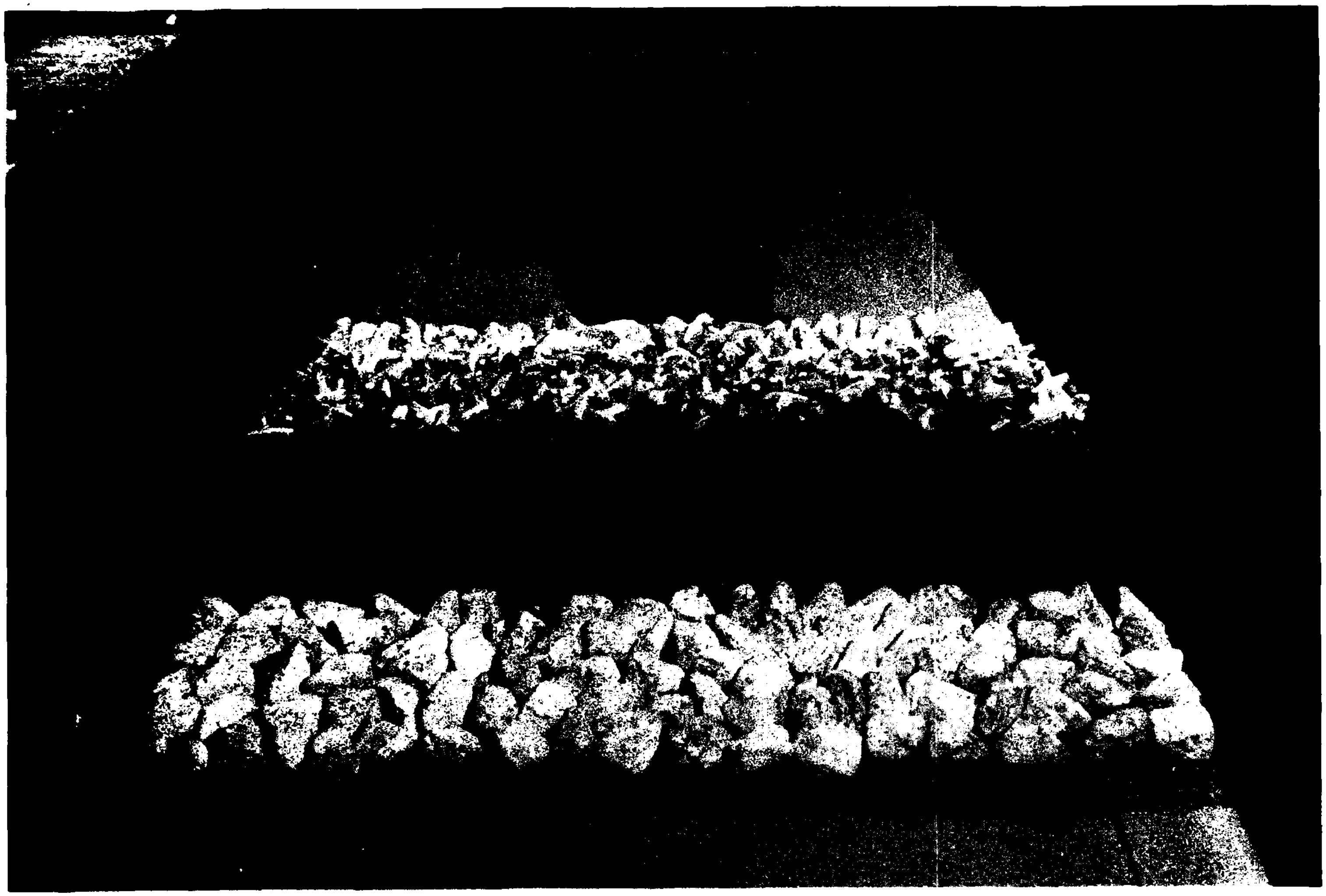

Photo 281. Channel-side view of Plan 16 after testing at swl's of +8, +6, and +4 ft NGVD; maximum wave heights = 16.0, 14.0, and 12.4 ft, respectively

Photo 282. Repeat test of Plan 16; sea-side view before wave attack

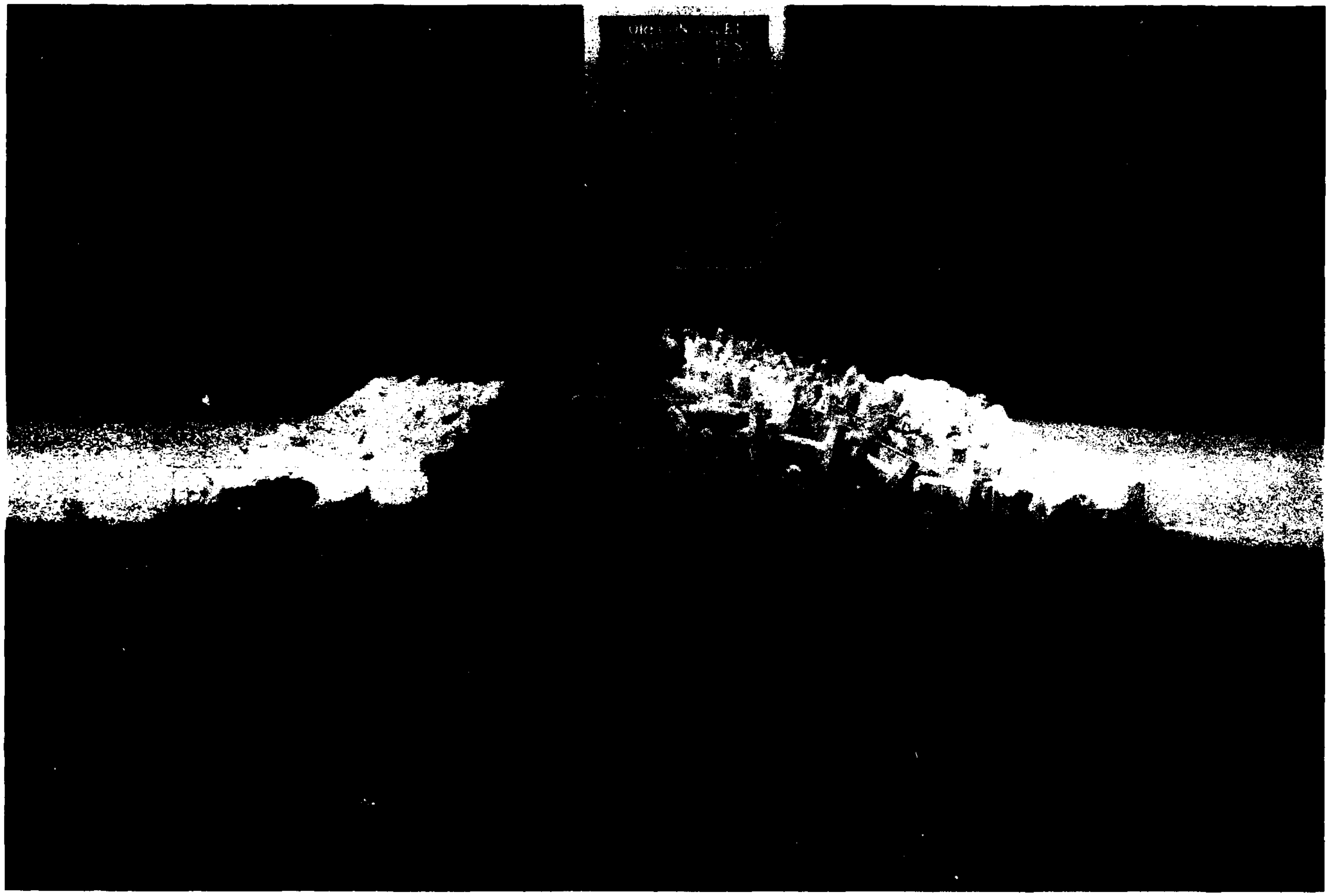

Photo 283. Repeat test of Plan 16; end view before wave attack

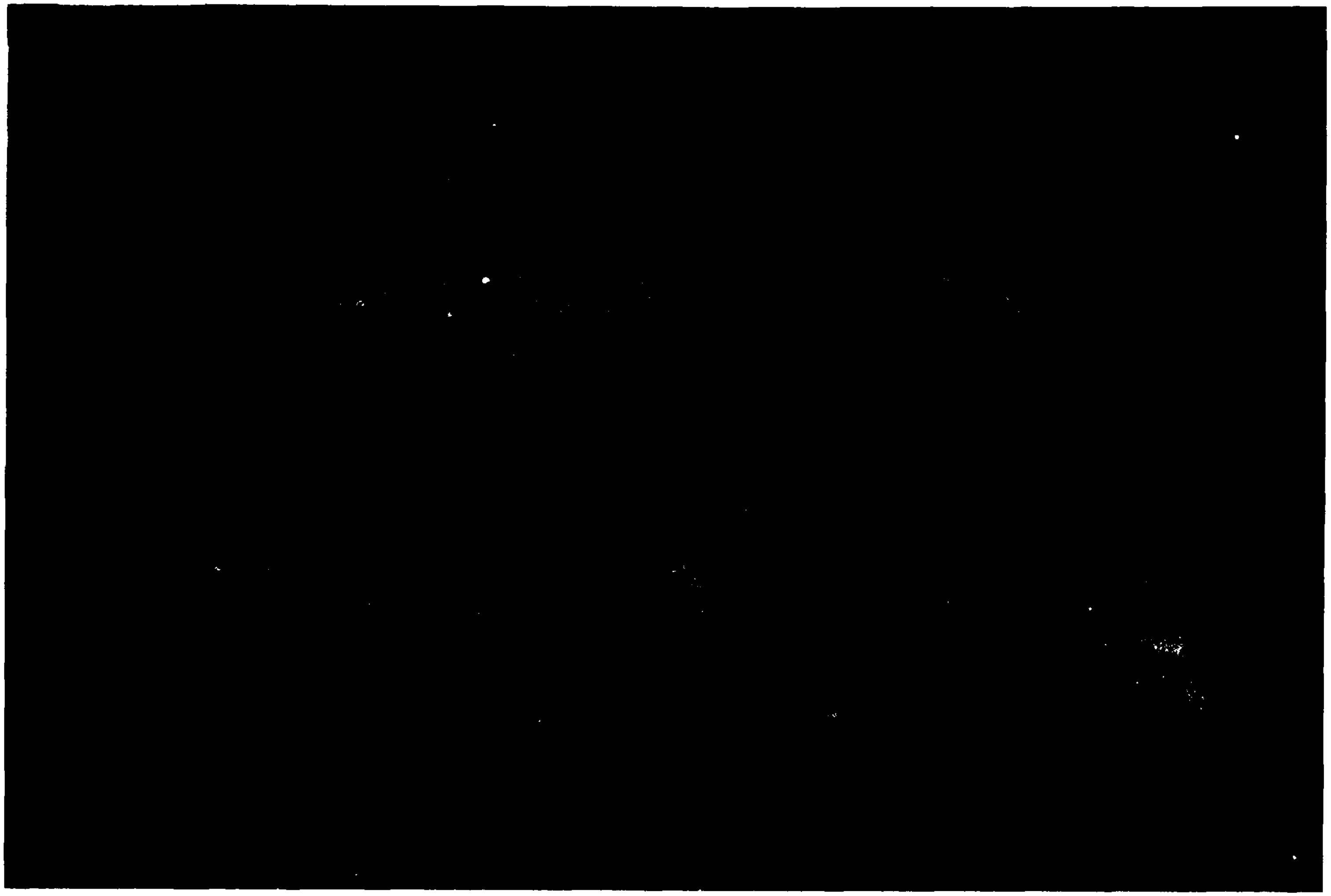

Photo 284. Repeat test of Plan 16; channel-side view before wave attack

Photo 285. Repeat test of Plan 16; sea-side view after testing at swl's of +4 and +6 ft NGVD; maximum wave heights = 12.4 and 14.0 ft, respectively

Photo 286. Repeat test of Plan 16; end view after testing at swl's of +4 and +6 ft NGVD; maximum wave heights = 12.4 and 14.0 ft, respectively

Photo 287. Repeat test of Plan 16; channel-side view after testing at swl's of +4 and +6 ft NGVD; maximum wave heights = 12.4 and 14.0 ft, respectively

Photo 288. Repeat test of Plan 16; sea-side view after testing at swl's of +4, +6, and +8 ft NGVD; maximum wave heights = 12.4, 14.0, and 16.0 ft, respectively

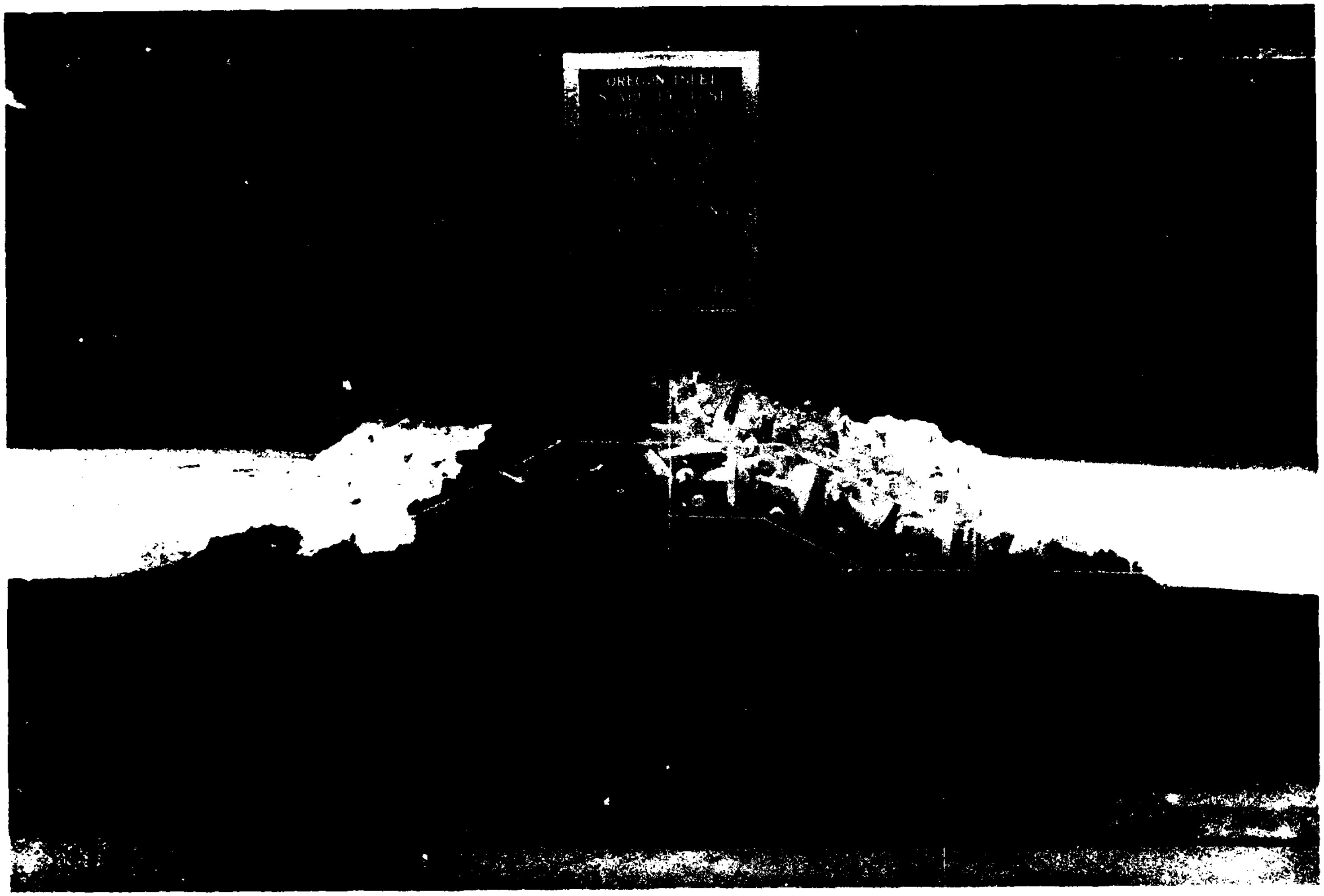

Photo 289. Repeat test of Plan 16; end view after testing at swl's of +4, +6, and +8 ft NGVD; maximum wave heights = 12.4, 14.0, and 16.0 ft, respectively

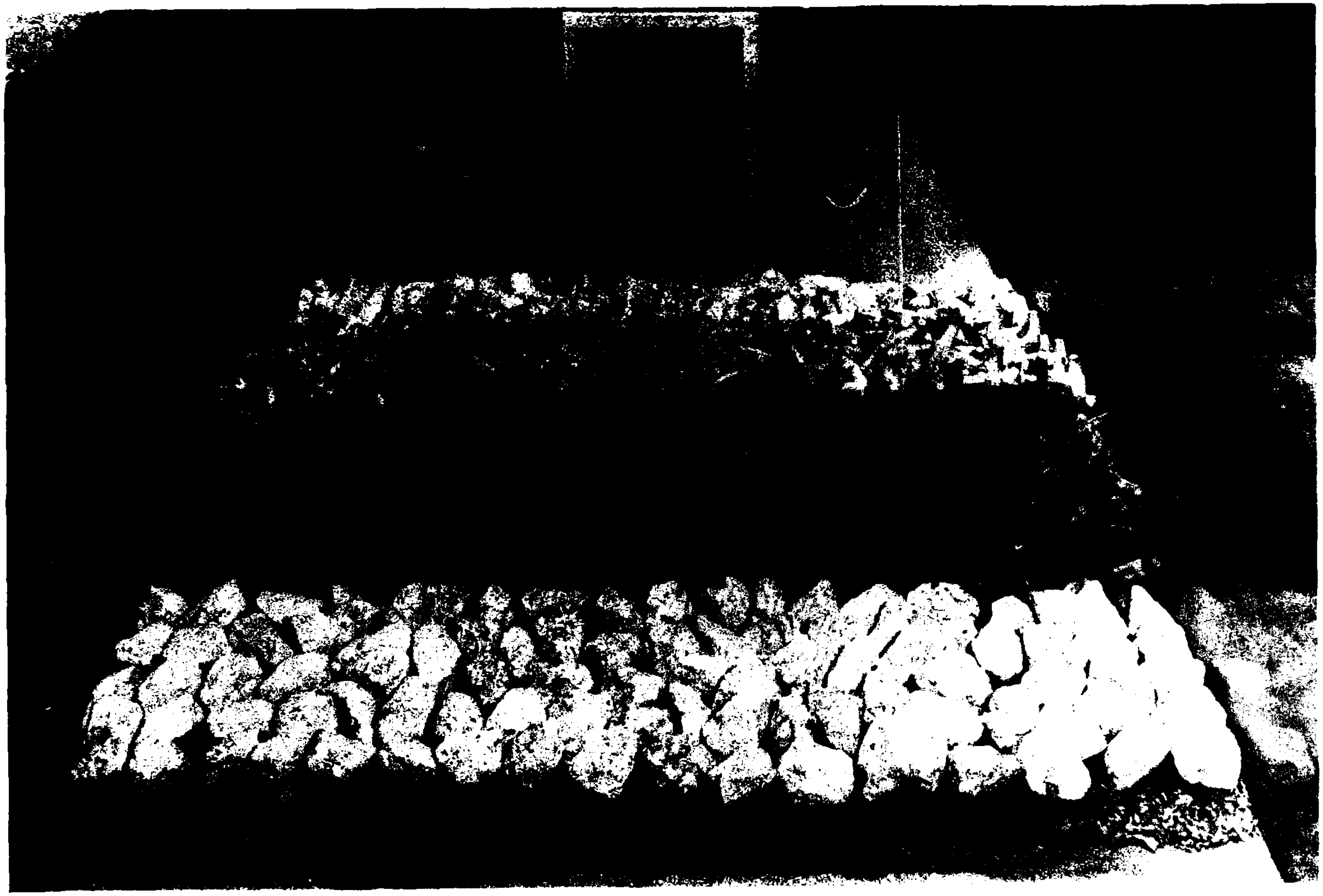

Photo 290. Repeat test of Plan 16; channel-side view after testing at swl's of +4, +6, and +8 ft NGVD; maximum wave heights = 12.4, 14.0, and 16.0 ft, respectively

Photo 291. End view of a 15.0-sec, 16.0-ft wave impinging on the seaward face of Plan 16; swl = +8 ft NGVD

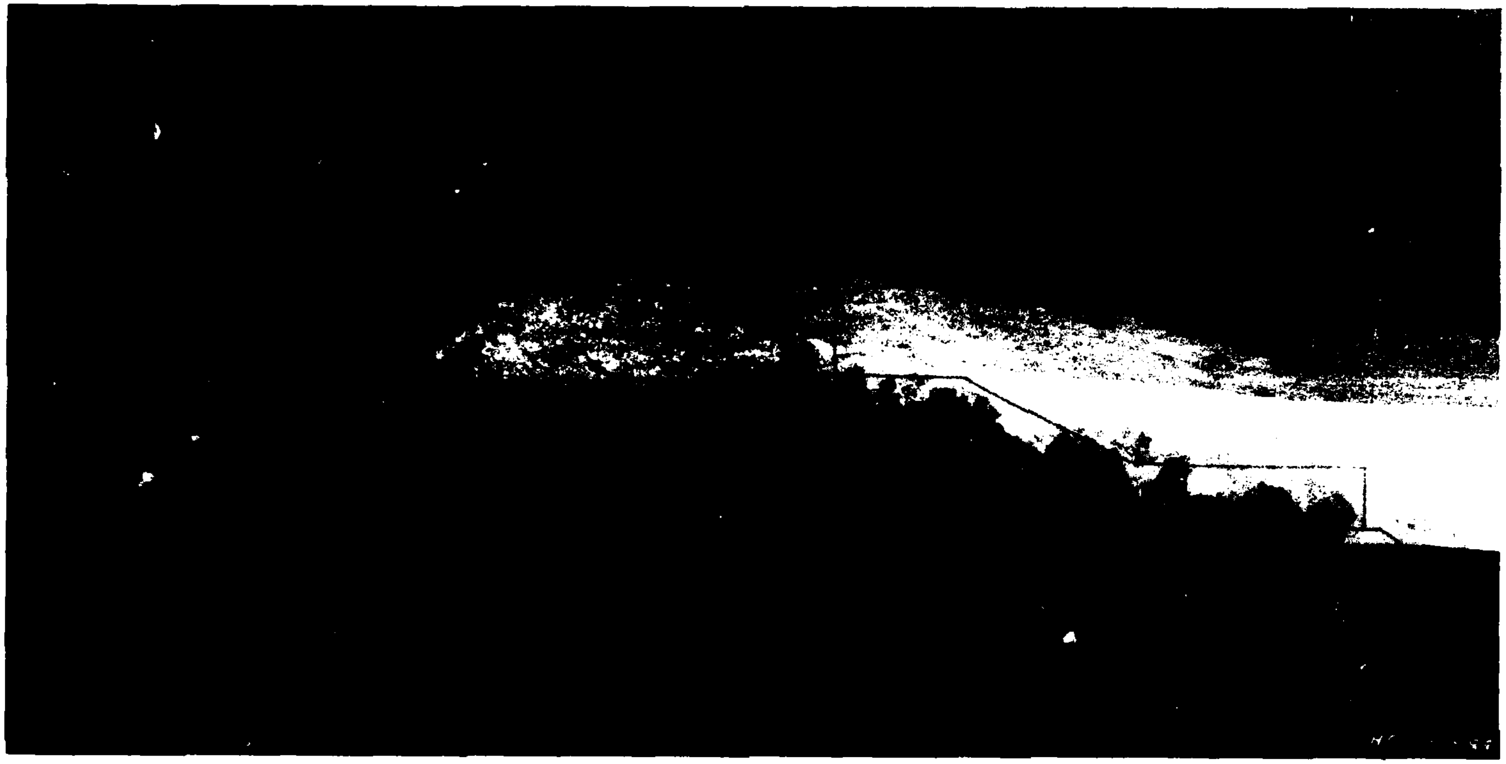

Photo 292. End view of a 15.0-sec, 16.0-ft wave overtopping Plan 16; swl = +8 ft NGVD

AD-A136 610 JETTY STABILITY STUDY OREGON INLET NORTH CAROLINA HYDRAULIC MODEL INVESTIGATION(U) COASTAL ENGINEERING RESEARCH CENTER VICKSBURG MS R D CARVER ET AL. SEP 83 5/5

UNCLASSIFIED CERC-TR-83-3 F/G 13/2 NL

END

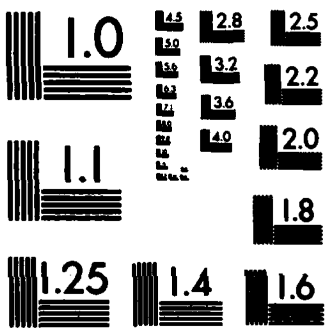

MICROCOPY RESOLUTION TEST CHART
NATIONAL BUREAU OF STANDARDS-1963-A

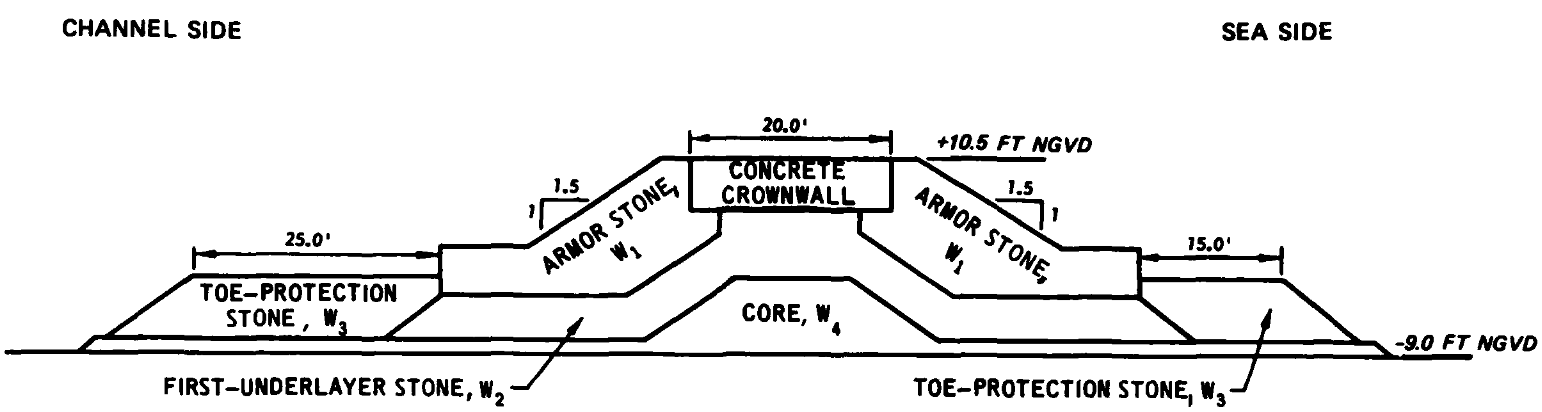

MATERIAL CHARACTERISTICS

MODEL	PROTOTYPE
W_1 = 0.38-LB STONE	W_1 = 8.0-TON STONE @ 165 PCF
W_2 = 0.038-LB STONE	W_2 = 0.8-TON STONE @ 165 PCF
W_3 = 0.095-LB STONE	W_3 = 2.0-TON STONE @ 165 PCF
W_4 = 0.00002- TO 0.004-LB STONE	W_4 = 1.0- TO 165.0-LB STONE @ 165 PCF

TYPICAL BREAKWATER CROSS SECTION
PLAN 1
MODEL SCALE 1:33

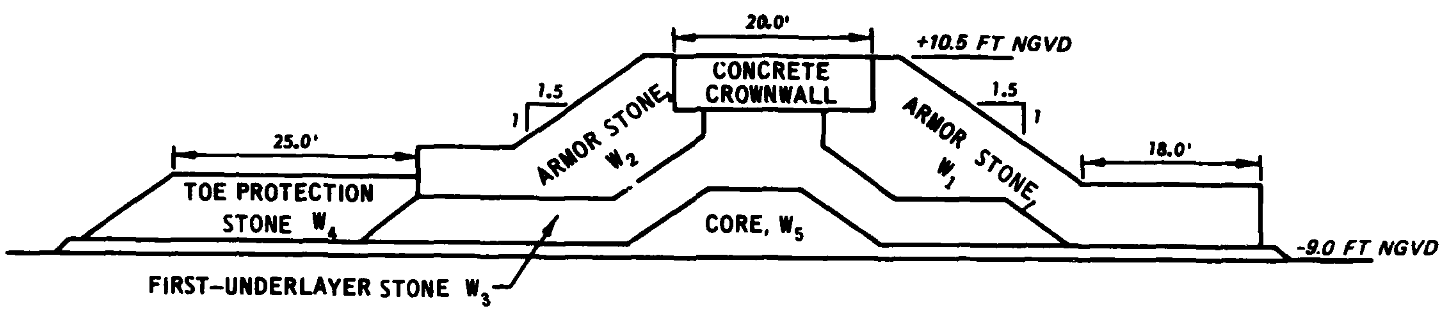

MATERIAL CHARACTERISTICS

MODEL	PROTOTYPE
W_1 = 0.55-LB STONE	W_1 = 11.5-TON STONE @ 165 PCF
W_2 = 0.38-LB STONE	W_2 = 8.0-TON STONE @ 165 PCF
W_3 = 0.047-LB STONE	W_3 = 0.98-TON STONE @ 165 PCF
W_4 = 0.095-LB STONE	W_4 = 2.0-TON STONE @ 165 PCF
W_5 = 0.00002- TO 0.004-LB STONE	W_5 = 1.0- TO 165.0-LB STONE @ 165 PCF

TYPICAL BREAKWATER CROSS SECTION

PLAN 2

MODEL SCALE 1:33

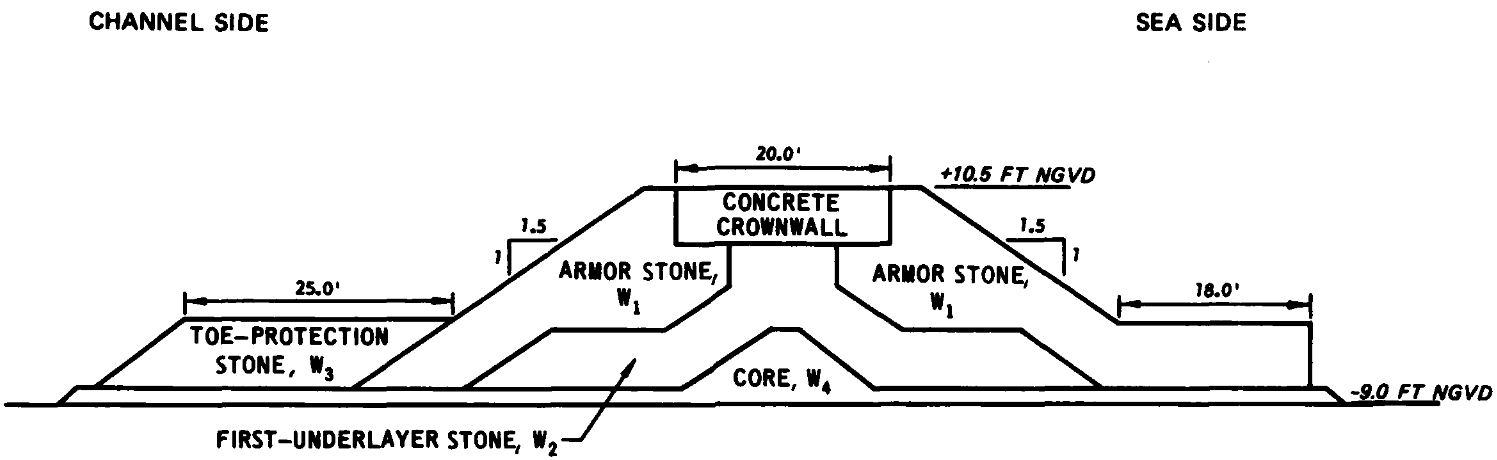

MATERIAL CHARACTERISTICS

MODEL	PROTOTYPE
W_1 = 0.55-LB STONE	W_1 = 11.5-TON STONE @ 165 PCF
W_2 = 0.055-LB STONE	W_2 = 1.15-TON STONE @ 165 PCF
W_3 = 0.095-LB STONE	W_3 = 2.0-TON STONE @ 165 PCF
W_4 = 0.00002- TO 0.004-LB STONE	W_4 = 1.0- TO 165-LB STONE @ 165 PCF

TYPICAL BREAKWATER CROSS SECTION

PLAN 3

MODEL SCALE 1:33

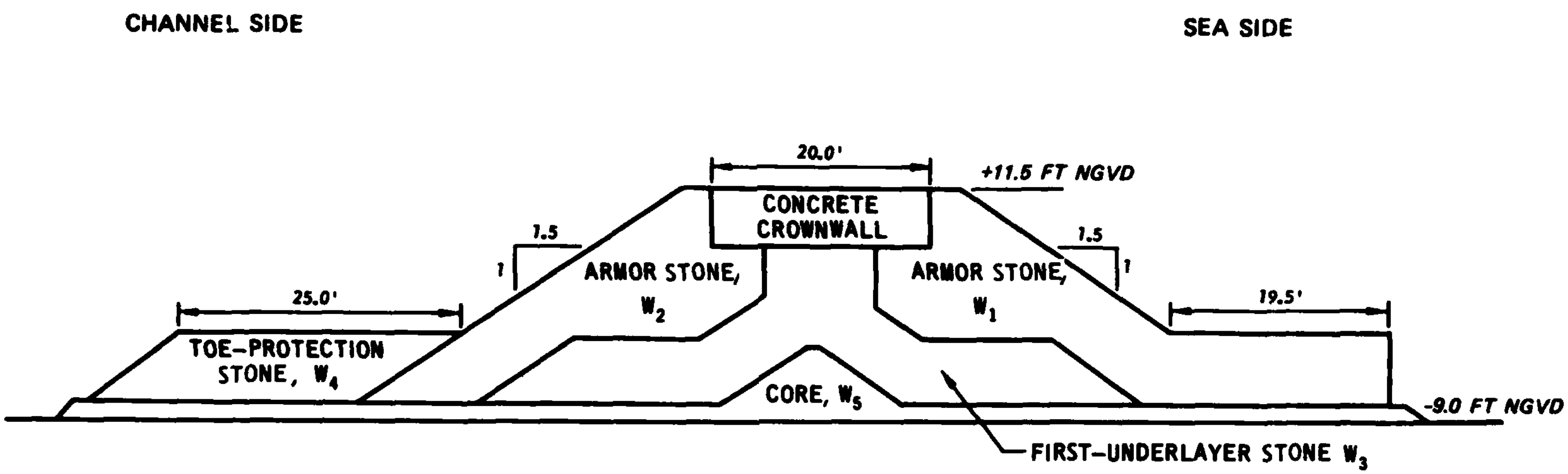

MATERIAL CHARACTERISTICS

MODEL	PROTOTYPE
W_1 = 0.71-LB STONE	W_1 = 15.0-TON STONE @ 165 PCF
W_2 = 0.55-LB STONE	W_2 = 11.5-TON STONE @ 165 PCF
W_3 = 0.063-LB STONE	W_3 = 1.33-TON STONE @ 165 PCF
W_4 = 0.095-LB STONE	W_4 = 2.0-TON STONE @ 165 PCF
W_5 = 0.00002- TO 0.004-LB STONE	W_5 = 1.0- TO 165.0-LB STONE @ 165 PCF

TYPICAL BREAKWATER CROSS SECTION

PLAN 4

MODEL SCALE 1:33

PLATE 4

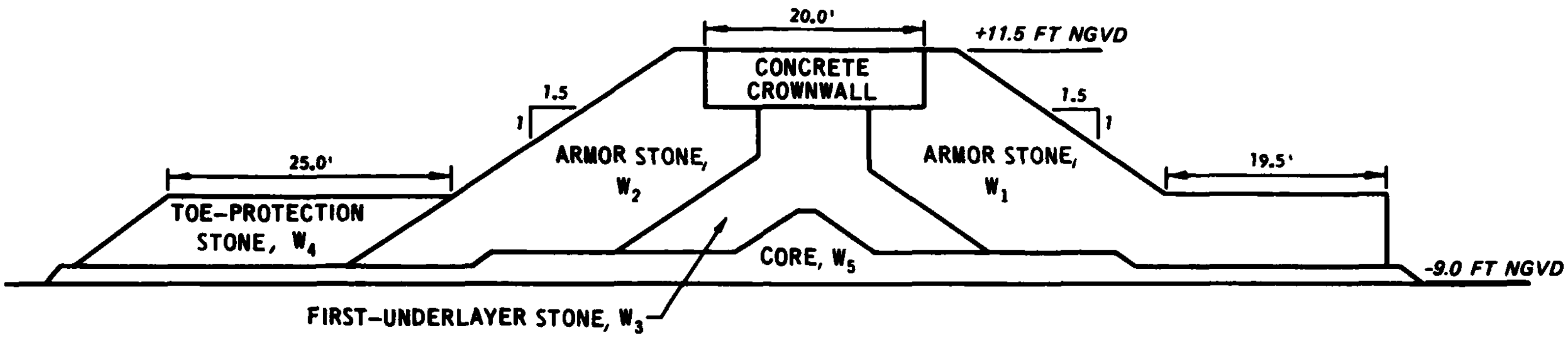

MATERIAL CHARACTERISTICS

MODEL	PROTOTYPE
W_1 = 0.71-LB STONE	W_1 = 15.0-TON STONE @ 165 PCF
W_2 = 0.55-LB STONE	W_2 = 11.5-TON STONE @ 165 PCF
W_3 = 0.063-LB STONE	W_3 = 1.33-TON STONE @ 165 PCF
W_4 = 0.095-LB STONE	W_4 = 2.0-TON STONE @ 165 PCF
W_5 = 0.00002- TO 0.004-LB STONE	W_5 = 1.0- TO 165.0-LB STONE @ 165 PCF

TYPICAL BREAKWATER CROSS SECTION

PLAN 4A

MODEL SCALE 1:33

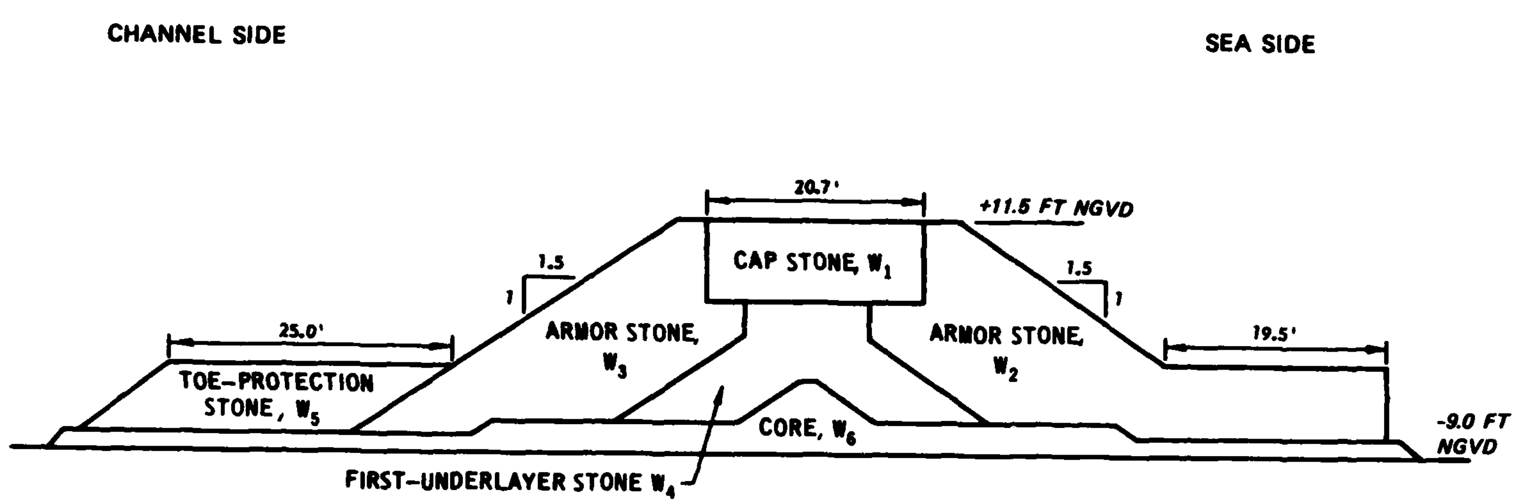

MATERIAL CHARACTERISTICS

MODEL	PROTOTYPE
W_1 = 0.86-LB STONE	W_1 = 18.0-TON STONE @ 165 PCF
W_2 = 0.71-LB STONE	W_2 = 15.0-TON STONE @ 165 PCF
W_3 = 0.55-LB STONE	W_3 = 11.5-TON STONE @ 165 PCF
W_4 = 0.063-LB STONE	W_4 = 1.33-TON STONE @ 165 PCF
W_5 = 0.095-LB STONE	W_5 = 2.0-TON STONE @ 165 PCF
W_6 = 0.00002- TO 0.004-LB STONE	W_6 = 1.0- TO 165-LB STONE @ 165 PCF

TYPICAL BREAKWATER CROSS SECTION

PLAN 4B

MODEL SCALE 1:33

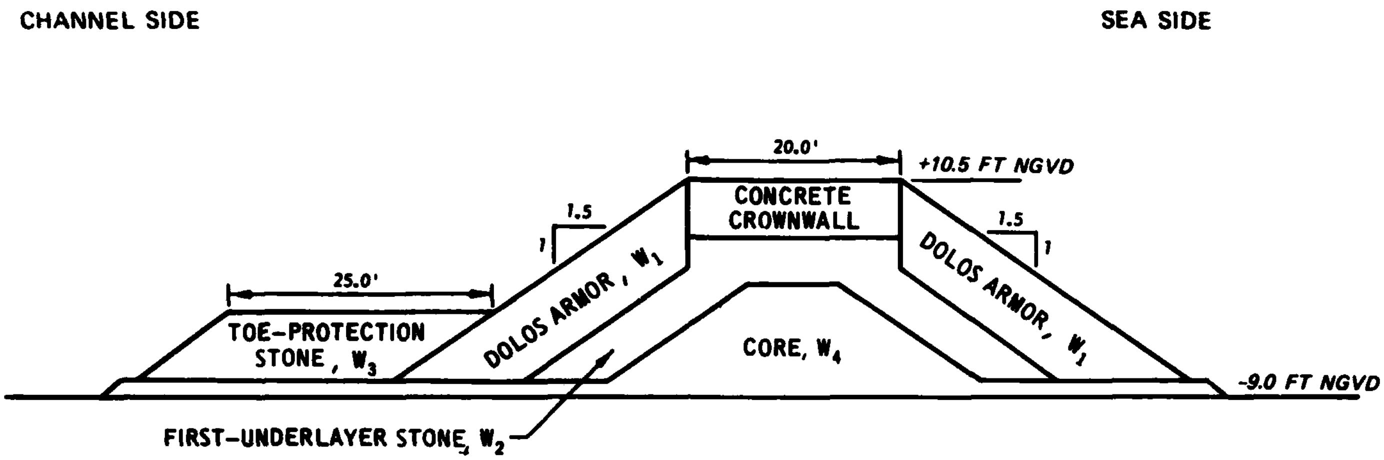

MATERIAL CHARACTERISTICS

MODEL	PROTOTYPE
W_1 = 0.24-LB DOLOS	W_1 = 3.25-TON DOLOS @ 150 PCF
W_2 = 0.048-LB STONE	W_2 = 0.65-TON STONE @ 165 PCF
W_3 = 0.095-LB STONE	W_3 = 2.0-TON STONE @ 165 PCF
W_4 = 0.00002- TO 0.004-LB STONE	W_4 = 1.0- TO 165-LB STONE @ 165 PCF

TYPICAL BREAKWATER CROSS SECTION

PLAN 5

MODEL SCALE 1:33

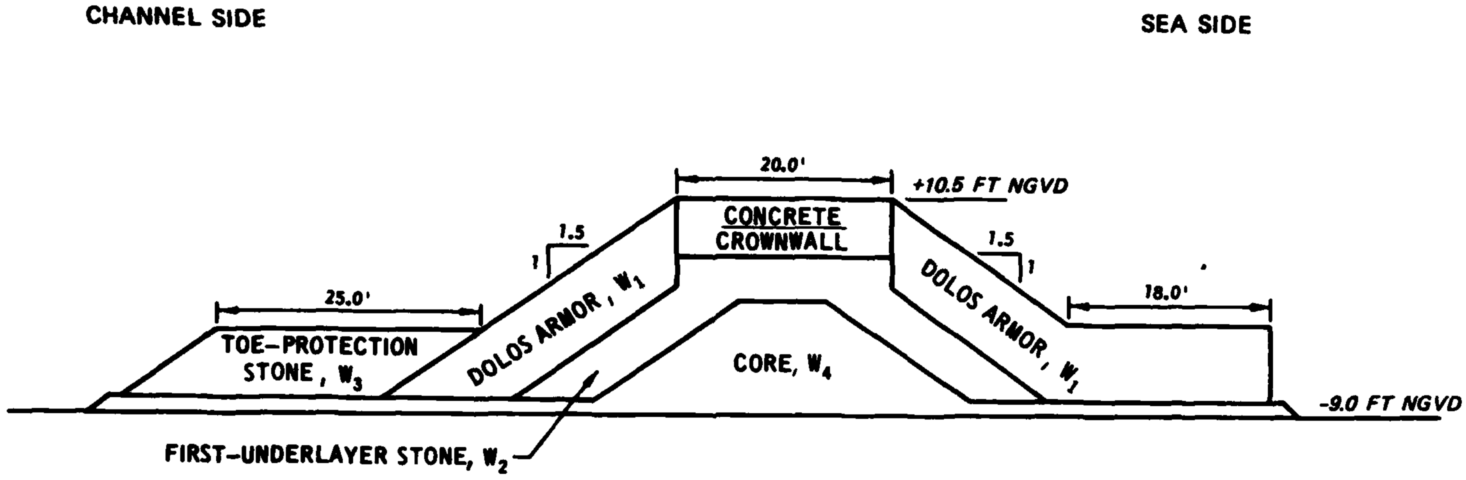

MATERIAL CHARACTERISTICS

MODEL	PROTOTYPE
W_1 = 0.24-LB DOLOS	W_1 = 3.25-TON DOLOS @ 150 PCF
W_2 = 0.048-LB STONE	W_2 = 0.65-TON STONE @ 165 PCF
W_3 = 0.095-LB STONE	W_3 = 2.0-TON STONE @ 165 PCF
W_4 = 0.00002- TO 0.004-LB STONE	W_4 = 1.0- TO 165-LB STONE @ 165 PCF

TYPICAL BREAKWATER CROSS SECTION

PLAN 6

MODEL SCALE 1:33

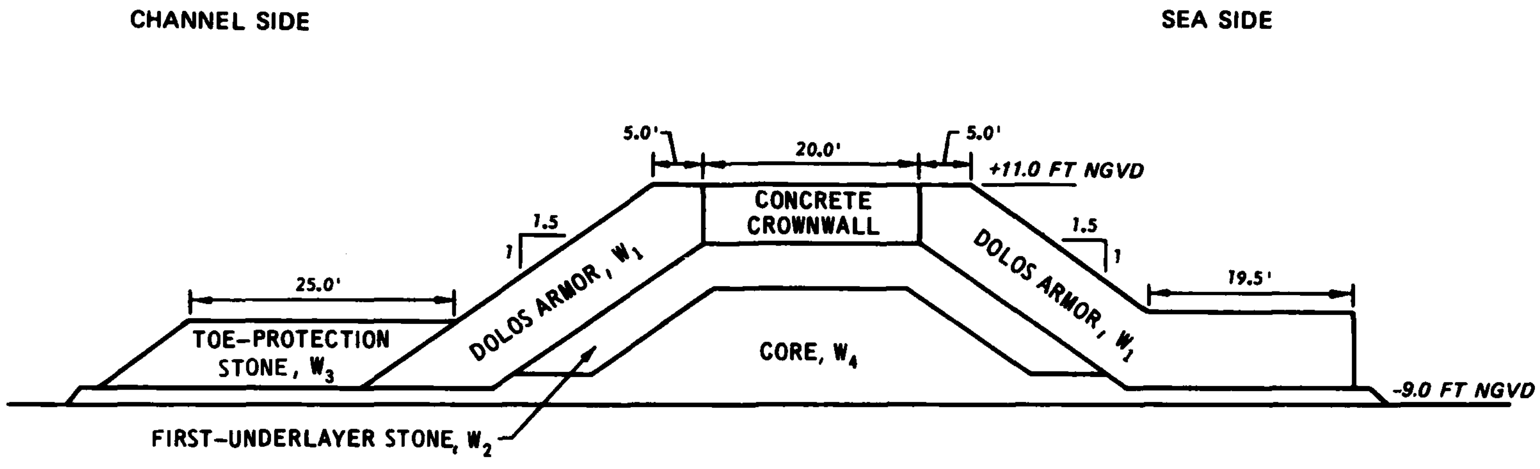

MATERIAL CHARACTERISTICS

MODEL	PROTOTYPE
W_1 = 0.24-LB DOLOS	W_1 = 3.25-TON DOLOS @ 150 PCF
W_2 = 0.048-LB STONE	W_2 = 0.65-TON STONE @ 165 PCF
W_3 = 0.095-LB STONE	W_3 = 2.0-TON STONE @ 165 PCF
W_4 = 0.00002- TO 0.004-LB STONE	W_4 = 1.0- TO 165-LB STONE @ 165 PCF

TYPICAL BREAKWATER CROSS SECTION

PLAN 7

MODEL SCALE 1:33

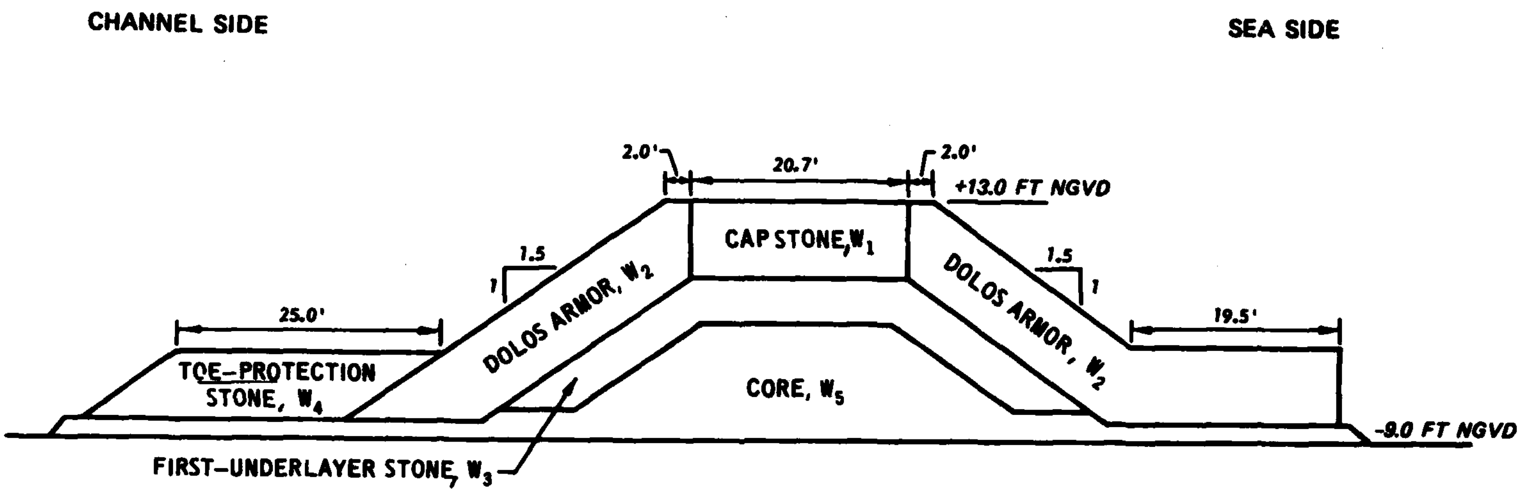

MATERIAL CHARACTERISTICS

MODEL	PROTOTYPE
W_1 = 0.86-LB STONE	W_1 = 18.0-TON STONE @ 165 PCF
W_2 = 0.24-LB DOLOS	W_2 = 3.25-TON DOLOS @ 150 PCF
W_3 = 0.048-LB STONE	W_3 = 0.65-TON STONE @ 165 PCF
W_4 = 0.095-LB STONE	W_4 = 2.0-TON STONE @ 165 PCF
W_5 = 0.00002- TO 0.004-LB STONE	W_5 = 1.0- TO 165-LB STONE @ 165 PCF

TYPICAL BREAKWATER CROSS SECTION

PLAN 8

MODEL SCALE 1:33

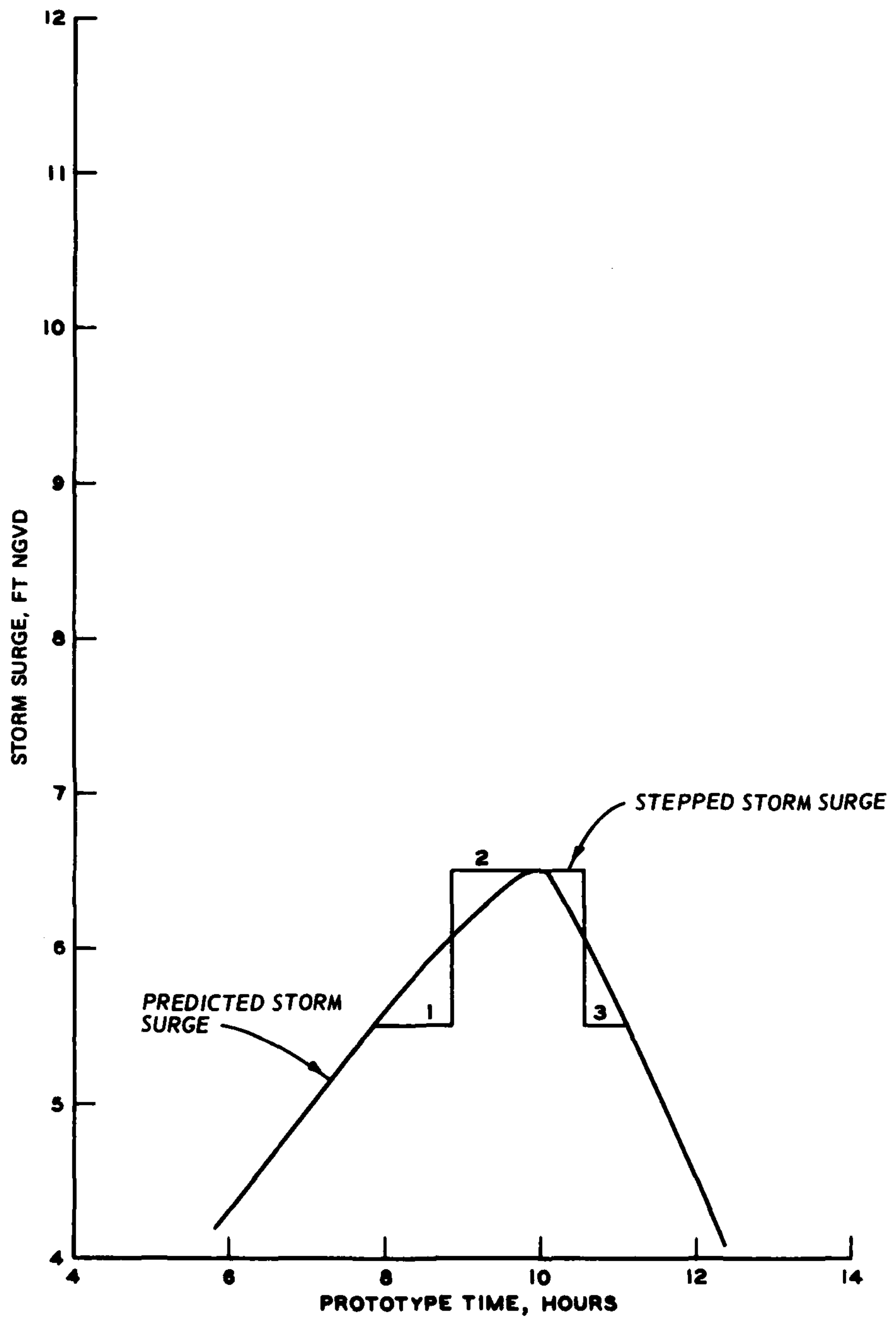

NOTE:

NUMBERS INDICATE HYDROGRAPH STEP NUMBER.

TEST CONDITIONS FOR EACH STEP ARE GIVEN IN TABLE 2.

STORM-SURGE HYDROGRAPH

MAXIMUM SURGE 6.5 FT NGVD
DESIGN SWL 5.5 FT NGVD

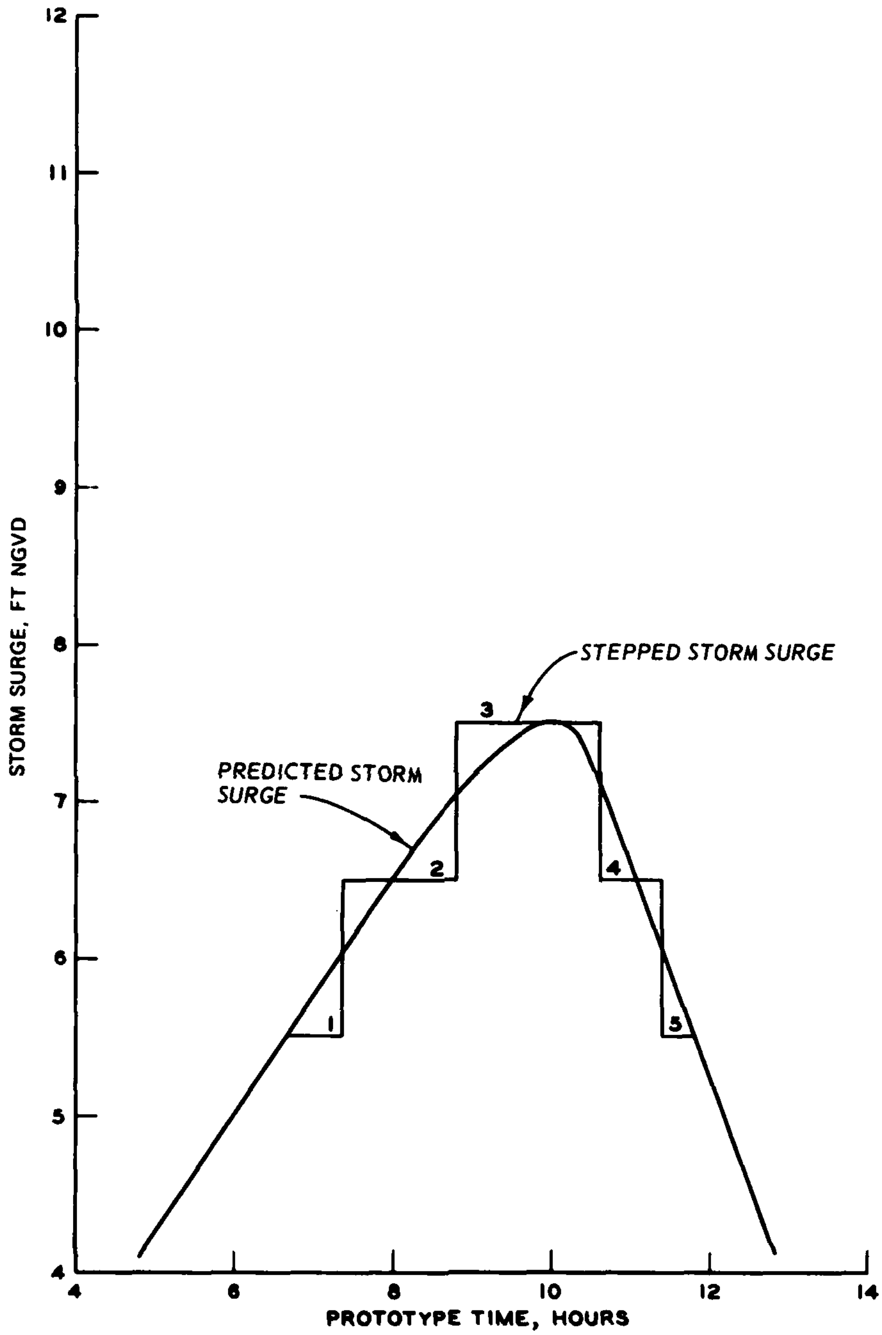

NOTE:

NUMBERS INDICATE HYDROGRAPH STEP NUMBER.

TEST CONDITIONS FOR EACH STEP ARE GIVEN IN TABLE 2.

STORM-SURGE HYDROGRAPH

MAXIMUM SURGE 7.5 FT NGVD

DESIGN SWL 5.5 FT NGVD

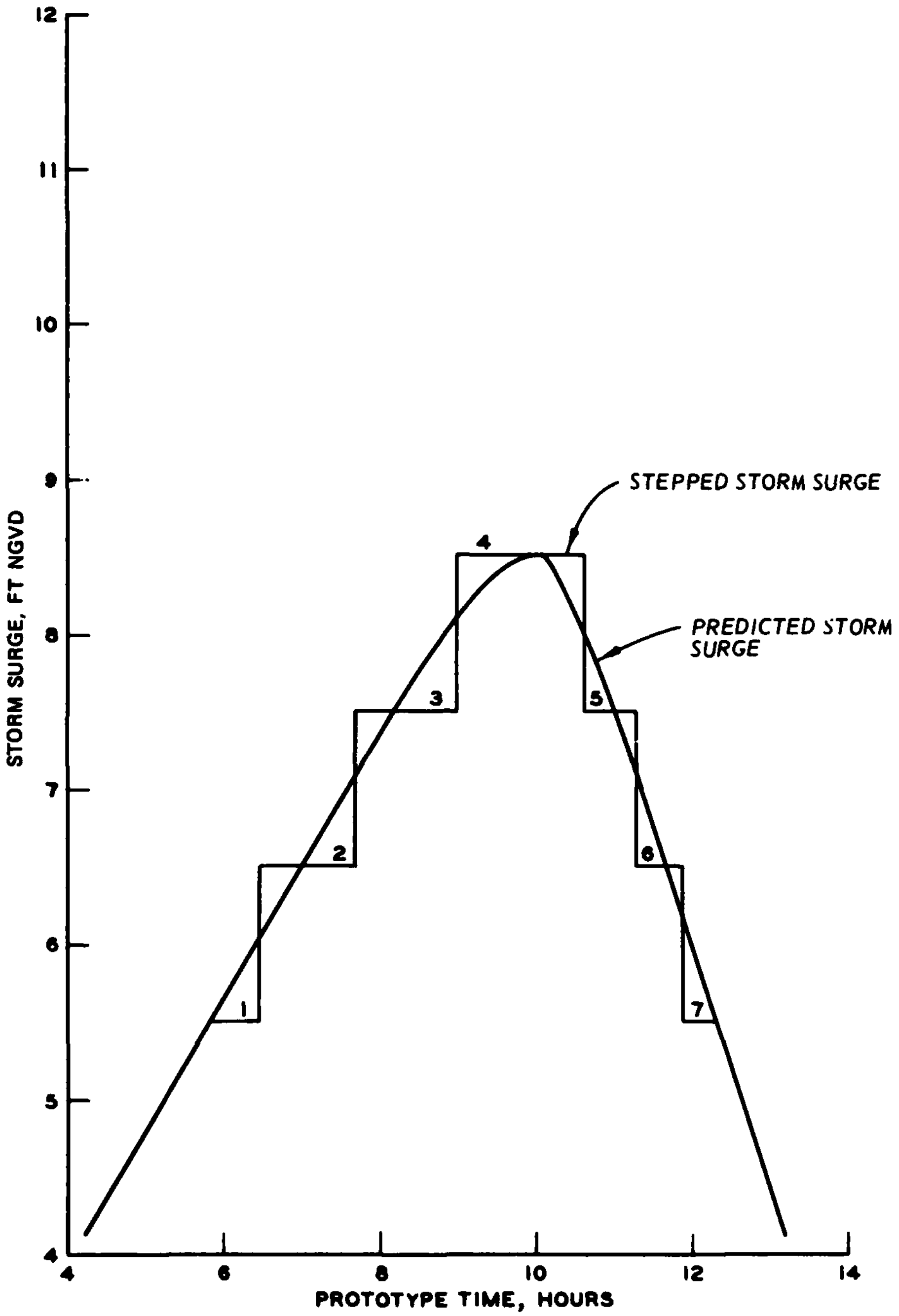

NOTE:

NUMBERS INDICATE HYDROGRAPH STEP NUMBER.

TEST CONDITIONS FOR EACH STEP ARE GIVEN IN TABLE 2.

STORM-SURGE HYDROGRAPH

MAXIMUM SURGE 8.5 FT NGVD

DESIGN SWL 5.5 FT NGVD

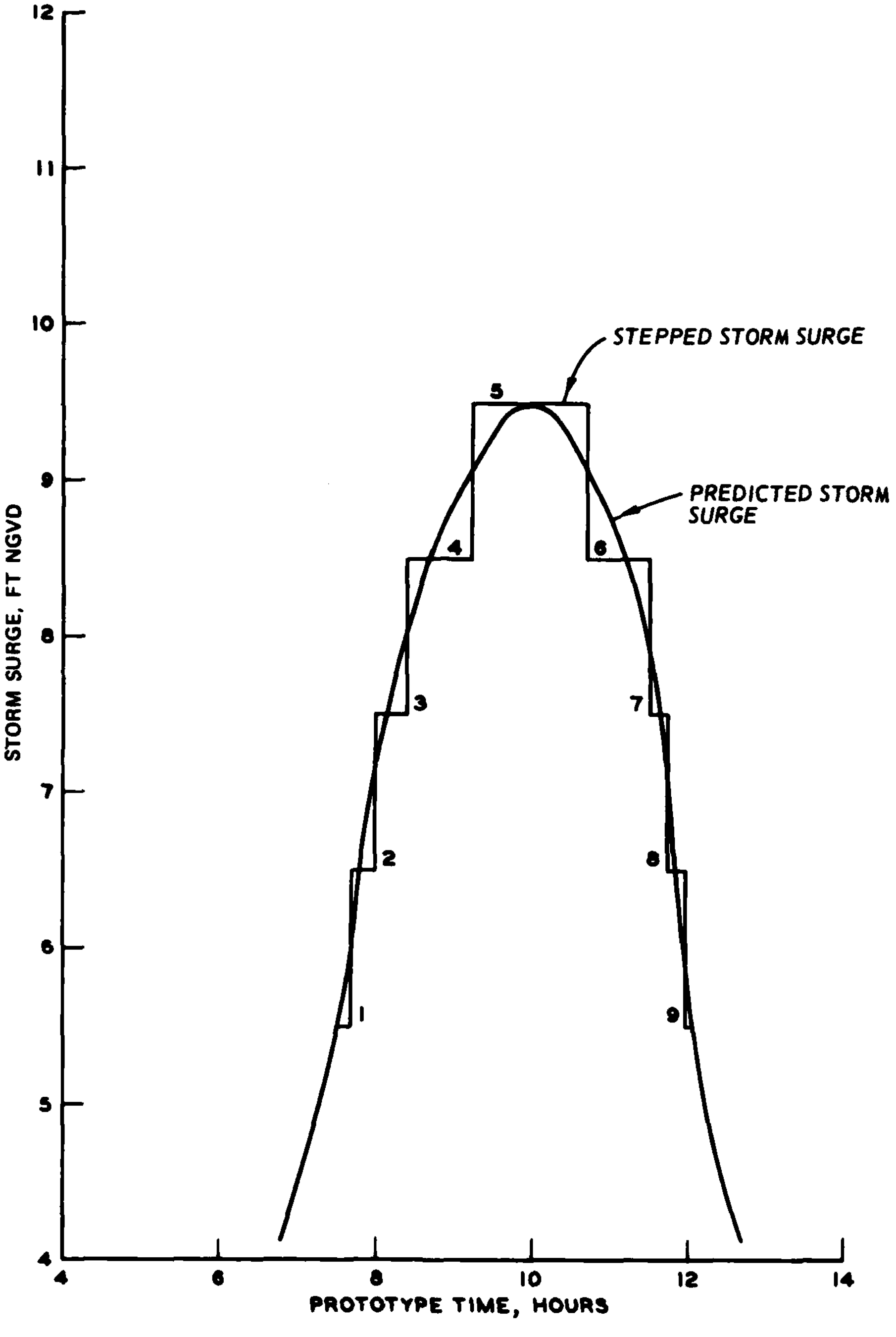

NOTE:

NUMBERS INDICATE HYDROGRAPH STEP NUMBER.

TEST CONDITIONS FOR EACH STEP ARE GIVEN IN TABLE 2.

STORM-SURGE HYDROGRAPH

MAXIMUM SURGE 9.5 FT NGVD

DESIGN SWL 5.5 FT NGVD

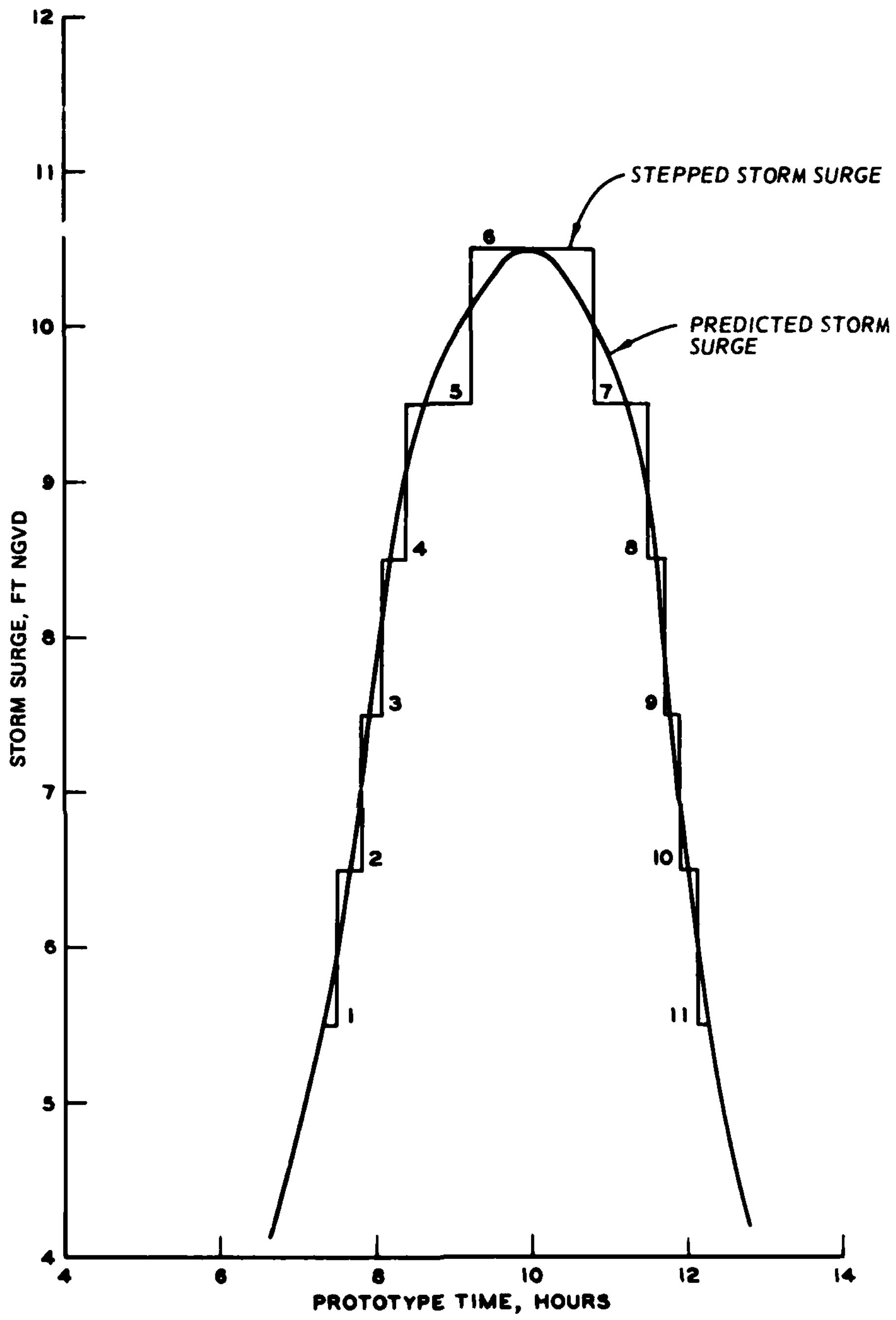

NOTE:
NUMBERS INDICATE HYDROGRAPH STEP NUMBER.
TEST CONDITIONS FOR EACH STEP ARE GIVEN IN TABLE 2.

STORM-SURGE HYDROGRAPH
MAXIMUM SURGE 10.5 FT NGVD
DESIGN SWL 5.5 FT NGVD

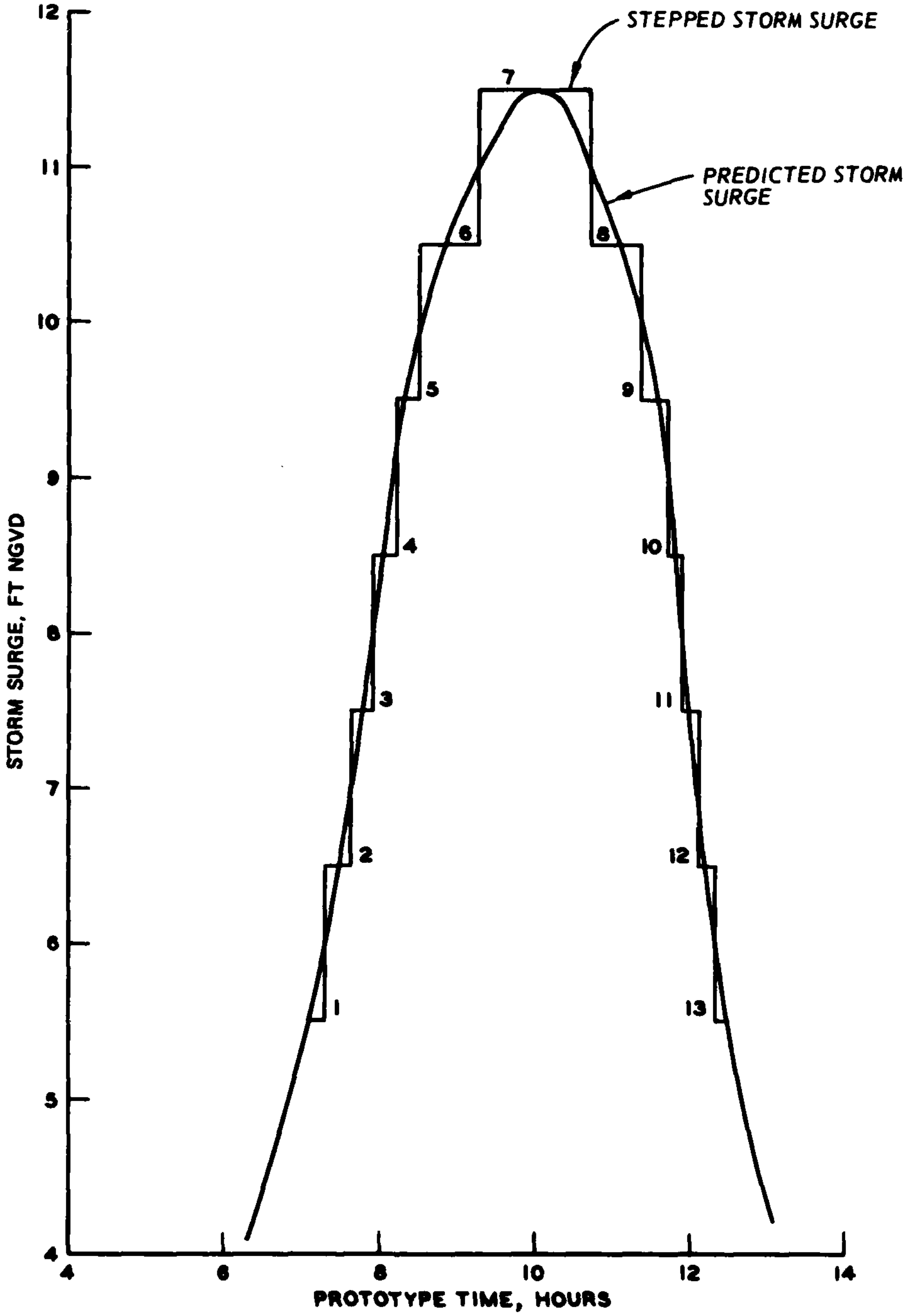

NOTE:

NUMBERS INDICATE HYDROGRAPH STEP NUMBER.

TEST CONDITIONS FOR EACH STEP ARE GIVEN IN TABLE 2.

STORM-SURGE HYDROGRAPH

MAXIMUM SURGE 11.5 FT NGVD

DESIGN SWL 5.5 FT NGVD

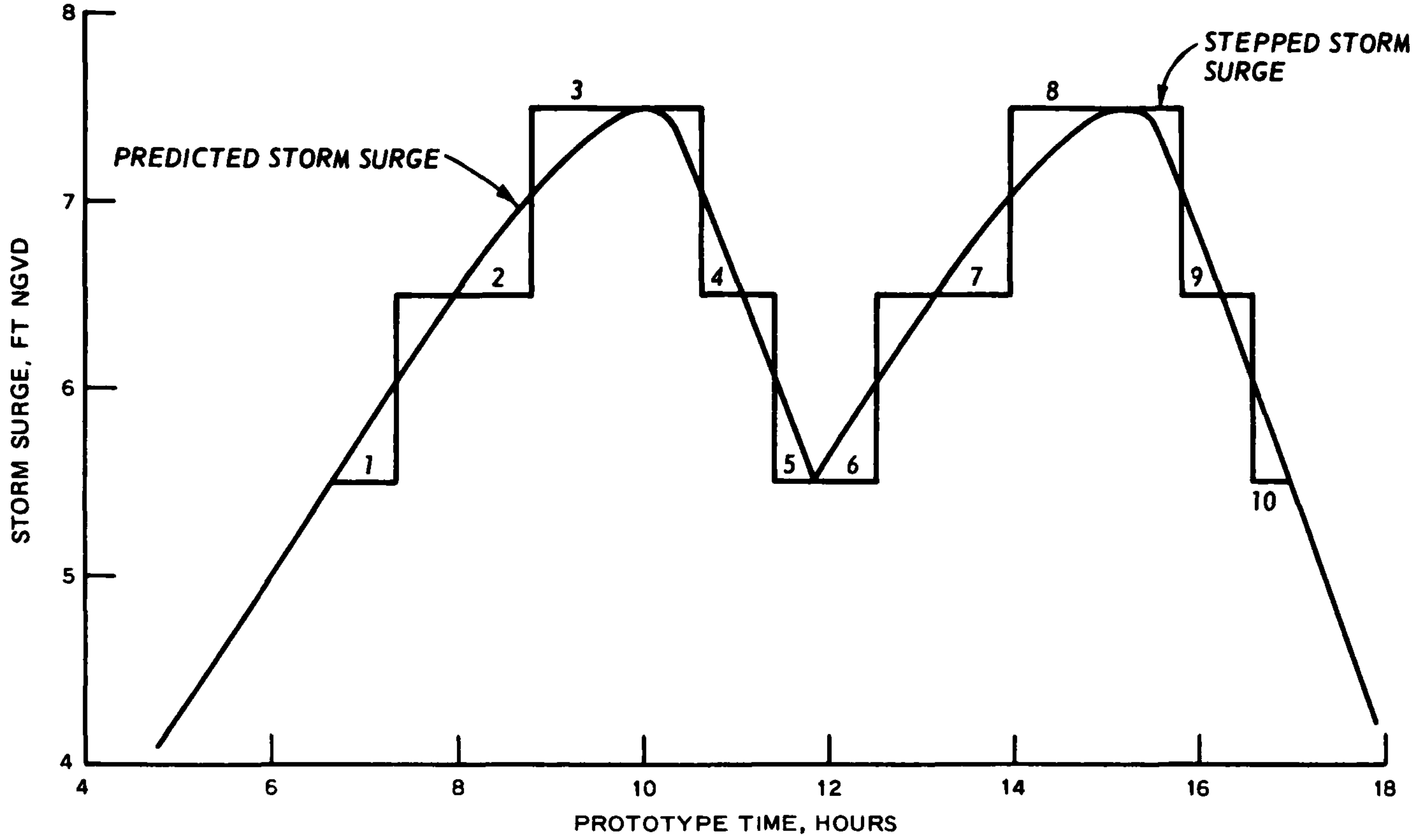

NOTE: NUMBERS INDICATE HYDROGRAPH STEP NUMBER

TEST CONDITIONS FOR EACH STEP ARE GIVEN IN TABLE 4

SIMULATION OF TWO SUCCESSIVE 7.5 FT NGVD HYDROGRAPHS

DESIGN SWL 5.5 FT NGVD

CHANNEL SIDE

SEA SIDE

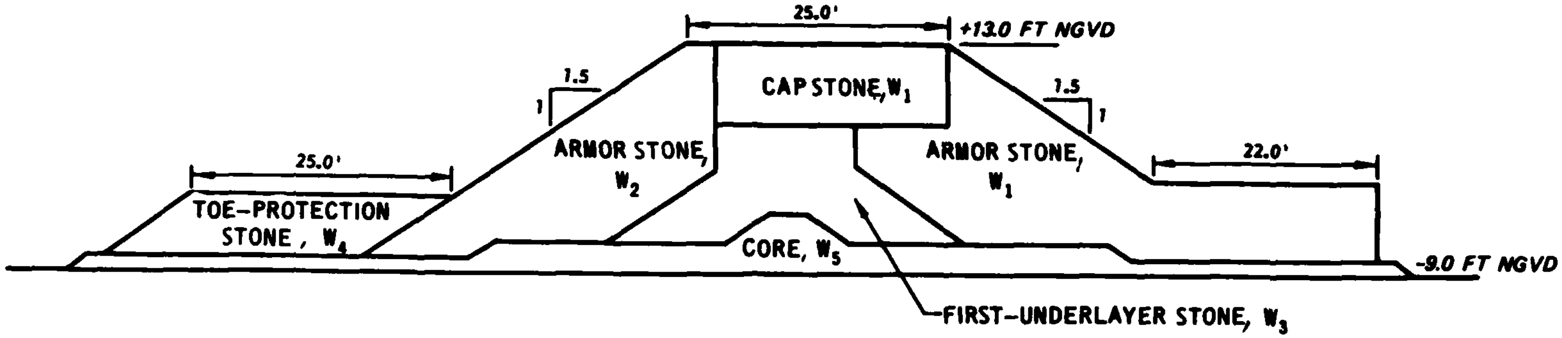

MATERIAL CHARACTERISTICS

MODEL	PROTOTYPE
W_1 = 1.05-LB STONE	W_1 = 22.0-TON STONE @ 165 PCF
W_2 = 0.55-LB STONE	W_2 = 11.5-TON STONE @ 165 PCF
W_3 = 0.08-LB STONE	W_3 = 1.68-TON STONE @ 165 PCF
W_4 = 0.095-LB STONE	W_4 = 2.0-TON STONE @ 165 PCF
W_5 = 0.00002- TO 0.004-LB STONE	W_5 = 1.0- TO 165-LB STONE @ 165 PCF

TYPICAL BREAKWATER CROSS SECTION

PLAN 4C

MODEL SCALE 1:33

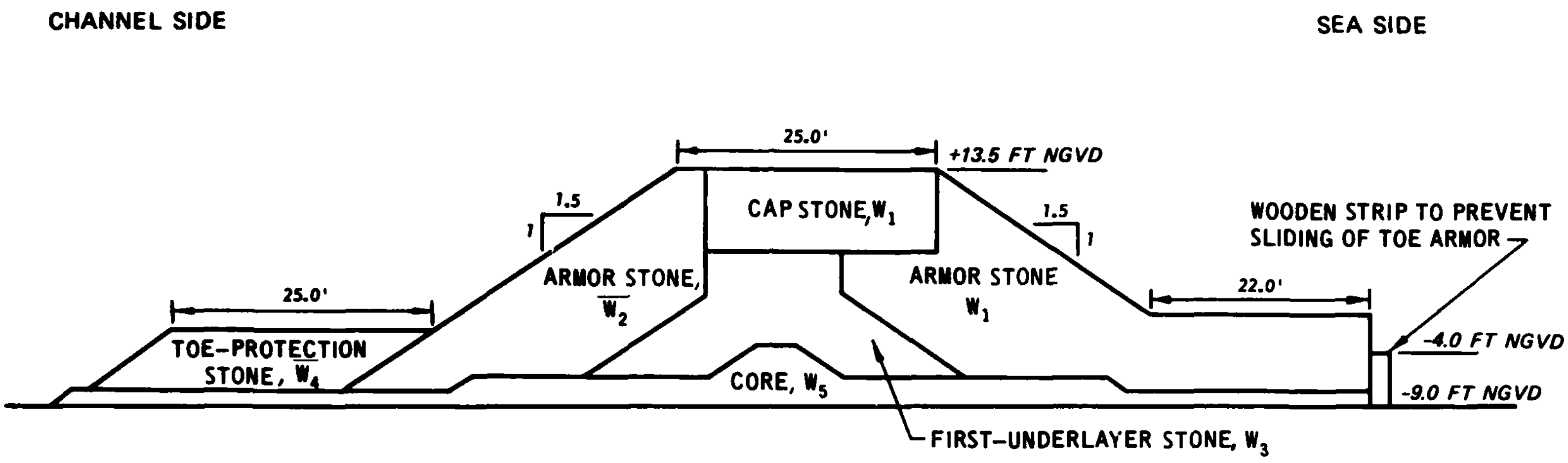

MATERIAL CHARACTERISTICS

MODEL	PROTOTYPE
W_1 = 1.05-LB STONE	W_1 = 22.0-TON STONE @ 165 PCF
W_2 = 0.55-LB STONE	W_2 = 11.5-TON STONE @ 165 PCF
W_3 = 0.08-LB STONE	W_3 = 1.68-TON STONE @ 165 PCF
W_4 = 0.095-LB STONE	W_4 = 2.0-TON STONE @ 165 PCF
W_5 = 0.00002- TO 0.004-LB STONE	W_5 = 1.0- TO 165-LB STONE @ 165 PCF

TYPICAL BREAKWATER CROSS SECTION

PLAN 4D

MODEL SCALE 1:33

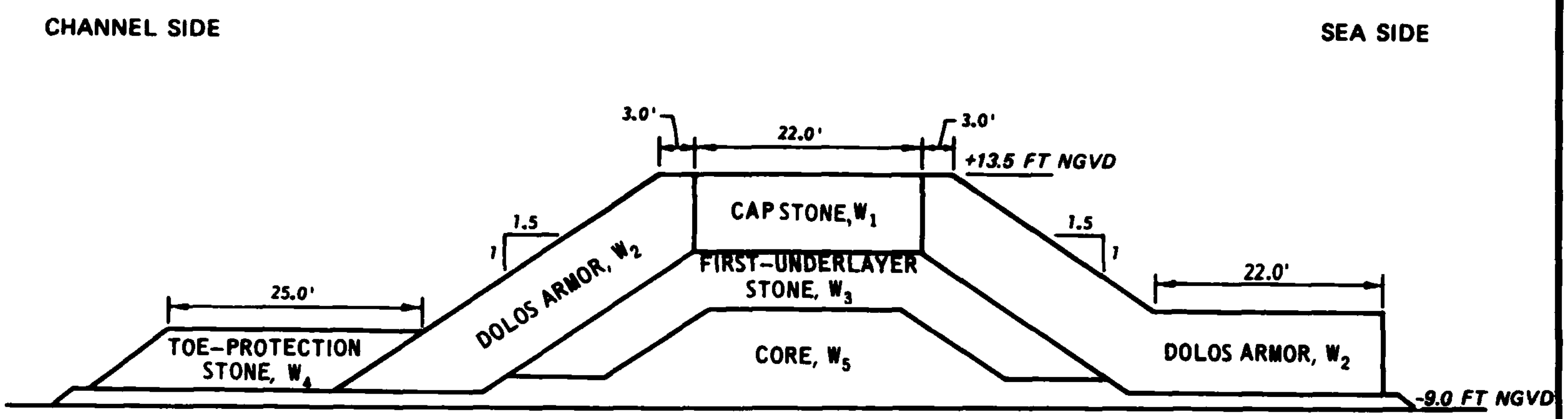

MATERIAL CHARACTERISTICS

MODEL	PROTOTYPE
W_1 = 1.05-LB STONE	W_1 = 22.0-TON STONE @ 165 PCF
W_2 = 0.31-LB DOLOS	W_2 = 5.0-TON DOLOS @ 150 PCF
W_3 = 0.062-LB STONE	W_3 = 1.0-TON STONE @ 165 PCF
W_4 = 0.095-LB STONE	W_4 = 2.0-TON STONE @ 165 PCF
W_5 = 0.00002- TO 0.004-LB STONE	W_5 = 1.0- TO 165-LB STONE @ 165 PCF

TYPICAL BREAKWATER CROSS SECTION

PLAN 9

MODEL SCALE 1:33

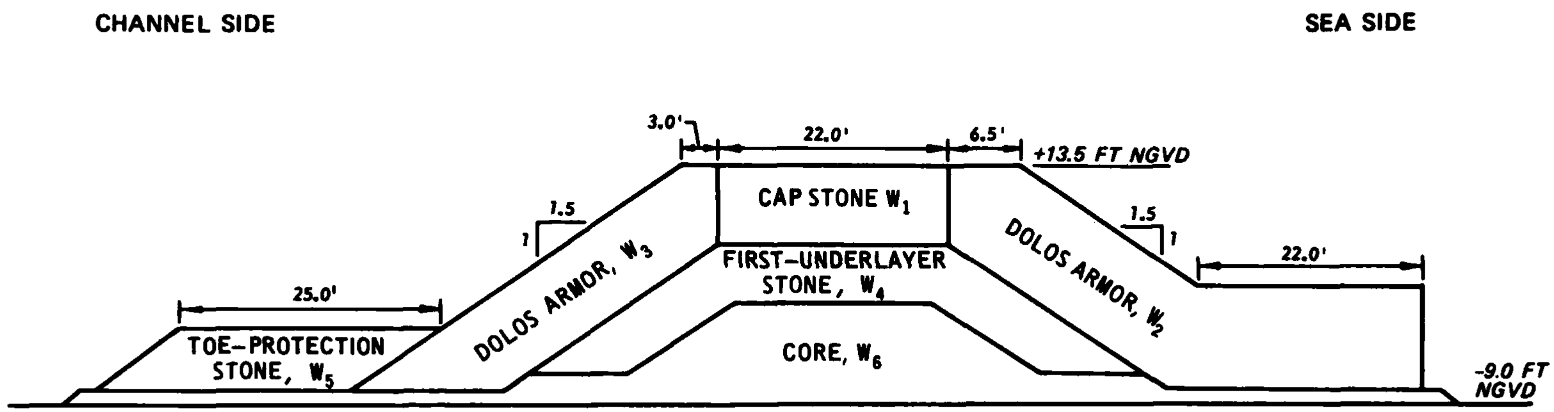

MATERIAL CHARACTERISTICS

MODEL	PROTOTYPE
W_1 = 1.05-LB STONE	W_1 = 22.0-TON STONE @ 165 PCF
W_2 = 0.59-LB DOLOS	W_2 = 9.25-TON DOLOS @ 150 PCF
W_3 = 0.31-LB DOLOS	W_3 = 5.0-TON DOLOS @ 150 PCF
W_4 = 0.062-LB STONE	W_4 = 1.0-TON STONE @ 165 PCF
W_5 = 0.095-LB STONE	W_5 = 2.0-TON STONE @ 165 PCF
W_6 = 0.00002- TO 0.004-LB STONE	W_6 = 1.0- TO 165-LB STONE @ 165 PCF

TYPICAL BREAKWATER CROSS SECTION

PLAN 10
MODEL SCALE 1:33

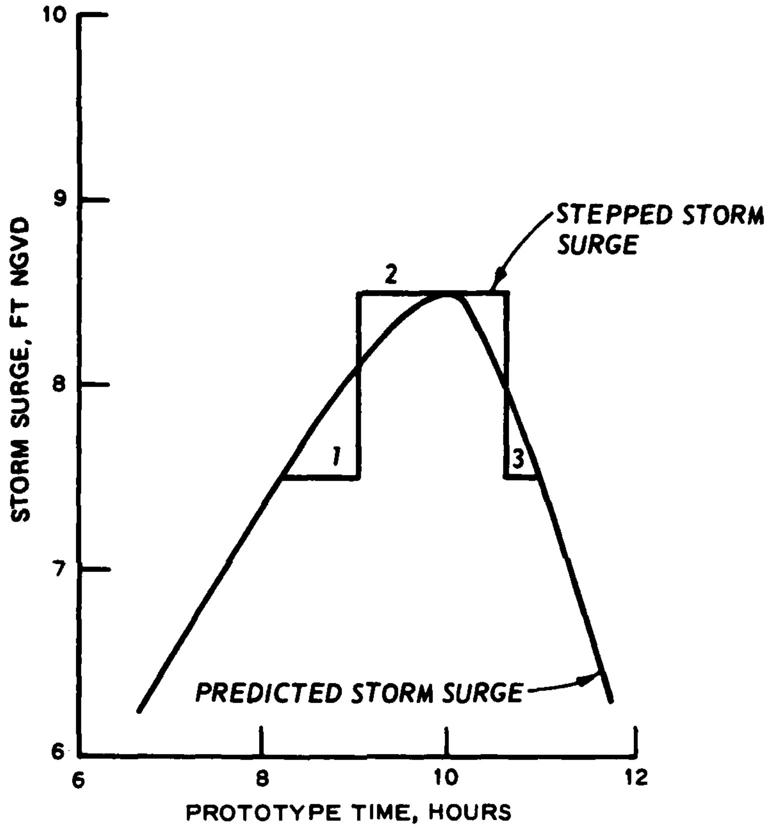

NOTE: NUMBERS INDICATE HYDROGRAPH STEP NUMBER

TEST CONDITIONS FOR EACH STEP ARE GIVEN IN TABLE 7

STORM-SURGE HYDROGRAPH

MAXIMUM SURGE 8.5 FT NGVD

DESIGN SWL 7.5 FT NGVD

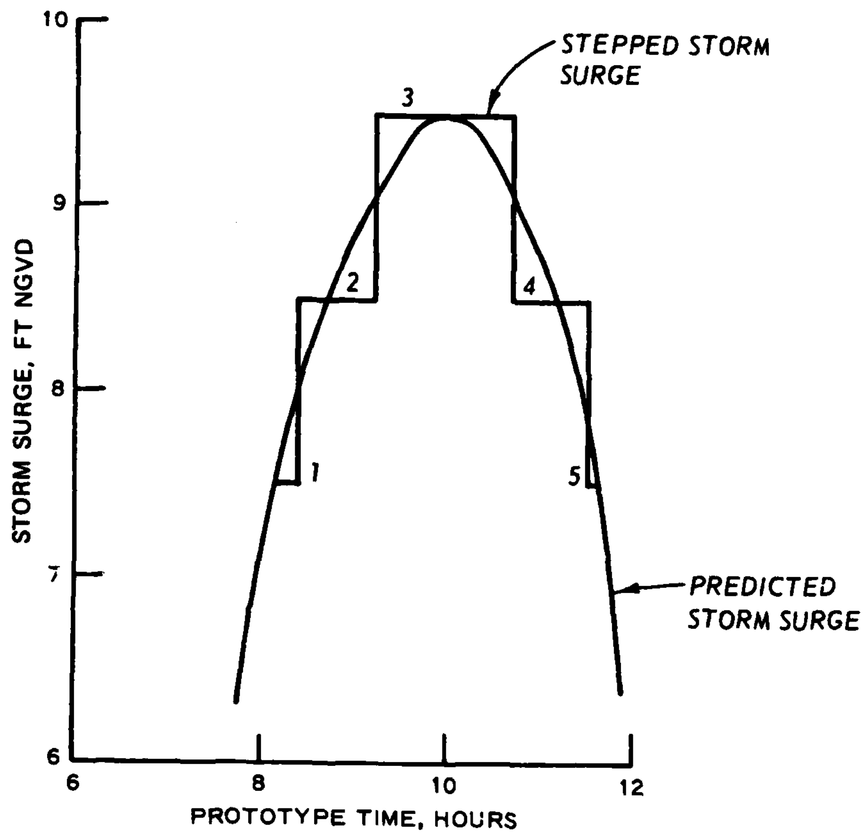

NOTE: NUMBERS INDICATE HYDROGRAPH STEP NUMBER

TEST CONDITIONS FOR EACH STEP ARE GIVEN IN TABLE 7

STORM-SURGE HYDROGRAPH

MAXIMUM SURGE 9.5 FT NGVD
DESIGN SWL 7.5 FT NGVD

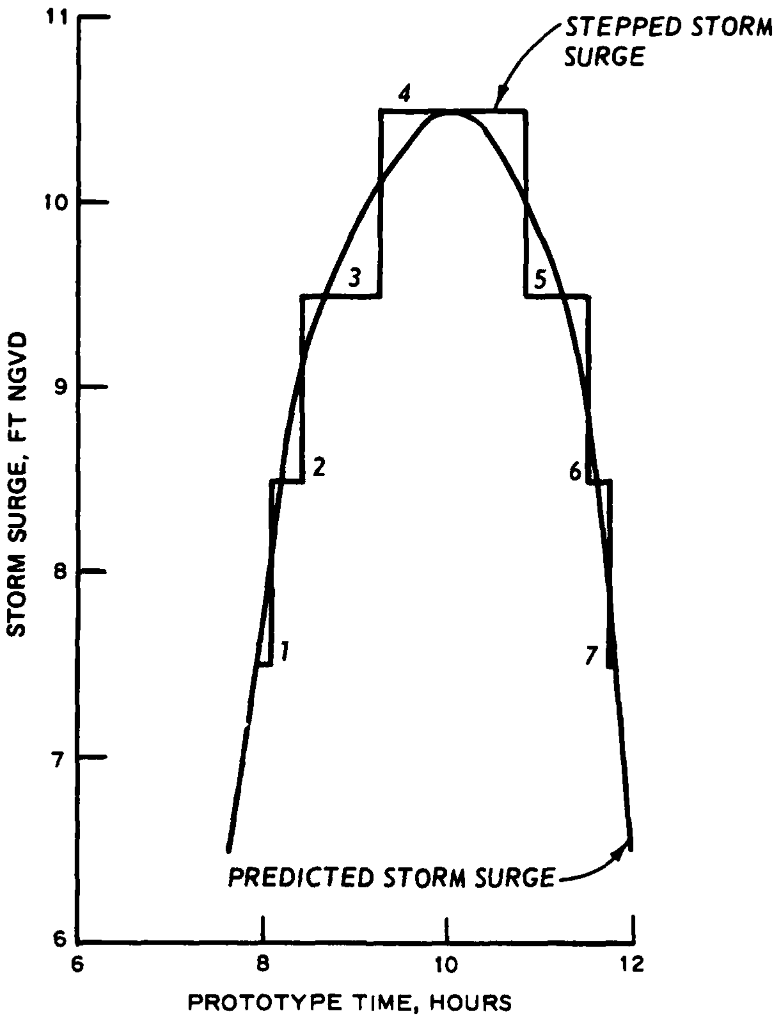

NOTE: NUMBERS INDICATE HYDROGRAPH STEP NUMBER

TEST CONDITIONS FOR EACH STEP ARE GIVEN IN TABLE 7

STORM-SURGE HYDROGRAPH

MAXIMUM SURGE 10.5 FT NGVD
DESIGN SWL 7.5 FT NGVD

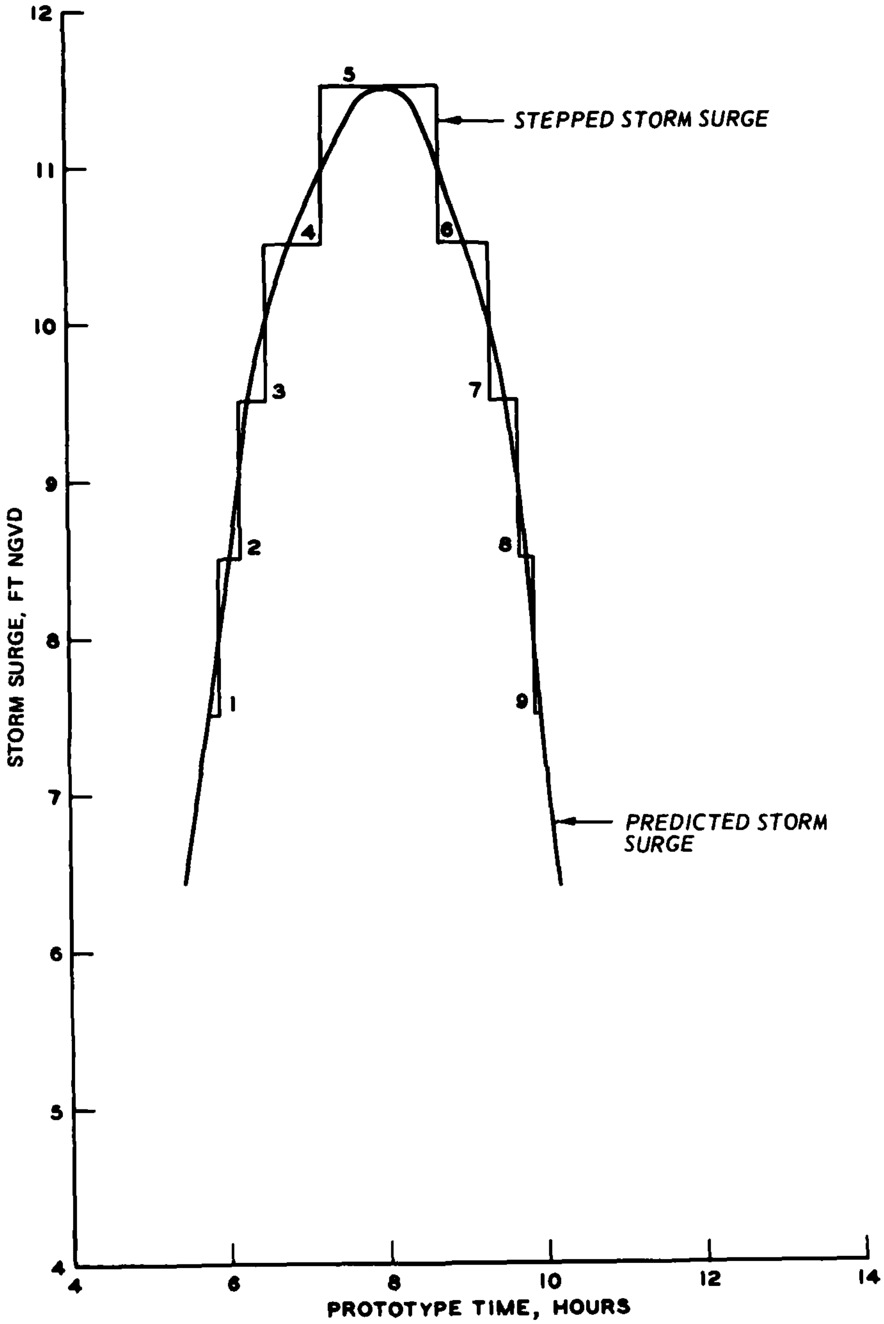

NOTE:
NUMBERS INDICATE HYDROGRAPH STEP NUMBER.
TEST CONDITIONS FOR EACH STEP ARE GIVEN IN TABLE 7.

STORM-SURGE HYDROGRAPH
MAXIMUM SURGE 11.5 FT NGVD
DESIGN SWL 7.5 FT NGVD

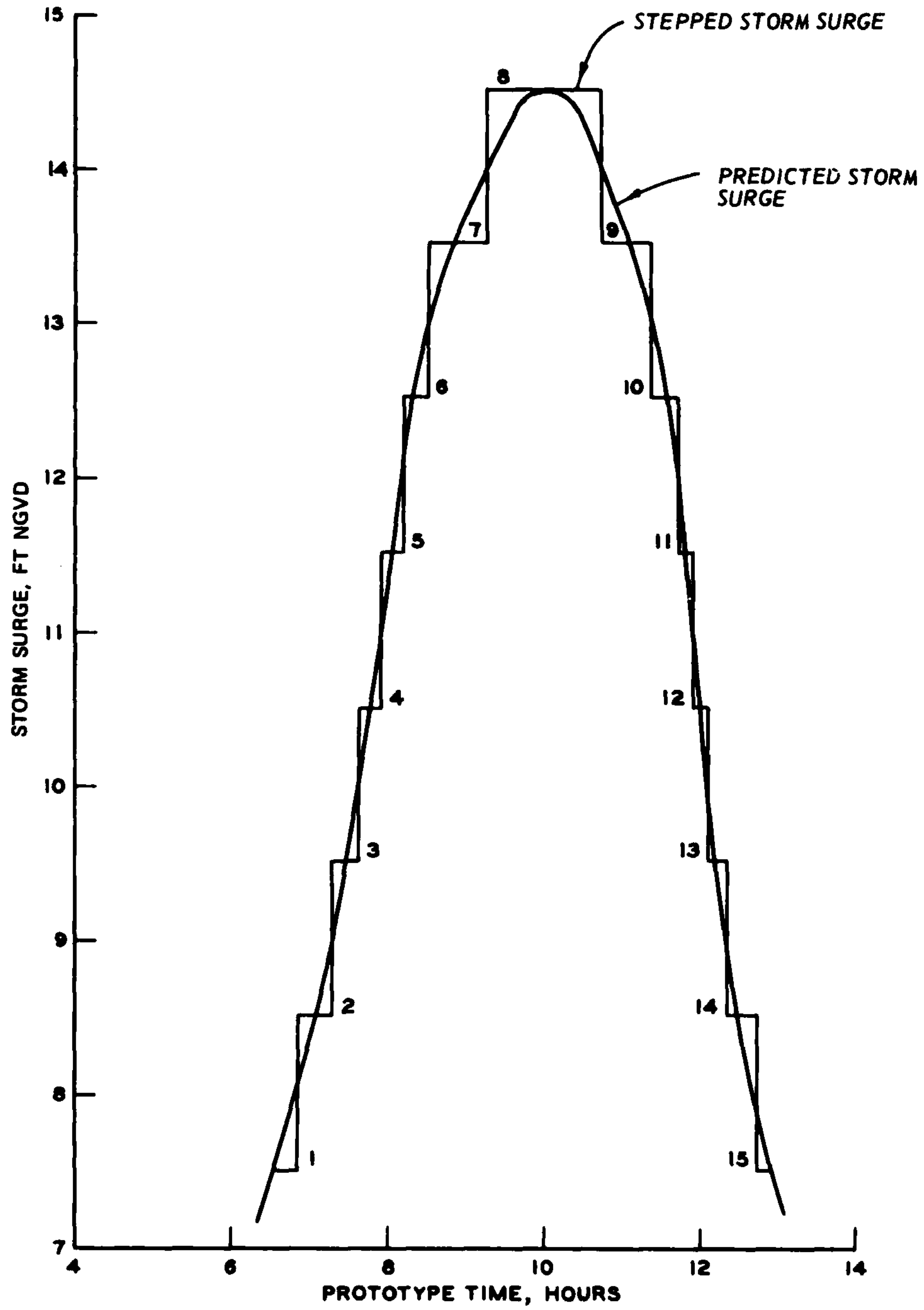

NOTE:

NUMBERS INDICATE HYDROGRAPH STEP NUMBER

TEST CONDITIONS FOR EACH STEP ARE GIVEN IN TABLE 7

STORM-SURGE HYDROGRAPH

MAXIMUM SURGE 14.5 FT NGVD
DESIGN SWL 7.5 FT NGVD

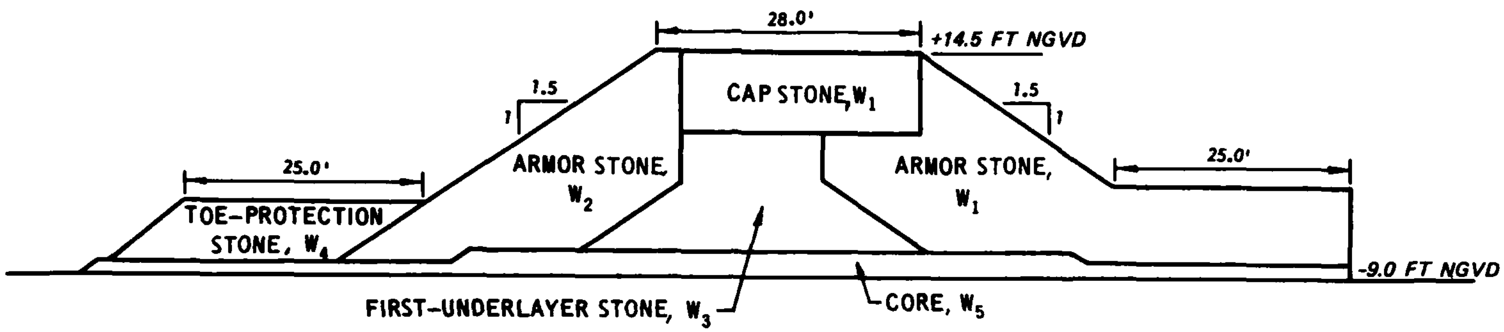

MATERIAL CHARACTERISTICS

MODEL	PROTOTYPE
W_1 = 1.45-LB STONE	W_1 = 30.5-TON STONE @ 165 PCF
W_2 = 0.71-LB STONE	W_2 = 15.0-TON STONE @ 165 PCF
W_3 = 0.11-LB STONE	W_3 = 2.3-TON STONE @ 165 PCF
W_4 = 0.095-LB STONE	W_4 = 2.0-TON STONE @ 165 PCF
W_5 = 0.00002- TO 0.004-LB STONE	W_5 = 1.0- TO 165-LB STONE @ 165 PCF

TYPICAL BREAKWATER CROSS SECTION

PLAN 4E

MODEL SCALE 1:33

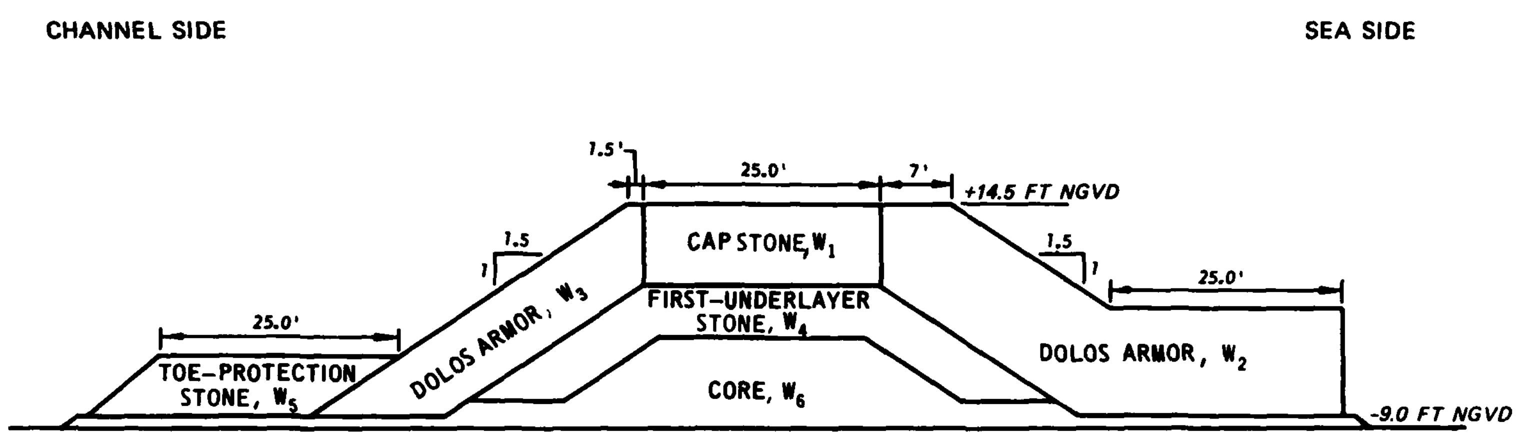

MATERIAL CHARACTERISTICS

MODEL	PROTOTYPE
W_1 = 1.45-LB STONE	W_1 = 30.5-TON STONE @ 165 PCF
W_2 = 0.86-LB DOLOS	W_2 = 12.5-TON DOLOS @ 150 PCF
W_3 = 0.31-LB DOLOS	W_3 = 5.0-TON DOLOS @ 150 PCF
W_4 = 0.062-LB STONE	W_4 = 1.0-TON STONE @ 165 PCF
W_5 = 0.095-LB STONE	W_5 = 2.0-TON STONE @ 165 PCF
W_6 = 0.00002- TO 0.004-LB STONE	W_6 = 1.0- TO 165-LB STONE @ 165 PCF

TYPICAL BREAKWATER CROSS SECTION

PLAN 11

MODEL SCALE 1:33

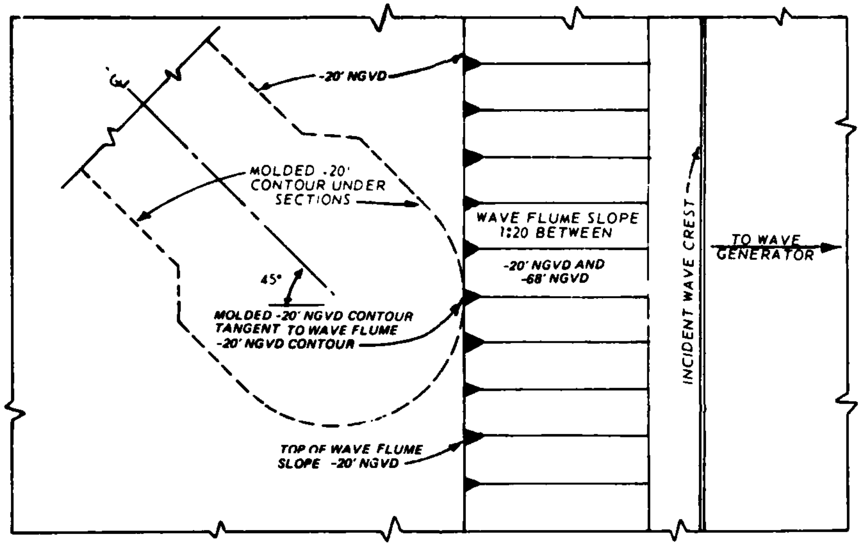

EXAMPLE OF MODEL SECTION ORIENTATION
IN WAVE FLUME FOR 45 DEG ANGLE
OF WAVE ATTACK

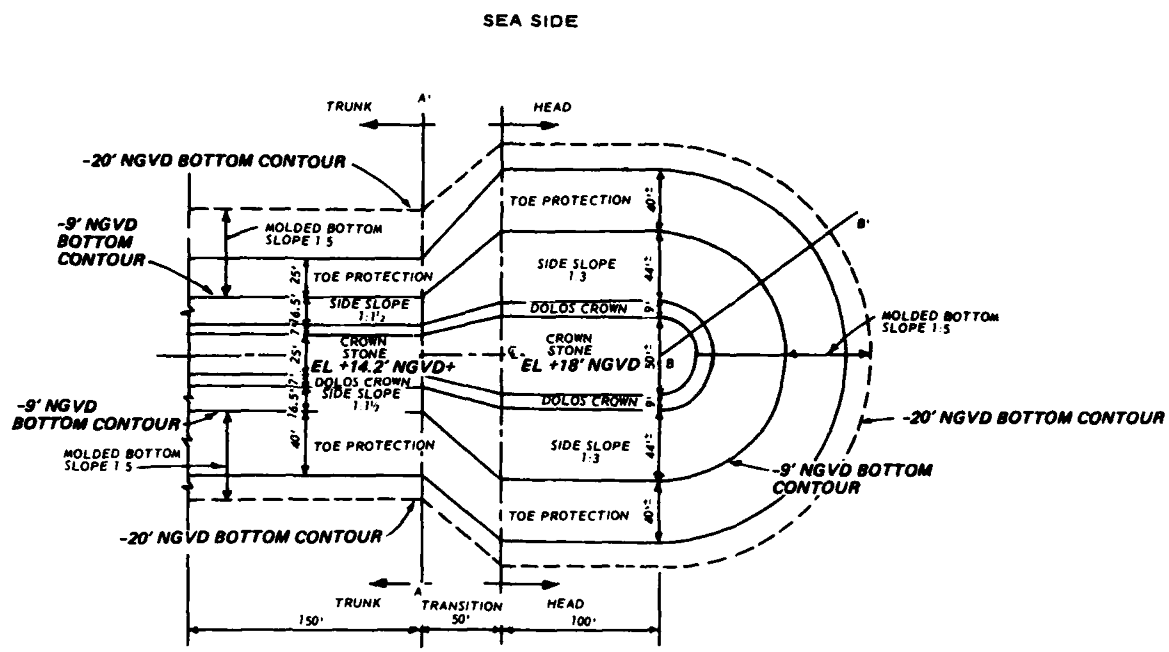

PLANS 3D-1 AND 3D-1A
PLAN VIEW
MODEL SCALE 1:48

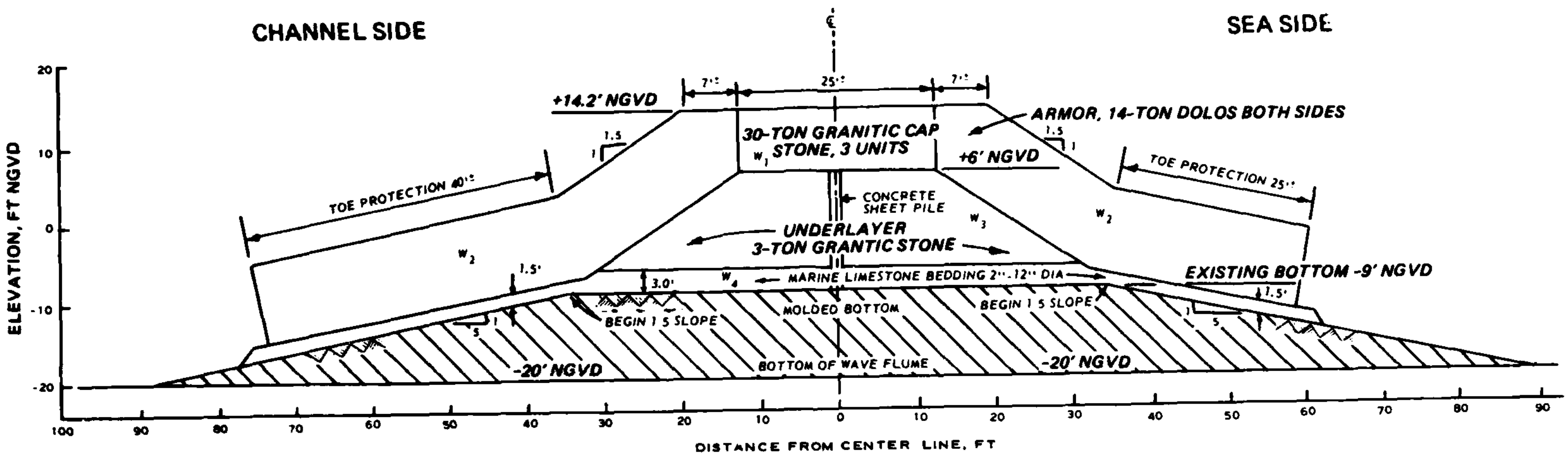

MATERIAL CHARACTERISTICS

MODEL	PROTOTYPE
W_1 = 0.46-LB STONE	W_1 = 30-TON STONE @ 165 PCF
W_2 = 0.28-LB DOLOS	W_2 = 14-TON DOLOS @ 150 PCF
W_3 = 0.046-LB STONE	W_3 = 3-TON STONE @ 165 PCF
W_4 = 0.000007-TO 0.001-LB STONE	W_4 = 1.0-TO 165.0-LB STONE @ 165 PCF

PLANS 3D-1, 3D-1A, 3D-1B, AND 3D-1C
SECTION A-A'
MODEL SCALE 1:48

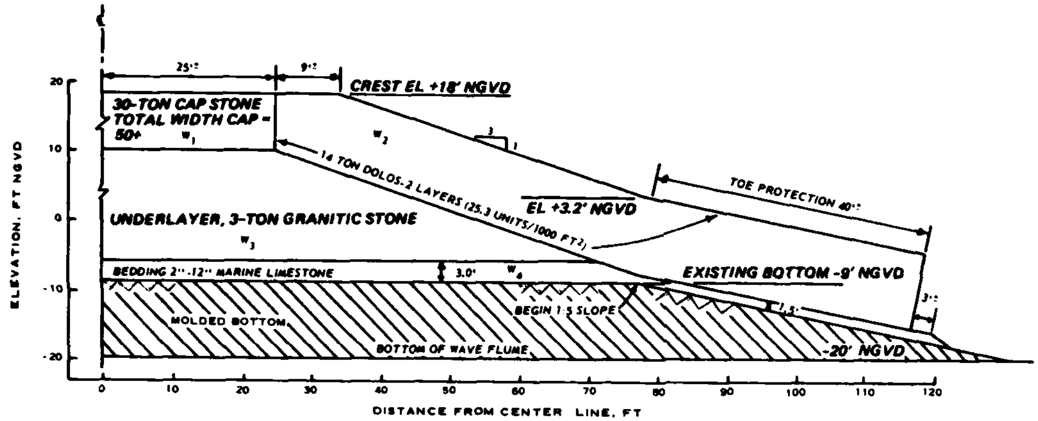

MATERIAL CHARACTERISTICS

MODEL	PROTOTYPE
W_1 = 0.46-LB STONE	W_1 = 30-TON STONE @ 165 PCF
W_2 = 0.28-LB DOLOS	W_2 = 14-TON DOLOS @ 150 PCF
W_3 = 0.046-LB STONE	W_3 = 3-TON STONE @ 165 PCF
W_4 = 0.000007-TO 0.001-LB STONE	W_4 = 1.0-TO 165.0-LB STONE @ 165 PCF

NOTE: HEAD SYMMETRICAL ABOUT CENTER LINE.

PLANS 3D-1, 3D-1A, AND 3D-1B
SECTION B-B'
MODEL SCALE 1:48

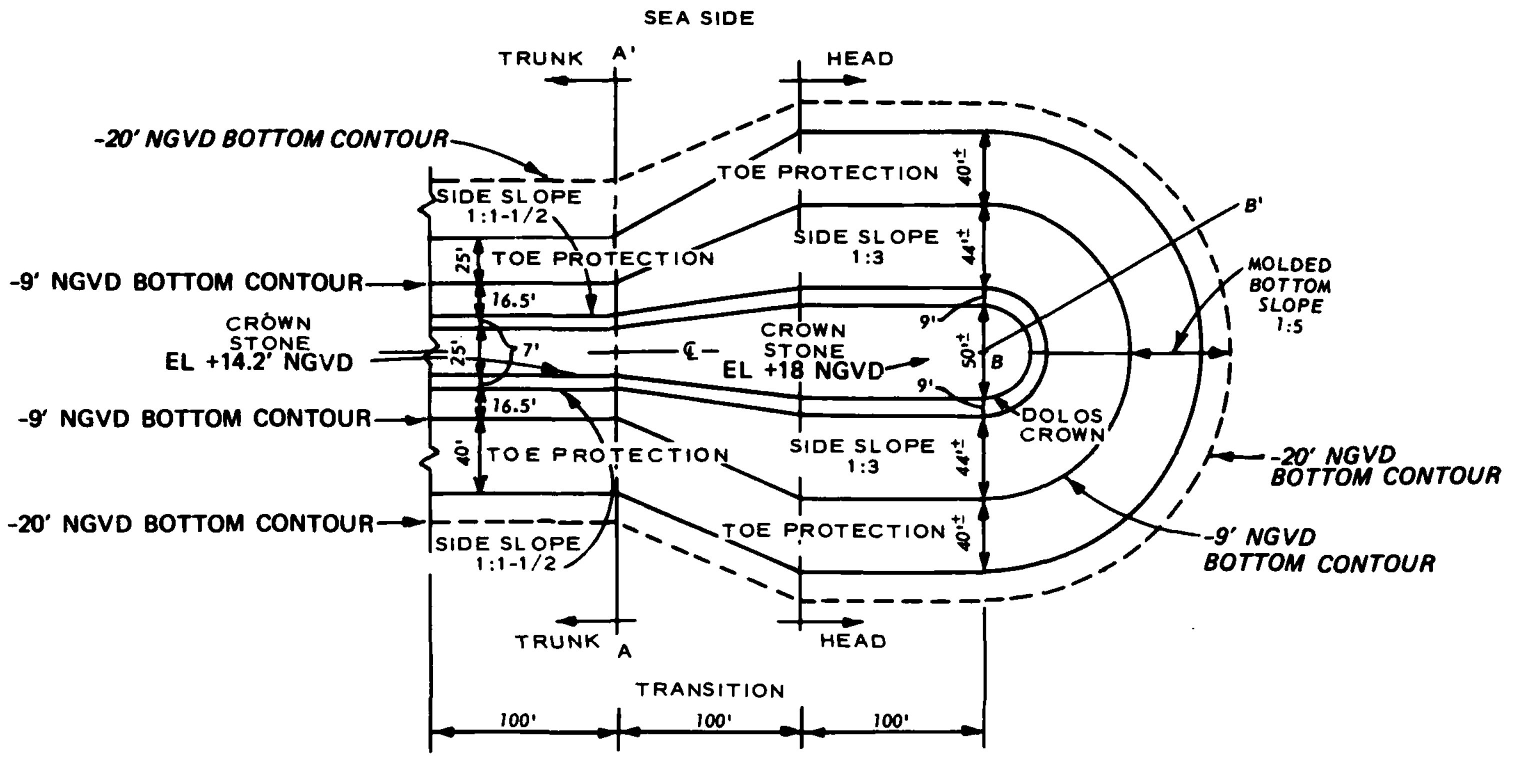

PLAN 3D-1B
PLAN VIEW
MODEL SCALE 1:48

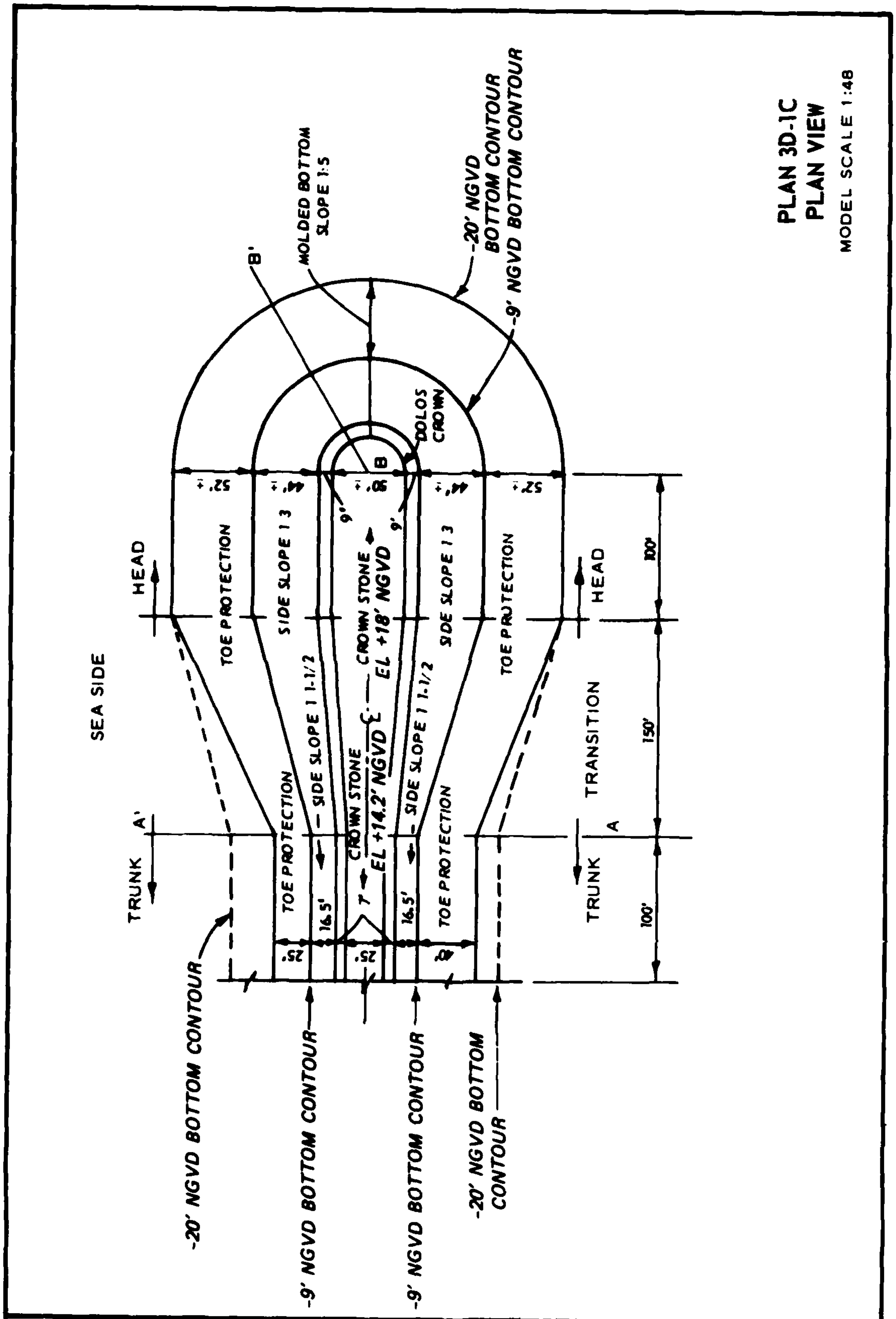

PLAN 3D-1C
PLAN VIEW
MODEL SCALE 1:48

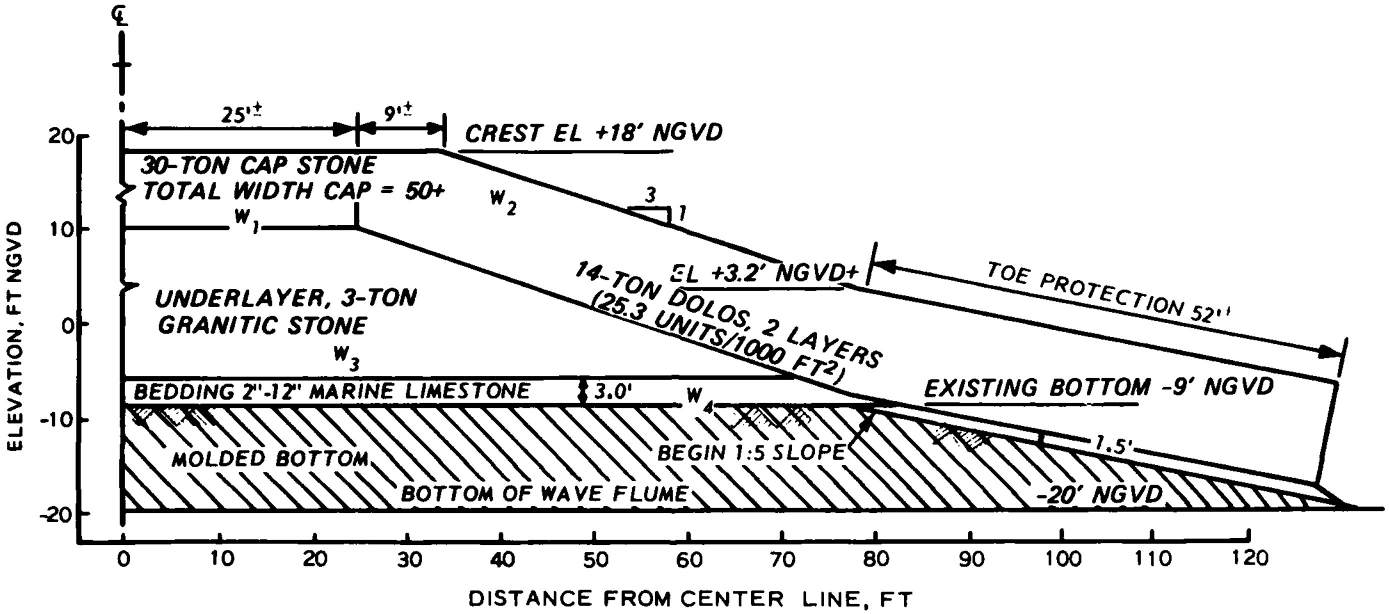

MATERIAL CHARACTERISTICS

MODEL	PROTOTYPE
W_1 = 0.46-LB STONE	W_1 = 30-TON STONE @ 165 PCF
W_2 = 0.28-LB DOLOS	W_2 = 14-TON DOLOS @ 150 PCF
W_3 = 0.046-LB STONE	W_3 = 3-TON STONE @ 165 PCF
W_4 = 0.000007- TO 0.001-LB STONE	W_4 = 1.0- TO 165.0-LB STONE @ 165 PCF

NOTE: HEAD SYMMETRICAL ABOUT CENTER LINE.

PLAN 3D-1C
SECTION B-B'
MODEL SCALE 1:48

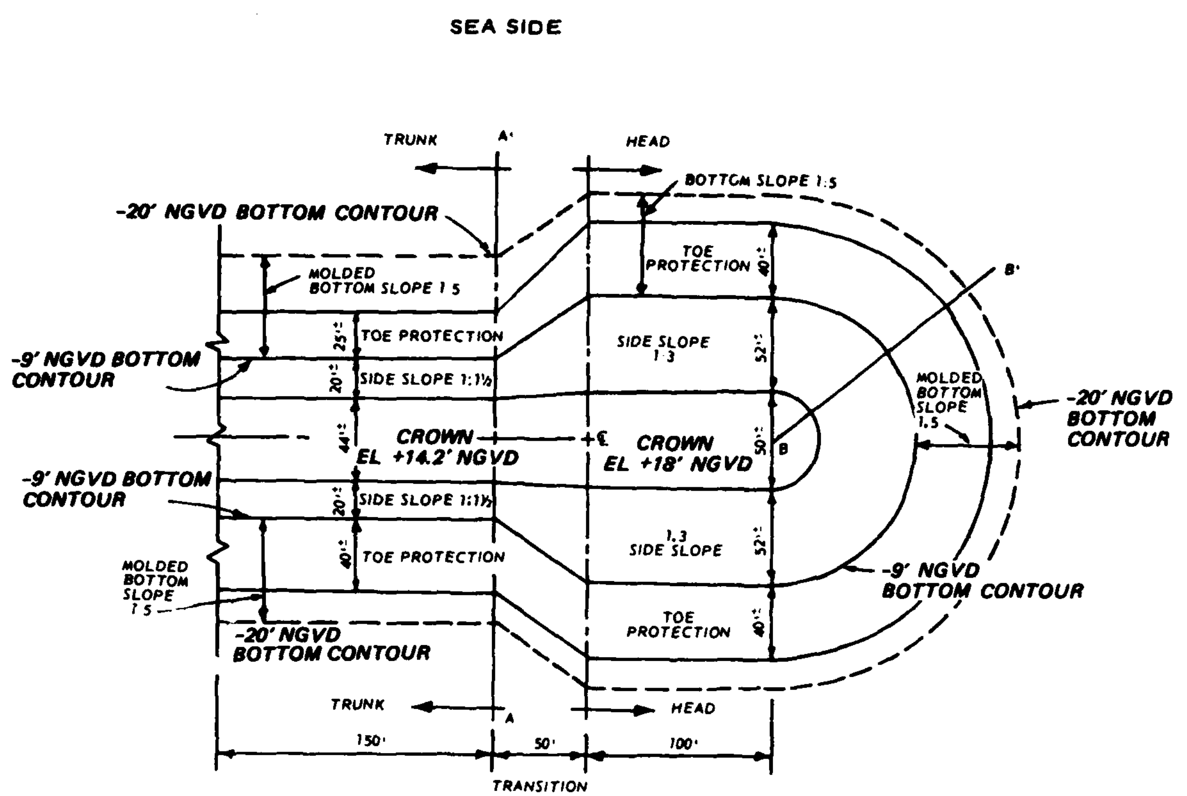

PLANS 3D-2 AND 3D-2A
PLAN VIEW
MODEL SCALE 1:48

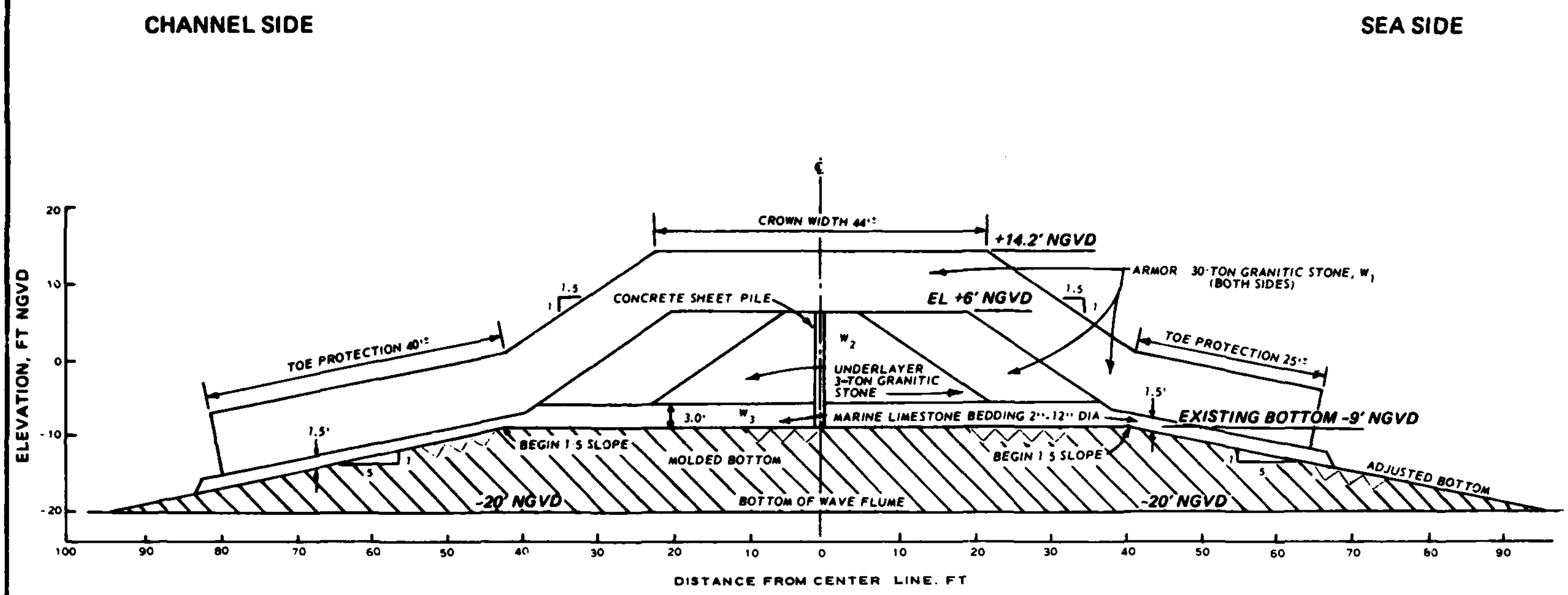

MATERIAL CHARACTERISTICS

MODEL	PROTOTYPE
W_1 = 0.46-LB STONE	W_1 = 30-TON STONE @ 165 PCF
W_2 = 0.046-LB STONE	W_2 = 3-TON STONE @ 165 PCF
W_3 = 0.000007-TO 0.001-LB STONE	W_3 = 1.0-TO 165.0-LB STONE @ 165 PCF

PLANS 3D-2, 3D-2A, 3D-2B, AND 3D-2C
SECTION A-A'
MODEL SCALE 1:48

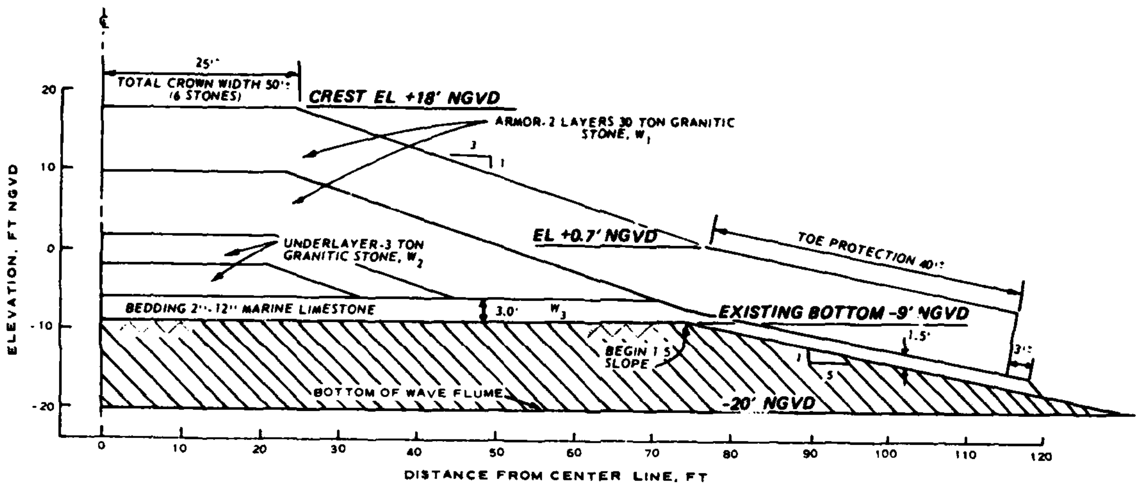

MATERIAL CHARACTERISTICS

MODEL	PROTOTYPE
W_1 = 0.46-LB STONE	W_1 = 30-TON STONE @ 165 PCF
W_2 = 0.046-LB STONE	W_2 = 3-TON STONE @ 165 PCF
W_3 = 0.000007- TO 0.001-LB STONE	W_3 = 1.0- TO 165.0-LB STONE @ 165 PCF

NOTE: HEAD SYMMETRICAL ABOUT CENTER LINE.

PLANS 3D-2 AND 3D-2A
SECTION B-B'
MODEL SCALE 1:48

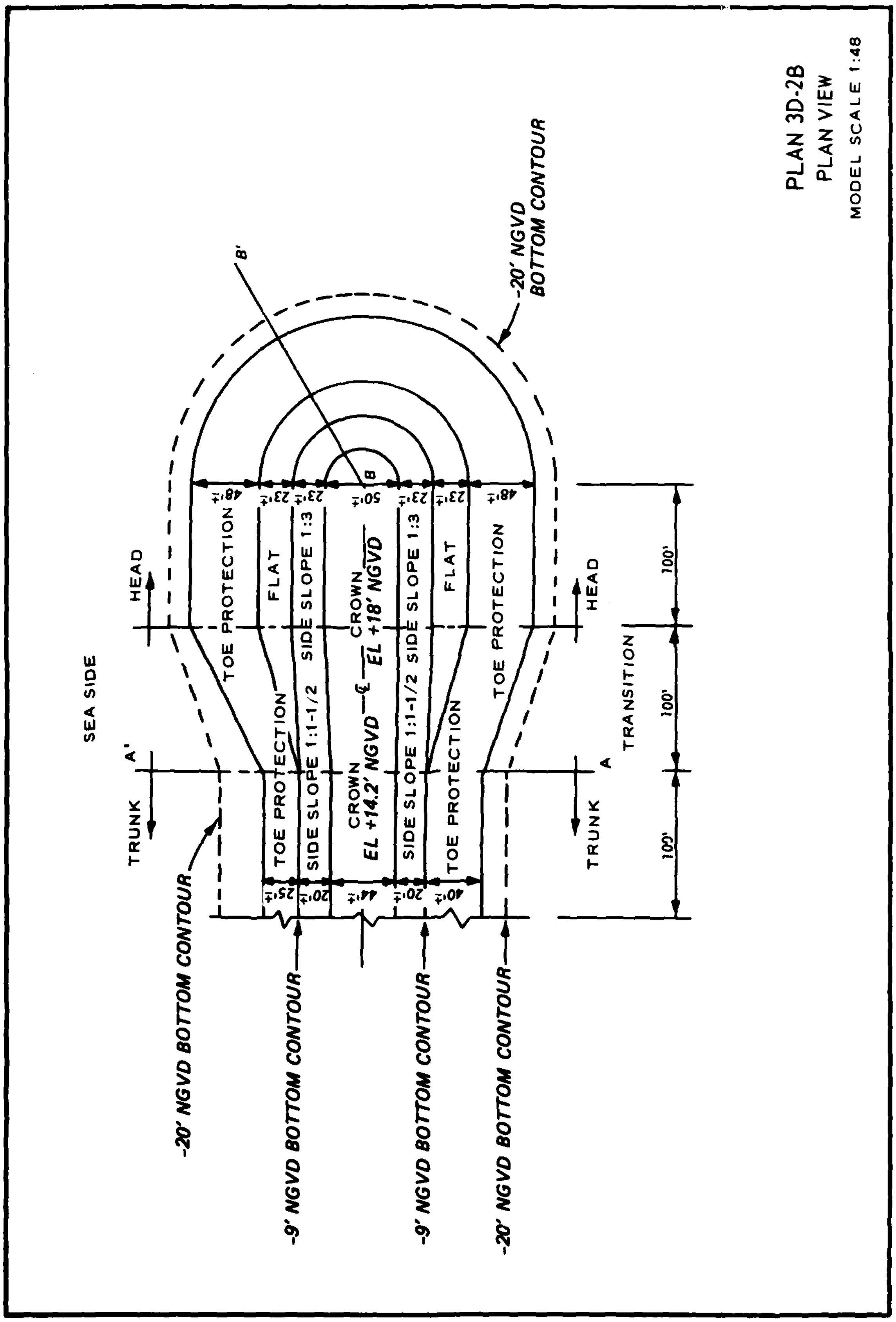
PLAN 3D-2B
PLAN VIEW
MODEL SCALE 1:48
SEA SIDE
HEAD
TRUNK
A'
A
B
B'
TRANSITION
100'
100'
100'
TOE PROTECTION
FLAT
SIDE SLOPE 1:3
CROWN
EL +18' NGVD
SIDE SLOPE 1:1-1/2
CROWN
EL +14.2' NGVD
48'±
23'±
50'±
25'±
20'±
44'±
40'±
-20' NGVD BOTTOM CONTOUR
-9' NGVD BOTTOM CONTOUR

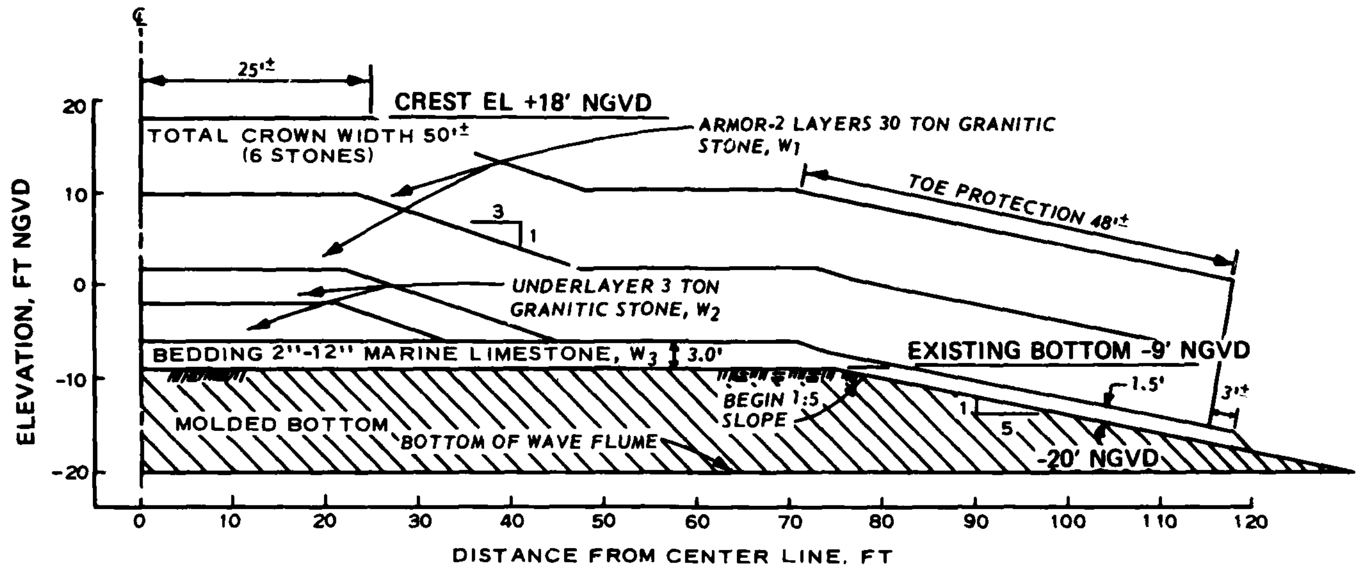

MATERIAL CHARACTERISTICS

MODEL	PROTOTYPE
W_1 = 0.46-LB STONE	W_1 = 30-TON STONE @ 165 PCF
W_2 = 0.046-LB STONE	W_2 = 3-TON STONE @ 165 PCF
W_3 = 0.000007- TO 0.001-LB STONE	W_3 = 1.0- TO 165.0-LB STONE @ 165 PCF

NOTE: HEAD SYMMETRICAL ABOUT CENTER LINE

PLAN 3D-2B
SECTION B-B'
MODEL SCALE 1:48

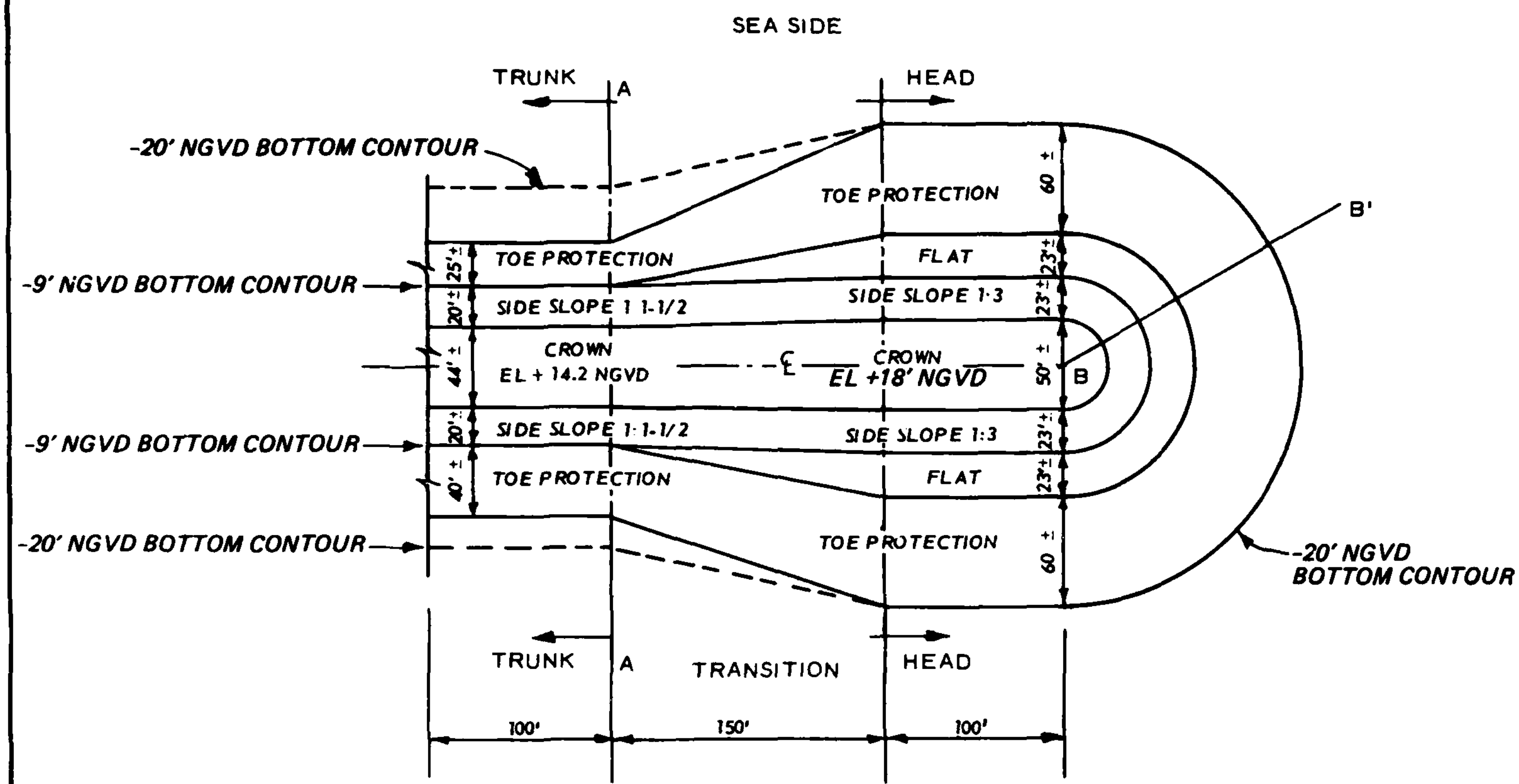

PLAN 3D-2C
PLAN VIEW
MODEL SCALE 1:48

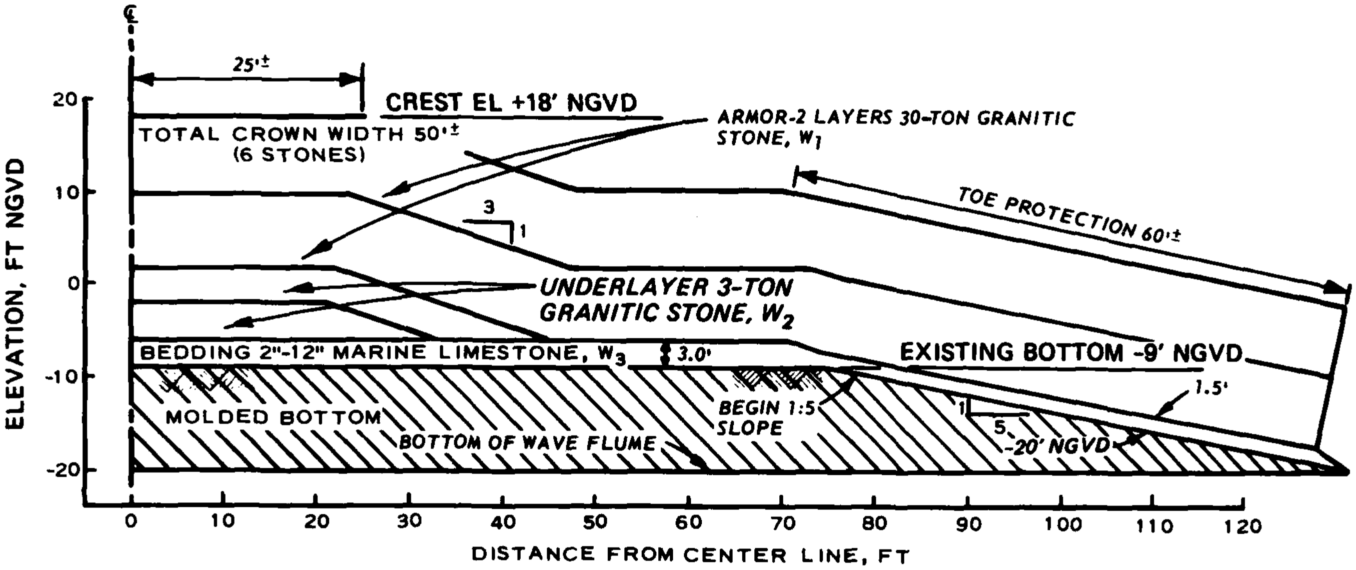

MATERIAL CHARACTERISTICS

MODEL	PROTOTYPE
W_1 = 0.46-LB STONE	W_1 = 30-TON STONE @ 165 PCF
W_2 = 0.046-LB STONE	W_2 = 3-TON STONE @ 165 PCF
W_3 = 0.000007- TO 0.001-LB STONE	W_3 = 1.0- TO 165.0-LB STONE @ 165 PCF

NOTE: HEAD SYMMETRICAL ABOUT CENTER LINE

PLAN 3D-2C
SECTION B-B'
MODEL SCALE 1:48

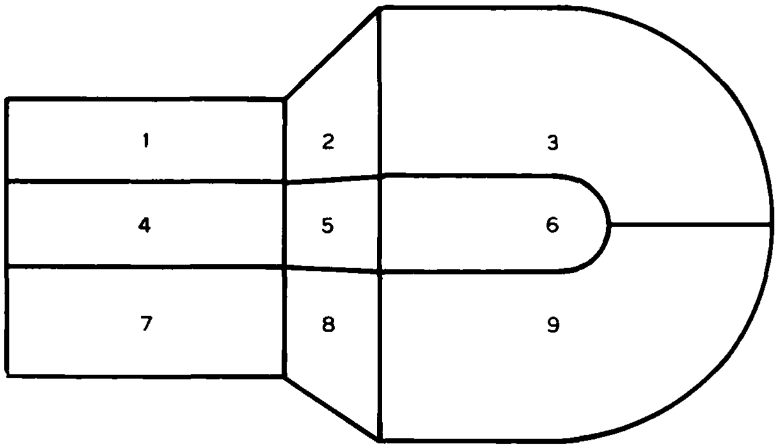

AREA NUMBER	SEGMENT	ARMOR AREA
1	TRUNK	SEA SIDE
2	TRANSITION	SEA SIDE
3	HEAD	SEA SIDE
4	TRUNK	CROWN
5	TRANSITION	CROWN
6	HEAD	CROWN
7	TRUNK	BEACH SIDE
8	TRANSITION	BEACH SIDE
9	HEAD	BEACH SIDE

SUBDIVISION OF TYPICAL TEST
SECTION FOR DETERMINING
DAMAGE BY NUMBER
METHOD

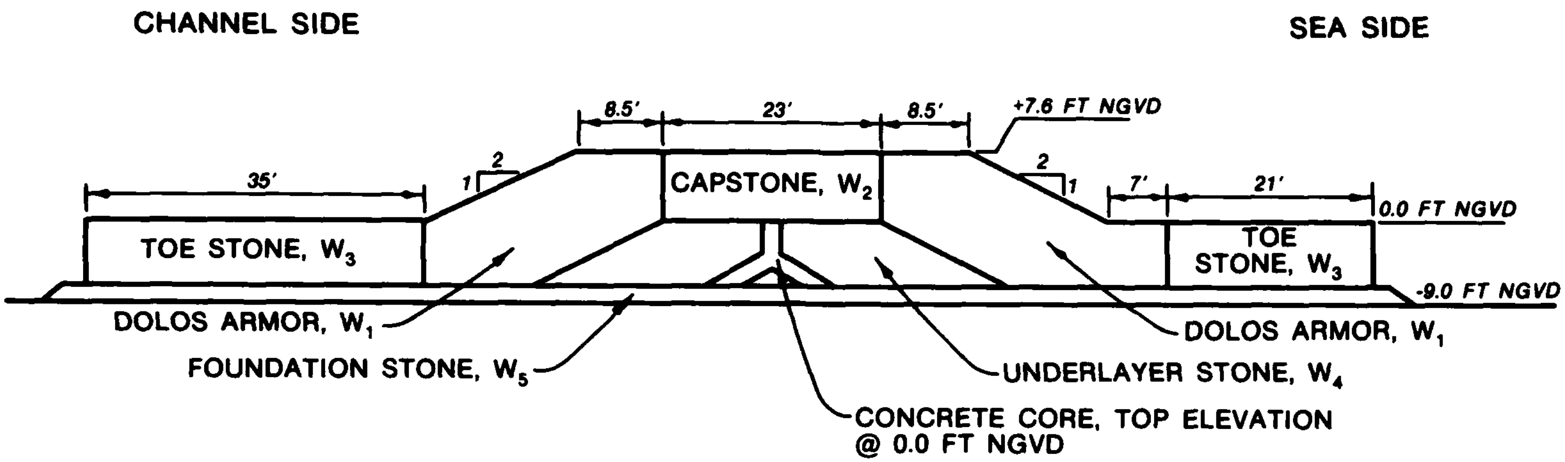

MATERIAL CHARACTERISTICS

MODEL	PROTOTYPE
W_1 = 0.59-LB DOLOS	W_1 = 10.5-TON DOLOS @ 140 PCF
W_2 = 1.42-LB STONE	W_2 = 24-TON STONE @ 165 PCF
W_3 = 1.13-LB STONE	W_3 = 19-TON STONE @ 165 PCF
W_4 = 0.024-LB STONE	W_4 = 3,500-LB STONE @ 120 PCF
W_5 = 0.000007- TO 0.00083-LB STONE	W_5 = 1.0- TO 120-LB STONE @ 120 PCF

TYPICAL BREAKWATER CROSS SECTION
PLAN 12
MODEL SCALE 1:31

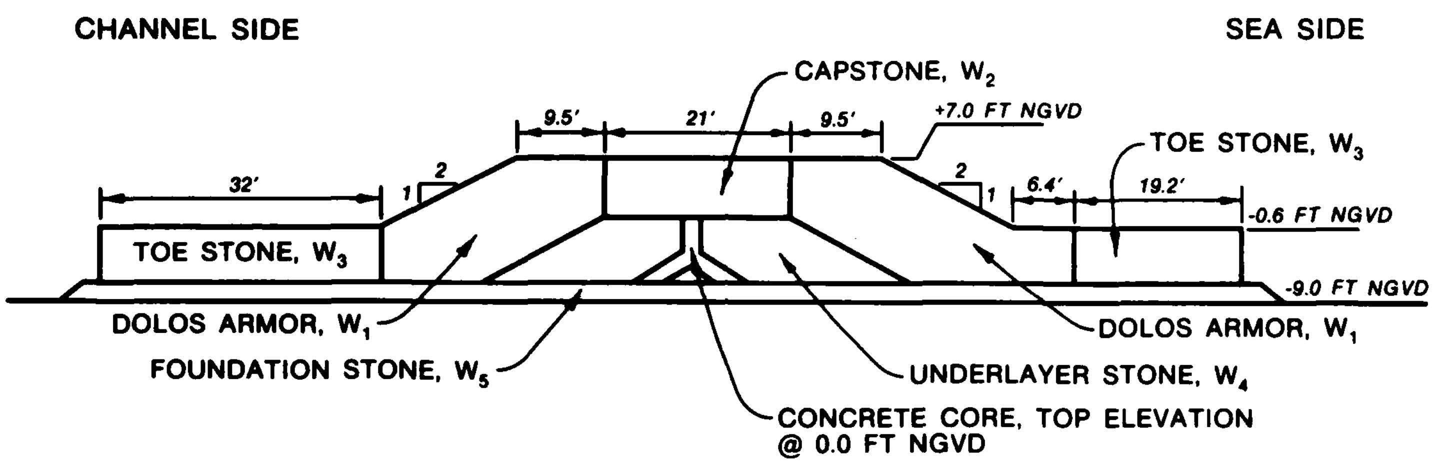

MATERIAL CHARACTERISTICS

MODEL	PROTOTYPE
W_1 = 0.59-LB DOLOS	W_1 = 10.5-TON DOLOS @ 140 PCF
W_2 = 1.13-LB STONE	W_2 = 19-TON STONE @ 165 PCF
W_3 = 0.86-LB STONE	W_3 = 14.5-TON STONE @ 165 PCF
W_4 = 0.024-LB STONE	W_4 = 3,500-LB STONE @ 120 PCF
W_5 = 0.000007- TO 0.00083-LB STONE	W_5 = 1.0- TO 120-LB STONE @ 120 PCF

TYPICAL BREAKWATER CROSS SECTION
PLAN 13
MODEL SCALE 1:31

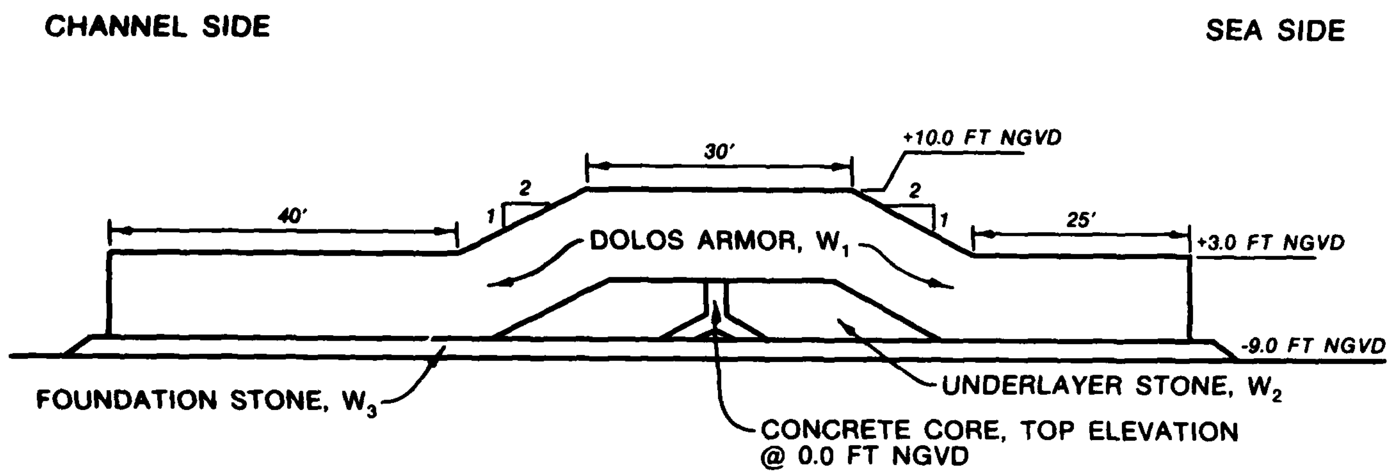

MATERIAL CHARACTERISTICS

MODEL	PROTOTYPE
W_1 = 0.59-LB DOLOS	W_1 = 10.5-TON DOLOS @ 140 PCF
W_2 = 0.024-LB STONE	W_2 = 3,500-LB STONE @ 120 PCF
W_3 = 0.000007- TO 0.00083-LB STONE	W_3 = 1.0- TO 120-LB STONE @ 120 PCF

TYPICAL BREAKWATER CROSS SECTION
PLAN 14
MODEL SCALE 1:31

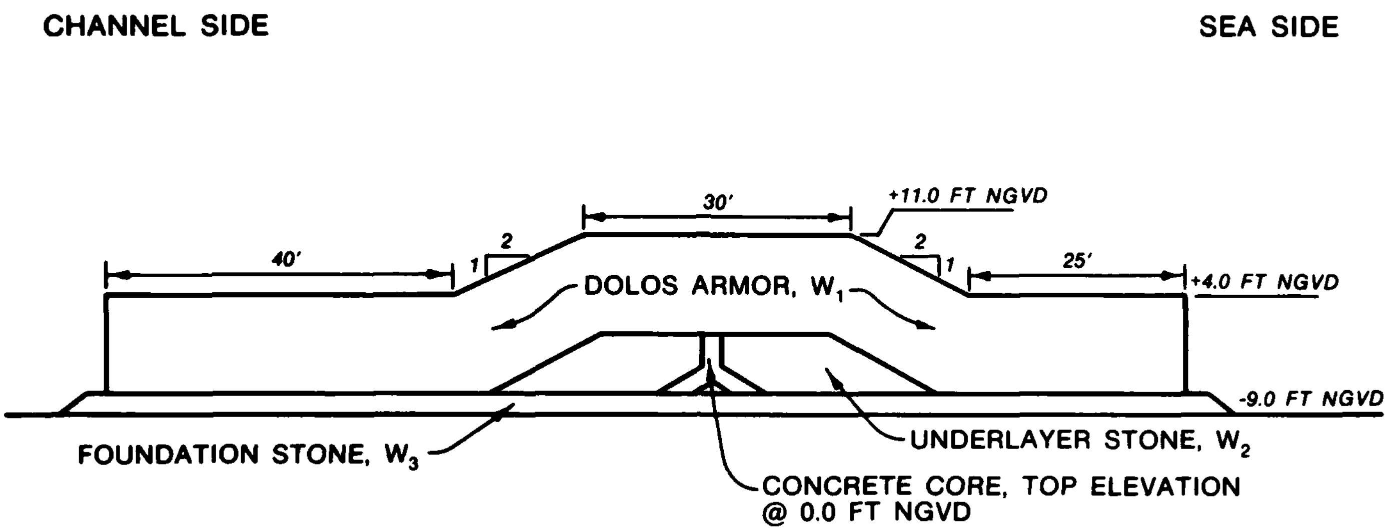

MATERIAL CHARACTERISTICS

MODEL	PROTOTYPE
W_1 = 0.86-LB DOLOS	W_1 = 14.0-TON DOLOS @ 140 PCF
W_2 = 0.031-LB STONE	W_2 = 4,500-LB STONE @ 120 PCF
W_3 = 0.000007- TO 0.00083-LB STONE	W_3 = 1.0- TO 120-LB STONE @ 120 PCF

TYPICAL BREAKWATER CROSS SECTION
PLAN 15
MODEL SCALE 1:31

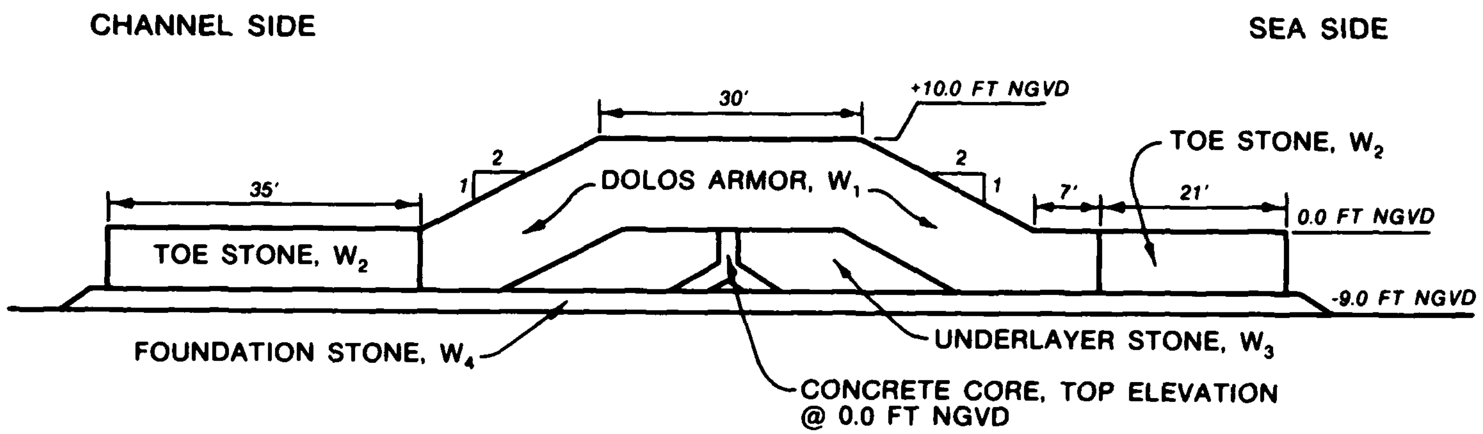

MATERIAL CHARACTERISTICS

MODEL	PROTOTYPE
W_1 = 0.59-LB DOLOS	W_1 = 10.5-TON DOLOS @ 140 PCF
W_2 = 1.13-LB STONE	W_2 = 19-TON STONE @ 165 PCF
W_3 = 0.024-LB STONE	W_3 = 3,500-LB STONE @ 120 PCF
W_4 = 0.000007- TO 0.00083-LB STONE	W_4 = 1.0- TO 120-LB STONE @ 120 PCF

TYPICAL BREAKWATER CROSS SECTION
PLAN 16
MODEL SCALE 1:31

APPENDIX A: COMPARISON OF JETTY CROSS SECTIONS BEFORE AND AFTER WAVE ATTACK

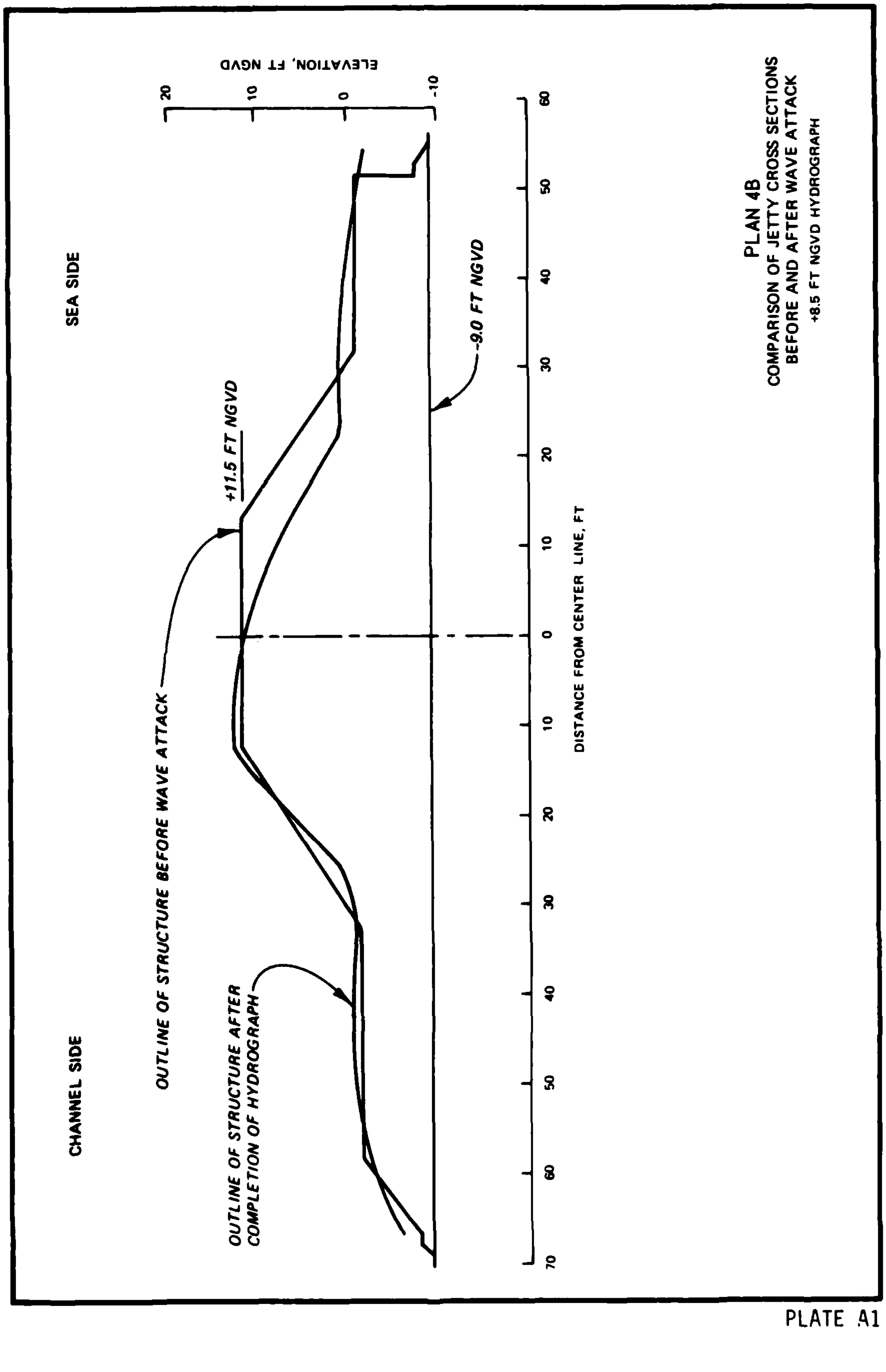

PLAN 4B
COMPARISON OF JETTY CROSS SECTIONS
BEFORE AND AFTER WAVE ATTACK
+8.5 FT NGVD HYDROGRAPH

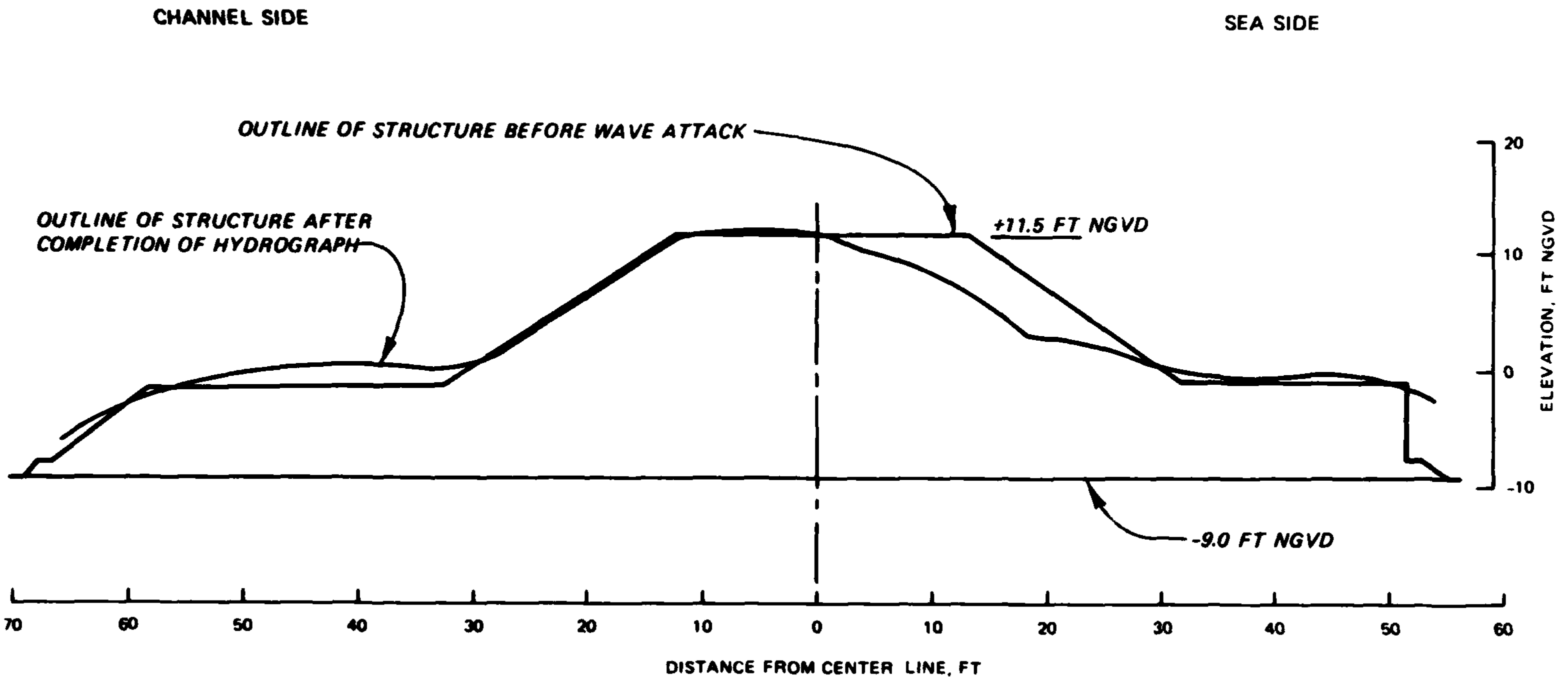

PLAN 4B
COMPARISON OF JETTY CROSS SECTIONS
BEFORE AND AFTER WAVE ATTACK
+9.5 FT NGVD HYDROGRAPH

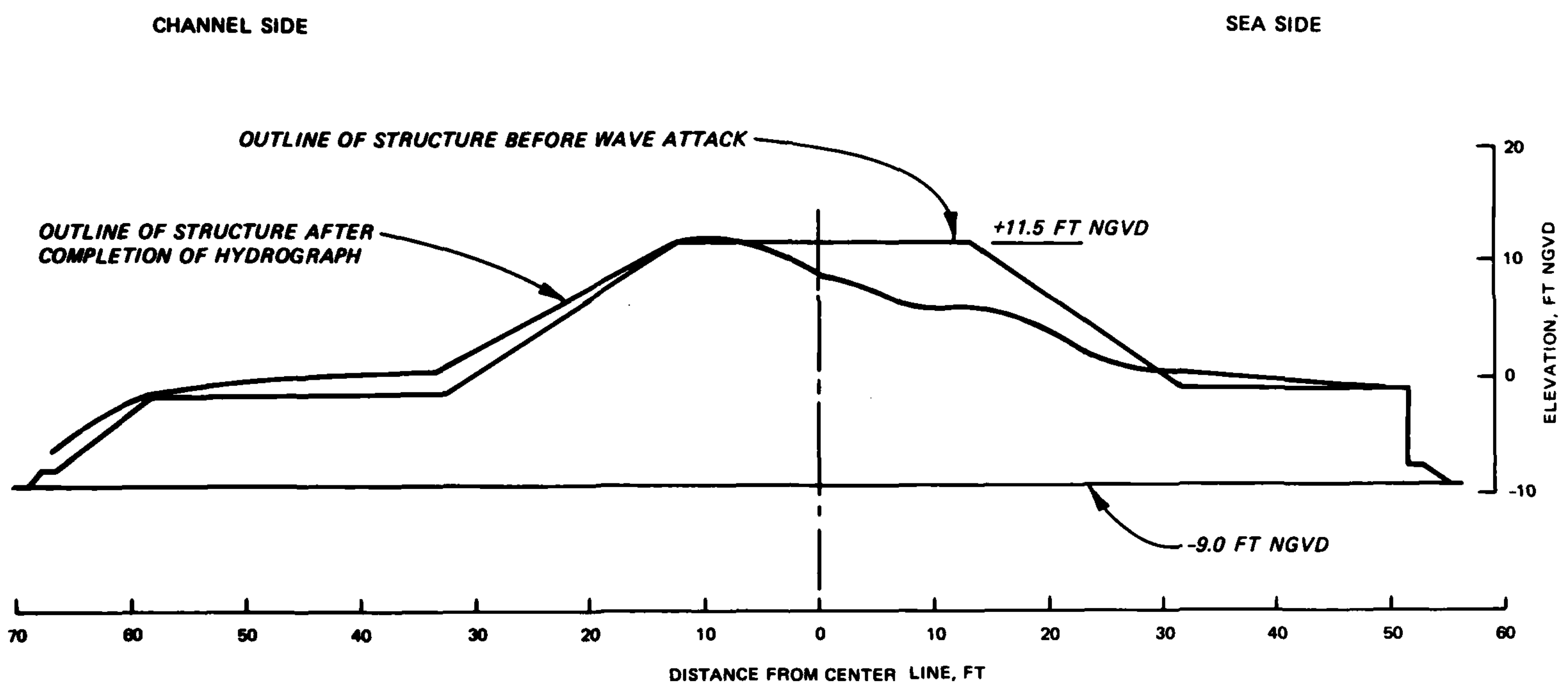

PLAN 4B
COMPARISON OF JETTY CROSS SECTIONS
BEFORE AND AFTER WAVE ATTACK
+10.5 FT NGVD HYDROGRAPH

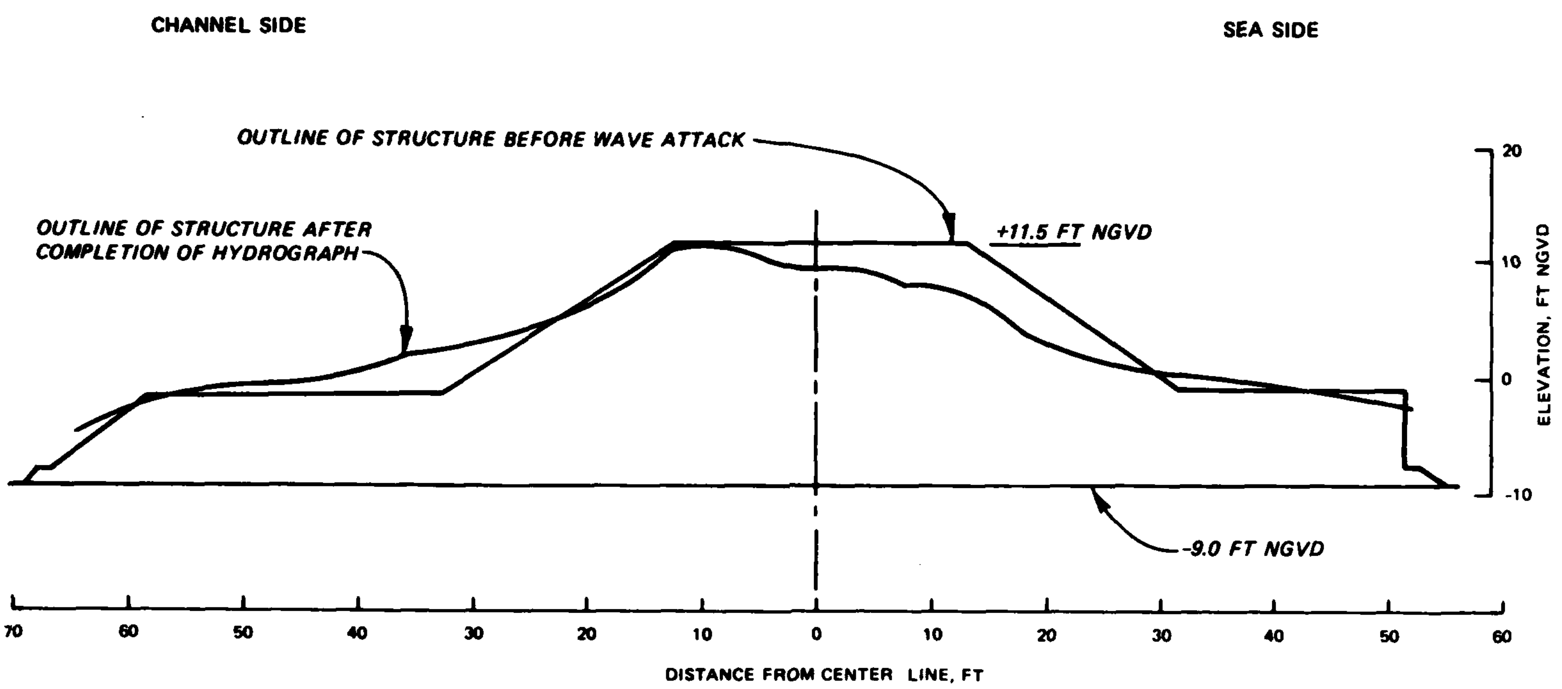

PLAN 4B
COMPARISON OF JETTY CROSS SECTIONS
BEFORE AND AFTER WAVE ATTACK
+11.5 FT NGVD HYDROGRAPH

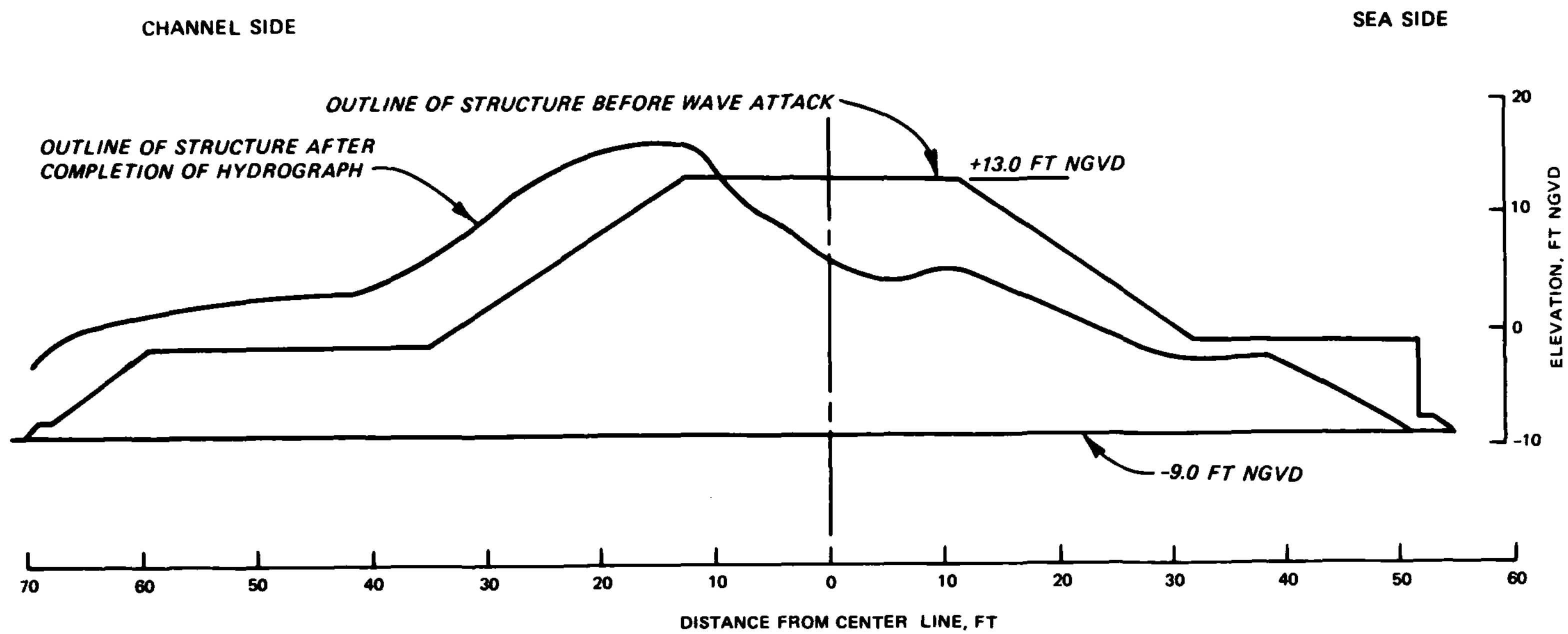

PLAN 8
COMPARISON OF JETTY CROSS SECTIONS
BEFORE AND AFTER WAVE ATTACK
+8.5 FT NGVD HYDROGRAPH

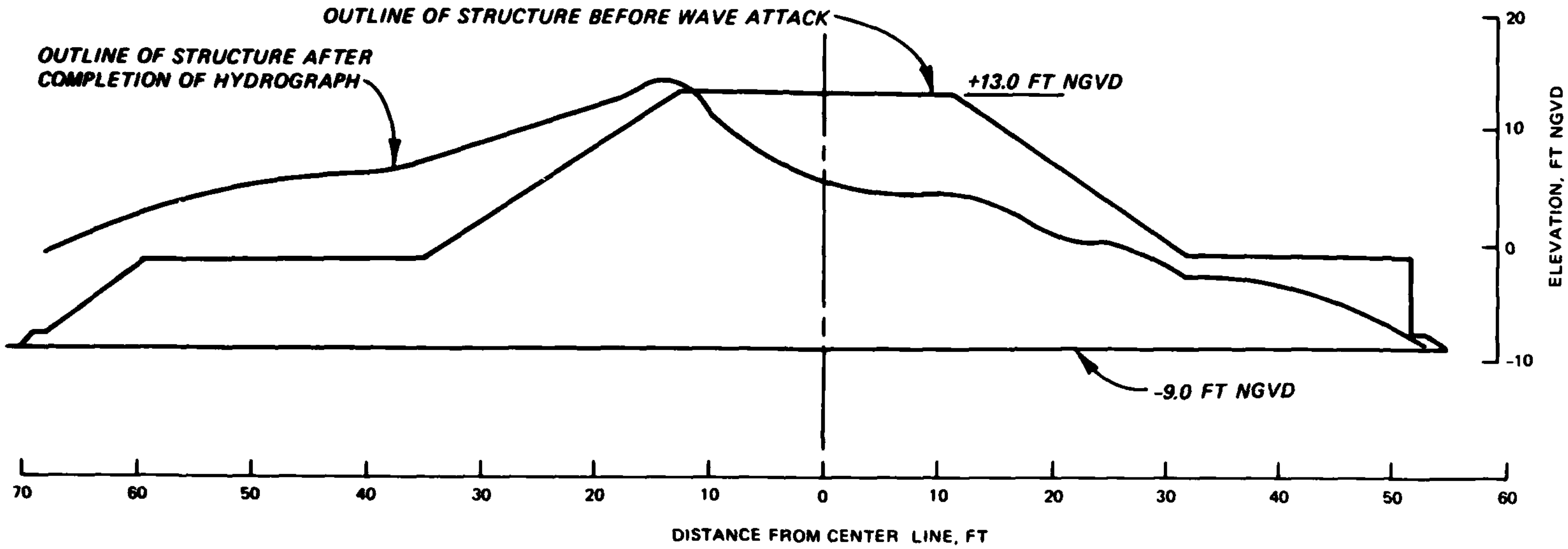

PLAN 8
COMPARISON OF JETTY CROSS SECTIONS
BEFORE AND AFTER WAVE ATTACK
+9.5 FT NGVD HYDROGRAPH

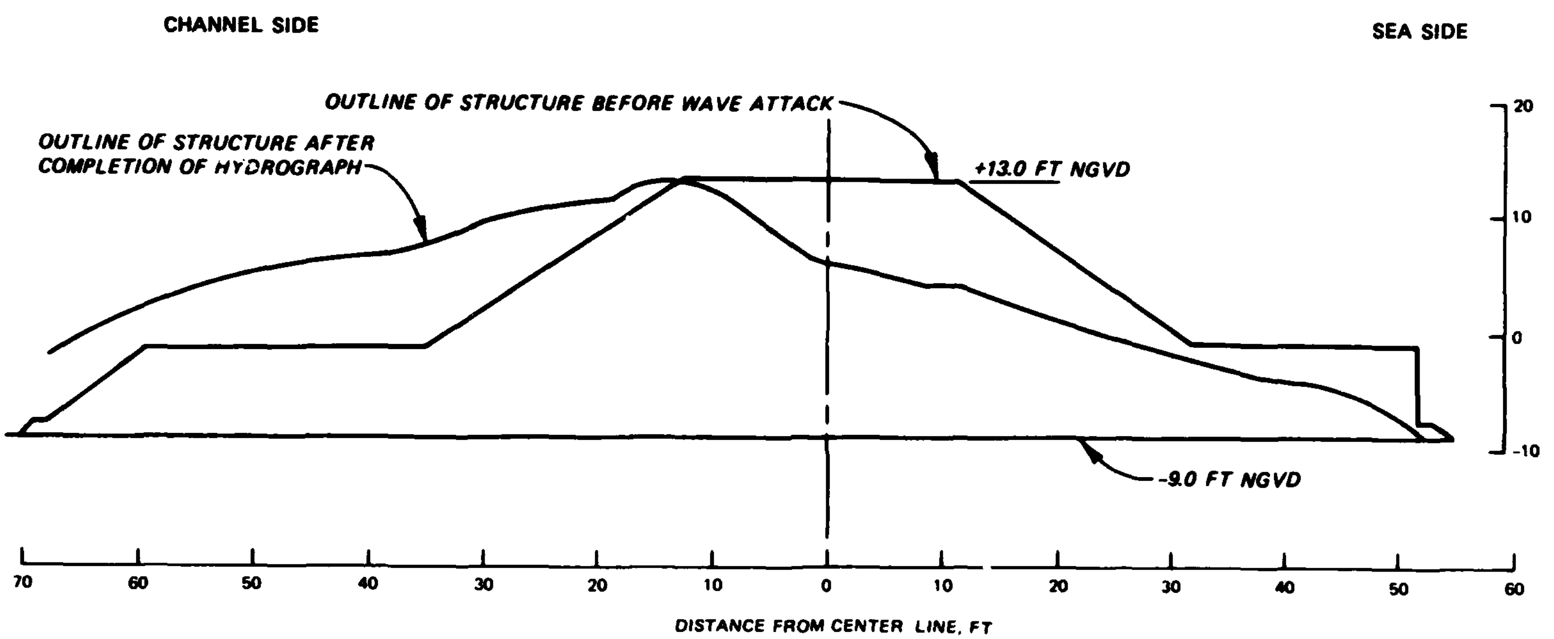

PLAN 8
COMPARISON OF JETTY CROSS SECTIONS
BEFORE AND AFTER WAVE ATTACK
+10.5 FT NGVD HYDROGRAPH

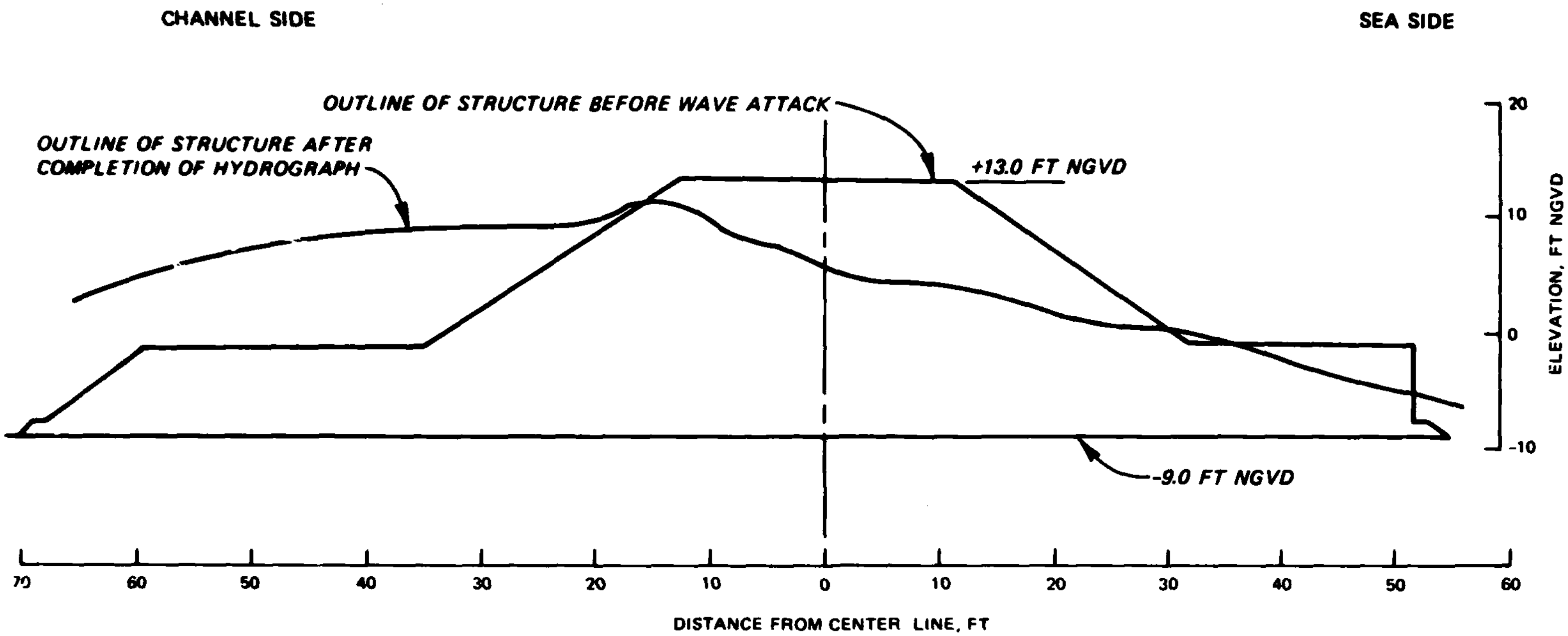

PLAN 8
COMPARISON OF JETTY CROSS SECTIONS
BEFORE AND AFTER WAVE ATTACK
+11.5 FT NGVD HYDROGRAPH

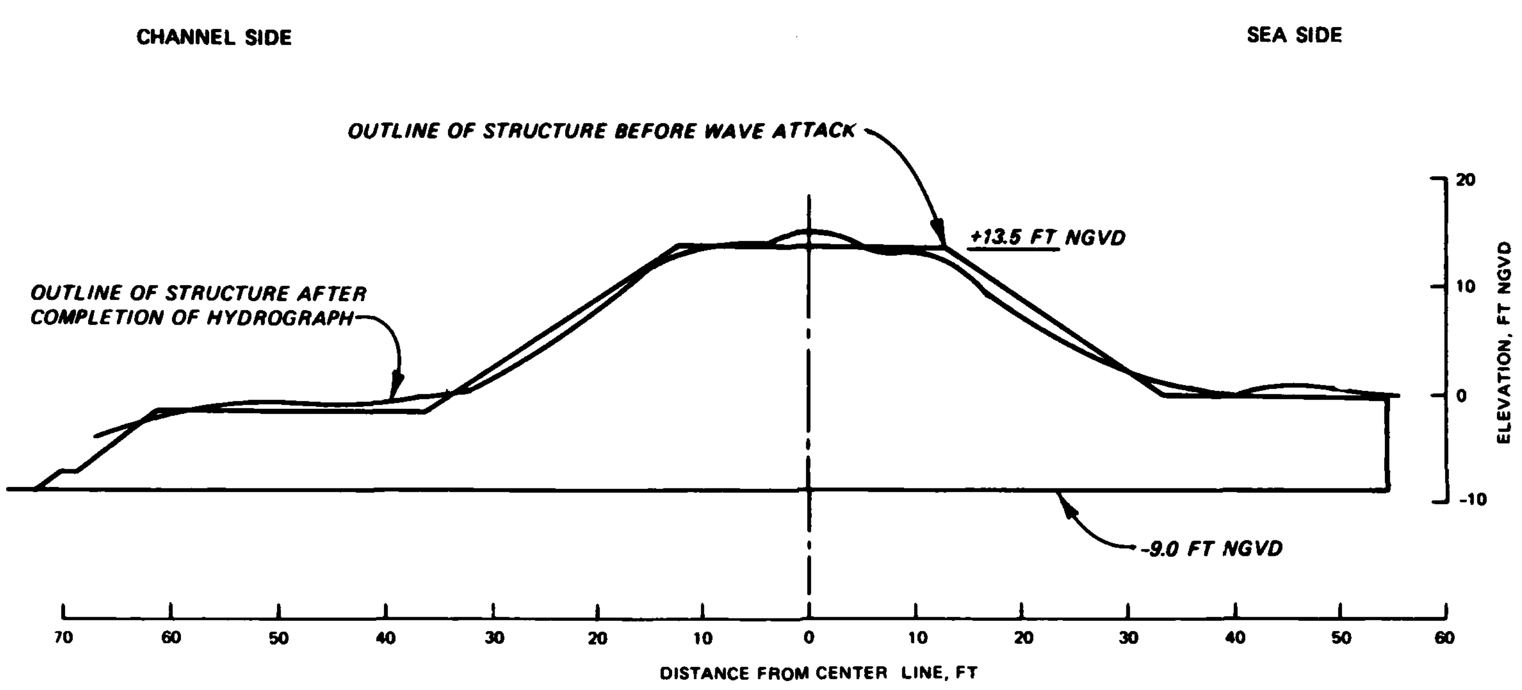

PLAN 4D

COMPARISON OF JETTY CROSS SECTIONS
BEFORE AND AFTER WAVE ATTACK
+8.5 FT NGVD HYDROGRAPH

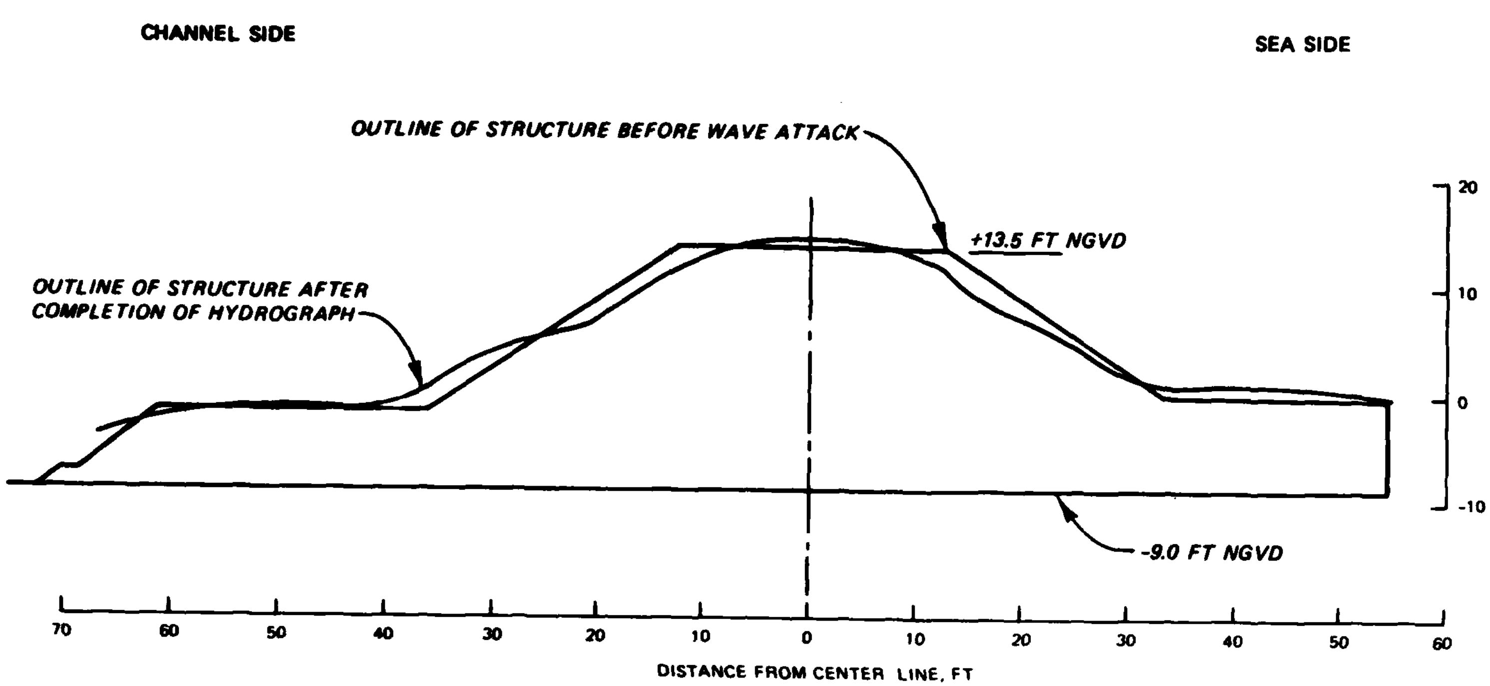

PLAN 4D
COMPARISON OF JETTY CROSS SECTIONS
BEFORE AND AFTER WAVE ATTACK
+9.5 FT NGVD HYDROGRAPH

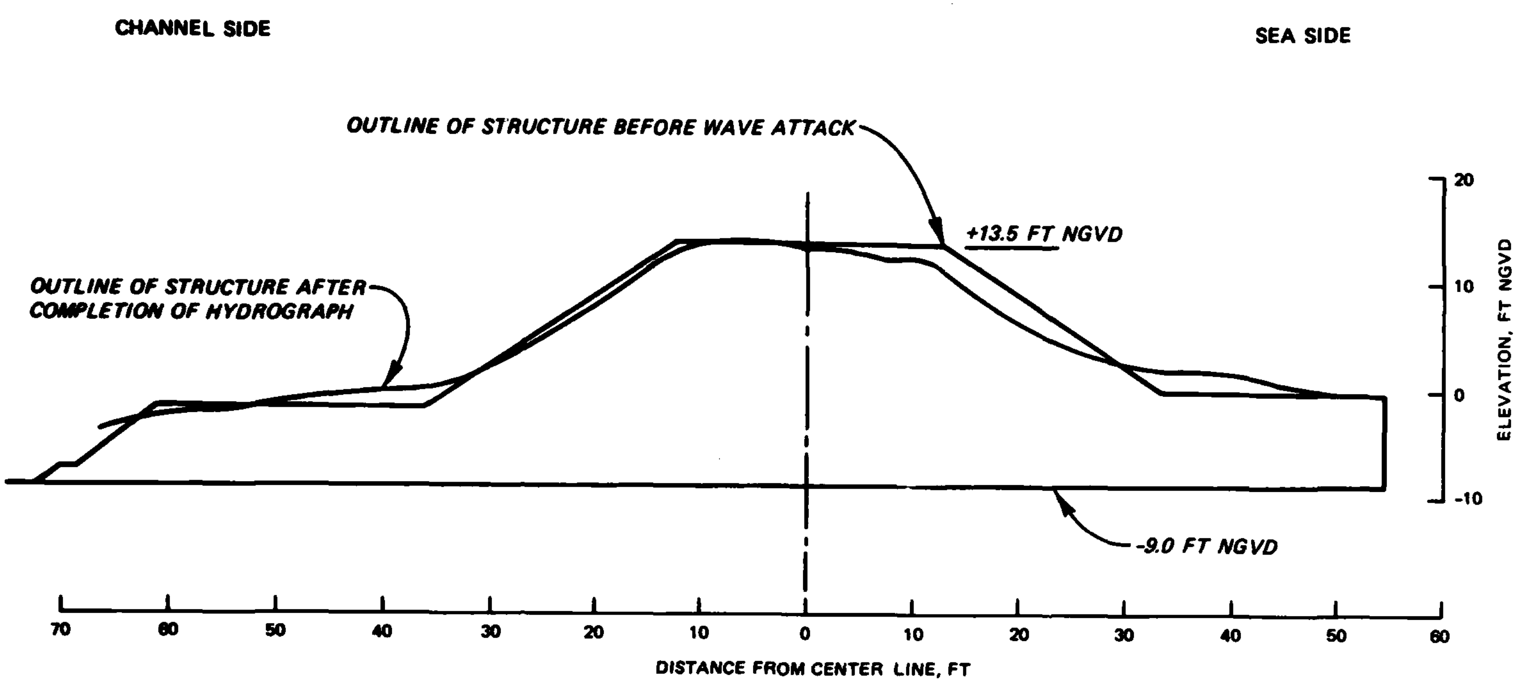

PLAN 4D

COMPARISON OF JETTY CROSS SECTIONS BEFORE AND AFTER WAVE ATTACK

+10.5 FT NGVD HYDROGRAPH

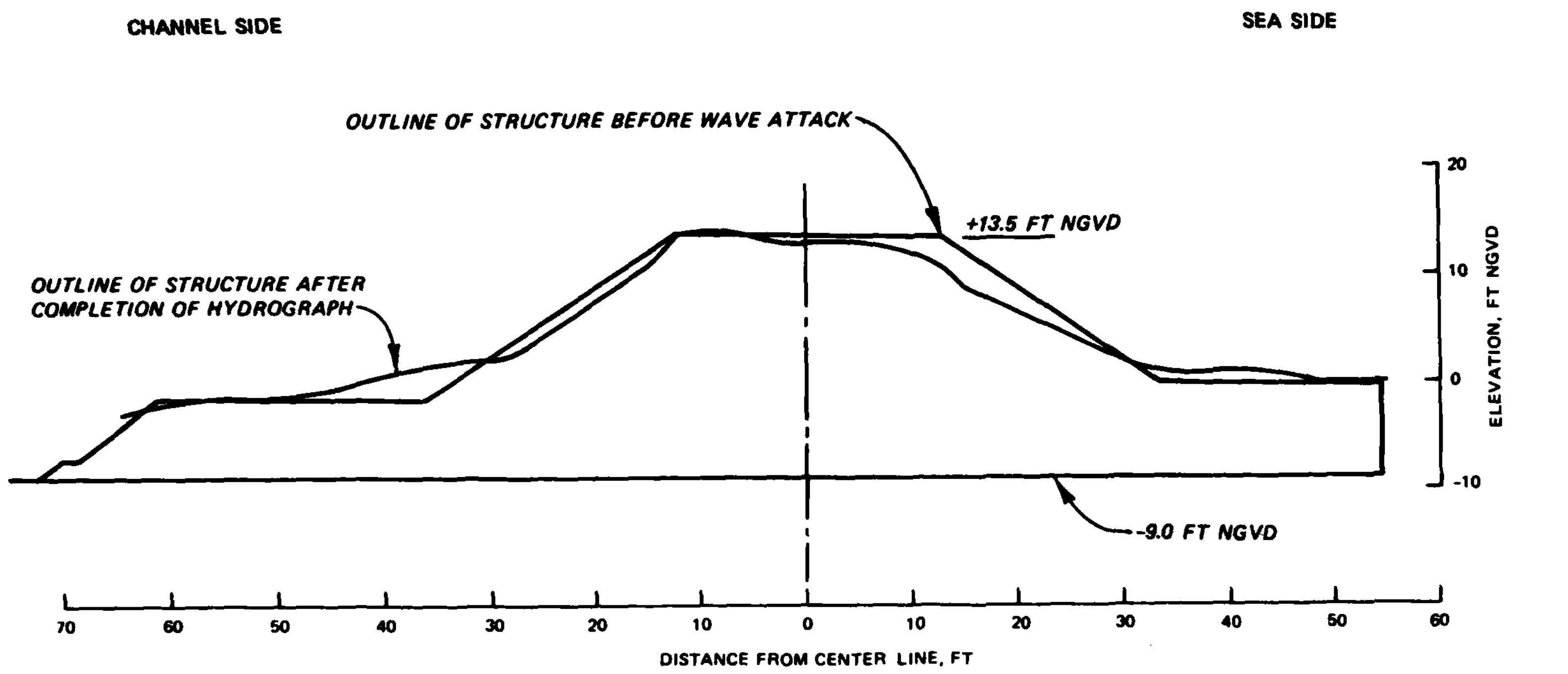

PLAN 4D
COMPARISON OF JETTY CROSS SECTIONS
BEFORE AND AFTER WAVE ATTACK
+11.5 FT NGVD HYDROGRAPH

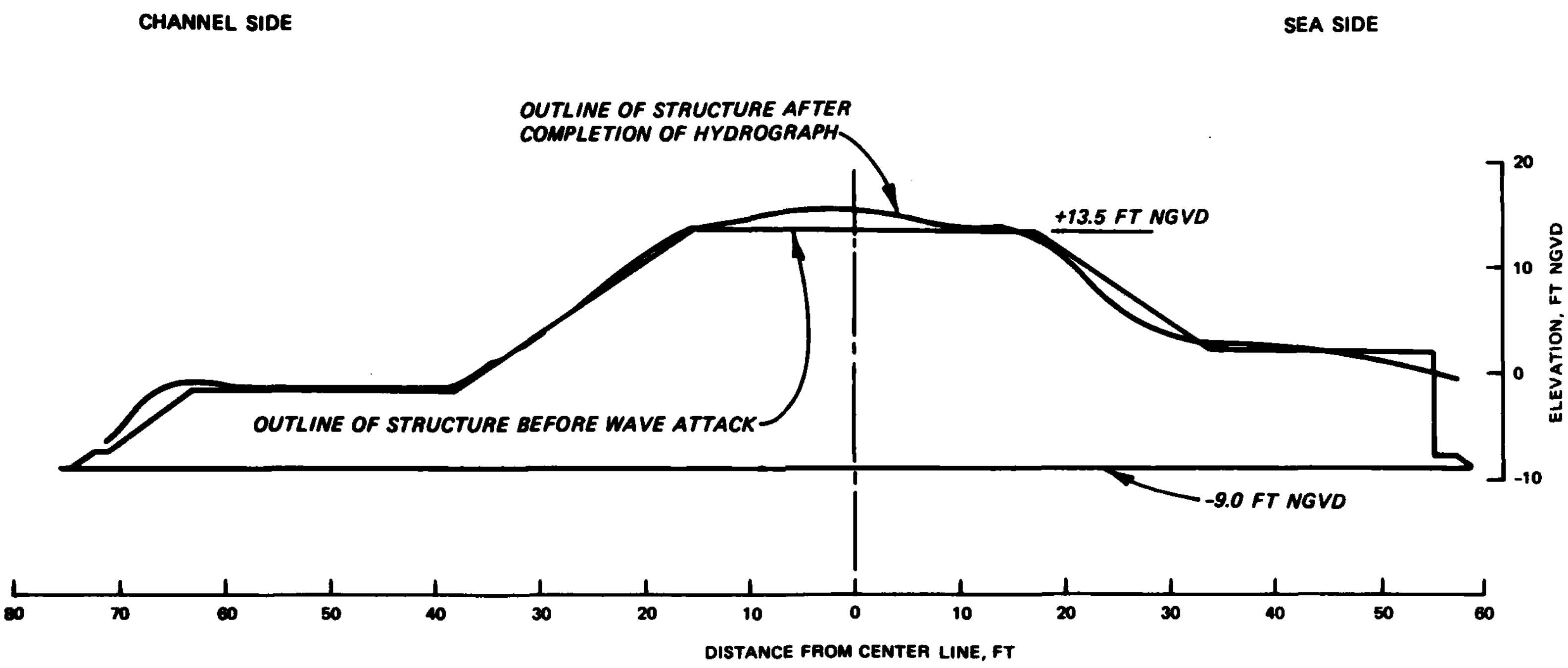

PLAN 10

COMPARISON OF JETTY CROSS SECTIONS
BEFORE AND AFTER WAVE ATTACK

+8.5 FT NGVD HYDROGRAPH

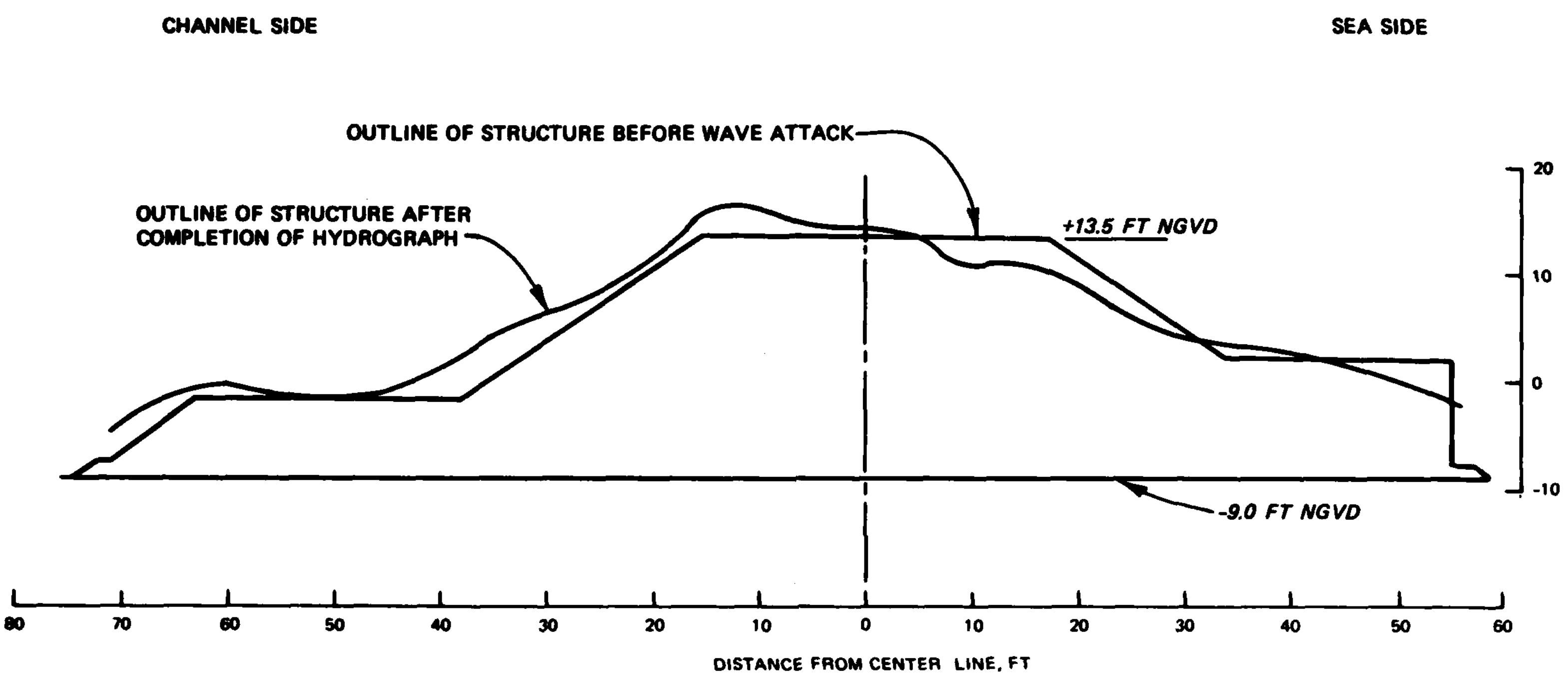

PLAN 10
COMPARISON OF JETTY CROSS SECTIONS
BEFORE AND AFTER WAVE ATTACK
+9.5 FT NGVD HYDROGRAPH

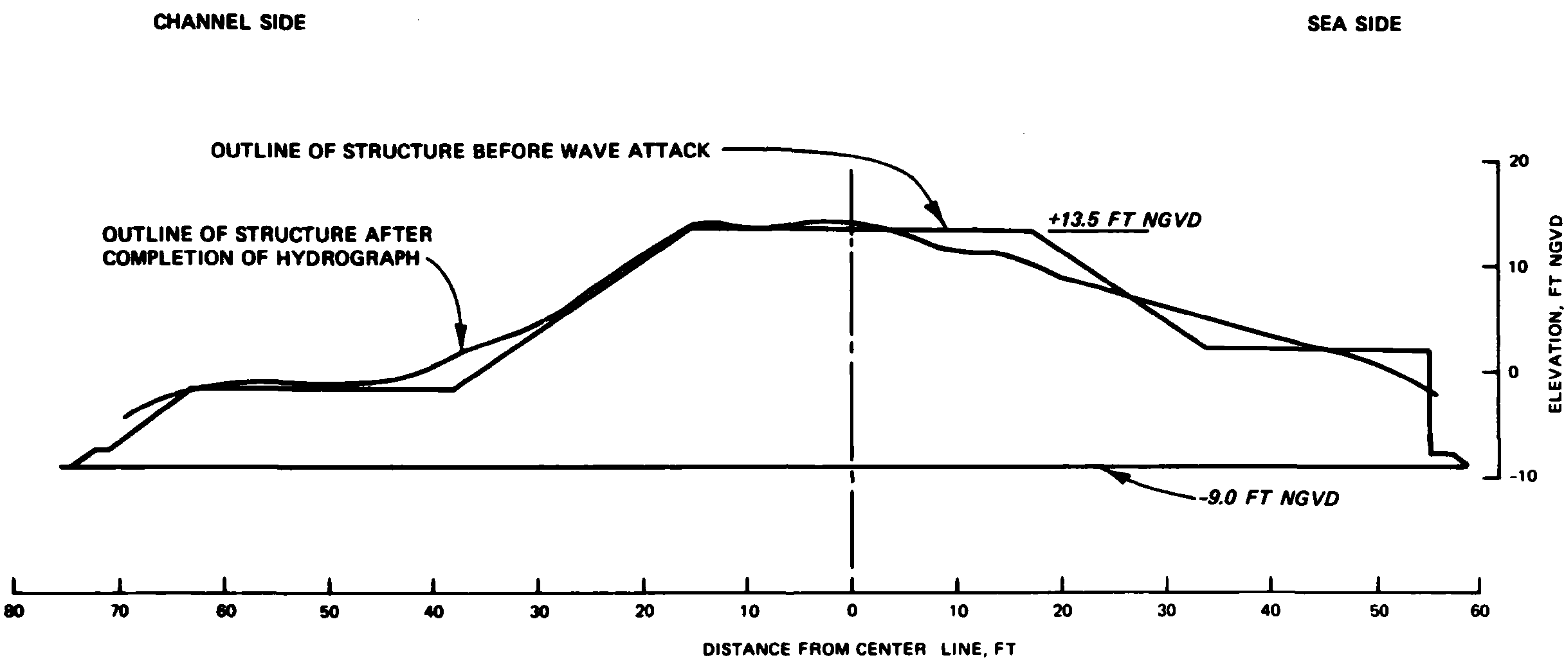

PLAN 10
COMPARISON OF JETTY CROSS SECTIONS
BEFORE AND AFTER WAVE ATTACK
+10.5 FT NGVD HYDROGRAPH

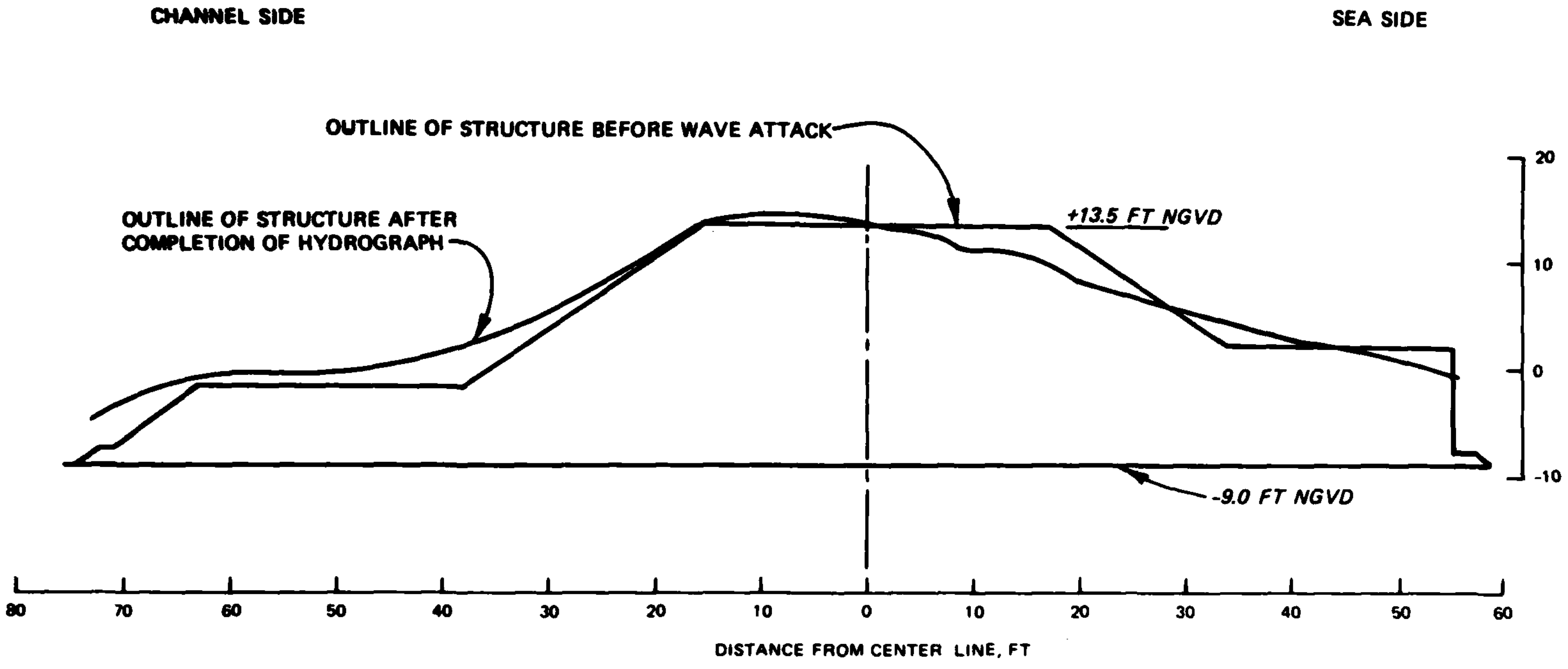

PLAN 10
COMPARISON OF JETTY CROSS SECTIONS
BEFORE AND AFTER WAVE ATTACK
+11.5 FT NGVD HYDROGRAPH

FILM

2 -8